

**DESIGN OF NOVEL DYES  
TOWARDS THE NEAR-INFRARED**

A Dissertation

by

AURORE LOUDET

Submitted to the Office of Graduate Studies of  
Texas A&M University  
in partial fulfillment of the requirements for the degree of

DOCTOR OF PHILOSOPHY

December 2007

Major Subject: Chemistry

**DESIGN OF NOVEL DYES TOWARDS  
THE NEAR-INFRARED**

A Dissertation

by

AURORE LOUDET

Submitted to the Office of Graduate Studies of  
Texas A&M University  
in partial fulfillment of the requirements for the degree of

DOCTOR OF PHILOSOPHY

Approved by:

Chair of Committee,  
Committee Members,

Head of Department,

Kevin Burgess  
Francois Gabbai  
Gyula Vigh  
Andy LiWang  
David Russell

December 2007

Major Subject: Chemistry

## ABSTRACT

Design of Novel Dyes Towards the Near-Infrared. (December 2007)

Aurore Loudet, B.S.; M.S., Université Paul Sabatier, Toulouse, France

Chair of Advisory Committee: Dr. Kevin Burgess

A series of seven functionalized near-infrared aza-BODIPY dyes have been synthesized and their spectroscopic properties measured. Their fluorescence emissions could be tuned by altering the electronic substituents on the aryl-groups. A through-bond energy transfer cassette featuring two fluorescein units as donor, and an aza-BODIPY dye as acceptor, was then synthesized and its preliminary spectroscopic properties examined. This cassette exhibited absorption and fluorescence characteristics that were highly dependent on the pH and the solvent polarity. Furthermore, no energy transfer was observed upon excitation of the donor.

Novel near-infrared aza-BODIPY were also synthesized via a one-pot, two step reaction. Upon demethylation and intermolecular cyclization onto the *B*-atom, a ~ 100 nm red-shift of both the absorption and fluorescence emission maxima could be observed.

Through-bond energy transfer cassettes based on squaraines have also been synthesized and their spectroscopic properties studied. These cassettes exhibited fast and efficient energy transfer from the donor to the acceptor.

In depth experiments have also been realized to correlate the rate of energy transfer and structure on 3 different sets of through-bond energy transfer cassettes. No correlations could be made between the rate of the energy transfer and the nature of the acceptor, and the distance between the donor and acceptor.

Finally, the use of DPP (diketo-pyrrolopyrrole) pigment as a potential donor for through-bond energy transfer cassettes was investigated. Three water-soluble DPPs dyes were prepared and studied. They all displayed weak fluorescence in water.

## DEDICATION

*To my husband, my daughter, my parents and grand-parents*



## ACKNOWLEDGEMENTS

I would like to thank my committee chair, Dr. Burgess, and my committee members, Dr. Gabbai, Dr. Vigh, and Dr. Li-Wang for their guidance and support throughout the course of this research.

Thanks to Jill Rutledge, Virginia Young and Laura Kulpa for all their assistance throughout all these years.

Thank you to the past and present members of the Burgess group for their support and friendship.

I will surely not forget to thank Dr. Karine Poullennec, “ma poule”, and Dr. Richard Duffy for all their help, fun time spend together and gossips. Thank you to B.J. Bench for introducing me to my husband.

A special *thank you* goes to Dr. Alexandre Picot for his love, friendship, support and care.

Finally *MERCI* to my parents, mamie Louise, my husband and daughter for their everlasting love, encouragement, support and patience.

## TABLE OF CONTENTS

|  | Page |
|--|------|
| ABSTRACT.....  | iii  |
| DEDICATION.....  | iv   |
| ACKNOWLEDGEMENTS.....  | v    |
| TABLE OF CONTENTS.....   | vi   |
| LIST OF FIGURES.....   | xi   |
| LIST OF TABLES.....  | xiv  |
| LIST OF SCHEMES.....   | xv   |
| CHAPTER  |      |
| I    BODIPY® DYES AND THEIR DERIVATIVES: SYNTHESSES AND                        |      |
| SPECTROSCOPIC PROPERTIES.....  | 1    |
| A. Introduction.....   | 1    |
| B. The BODIPY Core.....  | 2    |
| 1. Fundamental Properties.....   | 3    |
| 2. Syntheses From Pyrroles and Acid Chlorides or Anhydrides....                | 5    |
| 3. Syntheses From Pyrroles and Aldehydes.....                                  | 6    |
| 4. Syntheses From Ketopyrroles.....  | 10   |
| C. Modifications to <i>meso</i> -aromatic Substituents on the BODIPY Core..... | 12   |
| 1. Fluorescence Control via Photoinduced Electron Transfer.....                | 15   |
| D. BODIPY With Heteroatom Substituents.....                                    | 21   |
| 1. From Electrophilic Substitution Reactions.....                              | 21   |

| CHAPTER  | Page |
|--|------|
| 2. From Nucleophilic Attack on Halogenated BODIPYs.....  | 27   |
| 3. From Palladium Mediated C-H Functionalization.....  | 30   |
| 4. From Nucleophilic Attack at the <i>meso</i> -Position.....  | 32   |
| E. Aryl-, Alkenyl-, Alkynyl-Substituted BODIPYs.....   | 35   |
| 1. Aryl-substituted BODIPYs From Aryl-pyrroles.....  | 35   |
| 2. Condensation Reactions of the 3,5-Dimethyl Derivatives with<br>Benzaldehydes Derivatives to Give Alkenyl Systems..... | 38   |
| 3. From Palladium-catalyzed Coupling Reactions at the 3- and 5-<br>Positions.....  | 47   |
| F. Energy Transfer Cassettes.....  | 48   |
| 1. Through-space Energy Transfer Cassettes.....  | 48   |
| 2. Through-bond Energy Transfer Cassettes.....   | 54   |
| G. Substitution of Fluoride Atoms In the BF <sub>2</sub> -Group.....   | 67   |
| 1. With Alkyl Groups.....  | 67   |
| 2. With Aryl Groups.....   | 68   |
| 3. With Alkyne Groups.....   | 71   |
| 4. With Alkoxide Groups.....   | 76   |
| H. Use of Metals Other Than Boron.....   | 78   |
| I. BODIPY-analogs With Extended Aromatic Conjugation.....  | 82   |
| 1. Restricted Systems.....   | 82   |
| 2. Extended Aromatic Systems.....  | 86   |

| CHAPTER   | Page |
|---|------|
| J. Aza-BODIPY Dyes.....   | 92   |
| 1. Tetraaryl Systems.....   | 92   |
| 2. Extended Aza-BODIPY Systems.....   | 100  |
| K. Other Analogs of the BODIPYS.....  | 106  |
| 1. Biimidazol-2-yl-BF <sub>2</sub> Complexes.....   | 106  |
| 2. Pyridine-based Systems.....  | 107  |
| 3. 2-Ketopyrrole Complexes.....   | 109  |
| 4. Azobenzene Derivatives.....  | 110  |
| 5. Miscellaneous <i>N,N</i> -Bidentate Diphenyl Boron Chelates.....                       | 111  |
| 6. Boryl-substituted Thienylthiazoles.....  | 114  |
| L. Conclusions.....   | 118  |
| II FUNCTIONALIZED AZA-BODIPY DYES.....  | 121  |
| A. Introduction.....  | 121  |
| 1. Multiplexing Through-bond Energy Transfer Cassettes.....                               | 125  |
| B. Results and Discussion.....  | 129  |
| 1. Synthesis of Aza-BODIPY <b>288a-g</b> .....  | 129  |
| 2. Spectroscopic Properties of Aza-BODIPY derivatives <b>288a-g</b> .....                 | 133  |
| 3. Synthesis of Through-bond Energy Transfer Cassettes <b>289</b><br>and <b>290</b> ..... | 137  |
| 4. Spectroscopic Studies of Cassettes <b>289</b> and <b>290</b> .....                     | 141  |
| C. Conclusions.....   | 146  |

| CHAPTER   | Page |
|---|------|
| III RING CONSTRAINED NEAR-IR AZA-BODIPY DYES.....   | 147  |
| A. Introduction.....  | 147  |
| B. Results and Discussion.....  | 149  |
| 1. Synthesis.....   | 149  |
| 2. Spectroscopic Properties.....  | 149  |
| 3. Electrochemistry.....  | 151  |
| 4. Frontier Orbitals Calculations.....  | 153  |
| C. Conclusions.....   | 158  |
| IV SYNTHESSES AND SPECTROSCOPIC PROPERTIES OF ENERGY<br>TRANSFER SYSTEMS BASED ON SQUARAINES DYES .....     | 159  |
| A. Introduction.....  | 159  |
| 1. Squaraine Dyes.....  | 159  |
| 2. "Donor-acceptor" Cassettes.....  | 160  |
| B. Results and Discussion.....  | 162  |
| 1. Synthesis.....   | 162  |
| 2. Spectroscopic Studies.....   | 167  |
| C. Conclusions.....   | 171  |
| V CORRELATIONS OF STRUCTURE AND RATES OF ENERGY TRANSFER<br>FOR THROUGH-BOND ENERGY-TRANSFER CASSETTES..... | 172  |
| A. Introduction.....  | 172  |
| B. Results and Discussion.....  | 173  |
| 1. Synthesis.....   | 173  |
| 2. Transition Moments.....  | 176  |
| 3. Relaxation Times.....  | 182  |

| CHAPTER  | Page |
|--|------|
| 4. Anisotropy Measurements.....  | 185  |
| C. Conclusions.....  | 187  |
| VI DESIGN AND SYNTHESIS OF FLUORESCENT CASSETTES BASED ON<br>DIKETOPYRROLOPYRROLE..... | 190  |
| A. Introduction.....   | 190  |
| 1. DNA Sequencing: The State of the Art.....   | 190  |
| 2. Diketopyrrolopyrrole (DPP) Dyes.....  | 193  |
| B. Results and Discussion.....   | 202  |
| 1. Synthesis of <i>N</i> -alkylated DPPs.....  | 202  |
| 2. UV and Fluorescence Studies.....  | 208  |
| 3. DPP-based Cassettes.....  | 210  |
| C. Conclusions.....  | 215  |
| VII OUTLOOK AND CONCLUSION.....  | 216  |
| A. Outlook .....   | 216  |
| 1. Water-soluble Near-IR Dyes Based on Diketopyrrolopyrroles<br>(DPP) dyes.....        | 216  |
| 2. Water-soluble Cassettes Based on Aza-BODIPY .....                                   | 221  |
| B. Conclusion.....   | 224  |
| REFERENCES .....   | 226  |
| APPENDIX A.....  | 249  |
| APPENDIX B.....  | 350  |
| APPENDIX C.....  | 382  |
| APPENDIX D.....  | 401  |
| APPENDIX E.....  | 418  |
| VITA .....   | 465  |

## LIST OF FIGURES

|  | Page |
|--|------|
| Figure 1.1 Selected BODIPYs with <i>meso</i> -modifications to give: <b>a</b> selective sensors of particular redox active molecules; <b>b</b> pH probes; <b>c</b> metal-chelators; and <b>d</b> biomolecule conjugating groups.....   | 13   |
| Figure 1.2 The <i>meso</i> -substituent provides: <b>a</b> no significant electronic perturbation; <b>b</b> electrons to the excited state; and <b>c</b> a low lying LUMO to accept electrons from the excited state.....  | 16   |
| Figure 1.3 <b>a</b> Reductive PeT occurs when nitric oxide reacts with the diamine; <b>b</b> Calculated HOMO energy levels of <i>meso</i> -substituents for BODIPY <b>46</b> and <b>47</b> .....   | 18   |
| Figure 1.4 Reductive PeT increases in the order Et < H < CO <sub>2</sub> Et.....   | 20   |
| Figure 1.5 Electrophilic attack on tetramethyl-BODIPY.....   | 22   |
| Figure 1.6 Spectroscopic data for some BODIPYs formed by S <sub>N</sub> Ar reactions .....   | 28   |
| Figure 1.7 Structures of H-dimer and J-dimer.....  | 38   |
| Figure 1.8 Intramolecular B-N coordination of <i>N</i> -heteroaromatic systems .....   | 115  |
| Figure 2.1 Very few biological molecules possess intrinsic fluorescence in the near-IR.....  | 121  |
| Figure 2.2 A tetra-sulfonated indocyanine dye, with a carboxylic acid that can be used for conjugation to biomolecules.....  | 122  |
| Figure 2.3 Through-bond energy transfer cassette.....  | 126  |
| Figure 2.4 <b>a</b> Idealized fluorescence emissions from dyes used in DNA sequencing; <b>b</b> An approximate representation of data obtained from single dyes in DNA sequencing; <b>c</b> Diminished fluorescence intensities of the red dyes can be attributed to their lower extinction coefficients at the excitation wavelength, relative to the blue dyes. .... | 127  |
| Figure 2.5 First generation of through-bond energy transfer cassettes developed for DNA sequencing (top), and the corresponding acceptor rosamine fragments (bottom).....  | 128  |
| Figure 2.6 Fluorescence emission of the cassettes upon excitation at 488 nm. ....  | 129  |
| Figure 2.7 Thermal ellipsoid representation of <b>288a</b> . ....  | 132  |

|  | Page |
|--|------|
| Figure 2.8 <b>a</b> Normalized absorption and <b>b</b> fluorescence spectra of compounds <b>288a – g</b> in toluene at 5 $\mu$ M.....  | 136  |
| Figure 2.9 pH dependency of fluorescein fluorescence quantum yield.....  | 142  |
| Figure 2.10 Spectra of: <b>a</b> UV absorption and fluorescence spectra (excitation at 488 nm and 702 nm) in 1:1 THF:buffer pH 7.4; <b>b</b> UV absorption of <b>289</b> with increasing concentration of <b>289</b> in 1:1 THF:buffer pH 7.4; <b>c</b> fluorescence intensities (at 530 and 730 nm) versus concentration of compound <b>289</b> in 1:1 THF:buffer pH 7.4; <b>d</b> UV absorption of compound <b>289</b> in 1:1 THF:buffer pH 7.4 with increasing amount of Triton X-100; <b>e</b> fluorescence intensity of compound <b>289</b> upon excitation at 488 nm with increasing amount of Triton X-100; <b>f</b> fluorescence intensity of compound <b>289</b> upon excitation at 702 nm with increasing amount of Triton X-100 ..... | 143  |
| Figure 3.1 Comparison of fluorescence emission wavelength maxima and quantum yields (both in CHCl <sub>3</sub> ) for: <b>N</b> a “ring-extended” BODIPY; <b>O</b> an aryl-substituted BODIPY; <b>P</b> a similar, but constrained, aryl substituted BODIPY; <b>Q</b> a tetraphenyl-substituted azaBODIPY; and <b>R</b> a “ring extended” aza-BODIPY. Compound <b>300</b> is the focus of this research project.....  | 148  |
| Figure 3.2 Absorption (5 $\mu$ M in PhMe) spectra of <b>288c - d</b> and <b>300a - d</b> .....   | 150  |
| Figure 3.3 Fluorescence (5 $\mu$ M in PhMe) spectra of <b>288c - d</b> and <b>300a – d</b> .....   | 151  |
| Figure 3.4 Cyclic voltamogram of compound <b>288c</b> .....  | 152  |
| Figure 3.5 Cyclic voltamogram of compound <b>300a</b> .....  | 153  |
| Figure 3.6 HOMO and LUMO for compound <b>288c</b> , <b>300a</b> and <b>300d</b> .....  | 154  |
| Figure 3.7 X-Ray structure of compound <b>300d</b> .....   | 157  |
| Figure 4.1 Resonance structures of squaraine dyes.....   | 159  |
| Figure 4.2 <b>a</b> ) Through-space ET cassettes, <b>b</b> ) through-bond ET cassettes, <b>c</b> ) the acceptor fragments used in this study.....  | 161  |
| Figure 4.3 Donor-acceptor cassettes in this research.....  | 163  |
| Figure 4.4 <b>(a)</b> , <b>(c)</b> , <b>(e)</b> and <b>(g)</b> Overlaid absorption spectra of the donor fragments, the acceptor fragments, and the complete cassettes; all in CHCl <sub>3</sub> solution. <b>(b)</b> , <b>(d)</b> , <b>(f)</b> and <b>(h)</b> Fluorescence spectra of the cassettes; all excited at 300 nm or 590 (630) nm in CHCl <sub>3</sub> solution.....  | 169  |
| Figure 5.1 Sequence of anthracene-BODIPY cassettes having perpendicular donor and acceptor transition moments.....   | 177  |
| Figure 5.2 Indications of the S <sub>1</sub> $\leftrightarrow$ S <sub>0</sub> transition moments in the different energy-transfer cassettes.....   | 178  |



|  | Page |
|--|------|
| Figure 5.3 Sequence of anthracene-BODIPY cassettes having parallel donor and acceptor transition moments.....  | 178  |
| Figure 5.4 Sequence of fluorescein-rosamine cassettes. All have parallel donor and acceptor transition moments.....  | 180  |
| Figure 5.5 Sequence of fluorescein-rosamine cassettes with shorter linker. All also have parallel donor and acceptor transition moments.....                         | 181  |
| Figure 5.6 Commercial energy-transfer cassette Big ROX, obtained from ABI.....   | 182  |
| Figure 5.7 Sequence of gated emission spectra for compound <b>326</b> (in EtOH) following ultrashort-pulsed excitation at 405 nm.....                                | 183  |
| Figure 5.8 Gated fluorescence time profiles at 550 nm (donor) and 610 nm (acceptor) following ultrashort-pulsed excitation of compound <b>326</b> .....              | 183  |
| Figure 5.9 Polarized time profiles of compound <b>314</b> in chloroform following excitation at 405 nm. Signals monitored at 550 nm, on the BODIPY fluorescence...   | 186  |
| Figure 5.10 Polarized time profiles of compound <b>325</b> in ethanol following excitation at 495 nm. Signals monitored at 610 nm, on the rosamine fluorescence..... | 187  |
| Figure 6.1 Fluorescence intensities of JOE, ROX, FAM and TAMRA excited at 488 nm.....  | 191  |
| Figure 6.2 Through-space energy transfer cassettes (top), through-bond energy transfer cassettes (bottom).....   | 192  |
| Figure 6.3 Fluorescence intensities of ideal sequencing dyes: resolved and intense..   | 193  |
| Figure 6.4 Structural analogy of DPP with commercial pigments.....   | 194  |
| Figure 6.5 Centres of potential chemical reactivity.....   | 197  |
| Figure 6.6 Normalized UV absorption of DPP <b>347</b> , <b>351</b> and <b>352</b> in NaHCO <sub>3</sub> .....  | 208  |
| Figure 6.7 Normalized fluorescence emission of DPP <b>347</b> , <b>351</b> and <b>352</b> in NaHCO <sub>3</sub> .....  | 209  |

## LIST OF TABLES

|  | Page |
|--|------|
| Table 2.1 Selected bond lengths and angles for <b>288a</b> .....   | 132  |
| Table 2.2 Spectroscopic properties of the Aza-BODIPY derivatives <b>288 a - g</b> . ....   | 135  |
| Table 3.1 Spectroscopic properties of <b>288c-d</b> and <b>300a-d</b> .....  | 150  |
| Table 3.2 Electrochemical properties of <b>288c</b> and <b>300a</b> .....  | 152  |
| Table 3.3 Excitation energies from B3LYP calculations.....   | 155  |
| Table 3.4 Selected parameters for compounds <b>288c</b> and <b>300a</b> .....  | 156  |
| Table 3.5 Comparisons of some key parameters for <b>300d</b> .....   | 157  |
| Table 4.1 Spectroscopic data for the compounds <b>303a,b</b> and <b>304b-d</b> .....   | 168  |
| Table 4.2 The ratios of absorptions and fluorescence excitation spectra<br>{ $A(\lambda_{ex})/F(\lambda_{ex})$ } and the average lifetimes of the acceptor group upon<br>excitation of the donor and the acceptors of cassettes <b>303b</b> and<br><b>304b-d</b> ..... | 169  |
| Table 5.1 Emission characteristics of rigidly linked donor-acceptor cassettes<br>(solvent $\text{CHCl}_3$ for compounds <b>314 - 322</b> and ethanol for <b>323 - 330</b> ,<br>unless otherwise indicated).....  | 184  |
| Table 6.1 Physical properties of some DPP pigments .....   | 201  |
| Table 6.2 Spectroscopic data for the compounds <b>347</b> , <b>352</b> and <b>353</b> .....  | 208  |

## LIST OF SCHEMES

|             | Page   |    |
|-------------|--|----|
| Scheme 1.1  | <b>a</b> and <b>b</b> two different methods for production of ketopyrroles from magnesium derivatives of pyrrole, and application of these starting materials in the production of <b>c</b> symmetrical, and <b>d</b> unsymmetrical dyes.....  | 11 |
| Scheme 1.2  | Synthesis of diaminobenzene- and triazole-BODIPY derivatives <b>46</b> and <b>47</b> .....   | 19 |
| Scheme 1.3  | Preparation of 3,5-dichloro-BODIPY via chlorination of a dipyrromethane intermediate.....  | 26 |
| Scheme 1.4  | BODIPY dyes via S <sub>N</sub> Ar reactions .....  | 27 |
| Scheme 1.5  | Cyanopyrromethene-BF <sub>2</sub> complexes via addition of cyanide.....   | 33 |
| Scheme 1.6  | Synthesis of sulfur- and anilino- BODIPY derivatives.....  | 35 |
| Scheme 1.7  | Syntheses of BODIPY dyes anchored on xanthene units to test self-quenching: <b>a</b> a system with one BODIPY dye; <b>b</b> a similar compound with two, where only one has extended conjugation; and, <b>c</b> another where both have extended conjugation .....                           | 44 |
| Scheme 1.8  | Synthesis of C-BODIPYs using <b>a</b> aryl Grignard reagents; and, <b>b</b> aryl lithium reagents.....   | 69 |
| Scheme 1.9  | <b>a</b> Two-steps synthesis of bis(ethynyl)BODIPY <b>163</b> , and the monoprotected analog <b>164</b> ; and, <b>b</b> some examples of compounds that have been prepared via Sonogashira coupling of <b>163</b> .....  | 72 |
| Scheme 1.10 | Synthesis of homocoupled products .....  | 73 |
| Scheme 1.11 | Syntheses of the pyrrole-based starting materials.....   | 84 |
| Scheme 1.12 | Synthesis of more conjugated BODIPY derivatives .....  | 85 |
| Scheme 1.13 | Synthesis of a new NIR BODIPY dye .....  | 86 |
| Scheme 1.14 | Extended aromatic dyes from retro-Diels Alder reactions.....   | 87 |
| Scheme 1.15 | Synthesis of di(iso)indomethene dyes from 2-acylacetophenone derivatives.....  | 89 |
| Scheme 1.16 | Formation of azapyrromethene from <b>a</b> . nitroso pyrrole; and, <b>b</b> , nitrobutyrophenones <b>D</b> and keto-nitrile <b>E</b> ; <b>c</b> , postulated mechanism for the formation of azapyrromethene from nitrobutyrophenones <b>D</b> and <b>d</b> , from ket-nitrile <b>E</b> ..... | 93 |

|             | Page   |
|-------------|--|
| Scheme 1.17 | First syntheses of aza-BODIPY dyes..... 96   |
| Scheme 1.18 | Synthesis of cyclized/restricted 2,4-diarylpyrroles..... 101   |
| Scheme 1.19 | Synthesis of <b>a</b> , symmetrical and <b>b</b> , asymmetrical conformationally restricted azaBODIPY dyes..... 101  |
| Scheme 1.20 | Synthesis of biimidazol-2-yls BF <sub>2</sub> complexes ..... 106  |
| Scheme 1.21 | Two-step Fischer synthesis of <b>a</b> 2-(2'-pyridyl)indole; <b>b</b> 2-(2'-thiazoly) indole; <b>c</b> synthesis of 2-(8'-quinoly)indole or aza-indole via Negishi coupling..... 113 |
| Scheme 1.22 | Synthesis of the dimesityl-boryl substituted thienylthiazole <b>282</b> ..... 115  |
| Scheme 1.23 | Synthesis of <b>a</b> , head-to-head; <b>b</b> , head-to-tail, and <b>c</b> , tail-to-tail dimers 116  |
| Scheme 2.1  | Synthesis of azaBODIPYs <b>288</b> ..... 130   |
| Scheme 2.2  | Synthesis of <b>293h</b> from $\gamma$ -ketonitrile. .... 131  |
| Scheme 2.3  | <b>a</b> . Synthesis of cassettes <b>289</b> and <b>b</b> . <b>290</b> ..... 138   |
| Scheme 3.1  | Synthesis of target aza-BODIPY <b>300</b> ..... 149  |
| Scheme 4.1  | First synthesis of squaraine dyes..... 160   |
| Scheme 4.2  | Synthesis of cassette <b>303b</b> ..... 164  |
| Scheme 4.3  | Synthesis of cassettes <b>309c</b> ..... 165   |
| Scheme 4.4  | Synthesis of cassettes <b>304b-d</b> ..... 166   |
| Scheme 5.1  | Synthesis of 5-carboxaldehyde fluorescein diacetate <b>332</b> ..... 174   |
| Scheme 5.2  | Synthesis of cassettes <b>330</b> ..... 175  |
| Scheme 5.3  | Synthesis of cassette <b>331</b> ..... 176   |
| Scheme 6.1  | First report of DPP..... 194   |
| Scheme 6.2  | Synthesis of symmetrical DPP via the succinic route..... 195   |
| Scheme 6.3  | Synthesis of unsymmetrical DPP..... 196  |
| Scheme 6.4  | Examples of product that can be obtained by direct chemical transformations of diphenyl DPP..... 198   |

|             | Page   |
|-------------|--|
| Scheme 6.5  | Synthesis of N,N'-disubstituted DPP dyes..... 199  |
| Scheme 6.6  | Synthesis of trisubstituted DPP dyes..... 200  |
| Scheme 6.7  | Synthesis of DPPs derivatives..... 202   |
| Scheme 6.8  | Synthesis of $\beta$ -diketones..... 203   |
| Scheme 6.9  | Synthesis of diketofurofuranes..... 203  |
| Scheme 6.10 | Synthesis of symmetrical DPP <b>347</b> ..... 204  |
| Scheme 6.11 | Synthesis of the pyrrolinone <b>349</b> ..... 206  |
| Scheme 6.12 | Synthesis of unsymmetrical DPP <b>352</b> ..... 206                                      |
| Scheme 6.13 | Synthesis of bis-ethynyl DPP <b>355</b> ..... 211  |
| Scheme 6.14 | Synthesis of bis-fluoresceindiacetate-DPP cassette <b>356</b> ..... 213                  |
| Scheme 6.15 | Synthesis of bis-naphthofluoresceindiacetate-DPP cassette <b>357</b> ..... 214           |
| Scheme 7.1  | Synthesis of <b>a</b> , water-soluble donor; and <b>b</b> , a donor bearing a handle 217 |
| Scheme 7.2  | Alternative route to a water-soluble donor bearing a handle ..... 218                    |
| Scheme 7.3  | Synthesis of poly-ol BODIPY..... 219   |
| Scheme 7.4  | The Liebeskind-Srögl cross-coupling..... 219   |
| Scheme 7.5  | Synthesis of a near-IR DPP-BODIPY based cassette ..... 220                               |
| Scheme 7.6  | Synthesis of a cassette via the Liebeskind-Srögl cross-coupling ..... 223                |

# CHAPTER I

## BODIPY® DYES AND THEIR DERIVATIVES: SYNTHESSES AND SPECTROSCOPIC PROPERTIES\*

### A. Introduction

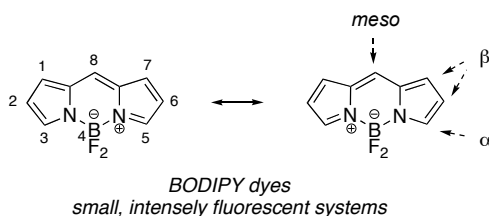
Advances in imaging techniques now make it feasible to do things that were not previously possible. Experiments in which interacting proteins are observed inside living cells are now common for dynamically averaged systems,<sup>1-3</sup> and the field is close to observation of similar events on a single molecule level.<sup>4-8</sup> Labels can be attached to proteins, *eg* antibodies, which accumulate in specific organs for imaging in animals and human subjects.<sup>9</sup> The technological advances in this area are remarkable. However, there is a growing realization that imaging events in cells and whole organisms by fluorescence is limited by the probes available. For instance, there are few that emit at 800 nm or above, yet living tissues are most transparent to light at and above this wavelength.

4,4-Difluoro-4-bora-3a,4a-diaza-s-indacene, or BODIPY® (hereafter abbreviated to BODIPY) dyes tend to be strongly UV-absorbing small molecules that emit relatively sharp fluorescence peaks with high quantum yields. They are relatively insensitive to the polarity and pH of their environment, and are reasonably stable to physiological conditions. Small modifications to their structures enable tuning of their fluorescence characteristics, consequently these dyes are widely used to label proteins<sup>10-14</sup> and DNA<sup>15</sup>. However, these compounds also have some undesirable characteristics for many applications in biotechnology. For instance, most emit at less than 600 nm, and only a handful of water-soluble derivatives has been made. Thus, there is the potential that modifications to the BODIPY framework will lead to probes that can be used more effectively for imaging in living cells and whole organisms, but that is largely unrealized.

---

This dissertation follows the style of *Journal of Organic Chemistry*.

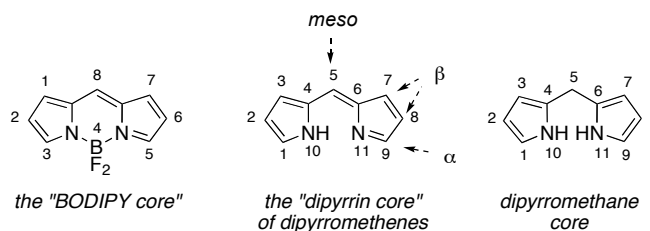
\*Reprinted with permission from "BODIPY® Dyes and Their Derivatives: Syntheses and Spectroscopic Properties" by Aurore Loudet, Kevin Burgess, 2007. *Chemical Reviews*, 107, 4891- 4932; copyright 2007, American Chemical Society.



Our research group is interested in making BODIPY-related probes that will realize some of their potential for intracellular imaging. This review is intended to facilitate this process by summarizing the basic chemistry and spectroscopic properties of common BODIPY-derivatives, and highlighting ways in which other interesting probes could be prepared. Readers particularly interested in applications of BODIPY dyes as labeling reagents,<sup>11,13,16-43</sup> fluorescent switches,<sup>44,45</sup> chemosensors<sup>46-83</sup> and as laser dyes<sup>84</sup> may be interested in this review as a guide to synthesis and spectroscopic properties, but details on use of the dyes in those ways are not included here. Readers interested in small amounts of commercially available dyes for labeling should also consult the Invitrogen (formerly Molecular Probes) catalog.<sup>11,85</sup>

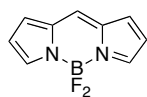
## B. The BODIPY Core

The IUPAC numbering system for BODIPY dyes is different to that used for dipyrromethenes,<sup>86</sup> and this can lead to confusion. However, the terms  $\alpha$ -,  $\beta$ -positions, and *meso*- are used in just the same way for both systems.

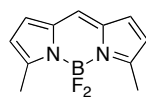


## 1. Fundamental Properties

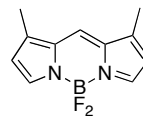
BODIPY **1**, which has no substituents, has not been reported in the literature. This may be because of synthetic difficulties obtaining this compound related to the fact that none of the pyrrole-based carbons are blocked from electrophilic attack. Synthesis of the corresponding dipyrromethene precursor has been reported, but this compound is unstable and decomposes above  $-30^{\circ}$  to  $-40^{\circ}$  C.<sup>87</sup> The symmetrical, dimethyl-substituted compound **2** has been prepared<sup>88</sup> and could be considered as a reference to which other simple alkylated BODIPYs can be compared. The symmetrically substituted systems **3** and **4** have apparently not been reported, reflecting synthetic limitations for even some simple BODIPY systems. However, the unsymmetrically substituted BODIPYs **5** and **6** have been prepared.<sup>89</sup> There are relatively minor differences in the reported UV-absorption maxima, fluorescence emission maxima, and quantum yields of these compounds, and these should not be over-interpreted because small calibration errors are common in these types of experiments. However, when the symmetrically-, tetra-, hexa-, and hepta-alkylated systems **7**,<sup>89,90</sup> **8**, and **9** are included in the comparison then an unambiguous trend towards red-shifted absorption and emission maxima with increased substitution becomes apparent.



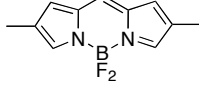
**1**  
unknown



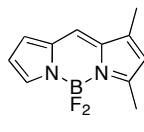
**2**  
EtOH,  $\Phi$  0.81  
 $\lambda_{\text{max abs}}$  507 nm  
 $\lambda_{\text{max emiss}}$  520 nm



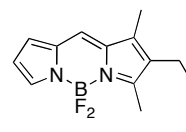
**3**  
unknown



**4**  
unknown

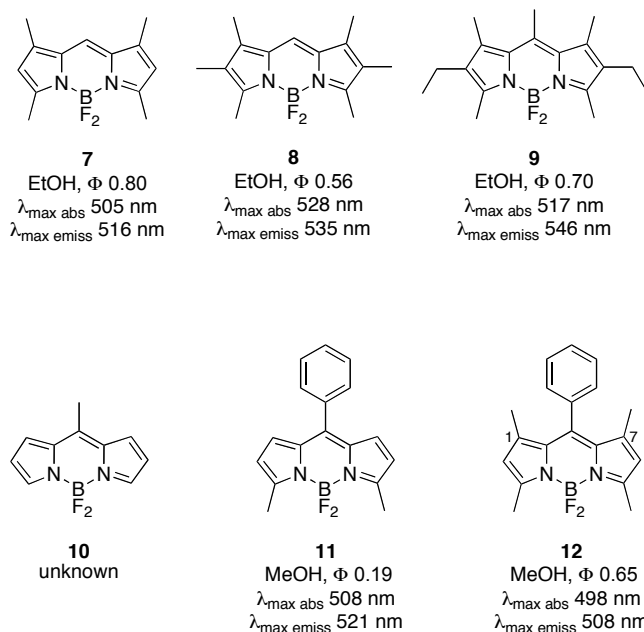


**5**  
EtOH,  $\Phi$  0.70  
 $\lambda_{\text{max abs}}$  499 nm  
 $\lambda_{\text{max emiss}}$  509 nm



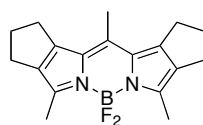
**6**  
EtOH,  $\Phi$  0.40  
 $\lambda_{\text{max abs}}$  510 nm  
 $\lambda_{\text{max emiss}}$  520 nm



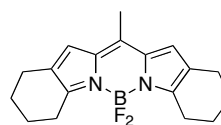


Alkylation or arylation at the *meso* position has no special effect on the absorption and emission wavelengths (compare **2** with **11**, and **7** with **12**) even though this substitution position is structurally unique. However, the quantum yield of the *meso*-phenyl compound **11** is appreciably less than the more substituted analog **12**. Such differences are widely attributed to 1,7-substituents preventing free rotation of the phenyl group reducing loss of energy from the excited states via non-irradiative molecular motions. Consistent with this, introduction of *ortho*-substituents on the phenyl ring has been observed to increase quantum yields, and similar explanations have been invoked.

BODIPY derivatives in which aliphatic rings have been fused to the pyrrole fragments are perhaps more constrained than ones bearing acyclic aliphatic substituents. Nevertheless, the effects on their emission maxima are not always easily rationalized. Compound **13** has a shorter emission wavelength maximum than **9** even though both have three substituents on the pyrrole rings. On the other hand, **14** has only two such attachments, yet it has the longest wavelength fluorescence emission.



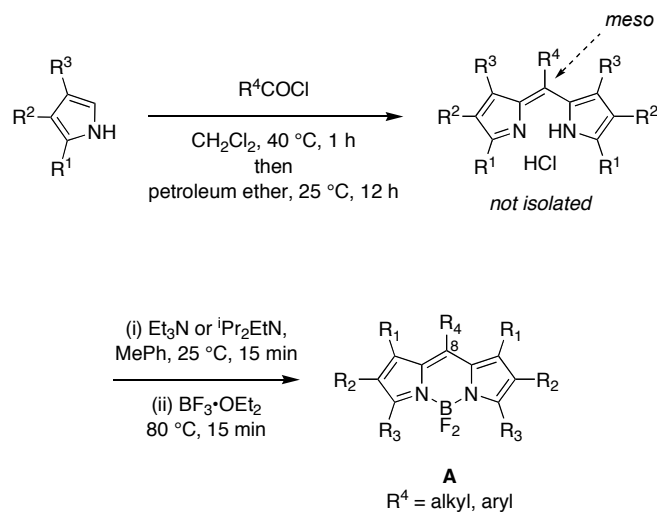
**13**  
EtOH,  $\Phi$  0.81  
 $\lambda_{\text{max abs}}$  512 nm  
 $\lambda_{\text{max emiss}}$  535 nm



**14**  
EtOH,  $\Phi$  0.84  
 $\lambda_{\text{max abs}}$  535 nm  
 $\lambda_{\text{max emiss}}$  560 nm

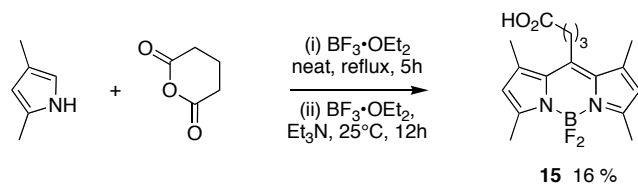
## 2. Syntheses From Pyrroles and Acid Chlorides or Anhydrides

8-Substituted BODIPY<sup>®</sup> dyes **A** (ie ones with substituents in the *meso* position) tend to be relatively easy to prepare via condensation of acyl chlorides with pyrroles (reaction 1).<sup>91,92</sup> These transformations involve unstable dipyrromethene hydrochloride salt intermediates. The intermediate dipyrromethene hydrochlorides are easier to handle and purify as C-substitution increases but, even so, these are not generally isolated in syntheses of BODIPY dyes.



reaction 1

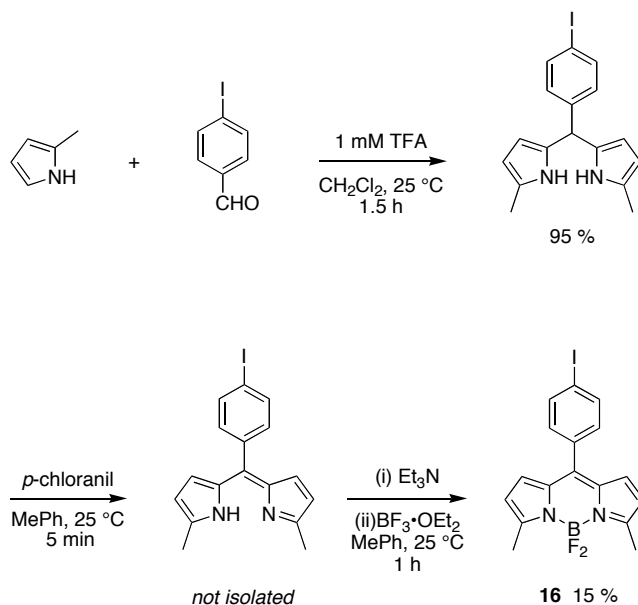
Other activated carboxylic acid derivatives could be used in place of acid chlorides in reaction 1. In the particular case of acid anhydrides, this concept has been reduced to practice. Reaction 2 shows how the BODIPY derivative **15** was prepared from glutaric anhydride.<sup>37</sup> An attractive feature of this chemistry is that a free carboxylic acid is produced, and this may later be used to attach the probe to target molecules.



reaction 2

### 3. Syntheses From Pyrroles and Aldehydes

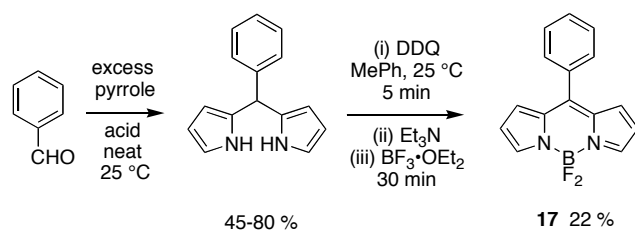
Syntheses similar to those depicted in reactions 1 and 2 but which use aromatic aldehydes<sup>14</sup> (to the best of our knowledge, *aliphatic* aldehydes have not been reported in this reaction) require oxidation steps. The reagents for these oxidations can introduce experimental complications. Thus in reaction 3 the oxidant used was *p*-chloranil and eventually the byproducts from this had to be removed (in fact, this was done after complexation with the boron).



reaction 3

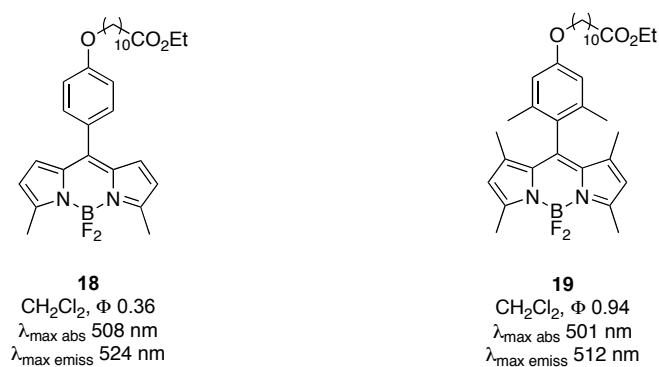
$\alpha,\beta$ -Unsubstituted BODIPYs eg **17** can also be prepared from aldehydes using neat conditions.<sup>14</sup> The aldehyde is dissolved in excess pyrrole at room temperature, and the

dipyrromethane intermediate (the reduced form of the dipyrromethene) was formed and isolated. The BODIPY dye was obtained after oxidation with DDQ and complexation with boron (reaction 4). Acid chlorides probably would be too reactive to use with pyrrole (since it is unsubstituted and more reactive) so this aldehyde-based approach is the method of choice.



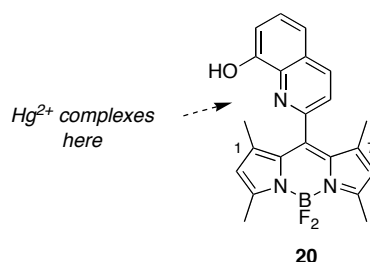
reaction 4

Use of, for instance, halogenated benzaldehydes (or halogenated acid chlorides above) broadens the scope of the reaction by offering the potential for elaboration of these groups in compounds like **16**. In another example, systems **18** and **19** were prepared from benzaldehyde derivatives that have long chain acid substituents. These probes were used to investigate dynamic effects in membranes.<sup>2</sup> Presumably *ortho*-substituents were included on the *meso*-aromatic group to restrict rotation of that ring and increase quantum yields.

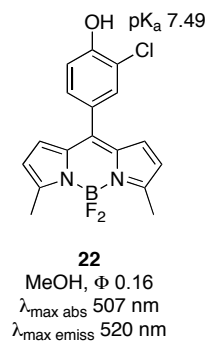
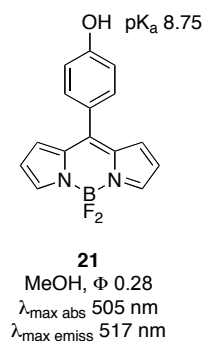


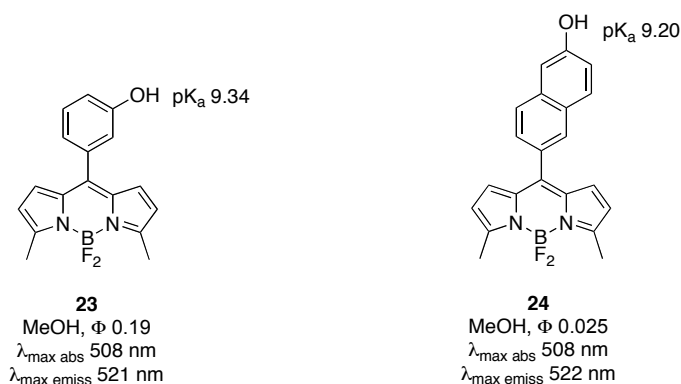
The fact that a diverse set of aldehydes could be used to prepare *meso*-substituted BODIPYs provides a means to introduce more sophisticated functionalities for specialized purposes. For instance, 8-hydroxyquinoline-2-carboxaldehyde was used to prepare the  $\text{Hg}^{2+}$ -

selective chromo- and fluoroionophore **20**.<sup>60</sup> This probe is highly fluorescent in the presence of transition-metal ions ( $\text{Co}^{2+}$ ,  $\text{Ni}^{2+}$ ,  $\text{Cu}^{2+}$ , and  $\text{Zn}^{2+}$ ) and heavy-metal ions ( $\text{Pb}^{2+}$ ,  $\text{Cd}^{2+}$ ), but 5 equiv. of mercuric ions reduced its emission by more than 98% (the color of the solution also changed from light amber to red enabling the progress of the complexation event to be visualized). A 1:1 complex with  $\text{Hg}^{2+}$  is formed in which the dipyrromethene core of **20** adopts a nearly orthogonal conformation with the 8-hydroxyquinoline moiety because of the methyl groups in positions 1- and 7- on the BODIPY core. This particular arrangement displays the binding site of 8-hydroxyquinoline for complexation of metal ions. The shape of these BODIPY-based ligand is such that 2:1 L:M complexes are sterically disfavored.

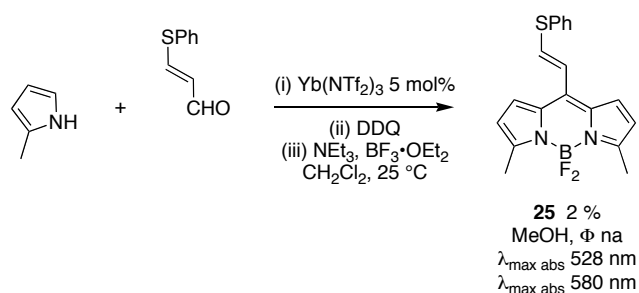


Fluorescent pH probes **21** - **24** have been prepared from phenolic benzaldehydes (a case where the acid chloride approach would have raised chemoselectivity issues).<sup>68</sup> These compounds are weakly fluorescent in the phenolate form presumably due to charge transfer from the phenolate donor to the excited-state indacene moiety. The pK<sub>a</sub> of the different derivatives was tuned by varying the aromatic substituent.

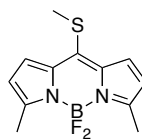




It is unusual to use any aldehydes that are not aromatic to prepare BODIPY derivatives. In this sense the vinylic thioether probe **25** is exceptional. A catalytic amount of ytterbium (III) trifluoromethane sulfonamide was used to mediate the condensation process, the intermediate dipyrromethane was oxidized with DDQ, and complexation with boron trifluoride gave the product, though in very poor yield.<sup>93</sup> The fluorescence emission of compound **25** was red-shifted relative to dyes with a phenyl group at the *meso* position (eg **11**). Compound **26** has a sulfide in conjugation with the BODIPY core, just as **25** does. The fluorescence emission maximum of **25** is 26 nm red-shifted compared to **26**, indicating that electron donating groups in this position tend to have that effect.



reaction 5

**26**

MeOH,  $\Phi$  0.37  
 $\lambda_{\text{max abs}}$  530 nm  
 $\lambda_{\text{max abs}}$  554 nm

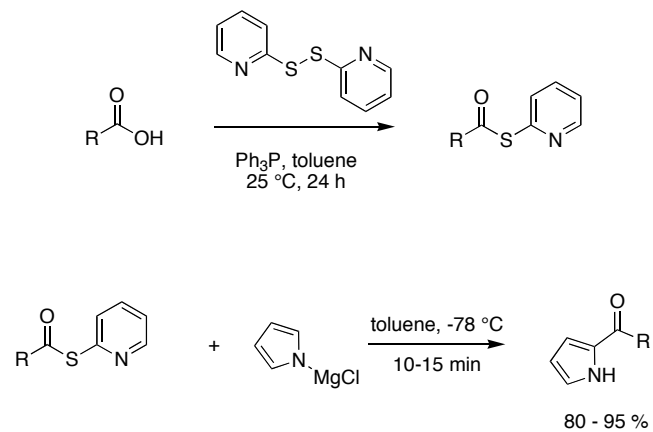
#### 4. Syntheses From Ketopyrroles

Condensations of pyrroles with acid chlorides or with benzaldehyde derivatives, as outlined above, are direct and convenient methods to access symmetrically substituted BODIPY dyes. However, another approach is required to form unsymmetrically substituted ones. Generally, this is achieved via preparations of ketopyrrole intermediates, followed by a Lewis acid mediated condensation of these with another pyrrole fragment.

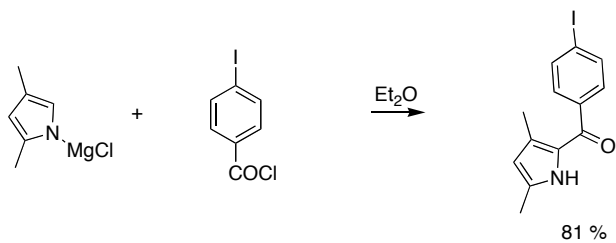
Schemes 1.1 a and b show reactions of magnesium anions of pyrroles with activated carboxylic acid derivatives to give the corresponding 2-ketopyrroles.<sup>94,95</sup> In part c, one such ketopyrrole is condensed with another pyrrole unit to give a BODIPY framework. That example gives a symmetrical product, but the method is particularly valuable for unsymmetrical ones, as in Scheme 1.1d.

**Scheme 1.1.** **a** and **b** two different methods for production of ketopyrroles from magnesium derivatives of pyrrole, and application of these starting materials in the production of **c** symmetrical, and **d** unsymmetrical dyes.

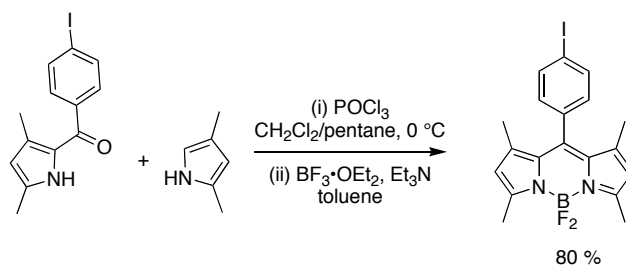
**a**



**b**



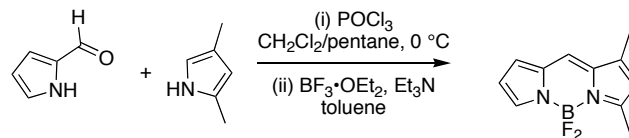
**c**





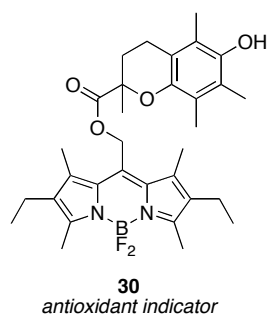
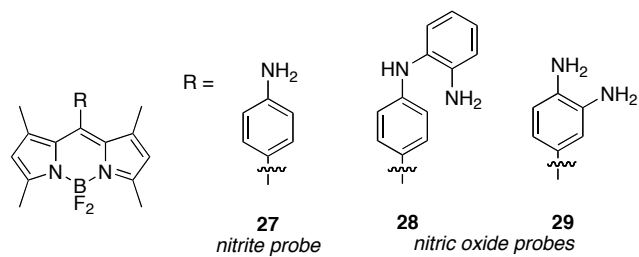
## Scheme 1.1. Continued.

d

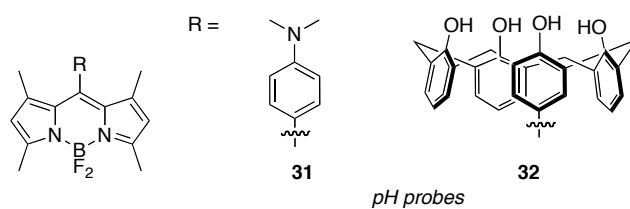
C. Modifications to *meso*-Aromatic Substituents On The BODIPY Core

The BODIPY core is robust enough to withstand a range of chemical transformations, and a variety of aromatic groups can be introduced at the *meso*-position for appropriately functionalized BODIPY dyes. Alternatively, dyes with special *meso*-groups can be produced via *in vivo* synthesis. These strategies have been used to produce several dyes for many different applications; just a few illustrative ones are shown in Figure 1.1. For instance, derivatives of this type have been formed as selective sensors of particular redox active molecules (**27**,<sup>62</sup> **28**,<sup>65</sup> **29**,<sup>48</sup> and **30**,<sup>96</sup> Figure 1.1a), pH probes (**31**<sup>55</sup> and **32**<sup>51</sup>, 1b), metal-chelators (**33**,<sup>79</sup> **34**,<sup>79</sup> **35**,<sup>74</sup> **36**,<sup>67</sup> **37**,<sup>66</sup> **38**,<sup>53</sup> **39**,<sup>80</sup> **40**,<sup>78</sup> **41**,<sup>82</sup> and **42**,<sup>71</sup> 1c), and as biomolecule conjugating groups (**43**,<sup>49</sup> **44**,<sup>81</sup> and **45**,<sup>97</sup> 1d).

a



b



c

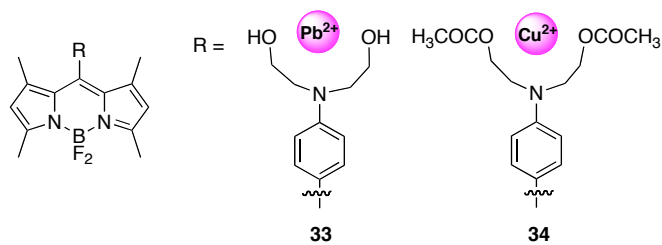


**Figure 1.1.** Selected BODIPYs with *meso*-modifications to give: **a** selective sensors of particular redox active molecules; **b** pH probes; **c** metal-chelators; and, **d** biomolecule conjugating groups.

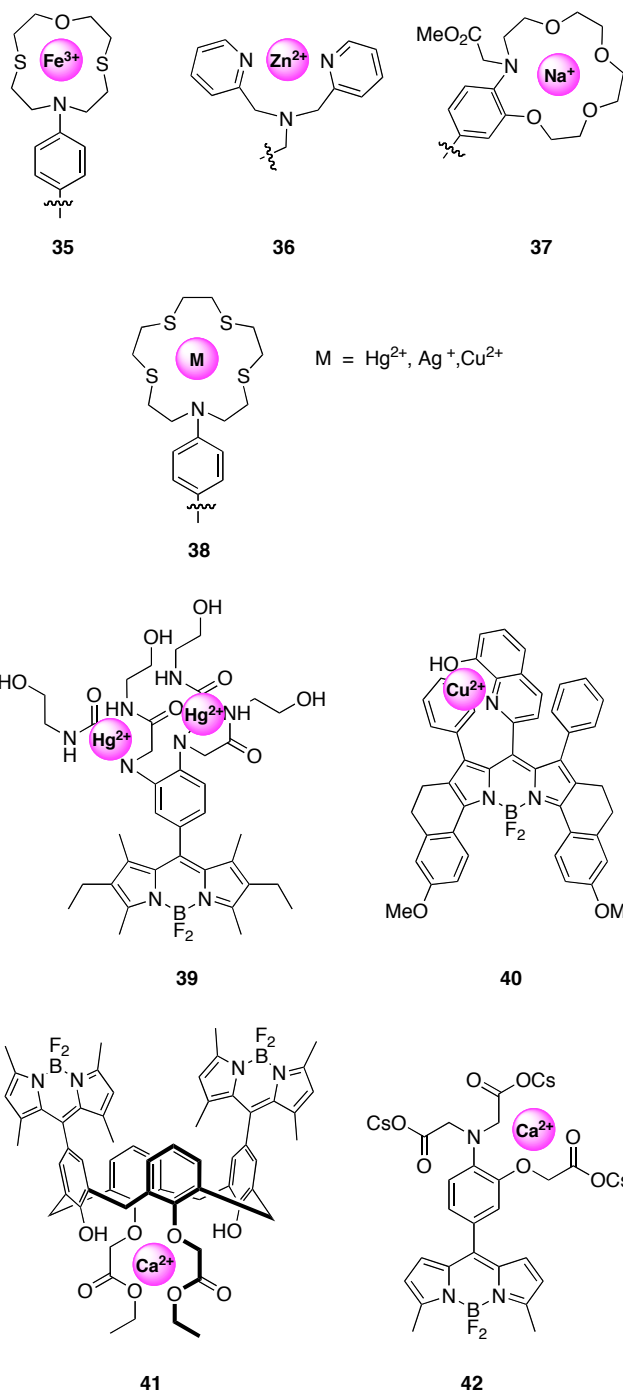


Figure 1.1. Continued

d

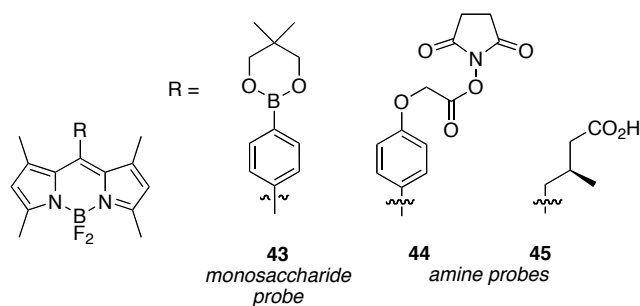


Figure 1.1. Continued

Here we intend to restrict the discussion to the general concepts that influence the fluorescence properties of *meso*-modified BODIPY dyes; this review does not attempt to give a comprehensive list of all the compounds made. Without exception, the chemosensors operate by perturbing the reduction potential of the *meso*-substituent. The next section discusses the electronic effects of these perturbations on fluorescence.

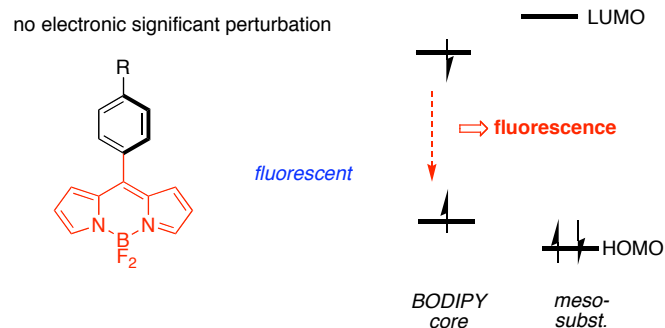
### 1. Fluorescence Control via Photoinduced Electron Transfer

Transfer of electrons between non-planar parts of fluorescent molecules modifies their fluorescence intensities.<sup>98</sup> This has been known for sometime but Nagano, Ueno and co-workers have skillfully applied calculated orbital energy levels and experimentally determined electrochemical data to rationalize quantum yields. Their initial work with fluorescein derivatives,<sup>99,100</sup> was later expanded to encompass BODIPY systems as described here.<sup>101</sup>

Some non-planar fluorescent molecules can be regarded as a highly fluorescent group with non- (or significantly less) fluorescent substituents (Figure 1.2a). Some such substituents, depending on their oxidation potentials relative to the excited state of the BODIPY core, can act as electron donors or acceptors. If electron transfer occurs then the fluorescence is diminished when the fluorescent group in its excited state is reduced. In this situation, the fluorescent group is acting as an acceptor, consequently this may be called reductive-PeT or a-PeT (“a” for acceptor; Figure 1.2b). However, if the energy states are such that the excited state of the fluorescent group can donate electrons to the substituent LUMO then oxidative-PeT, d-PeT, occurs (“d” for donor; Figure 1.2c). Indirectly, solvent polarity has an effect on this process. This

is because photoexcitation and oxidation processes involve modification of ground state dipoles, and solvents may stabilize or destabilize these changes according to polarity.

**a**



**b**

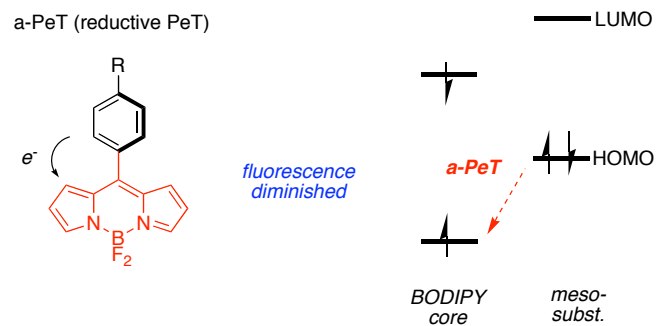


**Figure 1.2.** The meso-substituent provides: **a** no significant electronic perturbation; **b** electrons to the excited state; and, **c** a low lying LUMO to accept electrons from the excited state.

c

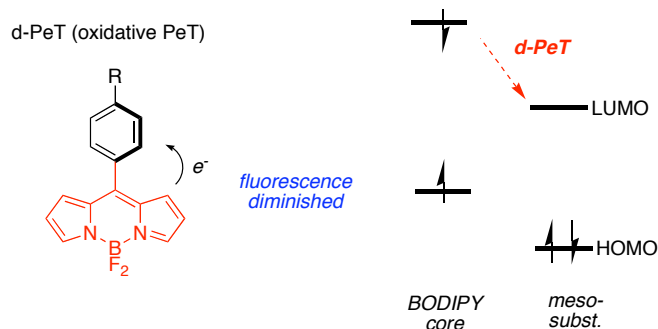


Figure 1.2. Continued

The feasibility of electron transfer can be judged from the change in free energy ( $\Delta G_{\text{PeT}}$ ), as described by the Rehm-Weller equation:<sup>102</sup>

$$\Delta G_{\text{PeT}} = E_{1/2}(\text{D}^+/\text{D}) - E_{1/2}(\text{A}/\text{A}^-) - \Delta E_{00} - C$$

where

$E_{1/2}(\text{D}^+/\text{D})$  = ground-state oxidation potential of the donor

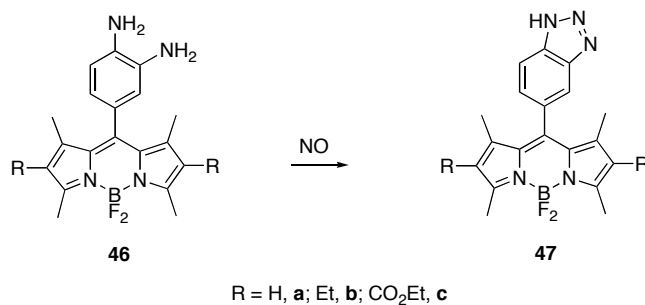
$E_{1/2}(\text{A}/\text{A}^-)$  = ground-state reduction potential of the acceptor

$\Delta E_{00}$  = excitation energy

$C$  = an electrostatic interaction term.

Nagano and co-workers applied these principles to the triazole-BODIPY derivative **47** to develop a nitric oxide probe.<sup>61</sup> The low fluorescence of the diamine **46** was explained in terms of reductive PeT (Figure 1.3). When nitric oxide converts the diamine into the benzotriazole **47** then reductive PeT does *not* occur and fluorescence is observed. Scheme 1.2 outlines the synthesis of the probe and the oxidized product.

a



b

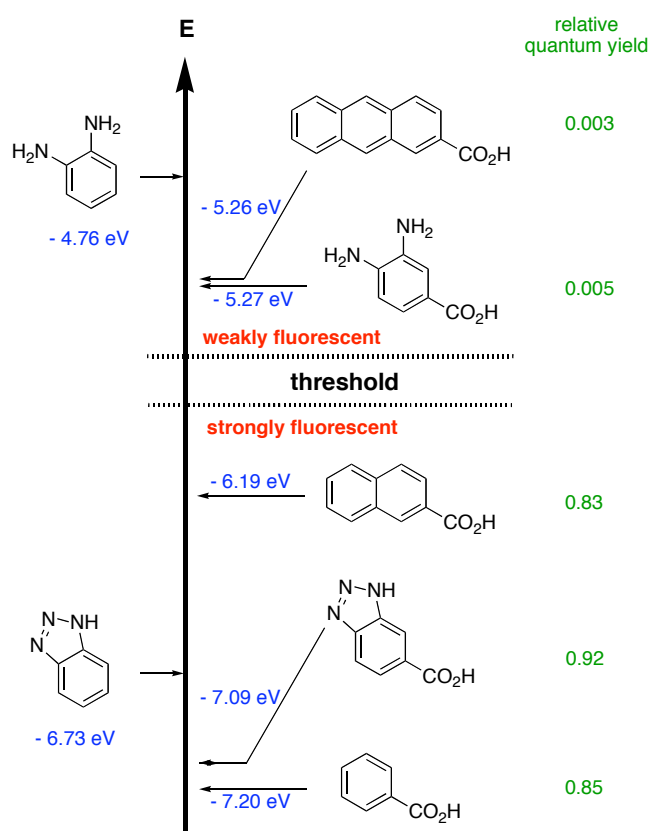
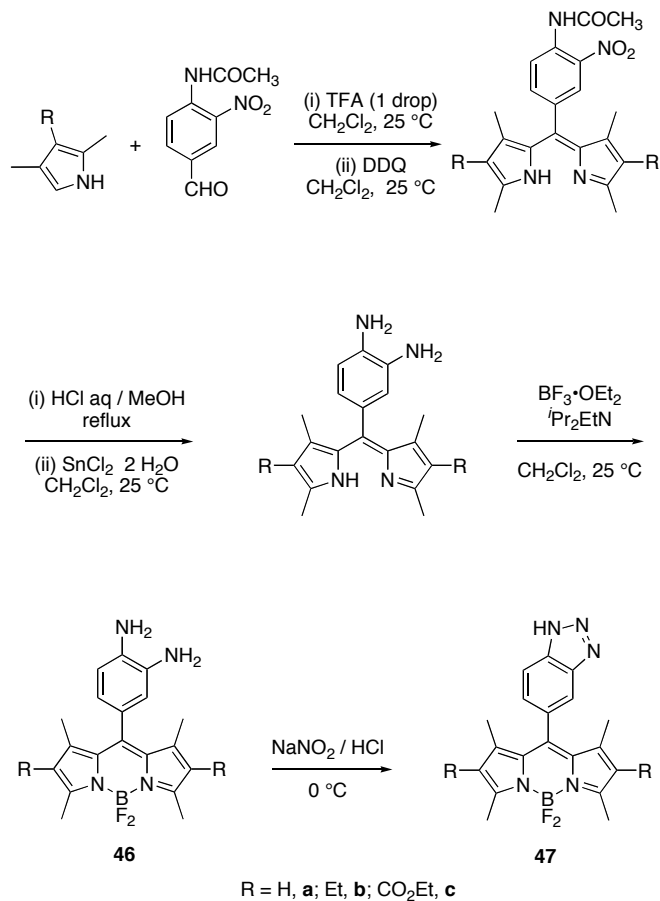


**Figure 1.3.** a Reductive PeT occurs when nitric oxide reacts with the diamine; b Calculated HOMO energy levels of *meso*-substituents for BODIPY **46** and **47**.

**Scheme 1.2.** Synthesis of diaminobenzene- and triazole- BODIPY derivatives **46** and **47**.



A refinement of the ideas presented above was used to explain the observation that fluorescence for the compounds **47** decreased in the order **b** > **a** > **c** (Figure 1.4). This is because the nature of the substituent impacts the reduction potential of the BODIPY core in that order (**b** is the most negative).



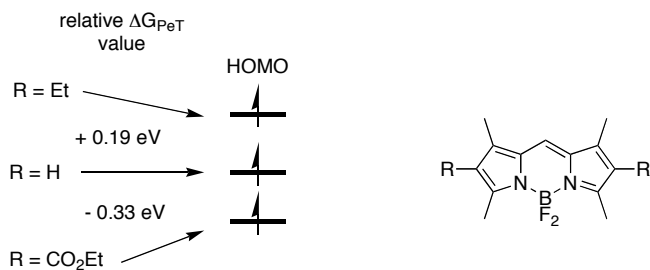
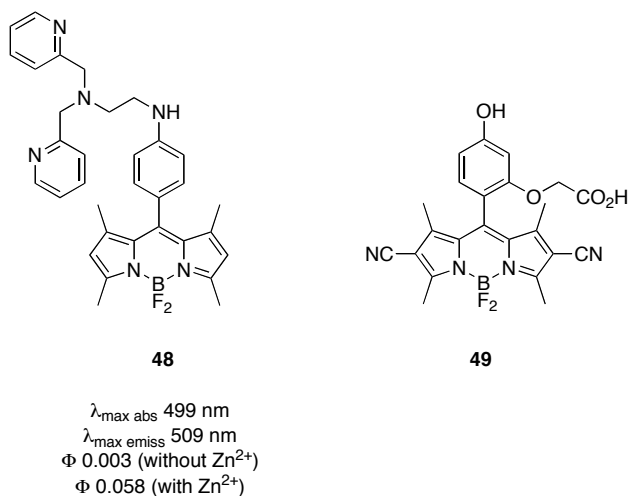


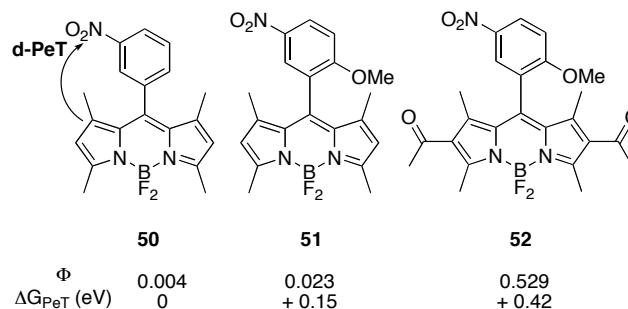
**Figure 1.4.** Reductive PeT increases in the order Et < H < CO<sub>2</sub>Et.

Fluorescence of the Zn<sup>2+</sup> and NO<sub>2</sub><sup>+</sup> chemosensors **48**<sup>63</sup> and **49**<sup>103</sup> has been explained using reductive PeT concepts outlined above. Chelation or nitration, respectively, makes the reduction potential of the *meso*-substituent more negative, PeT is switched-off, and the probes become fluorescent.



Strongly electron withdrawing substituents on aromatic *meso*-substituents lower the LUMO of the aromatic system to the level where it might accept electrons from the orbital containing the promoted electron in the BODIPY core (Figure 1.2c). In such cases *oxidative* PeT comes into play. Evidence for this is seen in the quantum yields of **50** - **52**.<sup>103</sup> For dye **52** oxidative PeT is

diminished because the ketones lower the energy of the BODIPY orbital containing the promoted electron.



There are at least two weaknesses associated with combining theoretical calculations and electrochemical data to rationalize quantum yields. First, the reduction potentials for the two components are calculated on isolated systems: the fact that they are attached to each other must perturb the actual orbital levels. Second, energies of excited states are notoriously difficult to calculate. Nevertheless, the approach emphasized by Nagano and co-workers helps dispel dogmas that surround fluorescent probes. For instance the assertion that nitro groups or heavy atom substituents always quench fluorescence is simply not true. The reality is that they tend to do so but only if their orbital energy levels interact with the fluorescent chromophore in a way that facilitates PeT.

## D. BODIPYs with Heteroatom Substituents

### 1. From Electrophilic Substitution Reactions

Simple considerations of mesomeric structures reveal that 2- and 6-positions of the BODIPY core bear the least positive charge so should be most susceptible to electrophilic attack (Figure 1.5). However, there is no definitive study of regioselectivities in these reactions for BODIPYs without pyrrole substituents; almost invariably some of the other positions are blocked by substituents.

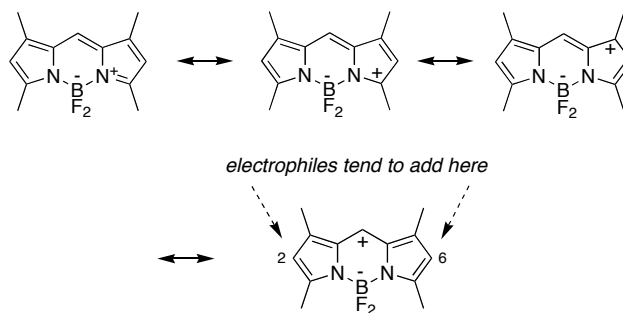
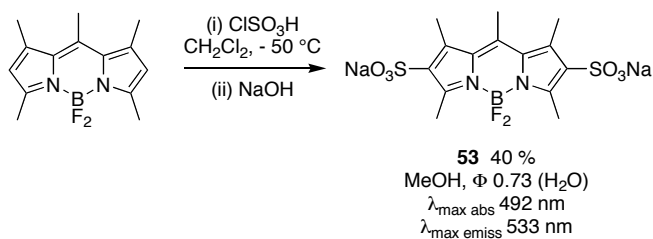


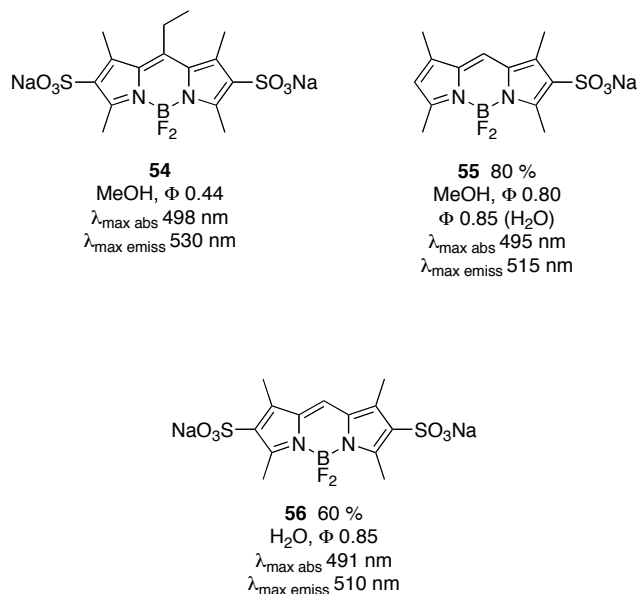
**Figure 1.5.** Electrophilic attack on tetramethyl-BODIPY.

### Sulfonation

To the best of our knowledge, less than a handful of sulfonated BODIPY dyes have been reported. They were obtained from tetra-, or penta-substituted BODIPYs via treatment with chlorosulfonic acid, then subsequent neutralization with a base (eg reaction 6). Monosulfonated systems can be obtained when only one equivalent of chlorosulfonic acid is used. Introduction of sulfonate groups do not change the absorption and fluorescence emission maxima significantly relative to the unsulfonated dye. The sulfonated BODIPY dyes **53** – **56** are strongly fluorescent in water and/or methanol, and are claimed to have even better stability than the parent dyes.<sup>91,104-109</sup>

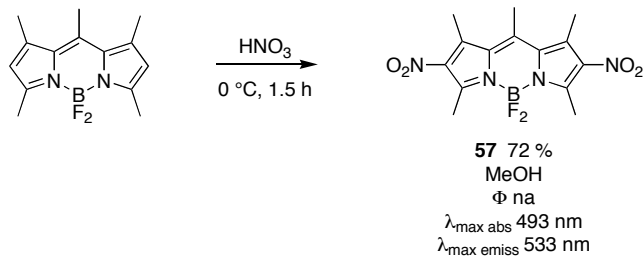


reaction 6



### Nitration

The 2,6-dinitro BODIPY dye **57** can be obtained via nitration with nitric acid at 0 °C (reaction 7). Introduction of the nitro groups drastically reduces the fluorescence quantum yield.<sup>91,110-112</sup> To the best of our knowledge, this is the only nitration of a BODIPY dye that has been reported in the literature.

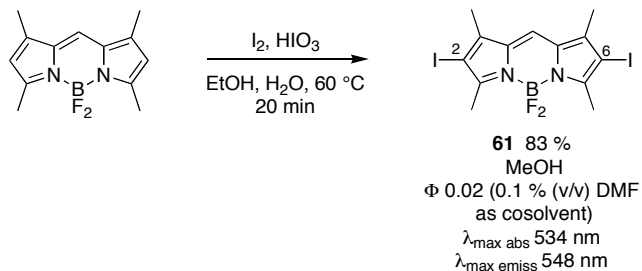


reaction 7

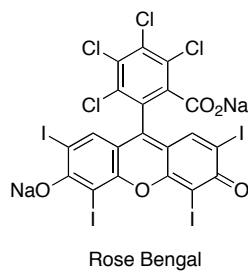
2,6-Dinitro-BODIPY **58**<sup>113</sup> and **59**<sup>114-118</sup> have also been reported in the Japanese patent literature for applications as sensitizers and inks. We were unable to find procedures for their syntheses and spectroscopic data.



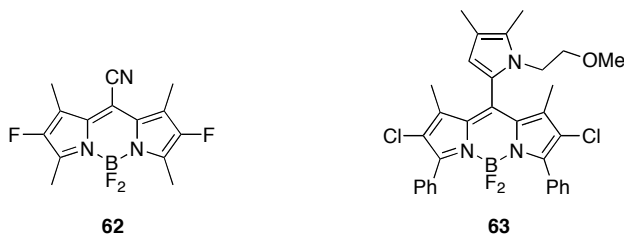
Bengal; this is because the BODIPY core has a more positive oxidation potential than the xanthone unit of Rose Bengal. Compound **61** is an efficient photosensitizer.



reaction 9

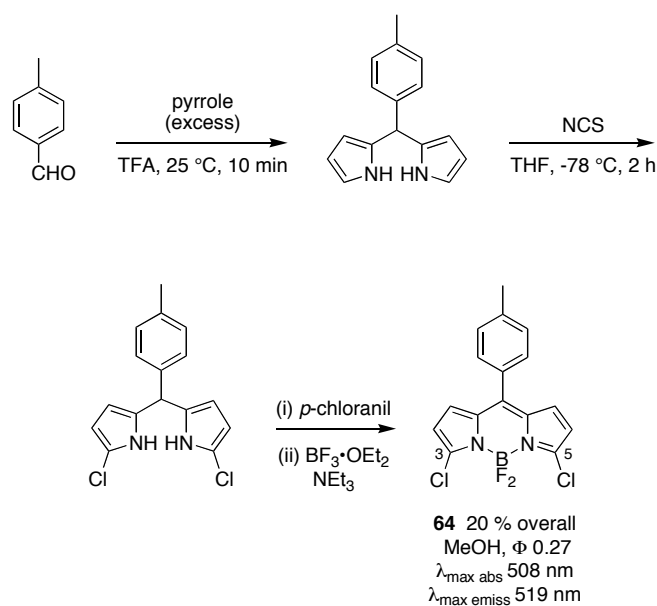


2,6-Difluoro- and 2,6-dichloro- BODIPY derivatives **62**<sup>113</sup> and **63**,<sup>114-118</sup> have found applications as electroluminescent devices and sensitizers. Their synthesis has not been reported.



Chlorination of the unsubstituted dipyrromethane shown in Scheme 1.3 occurs preferentially at the  $\alpha$ -positions. Thus the 3,5-dichloro BODIPY derivative **64** could be obtained after oxidation with *p*-chloranil and complexation with boron trifluoride etherate. Applications of such chlorinated materials as  $S_NAr$  electrophiles are described later in this review.

**Scheme 1.3.** Preparation of 3,5-dichloro-BODIPY via chlorination of a dipyrromethane intermediate.



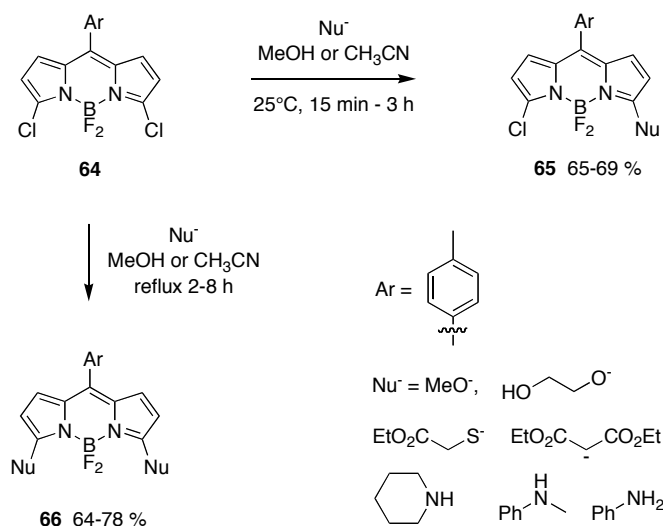
### Potential for Other Electrophilic Substitution Reactions

BODIPY dyes are intrinsically electron rich, and the reactions shown above illustrate that they will react with electrophiles. It is therefore surprising that the reactions shown above represent the state-of-the-art in this area. There are very few sulfonation reactions despite the importance of water-soluble dyes; most of the sulfonated BODIPY compounds in the Invitrogen catalog feature carboxylic acids with sulfonated leaving groups. There are no reports of some common electrophilic addition processes like Vilsmeier-Haack reactions, but our group has investigated this type of reaction, and the mono-formylated BODIPY dye could successfully be synthesized in excellent yield (unpublished results).

## 2. From Nucleophilic Attack on Halogenated BODIPYs

The most common approach to introduce substituents on the 3- and 5-positions of the BODIPY core involve *de novo* syntheses with appropriately substituted pyrroles, but an exciting recent development reaches the same goal via nucleophilic substitution on the 3,5-dichloro-BODIPY **64**.<sup>121,122</sup> The nucleophiles used so far include alkoxides, amines, thioalkoxides, and the diethyl malonate anion. These reactions can be stopped at the mono-substitution stage or forced to the disubstitution product (Scheme 1.4) hence they are useful for access to asymmetric **65** and symmetric **66**, hetero-substituted BODIPY dyes, which would be difficult to obtain by other routes.

**Scheme 1.4.** BODIPY dyes via  $S_NAr$  reactions.



The spectroscopic effects of electron donating groups attached to the BODIPY core for the compounds in Scheme 1.4 were studied. The 3- and 5-substituents had significant effects, shifting both the absorption and/or emission spectra, and changing the fluorescence quantum yields. For example, introduction of an amino- or sulfur-centered nucleophiles results in a significant bathochromic shift (red-shift) of both the absorption and emission.<sup>121</sup> Data were



collected in methanol (Figure 1.6); the absorption and emission maxima were red-shifted in cyclohexane but otherwise it was quite similar to that for methanol (data not shown). The quantum yields varied widely, but generally tended to be reduced relative to unsubstituted BODIPYs.

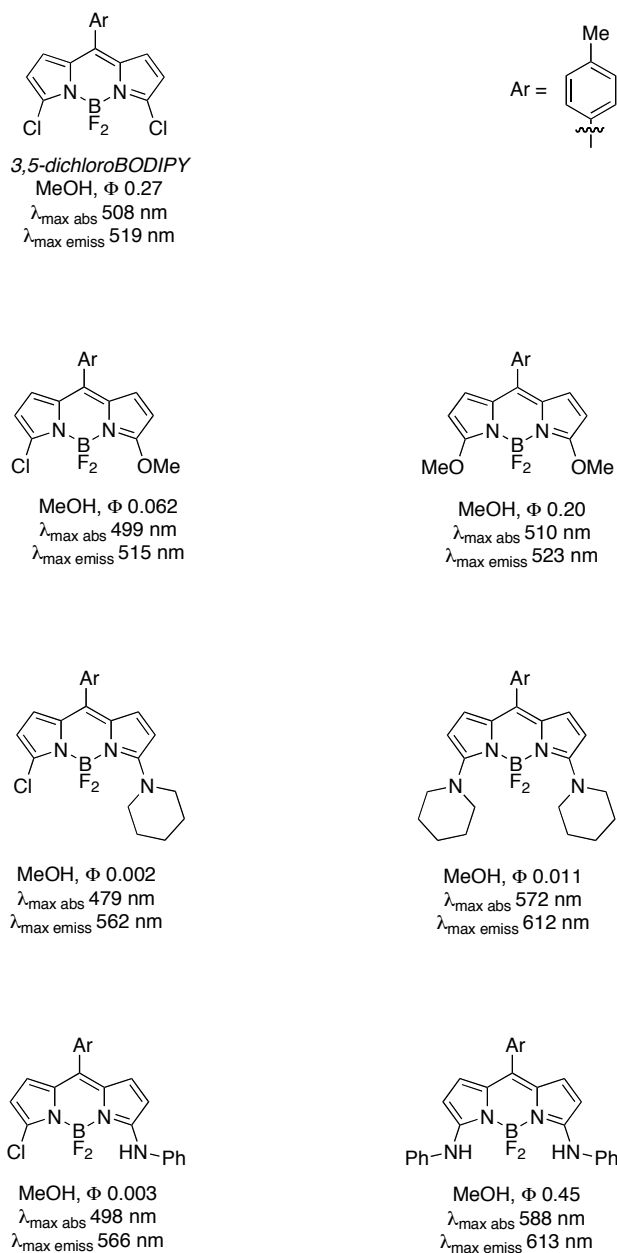


**Figure 1.6.** Spectroscopic data for some BODIPYs formed by  $S_NAr$  reactions.

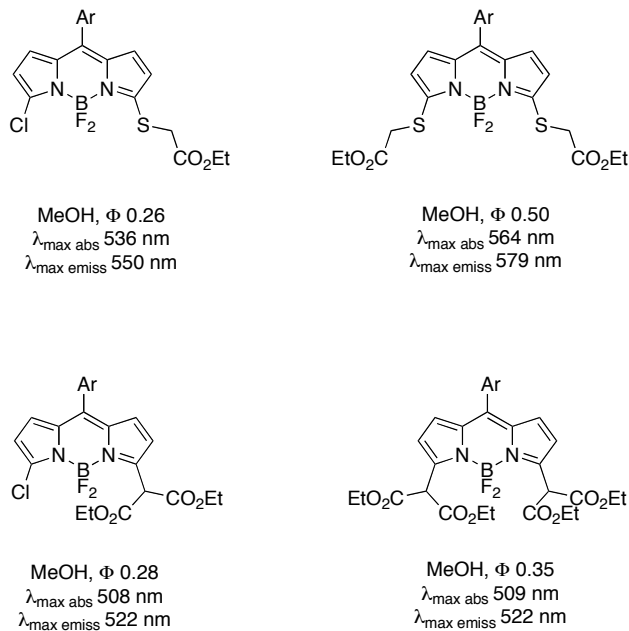
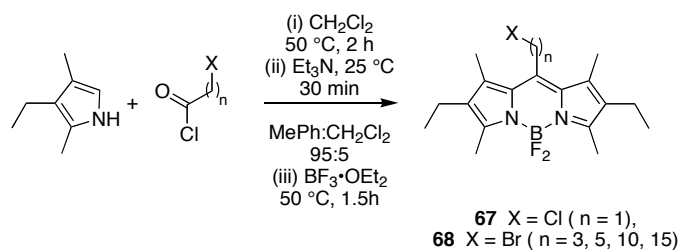


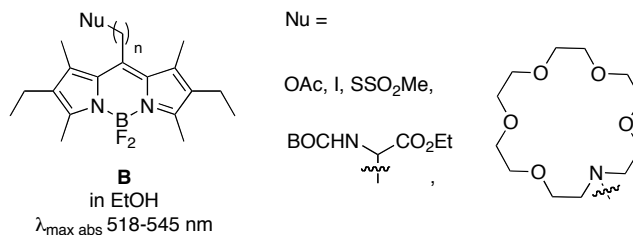
Figure 1.6. Continued

8-( $\omega$ -Haloalkyl)-BODIPY dyes **67** and **68** are useful starting materials. These are easily synthesized by condensation of a  $\omega$ -haloacyl chloride with 3-ethyl-2,4-dimethyl pyrrole (reaction 10).<sup>123</sup>



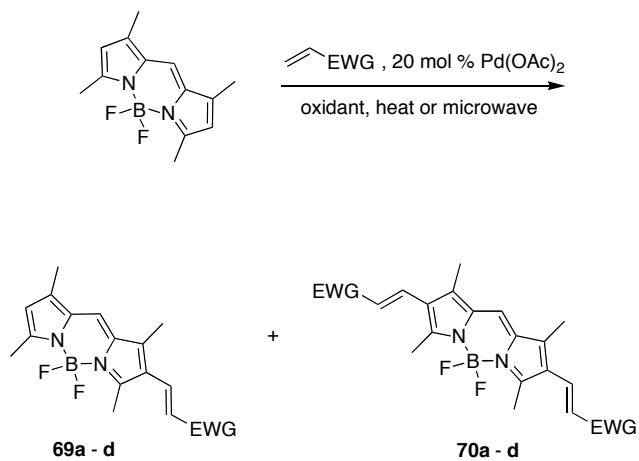
reaction 10

Compounds **67** and **68** can be functionalized by nucleophilic substitution reactions.<sup>58,123</sup> Thus **67** and **68** are precursors to a range of compounds **B** including fluorescent electrophiles, disulfides for chemoselective labeling of cysteine residues, fluorescent amino acids, and chemosensors for metal ions.<sup>58</sup>



### 3. From Palladium Mediated C-H Functionalization

Pyrroles can be functionalized via palladium catalyzed activation reactions.<sup>124-126</sup> Our group applied the same strategy to synthesize novel BODIPY dyes via palladium mediated C-H functionalization (reaction 11).<sup>127</sup> This route provides a direct way to extend the conjugation of the BODIPY core, without a halogenated or metallated intermediate prior to the coupling reaction. Highly fluorescent, mono- (**69**) or disubstituted (**70**) dyes can be obtained. A water-soluble, sulfonated BODIPY dye **69d** was also prepared via this route, but in low yield (2 %).



EWG =

**a** CO<sub>2</sub>Me  
EtOH,  $\Phi$  0.73  
 $\lambda_{\text{max abs}}$  527 nm  
 $\lambda_{\text{max emiss}}$  549 nm

**a** CO<sub>2</sub>Me  
CH<sub>3</sub>CO<sub>2</sub>Et,  $\Phi$  0.51  
 $\lambda_{\text{max abs}}$  559 nm  
 $\lambda_{\text{max emiss}}$  580 nm

**b** CO<sub>2</sub>Bu  
EtOH,  $\Phi$  0.73  
 $\lambda_{\text{max abs}}$  528 nm  
 $\lambda_{\text{max emiss}}$  551 nm

**b** CO<sub>2</sub>Bu  
EtOH,  $\Phi$  0.52  
 $\lambda_{\text{max abs}}$  560 nm  
 $\lambda_{\text{max emiss}}$  580 nm

**c** CO<sub>2</sub>H  
EtOH,  $\Phi$  0.42  
 $\lambda_{\text{max abs}}$  531 nm  
 $\lambda_{\text{max emiss}}$  570 nm

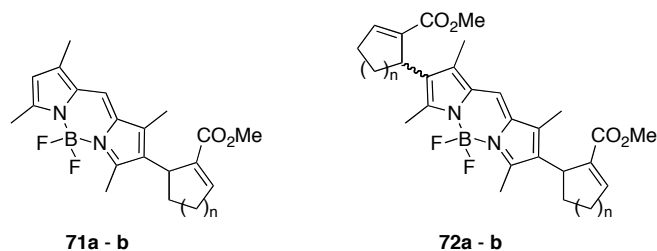
**c** *not formed*

**d** SO<sub>3</sub>H  
EtOH,  $\Phi$  0.25  
 $\lambda_{\text{max abs}}$  529 nm  
 $\lambda_{\text{max emiss}}$  560 nm

**d** *not formed*

reaction 11

The C-H functionalization process was also applied to  $\alpha$ ,  $\beta$ -unsaturated esters to form compounds **71** and **72**. Mono- and disubstituted products were obtained, but the alkene double bond was shifted out of conjugation with the BODIPY core.



**a** n = 1  
EtOH,  $\Phi$  0.72  
 $\lambda_{\text{max abs}}$  518 nm  
 $\lambda_{\text{max emiss}}$  525 nm

**b** n = 2  
EtOH,  $\Phi$  0.78  
 $\lambda_{\text{max abs}}$  517 nm  
 $\lambda_{\text{max emiss}}$  527 nm

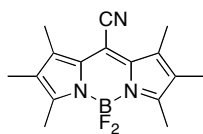
**a** n = 1  
EtOH,  $\Phi$  0.92  
 $\lambda_{\text{max abs}}$  530 nm  
 $\lambda_{\text{max emiss}}$  539 nm

**b** n = 2  
EtOH,  $\Phi$  0.89  
 $\lambda_{\text{max abs}}$  529 nm  
 $\lambda_{\text{max emiss}}$  540 nm

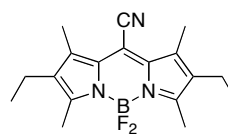
#### 4. From Nucleophilic Attack at the meso-Position

BODIPY systems with a *meso*-cyanide substituent are special insofar as they fluoresce at significantly longer wavelengths than the unsubstituted systems.<sup>128</sup> Further, they can be accessed by direct addition of cyanide anion to the dipyrromethene core, followed by oxidation. The first synthetic route developed gave poor overall yields, mainly due to loss of material in forming the dipyrromethene,<sup>92</sup> but an improved route was developed by Boyer (Scheme 1.5).<sup>129</sup> In that work, Knorr condensation of 3-ethylhexan-2,4-dione with diethyl aminomalonate give ethyl 3,4-diethyl-5-methylpyrrole-2-carboxylate. This pyrrole is then converted to the dipyrromethene hydrobromide via the presumed intermediacy of 2-methyl-3,4-diethylpyrrole and its condensation with the  $\alpha$ -formyl derivative that is formed *in situ*.

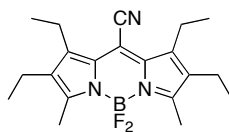




**74**  
MeOH,  $\Phi$  0.54  
 $\lambda_{\text{max abs}}$  588 nm  
 $\lambda_{\text{max emiss}}$  612 nm



**75**  
dioxane,  $\Phi$  0.55  
 $\lambda_{\text{max abs}}$  580 nm  
 $\lambda_{\text{max emiss}}$  620 nm

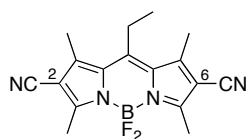


**76**  
MeOH,  $\Phi$  0.56  
 $\lambda_{\text{max abs}}$  592 nm  
 $\lambda_{\text{max emiss}}$  609 nm



**77**  
dioxane,  $\Phi$  0.82  
 $\lambda_{\text{max abs}}$  556 nm  
 $\lambda_{\text{max emiss}}$  589 nm

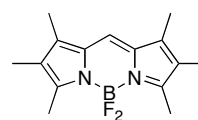
The red-shift in fluorescence observed when a cyano group is added to the *meso*-position is somewhat particular to that site. 2,6-Dicyano BODIPY **78** has two cyano groups, but neither occupies the *meso*-position. Fluorescence from this compound peaks at about the same wavelength as similar BODIPYs without nitrile substituents, *eg* **79** and **8**.<sup>129</sup> Similarly, substitution at the 2 and 6-positions with carboethoxy, acetamido, sulfonate anion, bromo or nitro groups do not produce any red-shift.<sup>92,129,130</sup>



**78**  
dioxane,  $\Phi$  0.79  
 $\lambda_{\text{max abs}}$  496 nm  
 $\lambda_{\text{max emiss}}$  511 nm



**79**  
dioxane,  $\Phi$  0.99  
 $\lambda_{\text{max abs}}$  493 nm  
 $\lambda_{\text{max emiss}}$  519 nm

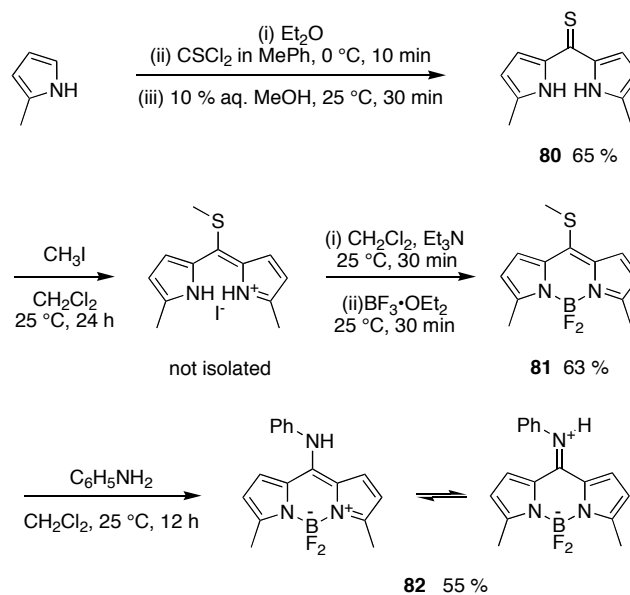


**8**  
MeOH,  $\Phi$  0.56  
 $\lambda_{\text{max abs}}$  528 nm  
 $\lambda_{\text{max emiss}}$  552 nm

A synthesis of sulfur containing BODIPYs under mild conditions was recently achieved via reaction of thiophosgene with substituted pyrroles to give the corresponding thioketone **80**. The latter can then react with various electrophiles to form the dipyrromethene intermediates that

were combined with boron trifluoride in presence of base to afford the thio-BODIPY derivatives **81**. These *meso*-thioalkyl groups can be displaced by nucleophiles to give anilino-substituted BODIPY derivative **82** (Scheme 1.6). Amine adduct **82** was not fluorescent, presumably because of electron transfer from the amine group to the BODIPY core in the excited state.

**Scheme 1.6.** Synthesis of sulfur- and anilino- BODIPY derivatives.

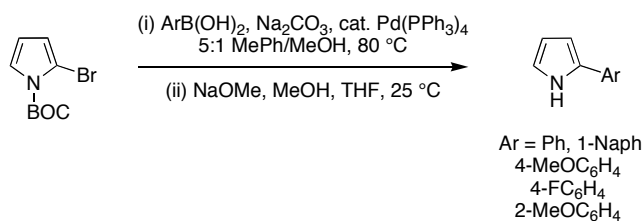


## E. Aryl-, Alkenyl-, Alkynyl-substituted BODIPYs

### 1. Aryl-substituted BODIPYs from Aryl-pyrroles

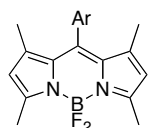
Aryl-substituted BODIPY dyes can be formed via condensation of the corresponding pyrroles with acyl chlorides.<sup>131,132</sup> The 2-aryl pyrroles used were prepared via Suzuki couplings<sup>133</sup> of *N*-*tert*-butoxycarbonyl-2-bromopyrrole (reaction 12); this was more convenient than starting with less accessible materials like 4-aryl-1-azidobutadienes<sup>134</sup> or a *N*-tosylarylimine.<sup>135,136</sup> Removal of the *N*-BOC protecting group under basic conditions gave the desired aryl pyrroles. These products were found to decompose on standing, rapidly under acidic conditions, and were therefore best formed immediately before use.





reaction 12

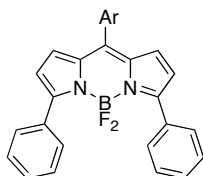
3,5-Diaryl BODIPY dyes were obtained from the pyrroles shown above, via a one pot, two-step process featuring 4-iodobenzoyl chloride. The 3,5-aryl groups extend the conjugation of the BODIPY systems. Compared to the alkyl-substituted derivatives *eg* **83** and **84** which have green, fluorescein-like emissions ( $\lambda_{\text{max emis}} = 510 \text{ nm}$ ), both the absorption and emission maxima of 3,5-diaryl substituted BODIPYs **85** – **89** are shifted to longer wavelengths ( $\lambda_{\text{max emis}} = 588 - 626 \text{ nm}$ ).<sup>131,132</sup> The *para*-electron-donating group of **87** gives a larger bathochromic shift and increased quantum yield, compared to the compound with that same substituents in the *ortho*-position **89**. Similarly, the extended aromatic substituent naphthalene of **86** red-shifted the emission maximum for this compound. However, the extinction coefficients for **85** – **89** were not markedly increased relative to the alkyl systems **83** and **84** and their fluorescence quantum yields were significantly lower due to non-radiative loss of energy via rotation around the C-Ar bonds.<sup>137</sup>



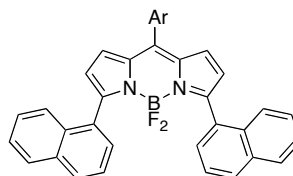
**83**  
CHCl<sub>3</sub>,  $\Phi$  0.64  
 $\lambda_{\text{max abs}}$  500 nm  
 $\lambda_{\text{max emiss}}$  510 nm



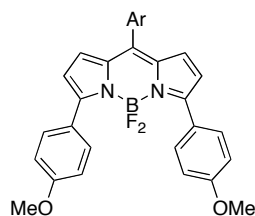
**84**  
CHCl<sub>3</sub>,  $\Phi$  0.78  
 $\lambda_{\text{max abs}}$  524 nm  
 $\lambda_{\text{max emiss}}$  537 nm



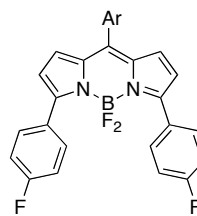
**85**  
CHCl<sub>3</sub>,  $\Phi$  0.20  
 $\lambda_{\text{max abs}}$  555 nm  
 $\lambda_{\text{max emiss}}$  588 nm



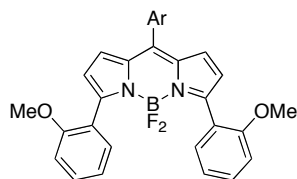
**86**  
CHCl<sub>3</sub>,  $\Phi$  0.38  
 $\lambda_{\text{max abs}}$  542 nm  
 $\lambda_{\text{max emiss}}$  607 nm



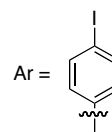
**87**  
 $\text{CHCl}_3$ ,  $\Phi$  0.42  
 $\lambda_{\text{max abs}}$  582 nm  
 $\lambda_{\text{max emiss}}$  626 nm



**88**  
 $\text{CHCl}_3$ ,  $\Phi$  0.22  
 $\lambda_{\text{max abs}}$  555 nm  
 $\lambda_{\text{max emiss}}$  590 nm



**89**  
 $\text{CHCl}_3$ ,  $\Phi$  0.08  
 $\lambda_{\text{max abs}}$  545 nm  
 $\lambda_{\text{max emiss}}$  598 nm



Fluorescence of BODIPYs in solution can be reduced at elevated concentrations due to intermolecular  $\pi$ -stacking. BODIPY dyes can stack in two geometrically distinct forms: H- and J-dimers (Figure 1.7). The former is most likely a result of intramolecular dimerization, with the stacking of two BODIPY planes with almost parallel  $S_0 \rightarrow S_1$  transition dipoles, and anti-parallel electric dipole moments. This dimer is practically non-fluorescent, and exhibits blue-shifted absorption relative to that of the monomer. The J-dimer, in which the  $S_0 \rightarrow S_1$  transition dipoles are oriented in planes at  $55^\circ$ , is fluorescent and shows a red-shifted absorption relative to that of the monomer.<sup>138-140</sup>

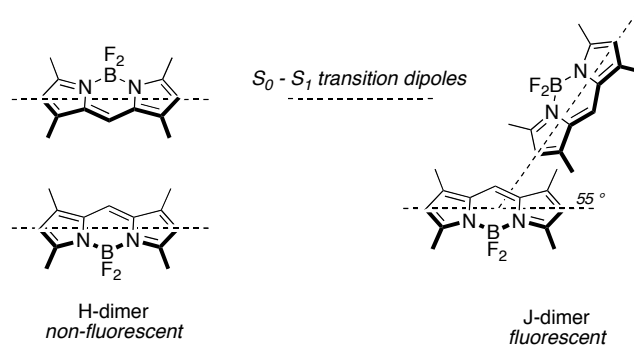
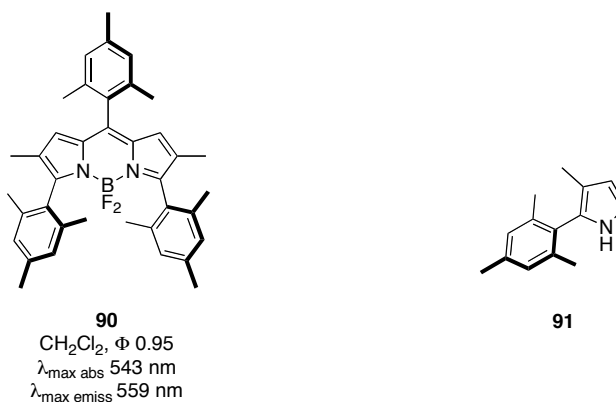


**Figure 1.7.** Structures of H-dimer and J-dimer.

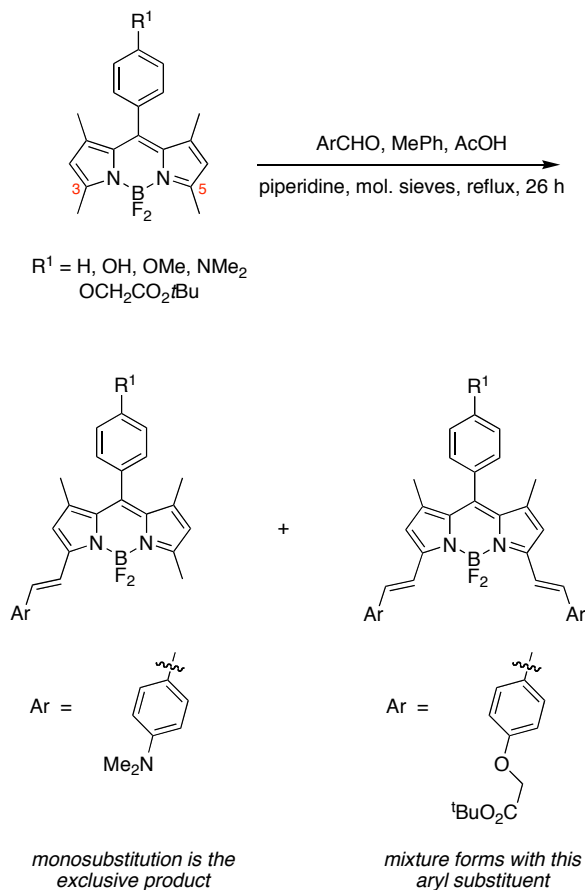
Compound **90** was designed as a probe that was sterically prevented from forming dimers in solution.<sup>141</sup> Further, the hindered internal rotation of the mesityl rings reduces non-radiative relaxation of excited states, enhancing fluorescence quantum yields. Dye **90** was prepared from mesityl aldehyde and pyrrole **91** (made via a Trofimov reaction).<sup>136</sup>



## 2. Condensation Reactions of the 3,5-Dimethyl Derivatives with Benzaldehyde Derivatives to Give Alkenyl Systems

In the last few years it has been shown that 3- and 5-methyl BODIPY substituents are acidic enough to participate in Knoevenagel reactions. Thus styryl-BODIPY derivatives can be

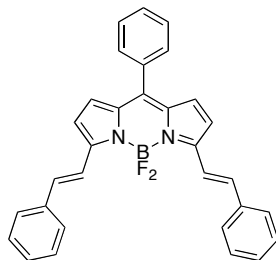
obtained by condensation of 3,5-dimethyl-BODIPYs with aromatic aldehydes (reaction 13).<sup>142,143</sup> With *p*-dialkylaminobenzaldehyde the reaction can be restricted to one condensation, but 4-alkoxybenzaldehydes tend to give mixtures corresponding to one and two condensations.<sup>144</sup> Di(dimethylamino)styryl-substituted BODIPY dyes can be obtained with longer reaction time (7 d).<sup>145</sup>



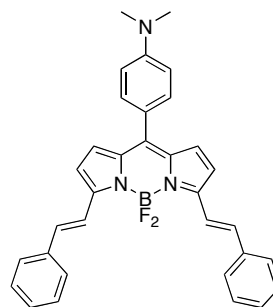
reaction 13

The condensation processes shown in reaction 13 provide direct entry into BODIPY derivatives that have red-shifted fluorescence properties, and functional groups that can be used in sensors and molecular logic gates. UV-absorption spectra of compounds from one condensation (eg **94** and **95**) tend to reach a maximum around 594 nm in MeOH, and their fluorescence emissions are similarly red-shifted. Both the absorption and, particularly, the fluorescence spectra are dependant upon solvent polarity.<sup>146,147</sup> The red-shift is more

pronounced in polar solvents indicating excitation of the dyes leads to more polarized excited states.

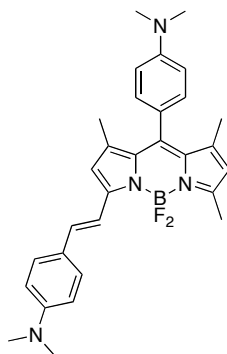


**92**  
 $\text{CH}_3\text{CN}$ ,  $\Phi$  0.84  
 $\lambda_{\text{max abs}}$  628 nm  
 $\lambda_{\text{max emiss}}$  642 nm



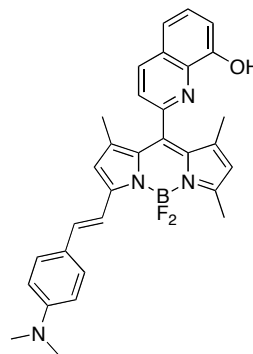
**93**  
 $\text{CH}_3\text{CN}$ ,  $\Phi$   $4 \times 10^{-4}$   
 $\lambda_{\text{max abs}}$  620 nm  
 $\lambda_{\text{max emiss}}$  636 nm

$\text{CH}_3\text{CN} + \text{H}^+$ ,  $\Phi$  0.75  
 $\lambda_{\text{max abs}}$  634 nm  
 $\lambda_{\text{max emiss}}$  652 nm



**94**  
 $\text{H}_2\text{O}$ ,  $\Phi$   $9 \times 10^{-4}$      $\text{MeOH}$ ,  $\Phi$  0.10  
 $\lambda_{\text{max abs}}$  578 nm     $\lambda_{\text{max abs}}$  594 nm  
 $\lambda_{\text{max emiss}}$  758 nm     $\lambda_{\text{max emiss}}$  699 nm

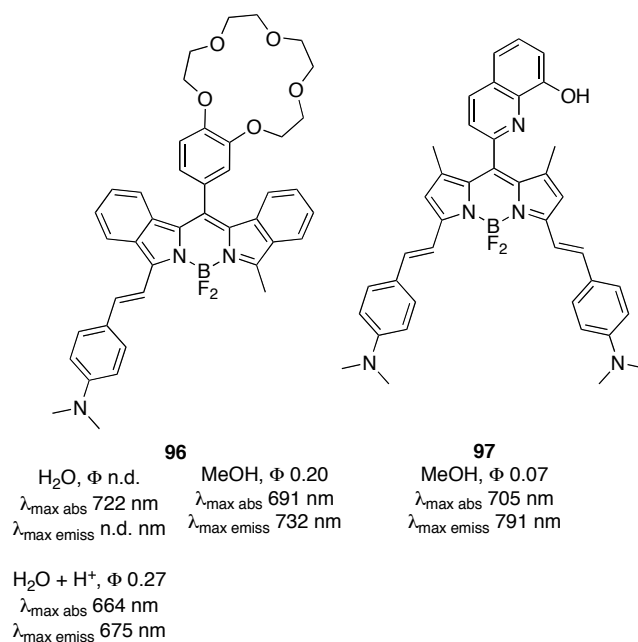
$\text{H}_2\text{O} + 2\text{H}^+$ ,  $\Phi$  0.55  
 $\lambda_{\text{max abs}}$  557 nm  
 $\lambda_{\text{max emiss}}$  565 nm



**95**  
 $\text{MeOH}$ ,  $\Phi$  0.04  
 $\lambda_{\text{max abs}}$  608 nm  
 $\lambda_{\text{max emiss}}$  738 nm

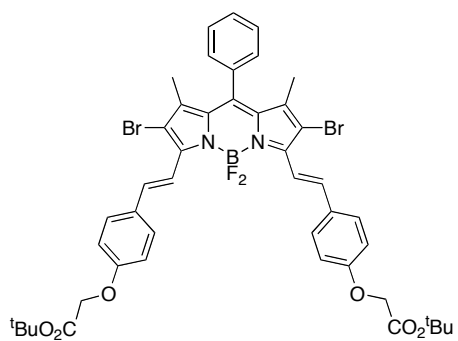
Structures **93** - **97** illustrate some effects of amino substituents in these styryl systems. When the amine is directly conjugated with the styryl group then a maximum red-shift is obtained, but when it is part of the *meso*-substituent then the bathochromic shift is less because

this *meso* substituent is non-planar. Quantum yields for these materials are only high when the amine is protonated disfavoring Intramolecular Charge Transfer (ICT) in the excited state.<sup>142,147</sup>

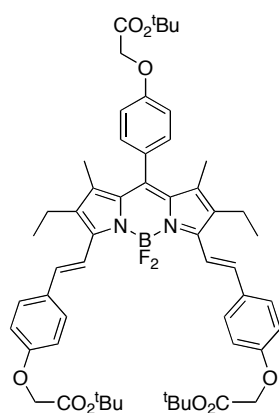


Structures **95** - **97** were prepared as metal sensors where complexation to ions alleviates ICT and increases the quantum yields. Comparison of the spectral data for **95** and **97** reveals a second styryl group gives a red-shift in the UV absorbance of almost 100 nm, and in about 50 nm in the fluorescence spectrum.<sup>145</sup>

There is no marked pH dependence for the alkoxy-substituted systems **98** and **99**.<sup>144</sup> However, the amino-phenol **100** has quenched fluorescence when the hydroxyl group is deprotonated, but the UV absorbance and fluorescence remain the same; fluorescence is enhanced and there is a blue shift when the amine group is protonated. This molecule has therefore been compared to a logic gate.<sup>75</sup>

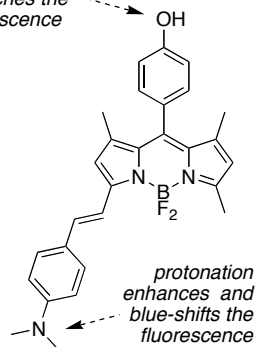
**98**

$i$ PrOH,  $\Phi$  0.42  
 $\lambda_{\text{max abs}}$  657 nm  
 $\lambda_{\text{max emiss}}$  679 nm  
 fwhm 41 nm

**99**

$i$ PrOH,  $\Phi$  0.40  
 $\lambda_{\text{max abs}}$  657 nm  
 $\lambda_{\text{max emiss}}$  679 nm  
 fwhm 43 nm

*deprotonation  
 quenches the  
 fluorescence*

**100**

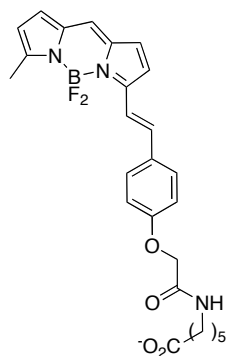
THF,  $\Phi$  0.25  
 $\lambda_{\text{max abs}}$  565 nm  
 $\lambda_{\text{max emiss}}$  660 nm

THF +  $\text{H}^+$ ,  $\Phi$  0.85  
 $\lambda_{\text{max abs}}$  525 nm  
 $\lambda_{\text{max emiss}}$  560 nm

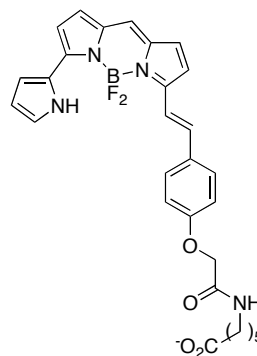
THF +  $\text{OH}^-$ ,  $\Phi$  0.032  
 $\lambda_{\text{max abs}}$  565 nm  
 $\lambda_{\text{max emiss}}$  660 nm

*protonation  
 enhances and  
 blue-shifts the  
 fluorescence*

Invitrogen's BODIPY 630/650 and BODIPY 650/665 probes are the longest-wavelength amine-reactive BODIPY fluorophores reported to date.



**BODIPY 630/650**



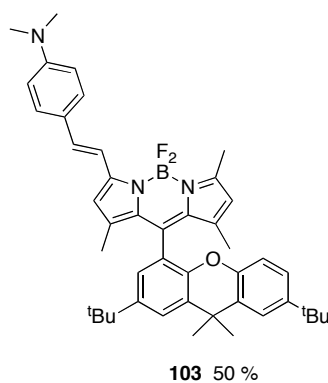
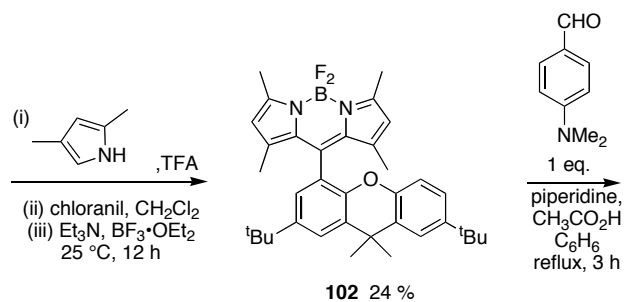
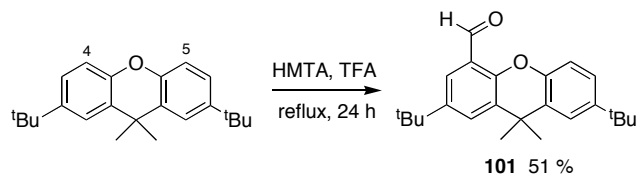
**BODIPY 650/665**

Biomolecules labeled at relatively large BODIPY:protein ratios can have diminished fluorescence due to interactions between the probes; the fluorescence can also be red-shifted for the same reason.<sup>148</sup> Small molecules containing two BODIPYs have been produced to test these types of effects. The first prepared were somewhat flexible being based on cyclohexane.<sup>138,139</sup> More recently, rigid test molecules with cofacial BODIPY dyes have been made and studied. Only one transition dipole moment is possible for these structures. The xanthane unit was chosen as a scaffold since it can be easily functionalized on its 4- and 5-positions. Aldehyde or bis-aldehyde functionalities on the xanthane (**101** or **105**, respectively) were used to construct the BODIPY units by condensation with 2,4-dimethylpyrrole. A 3-methyl substituent on the BODIPY was then reacted with *p*-dimethylaminobenzaldehyde to extend the conjugation (Scheme 1.7).<sup>149</sup>



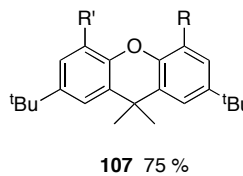
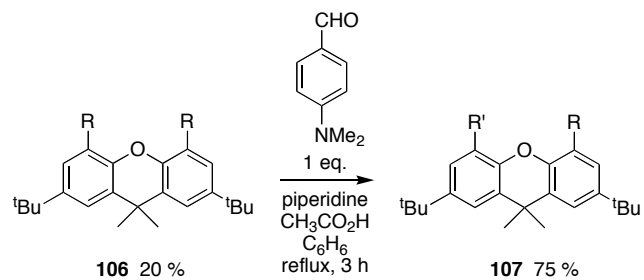
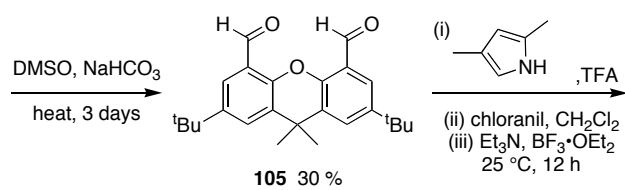
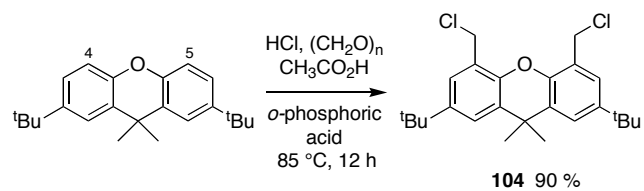
**Scheme 1.7.** Syntheses of BODIPY dyes anchored on xanthenes units to test self-quenching: **a** a system with one BODIPY dye; **b** a similar compound with two, where only one has extended conjugation; and, **c** another where both have extended conjugation.

**a**



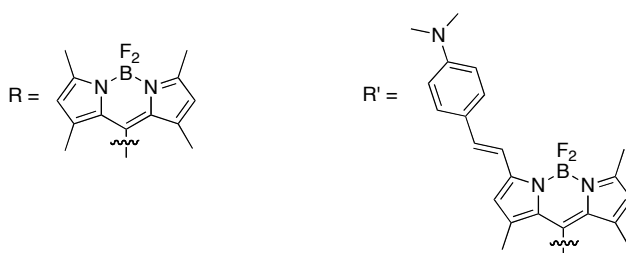
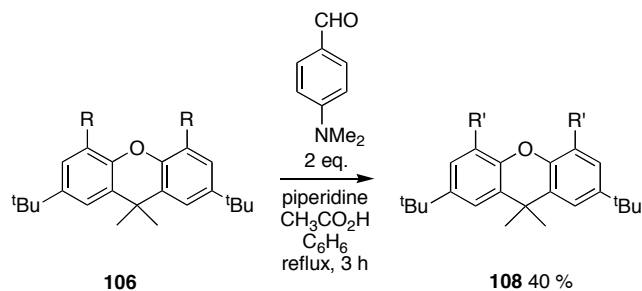
## Scheme 1.7. Continued.

b



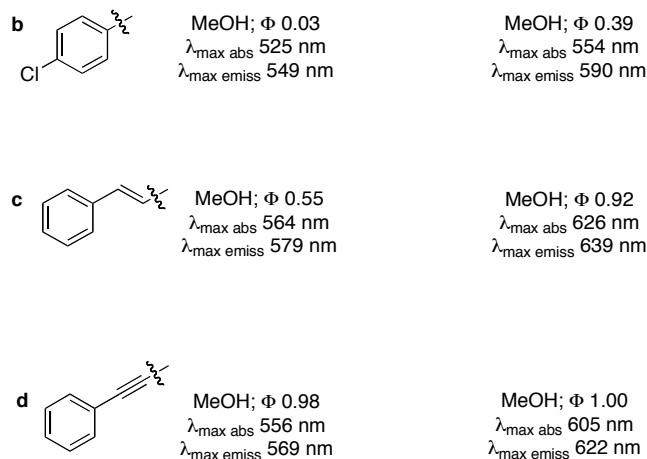
## Scheme 1.7. Continued.

c



Compound **106** has two cofacial BODIPY groups, and the UV absorption maximum of the BODIPY part is blue shifted (to 478 nm, with a shoulder at 504 nm) relative to 1,3,5,7-tetramethyl-BODIPY **7** and the control compound **102**. Compound **107** which has one styryl-extended BODIPY and one tetramethyl-BODIPY substituent has UV absorption peaks corresponding to both these substituents (455 nm and 575 nm). Upon excitation at 480 nm, the monochromophoric system **102** exhibits a very strong emission at 500 nm, while the fluorescence emission of the di-BODIPY system **106** is significantly quenched; it shows two peaks, one at 505 nm and a broader excimer-type emission at 590 nm. Efficient energy transfer from the donor (tetra-methyl BODIPY) to the acceptor (extended BODIPY) was observed for the system **107**. The cofacial chromophores are separated by approximately 4.5 Å, allowing both energy transfer and formation of an excimer-like state. Incidentally, system **107** acts as an energy transfer cassette; fluorescence emission could be observed at 650 nm from the extended





reaction 14

## F. Energy Transfer Cassettes

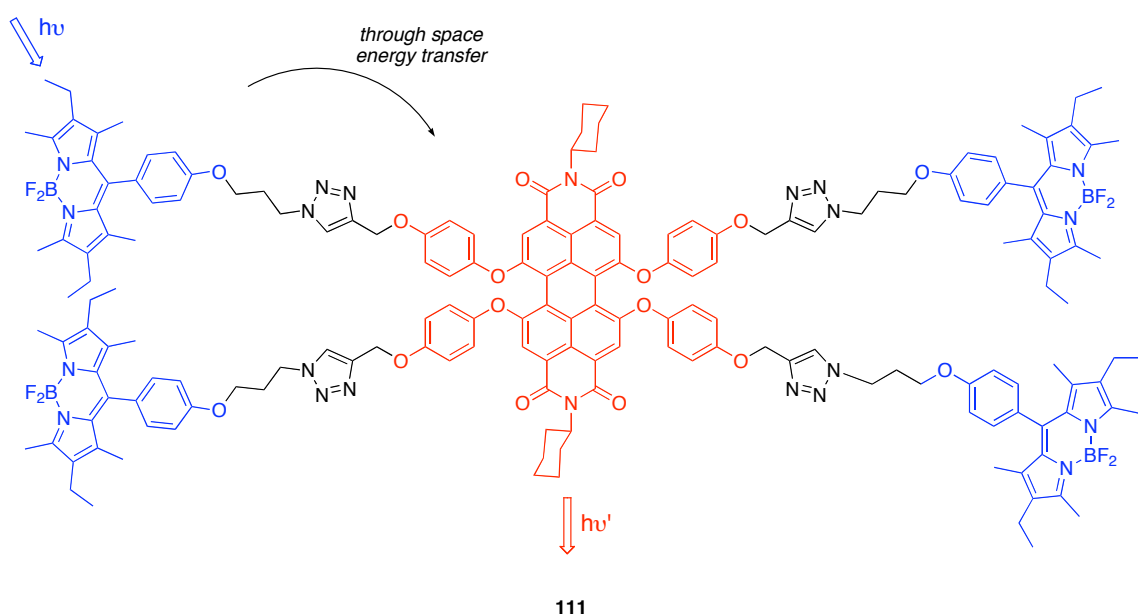
### 1. Through-space Energy Transfer Cassettes

Two fluorescent entities may be joined in the same molecule to give a “cassette”. One of these, the *donor*, may collect radiation efficiently at the excitation wavelength and pass this energy to the second fluorescent moiety that emits it at a longer wavelength. If the mechanism of energy transfer is through space then this system might be called a through-space energy transfer cassette. Through space-energy transfer cassettes are typically used to artificially enhance the Stokes' shift of a probe. Ones featuring BODIPY dyes have been somewhat useful for DNA sequencing on a genomic scale<sup>151</sup> where four distinct fluorescent outputs are required, and usually only one excitation wavelength is used.

Through-space energy transfer efficiencies depend on several factors, including: (i) spectral overlap of the donor emission with the acceptor absorbance; (ii) distance between the donor and the acceptor; (iii) the orientation factors; and, (iv) the effectiveness of alternative de-excitation modes. Cassettes described in this section have no obvious way to transfer energy from donors to acceptors via bonds.

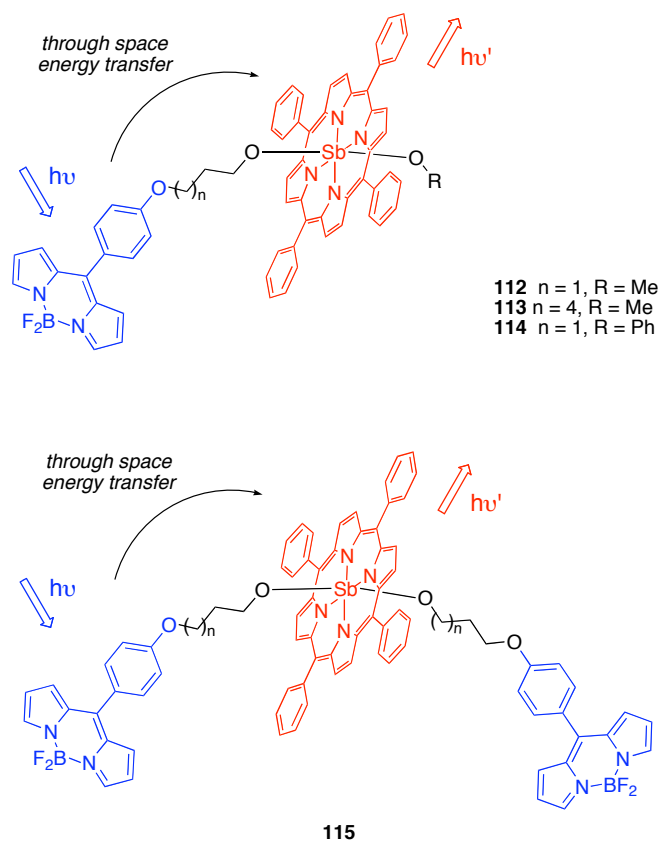
The dendritic light harvesting system **111** with four BODIPY donors and a perylenediimide (PDI) acceptor was constructed via click chemistry.<sup>152</sup> Its UV spectrum is equal to the sum of the donor and acceptor components indicating they are not electronically perturbing each other.<sup>153</sup>

The extinction coefficients of **111** at 526 nm (BODIPY  $\lambda_{\text{max}}$ ) and 582 nm (PDI  $\lambda_{\text{max}}$ ) are 240 000 and 45 000  $\text{M}^{-1}\text{cm}^{-1}$ , respectively, hence the donor absorption is huge simply because four BODIPY units are involved. No green fluorescence emission from BODIPY was observed upon excitation at 526 nm, indicating efficient energy transfer (99 %). Based on the energy transfer efficiency, the authors of this work calculated a Förster critical radius of 47 Å. An “antenna effect” {emission intensity at 618 nm when excited at 526 nm (BODIPY core) divided by that from excitation at 588 nm (at the PDI core)} gave approximately a 3.5 fold enhancement.

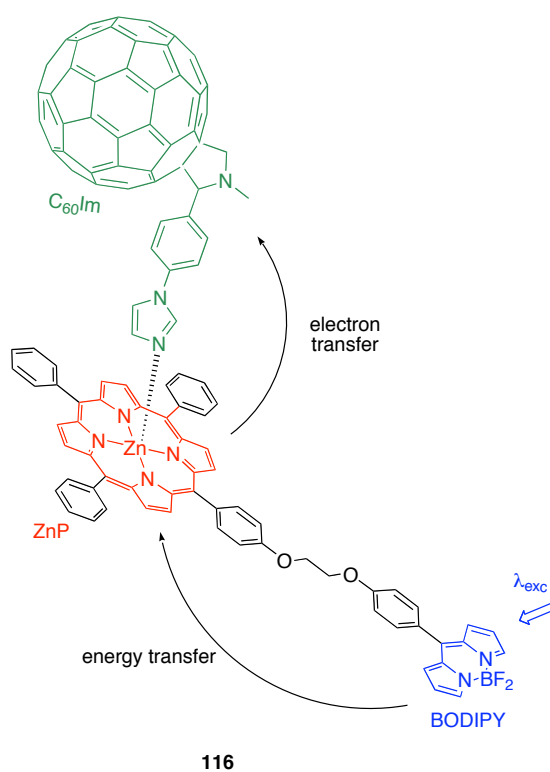


Most studies on energy transfer between porphyrins and other chromophores have focused on electron and energy transfer in the plane of the porphyrin. “Vertical” electron and energy transfer from axial ligands, on the other hand, has not been studied extensively but systems **112** – **115** were synthesized to study this phenomenon. An antimony porphyrin was chosen as the acceptor because this central metal can coordinate to ligands with oxygen, nitrogen, or sulfur atoms. Energy transfer from the excited singlet state of the BODIPY to the Sb(TPP) chromophore occurs for **112**, **113** and **115**. This happens with efficiencies in the 13 – 40 % range, decreasing as the length of the methylene bridge increases. Little or no evidence was seen for quenching of the porphyrin excited singlet state by the BODIPY. This was true even when polar solvents were used and the donor and acceptor fragments would be expected

to pack against each other. However, for system **114**, which differs from **112** only at the second axial ligand (phenoxy vs methoxy), the excited singlet state of the Sb(TPP)-acceptor was quenched by the BODIPY and phenoxy ligands. The quenching by the phenoxy group occurs, at least in part, via a non-radiative electron-transfer process.<sup>154</sup>

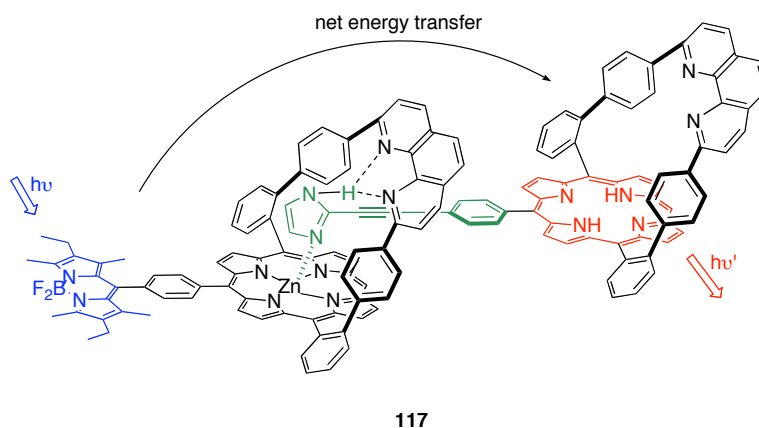


System **116** is another artificial light harvesting system with BODIPY dye donors, but here the energy is transferred to a zinc porphyrin (ZnP) then electron transfer occurs to a fullerene ( $\text{C}_{60}\text{-Im}$ ) unit; thus the molecule was called a “supramolecular triad”. The Zn-porphyrin connects to the fullerene component via metal to axial-ligand coordination. Both steps in the process were efficient. Overall, the system was said to mimic the “combined antenna-reaction center” events in natural photosynthesis.<sup>155</sup>

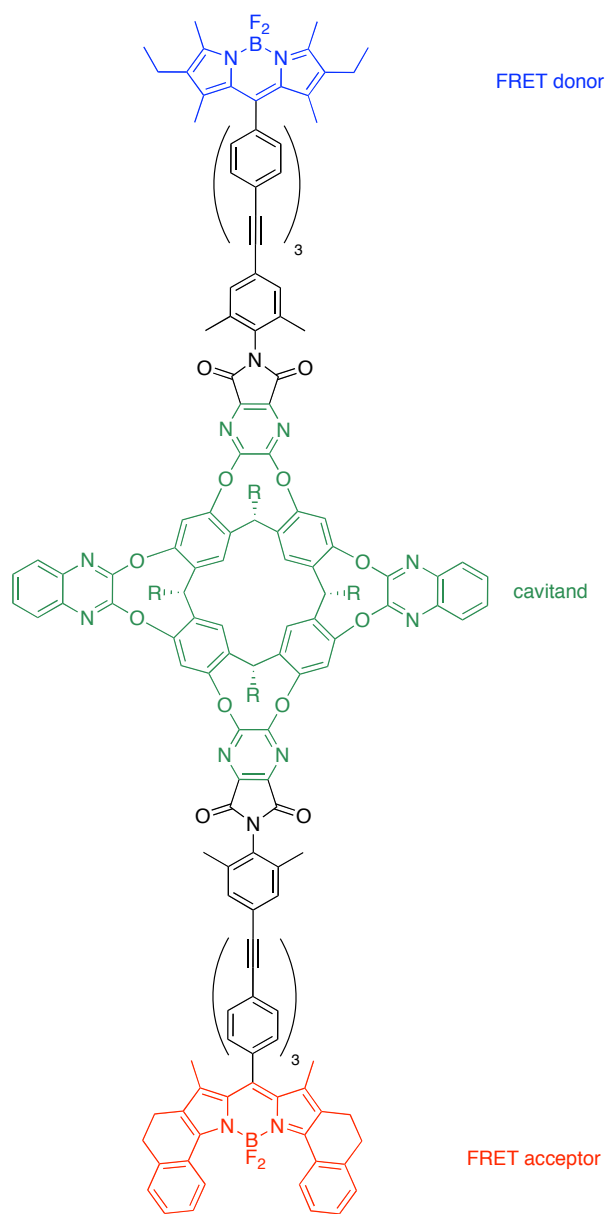


Like **112** - **116**, complex **117** also features a donor and an acceptor system linked via axial coordination to a zinc porphyrin.<sup>156</sup> This self-assembling system is based on the exceptional affinity of phenanthroline-strapped zinc porphyrins for *N*-unsubstituted imidazoles.<sup>157,158</sup> Efficient net energy transfer (80 %) was observed for excitation of the BODIPY at 495 nm and emission at the free porphyrin. Energy transfer from the excited ZnP-Im complex to the free porphyrin was calculated to be 85%.

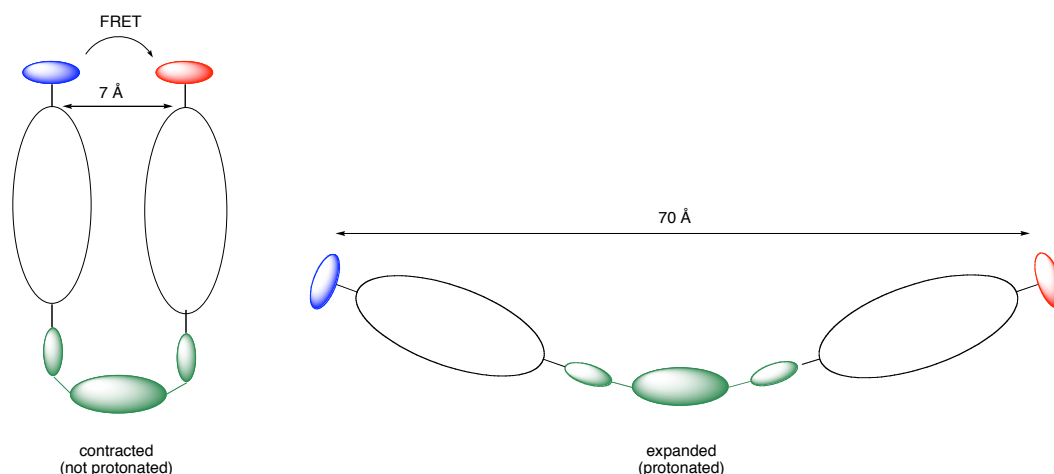




Compound **118** was designed to be a molecular switch. It has two stable conformations governed by the bridged resorcin<sup>159</sup> arene scaffold.<sup>160</sup> In the absence of protons (or perhaps other guest cations) the molecule exists in a contracted geometry maximizing FRET (fluorescence resonance energy transfer) between the two BODIPY based probes. Decreased pH values switch the molecule to the expanded conformation and this is evident by the reduced energy transfer. An advantage of using BODIPY dyes in this study is their low sensitivity to pH changes.



**118**  
 $R = n\text{-C}_6\text{H}_{13}$



The UV spectrum of **118** displays three strong absorption bands assigned to the spacer ( $\lambda_{\text{max}}$  332 nm), the donor ( $\lambda_{\text{max}}$  529 nm) and the acceptor dye ( $\lambda_{\text{max}}$  619 nm), respectively. Upon excitation at 490 nm, two emission bands at 542 nm (donor dye) and 630 nm (acceptor dye) are observed, in a ratio of the donor/acceptor fluorescence intensity of 45:55, indicating low FRET efficiency (possibly due to unfavorable orientations of the transition dipole moments, and/or to the dynamic behavior of the cavitaand part). Upon addition of TFA, the emission from the acceptor is nearly completely quenched, whereas the donor fluorescence intensity doubles.

## 2. Through-bond Energy Transfer Cassettes

### *Porphyrin-based Systems as Models of Photosynthesis*

The prevalent mechanism of through-space energy transfer is likely to be via dipolar couplings, *ie* Förster energy transfer. The rate and efficiency of this is governed by, among other things, the overlap integral between the donor fluorescence and the acceptor absorbance.

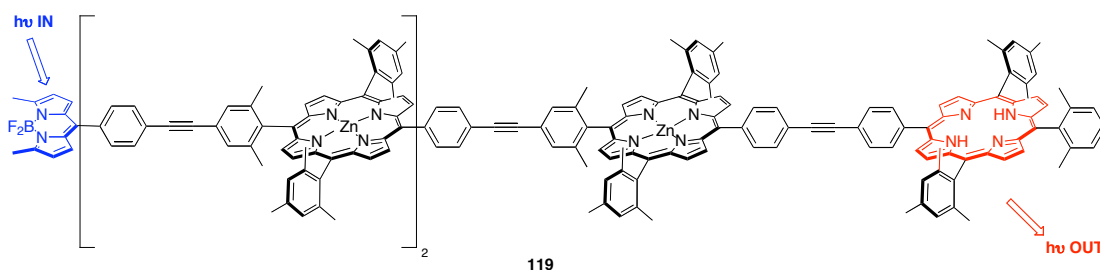
If the donor and acceptor dyes are coupled to each other via a conjugated but twisted  $\pi$ -system then the prevalent mechanism of energy transfer is likely to be through bonds. Constraints on through-bond energy transfer are not well understood, but it appears there is no requirement for a good overlap integral. This is important in the design of fluorescent cassettes because, if this is true, there is no obvious limitation on the energy gap between the donor fluorescence and the acceptor absorbance, hence cassettes with huge “apparent Stokes’ shifts” could be produced.

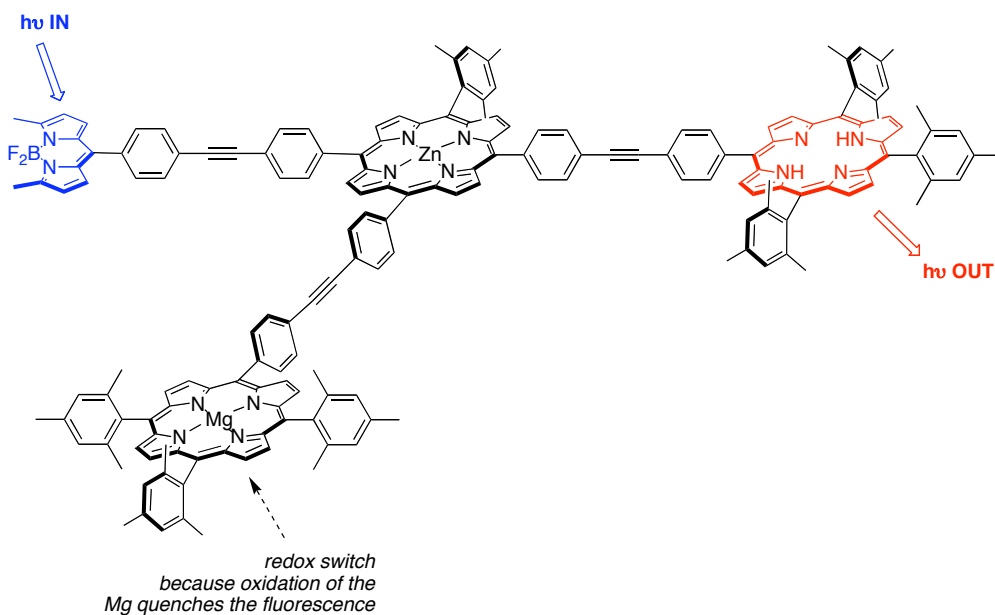
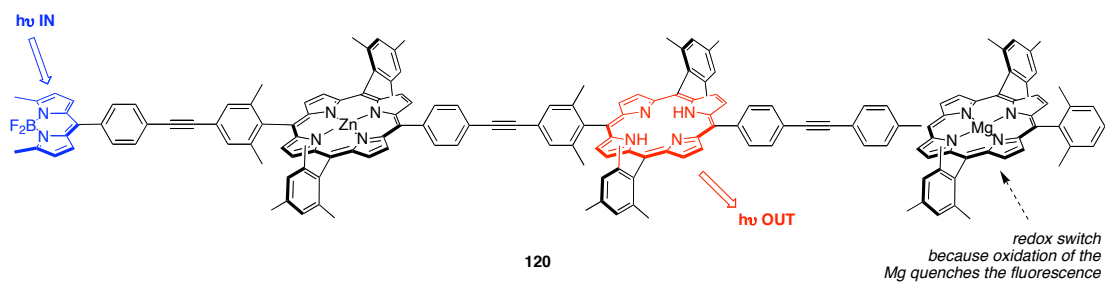
A pioneer of energy transfer systems featuring BODIPY donors was Lindsey who studied them in the context model porphyrin-based systems for photosynthesis.<sup>161</sup> He proposed that the rates and efficiencies of through-bond energy transfer are influenced by the following factors:

- steric interactions between the donor/acceptor wherein increased torsional constraints decrease rates and efficiencies of energy transfer;
- frontier orbital characteristics for the HOMO and LUMO; and related to that,
- the site of attachment of the donor/acceptor to the linker and the nature of the linker.

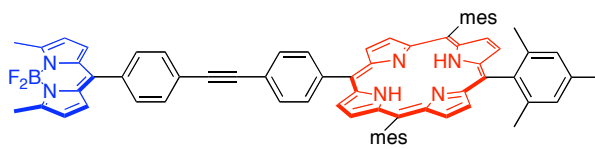
Lindsey has described the through-bond energy transfer cassette **119** as a “linear molecular photonic wire”. It features a BODIPY donor and a free base porphyrin acceptor. This donor-acceptor pair is separated by 90 Å. Efficient energy transfer (76 %) from the donor to the acceptor was observed upon excitation at 485 nm (*ie* the donor  $\lambda_{\text{max abs}}$ ).<sup>162</sup>

Systems **120** and **121** were described as “molecular optoelectronic linear- and T-gates”, respectively. In these cassettes, the emission of the acceptor can be turned on or off via reduction or oxidation of the attached magnesioporphyrin; the latter in its oxidized state quenches fluorescence via ICT. For each cassette more than 80% of energy transfer was observed upon excitation of the BODIPY donor part.<sup>163</sup>

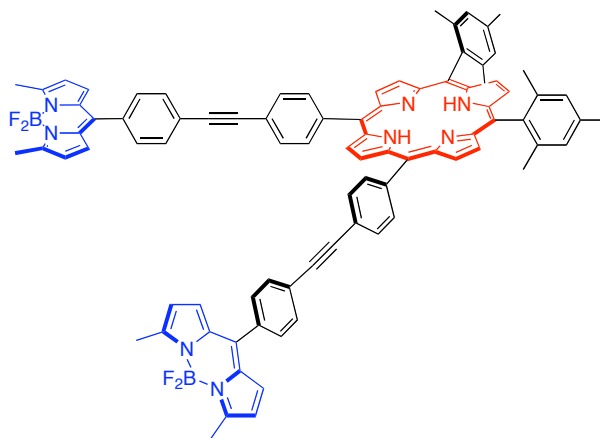




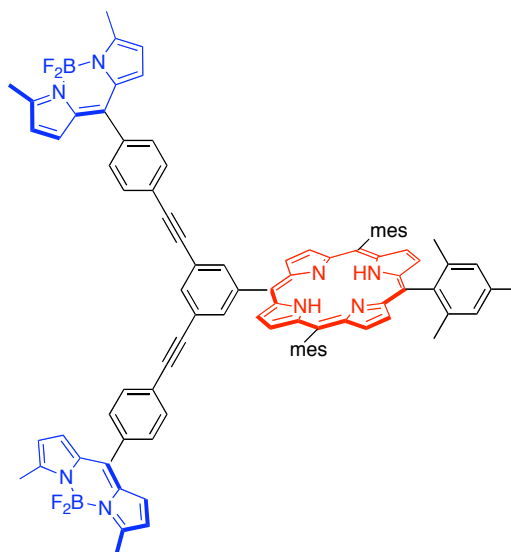
Compounds **122** - **125** are light-harvesting arrays featuring one, two, or eight BODIPY donors and one porphyrin acceptor. Increasing the number of BODIPY donors from one to eight only increases the relative absorption at 516 nm from 68 to 94 % (of a BODIPY standard) for the free base porphyrins **122** - **125**, and from 91 to 99 % for the Zn-porphyrin (not shown). Near quantitative energy transfer was observed for the systems containing one or two BODIPY units, but 80-90 % energy transfer was observed for the system bearing eight BODIPY units.<sup>164</sup>



122

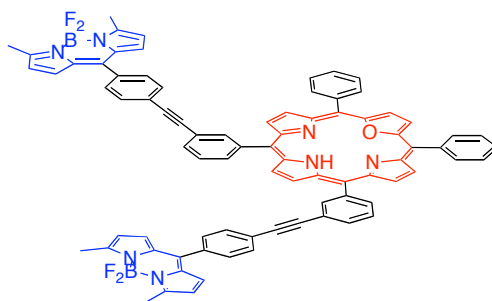


123

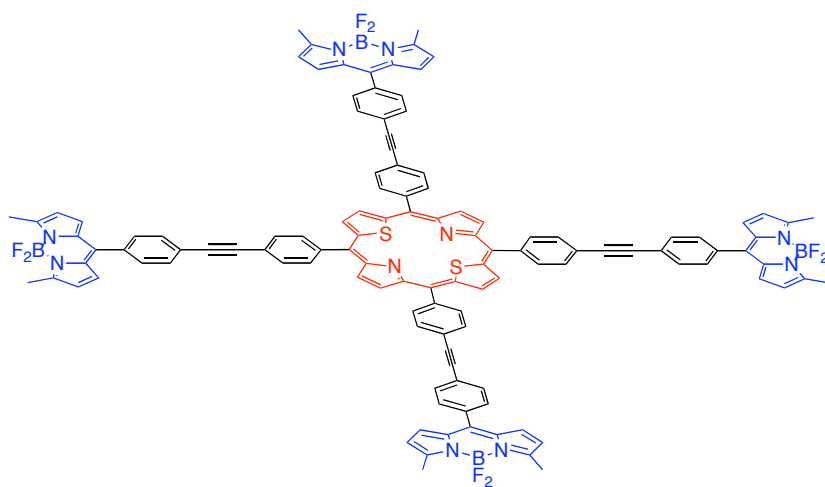


124



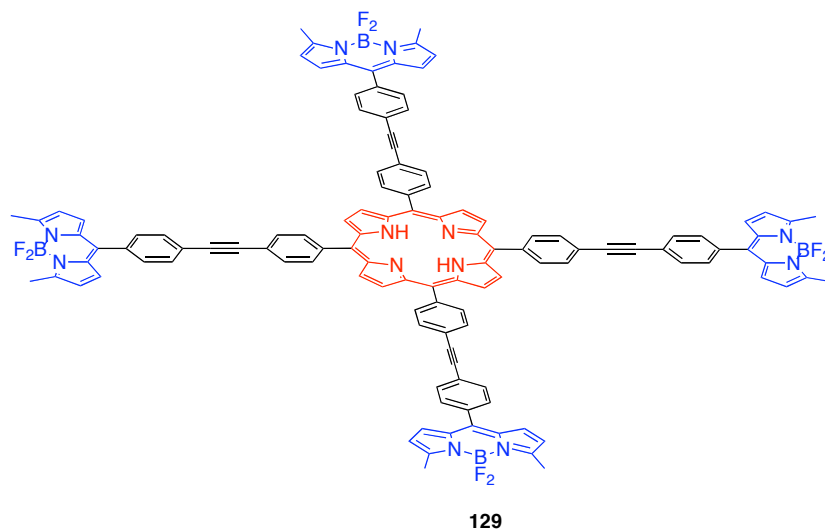


127



128

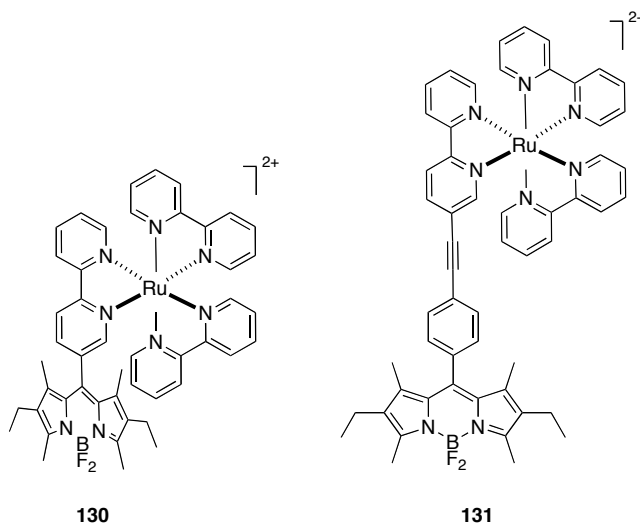
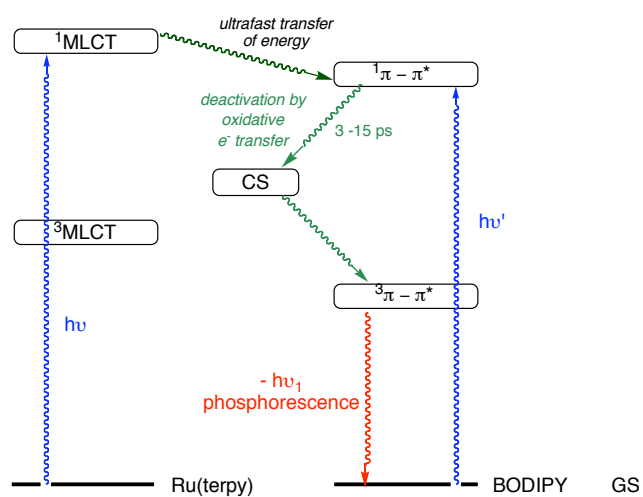


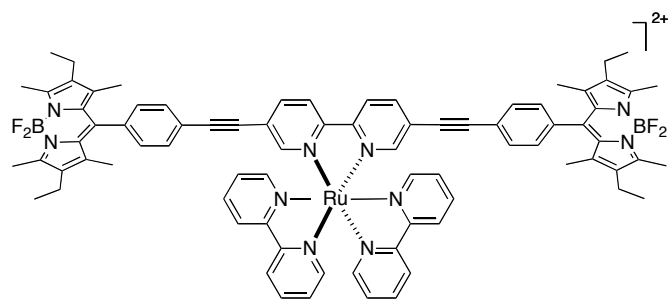


### ***Polypyridine Complexes Containing Accessory BODIPY Chromophores***

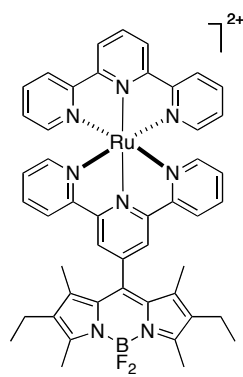
The dual-dye systems **130** – **137** featuring one or more BODIPY chromophores and a Ru(II) polypyridine complex have been synthesized as models for solar energy conversion and storage. The BODIPY chromophore was chosen for its strong fluorescence, whereas the Ru(II) polypyridine complex was chosen for its relatively intense and long-lived triplet metal-to-ligand charge transfer (MLCT) emission. The pyridine based BODIPY dyes were synthesized by condensation of formylpyridine with 3-ethyl-2,4-dimethylpyrrole.<sup>169-172</sup> The new compounds exhibit intense absorption in the visible region (acetonitrile solution), with a major sharp band at 523 nm assigned to the  $\pi - \pi^*$  transition for the dipyrromethene dye and a broader band of lower intensity between 450 and 500 nm. The free ligands are strongly fluorescent both in solution at room temperature and at 77 K in a rigid matrix, but no luminescence could be observed in solution for the Ru complexes, independently of the excitation wavelength. Nanosecond transient absorption spectra, however, revealed that a relatively long-lived (ms time scale) excited state was formed for all metal complexes. The latter was identified as the BODIPY-based triplet state, and is believed to be formed through a charge-separated level from the BODIPY-based  $^1\pi - \pi^*$  state. At 77 K, all the complexes studied except for **130**, exhibit the BODIPY-based fluorescence, although with a slightly shortened lifetime compared to the free ligands. However, the surprising finding was that **133** – **135** also exhibit a phosphorescence assigned to the BODIPY subunits (emission at 774 nm of 50 ms lifetime). This is the first report of phosphorescence for BODIPY based dyes. The authors propose that the phosphorescence is due to the presence of the heavy ruthenium metal, which facilitated intensity to be diverted into

the BODIPY  $^3\pi - \pi^*$  state from the closely lying metal-based  $^3\text{MLCT}$  level (for which luminescence decay is highly efficient at 77 K).<sup>170,173,174</sup> Phosphorescence from BODIPY units is certainly unusual. It only was observed here at 77 K for a system coupled with a ruthenium complex, and the efficiency of the process was not determined.

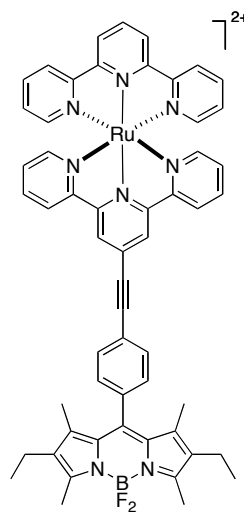




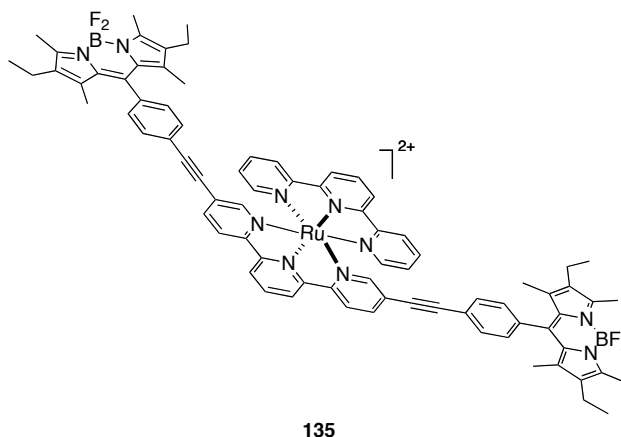
132



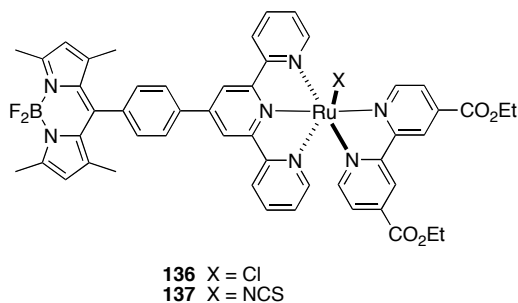
133



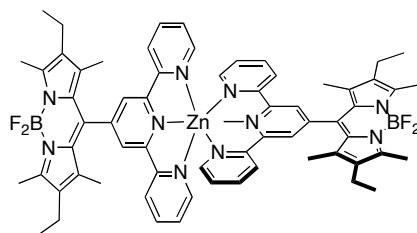
134



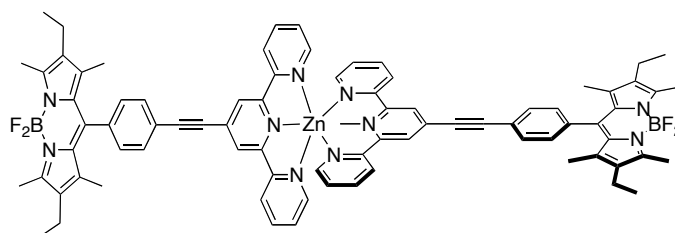
Compounds **136** and **137** combine ruthenium polypyridine units with BODIPY fragments. The BODIPY part ensures a high molar absorption coefficient of the system in the metal-to-ligand charge-transfer region (around 500 nm). The singlet excited states of **136** and **137** are strongly quenched by the presence of ruthenium: energy transfers to the Ru center with high efficiency (93 % and 73 % for **136** and **137**, respectively), where it is then dissipated via electron transfer and/or singlet to triplet intersystem crossing. The net effect is that these complexes are not fluorescent.<sup>175</sup>



Loss of fluorescence when BODIPY dyes are conjugated with metal complexes is common. For instance complexes **138** and **139** have greatly reduced fluorescence relative to the free ligands,<sup>171,172</sup> presumably due to intramolecular electron transfer.<sup>171,176</sup>



138



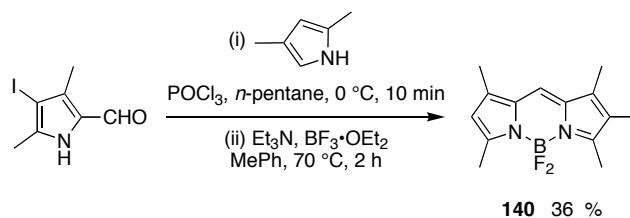
139

Other complexes, eg of platinum,<sup>177</sup> containing BODIPY-based ligands have been prepared, but without comment on their fluorescent properties. It is unlikely that such materials will be useful as probes.

### ***Relatively Compact Systems as Potential Probes in Biotechnology***

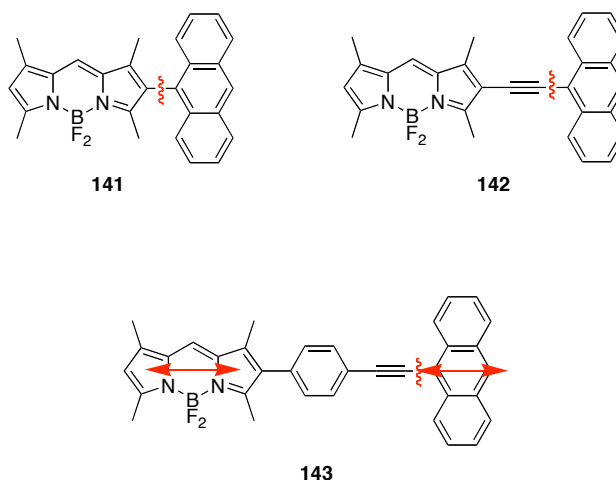
Porphyrin-based cassettes tend to be larger than is ideal for applications relating to labeling of biomolecules, but the through-bond energy transfer aspect could be very useful for applications wherein one source is used and several different outputs must be observed simultaneously. Thus, there has been interest in making smaller through-bond energy transfer cassettes.

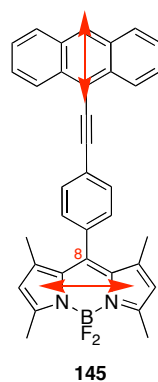
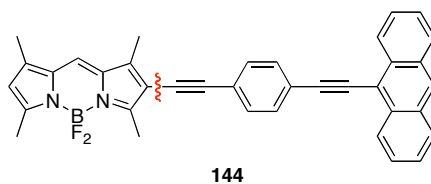
BODIPY-based cassettes featuring simple aromatic donors can be prepared from halogenated BODIPYs eg **140** via palladium mediated cross-coupling reactions.<sup>178</sup> Monoiodinated products can be quite useful for such syntheses. For instance, reaction 15 shows a typical stepwise BODIPY synthesis that was used for this.<sup>178</sup>



reaction 15

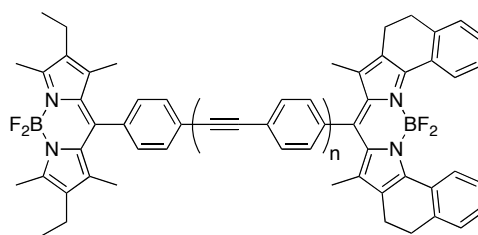
Fluorescence quantum yields of compounds **141** - **144** excited at the donor  $\lambda_{\max}$  range from 0.02 to 0.75 (in chloroform). In compound **145**, the  $S_1 \leftrightarrow S_0$  transition moments of the chromophores are mutually perpendicular in all conformations. Fast energy transfer, of the order of  $0.45 \pm 0.08$  ps, was observed for this compound. For **141** - **144**, the donor and acceptor  $S_1 \leftrightarrow S_0$  transition moments are mutually coaxial with the linker in all conformations. The transfer rate for this set of compounds was *even faster* than for **145**,  $\sim 200$  fs; in fact, this was too fast to be measured accurately.<sup>179</sup> Thus it appears from this data that parallel and aligned transition moments are ideal for extremely fast energy transfer. The length of the linker in this series of compounds was also varied but not enough derivatives were made to arrive at conclusions relating this parameter with energy-transfer rates.





More recently, energy transfer cassettes like **145** have been prepared; these are very similar except that the *meso*-donor group is one or two pyrene units linked with alkynes. It was shown that the energy transfer efficiency is reduced when alkyne units are added. Of course, use of conjugated pyrenes as the donor increases the UV absorption at shorter wavelengths and the  $\lambda_{\text{max}}$  for that donor-based band; the latter effect decreases the apparent Stokes' shift observed.<sup>180</sup>

Energy transfer cassettes like **146** – **148**, in which two BODIPY chromophores are linked via an acetylenic linker, have been prepared.<sup>160</sup> As the size of the linker increases, energy transfer efficiency decreases from about 98 % to ~ 35 %. These were described as FRET cassettes, but there is a strong possibility that some of the energy transfer takes place through bonds.

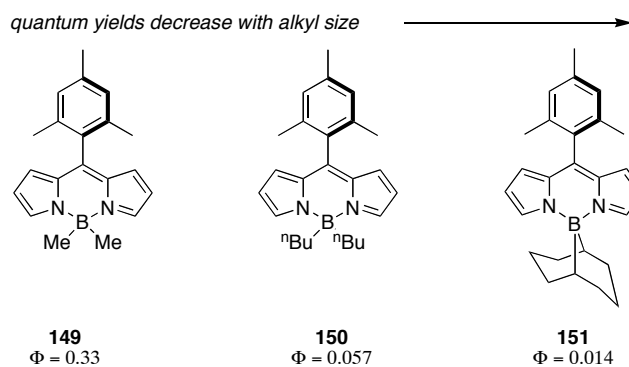


**146 - 148**  
n = 1, 3, and 6 respectively

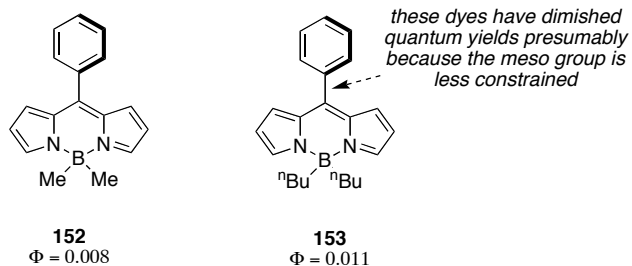
## G. Substitution of Fluoride Atoms in the BF<sub>2</sub>-Group

### 1. With Alkyl Groups

Some dialkyl-*B* BODIPY compounds have been prepared via reactions of the corresponding dipyrromethenes with bromodimethylborane, dibutylboron triflate, or 9-BBN triflate. Increased steric bulk at the boron atom along this series correlated with *decreased* fluorescence quantum yields. While the substituent at the *meso* position has no effect on the UV absorption and emission spectra, the fluorescence quantum yields strongly depend on the nature of the aryl group. Introduction of steric constraints on the aryl ring increases the quantum yield (compare **149** and **152**, **150** and **153**).<sup>181</sup>





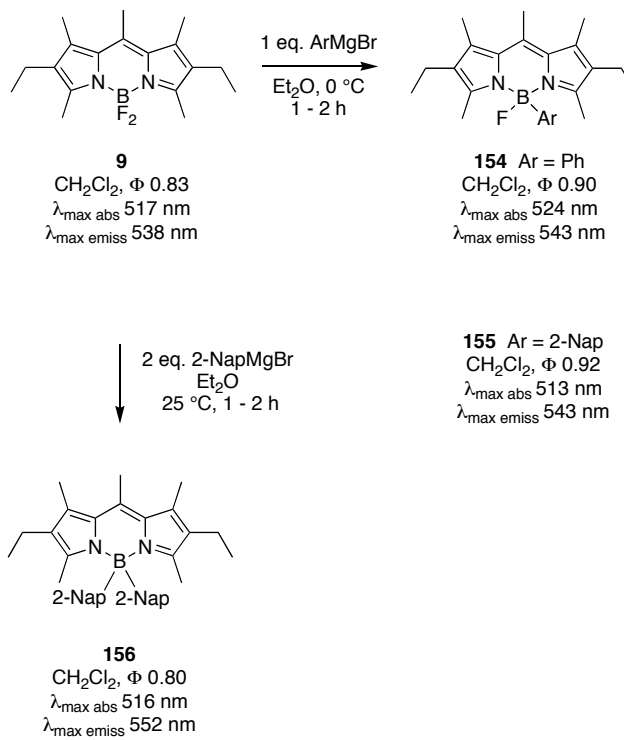


## 2. With Aryl Groups

Aryl Grignards can displace fluoride from the boron difluoride entity of BODIPY dyes. In Scheme 1.8a, at 0 °C, even with excess Grignard reagent, only the monosubstituted products **154** and **155** were obtained, but the disubstituted product **156** was formed by adding the Grignard reagent at room temperature. Reaction of aryl lithium reagents was much faster; these gave only the disubstituted products **157** - **159**, even when just one equivalent of anion was added (Scheme 1.8b).

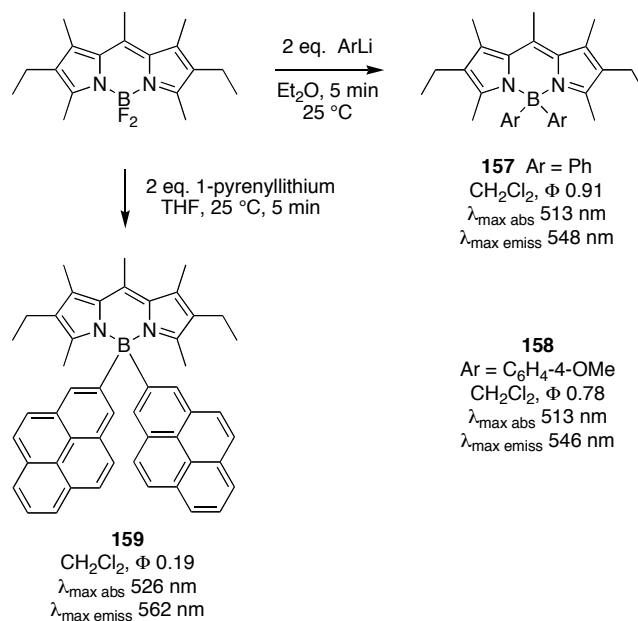
**Scheme 1.8.** Synthesis of C-BODIPYs using a aryl Grignard reagents; and, b aryl lithium reagents.

**a**



## Scheme 1.8. Continued.

b

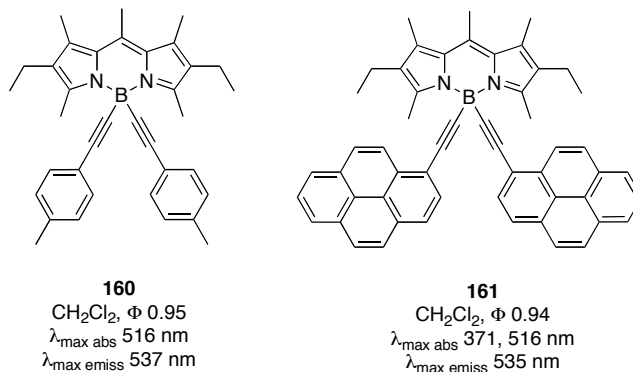


The new dyes **154** – **159** are highly fluorescent in solution. While the absorption maximum of the BF<sub>2</sub> parent dye is relatively insensitive to the solvent polarity, the *B*-Ar BODIPYs tend to undergo small red-shifts in more polar solvents. The origin of this solvent dependence may be minimization of interactions of the *B*-aryl groups with more polar media. The fluorescence emission maxima of **154** – **159** are also red-shifted relative to the parent BF<sub>2</sub> structures.

UV absorbance by the aromatic substituents means that these compounds can be regarded as energy transfer cassettes, and when the *B*-Ar groups have good extinction coefficients then there may be some value in this aspect of their properties. The dipyrrene system **159** absorbs in the range 230 - 317 nm corresponding to the  $\pi \leftrightarrow \pi^*$  transition of the pyrene units, and emits exclusively (100 % energy transfer) from the BODIPY part.<sup>182</sup> However, there is no immediate application of this effect.

### 3. With Alkyne Groups

Acetylide anions are also good nucleophiles for the displacement of fluoride from the borondifluoride entity of BODIPY dyes. The pyrromethene dialkynyl borane complexes **160** and **161**, for instance, were synthesized from 4-lithioethynyltoluene and 1-lithioethynylpyrene, respectively.<sup>183-185</sup>

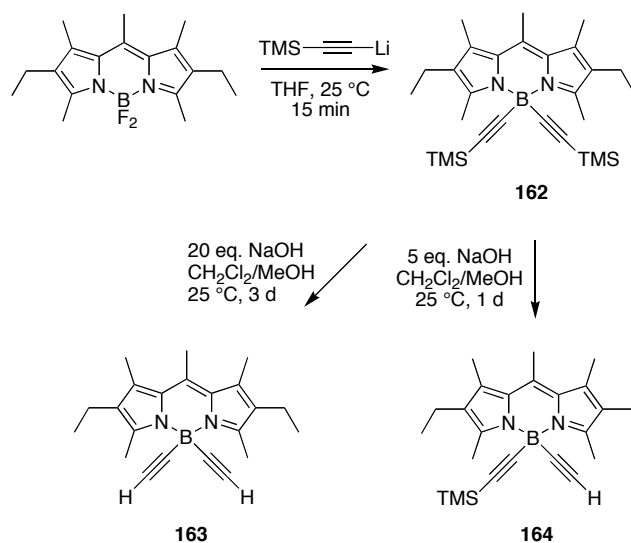


Adding groups to the boron atoms does not bring them into conjugation with the BODIPY core. Consistent with this, the absorption spectra of **160** and **161** have distinct BODIPY and ethynylaryl components. Upon excitation at 516 nm, both **160** and **161** emit strongly, with high fluorescence quantum yield, in the region 535-540 nm. For **161**, excitation at 371 nm (pyrene absorption band) did not lead to emission from the pyrene but instead to emission characteristic of the indacene core, indicating an efficient energy transfer from the pyrene to the indacene moiety.<sup>183,184,186</sup>

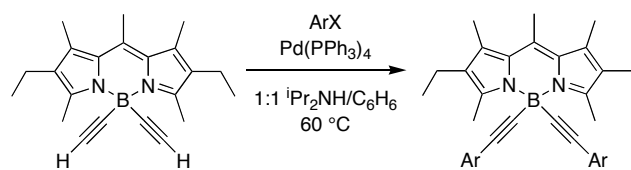
It is possible to add trimethylsilylacetylide to displace fluoride from BODIPYs, then desilylate under basic conditions and Sonogashira couple to the terminal alkyne eg **163** (Scheme 1.9). Whereas use of excess sodium hydroxide in the desilylation reaction affords the bis(ethynyl)BODIPY **163**, the monoprotected derivative **164** can be obtained using limited amounts of NaOH and shorter reaction times.<sup>187,188</sup> Access to the monoprotected derivative facilitates introduction of different substituents on the *B*-alkynes.<sup>184</sup>

**Scheme 1.9.** **a** Two-steps synthesis of bis(ethynyl)BODIPY **163**, and the monoprotected analog **164**; and, **b** some examples of compounds that have been prepared via Sonogashira coupling of **163**.

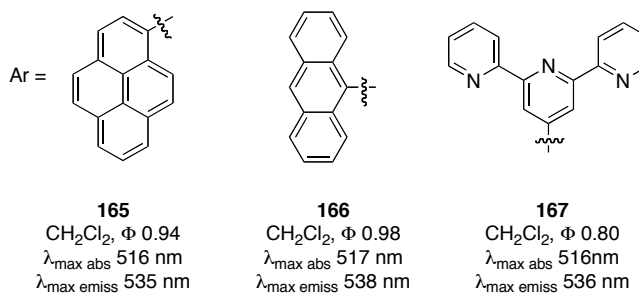
**a**



**b**



X = Br or OTf

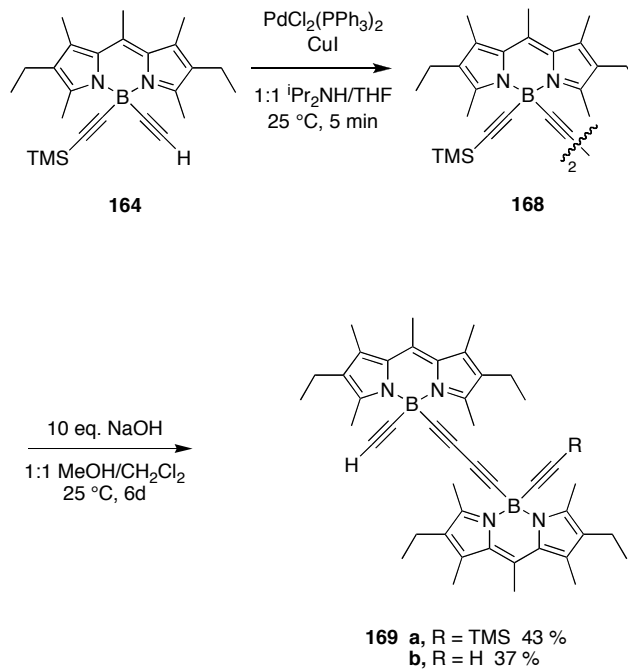


Compounds **165** – **166** can act as energy transfer cassettes, just like the *B*-aryl systems mentioned above. Irradiation of the donor (pyrene or anthracene) was observed to give only BODIPY emission, indicative of a near quantitative energy transfer.

Terminal alkynes like **164** and **170** can be oxidatively dimerized (Pd(II) and CuI under aerobic conditions) to give butadiynes **168** and **171** (Scheme 1.10).<sup>187</sup> Deprotection of the product butadiyne **168** was very slow, a mixture of monodeprotected **169a** and bisdeprotected **169b** was isolated after 6 days.<sup>187</sup>

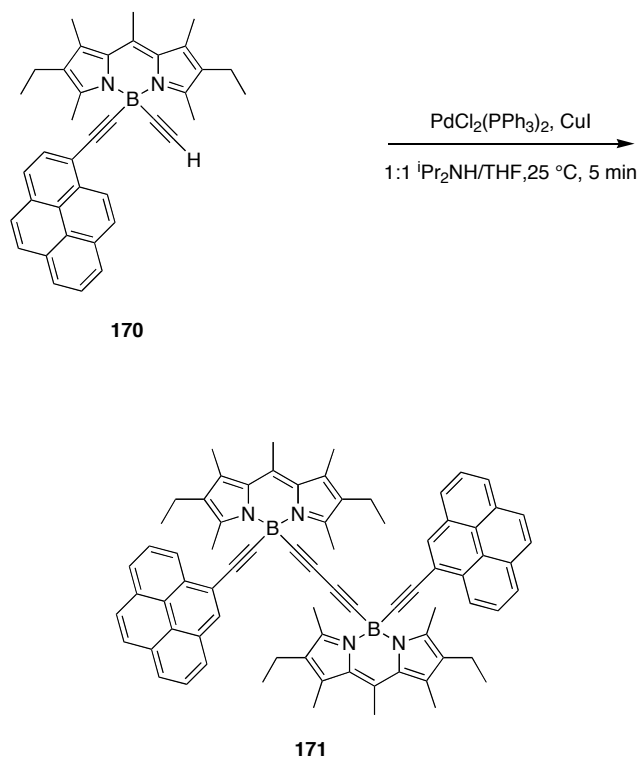
**Scheme 1.10.** Synthesis of homocoupled products.

**a**

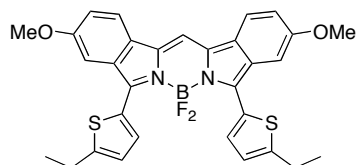


## Scheme 1.10. Continued.

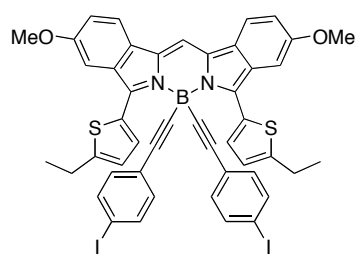
b



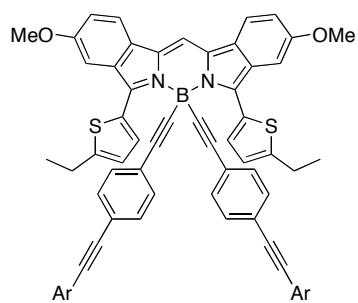
A very similar concept was explored by the same group but using diisoindolodithienylpyromethene-dialkynyl borane dyes.<sup>189</sup> These dyes have quite long wavelength emissions (over 750 nm); the parent  $\text{BF}_2$  dye **172** was known prior to this work.<sup>190</sup> Intermediate **173** was obtained by reaction of **172** with the appropriate alkynyl-Grignard reagent. Sonogashira coupling with various ethynyl-arene derivatives afforded the systems **174** - **178**. All the new dyes exhibit a UV absorption maximum at 708 nm with a molar absorptivity of  $\sim 80\,000 \text{ M}^{-1} \text{ cm}^{-1}$ . Higher energy absorption bands assigned to the pyrene, perylene, bis- and tri-pyridine were also observed near 350 and 450 nm. Upon excitation at 708 nm, a broad emission band at 750 nm, with quantum yields between 0.19 and 0.45 was observed in all cases. Fast energy transfer to the central dipyrromethene core was observed upon irradiation of the pyrene and perylene units in **177** and **178**, giving large virtual Stokes' shifts. The efficiency of the energy transfer for compounds **177** and **178** was estimated to 58% and 38%, respectively. Formation of aggregates was observed when the dyes were dissolved at concentrations higher than  $10^{-7} \text{ M}$ .

**172**

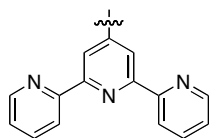
CH<sub>2</sub>Cl<sub>2</sub>, Φ 0.20  
 $\lambda_{\text{max abs}}$  727 nm  
 $\lambda_{\text{max emiss}}$  780 nm

**173**

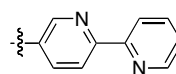
CH<sub>2</sub>Cl<sub>2</sub>, Φ 0.45  
 $\lambda_{\text{max abs}}$  709 nm  
 $\lambda_{\text{max emiss}}$  750 nm



Ar =

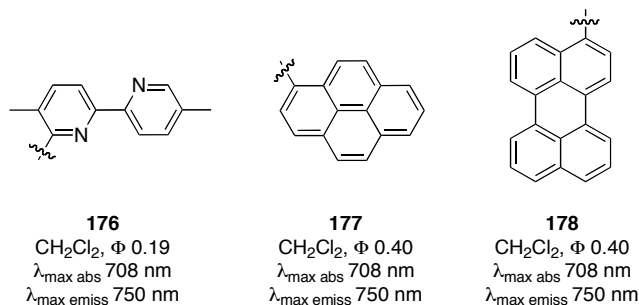
**174**

CH<sub>2</sub>Cl<sub>2</sub>, Φ 0.22  
 $\lambda_{\text{max abs}}$  709 nm  
 $\lambda_{\text{max emiss}}$  750 nm

**175**

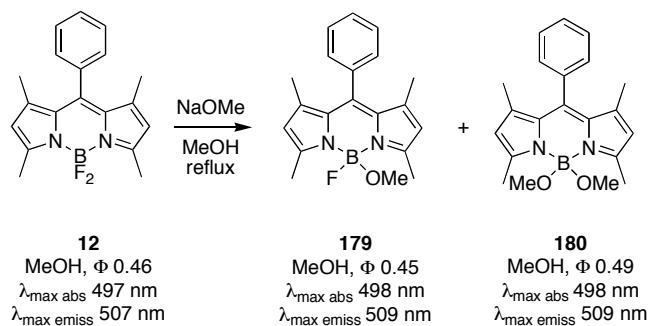
CH<sub>2</sub>Cl<sub>2</sub>, Φ 0.21  
 $\lambda_{\text{max abs}}$  708 nm  
 $\lambda_{\text{max emiss}}$  750 nm





#### 4. With Alkoxide Groups

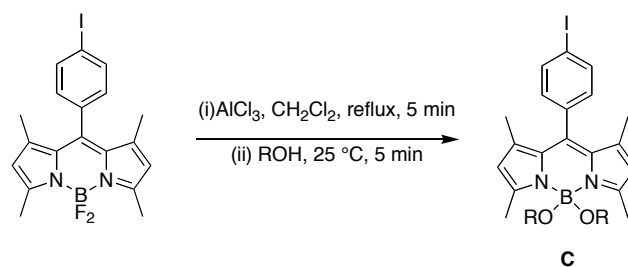
The first two *B*-methoxy BODIPYs prepared were **179** – **180**. These were made by reacting the corresponding BF<sub>2</sub> compound with sodium methoxide in methanol (reaction 16). The shape of the absorption and emission spectra were the same for the starting material **12** and the two products, suggesting the change in *B*-substituents had little effect on the electronic states of the borondiacene core. Interestingly, the monomethoxy and dimethoxy products were more water-soluble than the corresponding BF<sub>2</sub> compounds.<sup>83</sup>



reaction 16

The only other report of *B*-OR BODIPYs systems **C** describes their syntheses via treatment of the corresponding BODIPY with various alcohols in the presence of aluminum trichloride (reaction 17).<sup>95</sup> This study was more expansive than the first insofar as a more diverse

set of alcohols were studied. Thus the alcohols used included simple alkoxy **181** - **183**, aryloxy **184** - **187**, and several diol-derived systems **188** - **191**. Across this series there were only minor changes in the absorbance and emission spectra. The *dialkoxy*-BODIPYs **181** - **183** appear to have higher fluorescence quantum yields than the *diaryloxy*-ones **184** - **187**, and the systems binaphthol- and catechol-derived systems **188** and **189** have extremely poor quantum yields.



R =

**181**

CHCl<sub>3</sub>, Φ 0.55  
 $\lambda_{\text{max abs}}$  505 nm  
 $\lambda_{\text{max emiss}}$  519 nm

**182**

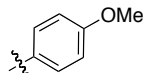
CHCl<sub>3</sub>, Φ 0.76  
 $\lambda_{\text{max abs}}$  504 nm  
 $\lambda_{\text{max emiss}}$  518 nm

**183**

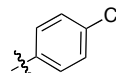
CHCl<sub>3</sub>, Φ 0.65  
 $\lambda_{\text{max abs}}$  506 nm  
 $\lambda_{\text{max emiss}}$  522 nm

**184**

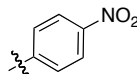
CHCl<sub>3</sub>, Φ 0.06  
 $\lambda_{\text{max abs}}$  506 nm  
 $\lambda_{\text{max emiss}}$  517 nm

**185**

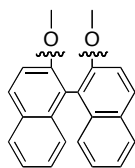
CHCl<sub>3</sub>, Φ 0.004  
 $\lambda_{\text{max abs}}$  507 nm  
 $\lambda_{\text{max emiss}}$  518 nm

**186**

CHCl<sub>3</sub>, Φ 0.065  
 $\lambda_{\text{max abs}}$  506 nm  
 $\lambda_{\text{max emiss}}$  520 nm

**187**

CHCl<sub>3</sub>, Φ 0.54  
 $\lambda_{\text{max abs}}$  504 nm  
 $\lambda_{\text{max emiss}}$  516 nm

(RO)<sub>2</sub> =

**188**  
CHCl<sub>3</sub>, Φ 0.002  
λ<sub>max</sub> abs 506 nm  
λ<sub>max</sub> emiss 516 nm



**189**  
CHCl<sub>3</sub>, Φ 0  
λ<sub>max</sub> abs 510 nm  
λ<sub>max</sub> emiss na



**190**  
CHCl<sub>3</sub>, Φ 0.14  
λ<sub>max</sub> abs 507 nm  
λ<sub>max</sub> emiss 521 nm

OH

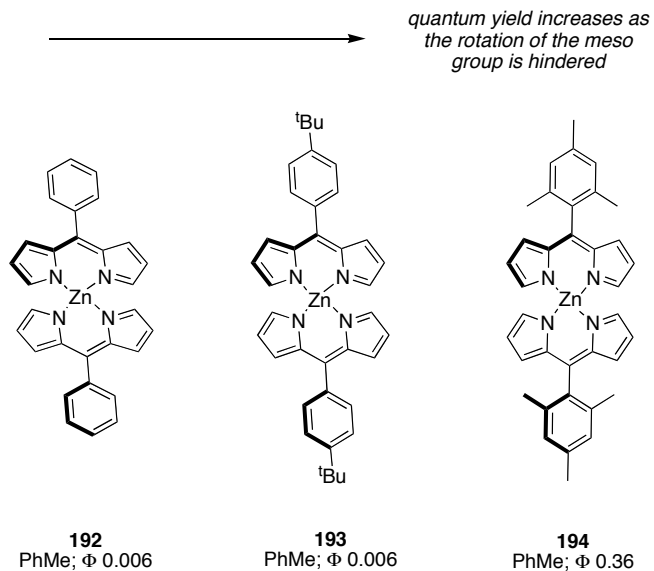
**191**  
CHCl<sub>3</sub>, Φ 0.54  
λ<sub>max</sub> abs 504 nm  
λ<sub>max</sub> emiss 522 nm

reaction 17

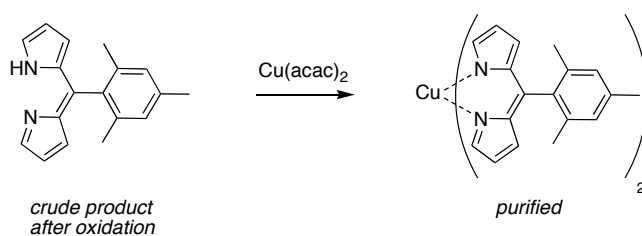
## H. Use of Metals Other Than Boron

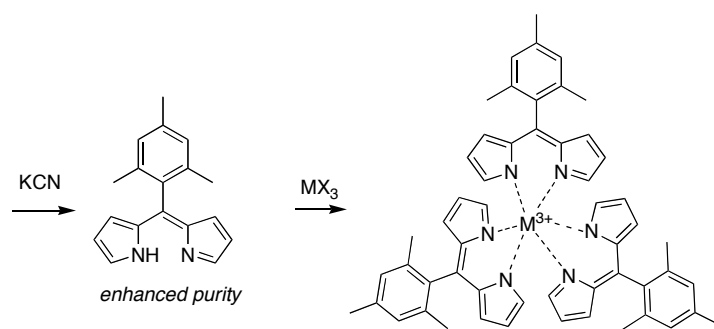
The BODIPY core features a boraindacene unit, so compounds where the boron has been substituted with other metals are, strictly speaking, beyond the scope of this review. However, there are a few dipyrromethene anion complexes of other metals that have highly fluorescent spectroscopic characteristics. These are covered here because they are clearly relevant as probes.

Free base dipyrins react readily with a variety of metals salts to form the corresponding bis(dipyrinato)-metal(II) or tris(dipyrinato)-metal(III) complexes, but their fluorescence properties have rarely been studied and they have generally been regarded as non-fluorescent.<sup>191-214</sup> The first report (2003) of fluorescent properties was for zinc complexes of the boraindacene fragment.<sup>215,216</sup> The complexes were prepared either from (i) treatment of a purified dipyrin with zinc acetate; or, (ii) a two-step one-flask approach involving oxidation of a dipyrromethane and complexation of the resulting crude dipyrin with a Zn(OAc)<sub>2</sub> in presence of triethylamine. Complexes **192** and **193** are weakly fluorescent but **194** is a stronger emitter (it has a multnanosecond excited-state lifetime); thus free rotation of the *meso*-phenyl is again implicated as a major pathway for non-radiative relaxation to the ground state for **192** and **193**.

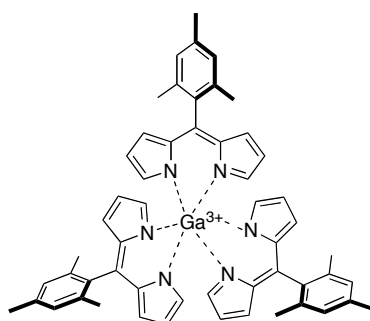
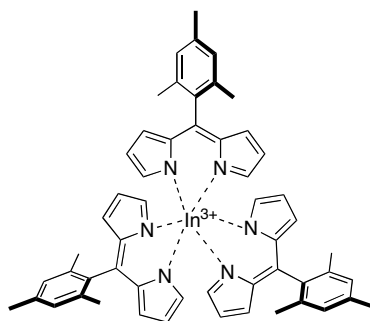


Porphyrin or phthalocyanine complexes of group 13 metals can be fluorescent; this inspired syntheses of two new dipyrromethenes **195** and **196** from gallium(III) and indium(III), respectively (reaction 18). In hexanes the new compounds fluoresce green light, with quantum yields of 0.024 and 0.074 for the gallium(III) and indium(III) complexes, respectively.<sup>217</sup>

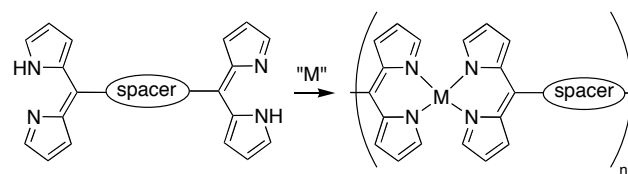




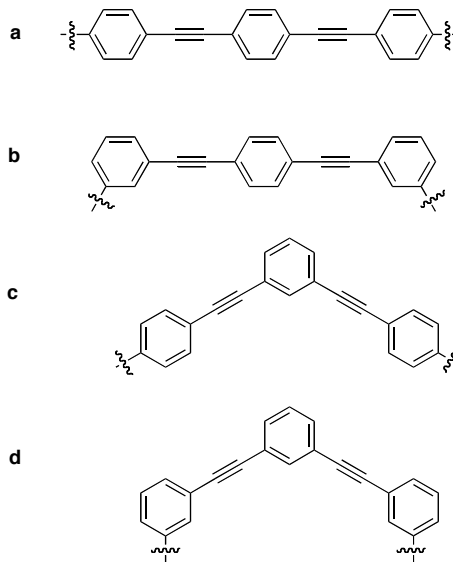
reaction 18

**195**hexanes,  $\Phi$  0.024 $\lambda_{\text{max abs}}$  448 nm $\lambda_{\text{max emiss}}$  528 nm**196**hexanes,  $\Phi$  0.074 $\lambda_{\text{max abs}}$  444 nm $\lambda_{\text{max emiss}}$  522 nm

“Nanoarchitectures” **197a-d** have been fabricated from Zn, Co, Ni, and Cu with dipyrromethene-based ligands, but are only strongly fluorescent with zinc.<sup>218</sup> The fluorescence emission maxima of the zinc complexes in THF and in the solid state are around 510 - 515 nm and 532 – 543 nm, respectively. In acetonitrile, no emission was observed possibly because of aggregation of the particles. Fluorescence emission could be observed at submicron scale for particles derived from Zn-bridged dipyrromethene oligomers; this is significant because quantum dots formed from clusters of inorganic compounds are considerably larger.



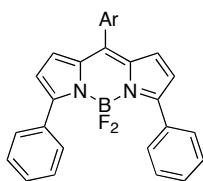
spacer =



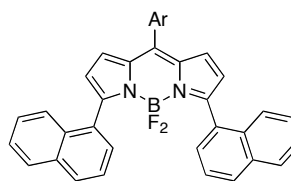
## I. BODIPY-analogs With Extended Aromatic Conjugation

### 1. Restricted Systems

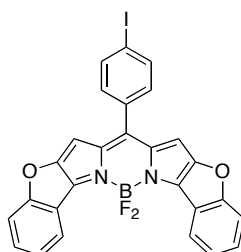
As mentioned previously, aryl-substituents on the BODIPY chromophore, *eg* in **85** and **86**, red-shift the absorption and emission spectra, but decrease the fluorescence intensity, presumably because of the free rotation of the aryl groups.<sup>131,132</sup> Consequently, more rigid systems like **198** and **199** were prepared and studied.<sup>219</sup> These absorb and fluoresce more intensely at longer wavelengths, and their quantum yields are generally higher, with the exception of **198b**.



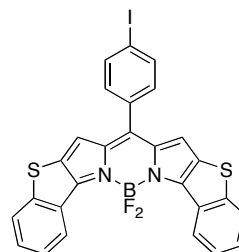
**85**  
CHCl<sub>3</sub>,  $\Phi$  0.20  
 $\lambda_{\text{max abs}}$  555 nm  
 $\lambda_{\text{max emiss}}$  588 nm



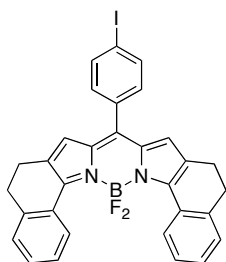
**86**  
CHCl<sub>3</sub>,  $\Phi$  0.38  
 $\lambda_{\text{max abs}}$  542 nm  
 $\lambda_{\text{max emiss}}$  607 nm



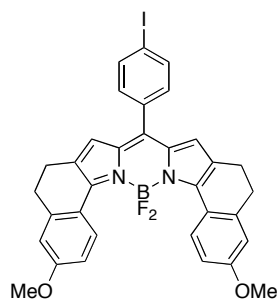
**198a**  
MeOH,  $\Phi$  0.34  
 $\lambda_{\text{max abs}}$  637 nm  
 $\lambda_{\text{max emiss}}$  647 nm



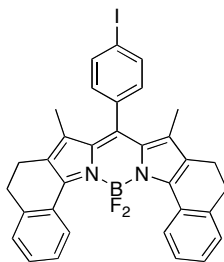
**198b**  
MeOH,  $\Phi$  0.05  
 $\lambda_{\text{max abs}}$  658 nm  
 $\lambda_{\text{max emiss}}$  673 nm



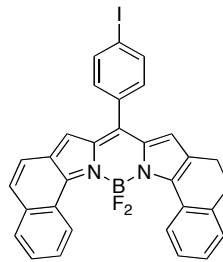
**199a**  
MeOH,  $\Phi$  0.38  
 $\lambda_{\text{max abs}}$  634 nm  
 $\lambda_{\text{max emiss}}$  647 nm



**199b**  
MeOH,  $\Phi$  0.13  
 $\lambda_{\text{max abs}}$  658 nm  
 $\lambda_{\text{max emiss}}$  673 nm



**199c**  
MeOH,  $\Phi$  0.72  
 $\lambda_{\text{max abs}}$  619 nm  
 $\lambda_{\text{max emiss}}$  629 nm



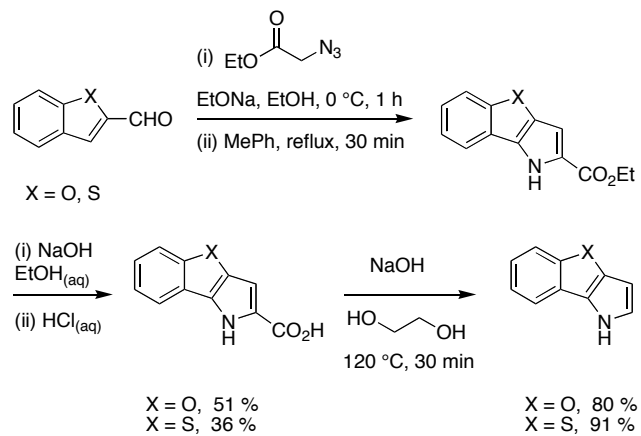
**200**  
MeOH,  $\Phi$  0.17  
 $\lambda_{\text{max abs}}$  634 nm  
 $\lambda_{\text{max emiss}}$  668 nm

The new derivatives **198** and **199** were obtained by condensation of 4-iodobenzoyl chloride with the corresponding pyrrole-based starting materials, which were prepared in several steps as described in Scheme 1.11. Most of the effort here is in the preparation of the pyrrole based starting materials. Part **a** of Scheme 1.11 shows a route that featured intramolecular C-H activation by a nitrene, **b** involves a Trofimov reaction,<sup>136</sup> and **c** shows a classical condensation route.<sup>220</sup>

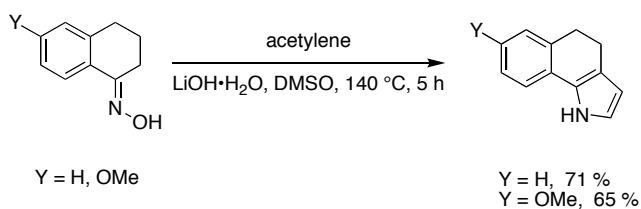


Scheme 1.11. Syntheses of the pyrrole-based starting materials.

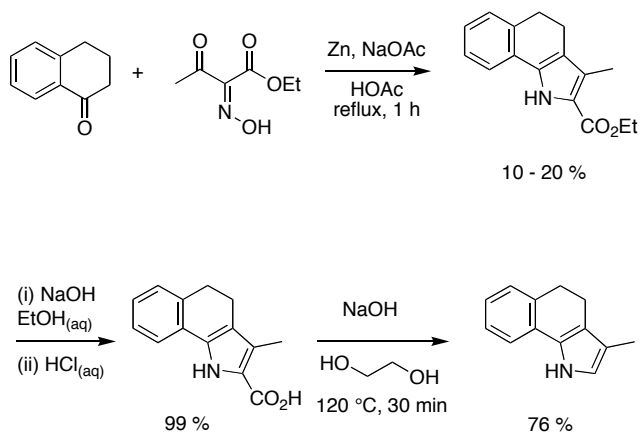
a



b

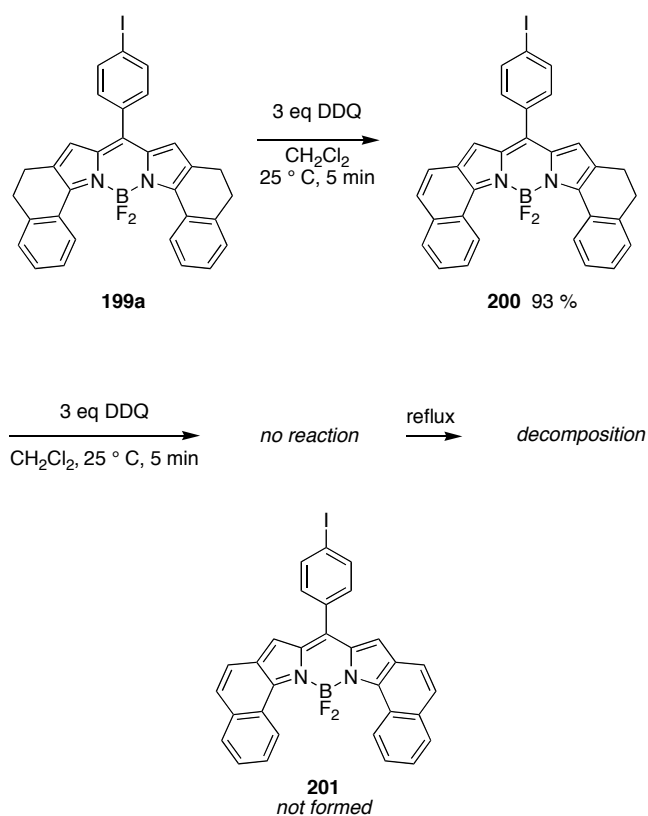


c



Oxidation of **199a** was attempted, but only the half-oxidized product **200** could be obtained; further treatment with excess DDQ at room temperature for overnight gave no reaction (Scheme 1.12). Semi-empirical calculations showed that the activation energy required to form **201** was excessive compared with the half oxidized form **200** due to steric reasons. The physical properties of the mono-oxidized product were somewhat surprising. First, the maximum absorbance was not shifted to the red relative to **199a**, only the fluorescence emission was shifted to the red by 21 nm. Second, although the conjugation of the system was extended, the extinction coefficient was three times smaller than the reduced form of the dye **199a** (41000 vs. 126250 respectively); the quantum yield was also less than half that of **199a**.

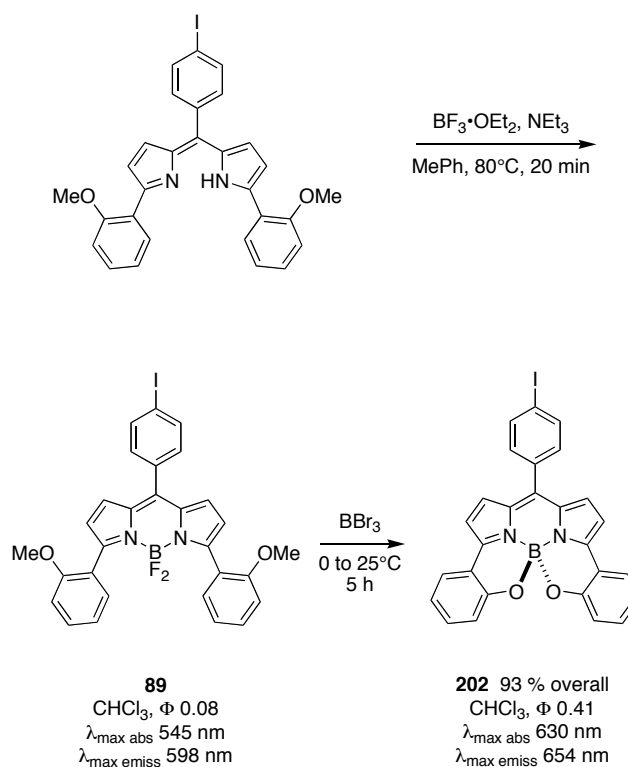
**Scheme 1.12.** Synthesis of more conjugated BODIPY derivatives.



2'-Methoxy groups on  $\alpha$ -aryl groups provide a special opportunity for syntheses of constrained BODIPY dyes. Thus **202**, wherein rotation around a C-Ar bond was prevented by B-

O bond formation, was conveniently obtained by demethylation and intramolecular cyclization of **89** (Scheme 1.13).<sup>221</sup> Dye **202** has a red-shifted, sharper fluorescence emission than the BF<sub>2</sub> parent dye and its quantum yield is 5.5-6.0 times larger.

**Scheme 1.13.** Synthesis of a new NIR BODIPY dye.



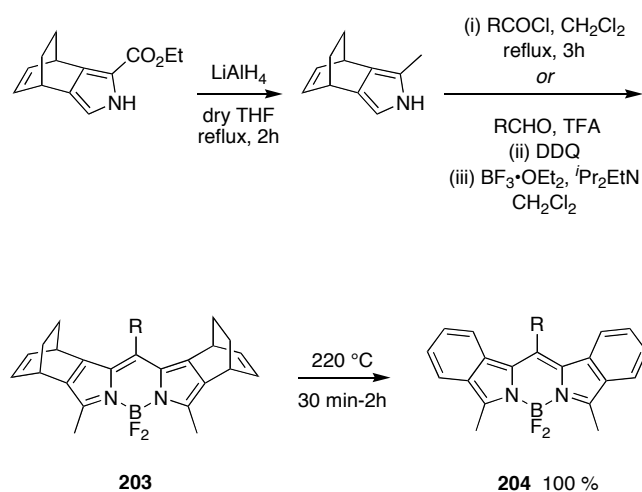
## 2. Extended Aromatic Systems

### *Di(iso)indomethene Dyes*

Aromatic ring-fused BODIPY derivatives, boron-di(iso)indomethene dyes **204** have been prepared via retro Diels-Alder reactions<sup>222,223</sup> featuring a norbornane-derived pyrrole (Scheme 1.14).<sup>224</sup> The spectroscopic data for the di(iso)indomethene derivatives **204** are shown below. The nature of the substituents at the *meso* position has no influence on the absorption and

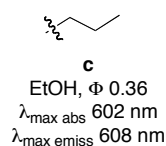
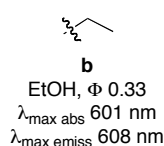
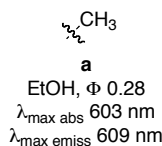
emission properties of the new dyes. The new di(iso)indomethene dyes display a red-shifted absorption compared to the bicyclic-BODIPY precursors **203**. The more expanded, conjugated, and rigid di(iso)indomethene BODIPY dyes **204** are also characterized by a significantly higher extinction coefficient relative to the bicyclic-BODIPY dyes **203**. Due to their rigid-fused system, which prevents a non-radiative deactivation of the excited state, bicyclic-BODIPY **203** and di(iso)indomethene BODIPY dyes **204** have small Stokes' shifts. The Stokes' shifts are, however, generally larger for bicyclic-BODIPY dyes **203** than for the di(iso)indomethene derivatives **204**. The absorption and emission spectra of bicyclic-BODIPY **203** and di(iso)indomethene BODIPY dyes **204** are independent of the solvent polarity. The fluorescence quantum yield of the bicyclic-BODIPY dyes **203** is much higher than the one for the corresponding di(iso)indomethene BODIPY dyes **204**.

**Scheme 1.14.** Extended aromatic dyes from retro-Diels Alder reactions.

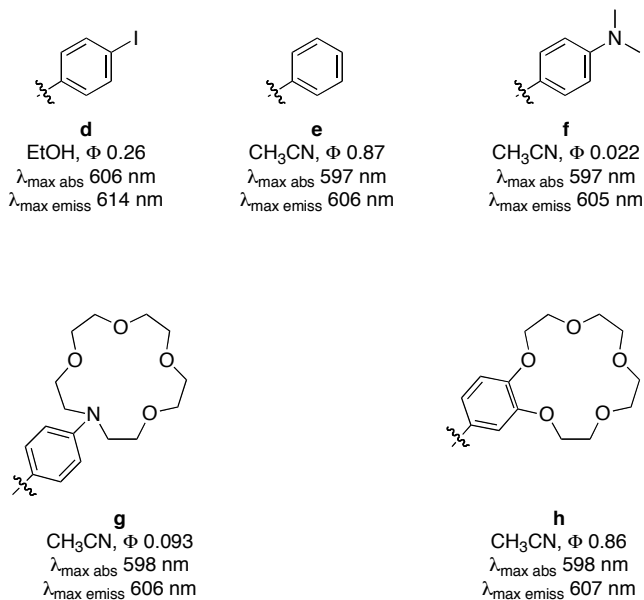


for **204** .....

R =

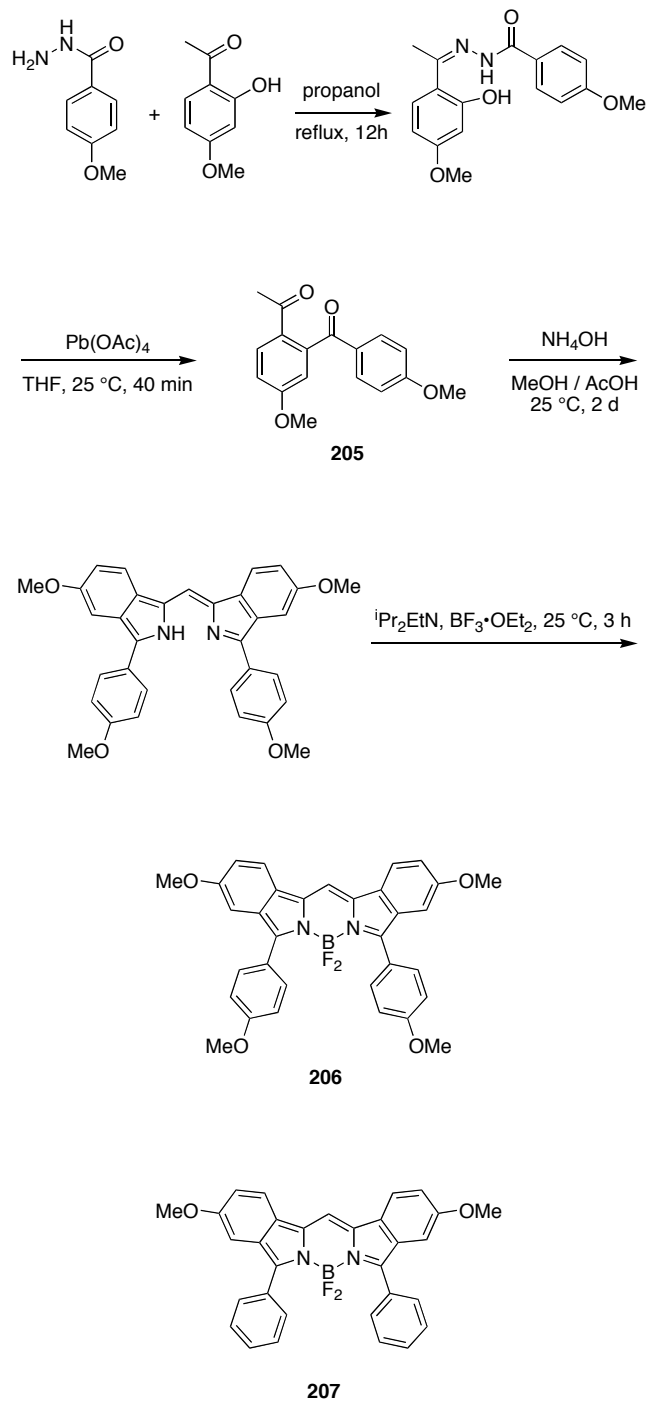


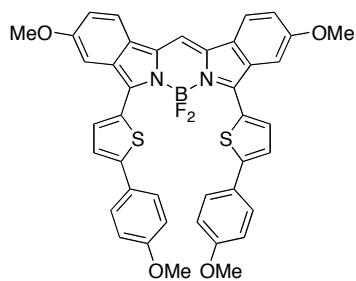
## Scheme 1.14. Continued.



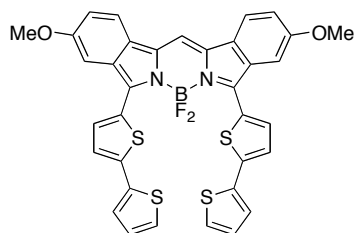
Other indomethene dyes including **172**<sup>190</sup> and **206 - 209**<sup>190,225</sup> have been prepared via a different route. Substituted 2-acylacetophenones **205**, obtained from 2-hydroxyacetophenones and hydrazines,<sup>226</sup> were condensed with ammonia to give the dibenzopyrromethene. These were treated with boron trifluoride to give the 3,4:3',4'-dibenzopyrrometheneboron difluoride core (Scheme 1.15). The new dyes exhibit very long wavelength absorption and emission bands, and are relatively stable to photobleaching.

**Scheme 1.15.** Synthesis of di(iso)indomethene dyes from 2-acylacetophenone derivatives.





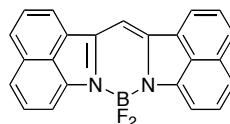
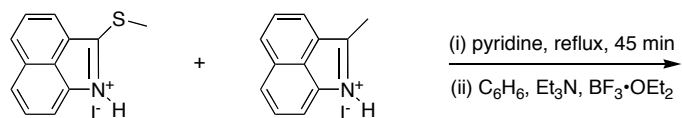
**208**  
 $\text{CH}_2\text{Cl}_2$   
 $\lambda_{\text{max abs}}$  765 nm  
 $\lambda_{\text{max emiss}}$  827 nm



**209**  
 $\text{CH}_2\text{Cl}_2$   
 $\lambda_{\text{max abs}}$  766 nm  
 $\lambda_{\text{max emiss}}$  831 nm

### ***Dyes Based On Benz[c,d]indole***

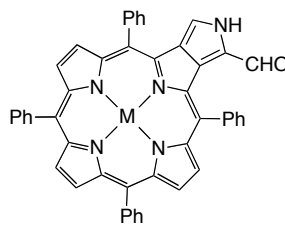
Benz[c,d]indole and its derivatives have been used to form deeply colored dyes. Compound **210**, for instance, was obtained by condensation of 2-methylthiobenz[c,d]indolium iodide and 2-methylbenz[c,d]indolium iodide, followed by complexation with boron trifluoride etherate. Its fixed planar structure exhibits a sharp absorption band at 618 nm, and fluoresces at 625 nm.<sup>227,228</sup>

**210**DMSO;  $\Phi$  0.52 $\lambda_{\text{max abs}}$  618 nm $\epsilon$  94 000 M<sup>-1</sup>cm<sup>-1</sup> $\lambda_{\text{max emiss}}$  625 nm

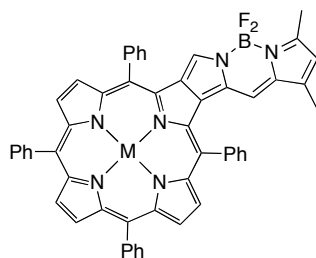
reaction 19

### ***Porphyrin-fused Systems***

Systems **212** – **214** have edge-shared porphyrin and BODIPY parts. They were synthesized from the formylated pyrroloporphyrin **211** via acid-catalyzed condensation with 2,4-dimethylpyrrole. Their UV spectra contain four quite intense bands in the 300 – 750 nm region, and do not resemble the sum of the spectra of tetraphenylporphyrin (TPP) and of BODIPY. Systems **212** and **214** emit respectively at 693 and 714 nm upon excitation over all the 240 – 700 nm region with low quantum yields, and **213** did not show any significant fluorescence.<sup>12</sup>

**211**





M = none  
**212**  
 CH<sub>2</sub>Cl<sub>2</sub>, Φ 0.04  
 $\lambda_{\text{max abs}}$  388, 413, 531, 640 nm  
 $\lambda_{\text{max emiss}}$  693 nm

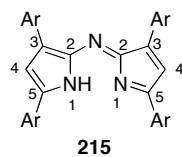
M = Cu  
**213**  
 CH<sub>2</sub>Cl<sub>2</sub>, Φ 0  
 $\lambda_{\text{max abs}}$  390, 412, 531, 675 nm  
 $\lambda_{\text{max emiss}}$  693 nm

M = Zn  
**214**  
 CH<sub>2</sub>Cl<sub>2</sub>, Φ 0.053  
 $\lambda_{\text{max abs}}$  392, 415, 539, 676 nm  
 $\lambda_{\text{max emiss}}$  714 nm

## J. Aza-BODIPY Dyes

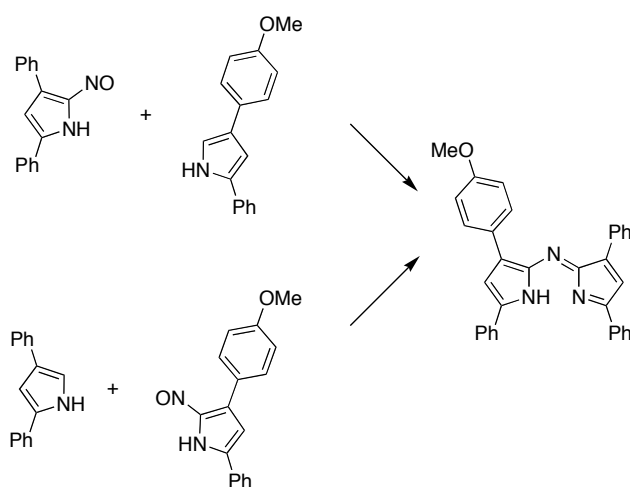
### 1. Tetraaryl Systems

Synthesis of the azadipyrromethene chromophore **215** (without boron, but with aryl substituents) was first described in the 1940s.<sup>229-231</sup> This, as described below, is the framework for a very interesting set of dyes called the aza-BODIPYs. Two general methods to prepare these compounds were developed. In one, 2,4-diarylpyrroles were converted into their 5-nitroso derivatives, then condensed with a second molecule of pyrrole (Scheme 1.16a). Scheme 1.16b shows the second method, in which Michael addition products **D** from chalcones and nitromethane,<sup>229</sup> or cyanide **E**,<sup>230,231</sup> were reacted with formamide (or other ammonia-sources) to give the core **215**. In the first instance, these reactions were performed neat, *ie* without solvent. Soon after, it was realized that use of alcohol solvents usually causes the azadipyrromethenes to precipitate from the reaction mixture, thus enhancing the ease of isolation and yields. The postulated mechanism for formation of the azadipyrromethene core from the nitromethane adducts is shown in Scheme 1.16c. It proceeds via pyrrole **217**, which is nitrosylated *in situ* to give **218** that then condenses with another molecule of the pyrrole.



**Scheme 1.16.** Formation of azapyrromethene from **a.** nitroso pyrrole; and **b.** nitrobutyrophenones **D** and keto-nitrile **E**; **c.** postulated mechanism for the formation of azapyrromethene from nitrobutyrophenones **D** and, **d.** from keto-nitrile **E**.

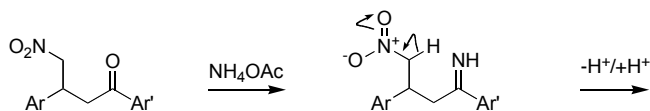
**a**



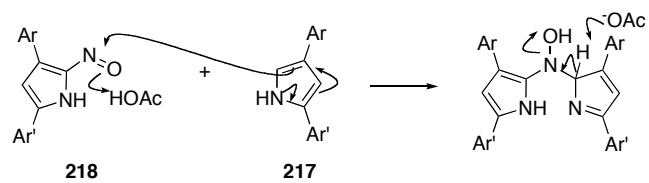
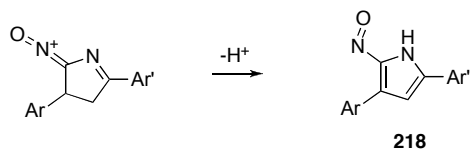
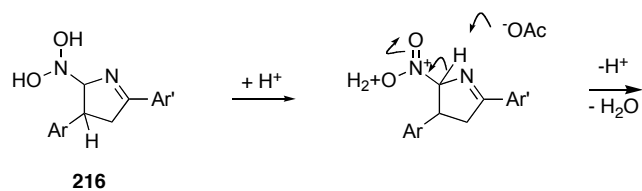
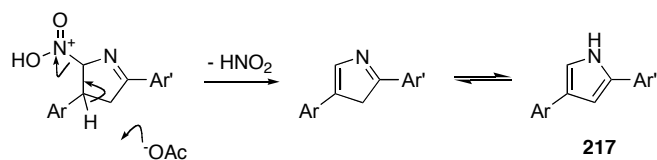
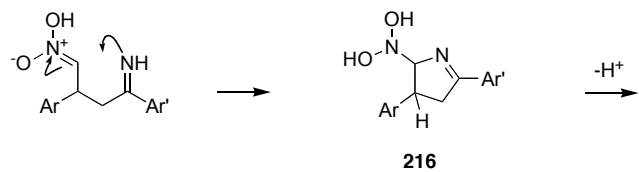
**b**



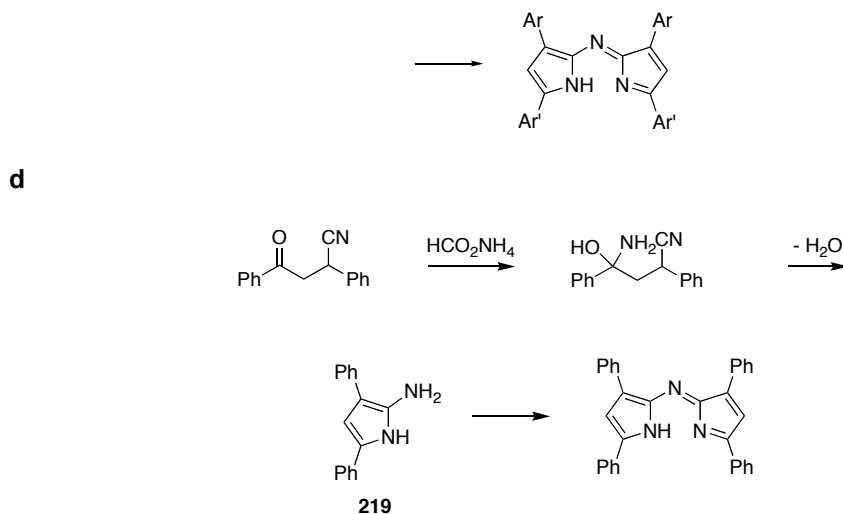
**c**



## Scheme 1.16. Continued.

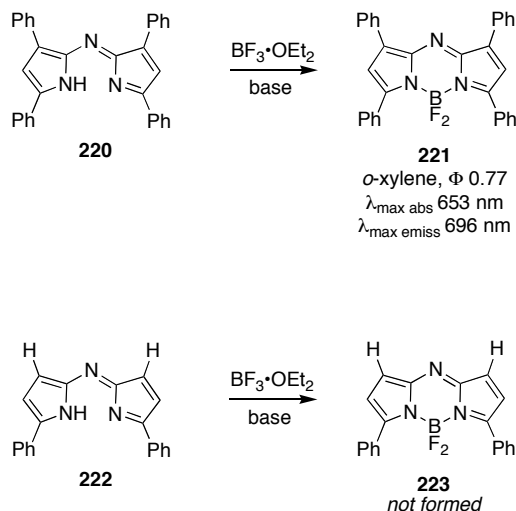


Scheme 1.16. Continued.



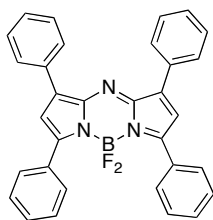
It is also possible to prepare the azadipyrrromethene chromophore from cyanide Michael addition products **E** as described in Scheme 1.16d. Ammonium formate serves as a source of ammonia in the pyrrole-forming condensation step. The 2-amino pyrrole intermediates **219** readily convert to the azadipyrrromethene core on heating in the air. Switching from acetate to formate in the dry melt process for the synthesis of **215** nearly doubled the yield to give approximately 50%.<sup>231</sup> Formation of this chromophore seems to be most facile when there are four phenyl substituents, but it is possible to obtain the diphenyl products **222** (below) by slight modification of the reaction conditions.<sup>231</sup>

The first reactions of azadipyrrromethenes with boron electrophiles were reported in the early 90's (Scheme 1.17).<sup>130,232</sup> The aza-BODIPY **221** was made from the 3,5-tetraphenyl azadipyrrromethene **220** in that way. It was reported that the less substituted aza-BODIPY **223** could not be obtained after treatment of the corresponding aza-dipyrrromethene **222** with boron trifluoride,<sup>232</sup> however, this might have been an artifact of the particular conditions screened.

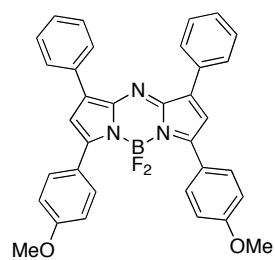
**Scheme 1.17.** First syntheses of aza-BODIPY dyes.

Beginning with research largely from O'Shea's group from 2002 onwards, there has been a resurgence of interest in aza-BODIPY dyes, and this has resulted in syntheses of dyes like **224** - **227**.<sup>233-235</sup> In this latest era of the field, the azadipyrromethene skeletons are still prepared from nitromethane adducts to the corresponding chalcone according to the route described in Scheme 1.16c but butanol, rather than methanol or solvent-free conditions, was the preferred medium.<sup>234</sup> The syntheses were completed by adding  $\text{BF}_3 \cdot \text{OEt}_2$  at room temperature; the intermediate azadipyrromethanes precipitated out in high purities and were not purified beyond washing with ethanol.<sup>233,234</sup>

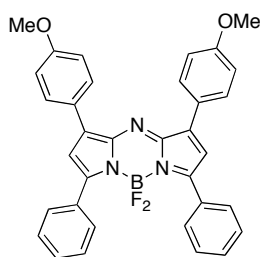
UV absorption maxima of the tetraarylazadipyrromethene- $\text{BF}_2$  chelates strongly depend on the Ar-substituents. *para*-Electron donating groups on the 5-Ar substituents gives increased extinction coefficients and significant red-shifts in the  $\lambda_{\text{max abs}}$  (149 nm for dimethylamino vs H, *cf* **227** vs **221**).<sup>235</sup> *para*-Substitution with an electron donating group on the 3-aryl ring has less impact, but still gives a bathochromic shift (*cf* **224** vs **225**).<sup>234</sup>



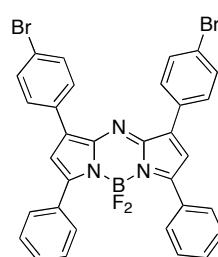
**221**  
 CHCl<sub>3</sub>,  $\Phi$  0.34  
 $\lambda_{\text{max abs}}$  650 nm  
 $\lambda_{\text{max emiss}}$  672 nm



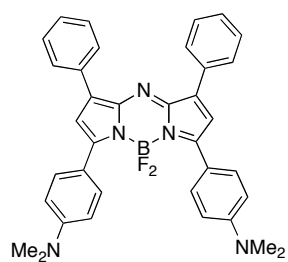
**224**  
 CHCl<sub>3</sub>,  $\Phi$  0.36  
 $\lambda_{\text{max abs}}$  688 nm  
 $\lambda_{\text{max emiss}}$  715 nm



**225**  
 CHCl<sub>3</sub>,  $\Phi$  0.23  
 $\lambda_{\text{max abs}}$  664 nm  
 $\lambda_{\text{max emiss}}$  695 nm



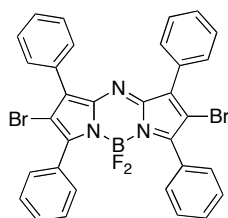
**226**  
 CHCl<sub>3</sub>,  $\Phi$  0.34  
 $\lambda_{\text{max abs}}$  658 nm  
 $\lambda_{\text{max emiss}}$  680 nm



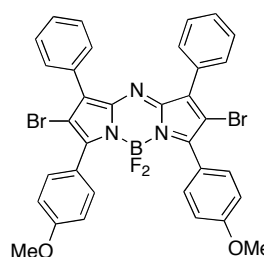
**227**  
 CHCl<sub>3</sub>,  $\Phi$  na  
 $\lambda_{\text{max abs}}$  799 nm  
 $\lambda_{\text{max emiss}}$  823 nm

The UV absorption maxima of the aza-BODIPY dyes are relatively insensitive to solvent polarity; only small blue-shifts tend to be observed (6 – 9 nm) when switching solvents from toluene to ethanol. Their absorptions are sharp, with a full width at half-maximum height (fwhm) varying from 51 to 67 nm in aqueous solution with an emulsifier called Cremophor EL, and 47 to 57 nm in chloroform indicating that the dyes do not aggregate under those conditions. The extinction coefficients range from 75,000 to 85,000 M<sup>-1</sup> cm<sup>-1</sup>, which is much greater than substituted porphyrins (3000 – 5000 M<sup>-1</sup> cm<sup>-1</sup>) for instance. This strong absorbance is one of the factors that facilitate efficient singlet-oxygen generation, hence these molecules are potentially useful photosensitizers for photodynamic therapy.<sup>236-239</sup>

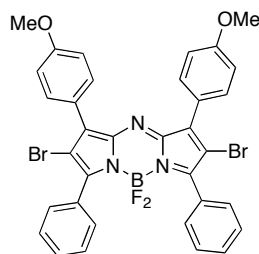
Fluorescence emission spectra of the aza-BODIPY dyes reported to date are also relatively insensitive to the solvent polarity. Compounds **221** and **224** to **226** have high fluorescence quantum yields. In the case of **226**, there is a bromine atom attached to the phenyl substituent, but no significant decrease in the quantum yield was observed.<sup>234</sup> On the other hand, introduction of bromine directly into the core of the dye eg compounds **228** to **230** results in a significant decrease of the fluorescence quantum yields, indicating a larger heavy-atom effect and an increased singlet oxygen production.<sup>234</sup> A quantum yield was not reported for **227**, but the compound became much more fluorescent under acidic conditions due to variation in the internal charge transfer.<sup>235</sup> Upon addition of acid, the absorption band at 799 nm disappears and a new band at 738 nm appears indicating the mono-protonated form. The later disappears with addition of more acid, and a new band characteristic of the bis-protonated species appears at 643 nm.



**228**  
CHCl<sub>3</sub>, Φ 0.01  
λ<sub>max</sub> abs 650 nm  
λ<sub>max</sub> emiss 673 nm

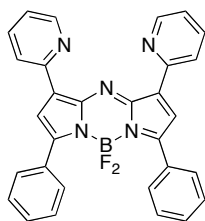


**229**  
CHCl<sub>3</sub>, Φ 0.10  
λ<sub>max</sub> abs 679 nm  
λ<sub>max</sub> emiss 714 nm

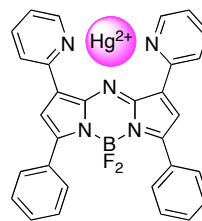
**230**

CHCl<sub>3</sub>,  $\Phi < 0.01$   
 $\lambda_{\text{max abs}}$  653 nm  
 $\lambda_{\text{max emiss}}$  679 nm

Aza-BODIPY dyes mostly have been discussed in the context of agents for photodynamic therapy, but chemosensors have also been made from these compounds. Compound **231** is highly selective for mercuric ions that become chelated between the 2'-pyridyl groups.<sup>240</sup> Mercuric ion complexation red-shifts both the UV-absorption and fluorescence emission maxima. The dissociation constant was determined to be  $5.4 \times 10^{-6}$  M, with a 1:1 binding stoichiometry.

**231**

CH<sub>3</sub>CN;  $\Phi$  0.19  
 $\lambda_{\text{max abs}}$  655 nm  
 $\lambda_{\text{max emiss}}$  682 nm

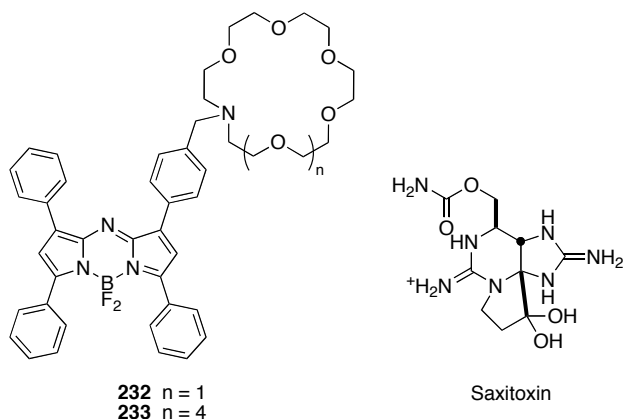


CH<sub>3</sub>CN;  $\Phi$  0.17  
 $\lambda_{\text{max abs}}$  696 nm  
 $\lambda_{\text{max emiss}}$  719 nm

Compound **232** and **233** are photoinduced electron transfer crown ether chemosensors featuring aza-BODIPY chromophore;<sup>241</sup> they are used as visible sensors for the paralytic shellfish toxin Saxitoxin. Saxitoxin contains guanidine groups, and it is these functional groups that interact with the crown ether part of these molecules. In the absence of Saxitoxin, PET from the crown ether to the fluorophore quenches the fluorescence. Upon complexation of the toxin, PET can no longer happen and fluorescence is turned on. At 1:1 toxin/crown stoichiometry, the fluorescence enhancement was over 100% for compound **232**. The average binding constant for **232** to Saxitoxin,  $6.2 \times 10^5 \text{ M}^{-1}$ , was among the highest observed for any chemosensor of that



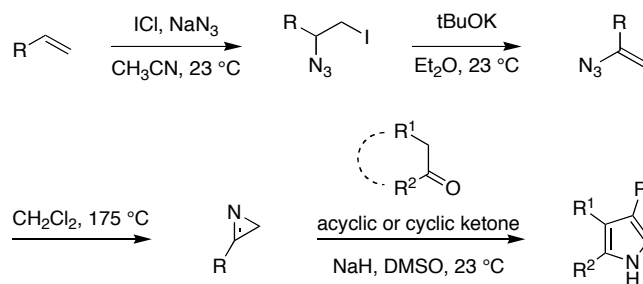
toxin. Compound **233**, which has a larger crown ether bound the toxin less strongly ( $1.4 \times 10^4 \text{ M}^{-1}$ ) and gave insignificant fluorescence enhancement. The putative PET mechanism in these systems involves  $\pi$ -stacking of one of the Saxitoxin's guanidiniums to the fluorophore.



## 2. Extended Aza-BODIPY Systems

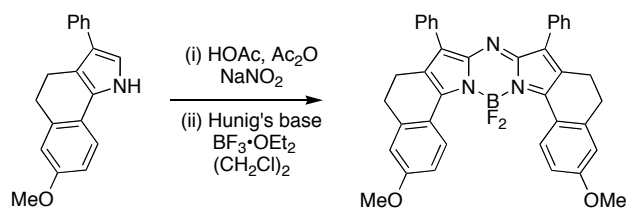
Strongly electron-donating groups, rigidifying structural modifications, and embellishments to extend the conjugation of the BODIPY dyes tend to red-shift their fluorescence emissions. Predictably then, similar modifications can be used to push the emission spectra of aza-BODIPY systems into the near-IR.

The “extended” aza-BODIPY systems **234** – **246** were synthesized from 2,4-diarylpyrroles. These starting materials were obtained in good overall yield over four steps from an alkene via (i) addition of iodo azide, (ii) dehydro-halogenation, (iii) pyrrolysis (azirine formation) and (iv) carbanion induced pyrrole formation as shown in Scheme 1.18.<sup>242,243</sup>

**Scheme 1.18.** Synthesis of cyclized/restricted 2,4-diarylpyrroles.

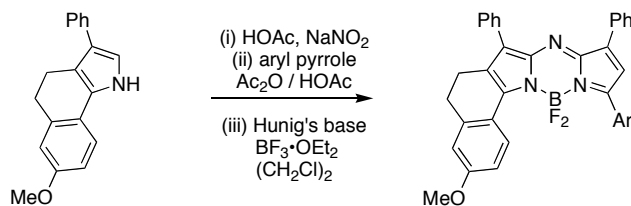
R = Ph; 4-MeOC<sub>6</sub>H<sub>4</sub>; phenylethyl

The conformationally restricted aza-BODIPY dyes were then prepared as shown in Scheme 1.19 via condensation of the pyrrole generated in Scheme 1.18 with a nitrosopyrrole generated *in situ*, followed by complexation with boron trifluoride. Attempts to condense 2,4-dimethylpyrrole with a nitrosated restricted 2,4-diarylpyrrole failed to give any product, suggesting that the 2-aryl substituent in the pyrrole is essential for the formation of these restricted aza-BODIPY dyes.

**Scheme 1.19.** Synthesis of **a**, symmetrical and **b**, asymmetrical conformationally restricted azaBODIPY dyes.**a**

## Scheme 1.19. Continued.

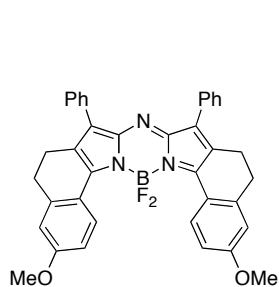
b



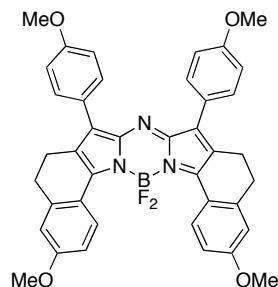
All the conformationally restricted systems **234** – **246** absorb over 650 nm. Dyes **234** – **236** with both sides incorporated in carbocyclic rings have narrow, intense (high  $\epsilon$ ) absorption bands at long wavelengths. In comparison to the “non-constrained” tetraaryl-azaBODIPY **224**, there is a bathochromic shift of up to 52 nm and a concomitant halving of the fwhm (27.1 nm for **236** vs 52.0 nm for **224**). The novel dyes were reported to possess excellent chemical and photostability. Furthermore, the fluorescence is insensitive to solvent polarity.<sup>242,243</sup>

There are also several details regarding the spectral properties of the dyes in this series. Substitution at the 3-position of the core does not affect the  $\epsilon$ -value of the dyes (compare **234** – **236**). Introduction of electron-donating groups results in a small blue-shift and a slightly higher fluorescence quantum yield (**234** vs **235**). Shorter  $\lambda_{\text{abs}}$ , lower  $\epsilon$ , broader absorption band, and lower fluorescence quantum yield were associated with the sulfur-containing dye **237**. The dehydrogenated carbocyclic restricted ring in system **239** decreases its quantum yield relative to **234**. Aza-BODIPYs with only one side restricted have much lower extinction coefficients (**240** – **246** vs **234**). The quantum yields of non-symmetric aza-BODIPY dyes are highly dependent on the substituents on the aromatic ring. Electron donating *para*-substituents give higher quantum yields (**240** and **241**), with shorter  $\lambda_{\text{abs}}$  indicating that the phenyl rings are twisted. *ortho*-Electron donating groups (eg in **242**) result in short  $\lambda_{\text{abs}}$ , low  $\epsilon$ , and broad absorption bands, indicating that the phenyl rings in **242** are twisted. Unexpectedly shorter  $\lambda_{\text{abs}}$ , low  $\epsilon$ , broader absorption bands and lower quantum yields were observed when two methoxy groups were present (**243** and **244**). The sharp and intense absorption, high quantum yield obtained in the special case of

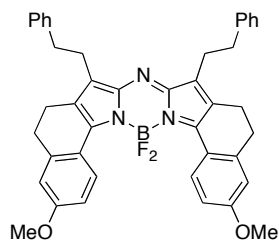
**245** wherein a 2-methoxy-1-naphthyl substituent is present indicates that the naphthyl ring is distorted so that electron transfer is suppressed.



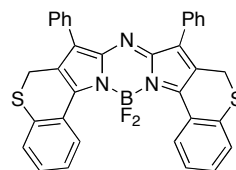
**234**  
 $\text{CHCl}_3$ ,  $\Phi$  0.28  
 $\lambda_{\text{max abs}}$  740 nm  
 $\epsilon$  159000  $\text{M}^{-1}\text{cm}^{-1}$   
 $\lambda_{\text{max emiss}}$  752 nm



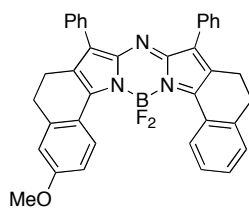
**235**  
 $\text{CHCl}_3$ ,  $\Phi$  0.29  
 $\lambda_{\text{max abs}}$  736 nm  
 $\epsilon$  157000  $\text{M}^{-1}\text{cm}^{-1}$   
 $\lambda_{\text{max emiss}}$  748 nm



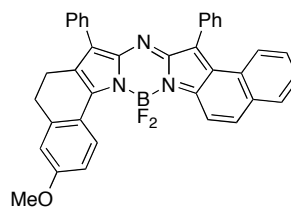
**236**  
 $\text{CHCl}_3$ ,  $\Phi$  0.31  
 $\lambda_{\text{max abs}}$  721 nm  
 $\epsilon$  162000  $\text{M}^{-1}\text{cm}^{-1}$   
 $\lambda_{\text{max emiss}}$  732 nm



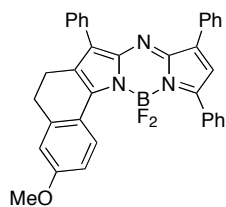
**237**  
 $\text{CHCl}_3$ ,  $\Phi$  0.11  
 $\lambda_{\text{max abs}}$  706 nm  
 $\epsilon$  115000  $\text{M}^{-1}\text{cm}^{-1}$   
 $\lambda_{\text{max emiss}}$  730 nm



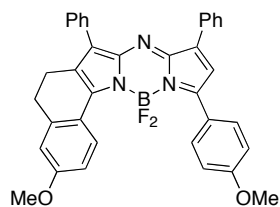
**238**  
 $\text{CHCl}_3$ ,  $\Phi$  0.32  
 $\lambda_{\text{max abs}}$  723 nm  
 $\epsilon$  157000  $\text{M}^{-1}\text{cm}^{-1}$   
 $\lambda_{\text{max emiss}}$  734 nm



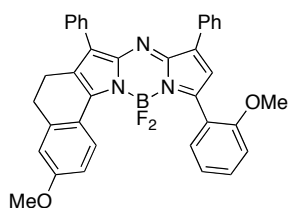
**239**  
 $\text{CHCl}_3$ ,  $\Phi$  0.11  
 $\lambda_{\text{max abs}}$  715 nm  
 $\epsilon$  141000  $\text{M}^{-1}\text{cm}^{-1}$   
 $\lambda_{\text{max emiss}}$  730 nm



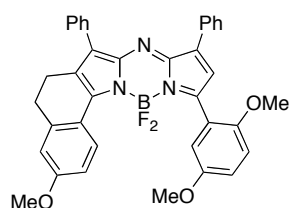
**240**  
 $\text{CHCl}_3$ ,  $\Phi$  0.44  
 $\lambda_{\text{max abs}}$  688 nm  
 $\epsilon$  108000  $\text{M}^{-1}\text{cm}^{-1}$   
 $\lambda_{\text{max emiss}}$  710 nm



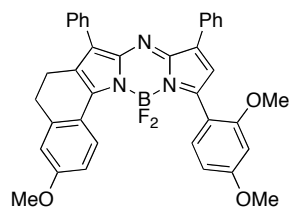
**241**  
 $\text{CHCl}_3$ ,  $\Phi$  0.38  
 $\lambda_{\text{max abs}}$  708 nm  
 $\epsilon$  96200  $\text{M}^{-1}\text{cm}^{-1}$   
 $\lambda_{\text{max emiss}}$  732 nm



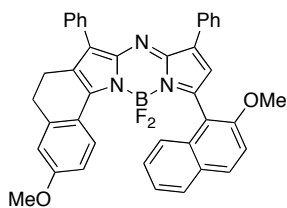
**242**  
 $\text{CHCl}_3$ ,  $\Phi$  0.38  
 $\lambda_{\text{max abs}}$  678 nm  
 $\epsilon$  83900  $\text{M}^{-1}\text{cm}^{-1}$   
 $\lambda_{\text{max emiss}}$  713 nm



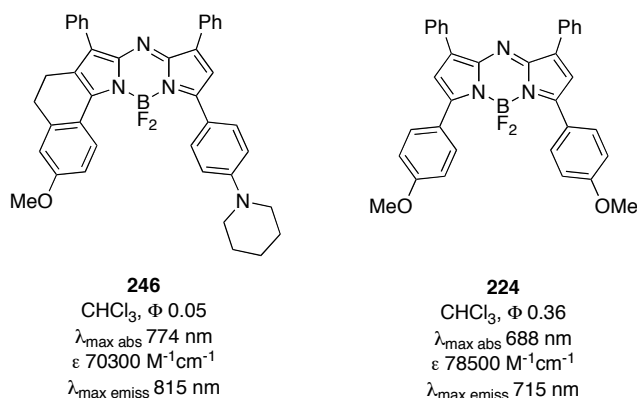
**243**  
 $\text{CHCl}_3$ ,  $\Phi$  0.24  
 $\lambda_{\text{max abs}}$  681 nm  
 $\epsilon$  66500  $\text{M}^{-1}\text{cm}^{-1}$   
 $\lambda_{\text{max emiss}}$  728 nm



**244**  
 $\text{CHCl}_3$ ,  $\Phi$  0.18  
 $\lambda_{\text{max abs}}$  707 nm  
 $\epsilon$  78000  $\text{M}^{-1}\text{cm}^{-1}$   
 $\lambda_{\text{max emiss}}$  735 nm



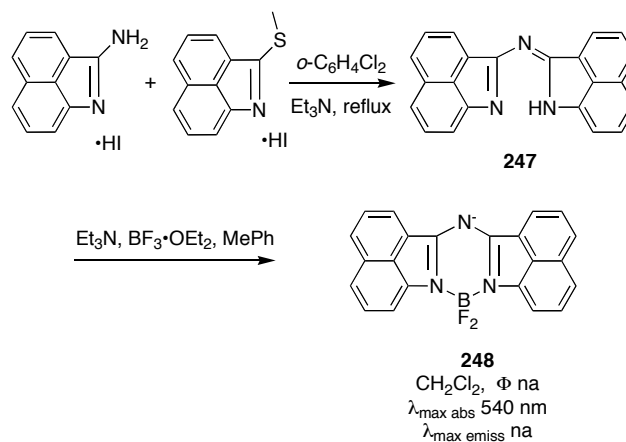
**245**  
 $\text{CHCl}_3$ ,  $\Phi$  0.46  
 $\lambda_{\text{max abs}}$  668 nm  
 $\epsilon$  113000  $\text{M}^{-1}\text{cm}^{-1}$   
 $\lambda_{\text{max emiss}}$  692 nm



### Dyes Based On Benz[c,d]indole

Synthesis of compound **248** involves refluxing 2-benz[c,d]indolamine hydroiodide with 2-(methylthio)benz[c,d]indole-hydroiodide in 1,2-dichlorobenzene in presence of triethylamine gives the amine **247**. Subsequent treatment with boron trifluoride etherate affords the desired product **248** (reaction 18).<sup>244</sup>

While the benz[c,d]indole based BODIPY dye **210** displays a red-shifted absorption and fluorescence, the aza-BODIPY analog **248** shows a blue-shifted absorption at 540 nm. Unfortunately, no fluorescence properties have been reported.

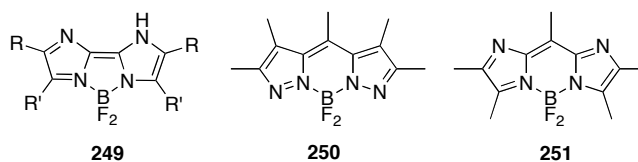


reaction 20

## K. Other Analogs of the BODIPYs

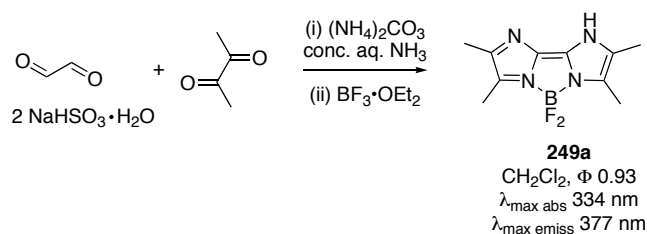
### 1. Biimidazol-2-yl-BF<sub>2</sub> Complexes

Biimidazol-2-yls difluoroborate complexes **249** have been obtained by: (i) reacting glyoxal bisulfite, 2,3-butanedione and concentrated aqueous NH<sub>3</sub> (Scheme 1.20a)<sup>245,246</sup>; (ii) condensation of 1,2-cyclohexanedione with 40% aqueous glyoxal in ethanol saturated with dry ammonia gas;<sup>246</sup> and, (iii) condensation of oxamide with *o*-phenylenediamine in refluxing ethylene glycol (Scheme 1.20c).<sup>247,248</sup> It would seem logical that similar dyes of the type **250** and **251** could be prepared, but attempts to do so have been reported as unsuccessful.<sup>249</sup>

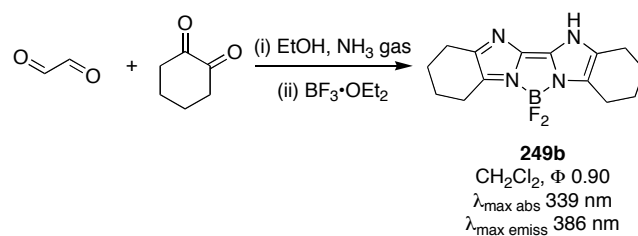


**Scheme 1.20.** Synthesis of biimidazol-2-yls BF<sub>2</sub> complexes.

**a**

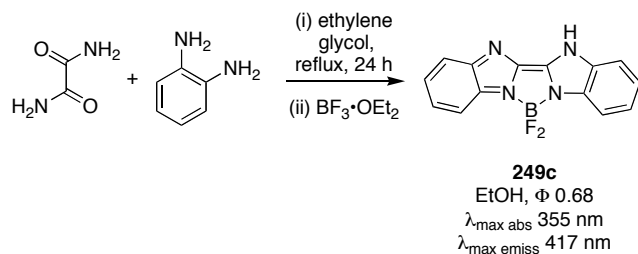


**b**



## Scheme 1.20. Continued.

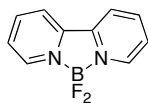
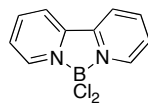
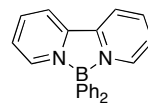
c



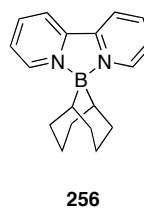
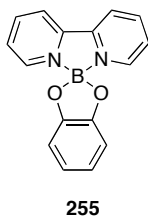
The parent, non-*B*-coordinated heterocyclic systems for molecules **249** are not significantly fluorescent, but the  $\text{BF}_2$  complexes display strong fluorescence as shown in the diagrams. Predictably, red shifts for both the absorption and emission maxima, and increased extinction coefficients are observed with increased conjugation and rigidity.

## 2. Pyridine-based Systems

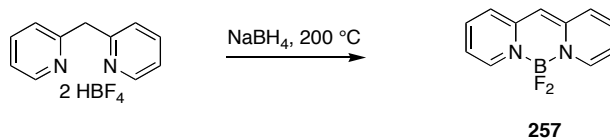
The dipyridyl-2-yl-boron complexes **252** - **256** have been prepared from reactions of bipyridines with boron electrophiles.<sup>250</sup> They absorb between 302-322 nm, with the exception of the complex **255**, which absorbs at 371 nm. No fluorescence was detected for these complexes.

**252****253****254**



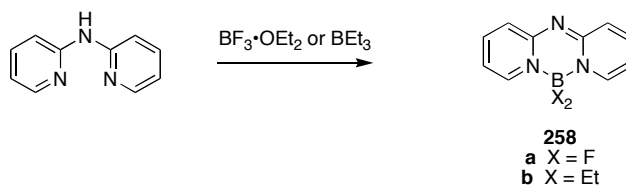


The pyridomethene-BF<sub>2</sub> complex **257** was synthesized as shown in reaction 19 from the 2,2'-dipyridylmethane by fusion with sodium borohydride.<sup>251</sup> The product shows a strong absorption at 468 nm, with a extinction coefficient of 17,783 M<sup>-1</sup>cm<sup>-1</sup> in chloroform, but does not fluoresce.



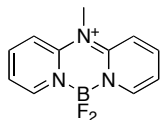
reaction 21

The 10-azapyridomethene-BF<sub>2</sub> complex **258a** was obtained via condensation between dipyrind-2-ylamine and boron trifluoride.<sup>232</sup> Similarly, 10-Azapyridomethene-B(Et)<sub>2</sub> **258b** was obtained by condensation with triethylboron (reaction 20). Complex **258a** absorbs at 382 nm (log ε = 4.47) in ethanol, and strongly fluoresces at 422 nm (Φ = 0.81).

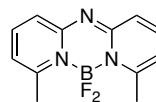


reaction 22

Treatment of dipyrro-2-ylamine with methyl iodide gives the methyl dipyrro-2-ylamine, which can be converted to the 10-methyl-10-azapyridomethene-BF<sub>2</sub> complex **259** by treatment with boron trifluoride. The homologous complex **260** was obtained by condensation between 2-amino-6-methylpyridine and 2-chloro-6-methylpyridine, and subsequent treatment with boron trifluoride. Both these complexes are fluorescent, but the neutral one, **260**, fluoresces at longer wavelength.



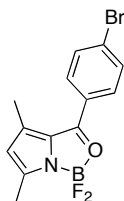
**259**  
EtOH,  $\Phi$  0.36  
 $\lambda_{\text{max abs}}$  325 nm  
 $\lambda_{\text{max emiss}}$  362 nm



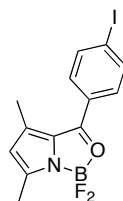
**260**  
EtOH,  $\Phi$  0.40  
 $\lambda_{\text{max abs}}$  396 nm  
 $\lambda_{\text{max emiss}}$  416 nm

### 3. 2-Ketopyrrole Complexes

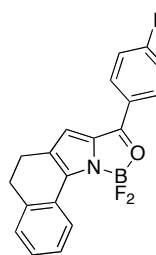
The 2-ketopyrrole complexes **261** - **265** were isolated as minor by-products (less than 5%) in the synthesis of the corresponding BODIPY analogs. The yield of **261** - **265** could be improved by increasing the amount of acid chloride used in the synthesis. 2-Ketopyrrole complexes are less conjugated than BODIPY dyes, hence their absorption, extinction coefficients and emission wavelengths are shorter/smaller. The Stokes' shifts for these compounds, however, are greater than for BODIPY systems (48 nm to 154 nm, *cf* approximately 10-15 nm for BODIPY dyes).



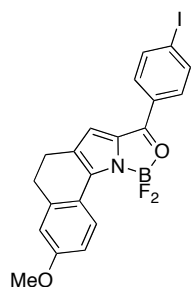
**261**  
CHCl<sub>3</sub>,  $\Phi$  na  
 $\lambda_{\text{max abs}}$  321 nm  
 $\epsilon$  19 000  
 $\lambda_{\text{max emiss}}$  475 nm



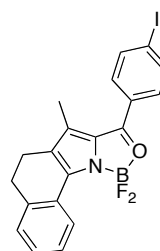
**262**  
CHCl<sub>3</sub>,  $\Phi$  na  
 $\lambda_{\text{max abs}}$  322 nm  
 $\epsilon$  16 000  
 $\lambda_{\text{max emiss}}$  475 nm



**263**  
CHCl<sub>3</sub>,  $\Phi$  0.89  
 $\lambda_{\text{max abs}}$  468 nm  
 $\epsilon$  48 000  
 $\lambda_{\text{max emiss}}$  516 nm



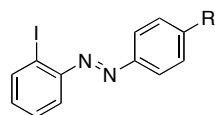
**264**  
 CHCl<sub>3</sub>,  $\Phi$  0.52  
 $\lambda_{\text{max abs}}$  488 nm  
 $\epsilon$  43 000  
 $\lambda_{\text{max emiss}}$  544 nm



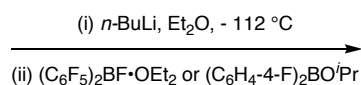
**265**  
 CHCl<sub>3</sub>,  $\Phi$  0.58  
 $\lambda_{\text{max abs}}$  445 nm  
 $\epsilon$  46 000  
 $\lambda_{\text{max emiss}}$  504 nm

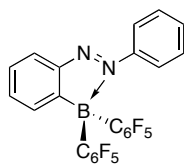
#### 4. Azobenzene Derivatives

Azobenzenes are the most common chromophores in commercial dyes and, because of photoinduced isomerization, they are used as photoresponsive molecular switches. A consequence of facile photoisomerization is that quantum yields for these compounds are so low that fluorescence tends only to be observed in a rigid matrix at low temperature. A recent innovation in this field, however, is fixation of the  $\pi$ -conjugate systems using boryl-entities to give the fluorescent compounds **266** – **268**.<sup>252</sup>

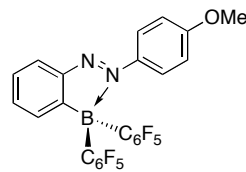


R = H, OMe

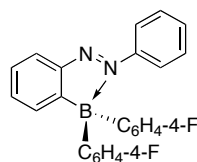




**266**  
hexanes;  $\Phi$  0.23  
 $\lambda_{\text{max abs}}$  386 nm  
 $\lambda_{\text{max emiss}}$  503 nm



**267**  
hexanes;  $\Phi$  0.76  
 $\lambda_{\text{max abs}}$  439 nm  
 $\lambda_{\text{max emiss}}$  524 nm



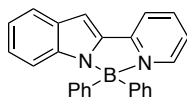
**268**  
no fluorescence

reaction 23

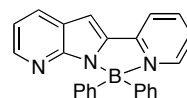
Azobenzene dyes **266** and **267** display a remarkable red shifted absorbance (386 nm and 439 nm, respectively) relative to unsubstituted (*E*)-azobenzene ( $\lambda = 315$  nm). Irradiation of **266** and **267** with a super-high-pressure mercury lamp did not cause photoisomerization. The azobenzene derivative **268**, bearing a fluorinated substituent on the boron atom, showed almost no fluorescence. We speculate that this could be due to intramolecular charge transfer from the least electron rich aryl substituent into the excited state of the complexed azobenzene system.

### 5. Miscellaneous *N, N*-Bidentate Diphenyl Boron Chelates

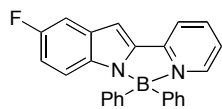
Luminescent *N, N*-bidentate diphenylboron chelates **269** - **281**<sup>253,254</sup> have emission maxima that vary with the nature of the parent organic system. Limited information was provided regarding the spectroscopic properties of these molecules, but the data presented are interesting because some of the dyes have high quantum yields and/or fluorescence emissions around 600 nm. These systems perhaps warrant further attention.



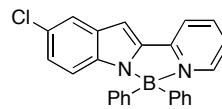
**269**  
 $\lambda_{\text{max emiss}}$  516 nm  
 $\Phi$  0.29



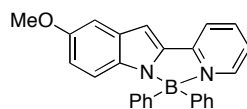
**270**  
 $\lambda_{\text{max emiss}}$  476 nm  
 $\Phi$  0.61



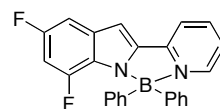
**271**  
 $\lambda_{\text{max emiss}}$  490 nm  
 $\Phi$  0.33



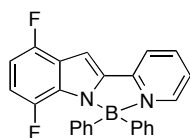
**272**  
 $\lambda_{\text{max emiss}}$  487 nm  
 $\Phi$  0.22



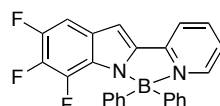
**273**  
 $\lambda_{\text{max emiss}}$  532 nm  
 $\Phi$  0.036



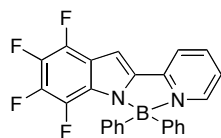
**274**  
 $\lambda_{\text{max emiss}}$  481 nm  
 $\Phi$  0.32



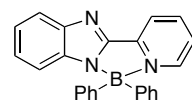
**275**  
 $\lambda_{\text{max emiss}}$  482 nm  
 $\Phi$  0.31



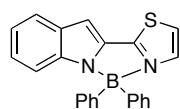
**276**  
 $\lambda_{\text{max emiss}}$  469 nm  
 $\Phi$  0.65



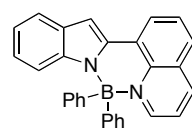
**277**  
 $\lambda_{\text{max emiss}}$  467 nm  
 $\Phi$  0.60



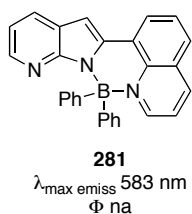
**278**  
 $\lambda_{\text{max emiss}}$  445 nm  
 $\Phi$  0.46



**279**  
 $\lambda_{\text{max emiss}}$  470 nm  
 $\Phi$  0.14



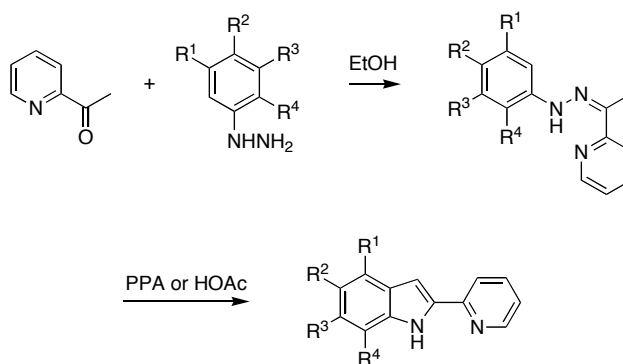
**280**  
 $\lambda_{\text{max emiss}}$  611 nm  
 $\Phi$  na



A variety of methods were used to produce the parent heterocycles for the dyes shown above (Scheme 1.21). The 2-(2'-pyridyl)indole and 2-(2'-thiazolyl)indole based ligands were synthesized by a two-step Fischer synthesis (Scheme 1.21a and b, respectively). Scheme 1.21c illustrates how a Negishi coupling<sup>255</sup> was used for the synthesis of the 2-(8'-quinolyl)indole or -azaindole. Treatment of the product heterocycles shown in Scheme 1.21 with triphenylboron (1:1 ratio) in toluene afforded the boron complexes **269** - **281** in good yields.

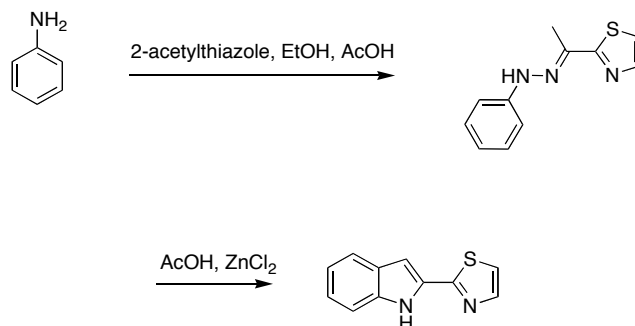
**Scheme 1.21.** Two-step Fischer synthesis of **a** 2-(2'-pyridyl)indole ; **b** 2-(2'-thiazolyl)indole; **c** synthesis of 2-(8'-quinolyl)indole or aza-indole via Negishi coupling.

**a**

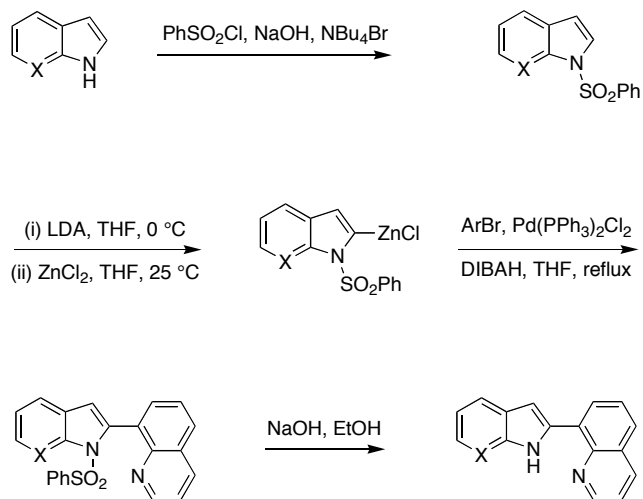


## Scheme 1.21. Continued.

b

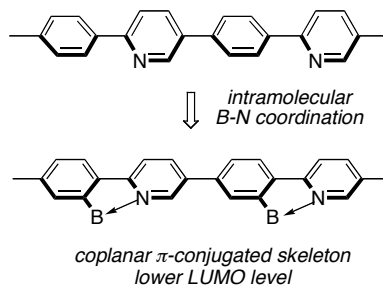


c

6. *Boryl-substituted Thienylthiazoles*

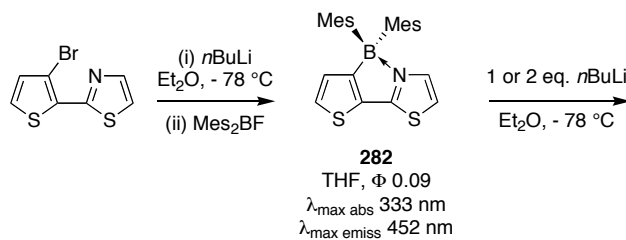
Finally, there are compounds that are even less closely related to the BODIPY core, formed by intramolecular B-N coordination in *N*-heteroaromatic systems. This new concept is illustrated for the development of new electronic materials. The interaction between the Lewis acid (boron) and Lewis base (nitrogen) not only constrain the  $\pi$ -conjugated framework in a

coplanar fashion, but also lower the LUMO level (Figure 1.8). Thus, (3-boryl-2-thienyl)-2-thiazole **282** was synthesized from (3-bromo-2-thienyl)-2-thiazole as shown in Scheme 1.22.<sup>256</sup> Compound **282** can easily be functionalized to the tin **283** or iodo **284** derivatives via the lithiated intermediates. Lithiation occurs regioselectively at the 5-position of the thiazole ring.



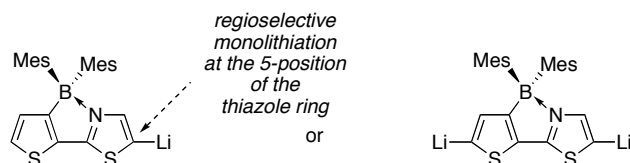
**Figure 1.8.** Intramolecular B-N coordination of *N*-heteroaromatic systems.

**Scheme 1.22.** Synthesis of the dimesityl-boryl substituted thienylthiazole **282**.

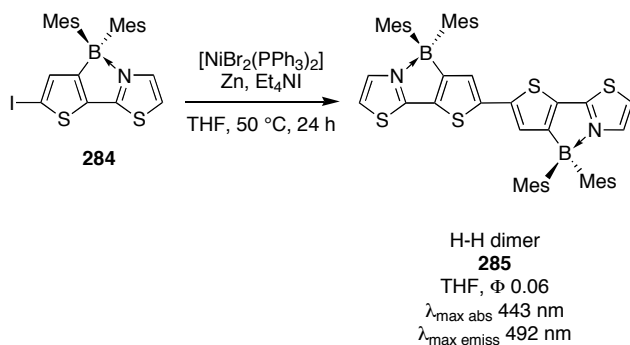




## Scheme 1.22. Continued.

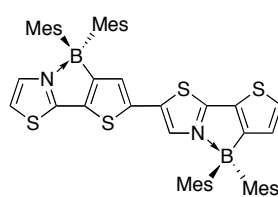
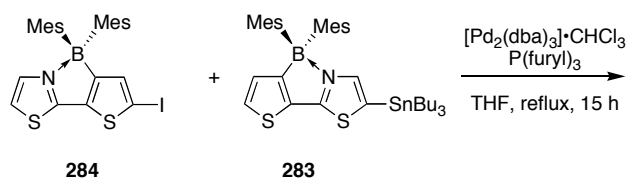


The corresponding tin and iodo derivatives can be used as building blocks in metal-catalyzed coupling reactions to prepare extended  $\pi$ -electron systems such as the head-to-head (H-H), head-to-tail (H-T), and tail-to-tail (T-T) dimers **285** - **287** (Scheme 1.23). The dimers display red-shifted absorption and emission relative to the monomer. The boryl-substituted thienylthiazoles **282** and **285**- **287** show weak fluorescence emission in the range 452 – 492 nm.<sup>256</sup>

Scheme 1.23. Synthesis of **a**, head-to-head; **b**, head-to-tail, and **c**, tail-to-tail dimers.**a**

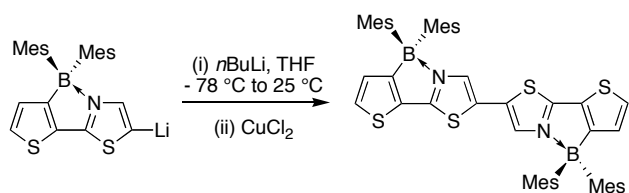
## Scheme 1.23. Continued.

b



H-T dimer  
**286**  
 THF,  $\Phi$  0.07  
 $\lambda_{\text{max abs}}$  427 nm  
 $\lambda_{\text{max emiss}}$  486 nm

c



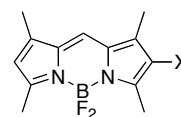
T-T dimer  
**287**  
 THF,  $\Phi$  0.09  
 $\lambda_{\text{max abs}}$  414 nm  
 $\lambda_{\text{max emiss}}$  472 nm

## L. Conclusion

Applications of BODIPY dyes outnumber, by far, studies of their fundamental chemistry and spectroscopic properties. This is unfortunate because they are such powerful tools for imaging, chemosensors, lasing materials, *etc.* There would be even more applications if some deficiencies in the area were addressed. For instance, there are very few water-soluble BODIPY dyes. In this review we mentioned compounds **53** – **56** and **69d**. The only other examples of water-soluble BODIPY dyes we found were lipophilic BODIPYs made water-soluble by activation with a sulfonated *N*-hydroxysuccinimide derivative.

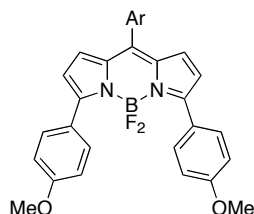


R = Me, **53**; Et, **54**; H, **56**

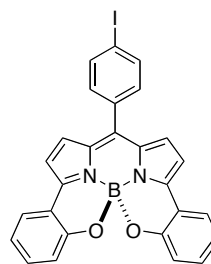


X = SO<sub>3</sub>Na, **55**  
CH=CHSO<sub>3</sub>H, **69d**

One conspicuous area for further research is the design and synthesis of BODIPY derivatives that emit further into the near-IR. Steps towards this can be taken by attaching aromatic groups, preferably with electron-donating substituents (*eg* **87**), rigidifying their structure (*eg* **202**), or producing ring-fused systems like **172**. One of the most innovative synthetic procedures for doing this involves condensation of BODIPY methyl substituents to give dyes similar to ones that Invitrogen markets such as “BODIPY 630/650” and “BODIPY 650/665”.



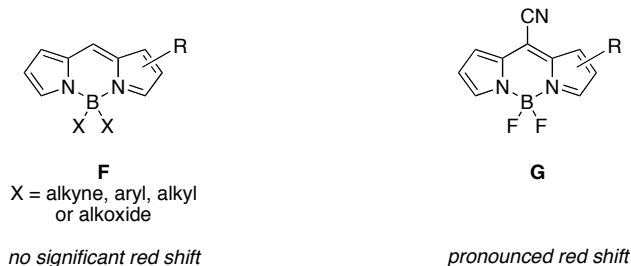
**87**  
CHCl<sub>3</sub>  
λ<sub>max emiss</sub> 626 nm



**202**  
CHCl<sub>3</sub>  
λ<sub>max emiss</sub> 654 nm

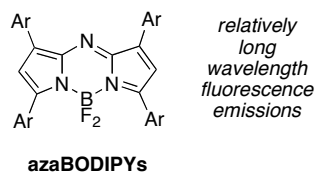


Many papers have been published on BODIPY-like systems in which fluorine atoms on the BODIPY dyes are replaced by a variety of C- or O-based nucleophiles to give products **F**. These modifications have proven useful as a means to make energy transfer systems. Substitutions of this kind may alter the quantum yields and fluorescence properties of the dyes, but they do not tend to shift their emissions to the red. Conversely, incorporation of a cyanide group at the *meso*-position gives a dramatic shift towards the near-IR.



Substitution of the boron atom in BODIPY dyes gives fluorescent Zn, In, and Ga derivatives, but other metals tend to quench the fluorescence. Quenching in such derivatives presumably occurs via electron-transfer mechanisms involving the dyes in their excited states.

Replacement of C-8 in the BODIPY with a nitrogen gives the so-called "AzaBODIPYs". These are an extremely interesting set of dyes because of their long fluorescence emissions wavelength. No water-soluble derivatives of these have been prepared, and nearly all the substituted compounds feature aryl groups in the 3,5-positions.



Overall, an abundance of relatively straightforward applications of BODIPY dyes have been reported. Some of the most significant synthetic procedures tend to be written in cryptic styles that are so often seen in the patent literature, but there have been some recent milestones in this area. The most important future developments with respect to applications in biotechnology will involve synthesis of water-soluble, easily functionalized systems, particularly those fluorescing above 600 nm.

## CHAPTER II

# FUNCTIONALIZED AZA-BODIPY DYES

### A. Introduction

Most fluorescence detection strategies use visible fluorophores, fluorescein being one of the most popular. However, autofluorescence from the cell can often be a problem when using visible fluorophores, and can result in both lower sensitivity and selectivity. “Green” autofluorescence of the skin and viscera, especially the gallbladder, small intestine, and bladder, is high when excited with blue light.<sup>257</sup> Tissue autofluorescence can be eliminated or reduced by use of NIR filter set. Imaging live cells deep in tissue is also difficult to accomplish using light microscopy because light scatters as it travels through tissue. There are two main type of scatters: Rayleigh scattering which is the scattering of light by particles much smaller than the wavelength of the light, and Mie scattering which can be describes as scattering by particles similar to or larger than a wavelength.<sup>257</sup> Light scatter is dependent on the wavelength of detection by  $1/\lambda^4$ .<sup>258,259</sup> Consequently, detection at 820 nm offers a sixfold reduction in scatter over detection at 500 nm. Very few biological molecules possess intrinsic fluorescence in the near-infrared (NIR) region of the spectrum (650-1100 nm) (Figure 2.1). Therefore, sensitivity and selectivity can significantly be improved by near-infrared laser induced fluorescence detection.

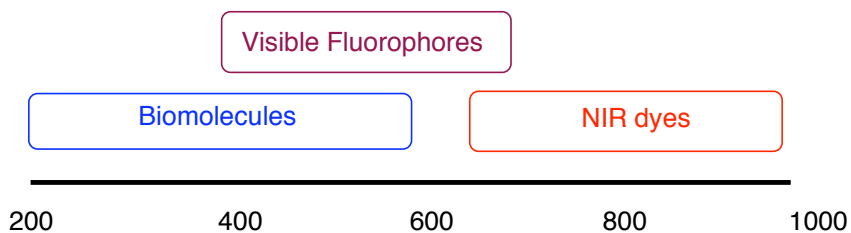


**Figure 2.1.** Very few biological molecules possess intrinsic fluorescence in the near-IR.

Due to the aforementioned factors, there is considerable interest in preparing new fluorescent dyes that emit towards the near-IR region.<sup>259-262</sup> Unfortunately, there are a very limited number of organic molecules that emit in this range and could be adapted to form probes for biomolecules. The most commonly NIR probes used in cell imaging are cyanines (Figure 2.2),<sup>263-267</sup>; whereas oxazines and squaraines have also been used. However, all NIR cyanine dyes have poor photostability, and in most cases possess low fluorescence quantum yields. The highest fluorescence quantum yield for NIR cyanine dyes in water was reported to be 0.28. Squaraines tend to be hydrophobic, causing aggregation and problems in bioconjugation. Thus, identification of stable and effective NIR probes has become urgent.

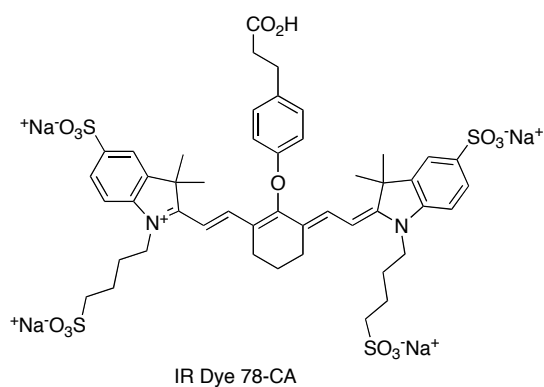


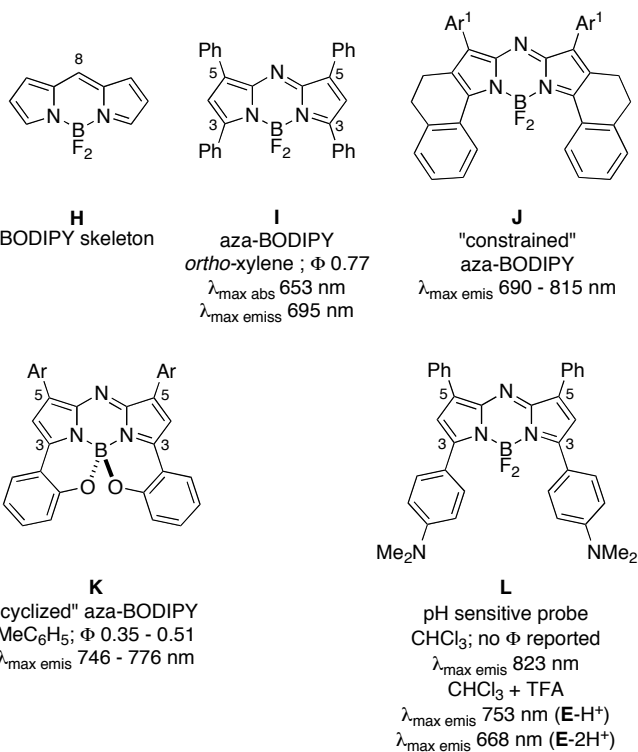
**Figure 2.2.** A tetra-sulfonated indocyanine dye, with a carboxylic acid that can be used for conjugation to biomolecules.

Few NIR fluorophores have been developed, and designing new NIR probes is a very difficult task. An ideal NIR probe should (i) fluoresce at 700-900 nm, (ii) have a high fluorescence quantum yield, (iii) have a narrow excitation/emission band, (iv) have high chemical and photo-stabilities, (v) have low cellular toxicity, and (vi) have excellent biocompatibility.

BODIPY (difluoroboradiaza-s-indacene) dyes **H** are highly fluorescent, stable, and insensitive to the solvents' polarity and pH. BODIPYs are unusual in that they are relatively non-

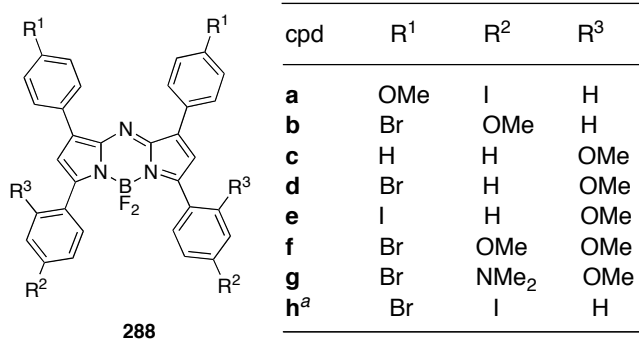
polar and are electronically neutral. They have found widespread applications as laser dyes, sensors, and molecular probes that emit in the region around 520 – 600 nm.<sup>268</sup> Modifications to the BODIPY core can lead to dyes that emit above 600 nm. Such modifications include appending strong electron-donating groups, rigidifying substituents around the core, and extending the conjugation of the system. The strategy of attaching electron-donating substituents, however, has limitations. For instance, amine groups make the probes sensitive to quenching via electron transfer to the excited state, and the fluorescence becomes pH sensitive.

There is a subset of BODIPY dyes that are related to the parent systems by *N*-for-*C* substitution at the C<sup>8</sup>-position. These are commonly called “aza-BODIPY” dyes, and most of the compounds reported to date have 3,3,5,5-aryl substituents, of which the tetraphenyl system **I** is the most widely studied. The parent heterocycle without a boron atom has been known since 1943,<sup>269-272</sup> but it was not until 1994 that a *B*-derivative was mentioned in the literature and its remarkable fluorescent properties were noted.<sup>273</sup> Specifically, the tetraphenyl compound **I** was shown to emit at 695 nm (in 1,2-Me<sub>2</sub>C<sub>6</sub>H<sub>4</sub>,  $\Phi = 0.77$ ), *ie* a marked red-shift relative to other BODIPY dyes.

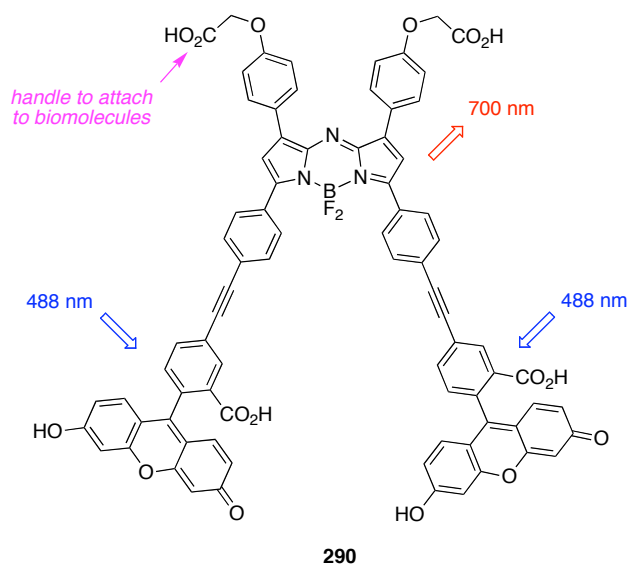
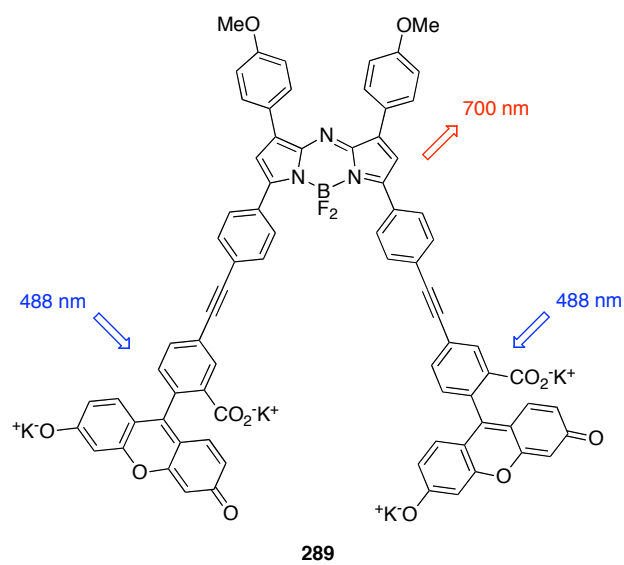




To date, there have been only two deliberate attempts to further extend the emission of aza-BODIPY dyes into the near IR-region. In the first, Carreira and co-workers used extended heterocycles to prepare constrained systems such as **J**; this gave molecules that emitted up to 815 nm with enhanced quantum yields.<sup>274,275</sup> Second, work from our laboratory focused on using *ortho*-oxygens on the 3,3-aryl substituents to constrain them giving systems **K**; this approach also shifts the fluorescence emissions to the red and increased the quantum yields.<sup>276</sup> Finally, when designing pH sensitive probes, O'Shea found that when 4-*N,N*-dimethylaminobenzene substituents were created at the 3,3-aza-BODIPY sites in molecule **L**, then an emission at 823 nm was observed under conditions where the amine groups were not protonated.<sup>277</sup> This was reported while the work described in this manuscript was in progress. Compound **L** has limited value as a potential core-structure for biomolecular probes unless protonated, in which case the red-shift is not observed. Nevertheless, that observation supported the hypothesis we were exploring, *ie* that strongly electron-withdrawing or -donating aryl-substituents could significantly shift the emissions of aza-BODIPY dyes. A second goal of this study was to prepare aza-BODIPY systems with halide substituents that could be substituted with “donor” fragments that absorb considerably shorter UV radiation. In the event, both these goals were realized, and the data are reported here. Specifically, a series of aza-BODIPY dyes **288a - g**, having a range of different substituted-aryl groups were prepared. One of these potential “acceptor” molecules, compound **288a** was elaborated into the donor-acceptor cassette<sup>278-280</sup> systems **289** and **290**. Important spectral parameters for all these dyes are reported here.



<sup>a</sup> compound **288h** could not be obtained. Compound **293h** could however be obtained.



### 1. Multiplexing and Through-bond Energy Transfer Cassettes

It is often desirable to simultaneously observe several fluorescently tagged components in a biochemical mixture, *ie* multiplexing. Our group has used the concept of *through-bond energy transfer* to design novel dye cassettes for multiplexing for DNA sequencing.<sup>281</sup> Multiplexing with one excitation source is, however, difficult as the sensitivity dramatically decreases with dyes

emitting in the red. This is because dyes that emit near the excitation source absorb the light most efficiently since they have a greatest absorption at that wavelength, while the dyes that have red-shifted absorption absorb less light and therefore fluoresce less at the excitation wavelength. To alleviate this problem, combinations of dyes that maximize FRET have been designed. The efficiency of the energy transfer in FRET systems is governed by the overlap integral between the donor emission and the acceptor absorption. If the overlap of the emission of the donor dye with the absorption of the acceptor dye is small, then the energy transfer will be small. Therefore, FRET is only a partial solution.

*Through-bond energy transfer* is mechanistically different from FRET. Notably, there is no known requirement for overlap of the emission of the donor fragment with the absorption of the acceptor part. Thus, in appropriately designed through-bond energy transfer cassettes, a donor part, or parts, could absorb photons at a convenient wavelength (eg 488 nm: excitation from an Ar-laser), transfer the energy rapidly through the conjugated linker to the acceptor fragment that emits at a far longer wavelength (Figure 2.3). The overlap between the donor emission and the acceptor absorbance is no longer required in through bond energy transfer cassettes. Thus, it is possible to design dyes that absorb strongly at a short wavelength and emit brightly with very similar intensities and excellent resolution. Coupling more than one donor in the conjugated system can increase the intensity of the emission from the acceptor. In summary, both the resolution and fluorescence intensities obtained from several probes excited at a single wavelength can be potentially increased by through bond energy transfer cassettes (Figure 2.4).

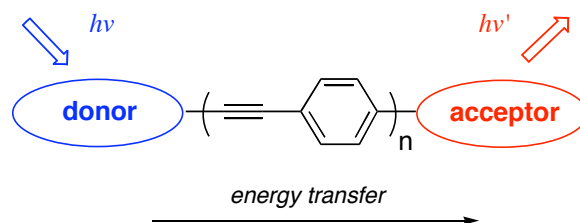


**Figure 2.3.** Through-bond energy transfer cassette

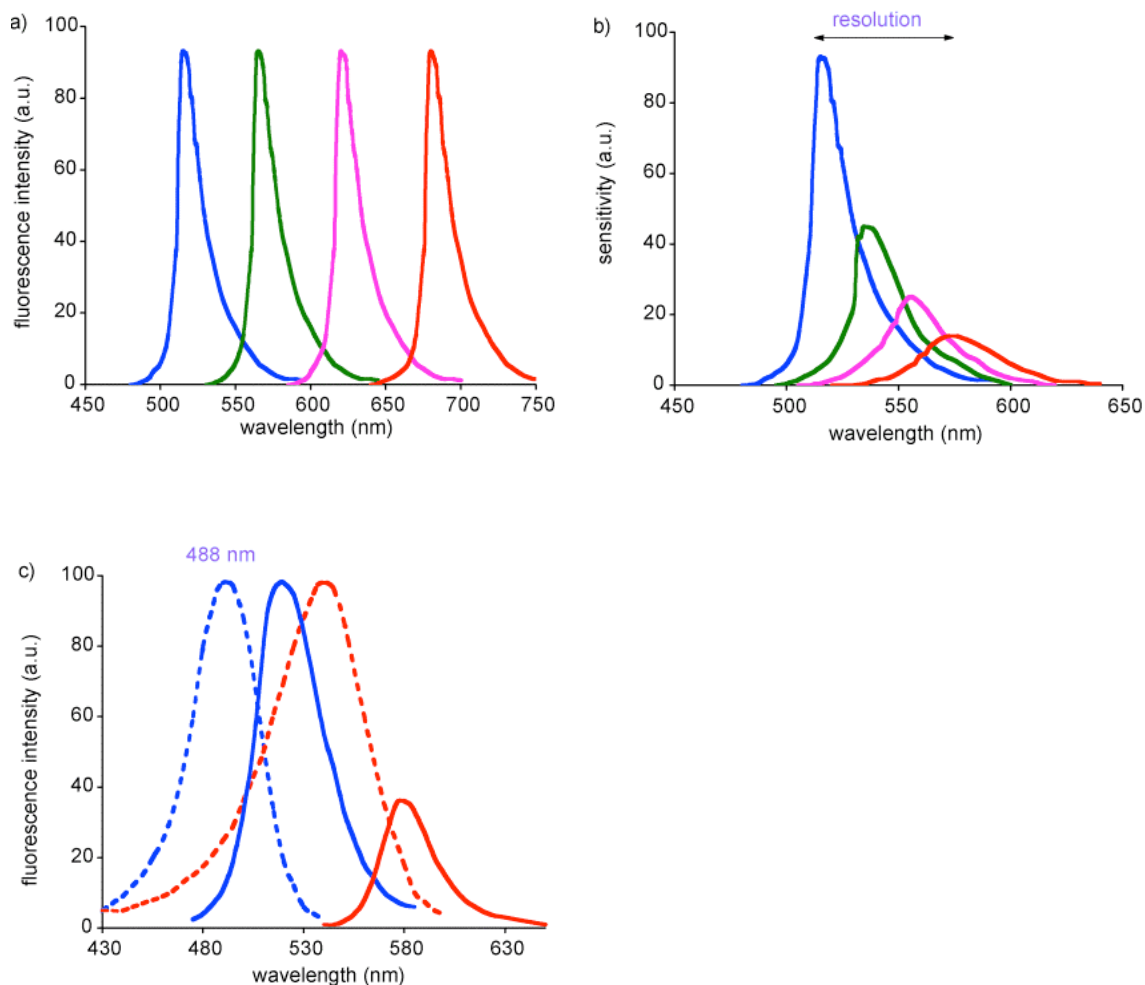


**Figure 2.4.** **a** Idealized fluorescence emissions from dyes used in DNA sequencing. **b** An approximate representation of data obtained from single dyes in DNA sequencing. **c** Diminished fluorescence intensities of the red dyes can be attributed to their lower extinction coefficients at the excitation wavelength, relative to the blue dyes.

A set of four through-bond energy transfer cassettes for use in automated fluorescence detected DNA sequencing has already been designed in our laboratories (Figure 2.5).<sup>282</sup> The cassettes feature fluorescein as a donor, and rosamines as acceptor dyes. They were shown to emit strongly, with highly efficient energy transfer. Upon excitation at 488 nm, sole fluorescence

typical of the acceptor was observed, proving 100% energy transfer from the donor to the acceptor (Figure 2.6). Furthermore, the four cassettes were considerably more stable to photobleaching than fluorescein, even though they each contain a fluorescein donor.

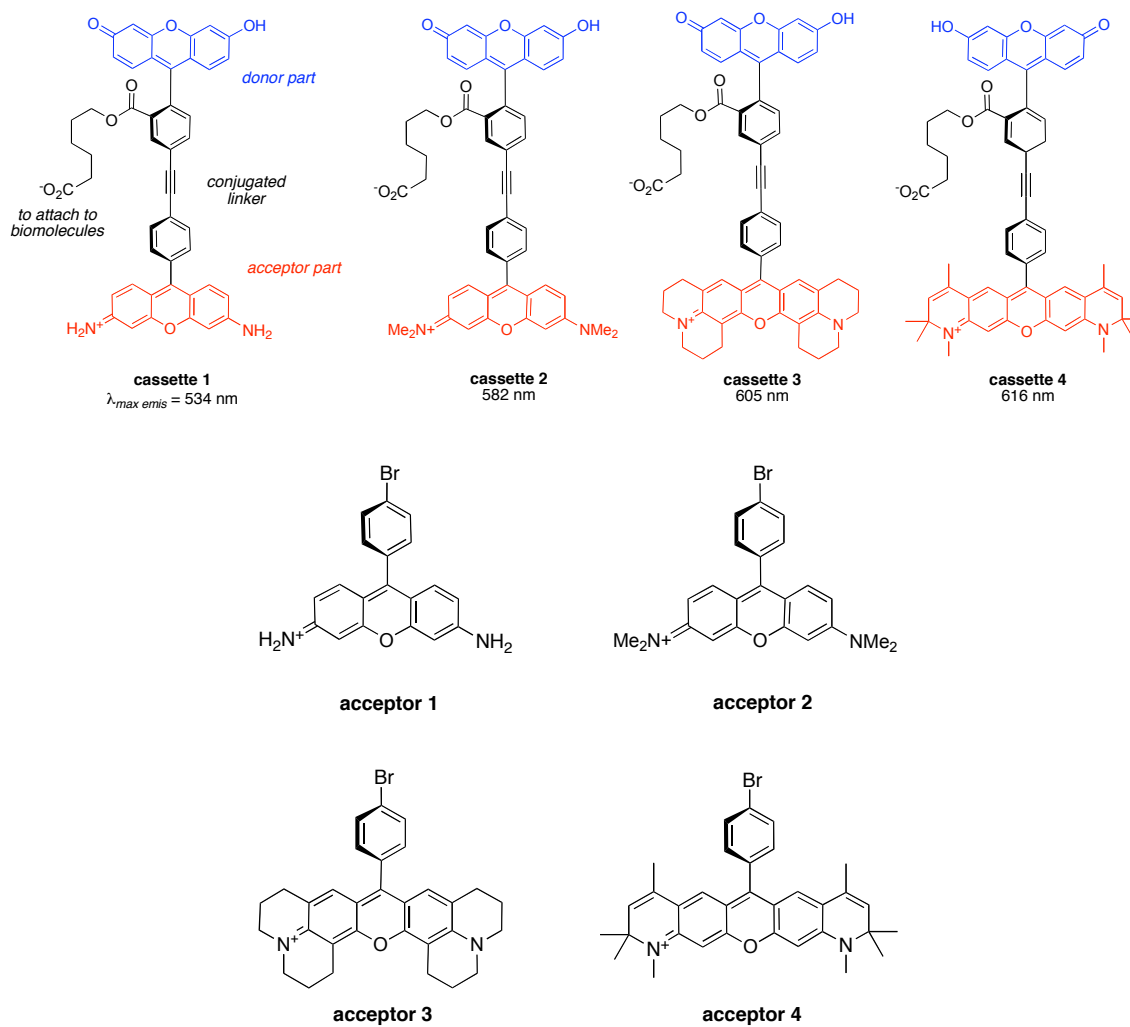


**Figure 2.5.** First generation of through-bond energy transfer cassettes developed for DNA sequencing (top), and the corresponding acceptor rosamine fragments (bottom).

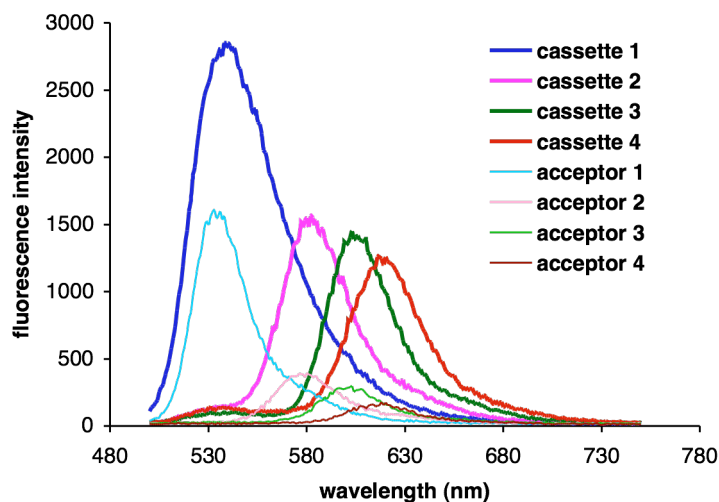


**Figure 2.6.** Fluorescence emission of the cassettes upon excitation at 488 nm.

This first generation of ET cassettes were a milestone in our research, but they were not very suitable for applications in biotechnology eg cellular imaging due to their poor water-solubility. Furthermore, probes emitting in the near-infrared region (650-850 nm) are preferred for cell imaging to avoid background fluorescence from flavins and other components in cell, and the emissions of these cassettes occurred at somewhat shorter wavelengths. We therefore decided to attempt preparations of water-soluble cassettes involving aza-BODIPY acceptors.

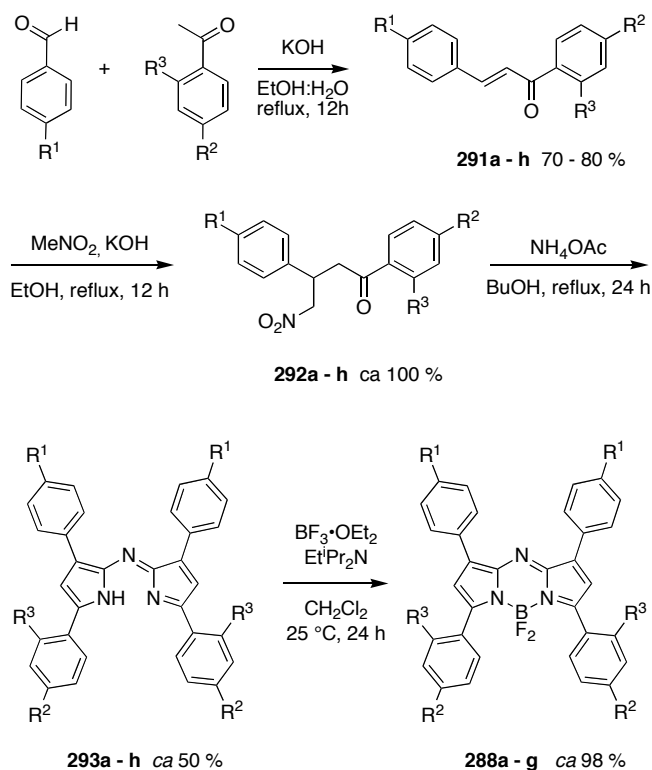
## B. Results and Discussion

### 1. Synthesis of Aza-BODIPYS 288a – g

Synthesis of dyes **288** began with diaryl  $\alpha,\beta$ -unsaturated ketones **291** (chalcones; readily prepared by an aldol/dehydration reaction of the corresponding benzaldehyde and acetophenone derivatives). O'Shea's modification<sup>283</sup> of an older Rogers' procedure was then used.<sup>284</sup> Thus, Michael addition of the anion from nitromethane to the chalcones **291** gave the 1,3-diaryl-4-nitrobutan-1-ones **292** in essentially quantitative yields after aqueous work-up; these were then used without further purification. Condensation with ammonium acetate in refluxing

butanol gave the azadipyrromethenes **293** via a cascade of events. Finally, complexation of the azadipyrromethenes with boron trifluoride gave the azaBODIPYs **288** in excellent yields.

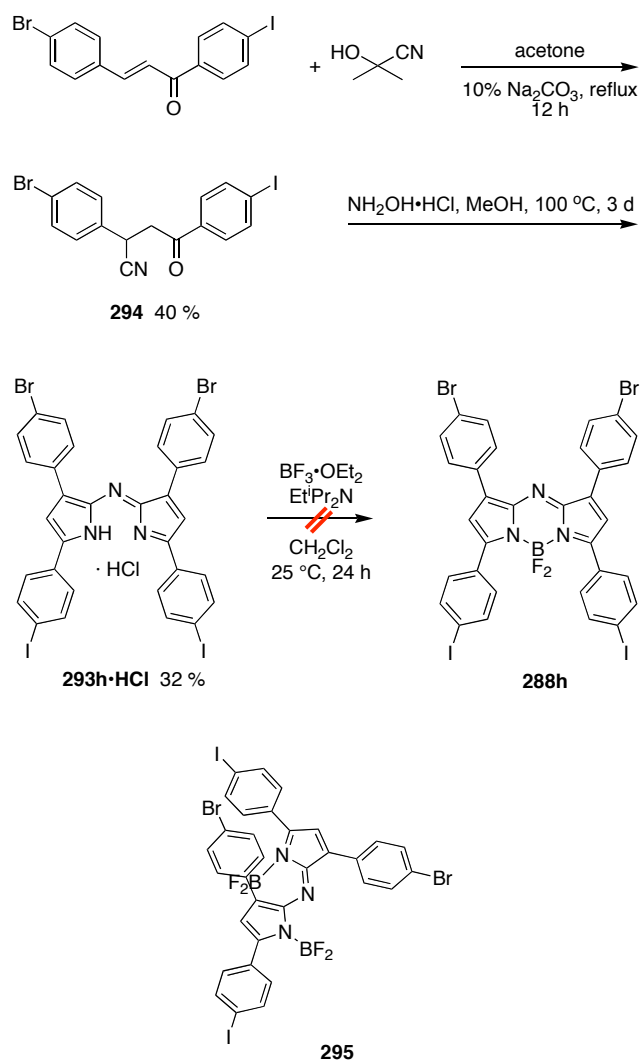
**Scheme 2.1.** Synthesis of azaBODIPYs **288**.



Using the procedure outlined in Scheme 1, dipyrromethene intermediate **293h** was only obtained in low yield (8%, crude) and in an impure form, so other conditions were developed (Scheme 2). Variations of solvent (butanol, pentanol, hexanol, neat), ammonia source ( $\text{HCONH}_2$  instead of  $\text{NH}_4\text{OAc}$ ) and heating conditions (conventional heating or microwave radiation) to make the reaction viable were unsuccessful. However, **293h·HCl** was obtained from the  $\gamma$ -ketonitrile **7** (made from the corresponding chalcone and acetone cyanohydrin) via condensation with hydroxylamine hydrochloride in methanol; this is one of the procedures developed by Rogers' in 1944.<sup>270,285</sup> Surprisingly, complexation of **293h** with boron trifluoride etherate did not

give the desired product, but instead led to a compound with two  $\text{BF}_2$  units ( $^{19}\text{F}$ ); the structure of this adduct was tentatively assigned as **295**. Presumably steric and/or electronic interactions within **293h** prevented formation of the desired aza-BODIPY **288h**, an observation supported by the fact that when the iodo groups were substituted (via Sonogashira for example) prior to complexation, formation of the aza-BODIPY proceeds easily and in good to excellent yield (data not shown).

**Scheme 2.2.** Synthesis of **293h** from  $\gamma$ -ketonitrile.





Compounds **288a - g** have good solubilities in most organic solvents (eg chloroform, toluene, tetrahydrofuran). An X-ray structure of compound **288a** is shown in Figure 2.7. Compound **288a** crystallized in the triclinic space group *P*-1 with two molecules in the asymmetric unit. The overall conjugated nature of the chromophore was confirmed from the analysis of the crystal structure with comparable bond lengths (Table 2.1).

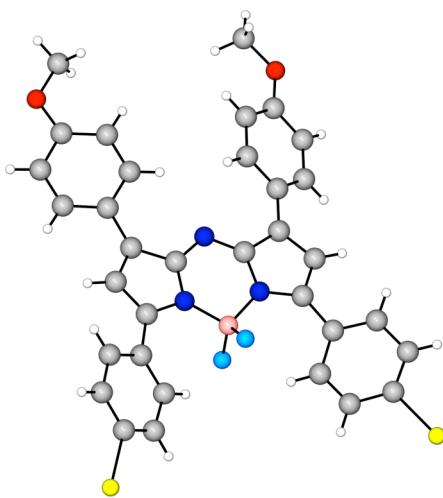


**Figure 2.7.** Thermal ellipsoid representation of **288a**.

**Table 2.1.** Selected bond lengths and angles for **288a**.

| Bond        | Length / Å | angle              | Angle / ° |
|-------------|------------|--------------------|-----------|
| C(1) – N(2) | 1.362      | F(1) – B(1) – F(2) | 111.6     |
| C(1) – N(1) | 1.353      | F(1) – B(1) – N(1) | 110.2     |
| C(1) – C(2) | 1.474      | F(2) – B(1) – N(1) | 109.9     |
| C(2) – C(3) | 1.36       | F(1) – B(1) – N(3) | 108.8     |

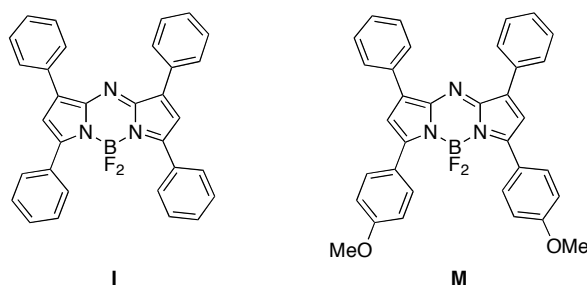
**Table 2.1.** Continued.

|             |       |                     |       |
|-------------|-------|---------------------|-------|
| C(3) – C(4) | 1.39  | F(2) – B(1) – N(3)  | 110.4 |
| C(4) – N(1) | 1.404 | N(1) – B(1) – N(3)  | 105.8 |
| N(1) – B(1) | 1.56  | N(1) – C(1) – N(2)  | 125.8 |
| B(1) – F(1) | 1.379 | N(1) – C(1) – C(2)  | 110.9 |
| C(5) – N(3) | 1.390 | N(2) – C(1) – C(2)  | 123.2 |
| C(5) – N(2) | 1.327 | C(3) – C(2) – C(1)  | 102.7 |
| C(5) – C(6) | 1.452 | C(3) – C(2) – C(9)  | 127.8 |
| C(6) – C(7) | 1.39  | C(1) – C(2) – C(9)  | 129.4 |
| C(7) – C(8) | 1.42  | C(2) – C(3) – C(4)  | 112.0 |
| C(8) – N(3) | 1.375 | C(3) – C(4) – N(1)  | 107.8 |
| N(3) – B(1) | 1.58  | C(3) – C(4) – C(29) | 126.7 |
| B(1) – F(2) | 1.387 | N(1) – C(4) – C(29) | 125.4 |

## 2. Spectroscopic Properties of Aza-BODIPY Derivatives **288 a – g**

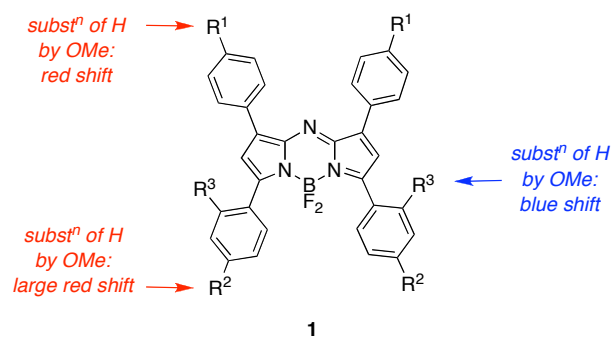
Compounds **288** were prepared mainly to facilitate syntheses of more elaborate molecules containing donor groups (eg **289** and **290**, *vide infra*), consequently most of them contain halogen atoms. However, this series of compounds does provide some non-systematic basis for comparing absorption and fluorescence properties.

Absorption spectra of compounds **288** show strong  $S_0 \rightarrow S_1$  transitions with absorbance maxima between 650 and 798 nm (Table 2.2 and Figure 2.8a). Entry 1 and 2 in Table 2.2 are literature data<sup>283</sup> for the tetra-aryl substituted aza-BODIPYs **I** and **M**.



Using these as references, the data collected on compounds **288** indicate that introduction of electron-donating groups onto the aryl substituents results in significant bathochromic shifts. The largest red-shift in the series was observed for compound **288g** (entry 9) which has two strongly electron donating groups attached to the 3-aryl substituents in *ortho*- and *para*-positions. This is consistent with the idea that the aza-BODIPY core is more conjugated with electron rich aryl substituents, presumably due to better orbital overlap. Comparison of molecules **288c** – **e** with the rest of those in the series implies that the presence of an *ortho*-methoxy group on the 3-aryl substituent correlates with a blue-shift in the absorbance, but this may be overridden by a strongly electron donating group in the *para*-position of that same aromatic ring. Throughout, the extinction coefficients for these new dyes are high, in the range of 55 000 to 109 000 M<sup>-1</sup>cm<sup>-1</sup>, characteristic of aza-BODIPY compounds.

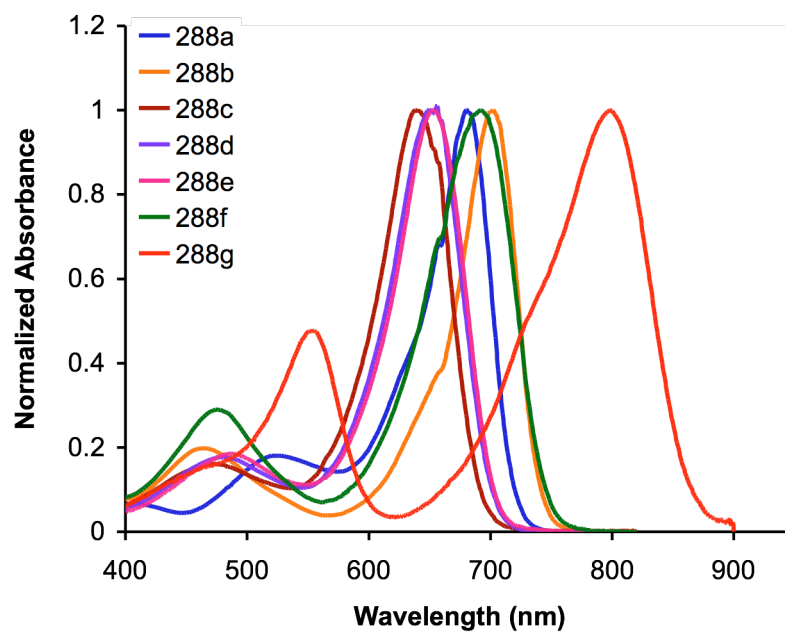
Fluorescence properties of the new dyes are also shown in Table 2.2, and the spectra are shown in Figure 2.8b. Their emission maxima range from 676 to 830 nm in toluene. Quantum yields for compounds in this series range from 0.07 to 0.41 in toluene. Interestingly, the fluorescence quantum yields of the bromoaryl-substituted derivatives were not significantly altered, while the fluorescence quantum yields of the iodoaryl-substituted derivatives show a significant decrease. There has been a tendency to over-generalize on the influence of some substituents on fluorescence, and the so-called “heavy atom effect” is a prime example of this. For compounds **288**, bromine-containing aryl-substituents do not reduce the quantum yields to trivial values (eg **288b**, entry 4). The only iodinated analogs in the series, **288a** and **288e**, also have reasonable quantum yields (0.18 and 0.10, respectively, entries 3 and 7). Most probably, the origins of the heavy atom effect are electron donation or acceptance from excited states of the chromophore, which often, but not always, occurs when heavy atoms are present. For the aza-BODIPY dyes **288** the halo-substituents are isolated from the chromophore by the aryl twist. Consequently, the main parameter influencing the fluorescence properties of the core is the *oxidation potentials* of those aryl substituents. This more sophisticated argument, rather than generalizations about “heavy atom effects”, is one advocated in other situations in several papers by Nagano and co-workers.<sup>286-292</sup>

**Table 2.2.** Spectroscopic properties of the Aza-BODIPY derivatives **288 a - g**.

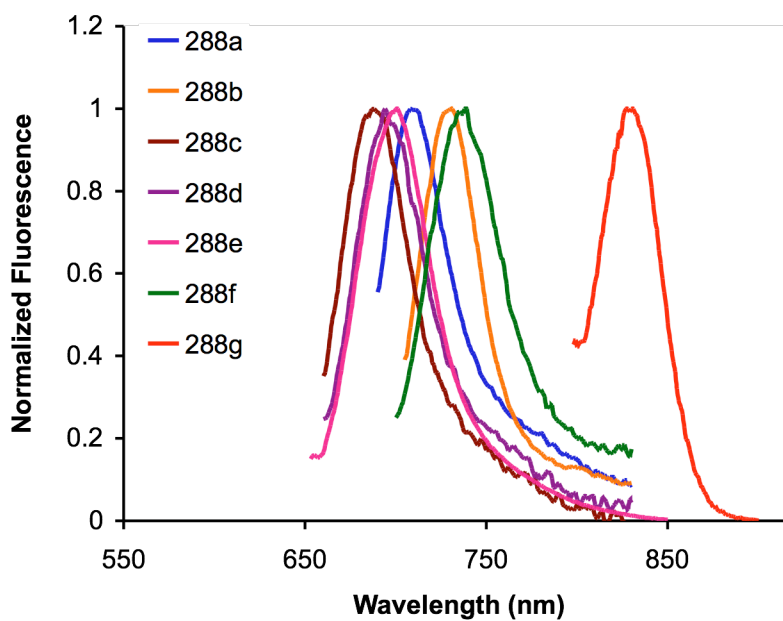
| entry | dye         | $\lambda_{\text{abs}}$ (nm) | $\epsilon$ ( $\text{M}^{-1} \text{cm}^{-1}$ ) | $\lambda_{\text{em}}$ (nm) | fwhm <sup>a</sup> (nm) | $\Phi$ <sup>b</sup> |
|-------|-------------|-----------------------------|---|----------------------------|------------------------|---------------------|
| 1     | <b>B</b>    | 655                         | 79 000  | 676                        | -                      | 0.34                |
| 2     | <b>F</b>    | 693                         | 85 000  | 717                        | -                      | 0.36                |
| 3     | <b>288a</b> | 680                         | 109 000                                       | 711                        | 47                     | 0.18 ± 0.01         |
| 4     | <b>288b</b> | 702                         | 84 120  | 731                        | 30                     | 0.42 ± 0.03         |
| 5     | <b>288c</b> | 640                         | 73 850  | 688                        | 47                     | 0.07 ± 0.01         |
| 6     | <b>288d</b> | 650                         | 55 000  | 694                        | 47                     | 0.10 ± 0.01         |
| 7     | <b>288e</b> | 653                         | 71 600  | 701                        | 35                     | 0.10 ± 0.01         |
| 8     | <b>288f</b> | 692                         | 66 200  | 738                        | 50                     | 0.20 ± 0.01         |
| 9     | <b>288g</b> | 798                         | 68 610  | 830                        | 30                     | 0.07 ± 0.01         |

<sup>a</sup>Full width at half maximum peak height. <sup>b</sup>Measured in 1% pyridine/toluene, Zn-phthalocyanine standard ( $\Phi = 0.30$  in the same solvent).

a



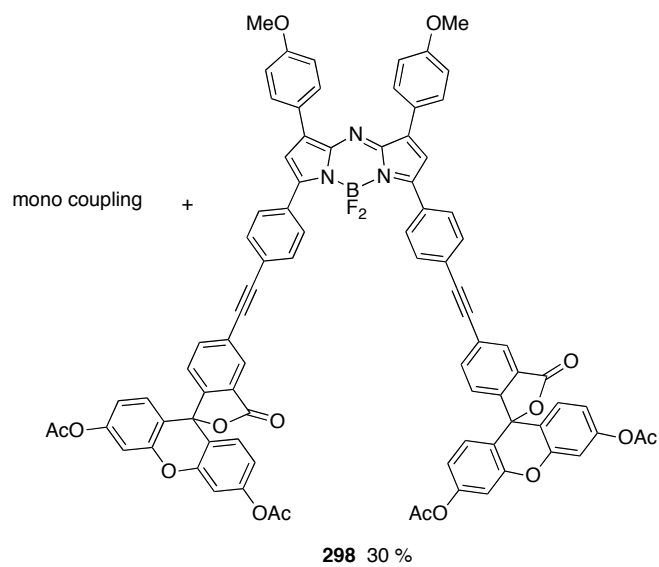
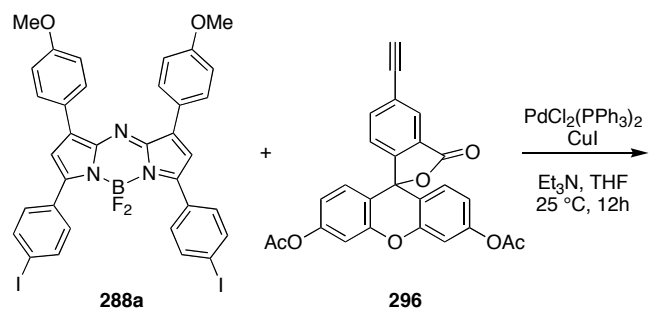
b



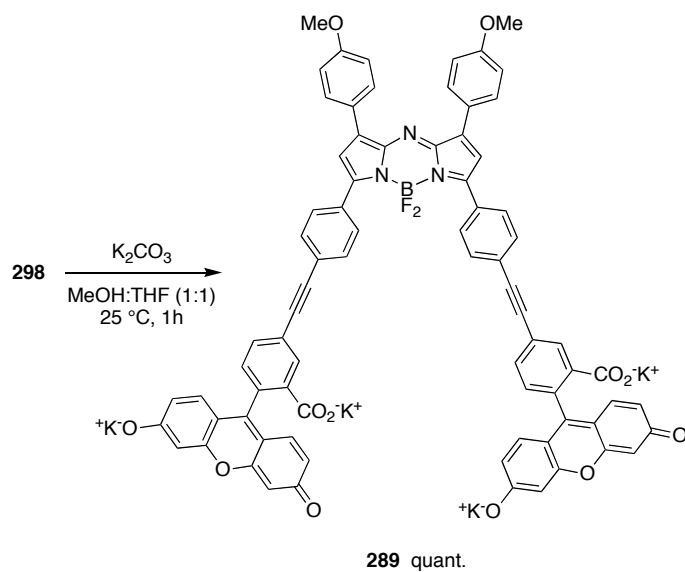
**Figure 2.8.** a Normalized absorption and b fluorescence spectra of compounds 288a – g in toluene at 5 μM.

### 3. Synthesis of Through-bond Energy Transfer Cassettes **289** and **290**

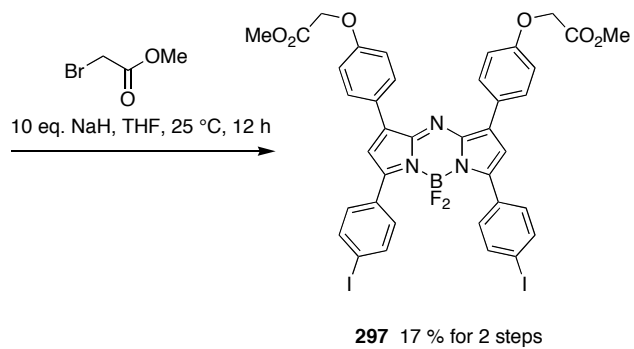
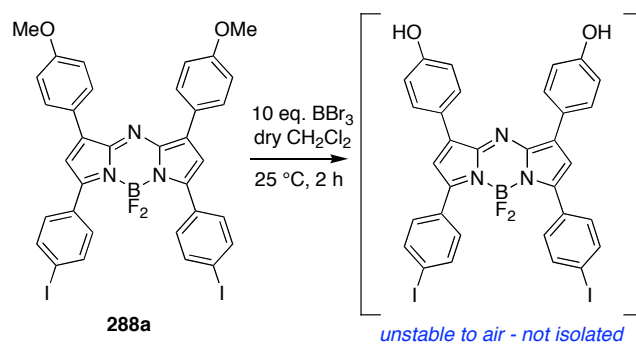
Scheme 3 shows syntheses of molecules **289** and **290** that have donor fluorescein-derived entities attached to BODIPY cores. These molecules were made to test their efficacy as energy transfer cassettes. The difference between compounds **289** and **290** is only a carboxylic acid linker in the acceptor part. Throughout this donor fragment was derived from the ethynyl fluorescein diacetate **296**<sup>280,293</sup> which served as a Sonogashira<sup>294</sup> coupling partner for the aza-BODIPYs **288a** or **297**, respectively. Compound **297** was obtained via a one-pot, two step procedure involving deprotection and alkylation of **288a**. In the synthesis of compound **297**, demethylation of the aza-BODIPY **288a** gave an intermediate with two phenolic-OH groups. This was unstable to air, hence it was alkylated without isolation at that stage. The final step in both syntheses was removal of the acetate groups from the fluorescein parts (potassium carbonate or TMSOK<sup>295</sup>); in the synthesis of compound **290** this also hydrolyzed the methyl ester functionality. Overall, the synthesis of cassette **289** was reasonably straightforward. However, cassette **290** was practically more difficult to prepare because of the instability of the intermediate mentioned above, and the need to isolate the final product via RP-HPLC. We were unable to fully and properly characterize compound **290** by NMR (<sup>1</sup>H and <sup>13</sup>C) in most organic solvents, including CD<sub>3</sub>CO<sub>2</sub>D and D<sub>2</sub>O, because the compound aggregated. However, compound **299** was fully characterized. Synthesis of compound **290** was supported by mass spectrometry analysis, and UV-fluorescence properties.

**Scheme 2.3. a. Synthesis of cassettes 289 and b. 290.****a**

## Scheme 2.3. Continued

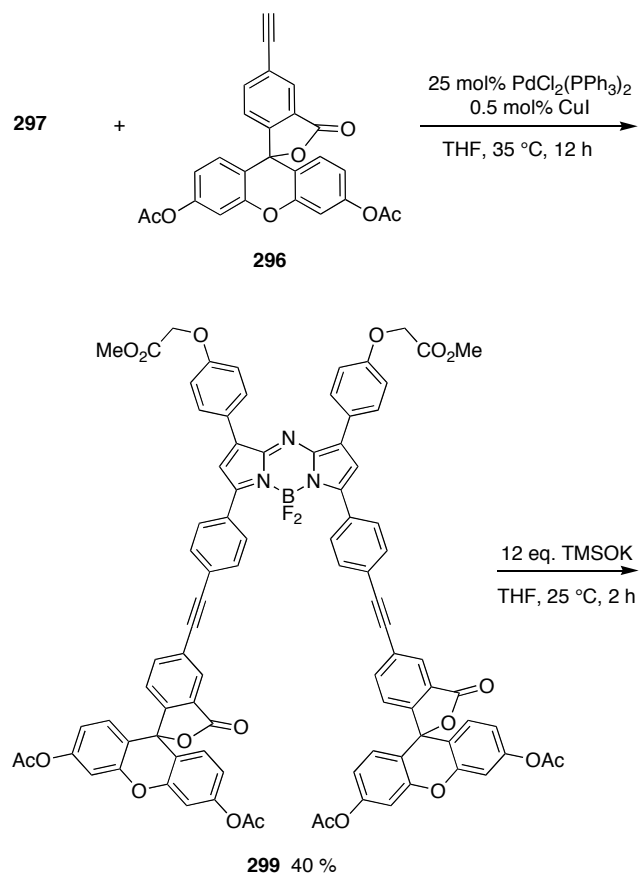


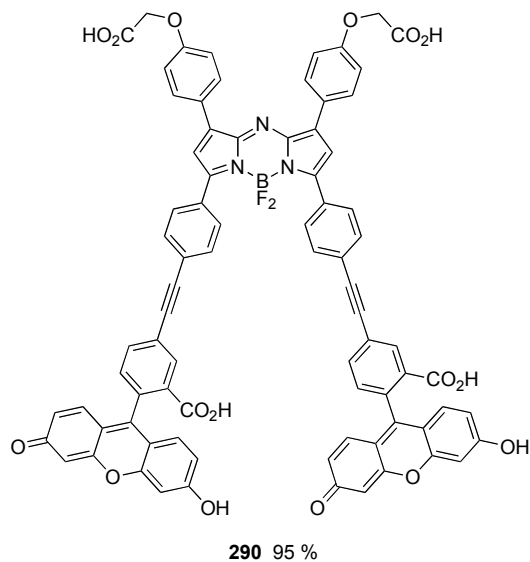
b





## Scheme 2.3. Continued



**Scheme 2.3. Continued****4. Spectroscopic Studies of Cassettes 289 and 290**

The absorption and emission spectra of cassettes **289** and **290** are solvent and pH dependent, reflecting the characteristics of the fluorescein part. This is consistent with the properties of fluorescein itself.<sup>85, 296-297</sup> Fluorescein tends to close to its lactone form at pH values of somewhat less than 6.5, and it is not particularly fluorescent in that state (Figure 2.9). Such pH-dependencies are undesirable if these cassettes were to be used as probes for imaging biomolecules.

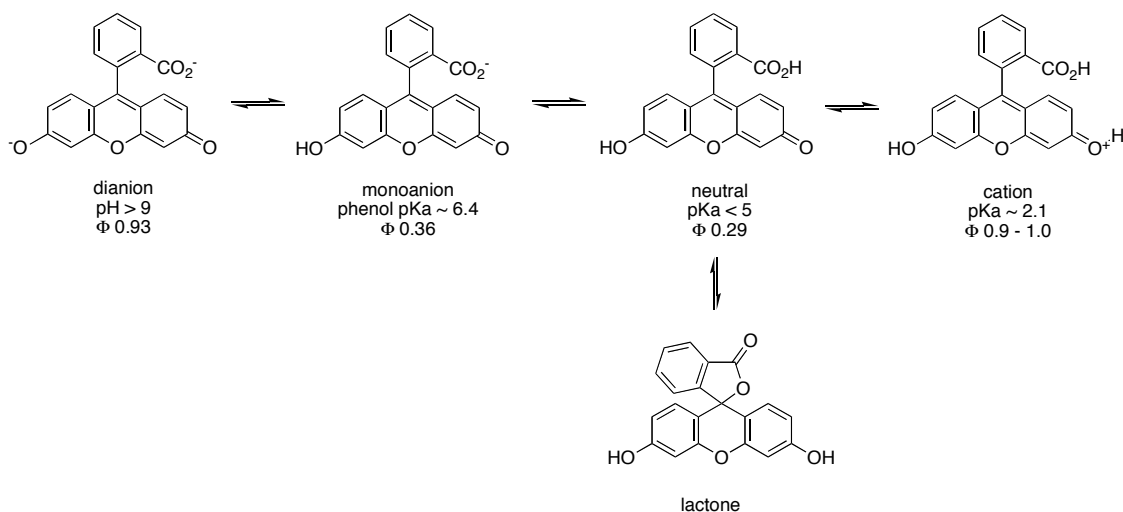
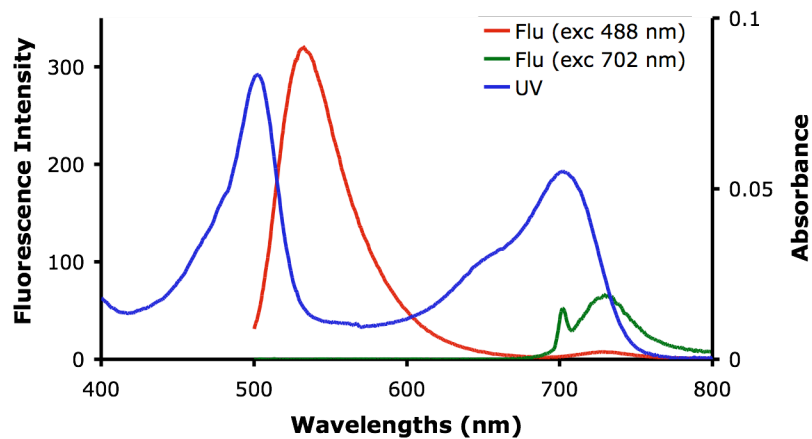


**Figure 2.9.** pH dependency of fluorescein fluorescence quantum yield.

Preliminary investigations of the spectroscopic properties of compound **289** showed little to no energy transfer from the donor to the acceptor in a 1:1 mixture of THF:buffer pH 7.4 (Figure 2.10a) *ie* little to no fluorescence from the aza-BODIPY (eg at 730 nm) was observed, and only fluorescence emission from the fluorescein was seen upon excitation of the donors at 488 nm,. To test if aggregation was responsible for this poor energy transfer, a concentration study was performed. No significant shift could be seen for both the absorption maxima of the donor and acceptor at 502 and 702 nm, respectively (Figure 2.10b). Further, the relationship between fluorescence intensity and concentration was essentially linear (Figure 2.10c). However, increasing concentrations of the non-ionic detergent Triton X-100 had significant effect on the system. The absorption peak of the fluorescein diminished with increased concentration of Triton X-100 (Figure 2.10d), and ultimately no peak was observed. The fluorescence emission of the donor showed the same tendency; no emission was observed at high concentration of Triton X-100 (Figure 2.10e). On the other hand, the fluorescence emission from the aza-BODIPY increased with increasing concentration of Triton X-100 (Figure 2.10f). It appears that in presence of the non-ionic detergent Triton X-100, the fluorescein is converted to its non-fluorescent lactone form. This change (from the quinoid to the lactone form) can occur due to the presence of the polyoxyethylene group in Triton X-100. It is well established that fluorescein dye retains its lactone form in presence of solvents having oxygen groups. Compound **290** showed similar results.

a



b

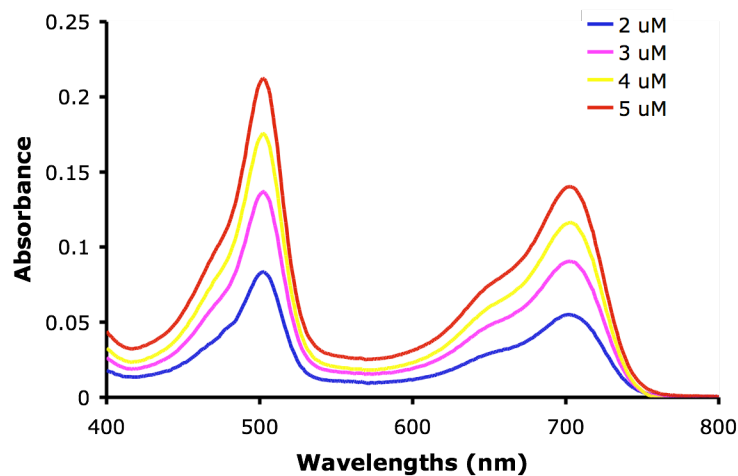
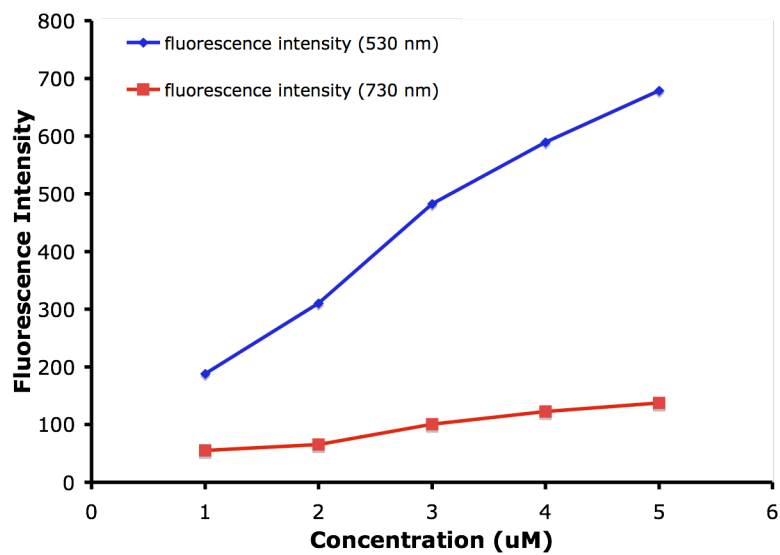


**Figure 2.10.** Spectra of: **a** UV absorption and fluorescence spectra (excitation at 488 and 702 nm) of **289** in 1:1 THF:buffer pH 7.4; **b** UV absorption of **289** with increasing concentration of **289** in 1:1 THF:buffer pH 7.4; **c** fluorescence intensities (at 530 and 730 nm) versus concentration of compound **289** in 1:1 THF:buffer pH 7.4; **d** UV absorption of compound **289** in 1:1 THF:buffer pH 7.4 with increasing amount of Triton-X 100; **e** fluorescence intensity of compound **289** upon excitation at 488 nm with increasing amount of Triton-X 100; **f** fluorescence intensity of compound **289** upon excitation at 702 nm with increasing amount of Triton-X 100.

c



d

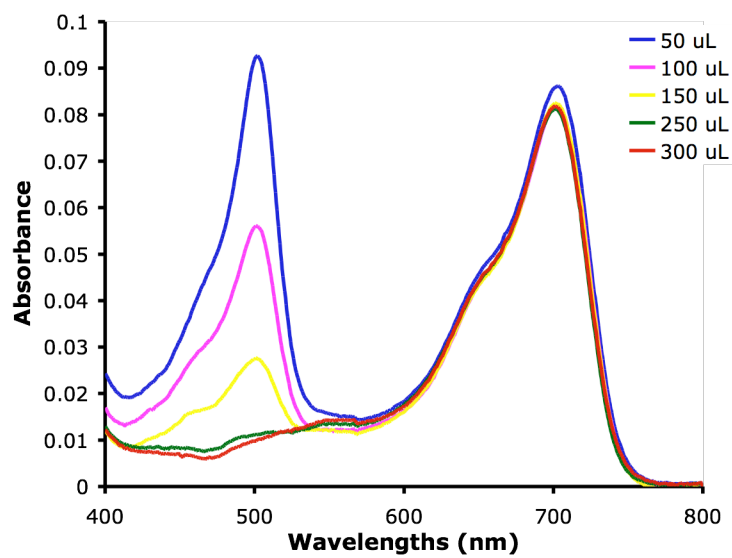
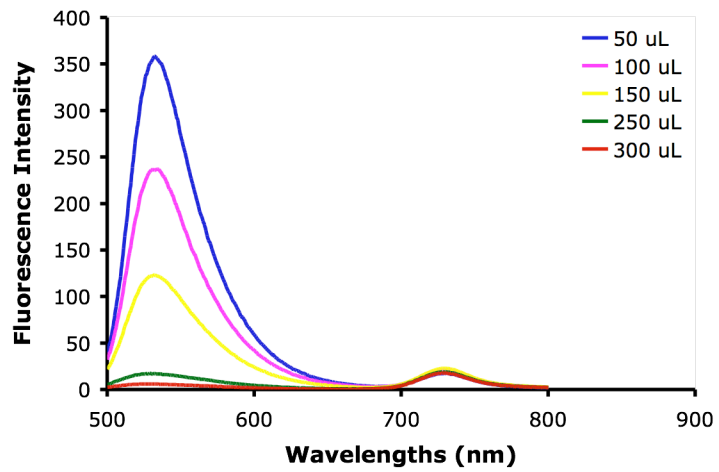


Figure 2.10. Continued.

e



f

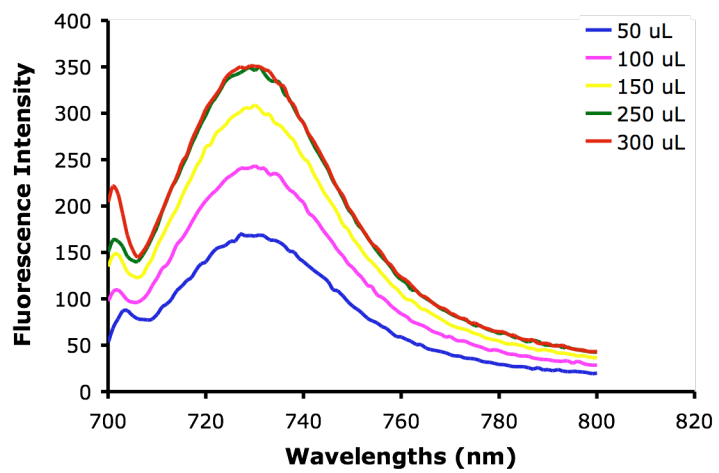


Figure 2.10. Continued.

### C. Conclusions

These studies show that the fluorescence emissions observed from aza-BODIPY dyes can be manipulated by altering the aryl-substituents. Red-shifts in the fluorescence tend to correspond to strongly electron donating *para*-groups, at least for the 3-aryl substituent. A series of seven functionalized aza-BODIPY dyes were prepared. Of these, compound **288a** proved to be a useful starting material for attachment of alkyne-based donor entities. In this study, the donor was a fluorescein-derived alkyne. Cassette **289** prepared from this coupling procedure exhibited absorption and fluorescence characteristics that were highly dependent on pH and solvent media. These observations correlate with equilibria at the fluorescein part corresponding to lactone formation, and to solvent polarity effects that seem to be influenced by the addition of a non-ionic detergent. Overall, fluorescein is probably not a good donor for cassettes designed for applications around physiological pH values. Aza-BODIPY dyes have great potential application as biomolecular probes if they can be modified to increase solubility in aqueous media thereby decreasing aggregation.

## CHAPTER III

### RING CONSTRAINED NEAR-IR AZA-BODIPY DYES

#### A. Introduction

Surprisingly few fluorescent probes emit in the near-IR region with high quantum yields.<sup>298</sup> Such compounds are valuable for intracellular imaging because autofluorescence in cells tend to obscure emissions at wavelengths below approximately 550 nm, but this factor becomes less of an issue at much longer wavelengths. Probes that emit in the 700 – 900 nm region are, therefore, relatively easy to visualize inside cells.<sup>299</sup> Cyanine dyes are currently the most widely used tags for visualization in this wavelength range, but they have relatively poor quantum yields.<sup>300</sup> Thus there is need for new fluorescent probes that emit efficiently above 700 nm.

BODIPY dyes are popular in biotechnology because they tend to have relatively sharp fluorescence emission characteristics, and high quantum yields.<sup>301</sup> However, the emission wavelengths of most BODIPY dyes are in the 530 – 630 nm range, and this is sub-optimal for intracellular or tissue imaging (*vide supra*). Previous work from our group explored two modification strategies for shifting BODIPY-fluorescence emissions to the red (Figure 3.1a). The first was to prepare “ring extended” BODIPY dyes, eg **N**, from heterocycles having more conjugated aromatic systems.<sup>302</sup> In the second, demethylation and intramolecular cyclization of the BODIPY **O** afforded a system **P** wherein non-radiative loss of energy via rotation around a C-Ar bond was prevented by B-O bond formation.<sup>303</sup> Comparison of data presented in Figure 3.1 for **O** with that for **N** and **P** indicates both strategies were effective, but still the emission wavelength was less than 700 nm.

Recent contributions from O’Shea and co-workers have elegantly demonstrated that tetraaryl-substituted aza-BODIPY dyes, like **Q** (Figure 3.1b), in solution fluoresces at significantly high wavelengths than typical BODIPY systems.<sup>304,305</sup> In an exciting development, Carreira et al prepared the ring-extended azaBODIPY dye **R** and showed it fluoresced at well over 740 nm.<sup>306</sup> We were therefore motivated to prepare compound **300** and study its fluorescence properties to complete this intriguing correlation of structure and fluorescence properties.



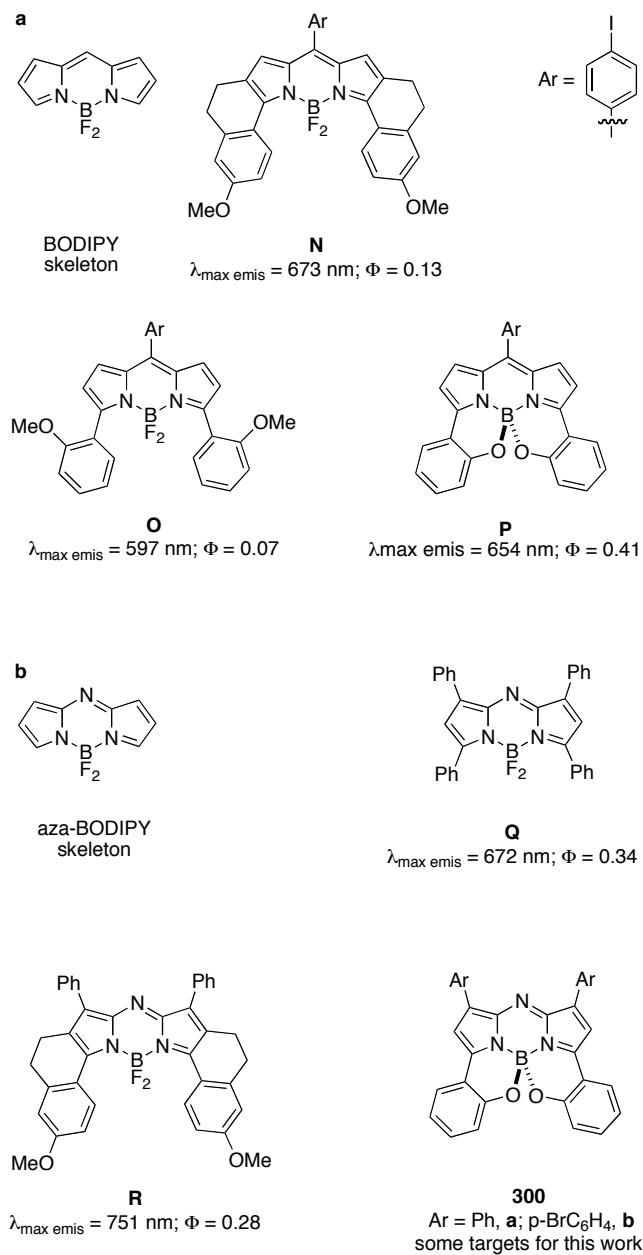


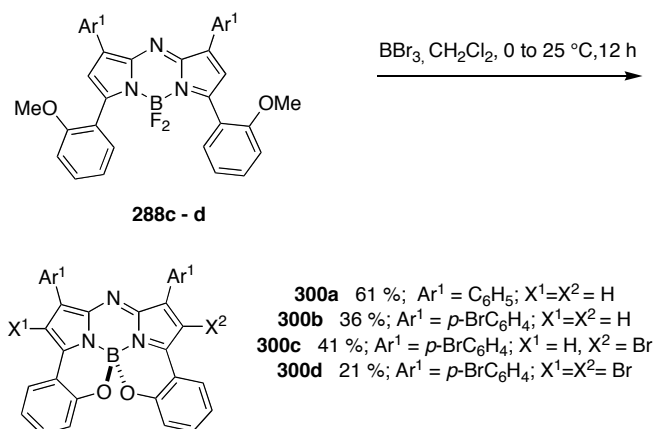
**Figure 3.1.** Comparison of fluorescence emission wavelength maxima and quantum yields (both in CHCl<sub>3</sub>) for: **N** a “ring-extended” BODIPY; **O** an aryl-substituted BODIPY; **P** a similar, but constrained, aryl substituted BODIPY; **Q** a tetraphenyl-substituted azaBODIPY; and **R** a “ring extended” aza-BODIPY. Compound **300** is the focus of this research project.

## B. Results and Discussion

### 1. Synthesis

Scheme 3.1 shows the synthesis of the target aza-BODIPY **300**. Compounds **300** are synthesized from the corresponding *ortho*-substituted aza-BODIPY dyes **288c** and **288d** by demethylation of the methoxide groups with boron tribromide. We anticipated this would lead to spontaneous cyclization giving the target materials **300a** - **b**. However, in addition to these, compounds corresponding to bromination of the azaBODIPY framework, *ie* **300c** - **d** were also observed. This is somewhat surprising since this did not occur for synthesis of **P**, but it is also potentially useful if the compounds are to be modified further.

**Scheme 3.1.** Synthesis of target aza-BODIPY **300**.



### 2. Spectroscopic Properties

Figure 3.2, figure 3.3 and Table 3.1 compare the electronic spectral characteristics of “less constrained” and “constrained” compounds **288c**, **288d** and **300a** - **d**. The constraint caused by forming the B-O bonds in **300** gave bathochromic shifts in both the absorption and emission maxima, and as much as a seven fold increase in the quantum yields. Introduction of bromine substituent in **300c** and **300d** did not result in a pronounced quenching of the fluorescence, contrary to some similar systems.<sup>304</sup>

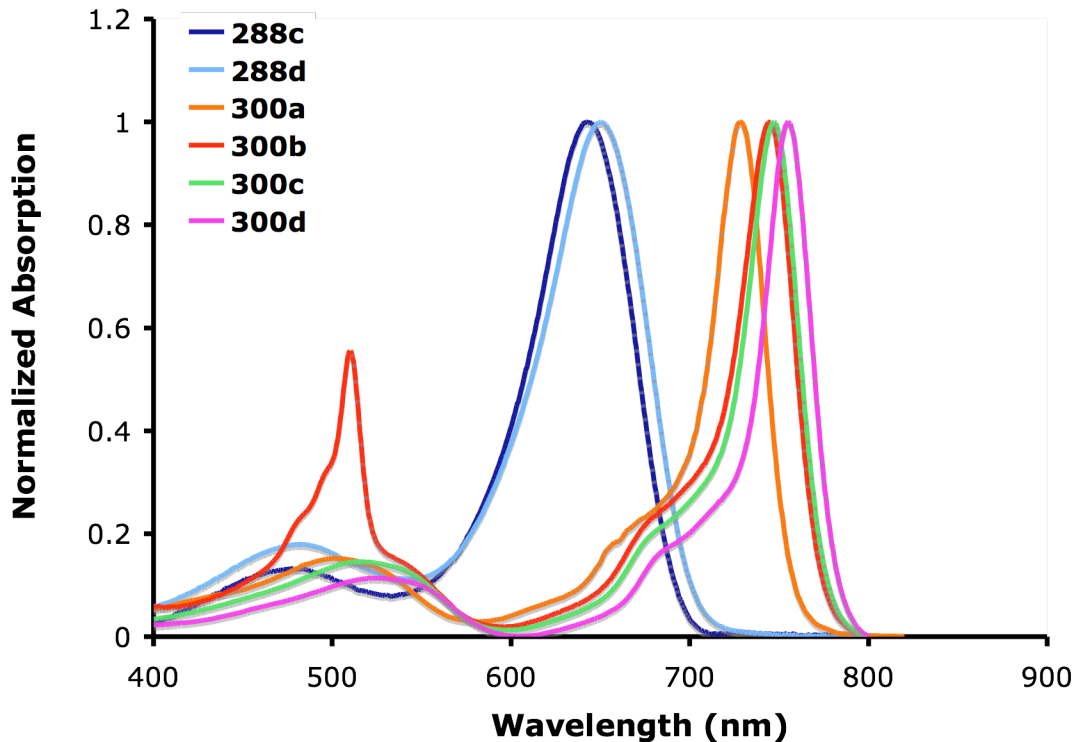


Figure 3.2. Absorption (5  $\mu$ M in PhMe) spectra of 288c - d and 300a - d.

Table 3.1. Spectroscopic properties of 288c–d and 300a–d.

|      | $\lambda_{\text{max}}/\text{nm}$<br>(abs) <sup>a</sup> | $\lambda_{\text{max}}/\text{nm}$<br>(flu) <sup>a</sup> | fwhm/nm | $\Phi^b$        |
|------|--|--|---------|-----------------|
| 288c | 642  | 688  | 43      | $0.07 \pm 0.01$ |
| 300a | 728  | 746  | 36      | $0.51 \pm 0.02$ |
| 288d | 650  | 699  | 45      | $0.10 \pm 0.01$ |
| 300b | 745  | 760  | 36      | 0.46            |
| 300c | 747  | 769  | 38      | 0.35            |
| 300d | 755  | 776  | 36      | 0.36            |

[a] a In PhMe [b] In 1% pyridine in PhMe, ZnPtc was used as a standard ( $\Phi=0.30$ )

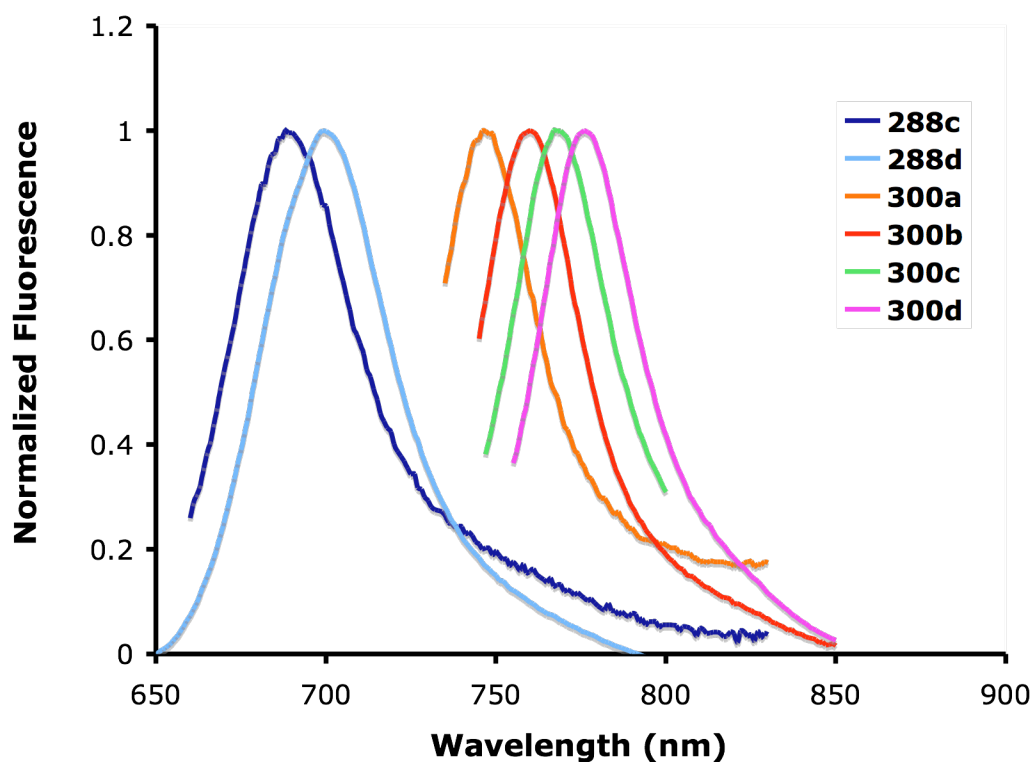


Figure 3.3. Fluorescence (5  $\mu$ M in PhMe) spectra of **288c - d** and **300a - d**.

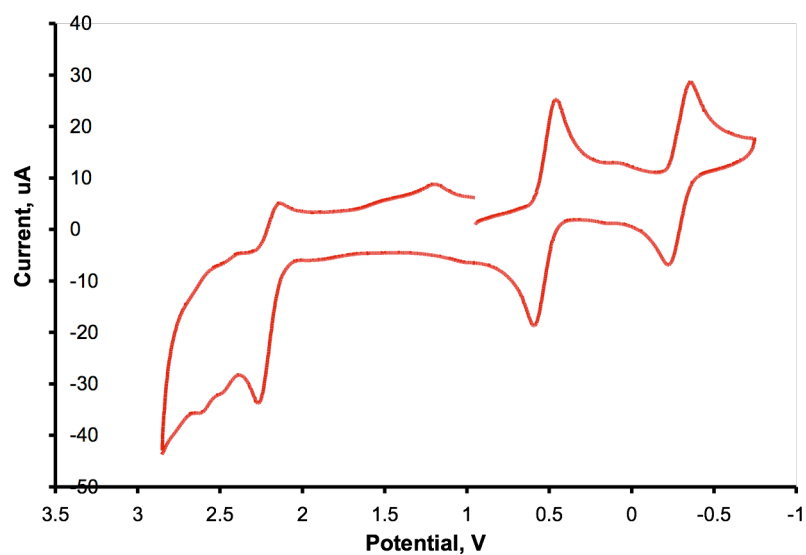
### 3. Electrochemistry

Electrochemical studies were performed for compounds **288a** (Figure 3.4) and **300a** (Figure 3.5) using dichloromethane as solvent and tetra-*n*-butylammonium tetrafluoroborate (TBA $\cdot$ BF $_4$ ) as supporting electrolyte; the data are summarized in Table 3.2. Both compounds displayed reversible oxidation waves, with half-wave potential of + 0.528 and + 0.934 V vs NHE (normal hydrogen electrode) for **288a** and **300a**, respectively. Reversible reduction waves with half-wave potentials of - 0.291 and -0.105 V vs NHE were observed for **288a** and **300a**, respectively. Compound **288a** is easier to oxidize than **300a** by 406 mV. Reduction of **288a** is more difficult (because the HOMO-LUMO gap is bigger, see above), with the corresponding half-wave potential being decreased by 186 mV relative to **300a**.

**Table 3.2.** Electrochemical properties of **288c** and **300a**.

|      | $E_{1/2}$ V vs NHE           |                              |
|------|------------------------------|------------------------------|
|      | bodipy <sup>•+</sup> /bodipy | bodipy Bodipy/ <sup>•+</sup> |
| 288c | 0.528                        | - 0.291                      |
| 300a | 0.934                        | - 0.105                      |

[a] The redox potentials were measured by cyclic voltammetry in CH<sub>2</sub>Cl<sub>2</sub>, containing 0.1 M TBA•BF<sub>4</sub> with a scan rate of 0.2 V/s [b] Ferrocene was used as internal reference [c] A Ag/AgCl was used as reference electrode, and a platinum coil served as a counter electrode.

**Figure 3.4.** Cyclic voltammogram of compound **288c**.

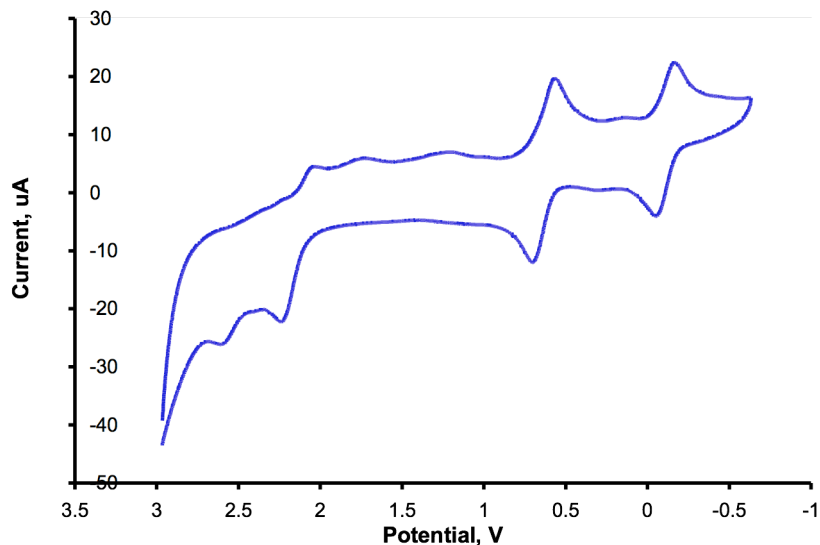


**Figure 3.5.** Cyclic voltammogram of compound **300a**.

#### **4. Frontier Orbitals Calculations**

B3LYP/6-31G\* calculations on compounds **288c**, **300a** and **300d** gave low energy conformers that have  $C_2$  symmetry axes passing through the *B*- and the bridging-*N*-atoms (Figure 3.6). The HOMO-LUMO energy gaps calculated were significantly less for compound **300a** and **300d** relative to **288a**, corresponding to a 2.19 to 2.11 and 2.05 eV drop on cyclization for **300a** and **300d**, respectively (Table 3.3). The dihedral angles between the aryl substituents and the heterocycle are almost the same, aligning them in near parallel orientations (Table 3.4). A crystal structure for compound **300d** (Figure 3.7) as a single crystal, and the structure in the solid state corresponded closely with those derived from the B3LYP calculations (Table 3.5).

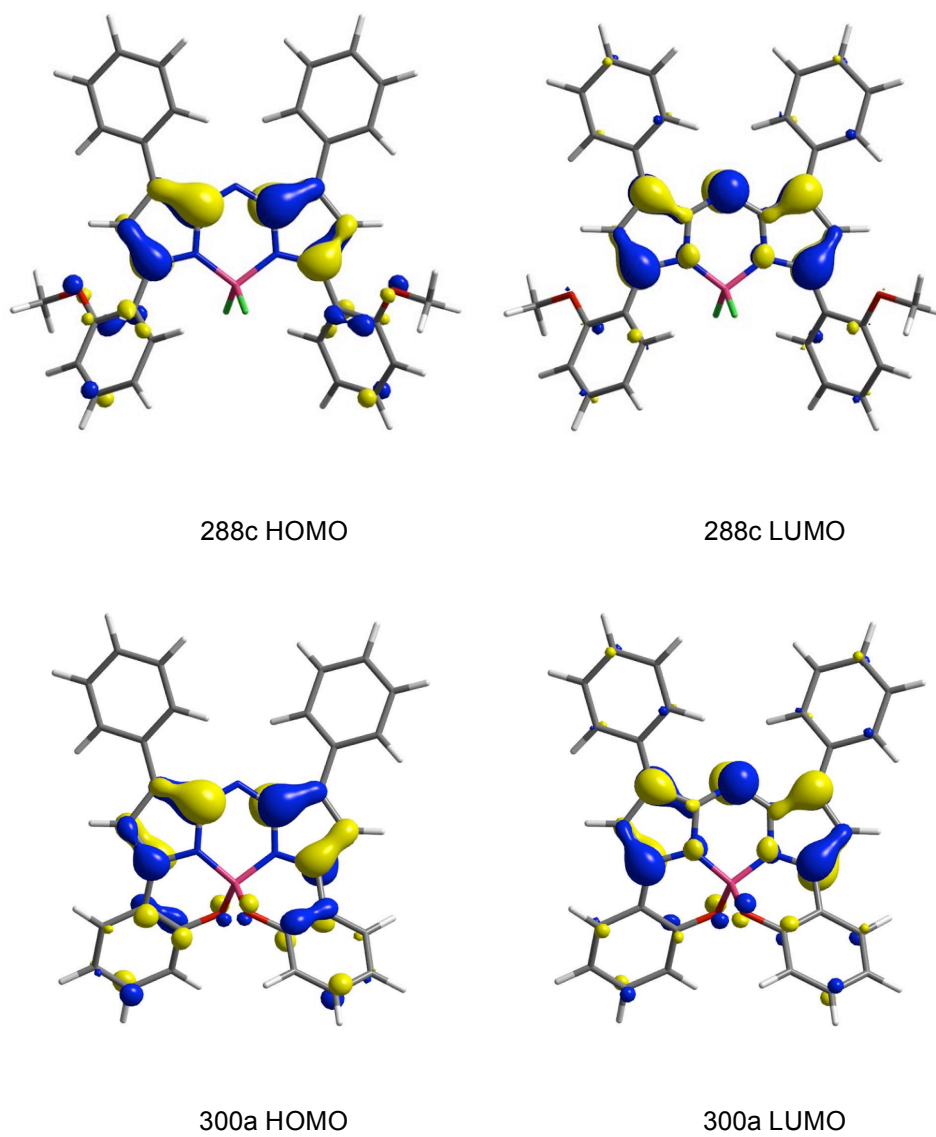


**Figure 3.6.** HOMO and LUMO for compound **288c**, **300a** and **300d**.

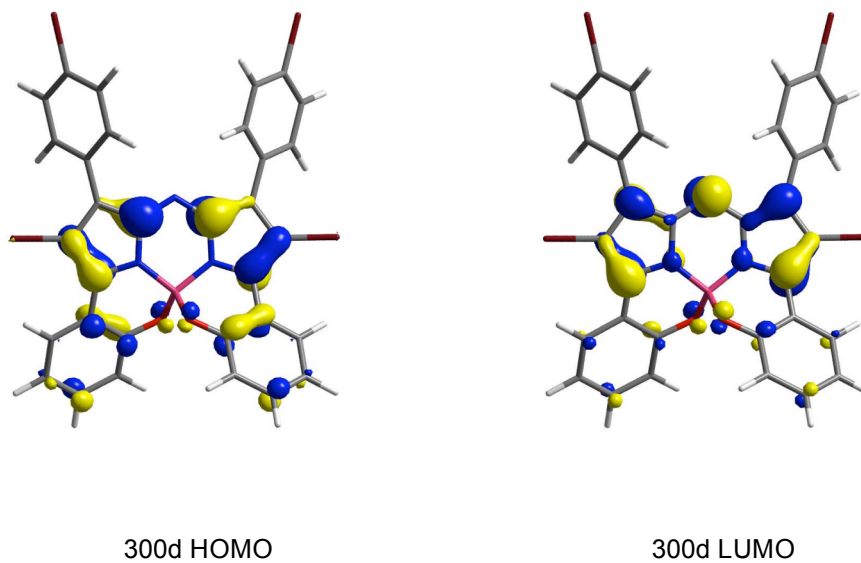


**Figure 3.6.** Continued.

**Table 3.3.** Excitation energies from B3LYP calculations.

| Comp'd | Excited state | Transition character       | $\Delta E$ (eV) |
|--------|---------------|----------------------------|-----------------|
| 288a   | 1             | HOMO $\rightarrow$ LUMO    | 2.197           |
|        | 2             | HOMO -1 $\rightarrow$ LUMO | 3.066           |
|        | 3             | HOMO -2 $\rightarrow$ LUMO | 3.07            |
| 300a   | 1             | HOMO $\rightarrow$ LUMO    | 2.111           |
|        | 2             | HOMO -1 $\rightarrow$ LUMO | 2.854           |
|        | 3             | HOMO -2 $\rightarrow$ LUMO | 3.122           |
| 300d   | 1             | HOMO $\rightarrow$ LUMO    | 2.047           |
|        | 2             | HOMO -1 $\rightarrow$ LUMO | 2.734           |
|        | 3             | HOMO -2 $\rightarrow$ LUMO | 2.886           |



**Table 3.4.** Selected parameters for compounds **288c** and **300a**.

|  | 288c  | 300a  |
|--|-------|-------|
|  |       |       |
| Bond lengths [Å]                                 |       |       |
| B – F  | 1.402 | -     |
| B – O  | -     | 1.476 |
| B – N  | 1.569 | 1.519 |
| N <sup>2</sup> – C <sup>1</sup>                  | 1.398 | 1.392 |
| C <sup>1</sup> – N <sup>1</sup>                  | 1.322 | 1.329 |
| C <sub>phenyl</sub> – O                          | 1.365 | 1.347 |
| Valence angles [°]                               |       |       |
| F – B – N  | 111.6 | -     |
| O – B – N  | -     | 106.2 |
| B – N <sup>2</sup> – C <sup>1</sup>              | 122.4 | 125.9 |
| F – B – F  | 110.9 | -     |
| O – B – O  | -     | 106.9 |
| C <sup>2</sup> – N <sup>1</sup> – C <sup>1</sup> | 120.4 | 118.5 |
| O – C – C  | 116.6 | -     |
| C – O – B  | -     | 116.5 |
| Torsion angles [°]                               |       |       |
| φ <sub>1</sub>                                   | 133.6 | 161.8 |
| φ <sub>2</sub>                                   | 133.6 | 161.8 |
| φ <sub>3</sub>                                   | 151.6 | 156.3 |

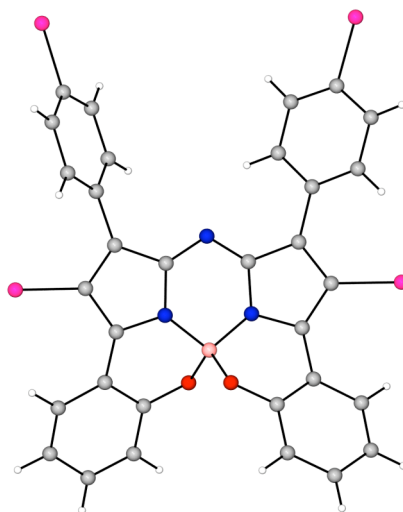


**Figure 3.7.** X-Ray structure of compound **300d**.

**Table 3.5.** Comparisons of some key parameters for **300d**.

| bond lengths [Å]                 | 300d (exp) | 300d (theoretical from B3YLP calc.) |
|----------------------------------|------------|-------------------------------------|
| B – O <sup>1</sup>               | 1.474      | 1.472                               |
| B – O <sup>2</sup>               | 1.459      | 1.473                               |
| B – N <sup>1</sup>               | 1.529      | 1.519                               |
| N <sup>2</sup> – C <sup>1</sup>  | 1.341      | 1.328                               |
| C <sup>1</sup> – N <sup>1</sup>  | 1.381      | 1.388                               |
| C <sup>3</sup> – N <sup>1</sup>  | 1.357      | 1.354                               |
| C <sup>1</sup> – C <sup>5</sup>  | 1.447      | 1.441                               |
| C <sup>5</sup> – C <sup>4</sup>  | 1.380      | 1.398                               |
| C <sup>4</sup> – C <sup>3</sup>  | 1.429      | 1.434                               |
| C <sup>4</sup> – Br <sup>1</sup> | 1.880      | 1.877                               |
| O <sup>2</sup> – C <sup>10</sup> | 1.364      | 1.348                               |

**Table 3.5.** Continued.

| valence angles [°]   |       |       |
|----------------------|-------|-------|
| $O^1 - B - O^2$      | 107.8 | 107.9 |
| $O^1 - B - N^1$      | 116.2 | 116.3 |
| $O^1 - B - N3^1$     | 106.8 | 106.1 |
| $C^3 - N^1 - C^1$    | 110.1 | 110.1 |
| $C^3 - N^1 - B^1$    | 122.4 | 122.6 |
| $C^1 - N^1 - B^1$    | 125.7 | 125.6 |
| $C^2 - N^2 - C^1$    | 117.0 | 118.1 |
| $C^{10} - O^2 - B^1$ | 114.2 | 115.6 |
| $N^2 - C^1 - N^1$    | 123.8 | 123.3 |
| $N^2 - C^1 - C^5$    | 127.7 | 128.5 |
| $N^1 - C^1 - C^5$    | 108.2 | 107.8 |
| $N^1 - C^3 - C^4$    | 106.4 | 106.9 |
| $N^1 - C^3 - C^9$    | 117.8 | 116.6 |

### C. Conclusion

In conclusion, the constrained azaBODIPYs **300** emit at longer wavelengths and with a higher quantum yields than comparable tetraaryl-substituted azaBODIPY dyes. Emission wavelengths of 746 - 776 nm are useful for applications in biotechnology. The azaBODIPY systems reported here are relatively<sup>307</sup> easy to prepare.

## CHAPTER IV

### SYNTHESES AND SPECTROSCOPIC PROPERTIES OF ENERGY TRANSFER SYSTEMS BASED ON SQUARAINES DYES\*

#### A. Introduction

##### 1. Squaraine Dyes

Squaraines are a novel class of organic dyes that are largely used for applications such as imaging, biological labeling, photodynamic therapy and nonlinear optics. They belong to the class of polymethyne dyes with resonance-stabilized zwitterionic structures (Figure 4.1).

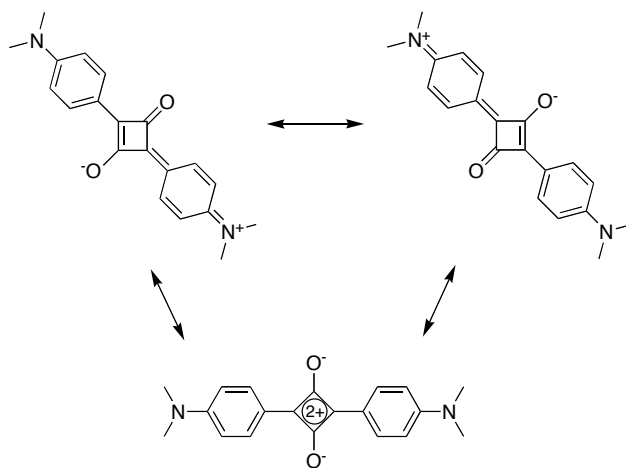


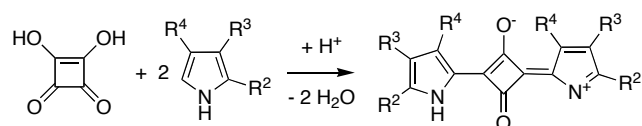
**Figure 4.1.** Resonance structures of squaraine dyes.

---

Reprinted with permission from "Syntheses and spectroscopic properties of energy transfer systems based on squaraines" by Guan-Sheng Jiao, Aurore Loudet, Hong Boon Lee, Stanislav Kalinin, Lennart B.-Å. Johansson and Kevin Burgess, 2003. *Tetrahedron*, 59, 3109-3116; copyright 2003, Elsevier Limited.

The first synthesis of squaraine dyes can be traced back to 1965 in the report of Triebs and Jacob, who were examining the action of pyrroles on squaric acid (Scheme 4.1).<sup>308</sup> Pyrroles reacted in a 2:1 molar ratio with squaric acid and produced an intensely colored condensation product.

**Scheme 4.1.** First synthesis of squaraine dyes.



Squaraines are generally prepared by condensation of electron-rich aromatic or heterocyclic compounds such as *N,N*-dialkylanilines, benzothiazoles, phenols, azulenes, and pyrroles with squaric acid.<sup>309-311</sup> Access to a variety of electron-rich aromatic and heterocyclic systems, which react with squaric acid, facilitated the design of symmetrical and unsymmetrical squaraine dyes with tunable optical properties. Furthermore, incorporating strong electron donors or extending the conjugation of the system allowed the synthesis of a large number of squaraines with near-IR absorption and emission. Because they emit in the near IR, and this region is far removed from the fluorescence of any biomolecules, squaraine are particularly attractive dyes for imaging, biological imaging.<sup>312</sup> The intense absorption and emission characteristic of squaraine dyes are associated with the donor-acceptor-donor type charge-transfer interaction.

## 2. “Donor acceptor” Cassettes

“Donor acceptor cassettes” (compounds in which a moiety absorbs at low wavelength and another emits at higher wavelength) based on through-space fluorescence energy transfer are common in biotechnology.<sup>313-319</sup> In such compounds, the ‘donor’, harvests energy from an excitation source and transmits it through space, via dipole–dipole coupling, to an ‘acceptor’ that then fluoresces. The donor and acceptor fragments in these cassettes are connected via a non-

conjugated linker (Figure 4.2.a). The efficiency of energy transfer in these systems depends on the distance between the donor and acceptor.

“Donor acceptor cassettes” in which the donor and acceptor fragments are conjugated<sup>278,320</sup> can have profound effects on the rates of energy transfer (ET) from the donor to the acceptor, and the ‘apparent Stokes’ shifts’ observed (Figure 4.2.b).<sup>321</sup> Conjugated ET systems of this kind have been investigated extensively in material science.<sup>322,323</sup> Such compounds can absorb at short wavelength and emit efficiently at much longer wavelengths, and can therefore be useful in applications that involve several multiplexed dyes, excited at one wavelength and observed at well dispersed longer wavelengths. Syntheses and spectral investigations of novel through-bond ET cassettes in which donors are directly conjugated to a squaraine acceptor (Figure 4.2.c) were therefore undertaken. Carbazole and similar heterocycles were used as donors since these absorb in the UV region at around 300 nm.

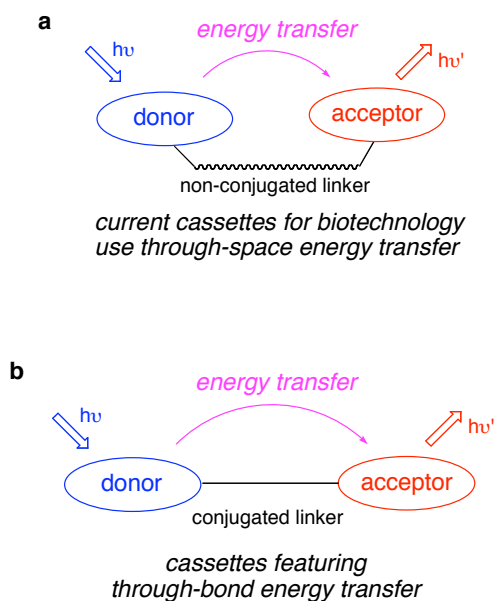


**Figure 4.2.** a) Through-space ET cassettes, b) through-bond ET cassettes, c) the acceptor fragments used in this study.

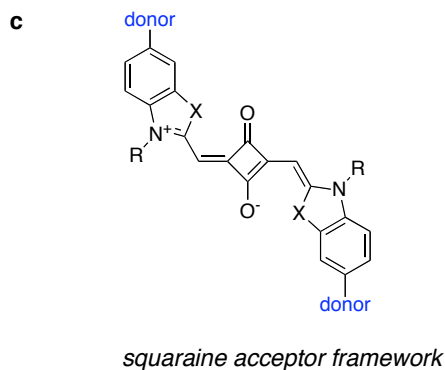


**Figure 4.2.** Continued.

## B. Results and Discussion

### 1. Synthesis

Compounds like **301** in which the squaraine fragment was formed from resorcinol derivatives were previously prepared in our laboratories; however, the products had low quantum yields. In retrospect, this is unsurprising because the 2,6-dihydroxyl substituents facilitate tautomerization processes, leading to radiationless decay.<sup>324</sup> Cassettes of type **302** were then prepared to avoid tautomerism problems. Quantum yields were not markedly increased, however, because another unfavorable characteristic comes into play for unsymmetrical squaraines; specifically, rotation about the bond labeled 'a' is facile because resonance favors single bond character here relative to bond 'b'. This effect makes electronic transmission through the squaraine system more difficult than it would otherwise be, depressing the quantum yield. Consequently, we focused on the synthesis of symmetrical squaraines **303** and **304** incorporating 3,3-dimethylindolenine and 2-methylbenzothiazole fragments, respectively (Figure 4.3).

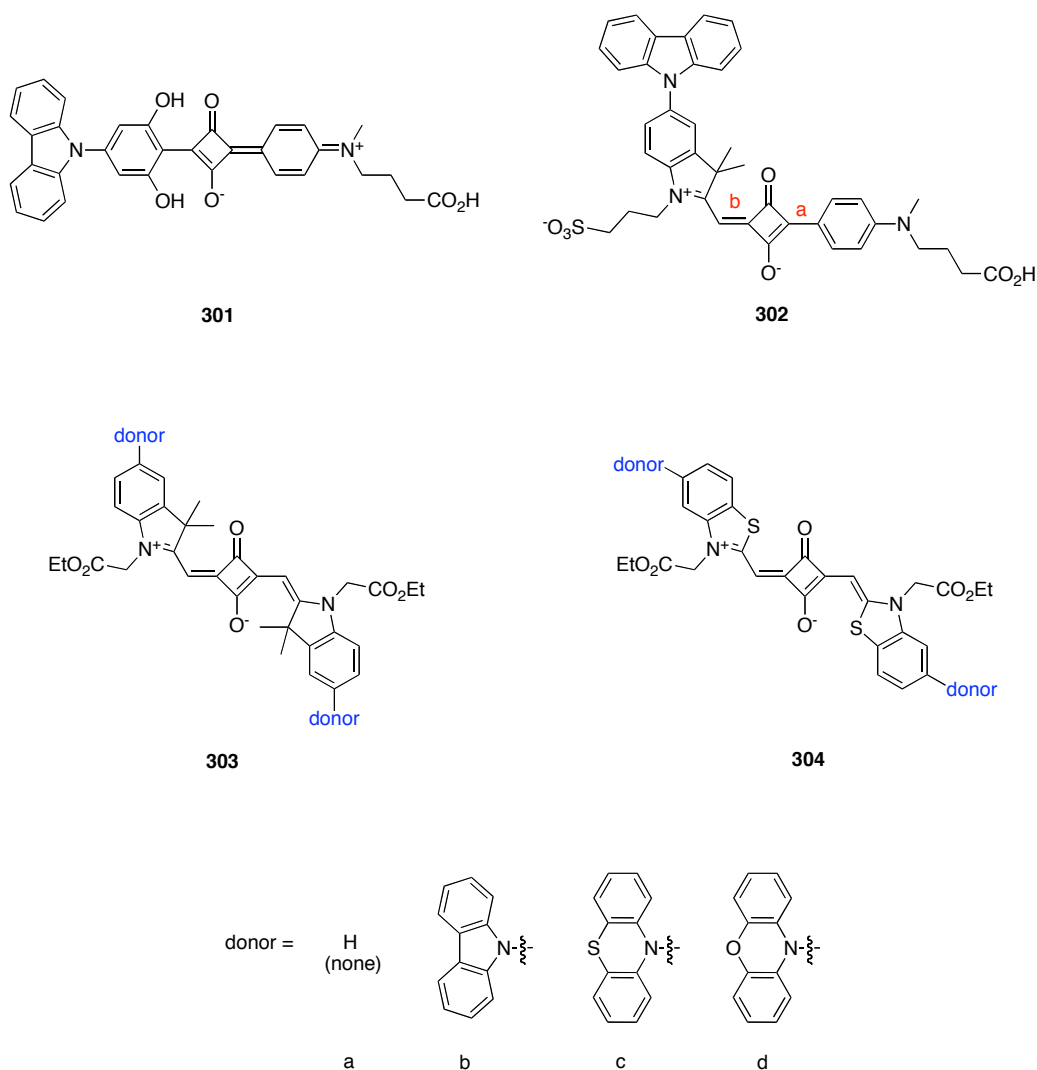
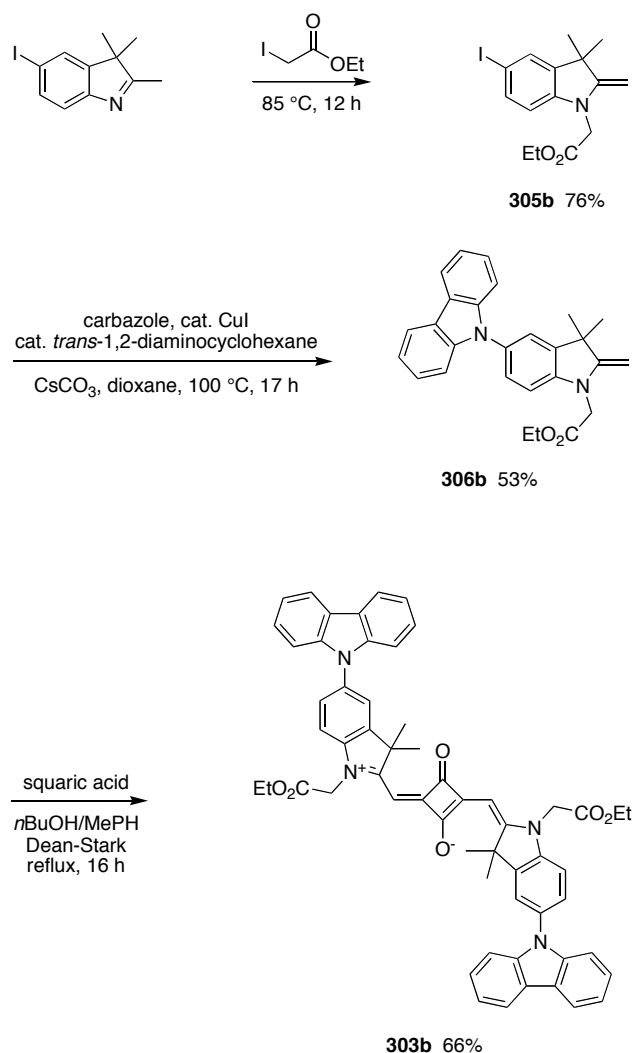


**Figure 4.3.** Donor-acceptor cassettes in this research.

Scheme 4.2 describes the syntheses of the cassettes **303b**. After N-alkylation of the iodoindolenine to give **305b**, copper-mediated couplings<sup>325</sup> were used to introduce the carbazole unit giving compounds **306b** in moderate yield (53%). Palladium-mediated couplings to achieve the same result were investigated briefly, but with little success.<sup>326</sup> Compound **306b** was condensed with squaric acid<sup>327</sup> to give the desired product **303b** as a blue metallic solid. The control compound **303a** was prepared via an abbreviated version of this sequence.



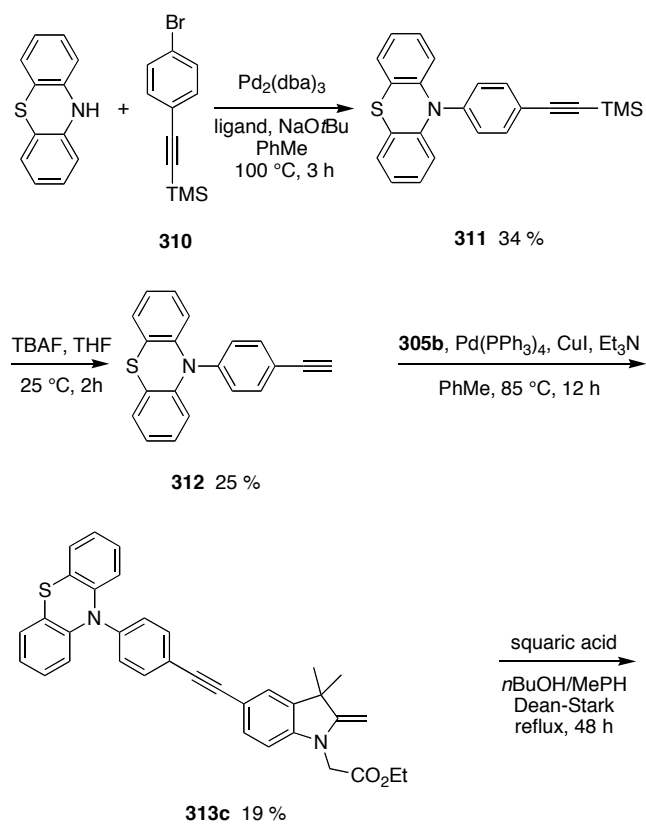
**Scheme 4.2.** Synthesis of cassette **303b**.



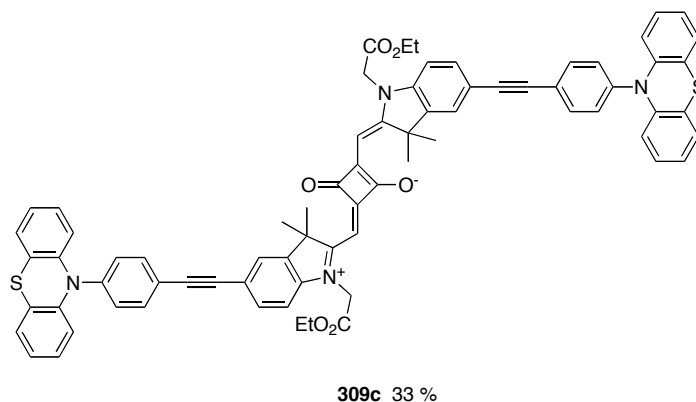
Attempt to synthesize **303c** eg. with phenothiazine as donor failed. We were unable to successfully couple the phenothiazine to the indolenine under the conditions developed for cassette **303b**. An alternative approach as shown in Scheme 4.3 was then undertaken to synthesize cassette **309c**. It started with the synthesis of 10-(4-ethynylphenyl)-10*H*-phenothiazine **312** via Sonogashira coupling between phenothiazine and **323**, and subsequent removal of the trimethyl silyl group in **311**. Compound **313c** was then obtained via another

Sonogashira coupling reaction with the indolenine derivative **305b**. Finally, compound **313c** was condensed with squaric acid to give the desired compound **309c** as a blue metallic solid.

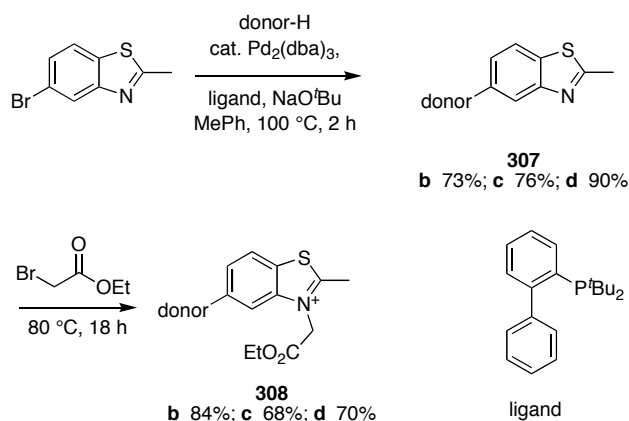
**Scheme 4.3.** Synthesis of cassettes **309c**.



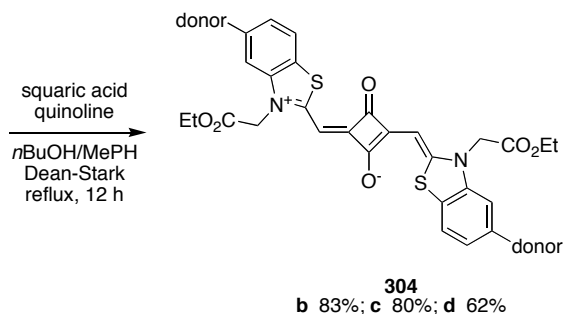
Scheme 4.3. Continued.



Cassettes **304b-d** were prepared by a post-doctoral associate in our laboratories, Dr. Guansheng Jiao. They were prepared via a similar procedure (Scheme 4.4) except that a palladium-mediated C–N coupling was used. The most notable difference between the two approaches is that the metal-catalyzed reactions gave higher yields in the second sequence (76–90%).<sup>329</sup>

Scheme 4.4. Synthesis of cassettes **304b-d**.

Scheme 4.4. Continued.



## 2. Spectroscopic Studies

A series of spectroscopic measurements were undertaken to test if compounds **303b** and **304b–d** behave as cassettes (rather than as simple conjugated molecules) and, if so, to quantitate their efficiencies. First, UV spectra of the molecules were recorded. If the UV spectrum of a particular system resembles that which would be obtained by superimposing UV spectra of the corresponding discrete donor and acceptor components, then the molecule is behaving as a cassette. Alternatively, if the UV is different, then the compound is behaving as a conjugated system. The UV spectra of compound **303b** overlaid with the spectrum of carbazole and **303a**, i.e. the donor and acceptor components, respectively is shown in Figure 4.4a. The UV spectrum of **303b** is very close to that which would be obtained by adding the donor (carbazole) and acceptor (**303a**) components. Consequently, this molecule behaves as a cassette with non-planar donor and acceptor systems in the ground state. Similar data were obtained for **304b–d** indicating they all function as cassettes (Figure 4.4).

Quenching of the donor fluorescence is one of the criteria that define a good cassette. If this quenching is complete then the ET efficiency is 100%, where:

$$ET_{\text{efficiency}} = \{100 \times [1 - (\text{fluorescence intensity of donor in cassette}) / (\text{fluorescence intensity of free donor})]\%$$

In our systems, the fluorescence of the free carbazole donor was so weak that accurate ET efficiency measurements proved to be impossible. In practice, it was also difficult to accurately measure the fluorescence quantum yield when exciting the donor group of the cassettes studied here. Thus, two important characteristics of the cassettes, ET efficiencies and fluorescence quantum yields, could not be measured directly.

ET efficiencies were therefore estimated using a different approach to circumvent the experimental difficulties outlined above; this involved the following line of reasoning:

The efficiency of ET in a cassette must be close to 100% if the fluorescence quantum yield of the acceptor group is the same when excited at the donor, or at the acceptor absorption;

If the ET efficiency is 1, then the ratio of the fluorescence excitation and the UV absorption spectra of the cassettes should be constant over the whole spectral region;

Fluorescence lifetimes of the cassettes **303b** and **304b-d** were measured upon excitation in the donor and acceptor regions. If the timescale of ET is 100 ps or slower, we expect to observe negative components in the fluorescence decay. No such component was found. It is also true that the average lifetimes must be longer when the donor is excited directly.

Table 4.1 summarizes the spectroscopic properties for **303b** and **304b-d**. The quantum yields values (0.23–0.37) show moderate fluorescence efficiencies. Rates of ET between the donor and the acceptor are likely to be fast relative to any thermal energy loss, so the quantum yields of the cassettes when irradiated in the donor region are likely to approximate to those of the acceptor components within them.

The average lifetimes are shown in Table 4.2. Fluorescence lifetime of the squaraine acceptor groups was very similar irrespectively of the excitation wavelength.

**Table 4.1.** Spectroscopic data for the compounds **303a,b** and **304b-d**

| Compound | $\lambda_{\max \text{ abs}}$ (nm) | $\lambda_{\max \text{ emiss}}$ (nm) | Apparent Stokes' shift (nm) | ET (%) <sup>a</sup> | $\Phi^b$ |
|----------|-----------------------------------|-------------------------------------|-----------------------------|---------------------|----------|
|          | below 350 nm                      |                                     |                             |                     |          |
| 303a     | 279, 344                          | 637                                 | 6 <sup>c</sup>              | -                   | 0.23     |
| 303b     | 293, 340                          | 659                                 | 366, 319                    | ~100                | 0.31     |
| 304a     | 310, 350                          | 679                                 | 10 <sup>c</sup>             | -                   | 0.33     |
| 304b     | 292, 339                          | 693                                 | 401, 354                    | ~100                | 0.37     |
| 304c     | 257, 315                          | 691                                 | 434, 376                    | ~100                | 0.33     |
| 304d     | 319                               | 688                                 | 369                         | ~100                | 0.36     |

<sup>a</sup> Determined indirectly,

<sup>b</sup> Excited at 590 nm for **303a, b** and 630 nm for **304a-d**,

<sup>c</sup> Actual Stokes' shift for **303a** and **304a**.

**Table 4.2.** The ratios of absorptions and fluorescence excitation spectra  $\{A(\lambda_{\text{ex}})/F(\lambda_{\text{ex}})\}$  and the average lifetimes of the acceptor group upon excitation of the donor and the acceptors of cassettes **303b** and **304b-d**

| Compound | Average $A(\lambda_{\text{ex}})/F(\lambda_{\text{ex}})$ , | Average lifetime (ns),                           | Average lifetime (ns),                |
|----------|---|--|---------------------------------------|
|          | $\lambda_{\text{ex}} = 300\text{-}400\text{ nm}$          | $\lambda_{\text{ex}} = 300\text{-}350\text{ nm}$ | $\lambda_{\text{ex}} = 630\text{ nm}$ |
| 304b     | 1.03  | 2.78   | 2.60                                  |
| 304c     | 1.33  | 3.04   | 2.83                                  |
| 304d     | 0.88  | 2.95   | 2.79                                  |
| 303b     | 0.99  | 1.56   | 1.46                                  |

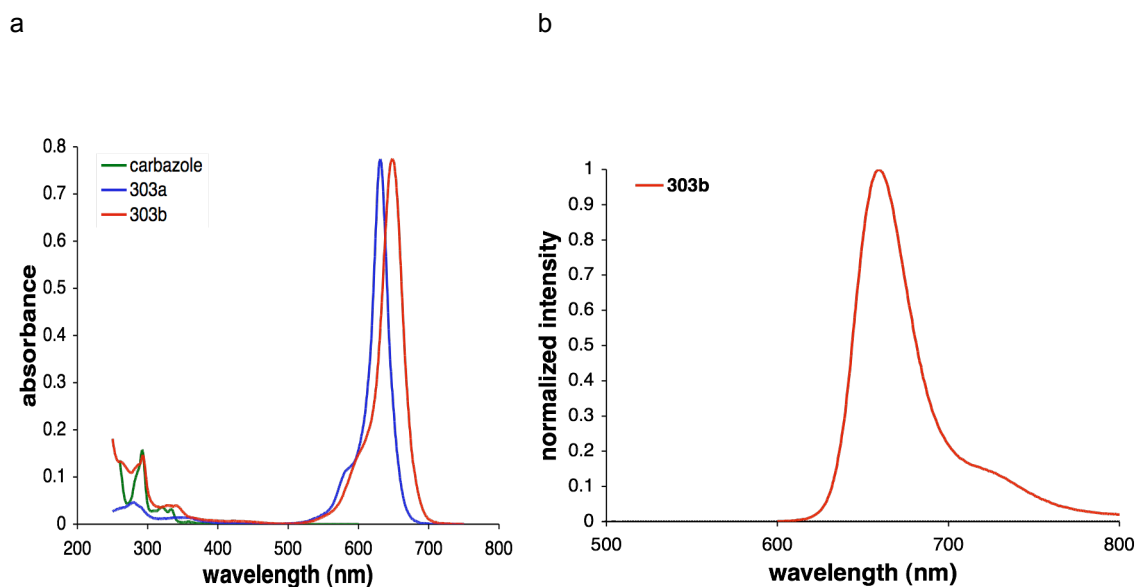


**Figure 4.4.** (a), (c), (e) and (g) Overlaid absorption spectra of the donor fragments, the acceptor fragments, and the complete cassettes; all in  $\text{CHCl}_3$  solution. (b), (d), (f) and (h) Fluorescence spectra of the cassettes; all excited at 300 nm or 590 (630) nm in  $\text{CHCl}_3$  solution.

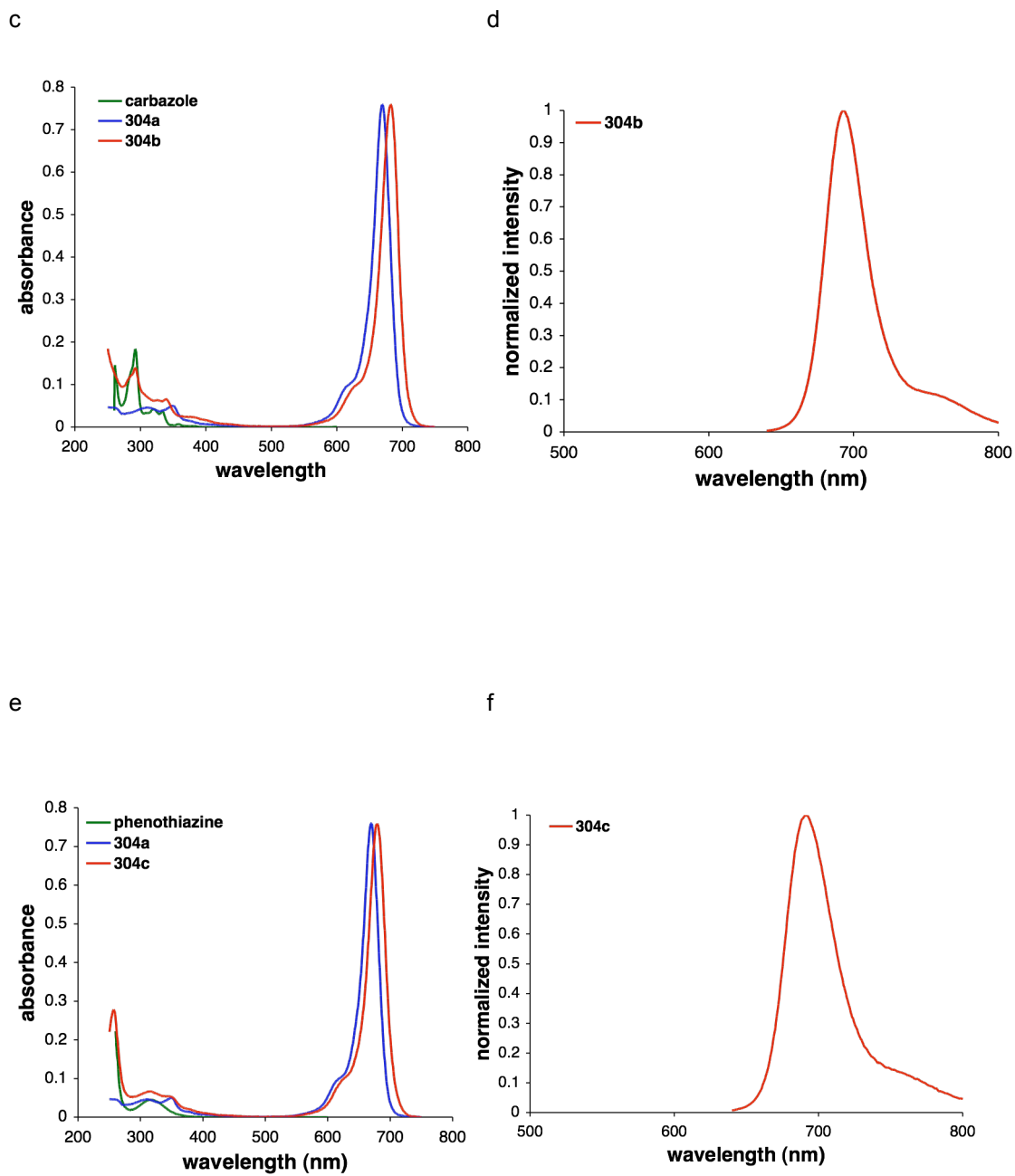


Figure 4.4. Continued.

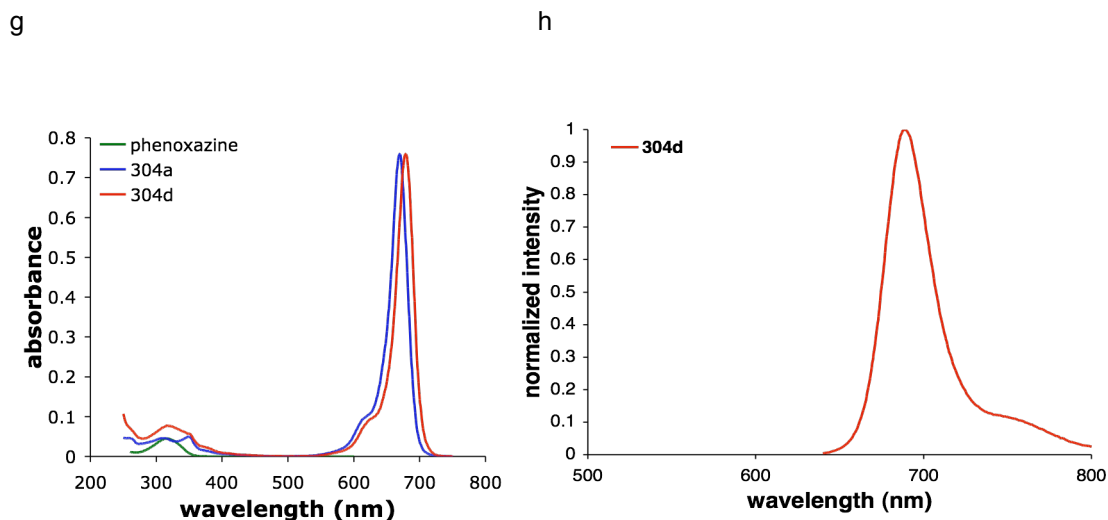


Figure 4.4. Continued.

### C. Conclusions

In conclusion, several cassettes based on squaraine fragments acting as acceptors (**303b** and **304b–d**) were prepared. These cassettes transfer energy very efficiently to their acceptor parts when irradiated in the donor absorption region (ca. 300 nm). With respect to fluorescence emission, the cassettes behave like dyes with a huge Stokes' shift, absorbing around 300 nm and fluorescing in the near IR region (637–693 nm). Emission at such long wavelengths is good for probing biological systems which do not fluoresce in this region, i.e. DNA, RNA, the majority of proteins, and many other biomolecular types. The quantum yields of the acceptors in the cassettes are high, and we infer that they are also high for the cassettes when irradiated in the donor region. Despite these attributes, cassettes **303b** and **304b–d** have some disadvantages with respect to tagging biological molecules. First, the donor fragments do not absorb very strongly, hence they cannot supply the acceptor well. Secondly, the molecules have poor water solubilities and this is likely to make their conjugation to biomolecules difficult. Our current research on similar ET cassettes is focused on solving these problems.



## CHAPTER V

### CORRELATIONS OF STRUCTURE AND RATES OF ENERGY TRANSFER FOR THROUGH-BOND ENERGY-TRANSFER CASSETTES\*

#### A. Introduction

A common problem in biotechnology is encountered when several biological molecules labeled with different fluorescent dyes are to be observed by using a single excitation wavelength. A typical example is in DNA sequencing, where termination by fluorescently labeled dideoxy-A, -T, -G, and -C bases must be differentiated.<sup>328,329</sup> The dye that fluoresces at the shortest wavelength typically has an absorption maximum wavelength,  $\lambda_{\text{abs max}}$ , close to that of the exciting source, hence it absorbs strongly and emits brightly. Conversely,  $\lambda_{\text{max}}$  for absorption by the "red dyes" is not close to the excitation wavelength; therefore those dyes harvest fewer photons and fluoresce relatively weakly. This problem can be partially alleviated by using two dyes arranged to maximize Förster energy transfer (FRET).<sup>330-332</sup> However, the resolution/brightness of such FRET systems is constrained by overlap of the donor emission with the acceptor absorption, corresponding to the overlap integral described in Förster theory.<sup>333</sup>

Our research focuses on donor-acceptor dye cassettes that are connected via a twisted, but otherwise conjugated,  $\pi$ -electron system. In such systems, energy transfer may occur through bonds as well as through space. If through-bond energy transfer is the dominant mechanism, then the resolution of multiplexed through-bond energy-transfer cassettes is not constrained by the spectral overlap integral. Thus, it should be possible to design brighter and better-resolved systems for multiplexing in biological systems. Through-bond energy transfer has been extensively investigated for development of optical materials,<sup>334-337</sup> and for photosynthetic models<sup>338</sup> but, prior to our work,<sup>339-341</sup> not for applications in biotechnology. Indeed, the types of linkers used in the cassettes described here (diphenylethynyl units) are similar to those employed in work on through-bond energy transfer in porphyrin molecular arrays.<sup>338</sup>

---

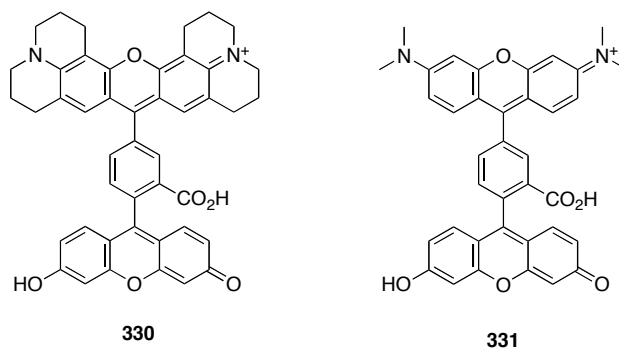
\*Reproduced in part with permission from "Correlations of Structure and Rates of Energy Transfer for Through-Bond Energy-Transfer Cassettes" by T. G. Kim, J. C. Castro, A. Loudet, J. G.-S. Jiao, R. M. Hochstrasser, K. Burgess, and M. R. Topp, 2006. *Journal of Physical Chemistry A*, 110, 20-27; copyright 2005, American Chemical Society.

## B. Results and Discussion

In this collaborative work, we sought to explore the correlation between structures and rates of energy transfer and fluorescence polarization for a range of through-bond energy-transfer cassettes. To do this, we compare the anthracene-BODIPY (BODIPY = 4,4-difluoro-1,3,5,7-tetramethyl-4-bora-3a,4a-diaza-s-indacene) systems **314** - **322**,<sup>339</sup> for which some data were reported previously, with the new fluorescein-rosamine cassettes **323** - **330**<sup>340</sup>. An important through-space energy-transfer cassette **344** was also studied for comparison. The compounds **314** - **330** were prepared in our laboratories by several students. The spectroscopic studies were realized in Prof. Hochstrasser's laboratories at the University of Pennsylvania.

### 1. Synthesis

Cassettes **314** - **329** were previously prepared by others group members over the past years.<sup>339,340</sup> Cassette **330** and **331** (not studied) featuring the shortest linker between the donor and acceptor were prepared for this study.

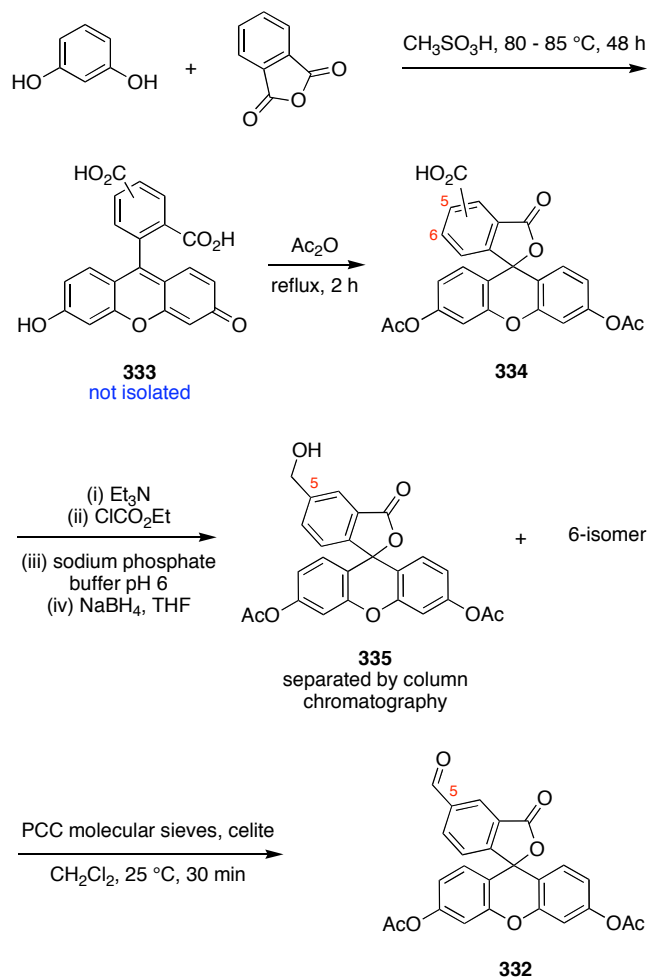


### Donor Synthesis

Fluorescein was chosen as the donor due to its favorable water-solubility, absorption spectrum, and high quantum yield. 5-Carboxyaldehyde fluorescein diacetate **332** was used as a starting block in the synthesis of these “short” cassette where a phenyl group only separates the donor and acceptor. Compound **332** was obtained in 4 steps from resorcinol and phthalic anhydride (Scheme 5.1). First, resorcinol and phthalic anhydride were condensed in methane sulfonic acid to give a mixture of both isomers, 5- and 6-carboxyfluorescein **333**. The crude

mixture was treated with acetic anhydride to give the 5- and 6-carboxyfluorescein diacetates **334**. The isomers were subsequently separated after reduction with sodium borohydride to the corresponding 5- and 6-(hydroxymethyl)fluorescein diacetate **335**. Finally, oxidation of the 5-isomer with PCC gave the desired 5-carboxyaldehyde fluorescein diacetate **332**.

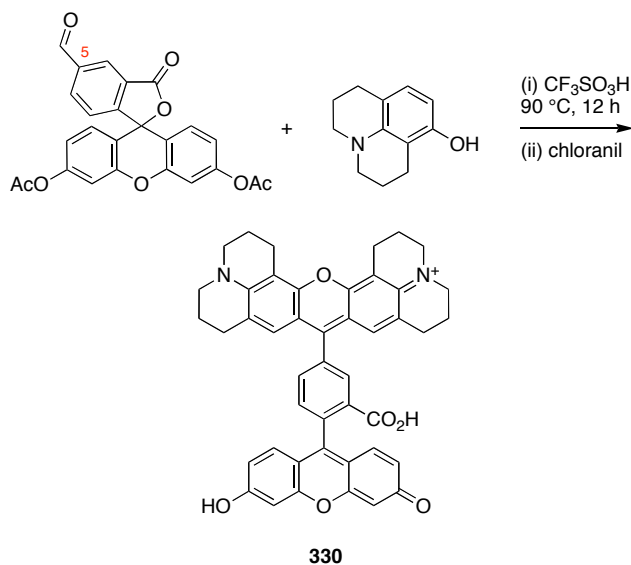
**Scheme 5.1.** Synthesis of 5-carboxyaldehyde fluorescein diacetate **332**.

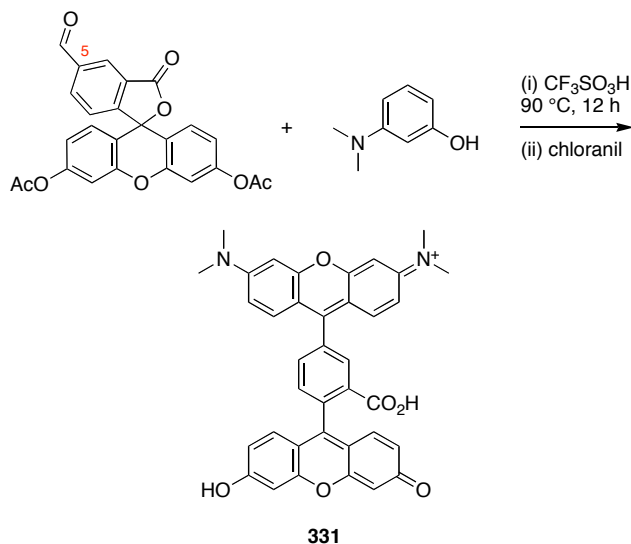


### Synthesis of the Energy Transfer Cassettes

The “short” cassettes were prepared by condensation of the 5-carboxaldehyde fluorescein diacetate **332** and the appropriate aminophenol in presence of trifluoromethane sulfonic acid, followed by oxidation with chloranil (Scheme 5.2 and 5.3). 8-Hydroxyjulolidinone and 3-dimethylaminophenol were thus successfully condensed to produce **330** and **331**, respectively. Condensation of 3-aminophenol under several different conditions revealed unsuccessful (data not shown). Condensation of protected 3-aminophenol derivatives was also attempted, but failed.

**Scheme 5.2.** Synthesis of cassettes **330**.



**Scheme 5.3.** Synthesis of cassette **331**.

## 2. Transition Moments

Cassettes **314 - 330** have donor and acceptor fragments linked by rigid,  $\pi$ -conjugated systems. They are designed to have a common absorbing chromophore matched to the exciting laser, but different emitters. Energy-transfer cassettes featuring fluorescein as the common donor and rhodamines as acceptors are commonly used in DNA sequencing. The fluorescence emission of the acceptor moieties ranges from 550 to 650 nm. Thus, different DNA bases excited by the same laser can be distinguished via the visible fluorescence of different attached labeling agents.

Usually, energy-transfer cassettes are selected for properties such as distinguishable emission (i.e., relatively narrow band) spectra, high-fluorescence quantum yields, relative ease of attachment to DNA strands, and not least, good photostability. In newer applications of labeling cassettes, which may involve experiments in single-molecule environments such as probe studies of single protein molecules, molecular orientation and fluorescence polarization also become important. Molecular motion and/or orientation of a probe can be sensed through time-resolved fluorescence polarization measurements.

The molecules examined in this study can be divided into three groups. In the first (Figure 5.1), compounds **314 - 318** have a 9- or 9,10-substituted anthracene donor species, excited near

405 nm, which transfers energy to a fluorescent BODIPY acceptor moiety. Most of the variation in this sequence involved tuning the emission of the BODIPY emitter via symmetrical structure modification.

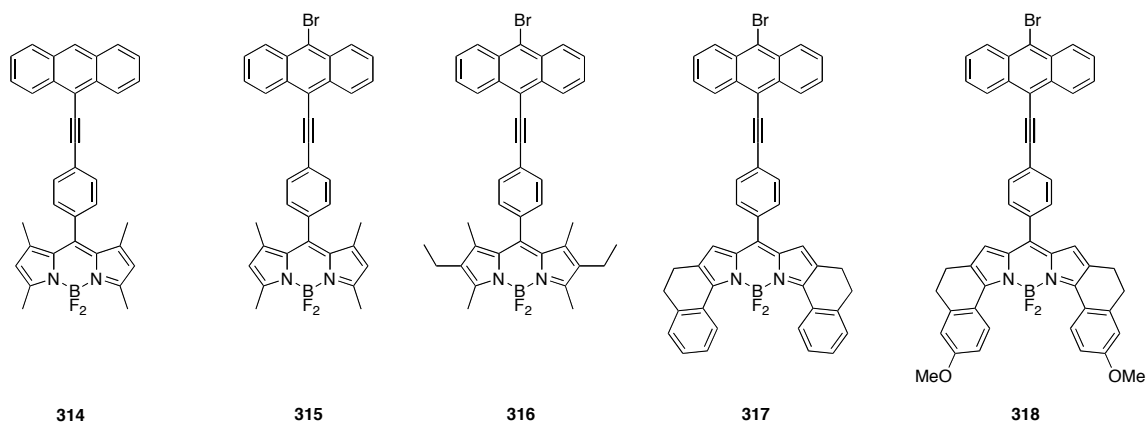


**Figure 5.1.** Sequence of anthracene-BODIPY cassettes having perpendicular donor and acceptor transition moments.

The  $S_1 \leftrightarrow S_0$  transition moments of the two chromophores are indicated in Figure 5.2. The anthracene  $S_1 \leftrightarrow S_0$  transition moment is directed along the axis of the phenylacetylene linker and perpendicular to the transition moment of the BODIPY acceptor. These transition moments are, therefore, mutually perpendicular, independently of the twist angle about the linker axis. Rate of energy-transfer in the range of  $0.42 \pm 0.12$  ps were found for those compounds.<sup>339</sup>

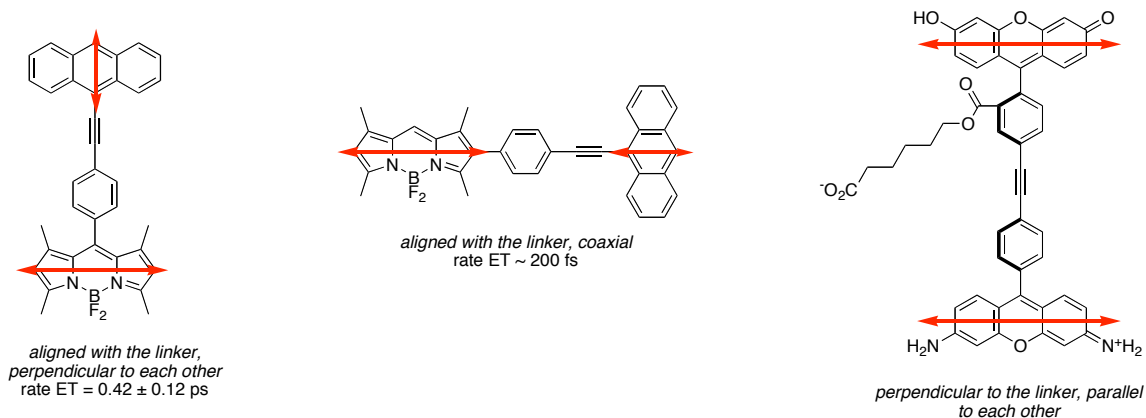


**Figure 5.2.** Indications of the  $S_1 \leftrightarrow S_0$  transition moments in the different energy-transfer cassettes.

The second set of molecules (compounds **319** - **322**; Figure 5.3) features the same donor and acceptor species, except that the long axis of BODIPY is aligned with the linker. This causes the transition moments (see Figure 5.2) to be mutually coaxial with the linker, again, independently of rotation about the linker axis. The length of the linker was also varied in this sequence to investigate the effects on energy-transfer rates, but the transfer rate for this set of compounds was found to be too fast to be measured accurately ( $\sim 200$  fs).<sup>339</sup>

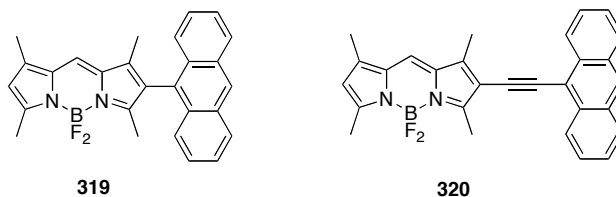


**Figure 5.3.** Sequence of anthracene-BODIPY cassettes having parallel donor and acceptor transition moments.

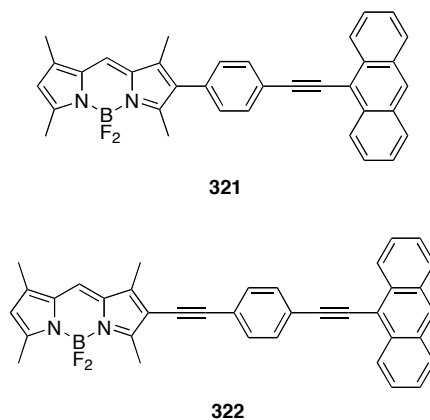


**Figure 5.3.** Continued.

The third set of compounds (**323 - 330**), shown in Figures 5.4 and 5.5, has fluorescein donors and rosamine derivatives as acceptor (the difference between rhodamine and rosamine lies in the presence or absence of an *o*-carboxyl substituent on the phenyl ring). Most of the cassettes in the third set, shown in Figure 5.4, have a diphenylacetylene linker, which maintains the spatial relationship of the donor and acceptor species and gives rise to polarized emission from the acceptor. The energy-transfer times were much longer than those for compounds **314 - 322**. Compounds **323 - 330** have in common that the donor and acceptor transition moments are close to mutually parallel and are perpendicular to the axis of the linker, as Figure 5.2 indicates.

Those compounds **323 - 327**, which were designed to have a steady evolution in the donor-acceptor energy gap, showed an unusually similar set of donor relaxation times, in pure ethanol, of  $6.2 \pm 0.4$  ps.



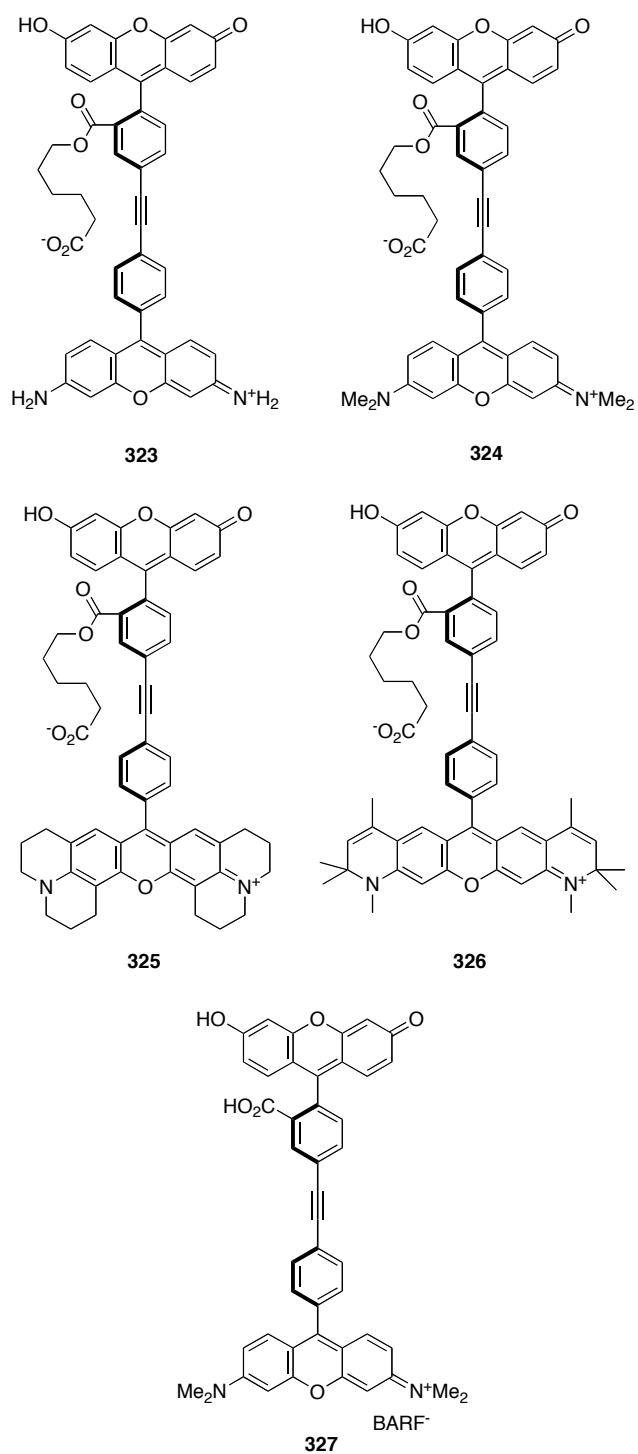


**Figure 5.4.** Sequence of fluorescein-rosamine cassettes. All have parallel donor and acceptor transition moments.

Compounds **328** – **330**, shown in Figure 5.5, were designed to investigate the effect of varying the length and type of the linker on energy-transfer time and polarization anisotropy. They showed a much greater variation in transfer time, with the most noticeable difference being for compound **330**. Despite having the shortest linker and parallel transition moments, compound **330** had a relaxation time 3 times longer than any of the other cassettes. Compound **331** (data not shown) showed the same behavior. Clearly, a less efficient energy-transfer mechanism exists for those two compounds.

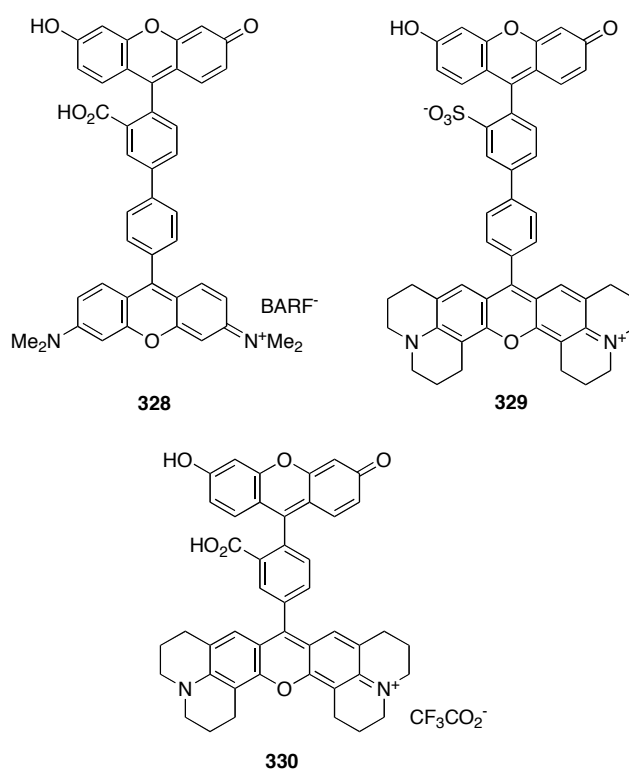


**Figure 5.5.** Sequence of fluorescein-rosamine cassettes with shorter linker. All also have parallel donor and acceptor transition moments.

Finally, the compounds shown above were compared to a commercial labeling cassette, "Big-ROX" (**336**, obtained from ABI), which is shown in Figure 5.6. Although having almost the same donor and similar acceptor species (rhodamine vs rosamine) to the other cassettes, the

two components are unsymmetrically linked by a flexible, partially saturated chain. A molecule of this type allows one to examine the dynamical consequences of removing the rigid linker. Compound **336** showed by far the longest transfer time (35 ps), suggesting that this is limited by FRET.

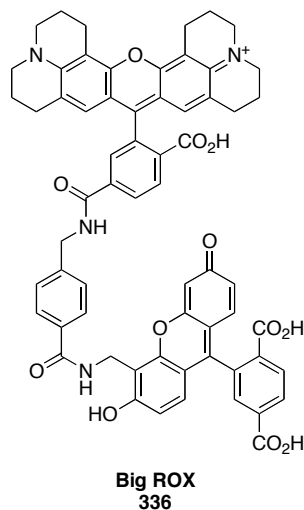


**Figure 5.6.** Commercial energy-transfer cassette Big ROX, obtained from ABI.

### 3. Relaxation Times

Time-resolved emission spectra for compound **326** could be obtained by scanning the gated spectrum at different delay times after irradiation. A clear decay of the donor emission near 530 nm (after excitation at 405 nm) and a complementary growth of the acceptor emission at 640 nm was observed on the time scale of 10 ps (Figure 5.7). Time profiles for both the donor and acceptor for compound **326** were also obtained by setting the detector at a particular wavelength while scanning the optical delay (Figure 5.8). The donor signal decayed with a time constant of ~5.8 ps.

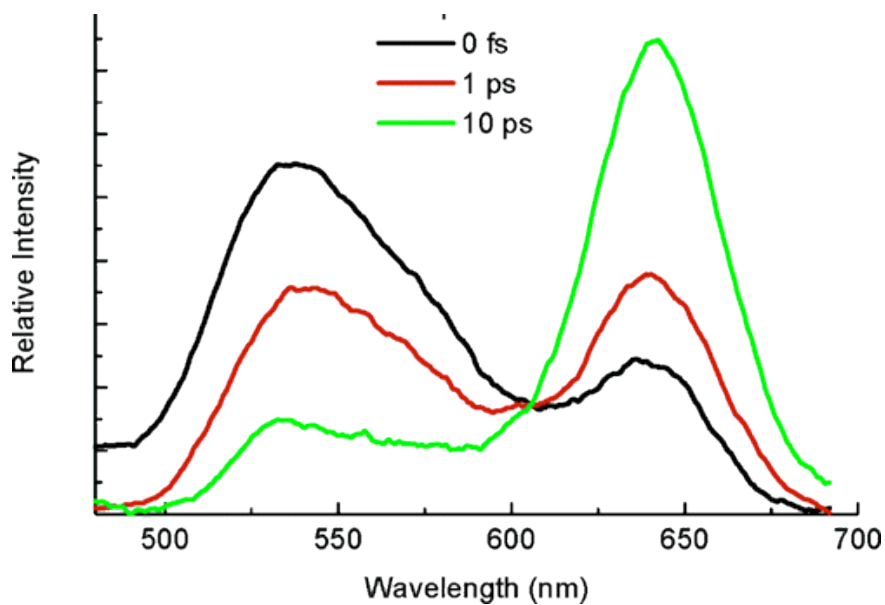


**Figure 5.7.** Sequence of gated emission spectra for compound **326** (in EtOH) following ultrashort-pulsed excitation at 405 nm.

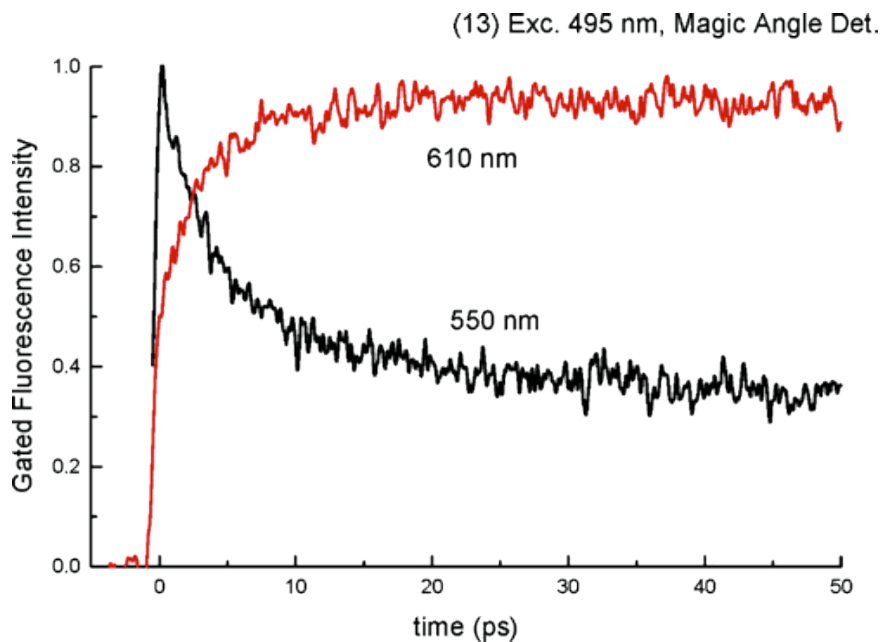


**Figure 5.8.** Gated fluorescence time profiles at 550 nm (donor) and 610 nm (acceptor) following ultrashort-pulsed excitation of compound **326**.

**Table 5.1.** Emission characteristics of rigidly linked donor-acceptor cassettes (solvent  $\text{CHCl}_3$  for compounds **314** - **322** and ethanol for **323** - **330**, unless otherwise indicated)

| Cpd no. | Acceptor<br>emission<br>maximum (nm) | Energy-<br>transfer<br>time (ps) | Acceptor<br>emission<br>Anisotropy r(t) |
|---------|--------------------------------------|----------------------------------|---|
| 314     | 515                                  | 0.4                              | - 0.1                                   |
| 315     | 520                                  | 0.49                             | n/m                                     |
| 316     | 545                                  | 0.55                             | n/m                                     |
| 317     | 660                                  | 0.33                             | - 0.1                                   |
| 318     | 690                                  | 0.47                             | - 0.09                                  |
| 319     | 615                                  | <0.2                             | + 0.23                                  |
| 320     | 650                                  | <0.2                             | + 0.31                                  |
| 321     | 570                                  | <0.2                             | n/m                                     |
| 322     | 590                                  | <0.2                             | + 0.22                                  |
| 323     | 535                                  | 6                                | n/m                                     |
| 324     | 580                                  | 6.8                              | + 0.27                                  |
| 325     | 605                                  | 6.3                              | + 0.25                                  |
| 326     | 620                                  | 5.8; 3.4 (basic<br>EtOH)         | + 0.20                                  |
| 327     | 580                                  | ~6                               | + 0.20                                  |
| 328     | 575                                  | 4.3                              | + 0.19                                  |
| 329     | 600                                  | 2.5                              | + 0.25                                  |
| 330     | 600                                  | 20                               | + 0.20                                  |
| Big     | ROX<br>590                           | 35                               | 0                                       |

(336)

#### 4. Anisotropy Measurements

Fluorescence anisotropy allows one to correlate the energy-transfer rates between the two chromophores with their relative transition moment orientations. Fluorescence anisotropy,  $r$ , can be found from:

$$r = (I_{//} - I_{\perp}) / (I_{//} + 2I_{\perp})$$

where  $I_{//}$  -  $I_{\perp}$  indicate intensity measurements parallel and perpendicular to the incident polarization, respectively. Ideal values of  $r$  are +0.4 for parallel and -0.2 for perpendicular.

Of all the samples studied (14 out of 18), only the commercial sample, compound **336** where the donor and acceptor chromophores are linked by a long flexible chain, showed unpolarized acceptor emission despite strong polarization of the donor moiety (Table 5.1).

The behavior of the anthracene-BODIPY cassettes, for which the sequence **314** - **318** show perpendicular polarizations and sequence **319** - **322** show parallel polarizations, has already been reviewed. We report here for the first time that all of compounds **323** - **330** also show parallel polarizations. Figure 5.9 shows the situation for compound **314**. During the rapid transfer process, the anisotropy quickly adopts a value of  $r(t)$  near -0.1, which remains constant during the 5-ps time scale of the scan. The negative anisotropy indicated a perpendicular orientation of the donor and acceptor transition moments.

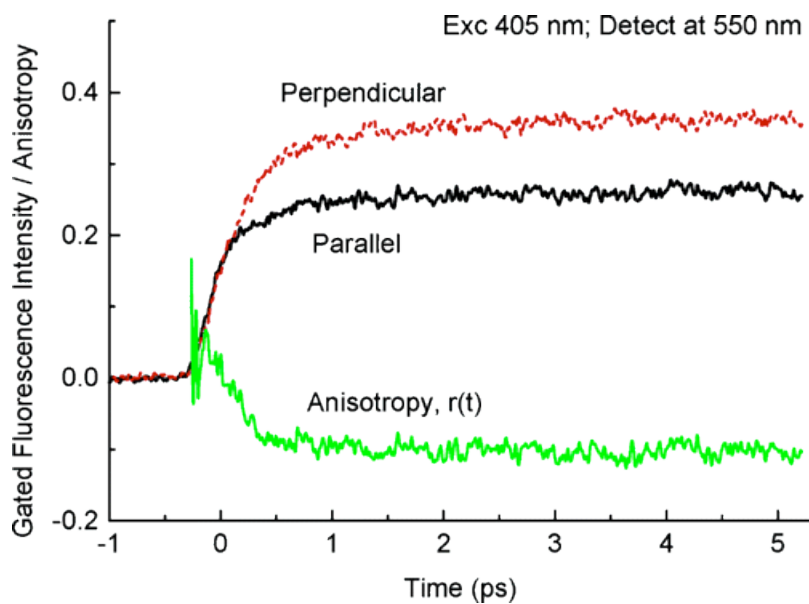


**Figure 5.9.** Polarized time profiles of compound **314** in chloroform following excitation at 405 nm. Signals monitored at 550 nm, on the BODIPY fluorescence.

The time profile of compound **325** monitored at 610 nm is shown in Figure 5.10. The fluorescence shows a positive anisotropy, decaying from the vicinity of + 0.33 (overlapping donor emission) to  $\sim +0.20$ , indicating a parallel orientation of the transition moments.

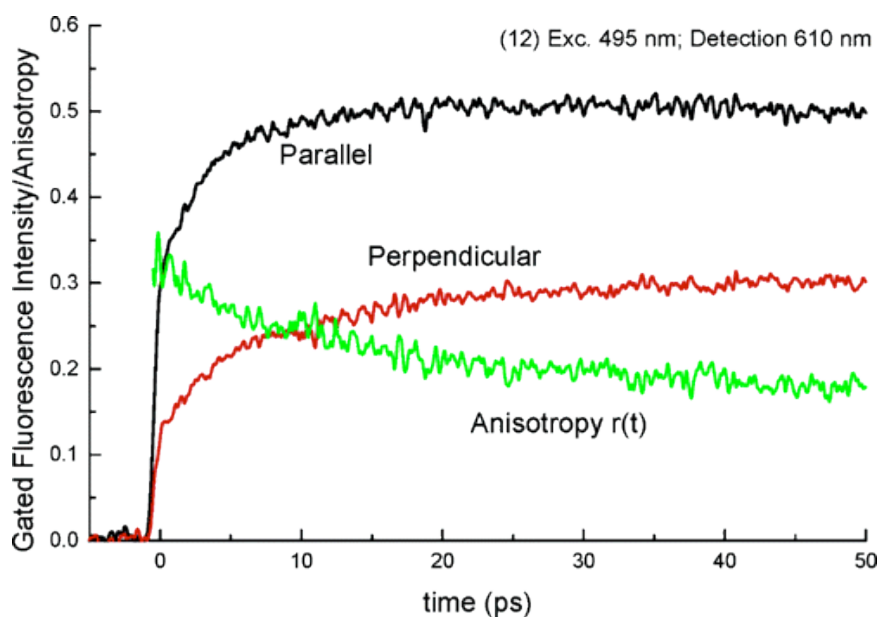


**Figure 5.10.** Polarized time profiles of compound **325** in ethanol following excitation at 495 nm. Signals monitored at 610 nm, on the rosamine fluorescence.

For reference, measurements following direct excitation of the acceptor species in compound **325** (exc ~ 530 nm) (Figure 5.10) showed a relatively slow depolarization, consistent with a diffusion-limited relaxation time (by extrapolation) on the order of 150-250 ps. Thus, any time-dependent change in the anisotropy on the time scale <20 ps, following donor excitation, is due to donor-acceptor energy transfer.

### C. Conclusions

Comparison of the series **314 - 318** and **323 - 327** shows no systematic correlation of the transfer rate with the nature of the acceptor, despite the differences in donor-acceptor energy gap. This also argues against the Förster mechanism, which depends somewhat critically on the overlap integral of the donor emission and acceptor absorption spectra, given by the above equation.

Experiments with cassettes having reduced donor-acceptor distances (**327**, **328**, **330**) also showed no significant increase in transfer rates, as would be predicted from Förster theory. On the contrary, results obtained for compound **330** showed that, when the linker is reduced to a



single carboxylated phenyl group, the transfer rate is much reduced. This indicates a significant reduction in the amount of coupling of the two chromophores, despite their continued parallel arrangement, which is currently unexplained. Similar variation of the donor-acceptor transfer distances in compounds **319** - **322** also did not reveal any correlations between the rates and the separation. In those cases, the transfer rates were faster than the experiments could reliably resolve (i.e., more than 30× faster than that for the similar fluorescein-rhodamine cases) and, again, not predicted by Förster theory. The donor and acceptor transition moments are both aligned with the linker axis, which is the case that clearly optimizes the transfer rates.

Fragment compounds were also synthesized, such as a fluorescein type of donor and several acceptors of the type seen in cassettes **323** - **327**. Calculations of the spectral overlap integrals between a given donor and several different acceptors show a variation of up to a factor of >2 for different cassettes, the maximum overlap being achieved for cassette **324**. If Förster transfer were significant, one would expect a similar variation in the transfer rates, which was not actually observed. Also, given the  $r^{-6}$  dependence of the Förster integral, one could expect a strong dependence on the separation of the two chromophores, which again, we do not see. Therefore, we conclude that Förster transfer is unlikely to represent the main mechanism for energy transfer in most of the cassettes shown here. Of all the synthetic cassettes in this study, just one, compound **330**, shows a slow energy transfer more consistent with a Förster type of mechanism.

The decay times of **328** and **329** were somewhat shorter than those of **323** - **327**, but within the variation observed in different solvents. Also, fluorescence polarization measurements clearly showed that the transition moment of the acceptor rosamine species remained parallel to that of the donor, indicating a canceling twist induced by the biphenyl linker. The surprise was with compound **330** (and a similar compound **331** not shown here), where the energy-transfer time increased to around 20 ps (i.e., nearly an order of magnitude slower than **328** and **329**). Note that, in compound **330**, the donor-acceptor separation is the closest for this entire family of molecules (**323** - **330**), and the polarization experiments again showed that the transition moments remain parallel. Despite the reduction in the physical distance between the chromophores, the coupling is significantly weaker. This behavior is consistent with through-bond energy transfer, which is influenced by the nature of the linker bonds intermediate between the donor and acceptor moieties.<sup>338,342</sup>

Finally, compound **336**, the commercial sample "Big-ROX", which contains flexibly linked fluorescein and rhodamine chromophores, shows a relaxation time nearly an order of magnitude longer than that for the other cassettes **323** - **329**. This is a case that more clearly reflects

through-space (FRET) as opposed to through-bond transfer. This is different behavior from compound **330**, which also shows slow energy transfer, but both the donor and acceptor emissions are polarized.

## CHAPTER VI

### DESIGN AND SYNTHESIS OF FLUORESCENT CASSETTES BASED ON DIKETOPYRROLOPYRROLE

#### A. Introduction

##### 1. DNA Sequencing: The State of The Art

In 1975, Maxam and Gilbert devised the first method for sequencing DNA fragments.<sup>343</sup> This method is reliable for sequencing up to ~250-300 nucleotides at a time; both single-stranded (ss) and double-stranded (ds) DNA can be sequenced. This technique involves the chemical cleavage of four samples of an end-labeled DNA restriction fragment at different specific nucleotides. The resulting fragments are separated by gel electrophoresis and the labeled fragments are detected by autoradiography.

In 1977, Sanger and his colleagues developed a second sequencing method, which now is more widely used.<sup>344</sup> The Sanger method or “dideoxy sequencing”, involves use of 2,3-dideoxynucleotidetriphosphates (ddNTPs). It is based on the ability of ddNTPs to terminate primer extension reactions catalyzed by a DNA polymerase due to their lack of 3-hydroxyl groups.

In a typical experiment, four separate reactions are performed, each containing primer, DNA template, polymerase, and the four deoxynucleotides (dNTPs). Addition of a different ddNTP to each reaction produces a nested set of oligonucleotides, each terminating with the specific ddNTP present in the reaction, that are then analyzed by gel electrophoresis (5' end-labelled with  $^{32}\text{P}$  or  $[\alpha\text{-}^{35}\text{S}]\text{dATP}$  are commonly used). Further elaboration of the Sanger method came with the replacement of radioactive nucleotides by fluorescent dyes, which can either be attached to the primer or to the terminating fragments.<sup>345,346</sup> In the dye-primer technology, four reactions can be set up and run in adjacent lanes, the sequencing primer having a fluorescent label. In the dye terminator chemistry, each of the ddNTPs has a different fluorescent label so that all four can be run in the same lane and distinguished by the wavelength at which they fluoresce. Four-color sequencing requires distinct emission maxima of the fluorophores, criterion that is met by the dyes (FAM, 5-carboxyfluorescein; JOE, 2',7'-dimethoxy-4',5'-dichloro-6-carboxyfluorescein; TAMRA, *N,N,N',N'*-tetramethyl-6-carboxyrhodamine; ROX, 6-carboxy-X-

rhodamine) currently used. Unfortunately these dyes do not have equal absorbance at any wavelength; rhodamine dye-labeled primers exhibit weaker signals than those labeled with fluorescein (Figure 6.1). To compensate this difference, more DNA template or multiple lasers must be used in the reactions run with rhodamine dye-labeled primers.

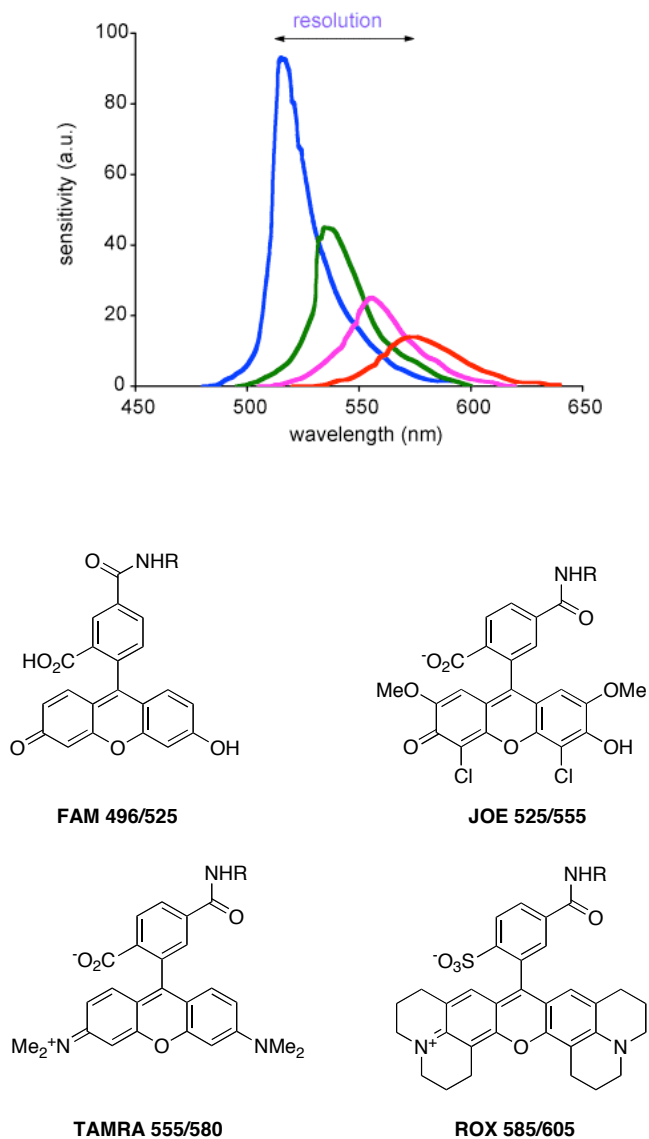


**Figure 6.1.** Fluorescence intensities of JOE, ROX, FAM and TAMRA excited at 488 nm.

In 1995, Ju et al. introduced energy transfer (ET) primers, which are far superior labels for DNA sequencing.<sup>347</sup> They have strong absorption at a common laser wavelength, high acceptor fluorescence emission at distinctive wavelength, and same relative electrophoretic mobility shift of the DNA fragments. Commonly, These primers carry a fluorescein derivative at the 5' end as a donor, and other fluorescein and rhodamine derivatives as acceptors within the primer sequence, on a thymidine residue. Energy (from an excitation source) is transmitted through space, via dipole-dipole coupling, from the donor to the acceptor that then fluoresces. Energy transfer from the donor (fluorescein) to the acceptor (rhodamine) leads to a more efficient excitation of the acceptor dyes than direct excitation by the laser, resulting in exceptional sensitivity and signal strengths several fold greater than those obtained with conventional single-dye labeled molecules. In these cassettes, the donor and acceptor are connected via a non-conjugated linker (Figure 6.2).

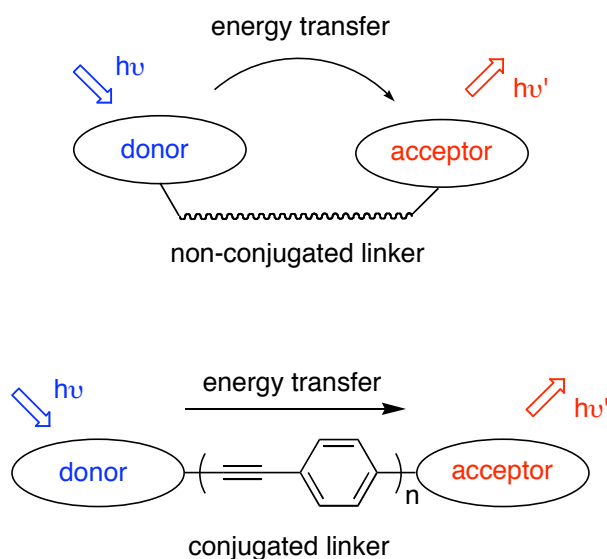


**Figure 6.2.** Through-space energy transfer cassettes (top), through-bond energy transfer cassettes (bottom)

However, through-space fluorescence ET does not solve the problem of resolution and intensity because the emission spectra of the donor dye must overlap with the absorption

spectra of the acceptor dye for ET to occur. However through-bond energy transfer (Figure 6.2) should allow for better resolution and intensities as demonstrated in Figure 6.3 since overlap of the donor fluorescence with the acceptor absorption is not required for ET.

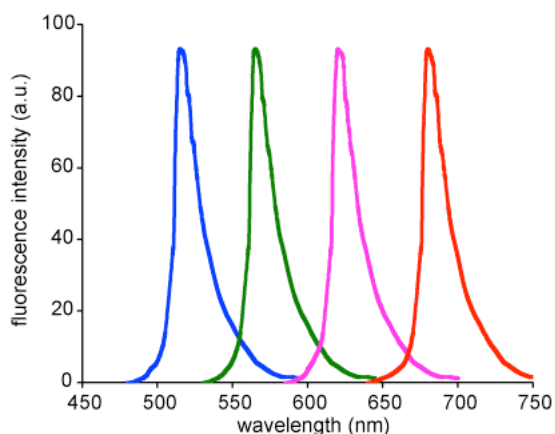


**Figure 6.3.** Fluorescence intensities of ideal sequencing dyes: resolved and intense.

## 2. Diketopyrrolopyrrole (DPP) Dyes<sup>348</sup>

### *DPP as Pigments*

1,4-Diketo-3,6-diarylpyrrolo[3,4-c]pyrroles, also called DPP is one of the most recent addition to the class of high performance pigments. The first synthesis of the DPP chromophore was reported in 1974 by Farnum, who while attempting to synthesize 2-azetionones **338** isolated a small amount of the diphenyl DPP derivative **337** (Scheme 6.1).<sup>348</sup> The underlying DPP chromophoric system bears strong structural resemblance to many well-known pigments, such as indigos, isoindolinones, epindolindione and quinacridones (Figure 6.4).

Despite their low molecular masses, the diaryl DPP pigments are highly insoluble and remarkably resistant to chemicals and heat. These properties can be attributed to the presence of strong intermolecular bonding forces e.g., H-bonding, van der Waal's contact,  $\pi - \pi$  interactions between molecular planes.

Scheme 6.1. First report of DPP.

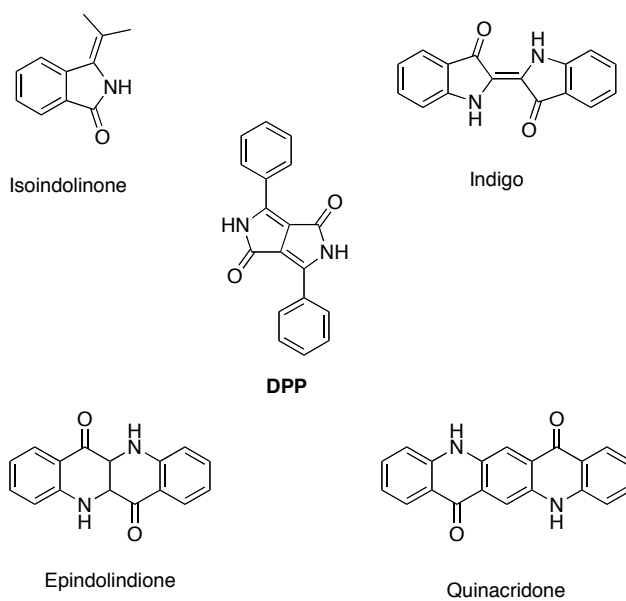
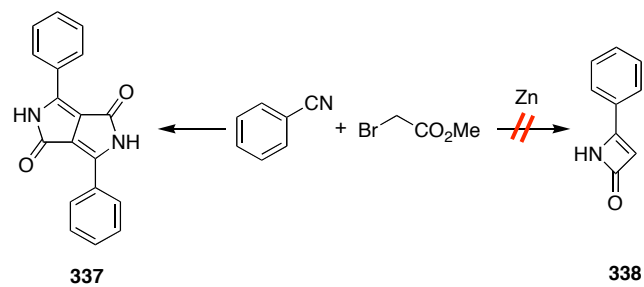


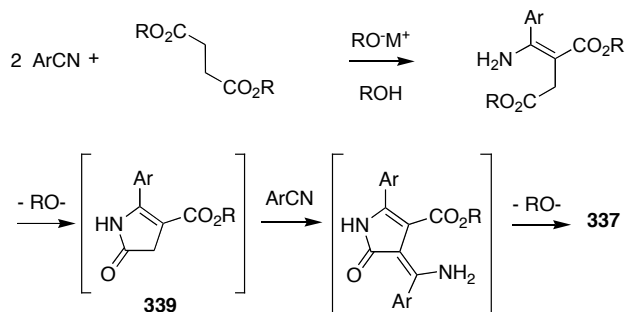
Figure 6.4. Structural analogy of DPP with commercial pigments.

### ***Syntheses, Mechanism of Formation and Reactivity of the DPP Chromophoric System***

In the original publication, Farnum postulated that the formation of the DPP 337 proceeded via an oxidative dimerization. In 1988, Iqbal and coworkers carefully reinvestigated

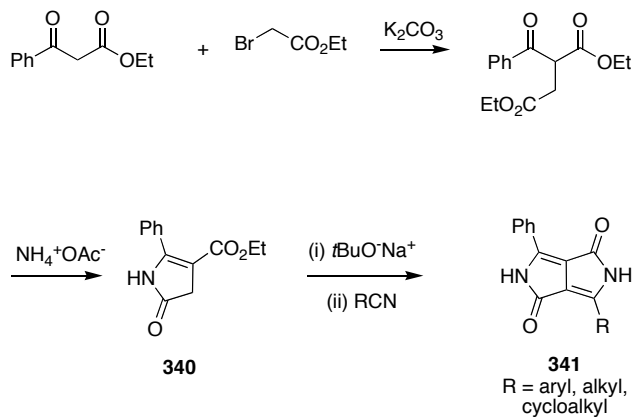
the Reformatsky route: synthesis of crucial intermediates and crossing experiments using two different benzonitriles strongly supported the formation of an intermediate lactam, and a new mechanism involving a pyrrolinone ester as the crucial intermediate was postulated.<sup>349</sup> However, the commercial viability of this process was hampered by the low yields of DPP formation (<30%). Continued search for alternative approaches to the DPP system led to the discovery of the elegant synthesis shown in Scheme 6.2.<sup>349</sup> Symmetrical DPP derivatives e.g. compounds bearing identical substituents at the 3- and 6- positions are obtained by condensation of succinic ester with 2 molar equivalents of nitriles in the presence of a strong and sterically hindered base.<sup>350</sup> The first step in the process presumably lead to the formation of the pyrroline-carboxylate ester 3, which after deprotonation, reacts with a second equivalent of nitrile to give the final product.

**Scheme 6.2.** Synthesis of symmetrical DPP via the succinic route



Asymmetrically substituted DPPs can be obtained from the pyrrolinone ester 340 with another benzonitrile in presence of a strong base such as sodium tert-butoxide as shown in Scheme 6.3.<sup>350-353</sup>



**Scheme 6.3.** Synthesis of unsymmetrical DPP

Although a number of modified methods have been reported, most of them suffer from low yield, high temperature and very long reaction times. Very recently, microwave assisted synthesis of DPPs was elaborated and allowed preparation of the compounds in higher yields and much shorter reaction times (10 min only).<sup>354</sup> The experimental procedure simply called for grinding and mixing ethyl bromoacetate, benzonitrile and zinc-copper couple. The reaction proceeded efficiently for moderate electron-donating substituted benzonitriles, but did not work for electron-withdrawing or strong electron-donating substituted benzonitriles.

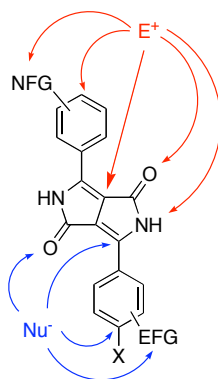
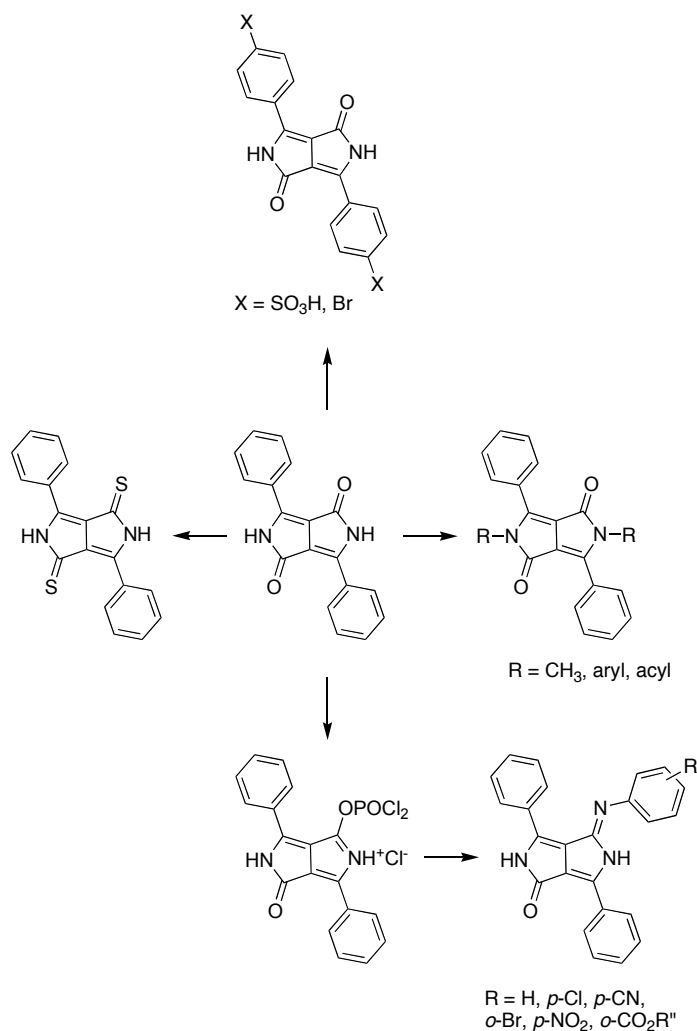


**Figure 6.5.** Centres of potential chemical reactivity.

There are several centres of reactivity in the DPP chromophoric system (Figure 6.5).<sup>355</sup> Appropriately substituted aryl groups could undergo diverse electrophilic and nucleophilic reactions. The bicyclic lactam chromophore which incorporates three different functional groups, is also susceptible to chemical transformations. Synthetic efforts have focused essentially on electrophilic aromatic substitution, *N*-substitution and nucleophilic transformations of the carbonyl group without incurring concomitant rupture of the heterocyclic nucleus (Scheme 6.4).

**Scheme 6.4.** Examples of product that can be obtained by direct chemical transformations of diphenyl DPP.

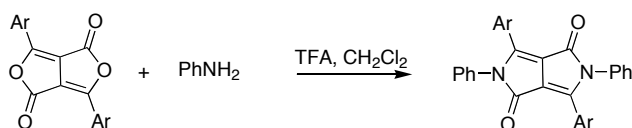


*N*, *N'*-Unsubstituted DPP find commercial application as red pigments because of their low solubility in most common solvents. *N*, *N'*-disubstitution prevents the formation of intermolecular hydrogen-bonding, and thus increases the solubility of DPP derivatives in organic solvents. *N*, *N'*-disubstituted DPP derivatives can be prepared by condensation of diketofurfurane with anilines (Scheme 6.5a), by oxidative dimerization of  $\beta$ -ketoamides (Scheme 6.5b) or by direct *N*-arylation or *N*-alkylation of the amide (Scheme 6.5c). In contrast to

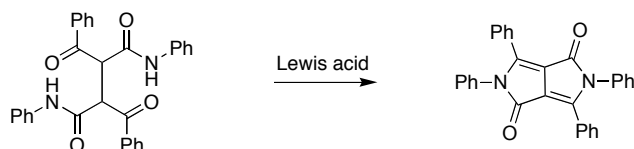
*N*-alkylation, *N*-arylation of amides required highly electron deficient aryl electrophiles such as 1-fluoro-2,4-dinitrobenzene, and necessitates reaction times of several days. 2,3,6-Triaryl-DPPs can be obtained from acylation of ethyl 2-aryl-4,5-dihydro-5-oxopyrrole-3-carboxylates with *N*-arylbenzimidoyl chlorides in the presence of a strong base (Scheme 6a) or by reaction of benzonitrile under basic conditions with 1,2-diaryl-4,5-dihydro-5-oxopyrrole-3-carboxylates (Scheme 6.b).<sup>356</sup>

**Scheme 6.5.** Synthesis of *N,N'*-disubstituted DPP dyes.

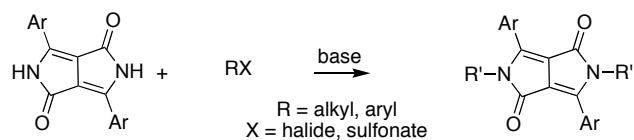
**a**

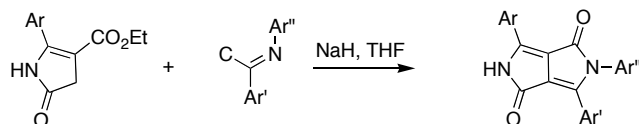
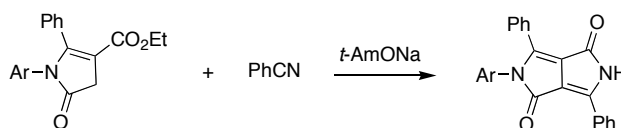


**b**

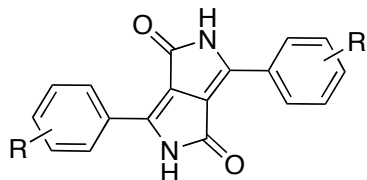


**c**



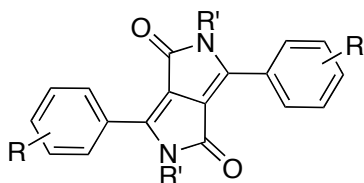
**Scheme 6.6.** Synthesis of trisubstituted DPP dyes.**a****b****Spectral Properties**

The characteristic physical properties of DPP **337** are the high melting point ( $> 350^{\circ}\text{C}$ ), low solubility ( $< 110 \text{ mgL}^{-1}$  in DMF at  $25^{\circ}\text{C}$ ) and an absorption in the visible region with a molar extinction coefficient of 33,000. In solution, DPP **337** gives a yellow fluorescing solution, whereas in the solid state it is a vivid red. Table 6.1 shows the absorption maxima ( $\lambda_{\text{max}}$ ) and the  $\epsilon$  values of differently substituted DPPs measured in solution, as well as the absorption maxima in the solid state. All aryl DPP pigments investigated exhibited a bathochromic shift (shift to longer wavelength) of the maximum absorption in solution. In the solid state, however, the absorption maxima depend strongly on the substituents and their position on the aromatic rings. Meta- substituted DPPs often show a blue shift (entries 1,2 vs. 3), while para- substituted DPPs experience a red shift of the wavelength of maximum absorption (entries 4,5 vs. 3). The large bathochromic shift of the  $\lambda_{\text{max}}$  in the solid state compared to that in solution is due to the strong intermolecular interactions, i.e. the hydrogen bonding,  $\pi$ -stacking and van der Waals interactions in the solid state.

**Table 6.1.** Physical properties of some DPP pigments.

| Entry | R                          | Shade         | $\lambda_{\max}$ (nm) | $\lambda_{\max}$ (nm) | $\Delta\lambda_{\max}$ | $\epsilon_{\max}$ |
|-------|----------------------------|---------------|-----------------------|-----------------------|------------------------|-------------------|
|       |                            |               | in solution           | in solid state        |                        |                   |
| 1     | <i>m</i> -CF <sub>3</sub>  | Orange-yellow | 509                   | 518                   | 9                      | 21500             |
| 2     | <i>m</i> -Cl               | Orange        | 512                   | 528                   | 16                     | 27000             |
| 3     | H                          | Yellow-red    | 504                   | 538                   | 34                     | 33000             |
| 4     | <i>p</i> -Br               | Blue-red      | 515                   | 555                   | 40                     | 35000             |
| 5     | <i>p</i> -NMe <sub>2</sub> | Violet-blue   | 554                   | 603                   | 51                     | 81500             |

DPP pigments fluoresce in solution. The Stokes shifts are in the range 10-15 nm and the fluorescence quantum yields ca. 60%. Through *N*-substitution, both the solubility and the Stokes shift can be increased



R = H; Me  
R' = H; 4-*t*Bu; 3,5-*t*Bu; 2-Me

$\lambda_{\max \text{ flu}} = 509\text{-}528 \text{ nm}$   
 $\Phi = 60\%$

## B. Results and Discussion

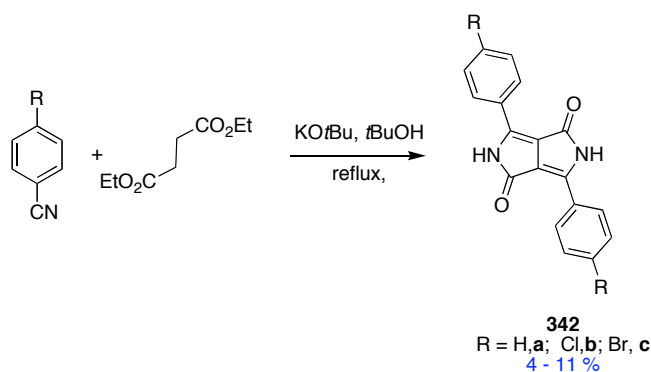
DPP belong to the most recently developed classes of technical pigments. Its major application is in the painting and plastic industry. To date, only three “water-soluble” DPPs have been made, but no UV and fluorescence studies have been realized on these compounds. However, the spectroscopic data reported on the pigment make this compound attractive for the purpose of our research project. We propose here to turn this pigment into a dye and to use it for fluorescence applications. In particular, DPP could be used as a donor in the cassette for DNA sequencing due to its absorption around 500 nm. Our strategy toward this challenging objective is to introduce water-solubilizing group on the nitrogen of the pyrrolinone or on the aromatic rings. *N*-Alkylation will also contribute to increase the solubility of these compounds by preventing the formation of intermolecular hydrogen bonds.

### 1. Synthesis of *N*-alkylated DPP

#### Synthesis of DPPs Derivatives

A short series of DPPs **342a - c** was synthesized from benzonitriles and diethyl succinate in presence of potassium *tert*-butoxide in *tert*-butanol (Scheme 6.7). In a first time, the benzonitrile derivatives were treated with the base in freshly distilled *tert*-butanol, and heated to reflux. Then, to this solution diethyl succinate was added dropwise. The products, isolated by filtration, were obtained in poor yields (4 – 11 %).

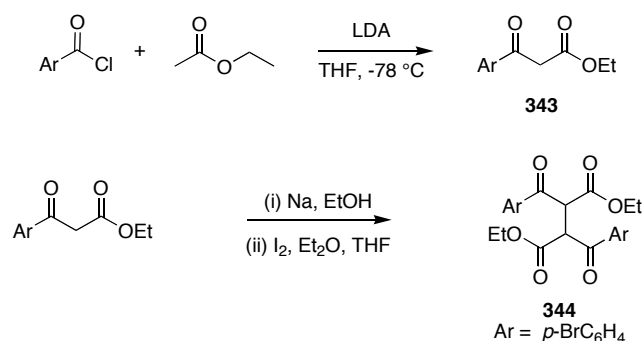
Scheme 6.7. Synthesis of DPPs derivatives.



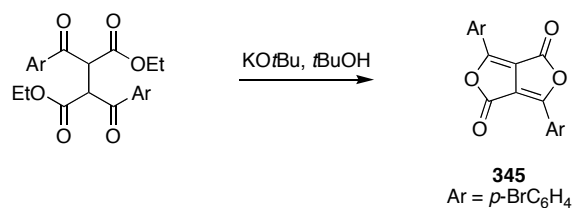
### *N,N*-Dialkylation of DPPs

Several attempts to alkylate DPP **342a** or **342c** were made, but none revealed successful. Alternative approaches were therefore undertaken. These involved condensation of an amine with  $\beta$ -diketones or diketofurofuran as outlined in Scheme 6.5a and b. The synthesis of the corresponding  $\beta$ -diketones and diketofurofuran are described in Scheme 6.8 and 6.9, respectively.  $\beta$ -Ketoesters **343** were obtained by reaction of ethyl acetate and benzoyl chlorides in presence of LDA in ether and base. Next, a modified procedure of the Knorr oxidative coupling of the  $\beta$ -ketoesters,<sup>357</sup> using NaOEt and iodine, afforded the 1,4-diketones **344** (Scheme 6.8). Diketofurofurans **345** were obtained by refluxing the corresponding 1,4-diketones in *tert*-butanol in presence of potassium *tert*-butoxide (Scheme 6.9).

**Scheme 6.8.** Synthesis of  $\beta$ -diketones



**Scheme 6.9.** Synthesis of diketofurofuranes.





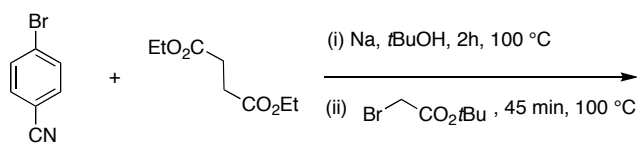
Finally, condensation of amines (alkyl or aryl) with either **344** or **345** should have given the corresponding DPP derivatives. However, no product could be obtained although several conditions were attempted. The fact that no product was obtained was most likely due to a bad choice of amines; the latter used not being reactive enough. Also, it has been shown that this kind of reaction requires very long reaction time and maybe the reactions were not run for long enough at that time.

#### ***In situ* Synthesis of *N,N'*-Disubstituted Symmetrical DPPs**

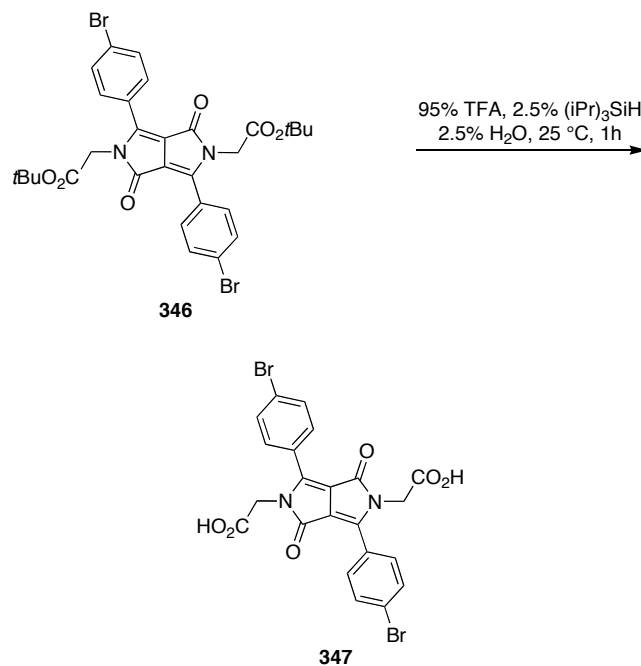
While the methodology described for the synthesis of *N*-alkylated DPP uses harsh conditions, we have elaborated a new route, easier and more convenient, toward the synthesis of *N*-alkylated DPP.

As shown in Scheme 6.10, the synthesis of symmetrical DPP **347** started with condensation of 4-bromobenzonitrile with diethyl succinate in presence of sodium *tert*-butoxide, followed by alkylation *in situ* with *tert*-butyl bromoacetate to yield the DPP **346**. Subsequent deprotection of the *tert*-butyl ester groups delivered the targeted compound **347** in clean manner with good overall yield.

**Scheme 6.10.** Synthesis of symmetrical DPP **347**.

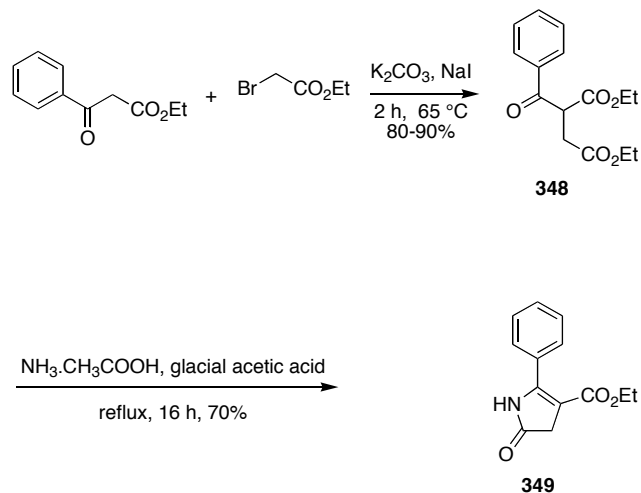


## Scheme 6.10. Continued.

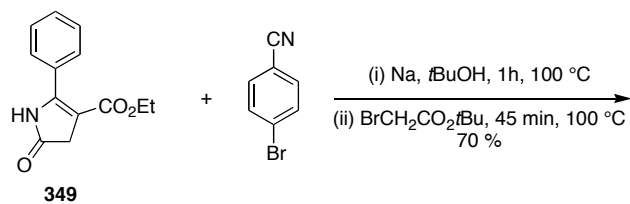
**Unsymmetrical DPP**

Unsymmetrical DPP could also be obtained with the same procedure; only 2 different benzonitriles were mixed with diethyl succinate. However this method leads to a mixture of symmetrical and unsymmetrical DPPs.

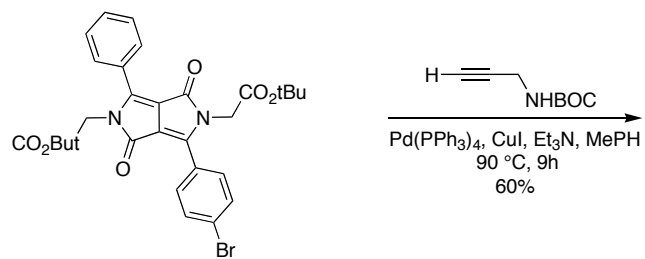
On the other hand, reaction of a pyrrolinone moiety **349** (obtained by condensation of diethyl benzoylsuccinate with ammonium acetate) with a benzonitrile derivative (Scheme 6.11), represents a clean access to unsymmetrical DPP.

**Scheme 6.11.** Synthesis of the pyrrolinone **349**.

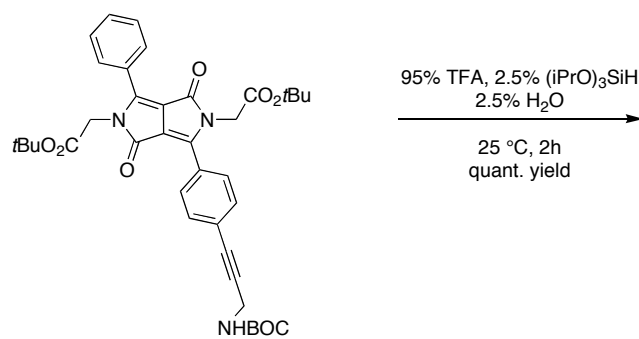
Subsequent reaction of the pyrrolinone **349** with 4-bromobenzonitrile in presence of sodium *tert*-butoxide, followed by alkylation *in situ* with *tert*-butyl bromoacetate afforded the unsymmetrical DPP **350** in a good yield (Scheme 6.12). Subsequent Sonogashira coupling with Boc protected propargyl amine, followed by removal of the *tert*-butyl ester and Boc groups finally afforded the unsymmetrical DPP **352** (Scheme 6.12).

**Scheme 6.12.** Synthesis of unsymmetrical DPP **352**.

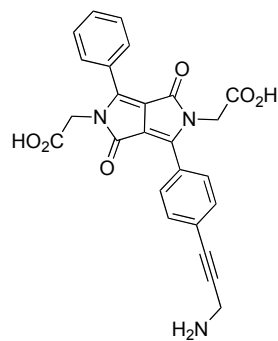
## Scheme 6.12. Continued.



350



351



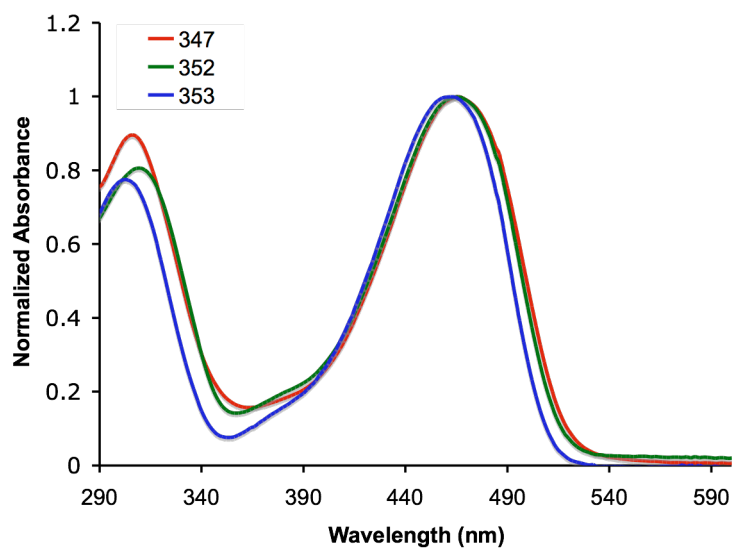
352

## 2. UV and Fluorescence Studies

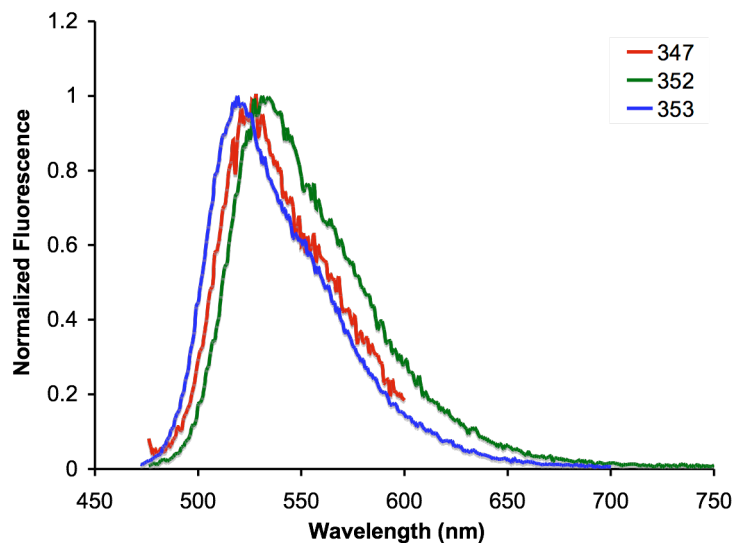
Table 6.2, Figure 6.6 and Figure 6.7 show UV and fluorescence data for the symmetrical DPP **347**, and the unsymmetrical DPPs **352**, and **353** in aqueous sodium bicarbonate solution. Compound **353** was obtained by cleavage of the *tert*-butyl group in compound **350**.

**Table 6. 2.** Spectroscopic data for the compounds **347**, **352**, and **353**.

| compound   | $\lambda_{\max}$<br>abs (nm) | $\lambda_{\max}$ emis (nm) (excited at<br>the $\lambda_{\max}$ abs ) |
|------------|------------------------------|--|
| <b>347</b> | 466                          | 528  |
| <b>352</b> | 466                          | 531  |
| <b>353</b> | 462                          | 519  |



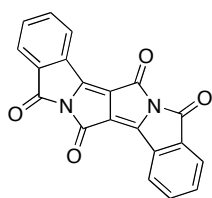
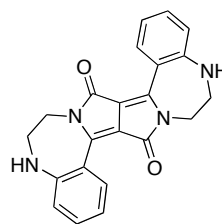
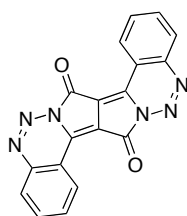
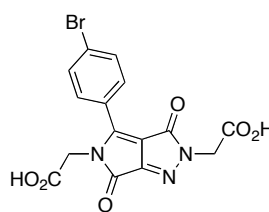
**Figure 6.6.** Normalized UV Absorption of DPP **347**, **351** and **352** in NaHCO<sub>3</sub>.



**Figure 6.7.** Normalized Fluorescence Emission of DPP **347**, **352** and **353** in  $\text{NaHCO}_3$ .

From these results, we concluded that DPP dyes could act as a donor in cassette for DNA sequencing, due to its absorption close to the wavelength used in argon laser (488 nm). Introduction of the propargyl amine moiety in an attempt to extend the conjugation (**352**) and thus displace the maximum absorption wavelength toward longer wavelength only gave a small red shift suggesting that the diketopyrrolopyrrole core is the component to be modified in the dye in order to change its physical properties.

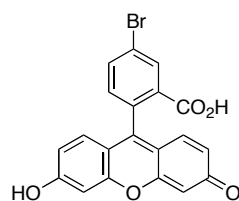
Thus, the properties of the DPP derived dyes could be tuned to longer wavelengths by introducing a more constraint, rigid system. Polycyclic systems such as **S**, **T** and **U** from 2-cyano-benzoic methyl ester and 2-nitro benzonitrile could be near-IR derivatives of DPPs. We have also considered the synthesis of aza-DPP **V** but condensation of the corresponding oxo-dihydro-pyrazole with 4-bromobenzonitrile failed to produce the pyrazolone **V** due to the lower reactivity of the pyrazole toward nucleophilic attack.

**S****T****U****V**

### 3. DPP-based Cassettes

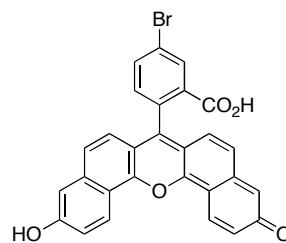
Synthesis of DPP based cassettes was undertaken in order to improve the  $\lambda$  maximum absorption (from 466 nm to 488 nm) and the molar extinction coefficient  $\epsilon$  of DPP. Fluorescein and naphthofluorescein were chosen as acceptor due to their relatively high absorptivity, and good water solubility.

Dibromo-DPP was first synthesized following the previously described procedure. Subsequent Sonogashira coupling with trimethylsilylacetylene, followed by TBAF removal of the TMS group yielded diacetylene derivative DPP **355**. Attachment of the acceptor, 5-bromofluorescein diacetate and 5-bromonaphthofluorescein diacetate, was accomplished using Sonogashira coupling (Scheme 6.13).



5-bromofluorescein

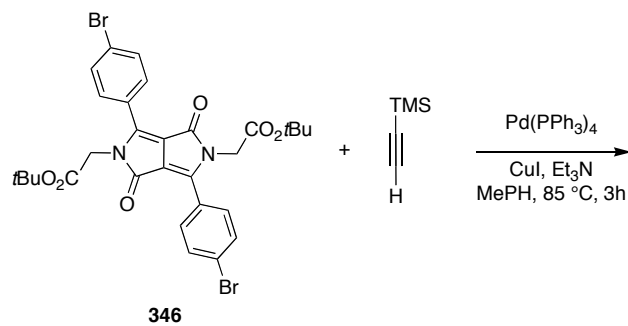
$\lambda_{\text{abs}}$  492 nm  
 $\lambda_{\text{flu}}$  518 nm



5-bromo naphthofluorescein

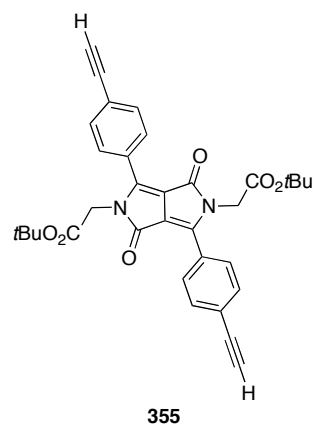
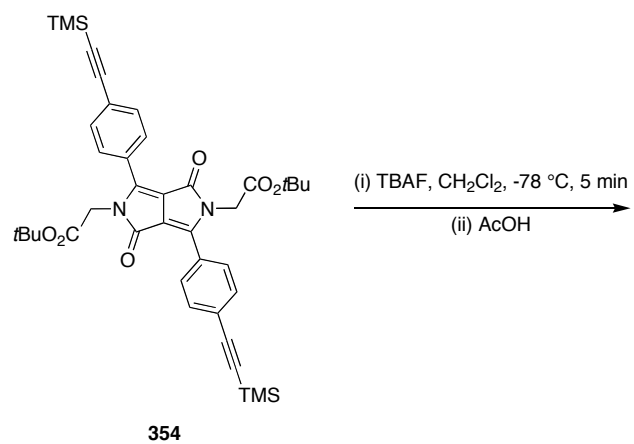
$\lambda_{\text{abs}}$  602 nm  
 $\lambda_{\text{flu}}$  666 nm

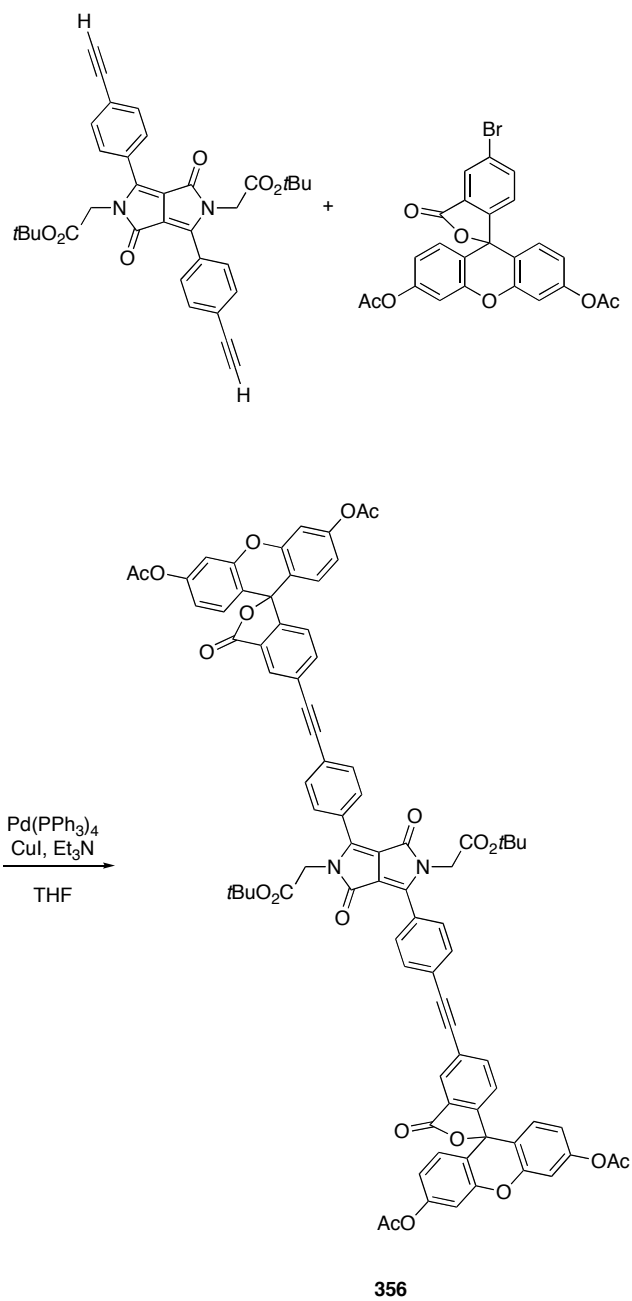
**Scheme 6.13.** Synthesis of bis-ethynyl DPP **355**.

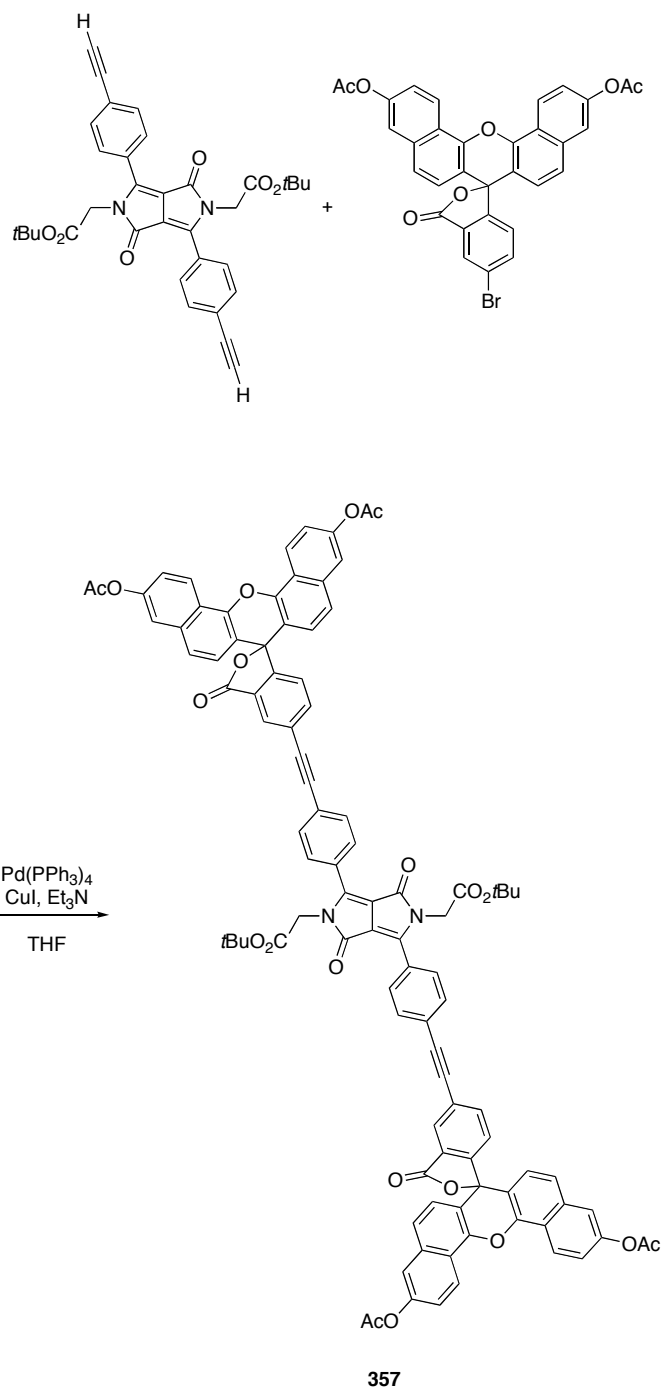




## Scheme 6.13. Continued.



**Scheme 6.14.** Synthesis of bis-fluoresceindiacetate-DPP cassette **356**.

**Scheme 6.15.** Synthesis of bis-naphthofluoresceindiactetate-DPP cassette **357**.

The final cassettes could be obtained by simultaneous removal of the acetate and the *tert*-butyl groups.

### C. Conclusion

An efficient route (two steps, one pot reaction) to *N,N*-disubstituted DPP was designed and used to produce compound **346** on a large scale. *N*-Alkylation not only increased the solubility of the DPP derivatives prepared, but also provided an easy access to a linker for attachment to biomolecules by deprotection of the *tert*-butyl functionality. Unsymmetrical DPPs **352** and **353** were also prepared and studied. DPPs **347**, **352** and **353** represent some of the few water-soluble DPPs. As illustrated with the preparation of cassettes **356** and **357**, compound **346** is a useful synthon for the preparation of through-bond energy-transfer cassette via Palladium mediated cross-coupling. However, because of their low extinction coefficient and low fluorescence intensity in aqueous media, we decided to stop this project and focus on different dyes more suitable for DNA sequencing and/or cell imaging.

## CHAPTER VII

### OUTLOOK AND CONCLUSION

#### A. Outlook

Designing new near-IR dyes consists of a lot of trial-error and is a very challenging task as it is hard to predict their quantum yields and extinction coefficients. Aza-BODIPYs have potential as biomolecular probes since they emit around 700 nm and above. However, as illustrated in Chapter II, a lot remains to be done to increase their water-solubilities, and reduce their overall hydrophobicity. There is therefore a need to design new water-soluble near-IR dyes. Cyanines dyes are the most common near-IR, but they have low quantum yield in water, and they are not ideal for single molecule detection.

#### 1. *Water-soluble Near-IR Dyes Based on Diketopyrrolopyrroles (DPP) Dyes*

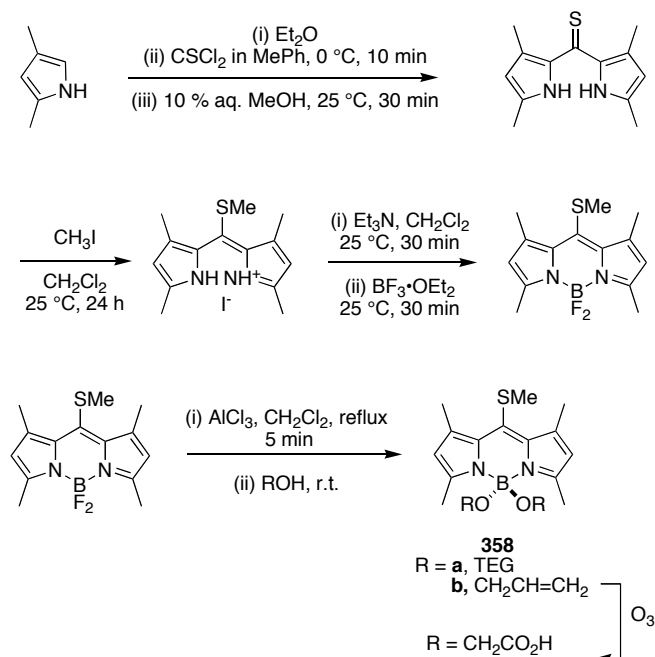
Although our first attempt to use DPPs in through-bond energy transfer cassettes failed, a recent report on near-IR DPPs<sup>358</sup> prompted our interest again. DPPs, as mentioned in the previous chapter, are highly insoluble in most organic solvents due to the network of hydrogen bonds they form with each other. By *N*-alkylation, their solubility can significantly be increased by suppressing the formation of these hydrogen bonds. Similarly, activation of the carbonyl groups, followed by reaction with nucleophile can be used to increase the solubilities of DPPs, but often, this only led to monosubstitution or to ring opening.<sup>359,360</sup> Daltrozzo and coworkers, have, however, recently reported the synthesis of disubstituted near-IR DPP dyes, by condensation of DPP with heteroarylacetonitriles in an excess of POCl<sub>3</sub>, followed by complexation with BF<sub>3</sub>•OEt<sub>2</sub> or BPh<sub>2</sub>Cl.<sup>360</sup> The new dyes thus formed emitted at 773 and 831 nm, with high quantum yield (0.59 and 0.53) and high extinction coefficient. Inspired by this work, we want to investigate the ability of these new dyes to act as acceptor in through-bond energy transfer cassettes. To be used as bio-molecular probes, cassettes must be water-soluble, and have a handle to attach to biomolecules. The absorption and fluorescence emission of fluorescein being pH dependent, we propose to use a BODIPY dye as donor. Our group has recently developed a methodology to synthesize sulfonated BODIPY dyes; however, it

appears that those dyes are not very stable. Therefore, we need to design new water-soluble dyes.

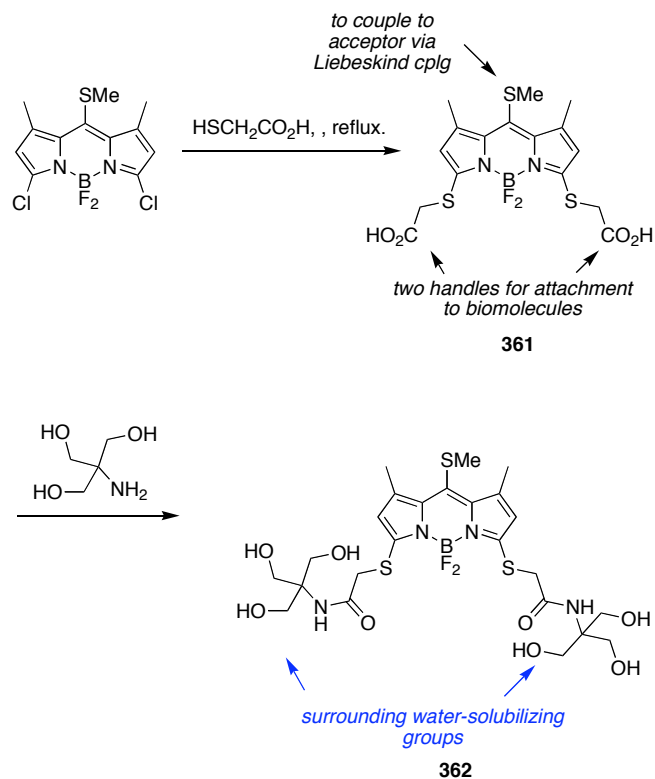
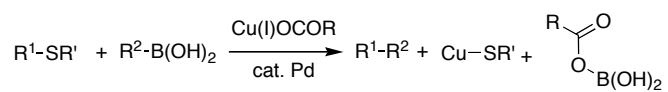
Triton X-100, the surfactant used to increase the solubility of our cassettes and/or dyes, is nothing else than a phenyl polyethylene glycol derivative. Therefore, we envisage use of the polyethylene glycol motif as our solubilizing group. In addition to increasing water-solubilities of our dyes, introducing triethylene glycol chains instead of sulfonic acids should greatly increase the ease of purification.

There are several ways to introduce a polyethylene glycol chain onto a BODIPY core. The first one is the substitution of the *F*-atoms with polyethylene glycol (Scheme 7.1). The second way is nucleophilic substitution onto 3,5-dichloroBODIPY. Scheme 7.1 describes the synthesis of *B*-alkoxides derivatives **358** from triethylene glycol (**358a**) or allyl alcohol (**358b**). Allyl alcohol is chosen because a handle to attach to biomolecules could be easily obtained via ozonolysis. The thio-ether BODIPY could be obtained following the procedure developed by Biellmann and co-workers.<sup>361</sup>

**Scheme 7.1.** Synthesis of **a**, a water-soluble donor; and **b**, a donor bearing a handle.





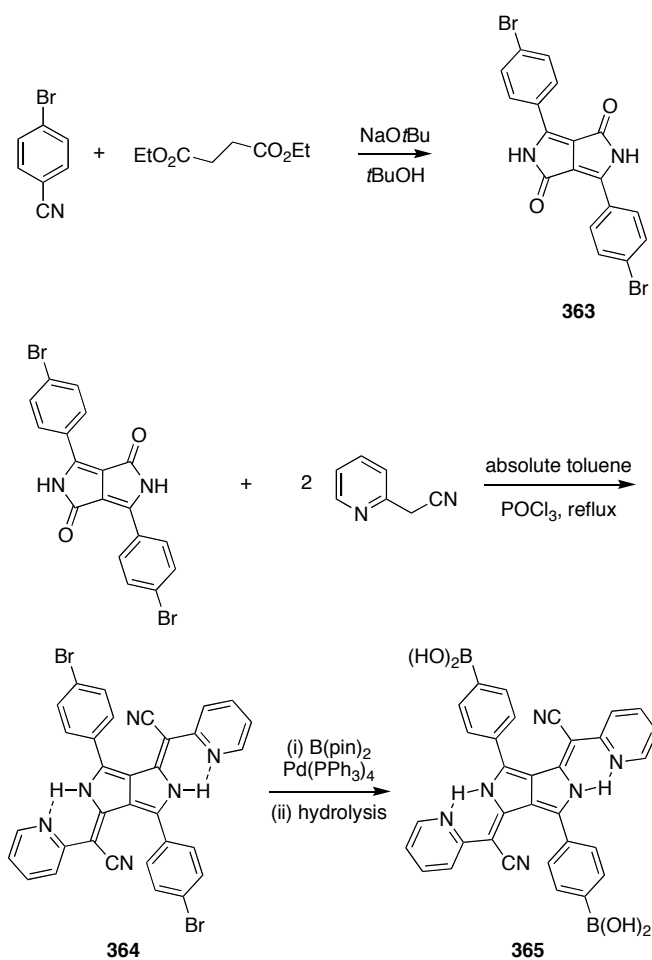
**Scheme 7.3.** Synthesis of a poly-ol BODIPY.**Scheme 7.4.** The Liebeskind-Srögl cross-coupling.**Synthesis of the cassette**

Synthesis of our first target is described in Scheme 7.5. In the first step, the dibromo-DPP has to be prepared. This will be achieved by condensation of 4-bromobenzonitrile with diethyl

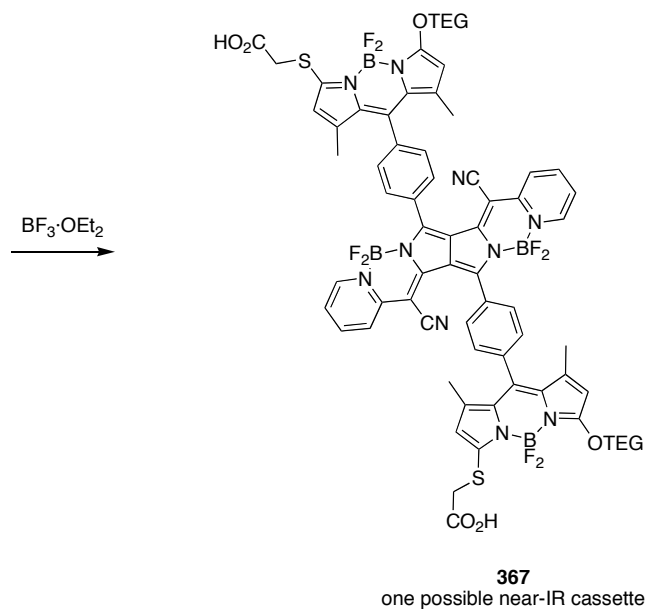
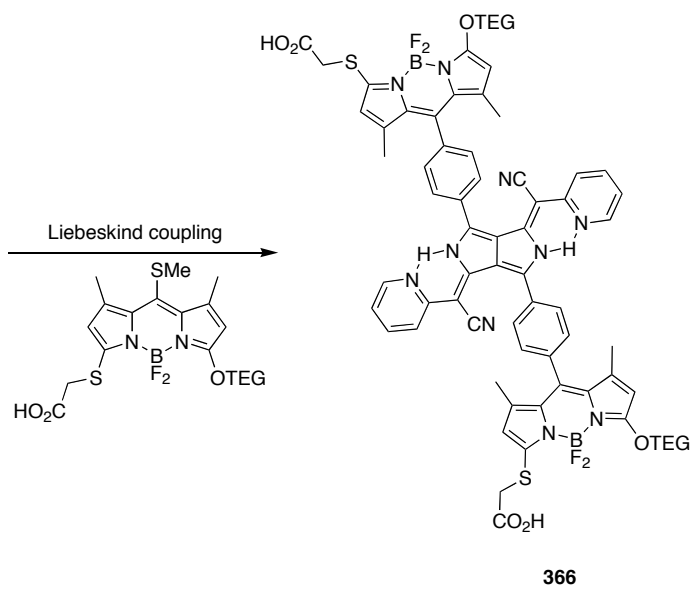


succinate in presence of a strong base. Next, condensation of 2-(pyridin-2-yl)acetonitrile in presence of  $\text{POCl}_3$  with **363** will provide compound **364**. The latter can then be converted to the boronic acid **365** and coupled to any donor described above via the Liebeskind-Srögl cross-coupling to form **366** which upon complexation with  $\text{BF}_3 \cdot \text{OEt}_2$  will afford the target compound **367**.<sup>362-365</sup> Upon excitation at 498 nm, emission at around 780 nm should be observed. Compound **367** is an illustrative example of cassettes that could be obtained via this route.

**Scheme 7.5.** Synthesis of a near-IR DPP-BODIPY based cassette.



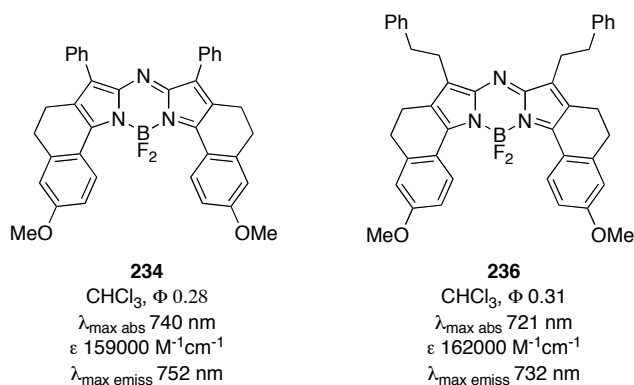
## Scheme 7.5. Continued.



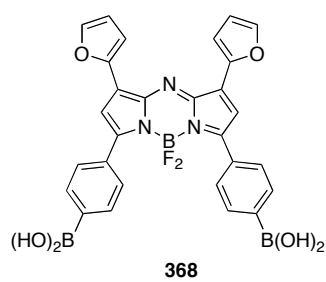
## 2. Water-soluble cassettes based on aza-BODIPY

As mentioned earlier, aza-BODIPY dyes tend to aggregate in aqueous solution or polar solvents in general. Therefore, there is a need to increase their solubility while trying to

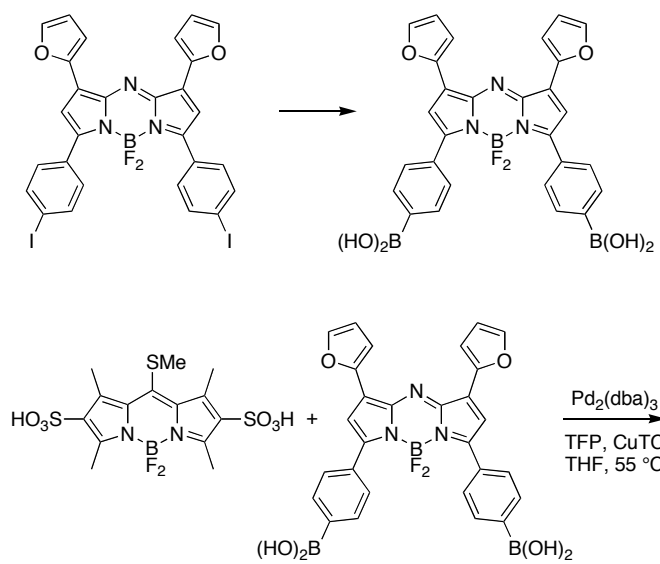
maintain their interesting properties, e.g. NIR absorption and emission, good quantum yields. In his latest work, Carreira reported that aryl groups at the 3,3-positions were required to form the dye, without them, no product could be obtained. The 5-position could however be altered. Thus, a 3,3-diaryl-5,5-dialky azaBODIPY dye **234** was synthesized. Introduction of alkyls groups resulted only in a small blue shift of both the absorption and emission relative to **236**.



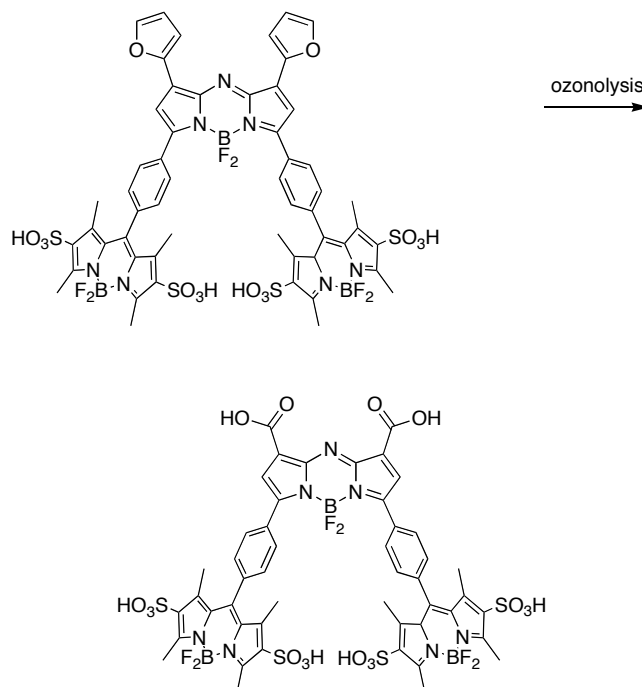
Therefore, we propose to synthesize the furan-based aza-BODIPY dye **368**. Compound **368** is particularly interesting as it easily allows introduction of carboxylic acid group onto the aza-BODIPY core via ozonolysis. Compound **368** could be prepared via the classical route from 2-furaldehyde and 4-iodoacetophenone. Compound **369** is an example of near-IR cassette that could be prepared from **368** via the Liebeskind cross-coupling. A bis-sulfonated BODIPY is shown in this case as a donor, but any of the BODIPYs mentioned above could be used as well. The synthesis of the cassette is shown in Scheme 7.6.



**Scheme 7.6.** Synthesis of a cassette via the Liebeskind- Srögl cross-coupling reaction.



## Scheme 7.6. Continued.



## B. Conclusion

A series of near-infrared aza-BODIPY dyes have been synthesized, and their spectroscopic properties measured. Through-bond energy transfer cassettes featuring two fluorescein units as donor, and an aza-BODIPY dye as acceptor, were then synthesized and their preliminary spectroscopic properties examined. For both cassettes, little to no energy transfer was observed in buffer pH 7.4. Addition of the non-ionic surfactant Triton X-100 (5%) to buffer pH 7.4 resulted in an increased energy transfer from the donor to the acceptor upon excitation at 488 nm. Cassettes **289** and **290**, although emitting near-IR are really not ideal for cell imaging. The combination of a fluorescein moiety as a donor with an aza-BODIPY as the acceptor, appeared to be a poor choice as they are of opposite nature (hydrophobic acceptor and hydrophilic, pH dependent donor). A lot remain to be done to make aza-BODIPY dyes useful for cell imaging.

Novels near-infrared aza-BODIPYs **300** were synthesized via a one-pot, two steps reaction. Upon demethylation, and intermolecular cyclization onto the *B*-atom, a  $\sim 100$  nm red-shift of both the absorption and fluorescence emission maxima could be observed. Furthermore, as much as a seven fold increase in the fluorescence quantum yield was obtained upon cyclization. Electrochemical studies were realized for the first time on aza-BODIPY **288a** and **300a**. Both compounds displayed a reversible oxidation and reduction waves.

Through-bond energy transfer cassettes **303** and **304** featuring a squaraine as the acceptor have been synthesized and their spectroscopic properties studied. Efficient energy transfer was observed for those cassettes upon excitation of the donor (ca. 300 nm). Although compounds **303** and **304** fluoresced brightly in the near-IR region, their lack of handle to attach to biomolecules and their poor water-solubilities made them unsuitable for cell imaging.

In Chapter III, our collaborative work with Dr Hochstraser found no systematic correlation of the transfer rate with the nature of the acceptor. No correlation was found either between the rates and the distance separating the donor and acceptor. Looking at the transition moments of the donor and acceptor, a general trend was observed for each series. When the transition moments of the donor and acceptor were aligned with the linker, and coaxial, fast energy transfer was observed ( $\sim 200$  fs). When the transition moments were aligned with the linker, but perpendicular, the observed rate of energy transfer was 0.42 ps. For parallel transition moments, perpendicular to the linker, the rate of energy transfer was around 6 ps with the exception of compound **330** for which the transfer rate was much reduced (20 ps).

Finally, we investigated the use of DPP (diketo-pyrrolopyrrole) pigment as a potential donor for through-bond energy transfer cassette. A convenient route to *N,N*-alkylated DPP was designed and allowed preparation of compound **346** in good yield on a large scale. This compound was a useful synthon for the preparation of cassette **356** and **357**. Three water-soluble DPPs, whom two of them were unsymmetrical were also prepared. The new DPP dyes thus prepared showed weak fluorescence emission and poor extinction coefficient. For these reasons, this project was stopped.

## REFERENCES

- (1) Nakanishi, J.; Nakajima, T.; Sato, M.; Ozawa, T.; Tohda, K.; Umezawa, Y. *Anal. Chem.* **2001**, *73*, 2920-2928.
- (2) Yamada, K.; Toyota, T.; Takakura, K.; Ishimaru, M.; Sugawara, T. *New J. Chem.* **2001**, *25*, 667-669.
- (3) Frangioni, J. V. *Curr. Opin. Chem. Biol.* **2003**, *7*, 626-34.
- (4) Weiss, S. *Science* **1999**, *283*, 1676-83.
- (5) Moerner, W. E.; Orrit, M. *Science* **1999**, *283*, 1670-6.
- (6) Ha, T. *Methods* **2001**, *25*, 78-86.
- (7) Nie, S.; Zare, R. N. *Annu. Rev. Biophys. Biomol. Struct.* **1997**, *26*, 567-596.
- (8) Tamarat, P.; Maali, A.; Lounis, B.; Orrit, M. *J. Phys. Chem.* **2000**, *104*, 1-16.
- (9) Ross, A. H.; Daou, M.-C.; McKinnon, C. A.; Condon, P. J.; Lachyankar, M. B.; Stephens, R. M.; Kaplan, D. R.; Wolf, D. E. *J. Cell Biol.* **1996**, *132*, 945-53.
- (10) Karolin, J.; Johansson, L. B.-A.; Strandberg, L.; Ny, T. *J. Am. Chem. Soc.* **1994**, *116*, 7801-6.
- (11) Haugland, R. P. *Handbook of Fluorescent Probes and Research Chemicals*; 6th ed.; Molecular Probes: Eugene, OR, 1996.
- (12) Tan, K.; Jaquinod, L.; Paolesse, R.; Nardis, S.; Di Natale, C.; Di Carlo, A.; Prodi, L.; Montalti, M.; Zaccheroni, N.; Smith, K. M. *Tetrahedron* **2004**, *60*, 1099-1106.
- (13) Yee, M.-c.; Fas, S. C.; Stohlmeyer, M. M.; Wandless, T. J.; Cimprich, K. A. *J. Biol. Chem.* **2005**, *280*, 29053-29059.
- (14) Wagner, R. W.; Lindsey, J. S. *Pure Applied Chem.* **1996**, *68*, 1373-80.
- (15) Metzker, M. L. Substituted 4,4-difluoro-4-bora-3a, 4a-diaza-s-indacene compounds for 8-color DNA sequencing. WO Patent 2003066812, February 5, 2003.

- (16) Fa, M.; Bergstrom, F.; Hagglof, P.; Wilczynska, M.; Johansson, L. B. A.; Ny, T. *Structure* **2000**, *8*, 397-405.
- (17) Bergstrom, F.; Hagglof, P.; Karolin, J.; Ny, T.; Johansson, L. B. A. *Proc. Natl. Acad. Sci. U.S.A.* **1999**, *96*, 12477-12481.
- (18) Wagner, R. W.; Lindsey, J. S. *Pure Applied Chem.* **1996**, *68*, 1373-1380.
- (19) Katayama, M.; Nakane, R.; Matsuda, Y.; Kaneko, S.; Hara, I.; Sato, H. *Analyst* **1998**, *123*, 2339-2342.
- (20) Karolin, J.; Johansson, L. B. A.; Strandberg, L.; Ny, T. *J. Am. Chem. Soc.* **1994**, *116*, 7801-6.
- (21) Drummen, G. P. C.; van Liebergen, L. C. M.; Op den Kamp, J. A. F.; Post, J. A. *Free Radical Biol. Med.* **2002**, *33*, 473-490.
- (22) Johnson, I. D.; Kang, H. C.; Haugland, R. P. *Anal. Biochem.* **1991**, *198*, 228-37.
- (23) Kurata, S.; Kanagawa, T.; Yamada, K.; Torimura, M.; Yokomaku, T.; Kamagata, Y.; Kurane, R. *Nucleic Acids Res.* **2001**, *29*, e34/1-e34/5.
- (24) Luo, Y.; Prestwich, G. D. *Bioconj. Chem* **1999**, *10*, 755-763.
- (25) Yamada, K.; Toyota, T.; Takakura, K.; Ishimaru, M.; Sugawara, T. *New J. Chem.* **2001**, *25*, 667-669.
- (26) Pagano, R. E.; Chen, C.-S. *Ann. NY Acad. Sci.* **1998**, *845*, 152-160.
- (27) Samsonov, A. V.; Mihalyov, I.; Cohen, F. S. *Biophys. J.* **2001**, *81*, 1486-1500.
- (28) Boldyrev, I. A.; Molotkovsky, J. G. *Russian J. Bioorg. Chem.* **2006**, *32*, 78-83.
- (29) Tahtaoui, C.; Parrot, I.; Klotz, P.; Guillier, F.; Galzi, J.-L.; Hibert, M.; Ilien, B. *J. Med. Chem.* **2004**, *47*, 4300-4315.
- (30) Shute, T. S.; Matsushita, M.; Dickerson, T. J.; La Clair, J. J.; Janda, K. D.; Burkart, M. D. *Bioconjugate Chem.* **2005**, *16*, 1352-1355.
- (31) Rostron, J. P.; Ulrich, G.; Retailleau, P.; Harriman, A.; Ziessel, R. *New J. Chem.* **2005**, *29*, 1241-1244.



- (32) Lawrie, G.; Grondahl, L.; Battersby, B.; Keen, I.; Lorentzen, M.; Surawski, P.; Trau, M. *Langmuir* **2006**, *22*, 497-505.
- (33) Merino, E. J.; Weeks, K. M. *J. Am. Chem. Soc.* **2005**, *127*, 12766-12767.
- (34) Fang, Y.; Peng, J.; Ferrie, A. M.; Burkhalter, R. S. *Anal. Chem.* **2006**, *78*, 149-155.
- (35) Worthington, A. S.; Burkart, M. D. *Org. Biomol. Chem.* **2006**, *4*, 44-46.
- (36) Li, J.; Kim, I. H.; Roche, E. D.; Beeman, D.; Lynch, A. S.; Ding, C. Z.; Ma, Z. *Bioorg. Med. Chem. Lett.* **2006**, *16*, 794-797.
- (37) Li, Z.; Mintzer, E.; Bittman, R. *J. Org. Chem.* **2006**, *71*, 1718-1721.
- (38) Toyota, T.; Tsuchi, H.; Yamada, K.; Takakura, K.; Yasuda, K.; Sugawara, T. *Langmuir* **2006**, *22*, 1976-1981.
- (39) Rose, T. M.; Prestwich, G. D. *ACS Chemical Biology* **2006**, *1*, 83-92.
- (40) Meng, Q.; Kim, D. H.; Bai, X.; Bi, L.; Turro, N. J.; Ju, J. *J. Org. Chem.* **2006**, *71*, 3248-3252.
- (41) Ferguson, C. G.; Bigman, C. S.; Richardson, R. D.; Van Meeteren, L. A.; Moolenaar, W. H.; Prestwich, G. D. *Org. Lett.* **2006**, *8*, 2023-2026.
- (42) Sculimbrene, B. R.; Imperiali, B. *J. Am. Chem. Soc.* **2006**, *128*, 7346-7352.
- (43) Peters, C.; Billich, A.; Ghobrial, M.; Hoegenauer, K.; Ullrich, T.; Nussbaumer, P. *J. Org. Chem.* **2007**, *72*, 1842-1845.
- (44) Golovkova, T. A.; Kozlov, D. V.; Neckers, D. C. *J. Org. Chem.* **2005**, *70*, 5545-5549.
- (45) Trieflinger, C.; Rurack, K.; Daub, J. *Angew. Chem. Int. Ed.* **2005**, *44*, 2288-2291.
- (46) Turfan, B.; Akkaya, E. U. *Org. Lett.* **2002**, *4*, 2857-9.
- (47) Gee, K. R.; Rukavishnikov, A.; Rothe, A. *Combinatorial Chemistry and High Throughput Screening* **2003**, *6*, 363-366.
- (48) Zhang, X.; Wang, H.; Li, J.-S.; Zhang, H.-S. *Anal. Chim. Act.* **2003**, *481*, 101-108.
- (49) DiCesare, N.; Lakowicz, J. R. *Tetrahedron Lett.* **2001**, *42*, 9105-9108.
- (50) Rurack, K.; Kollmannsberger, M.; Daub, J. *Angew. Chem. Int. Ed.* **2001**, *40*, 385-387.
- (51) Baki, C. N.; Akkaya, E. U. *J. Org. Chem.* **2001**, *66*, 1512-1513.

- (52) Kollmannsberger, M.; Rurack, K.; Resch-Genger, U.; Rettig, W.; Daub, J. *Chem. Phys. Lett.* **2000**, 329, 363-369.
- (53) Rurack, K.; Kollmannsberger, M.; Resch-Genger, U.; Daub, J. *J. Am. Chem. Soc.* **2000**, 122, 968-9.
- (54) Cha, N. R.; Moon, S. Y.; Chang, S.-K. *Tetrahedron Lett.* **2003**, 44, 8265-8268.
- (55) Werner, T.; Huber, C.; Heintl, S.; Kollmannsberger, M.; Daub, J.; Wolfbeis, O. S. *Fresenius' J. Anal. Chem.* **1997**, 359, 150-154.
- (56) Kollmannsberger, M.; Gareis, T.; Heintl, S.; Breu, J.; Daub, J. *Angew. Chem. Int. Ed.* **1997**, 36, 1333-1335.
- (57) Knaus, H. G.; Moshhammer, T.; Kang, H. C.; Haugland, R. P.; Glossmann, H. *J. Biol. Chem.* **1992**, 267, 2179-89.
- (58) Kalai, T.; Hideg, K. *Tetrahedron* **2006**, 62, 10352-10360.
- (59) Kalai, T.; Hideg, E.; Jeko, J.; Hideg, K. *Tetrahedron Lett.* **2003**, 44, 8497-8499.
- (60) Moon, S. Y.; Cha, N. R.; Kim, Y. H.; Chang, S.-K. *J. Org. Chem.* **2004**, 69, 181-183.
- (61) Gabe, Y.; Urano, Y.; Kikuchi, K.; Kojima, H.; Nagano, T. *J. Am. Chem. Soc.* **2004**, 126, 3357-67.
- (62) Li, M.; Wang, H.; Zhang, X.; Zhang, H. *Spectrochim. Acta, Part A: Mol. and Biomol. Spectroscopy* **2004**, 60A, 987-993.
- (63) Koutaka, H.; Kosuge, J.; Fukasaku, N.; Hirano, T.; Kikuchi, K.; Urano, Y.; Kojima, H.; Nagano, T. *Chem. Pharm. Bull.* **2004**, 52, 700-703.
- (64) Martin, V. V.; Rothe, A.; Diwu, Z.; Gee, K. R. *Bioorg. Med. Chem. Lett.* **2004**, 14, 5313-5316.
- (65) Zhang, X.; Zhang, H. *Spectrochim. Acta, Part A: Mol. Biomol. Spectroscopy* **2005**, 61A, 1045-1049.
- (66) Martin, V. V.; Rothe, A.; Gee, K. R. *Bioorg. Med. Chem. Lett.* **2005**, 15, 1851-1855.
- (67) Wu, Y.; Peng, X.; Guo, B.; Fan, J.; Zhang, Z.; Wang, J.; Cui, A.; Gao, Y. *Org. Biomol. Chem.* **2005**, 3, 1387-1392.

- (68) Baruah, M.; Qin, W.; Basaric, N.; De Borggraeve Wim, M.; Boens, N. *J. Org. Chem.* **2005**, *70*, 4152-7.
- (69) Yamada, K.; Nomura, Y.; Citterio, D.; Iwasawa, N.; Suzuki, K. *J. Am. Chem. Soc.* **2005**, *127*, 6956-6957.
- (70) Coskun, A.; Akkaya, E. U. *J. Am. Chem. Soc.* **2005**, *127*, 10464-10465.
- (71) Basaric, N.; Baruah, M.; Qin, W.; Metten, B.; Smet, M.; Dehaen, W.; Boens, N. *Org. Biomol. Chem.* **2005**, *3*, 2755-2761.
- (72) Malval, J.-P.; Leray, I.; Valeur, B. *New J. Chem.* **2005**, *29*, 1089-1094.
- (73) Baruah, M.; Qin, W.; Vallee, R. A. L.; Beljonne, D.; Rohand, T.; Dehaen, W.; Boens, N. *Org. Lett.* **2005**, *7*, 4377-4380.
- (74) Bricks, J. L.; Kovalchuk, A.; Trieflinger, C.; Nofz, M.; Bueschel, M.; Tolmachev, A. I.; Daub, J.; Rurack, K. *J. Am. Chem. Soc.* **2005**, *127*, 13522-13529.
- (75) Coskun, A.; Deniz, E.; Akkaya, E. U. *Org. Lett.* **2005**, *7*, 5187-5189.
- (76) Zeng, L.; Miller, E. W.; Pralle, A.; Isacoff, E. Y.; Chang, C. J. *J. Amer. Chem. Soc.* **2006**, *128*, 10-11.
- (77) Meallet-Renault, R.; Herault, A.; Vachon, J.-J.; Pansu, R. B.; Amigoni-Gerbier, S.; Larpent, C. *PhotoChem. Photobiol.* **2006**, *5*, 300-310.
- (78) Mei, Y.; Bentley, P. A.; Wang, W. *Tetrahedron Lett.* **2006**, *47*, 2447-2449.
- (79) Qi, X.; Jun, E. J.; Xu, L.; Kim, S.-J.; Hong, J. S. J.; Yoon, Y. J.; Yoon, J. *J. Org. Chem.* **2006**, *71*, 2881-2884.
- (80) Wang, J.; Qian, X. *Org. Lett.* **2006**, *8*, 3721-3724.
- (81) Li, J.-S.; Wang, H.; Huang, K.-J.; Zhang, H.-S. *Anal. Chim. Acta* **2006**, *575*, 255-261.
- (82) Kim, H. J.; Kim, J. S. *Tetrahedron Lett.* **2006**, *47*, 7051-7055.
- (83) Gabe, Y.; Ueno, T.; Urano, Y.; Kojima, H.; Nagano, T. *Anal. Biochem.* **2006**, *386*, 621-626.
- (84) Arbeloa, T. L.; Arbeloa, F. L.; Arbeloa, I. L.; Garcia-Moreno, I.; Costela, A.; Sastre, R.; Amat-Guerri, F. *Chem. Phys. Lett.* **1999**, *299*, 315-321.

- (85) <http://probes.invitrogen.com> In *Molecular Probes*; Invitrogen Corporation, 2006.
- (86) Dixon, H. B. F.; Cornish-Bowden, A.; Liebecq, C.; Loening, K. L.; Moss, G. P.; Reedijk, J.; Velick, S. F.; Venetianer, P.; Vliegthart, J. F. G.; et al. *Pure Appl. Chem.* **1987**, *59*, 779-832.
- (87) Van Koeveringe, J. A.; Lugtenburg, J. *Recl. Trav. Chim. Pays-Bas* **1977**, *96*, 55-58.
- (88) Vos de Wael, E.; Pardoën, J. A.; Van Koeveringe, J. A.; Lugtenburg, J. *Recl Trav. Chim. Pays-Bas* **1977**, *96*, 306-9.
- (89) Wael, E. V. d.; Pardoën, J. A.; Koeveringe, J. A. v.; Lugtenburg, J. *Recl. Trav. Chim. Pays-Bas* **1977**, *96*, 306-9.
- (90) Bandichhor, R.; Thivierge, C.; Bhuvanesh, N. S. P.; Burgess, K. *Acta Crystallogr. Sect. E: Struct. Rep. Online* **2006**, *E62*, o4310-o4311.
- (91) Shah, M.; Thangaraj, K.; Soong, M.-L.; Wolford, L. T.; Boyer, J. H.; Politzer, I. R.; Pavlopoulos, T. G. *Heteroat. Chem.* **1990**, *1*, 389-99.
- (92) Boyer, J. H.; Haag, A. M.; Sathyamoorthi, G.; Soong, M. L.; Thangaraj, K.; Pavlopoulos, T. G. *Heteroat. Chemistry* **1993**, *4*, 39-49.
- (93) Goud, T. V.; Tutar, A.; Biellmann, J.-F. *Tetrahedron* **2006**, *62*, 5084-5091.
- (94) Nicolaou, K. C.; Claremon, D. A.; Papahatjis, D. P. *Tetrahedron Lett.* **1981**, *22*, 4647-50.
- (95) Tahtaoui, C.; Thomas, C.; Rohmer, F.; Klotz, P.; Duportail, G.; Mely, Y.; Bonnet, D.; Hibert, M. *J. Org. Chem.* **2007**, *72*, 269-272.
- (96) Oleynik, P.; Ishihara, Y.; Cosa, G. *J. Am. Chem. Soc.* **2007**, *139*, 1842-1843.
- (97) Matsui, M.; Funabiki, K.; Nakaya, K.-i. *Bull. Chem. Soc. Jpn.* **2005**, *78*, 464-467.
- (98) DeSilva, A. P.; Gunaratne, H. G. N.; Gunnlaugsson, T.; Huxley, A. J. M.; McCoy, C. P.; Rademacher, J. T.; Rice, T. E. *Chem. Rev.* **1997**, *97*, 1515-66.
- (99) Tanaka, K.; Miura, T.; Umezawa, N.; Urano, Y.; Kikuchi, K.; Higuchi, T.; Nagano, T. *J. Am. Chem. Soc.* **2001**, *123*, 2530-2536.
- (100) Ueno, T.; Urano, Y.; Setsukinai, K.; Takakusa, H.; Kojima, H.; Kikuchi, K.; Ohkubo, K.; Fukuzumi, S.; Nagano, T. *J. Am. Chem. Soc.* **2004**, *126*, 14079-14085.

- (101) Sunahara, H.; Urano, Y.; Kojima, H.; Nagano, T. *J. Am. Chem. Soc.* **2007**, *129*, 5597-5604.
- (102) Rehm, D.; Weller, A. *Isr. J. Chem.* **1970**, *8*, 259-71.
- (103) Ueno, T.; Urano, Y.; Kojima, H.; Nagano, T. *J. Am. Chem. Soc.* **2006**, *128*, 10640-10641.
- (104) Worries, H. J.; Koek, J. H.; Lodder, G.; Lugtenburg, J.; Fokkens, R.; Driessen, O.; Mohn, G. R. *Recl. Trav. Chim. Pays-Bas* **1985**, *104*, 288-91.
- (105) Morgan, L. R.; Boyer, J. H. Boron difluoride compounds useful in photodynamic therapy and production of laser light. US Patent 5,189,029, 1995.
- (106) Morgan, L. R.; Boyer, J. H. Heterocyclic compounds and their use in photodynamic therapy. WO Patent 9419355, February 18, 1994.
- (107) Urano, T.; Nagasaka, H.; Tsuchiyama, M.; Ide, H. Photopolymerizable composition. US Patent 5498641, April 7, 1994.
- (108) Boyer, J. H.; Morgan, L. R. Preparation of difluoroboradiaza-s-indacene compounds and methods for using them. US Patent 5189029, 1993.
- (109) Boyer, J. H.; Morgan, L. R. Fluorescent chemical compositions useful as laser dyes and photodynamic therapy agents, and methods for their use. US Patent 361936, 1990.
- (110) Pavlopoulos, T. G.; Boyer, J. H.; Shah, M.; Thangaraj, K.; Soong, M. L. *Appl. Opt.* **1990**, *29*, 3885-6.
- (111) Boyer, J. H.; Thangaraj, K.; Soong, M. L.; Sathyamoorthi, G.; Ross, T. M.; Haag, A. M. *Proceedings of the International Conference on Lasers* **1991**, 739-41.
- (112) Pavlopoulos, T. G. *Proc. SPIE- Int. Soc. Opt. Eng.* **1999**, *3613*, 112-118.
- (113) Suzuki, T.; Tanaka, T.; Higashiguchi, I.; Oda, A. Organic electroluminescent device elements. JP Patent 11176572, 1999.
- (114) Takuma, K.; Misawa, T.; Sugimoto, K.; Nishimoto, T.; Tsukahara, H.; Tsuda, T.; Imai, G.; Kogure, H. Visible light-curable resin compositions and their use in inks. JP Patent 10273504, January 29, 1998.

- (115) Imai, G.; Kogure, H.; Ogiso, A.; Misawa, T.; Nishimoto, T.; Tsukahara, H.; Takuma, K. Visible light-curable resin compositions and their use in electrophotographic material. JP Patent 2000001509, 2000.
- (116) Imai, G.; Kogure, H.; Ogiso, A.; Misawa, T.; Nishimoto, T.; Tsukahara, H.; Takuma, K. Visible light-curable resin compositions and their use in electrophotographic material. JP Patent 2000001510, 2000.
- (117) Imai, G.; Kogure, H.; Ogiso, A.; Misawa, T.; Nishimoto, T.; Tsukahara, H.; Takuma, K. Positive-working visible ray-sensitive resin composition containing pyromethene boron complex sensitizer and its usage. JP Patent 2000039715, 2000.
- (118) Imai, G.; Kogure, H.; Ogiso, A.; Misawa, T.; Nishimoto, T.; Tsukahara, H.; Takuma, K. Positive-working visible ray-sensitive resin composition containing pyromethene boron complex sensitizer and its usage. JP Patent 2000039716, 2000.
- (119) Haugland, R. P.; Kang, H. C. Reactive fluorescent dipyrrometheneboron difluoride dyes as molecular probes for biopolymers. US Patent 4774339, 1988.
- (120) Yogo, T.; Urano, Y.; Ishitsuka, Y.; Maniwa, F.; Nagano, T. *J. Am. Chem. Soc.* **2005**, *127*, 12162-63.
- (121) Rohand, T.; Baruah, M.; Qin, W.; Boens, N.; Dehaen, W. *Chem. Commun.* **2006**, 266-8.
- (122) Baruah, M.; Qin, W.; Vallee, R. A. L.; Beljonne, D.; Rohand, T.; Dehaen, W.; Boens, N. *Org. Lett.* **2005**, *7*, 4377-80.
- (123) Amat-Guerri, F.; Liras, M.; Carrascoso, M. L.; Sastre, R. *Photochem. Photobiol.* **2003**, *77*, 577-584.
- (124) Rieth, R. D.; Mankad, N. P.; Calimano, E.; Sadighi, J. P. *Org. Lett.* **2004**, *6*, 3981-3983.
- (125) Bowie, A. L.; Hughes, C. C.; Trauner, D. *Org. Lett.* **2005**, *7*, 5207-5209.
- (126) Beck, E. M.; Grimster, N. P.; Hatley, R.; Gaunt, M. J. *J. Am. Chem. Soc.* **2006**, *128*, 2528-2529.
- (127) Thivierge, C.; Bandichhor, R.; Burgess, K. *Org. Lett.* **2007**, ASAP.
- (128) Treibs, A.; Kreuzer, F.-H. *Liebigs Ann. Chem.* **1968**, *718*, 208-23.

- (129) Sathyamoorthi, G.; Boyer, J. H.; Allik, T. H.; Chandra, S. *Heteroat. Chemistry* **1994**, *5*, 403-7.
- (130) Allik, T. H.; Hermes, R. E.; Sathyamoorthi, G.; Boyer, J. H. *Proc. SPIE-Int. Soc. Opt. Eng.* **1994**, *2115*, 240-8.
- (131) Thoresen, L. H.; Kim, H.; Welch, M. B.; Burghart, A.; Burgess, K. *Synlett* **1998**, 1276-8.
- (132) Burghart, A.; Kim, H.; Welch, M. B.; Thoresen, L. H.; Reibenspies, J.; Burgess, K.; Bergström, F.; Johansson, L. B.-A. *J. Org. Chem.* **1999**, *64*, 7813-9.
- (133) Miyaura, N.; Yanagi, T.; Suzuki, A. *TL* **1981**, *11*, 513-9.
- (134) Boukou-Poba, J. P.; Farnier, M.; Guillard, R. *Tetrahedron Lett.* **1979**, *20*, 1717-1720.
- (135) Katrizky, A. R.; Li, J.; Gordeev, M. F. *Synthesis* **1994**, 93-96.
- (136) Trofimov, B. A. *Adv. Heterocycl. Chem* **1990**, *51*, 177-301.
- (137) Rettig, W. *Angew. Chem.* **1986**, *98*, 969-86.
- (138) Bergstroem, F.; Mikhalyov, I.; Haeggloef, P.; Wortmann, R.; Ny, T.; Johansson, L. B. A. *J. Am. Chem. Soc.* **2002**, *124*, 196-204.
- (139) Mikhalyov, I.; Gretskaya, N.; Bergstroem, F.; Johansson, L. B. A. *Phys. Chem. Chem Phys.* **2002**, *4*, 5663-5670.
- (140) Marushchak, D.; Kalinin, S.; Mikhalyov, I.; Gretskaya, N.; Johansson, L. B. A. *Spectrochim. Acta, Part A: Molecular and Biomolecular Spectroscopy* **2006**, *65A*, 113-122.
- (141) Zaitsev, A. B.; Meallet-Renault, R.; Schmidt, E. Y.; Mikhaleva, A. I.; Badre, S.; Dumas, C.; Vasil'tsov, A. M.; Zorina, N. V.; Pansu, R. B. *Tetrahedron* **2005**, *61*, 2683-88.
- (142) Rurack, K.; Kollmannsberger, M.; Daub, J. *New J. Chem.* **2001**, *25*, 289-292.
- (143) Coskun, A.; Akkaya, E. U. *Tetrahedron Lett.* **2004**, *45*, 4947-9.
- (144) Dost, Z.; Atilgan, S.; Akkaya, E. U. *Tetrahedron* **2006**, *62*, 8484-8488.
- (145) Yu, Y.-H.; Descalzo, A. B.; Shen, Z.; Rohr, H.; Liu, Q.; Wang, Y.-W.; Spieles, M.; Li, Y.-Z.; Rurack, K.; You, X.-Z. *Chemistry--An Asian Journal* **2006**, *1*, 176-187.

- (146) Baruah, M.; Qin, W.; Flors, C.; Hofkens, J.; Vallee, R. A. L.; Beljonne, D.; Van der Auweraer, M.; De Borggraeve, W. M.; Boens, N. *J. Phys. Chem. A* **2006**, *110*, 5998-6009.
- (147) Rurack, K.; Kollmannsberger, M.; Daub, J. *Angew. Chem. Int. Ed.* **2001**, *40*, 385-7.
- (148) Dahim, M.; Mizuno, N. K.; Li, X.-M.; Momsen, W. E.; Momsen, M. M.; Brockman, H. L. *Biophys. J.* **2002**, *83*, 1511-1524.
- (149) Saki, N.; Dinc, T.; Akkaya, E. U. *Tetrahedron* **2006**, *62*, 2721-2725.
- (150) Rohand, T.; Qin, W.; Boens, N.; Dehaen, W. *Eur. J. Org. Chem.* **2006**, 4658-4663.
- (151) Metzker, M. L.; Lu, J.; Gibbs, R. A. *Science* **1996**, *271*, 1420-2.
- (152) Kolb, H. C.; Finn, M. G.; Sharpless, K. B. *Angew. Chem. Int. Ed.* **2001**, *40*, 2004-21.
- (153) Yilmaz, M. D.; Bozdemir, O. A.; Akkaya, E. U. *Org. Lett.* **2006**, *8*, 2871-2873.
- (154) Shiragami, T.; Tanaka, K.; Andou, Y.; Tsunami, S.-i.; Matsumoto, J.; Luo, H.; Araki, Y.; Ito, O.; Inoue, H.; Yasuda, M. *J. Photochem. Photobiol., A* **2005**, *170*, 287-297.
- (155) D'Souza, F.; Smith, P. M.; Zandler, M. E.; McCarty, A. L.; Itou, M.; Araki, Y.; Ito, O. *J. Am. Chem. Soc.* **2004**, *126*, 7898-7907.
- (156) Koepf, M.; Trabolsi, A.; Elhabiri, M.; Wytko, J. A.; Paul, D.; Albrecht-Gary, A. M.; Weiss, J. *Org. Lett.* **2005**, *7*, 1279-1282.
- (157) Paul, D.; Wytko, J. A.; Koepf, M.; Weiss, J. *Inorg. Chem.* **2002**, *41*, 3699-3704.
- (158) Leray, I.; Valeur, B.; Paul, D.; Regnier, E.; Koepf, M.; Wytko, J. A.; Boudon, C.; Weiss, J. *Photochem. Photobiol.* **2005**, *4*, 280-286.
- (159) Leray, I.; Valeur, B.; Paul, D.; Regnier, E.; Koepf, M.; Wytko, J. A.; Boudon, C.; Weiss, J. *Photochem. Photobiol.* **2005**, *4*, 280.
- (160) Azov, V. A.; Schlegel, A.; Diederich, F. *Angew. Chem. Int. Ed.* **2005**, *44*, 4635-4638.
- (161) Holten, D.; Bocian, D.; Lindsey, J. S. *Acc. Chem. Res.* **2002**, *35*, 57-69.
- (162) Wagner, R. W.; Lindsey, J. S. *J. Am. Chem. Soc.* **1994**, *116*, 9759-60.
- (163) Wagner, R. W.; Lindsey, J. S.; Seth, J.; Palaniappan, V.; Bocian, D. F. *J. Am. Chem. Soc.* **1996**, *118*, 3996-7.



- (164) Li, F.; Yang, S. I.; Ciringh, Y.; Seth, J.; Martin, C. H.; Singh, D. L.; Kim, D.; Birge, R. R.; Bocian, D. F.; Holten, D.; Lindsey, J. S. *J. Am. Chem. Soc.* **1998**, *120*, 10001-17.
- (165) Kumaresan, D.; Agarwal, N.; Gupta, I.; Ravikanth, M. *Tetrahedron* **2002**, *58*, 5347-5356.
- (166) Kumaresan, D.; Gupta, I.; Ravikanth, M. *Tetrahedron Lett.* **2001**, *42*, 8547-8550.
- (167) Ravikanth, M.; Agarwal, N.; Kumaresan, D. *Chem. Lett.* **2000**, 836-837.
- (168) Li, F.; Yang, S. I.; Ciringh, Y.; Seth, J.; Martin, C. H., III; Singh, D. L.; Kim, D.; Birge, R. R.; Bocian, D. F.; Holten, D.; Lindsey, J. S. *J. Am. Chem. Soc.* **1998**, *120*, 10001-10017.
- (169) Ulrich, G.; Ziesel, R. *Tetrahedron Lett.* **2004**, *45*, 1949-53.
- (170) Ulrich, G.; Ziesel, R. *J. Org. Chem.* **2004**, *69*, 2070-2083.
- (171) Goze, C.; Ulrich, G.; Charbonniere, L.; Cesario, M.; Prange, T.; Ziesel, R. *Chem. Eur. J.* **2003**, *9*, 3748-3755.
- (172) Ulrich, G.; Ziesel, R. *Synlett* **2004**, 439-444.
- (173) Galletta, M.; Campagna, S.; Quesada, M.; Ulrich, G.; Ziesel, R. *Chem. Commun.* **2005**, 4222-4224.
- (174) Galletta, M.; Puntoriero, F.; Campagna, S.; Chiorboli, C.; Quesada, M.; Goeb, S.; Ziesel, R. *J. Phys. Chem. A* **2006**, *110*, 4348-4358.
- (175) Odobel, F.; Zabri, H. *Inorg. Chem.* **2005**, *44*, 5600-5611.
- (176) Harriman, A.; Rostron, J. P.; Cesario, M.; Ulrich, G.; Ziesel, R. *J. Phys. Chem. A* **2006**, *110*, 7994-8002.
- (177) Ziesel, R.; Diring, S.; Retailleau, P. *J. Chem. Soc. Dalton Trans.* **2006**, 3285-3290.
- (178) Wan, C.-W.; Burghart, A.; Chen, J.; Bergstroem, F.; Johansson, L. B.-A.; Wolford, M. F.; Kim, T. G.; Topp, M. R.; Hochstrasser, R. M.; Burgess, K. *Chem. Eur. J.* **2003**, *9*, 4430-41.
- (179) Kim, T. G.; Castro, J. C.; Loudet, A.; Jiao, J. G.-S.; Hochstrasser, R. M.; Burgess, K.; Topp, M. R. *J. Phys. Chem.* **2006**, *110*, 20-7.
- (180) Ziesel, R.; Goze, C.; Ulrich, G.; Cesario, M.; Retailleau, P.; Harriman, A.; Rostron, J. P. *Chem. Eur. J.* **2005**, *11*, 7366-7378.

- (181) Kee, H. L.; Kirmaier, C.; Yu, L.; Thamyongkit, P.; Youngblood, W. J.; Calder, M. E.; Ramos, L.; Noll, B. C.; Bocian, D. F.; Scheidt, W. R.; Birge, R. R.; Lindsey, J. S.; Holten, D. *J. Phys. Chem. B* **2005**, *109*, 20433-20443.
- (182) Goze, C.; Ulrich, G.; Mallon, L. J.; Allen, B. D.; Harriman, A.; Ziessel, R. *J. Am. Chem. Soc.* **2006**, *128*, 10231-10239.
- (183) Ulrich, G.; Goze, C.; Guardigli, M.; Roda, A.; Ziessel, R. *Angew. Chem. Int. Ed.* **2005**, *117*, 3760-3764.
- (184) Ziessel, R.; Goze, C.; Ulrich, G. *Synthesis* **2007**, *6*, 936-949.
- (185) Ziessel, R.; Ulrich, G.; Harriman, A. *New J. Chem.* **2007**, *31*, 496-501.
- (186) Harriman, A.; Izzet, G.; Ziessel, R. *J. Am. Chem. Soc.* **2006**, *128*, 10868-10875.
- (187) Goze, C.; Ulrich, G.; Ziessel, R. *Org. Lett.* **2006**, *8*, 4445-4448.
- (188) Goze, C.; Ulrich, G.; Ziessel, R. *J. Org. Chem.* **2006**, *ASAP Articles*.
- (189) Goeb, S.; Ziessel, R. *Organic Letters* **2007**, *9*, 737-740.
- (190) Kang, H. C.; Haugland, R. P. Dibenzopyrrometheneboron Difluoride Dyes. US Patent 5,433,896, July 18, 1995.
- (191) Fischer, H.; Schubert, M. *Berichte der Deutschen Chemischen Gesellschaft [Abteilung] B: Abhandlungen* **1924**, *57B*, 610-7.
- (192) Fischer, H.; Klarer, J. *Ann.* **1926**, *448*, 178-93.
- (193) Corwin, A. H.; Melville, M. H. *J. Am. Chem. Soc.* **1955**, *77*, 2755-9.
- (194) Motekaitis, R. J.; Martell, A. E. *Inorg. Chem.* **1970**, *9*, 1832-9.
- (195) Corwin, A. H.; Sydow, V. L. *J. Am. Chem. Soc.* **1953**, *75*, 4484-6.
- (196) Porter, C. R. *J. Chem. Soc.* **1938**, 368-72.
- (197) Fergusson, J. E.; March, F. C.; Couch, D. A.; Emerson, K.; Robinson, W. T. *J. Chem. Soc. A* **1971**, 440-8.
- (198) March, F. C.; Fergusson, J. E.; Robinson, W. T. *J. Chem. Soc. Dalton Trans.* **1972**, 2069-76.
- (199) Fergusson, J. E.; Ramsay, C. A. *J. Chem. Soc.* **1965**, 5222-5.

- (200) Murakami, Y.; Sakata, K.; Harada, K.; Matsuda, Y. *Bull. Chem. Soc. Jpn.* **1974**, *47*, 3021-4.
- (201) Murakami, Y.; Sakata, K. *Bull. Chem. Soc. Jpn.* **1974**, *47*, 3025-8.
- (202) Murakami, Y.; Matsuda, Y.; Sakata, K.; Harada, K. *Bull. Chem. Soc. Jpn.* **1974**, *47*, 458-62.
- (203) Murakami, Y.; Matsuda, Y.; Sakata, K. *Inorg. Chem.* **1971**, *10*, 1728-34.
- (204) Murakami, Y.; Matsuda, Y.; Sakata, K. *Inorg. Chem.* **1971**, *10*, 1734-8.
- (205) Murakami, Y.; Matsuda, Y.; Iiyama, K. *Chem. Lett.* **1972**, 1069-72.
- (206) Murakami, Y.; Sakata, K. *Inorg. Chim. Acta* **1968**, *2*, 273-9.
- (207) Murakami, Y.; Kohno, Y.; Matsuda, Y. *Inorg. Chim. Acta* **1969**, *3*, 671-5.
- (208) Murakami, Y.; Matsuda, Y.; Sakata, K.; Martell, A. E. *J. Chem. Soc. Dalton Trans.* **1973**, 1729-34.
- (209) Murakami, Y.; Matsuda, Y.; Kobayashi, S. *J. Chem. Soc. Dalton Trans.* **1973**, 1734-7.
- (210) Murakami, Y.; Matsuda, Y.; Kanaoka, Y. *Bull. Chem. Soc. Jpn.* **1971**, *44*, 409-15.
- (211) Cotton, F. A.; DeBoer, B. G.; Pipal, J. R. *Inorg. Chem.* **1970**, *9*, 783-8.
- (212) Johnson, A. W.; Kay, I. T.; Markham, E.; Price, R.; Shaw, K. B. *J. Chem. Soc.* **1959**, 3416-24.
- (213) Ferguson, J.; West, B. O. *J. Chem. Soc. A* **1966**, 1565-8.
- (214) Ferguson, J.; West, B. O. *J. Chem. Soc. A* **1966**, 1569-72.
- (215) Yu, L.; Muthukumar, K.; Sazanovich, I. V.; Kirmaier, C.; Hindin, E.; Diers, J. R.; Boyle, P. D.; Bocian, D. F.; Holten, D.; Lindsey, J. S. *Inorg. Chem.* **2003**, *42*, 6629-6647.
- (216) Sazanovich, I. V.; Kirmaier, C.; Hindin, E.; Yu, L.; Bocian, D. F.; Lindsey, J. S.; Holten, D. *J. Amer. Chem. Soc.* **2004**, *126*, 2664-65.
- (217) Thoi, V. S.; Stork, J. R.; Magde, D.; Cohen, S. M. *Inorg. Chem.* **2006**, *45*, 10688-10697.
- (218) Maeda, H.; Hasegawa, M.; Hashimoto, T.; Kakimoto, T.; Nishio, S.; Nakanishi, T. *J. Amer. Chem. Soc.* **2006**, *128*, 10024-10025.

- (219) Chen, J.; Burghart, A.; Derecskei-Kovacs, A.; Burgess, K. *J. Org. Chem.* **2000**, *65*, 2900-2906.
- (220) Li, J. J. *Name Reactions in Heterocyclic Chemistry*; Wiley, Hoboken, NJ, 2005.
- (221) Kim, H.; Burghart, A.; Welch, M. B.; Reibenspies, J.; Burgess, K. *Chem. Commun.* **1999**, 1889-1890.
- (222) Wada, M.; Ito, S.; Uno, H.; Murashima, T.; Ono, N.; Urano, T.; Urano, Y. *Tetrahedron Lett.* **2001**, *42*, 6711-6713.
- (223) Shen, Z.; Röhr, H.; Rurack, K.; Uno, H.; Spieles, M.; Schulz, B.; Reck, G.; Ono, N. *Chem. Eur. J.* **2004**, *10*, 4853-4871.
- (224) Ito, S.; Murashima, T.; Ono, N.; Uno, H. *Chem. Commun.* **1998**, 1661-1662.
- (225) Wu, Y.; Klaubert, D. H.; Kang, H. C.; Zhang, Y.-z. Long-wavelength dyes for infrared tracing and their use. US Patent 6005113, 1999.
- (226) Kotali, A.; Tsoungas, P. G. *Tetrahedron Lett.* **1987**, *28*, 4321-4322.
- (227) Vasilenko, N. P.; Mikhailenko, F. A.; Rozhinskii, Y. I. *Dyes Pigm.* **1981**, *2*, 231-7.
- (228) Posokh, S. V.; Gavrilov, O. D.; Mikhailenko, F. A.; Ryl'kov, V. V.; Slominskii, Y. L.; Stepanov, A. I. *Zhurnal Prikladnoi Spektroskopii* **1984**, *40*, 218-22.
- (229) Rogers, M. A. T. *J. Chem. Soc.* **1943**, 590-6.
- (230) Davies, W. H.; Rogers, M. A. T. *J. Chem. Soc.* **1944**, 126-31.
- (231) Knott, E. B. *J. Chem. Soc.* **1947**, 1196-1201.
- (232) Sathyamoorthi, G.; Soong, M. L.; Ross, T. W.; Boyer, J. H. *Heteroat. Chem.* **1993**, *4*, 603-8.
- (233) Killoran, J.; Allen, L.; Gallagher, J.; Gallagher, W.; O'Shea, D. *Chem. Commun.* **2002**, 1862-3.
- (234) Gorman, A.; Killoran, J.; O'Shea, C.; Kenna, T.; Gallagher, W. M.; O'Shea, D. F. *J. Am. Chem. Soc.* **2004**, *126*, 10619-31.
- (235) McDonnell, S. O.; O'Shea, D. F. *Org. Lett.* **2006**, *8*, 3493-3496.

- (236) Gallagher, W. M.; Allen, L. T.; O'Shea, C.; Kenna, T.; Hall, M.; Gorman, A.; Killoran, J.; O'Shea, D. F. *Br. J. Cancer* **2005**, *92*, 1702-1710.
- (237) McDonnell, S. O.; Hall, M. J.; Allen, L. T.; Byrne, A.; Gallagher, W. M.; O'Shea, D. F. *J. Am. Chem. Soc.* **2005**, *127*, 16360-16361.
- (238) Hall, M. J.; Allen, L. T.; O'Shea, D. F. *Org. Biomol. Chem.* **2006**, *4*, 776-780.
- (239) Killoran, J.; O'Shea, D. F. *Chem. Commun.* **2006**, 1503-1505.
- (240) Coskun, A.; Yilmaz, M. D.; Akkaya, E. U. *Org. Lett.* **2007**, *9*, 607-609.
- (241) Gawley, R. E.; Mao, H.; Haque, M. M.; Thorne, J. B.; Pharr, J. S. *J. Org. Chem.* **2007**, ACS ASAP.
- (242) Zhao, W.; Carreira, E. M. *Angew. Chem. Int. Ed.* **2005**, *44*, 1677-1679.
- (243) Zhao, W.; Carreira, E. M. *Chemistry* **2006**, *12*, 7254-7263.
- (244) Vasilenko, N. P.; Mikhailenko, F. A. *Ukrainskii Khimicheskii Zhurnal (Russian Edition)* **1986**, *52*, 308-11.
- (245) Ronzio, A. R.; Waugh, T. D. In *Org. Synth.* **1955**, *3*, 438-441.
- (246) Bernarducci, E. E.; Bharadwaj, P. K.; Lalancette, R. A.; Krogh-Jespersen, K.; Potenza, J. A.; Schugar, H. J. *Inorg. Chem.* **1983**, *22*, 3911-20.
- (247) Lane, E. S. *J. Chem. Soc.* **1953**, 2238-40.
- (248) Fieselmann, B. F.; Hendrickson, D. N.; Stucky, G. D. *Inorg. Chem.* **1978**, *17*, 2074-84.
- (249) Ross, T. W.; Sathyamoorthi, G.; Boyer, J. H. *Heteroat. Chem.* **1993**, *4*, 609-12.
- (250) Huenig, S.; Wehner, I. *Heterocycles* **1989**, *28*, 359-63.
- (251) Douglass, J. E.; Barelski, P. M.; Blankenship, R. M. *J. Heterocycl. Chem.* **1973**, *10*, 255-7.
- (252) Yoshino, J.; Kano, N.; Kawashima, T. *Chem. Commun.* **2007**, 559-561.
- (253) Liu, S.-F.; Wu, Q.; Schmider, H. L.; Aziz, H.; Hu, N.-X.; Popovic, Z.; Wang, S. *J. Am. Chem. Soc.* **2000**, *122*, 3671-3678.
- (254) Liu, Q.-D.; Mudadu, M. S.; Thummel, R.; Tao, Y.; Wang, S. *Adv. Funct. Mater.* **2005**, *15*, 143-154.

- (255) Zeng, X.; Qian, M.; Hu, Q.; Negishi, E. *Angew. Chem. Int. Ed.* **2004**, *43*, 2259-2263.
- (256) Wakamiya, A.; Taniguchi, T.; Yamaguchi, S. *Angew. Chem. Int. Ed.* **2006**, *45*, 3170-3173.
- (257) Frangioni, J. V. *Curr. Opin. Chem. Biol.* **2003**, *7*, 626-34.
- (258) Michalet, X.; Kapanidis Achillefs, N.; Laurence, T.; Pinaud, F.; Doose, S.; Pflughoefft, M.; Weiss, S. *Annu. Rev. Biophys. Biomol. Struct.* **2003**, *32*, 161-82.
- (259) Weijer, C. J. *Science* **2003**, *300*, 96-100.
- (260) Stephens, D. J.; Allan, V. J. *Science* **2003**, *300*, 82-86.
- (261) Lippincott-Schwartz, J.; Patterson, G. H. *Science* **2003**, *300*, 87-91.
- (262) Rieder, C. L.; Khodjakov, A. *Science* **2003**, *300*, 91-96.
- (263) Mishra, A.; Behera, R. K.; Behera, P. K.; Mishra, B. K.; Behera, G. B. *Chem. Rev.* **2000**, *100*, 1973-2011.
- (264) Narayanan, N.; Little, G.; Raghavachari, R.; Patonay, G. *SPIE* **1995**, *2388*, 6-15.
- (265) McKeown, N. B. *Chem. Ind.* **1999**, 92-8.
- (266) Halik, M.; Hartmann, H. *Chem. Eur. J.* **1999**, *5*, 2511-7.
- (267) Kenworthy, A. K. *Methods* **2001**, *24*, 289-96.
- (268) Loudet, A.; Burgess, K. *Chem. Rev.* **2007**, *107*, 4891-4932.
- (269) Rogers, M. A. T. *J. Chem. Soc.* **1943**, 590-6.
- (270) Davies, W. H.; Rogers, M. A. T. *J. Chem. Soc.* **1944**, 126-31.
- (271) Rogers, M. A. T. *Nature* **1943**, *151*, 504.
- (272) Rogers, M. A. T. Azadipromethines, A New Class of Dyes. U.S. Patent 2,382,914, 1945.

- (273) Allik, T. H.; Hermes, R. E.; Sathyamoorthi, G.; Boyer, J. H. *Proc. SPIE-Int. Soc. Opt. Eng.* **1994**, 2115, 240-8.
- (274) Zhao, W.; Carreira, E. M. *Angew. Chem. Int. Ed.* **2005**, 44, 1677-1679.
- (275) Zhao, W.; Carreira, E. M. *Chem. -Eur. J.* **2006**, 12, 7254-7263.
- (276) Loudet, A.; Bandichhor, R.; Burgess, K. *Angew Chem Int Ed* **2007**, submitted.
- (277) McDonnell, S. O.; O'Shea, D. F. *Org. Lett.* **2006**, 8, 3493-3496.
- (278) Burgess, K.; Burghart, A.; Chen, J.; Wan, C.-W. *Proc. SPIE-Int. Soc. Opt. Eng.*, Conference in San Jose, CA, 2000.
- (279) Burghart, A.; Thoresen, L. H.; Chen, J.; Burgess, K.; Bergström, F.; Johansson, L. B.-A. *Chem. Commun.* **2000**, 2203-4.
- (280) Jiao, G.-S.; Thoresen, L. H.; Kim, T. G.; Haaland, W. C.; Gao, F.; Topp, M. R.; Hochstrasser, R. M.; Metzker, M. L.; Burgess, K. *Chem. Eur. J.* **2006**, 12, 7616-26.
- (281) Metzker, M. L.; Lu, J.; Gibbs, R. A. *Science* **1996**, 271, 1420-2.
- (282) Jiao, G.-S.; Thoresen, L. H.; Burgess, K. *J. Am. Chem. Soc.* **2003**, 125, 14668-9.
- (283) Gorman, A.; Killoran, J.; O'Shea, C.; Kenna, T.; Gallagher, W. M.; O'Shea, D. F. *J. Am. Chem. Soc.* **2004**, 126, 10619-31.
- (284) Rogers, M. A. T. *J. Chem. Soc.* **1943**, 590-6.
- (285) Rio, G.; Masure, D. *Bull. Soc. Chim. Fr.* **1972**, 4604-10.
- (286) Miura, T.; Urano, Y.; Tanaka, K.; Nagano, T.; Ohkubo, K.; Fukuzumi, S. *J. Am. Chem. Soc.* **2003**, 125, 8666-71.
- (287) Gabe, Y.; Urano, Y.; Kikuchi, K.; Kojima, H.; Nagano, T. *J. Am. Chem. Soc.* **2004**, 126, 3357-67.

- (288) Ueno, T.; Urano, Y.; Setsukinai, K.-i.; Takakusa, H.; Kojima, H.; Kikuchi, K.; Nagano, T. *J. Am. Chem. Soc.* **2004**, *126*, 14079-14085.
- (289) Urano, Y.; Kamiya, M.; Kanda, K.; Ueno, T.; Hirose, K.; Nagano, T. *J. Am. Chem. Soc.* **2005**, *127*, 4888-4894.
- (290) Tanaka, K.; Miura, T.; Umezawa, N.; Urano, Y.; Kikuchi, K.; Higuchi, T.; Nagano, T. *J. Am. Chem. Soc.* **2001**, *123*, 2530-2536.
- (291) Gabe, Y.; Ueno, T.; Urano, Y.; Kojima, H.; Nagano, T. *Anal. Biochem.* **2006**, *386*, 621-626.
- (292) Sunahara, H.; Urano, Y.; Kojima, H.; Nagano, T. *J. Am. Chem. Soc.* **2007**, *129*, 5597-5604.
- (293) Jiao, G.-S.; Han, J. W.; Burgess, K. *J. Org. Chem.* **2003**, *68*, 8264-7.
- (294) Sonogashira, K.; Tohda, Y.; Hagihara, N. *Tetrahedron Lett.* **1975**, 4467-70.
- (295) Cox, R. J.; Durston, J.; Roper, D. I. *J. Chem. Soc., Perkin Trans. 1*, **2002**, 1029-1035.
- (296) Zanker, V.; Peter, W. *Chem. Ber.* **1958**, *91*, 572-80.
- (297) Klonis, N.; Sawyer, W. H. *J. Fluoresc.* **1996**, *6*, 147-157.
- (298) Sun, C.; Yang, J.; Li, L.; Wu, X.; Liu, Y.; Liu, S. *J. Chromatogr., B* **2004**, *803*, 173-90.
- (299) Frangioni, J. V. *Curr. Opin. Chem. Biol.* **2003**, *7*, 626-34.
- (300) Benson, R. C.; Kues, H. A. *J. Chem. Eng. Data.* **1977**, *22*, 379-83.
- (301) Boyer, J. H.; Haag, A. M.; Sathyamoorthi, G.; Soong, M. L.; Thangaraj, K.; Pavlopoulos, T. G. *Heteroat. Chem.* **1993**, *4*, 39-49.
- (302) Chen, J.; Burghart, A.; Derecskei-Kovacs, A.; Burgess, K. *J. Org. Chem.* **2000**, *65*, 2900-2906.



- (303) Kim, H.; Burghart, A.; Welch, M. B.; Reibenspies, J.; Burgess, K. *Chem. Commun.* **1999**, 18, 1889-90.
- (304) Gorman, A.; Killoran, J.; O'Shea, C.; Kenna, T.; Gallagher, W. M.; O'Shea, D. F. *J. Am. Chem. Soc.* **2004**, 126, 10619-31.
- (305) Killoran, J.; Allen, L.; Gallagher, J.; Gallagher, W.; O'Shea, D. *Chem. Commun.* **2002**, 1862-3.
- (306) Zhao, W.; Carreira, E. M. *Angew. Chem. Int. Ed.* **2005**, 44, 1677-9.
- (307) Zhao, W.; Carreira, E. M. *Chem. -Eur. J.* **2006**, 12, 7254-7263.
- (308) Treibs, A.; Jacob, K. *Angew. Chem.* **1965**, 77, 680-1.
- (309) Maahs, G.; Hegenberg, P. *Angew. Chem. Int. Ed.* **1966**, 5, 888-93.
- (310) Sprenger, H.-E.; Ziegenbein, W. *Angew. Chem. Int. Ed.* **1968**, 7, 530-5.
- (311) Ziegenbein, W.; Sprenger, H. E. *Angew. Chem.* **1966**, 78, 937.
- (312) Slavik, J. In *Near-Infrared Dyes for High Technology Applications*; Daehne, S., Resch-Genger, U., Wolfbeis, O. S., Eds.; Kluwer Academic Publishers: Dordrecht, The Netherlands, 1998; Vol. 52.
- (313) Hung, S.-C.; Ju, J.; Mathies, R. A.; Glazer, A. N. *Anal. Biochem.* **1996**, 243, 15-27.
- (314) Lee, L. G.; Spurgeon, S. L.; Rosenblum, B. Energy Transfer Dyes with Enhanced Fluorescence. EP Patent 0805190 A2, 1997.
- (315) Lee, L. G.; Rosenblum, B.; Spurgeon, S. L. Fluorescent energy transfer dyes - useful for labelling dideoxynucleotides, oligonucleotides, etc. EP Patent 805190A, 1998.
- (316) Berti, L.; Xie, J.; Medintz, I. L.; Glazer, A. N.; Mathies, R. A. *Anal. Biochem.* **2001**, 292, 188-197.

- (317) Nampalli, S.; Zhang, W.; Rao, T. S.; Xiao, H.; Kotra, L. P.; Kumar, S. *Tetrahedron Lett.* **2002**, *43*, 1999-2003.
- (318) Lee, L. G.; Spurgeon, S. L.; Heiner, C. R.; Benson, S. C.; Rosenblum, B. B.; Menchen, S. M.; Graham, R. J.; Constantinescu, A.; Upadhya, K. G.; Cassel, J. M. *Nucleic Acids Res.* **1997**, *25*, 2816-22.
- (319) Rosenblum, B. B.; Lee, L. G.; Spurgeon, S. L.; Khan, S. H.; Menchen, S. M.; Heiner, C. R.; Chen, S. M. *Nucleic Acids Res.* **1997**, *25*, 4500-4.
- (320) Burghart, A.; Thoresen, L. H.; Chen, J.; Burgess, K.; Bergström, F.; Johansson, L. B.-A. *Chem. Commun.* **2000**, 2203-4.
- (321) Speiser, S. *Chem. Rev.* **1996**, *96*, 1953-76.
- (322) Wagner, R. W.; Lindsey, J. S. *J. Am. Chem. Soc.* **1994**, *116*, 9759-60.
- (323) McQuade, D. T.; Pullen, A. E.; Swager, T. M. *Chem. Rev.* **2000**, *100*, 2537-74.
- (324) Law, K.-Y. In *Organic Photochemistry*; Ramamurthy, V., Ed.; Marcel Dekker, Inc.: New York, 1997; Vol. 1.
- (325) Klapars, A.; Antilla, J. C.; Huang, X.; Buchwald, S. L. *J. Am. Chem. Soc.* **2001**, *123*, 7727-9.
- (326) Old, D. W.; Harris, M. C.; Buchwald, S. L. *Org. Lett.* **2000**, *2*, 1403-6.
- (327) Sprenger, H.-E.; Ziegenbein, W. *Angew. Chem. Int. Ed.* **1967**, *6*, 553-4.
- (328) Hood, L. E.; Hunkapiller, M. W.; Smith, L. M. *Genomics* **1987**, *1*, 201-12.
- (329) Smith, L. M.; Sanders, J. Z.; Kaiser, R. J.; Hughes, P.; Dodd, C.; Connell, C. R.; Heiner, C.; Kent, S. B.; Hood, L. E. *Nature* **1986**, *321*, 674-9.
- (330) Ju, J.; Kheterpal, I.; Scherer, J. R.; Ruan, C.; Fuller, C. W.; Glazer, A. N.; Mathies, R. A. *Anal. Biochem.* **1995**, *231*, 131-40.

- (331) Ju, J.; Glazer, A. N.; Mathies, R. A. *Nature Med.* **1996**, *2*, 246-9.
- (332) Nampalli, S.; Khot, M.; Kumar, S. *Tetrahedron Lett.* **2000**, *41*, 8867-71.
- (333) Lakowicz, J. R. *Principles of Fluorescence Spectroscopy*; Plenum: New York, 1983.
- (334) Weder, C.; Wrighton, M. S. *Macromolecules* **1996**, *29*, 5157-65.
- (335) Swager, T. M.; Gil, C. J.; Wrighton, M. S. *J. Phys. Chem.* **1995**, *99*, 4886-93.
- (336) McQuade, D. T.; Pullen, A. E.; Swager, T. M. *Chem. Rev.* **2000**, *100*, 2537-74.
- (337) Tour, J. M. *Chem. Rev.* **1996**, *96*, 537-53.
- (338) Holten, D.; Bocian, D.; Lindsey, J. S. *Acc. Chem. Res.* **2002**, *35*, 57-69.
- (339) Wan, C.-W.; Burghart, A.; Chen, J.; Bergstroem, F.; Johansson, L. B.-A.; Wolford, M. F.; Kim, T. G.; Topp, M. R.; Hochstrasser, R. M.; Burgess, K. *Chem. Eur. J.* **2003**, *9*, 4430-41.
- (340) Jiao, G.-S.; Thoresen, L. H.; Burgess, K. *J. Am. Chem. Soc.* **2003**, *125*, 14668-9.
- (341) Burghart, A.; Thoresen, L. H.; Chen, J.; Burgess, K.; Bergström, F.; Johansson, L. B.-A. *Chem. Commun.* **2000**, 2203-4.
- (342) Speiser, S. *Chem. Rev.* **1996**, *96*, 1953-76.
- (343) Maxam, A. M.; Gilbert, W. *Proc. Natl. Acad. Sci. U.S.A.* **1977**, *74*, 560-4.
- (344) Sanger, F.; Nicklen, S.; Coulson, A. R. *Proc. Natl. Acad. Sci.* **1977**, *74*, 5463-5467.
- (345) Smith, L. M.; Sanders, J. Z.; Kaiser, R. J.; Hughes, P.; Dodd, C.; Connell, C. R.; Heiner, C.; Kent, S. B.; Hood, L. E. *Nature* **1986**, *321*, 674-9.
- (346) Metzker, M. L.; Lu, J.; Gibbs, R. A. *Science* **1996**, *271*, 1420-2.
- (347) Ju, J.; Kheterpal, I.; Scherer, J. R.; Ruan, C.; Fuller, C. W.; Glazer, A. N.; Mathies, R. A. *Anal. Biochem.* **1995**, *231*, 131-40.

- (348) Farnum, D. G.; Mehta, G.; Moore, G. G. I.; Siegal, F. P. *Tetrahedron Lett.* **1974**, 2549-52.
- (349) Iqbal, A.; Jost, M.; Kirchmayr, R.; Pfenninger, J.; Rochat, A.; Wallquist, O. *Bull. Soc. Chim. Belg.* **1988**, 97, 615-43.
- (350) Morton, C. J. H.; Gilmour, R.; Smith, D. M.; Lightfoot, P.; Slawin, A. M. Z.; MacLean, E. *J. Tetrahedron* **2002**, 58, 5547-5565.
- (351) Morton, C. J. H.; Riggs, R. L.; Smith, D. M.; Westwood, N. J.; Lightfoot, P.; Slawin, A. M. *Z. Tetrahedron* **2005**, 61, 727-738.
- (352) Ruffieux, V.; Modoux, F. Process for the direct preparation of diketopyrrolo [3,4-c]pyrroles (DPPs) from disuccinates and aromatic nitriles in the presence of particle growth regulators. WO Patent 2003022847, 2003.
- (353) Wooden, G.; De Weck, G.; Wallquist, O. D. [(aminoalkoxy)phenyl]-1,4-pyrrolo [3,4-c]pyrroledione derivatives, a method for their preparation and their use in pigment compositions (Ciba-Geigy A.-G., Switz.). Application: EP Patent 92-810285, 1992.
- (354) Shaabani, A.; Dabiri, M.; Bazgir, A.; Gharanjig, K. *Dyes Pigm.* **2005**, 71, 68-72.
- (355) Hao, Z.; Iqbal, A. *Chem. Soc. Rev.* **1997**, 26, 203-213.
- (356) Riggs, R. L.; Morton, C. J. H.; Slawin, A. M. Z.; Smith, D. M.; Westwood, N. J.; Austen, W. S. D.; Stuart, K. E. *Tetrahedron* **2005**, 61, 11230-11243.
- (357) Wu, A.; Zhao, Y.; Chen, N.; Pan, X. *Synth. Commun.* **1997**, 27, 331-336.
- (358) Fischer, G. M.; Ehlers, A. P.; Zumbusch, A.; Daltrozzo, E. *Angew. Chem. Int. Ed.* **2007**, 46, 3750-3753.
- (359) Iqbal, A.; Jost, M.; Kirchmayr, R.; Pfenninger, J.; Rochat, A.; Wallquist, O. *Bull. Soc. Chim. Belg.* **1988**, 97, 615-43.

- (360) Closs, F.; Gompper, R. *Angew. Chem.* **1987**, *99*, 564-7.
- (361) Goud, T. V.; Tutar, A.; Biellmann, J.-F. *Tetrahedron* **2006**, *62*, 5084-5091.
- (362) Liebeskind, L. S.; Srogl, J. *J. Am. Chem. Soc.* **2000**, *122*, 11260-11261.
- (363) Wittenberg, R.; Srogl, J.; Egi, M.; Liebeskind, L. S. *Org. Lett.* **2003**, *5*, 3033-3035.
- (364) Yang, H.; Li, H.; Wittenberg, R.; Egi, M.; Huang, W.; Liebeskind, L. S. *J. Am. Chem. Soc.* **2007**, *129*, 1132-1140.
- (365) Lory, P.; Gilbertson, S. R. *Chemtracts* **2005**, *18*, 569-583

## APPENDIX A

### EXPERIMENTAL DATA FOR CHAPTER II

#### General Experimental Procedures.

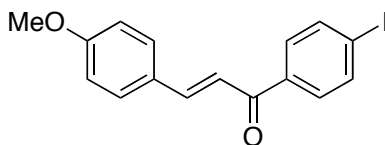
All chemicals were obtained from commercial suppliers and used without further purification. Thin layer chromatography was performed using silica gel 60F254 flash. Chromatography on silica gel was performed using a forced flow of the indicated solvent on EM reagents silica gel 60 (230-400 mesh). The solvents were dried/degassed by passing them down an alumina column.  $^1\text{H}$  and  $^{13}\text{C}$  NMR spectra were recorded on an Inova Instrument at 500 MHz ( $^1\text{H}$ ), 125 MHz ( $^{13}\text{C}$ ).  $^{11}\text{B}$  and  $^{19}\text{F}$  NMR spectra were recorded on a Inova 400 Broad Band instrument at 128 MHz ( $^{11}\text{B}$ ) and 376 MHz ( $^{19}\text{F}$ ). NMR chemical shifts are expressed in ppm relative to internal solvent peaks ( $\text{CDCl}_3$ : 7.27 ppm for  $^1\text{H}$  and 77.0 ppm for  $^{13}\text{C}$ ;  $\text{DMSO-}d_6$ : 2.50 ppm for  $^1\text{H}$  and 39.5 ppm for  $^{13}\text{C}$ ;  $\text{CD}_3\text{OD}$ : 3.30 ppm for  $^1\text{H}$  and 49.0 ppm for  $^{13}\text{C}$ ) and coupling constants were measured in Hz. For  $^{11}\text{B}$  NMR,  $\text{BF}_3\cdot\text{OEt}_2$  has been used as an external reference; similarly,  $\text{CFCl}_3$  was used as an external standard for the  $^{19}\text{F}$  spectra.

UV spectra were recorded in 1 cm path length quartz cuvettes on a Cary 100 Bio UV-Visible spectrophotometer at 5  $\mu\text{M}$ . Fluorescence emission spectra were recorded in 1 cm path length quartz cuvettes on a Photon Counting Spectrofluorometer PC1 SSI instrument equipped with an R928P photomultiplier tube which is sensitive up to  $\sim 850\text{-}900$  nm. Fluorescence spectra were recorded at concentrations between 1 and 5  $\mu\text{M}$ . Fluorescence quantum yield measurements were performed on the same instrument. The slit width was 0.5 nm for both excitation and emission. Relative quantum efficiencies of fluorescence of BODIPY derivatives were obtained by comparing the areas under the corrected emission spectrum of the test sample in 1% pyridine in toluene with that of a solution of zinc phthalocyanine, which has a quantum efficiency of 0.30 according to the literature.<sup>1</sup> Non-degassed, spectroscopic grade toluene and a 10 mm quartz cuvette were used. Dilute solutions ( $0.01 < A < 0.05$ ) were used to minimize reabsorption effects. The excitation wavelength was 671 nm for both compound **4** and **1**, and the reference.

Quantum yields were determined using the equation (1):<sup>2</sup>

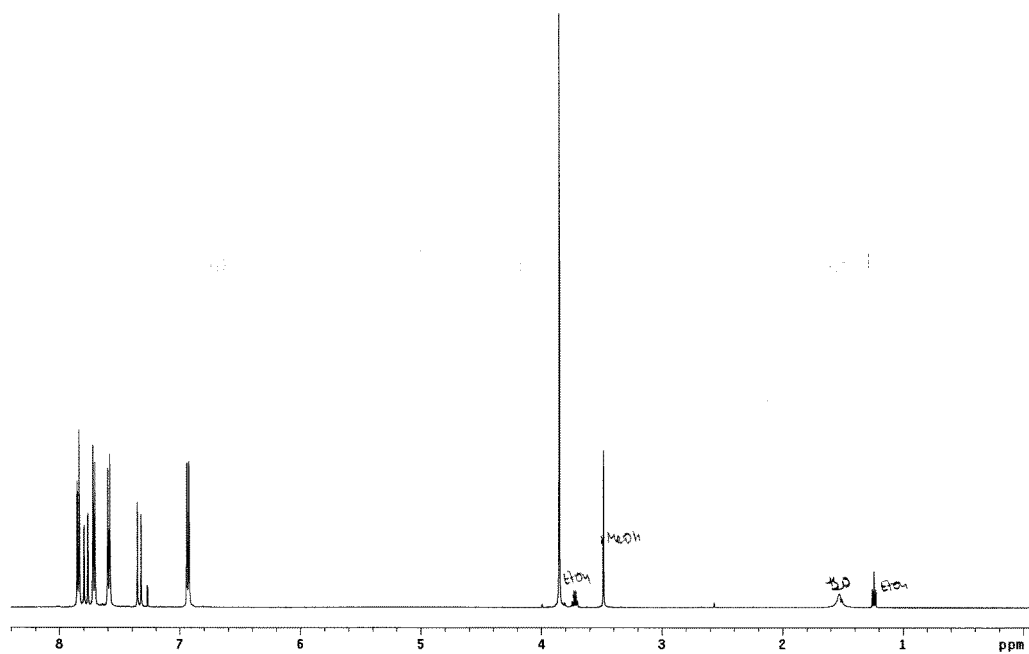
$$\text{equation (1)} \quad \Phi_X = \Phi_{\text{st}} (I_X/I_{\text{st}}) (A_{\text{st}}/A_X) (\eta_X^2/\eta_{\text{st}}^2)$$

Where  $\Phi_{st}$  is the reported quantum yield of the standard,  $I$  is the integrated emission spectra,  $A$  is the absorbance at the excitation wavelength and  $n$  is the refractive index of the solvent used ( $n=1$  if same solvent).  $X$  subscript denotes unknown, and  $st$  denotes standard.

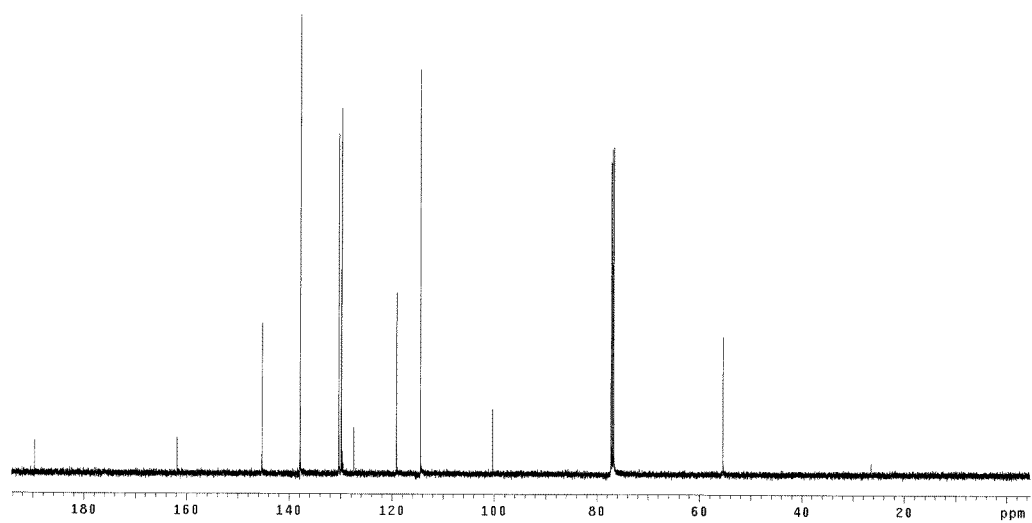
**1-(4-Iodophenyl)-3-(4-methoxyphenyl)prop-2-en-1-one (291a).**<sup>3,4</sup>

4-Methoxybenzaldehyde (5.53 g, 0.04 mol), 4-iodoacetophenone (10.00 g, 0.04 mol) and potassium hydroxide (0.16 g, 4.06 mmol) were dissolved in methanol / H<sub>2</sub>O (1:1 v/v, 120 mL) and stirred under reflux for 12 h. During the course of the reaction, the product precipitated from the reaction mixture. After cooling, the reaction mixture was filtered and washed with methanol to give the product as a white solid (11.35 g, 77%), m.p. (non corrected) 162.2-163.3 °C.  $\delta_{\text{H}}$  (500 MHz, CDCl<sub>3</sub>): 7.84 (d,  $J$ = 8.1 Hz, 2H), 7.78 (d,  $J$ = 15.6 Hz, 1H), 7.71 (d,  $J$ = 8.1 Hz, 2H), 7.59 (d,  $J$ = 8.3 Hz, 2H), 7.33 (d,  $J$ = 15.6 Hz, 1H), 6.93 (d,  $J$ = 8.3 Hz, 2H), 3.85 (s, 3H);  $\delta_{\text{C}}$  (125 MHz, CDCl<sub>3</sub>): 189.6, 161.8, 145.2, 137.8, 137.7, 130.3, 129.8, 127.3, 118.9, 114.4, 100.3, 55.4;  $m/z$  (ESI): theoretical mass (M+H)<sup>+</sup>: 365.00; found : 365.01.

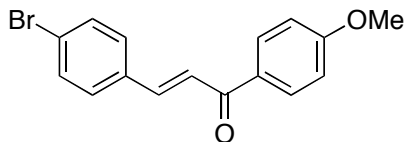




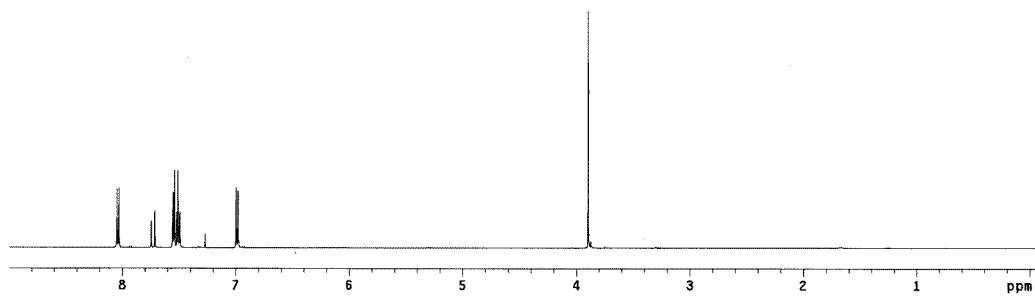
$^1\text{H}$  NMR for compound **291a** (500 MHz,  $\text{CDCl}_3$ )



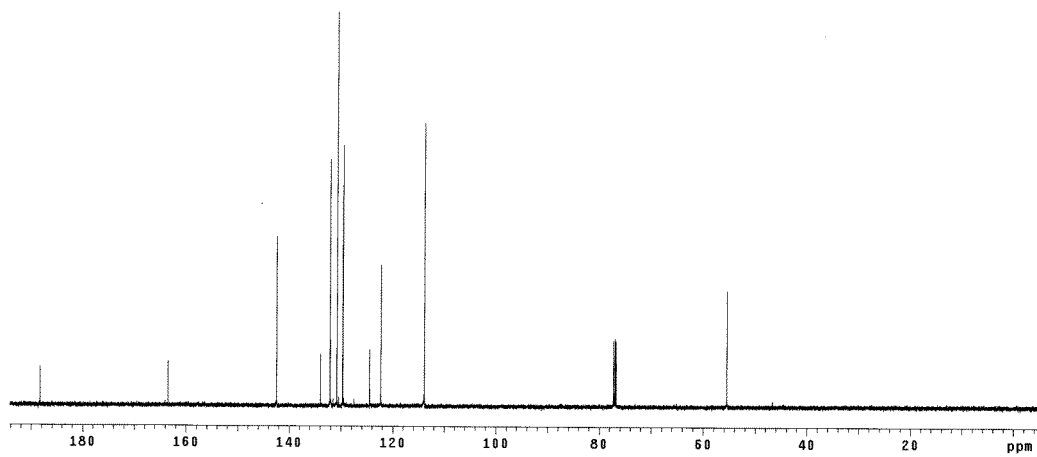
$^{13}\text{C}$  NMR for compound **291a** (125 MHz,  $\text{CDCl}_3$ )

**3-(4-Bromophenyl)-1-(4-methoxyphenyl)prop-2-en-1-one (291b).<sup>5</sup>**

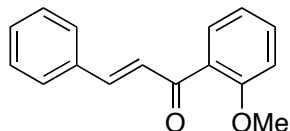
4-Bromobenzaldehyde (5.00 g, 0.027 mol), 4-methoxyacetophenone (3.22 g, 0.027 mol) and potassium hydroxide (0.108 g, 2.7 mmol) were dissolved in ethanol (30 mL) and stirred at room temperature for 12 h. The product which precipitated upon formation was filtered and washed with ethanol and water. The titled product was obtained as a white solid (7.3 g, 85 %), m.p. (non corrected) 149-150 ° C.  $\delta_{\text{H}}$  (500 MHz,  $\text{CDCl}_3$ ): 8.04 (d,  $J= 8.8$  Hz, 2H), 7.73 (d,  $J= 15.6$  Hz, 1H), 7.49-7.55 (m, 5 H), 6.99 (d,  $J= 8.8$  Hz, 2H), 3.89 (s, 3H);  $\delta_{\text{C}}$  (125 MHz,  $\text{CDCl}_3$ ): 188.3, 163.5, 142.4, 133.9, 132.1, 130.8, 130.7, 129.7, 124.5, 122.3, 113.8, 55.5; m/z (ESI): theoretical mass (M+H)<sup>+</sup>: 317.01; found : 317.02-319.02 (Br isotope).



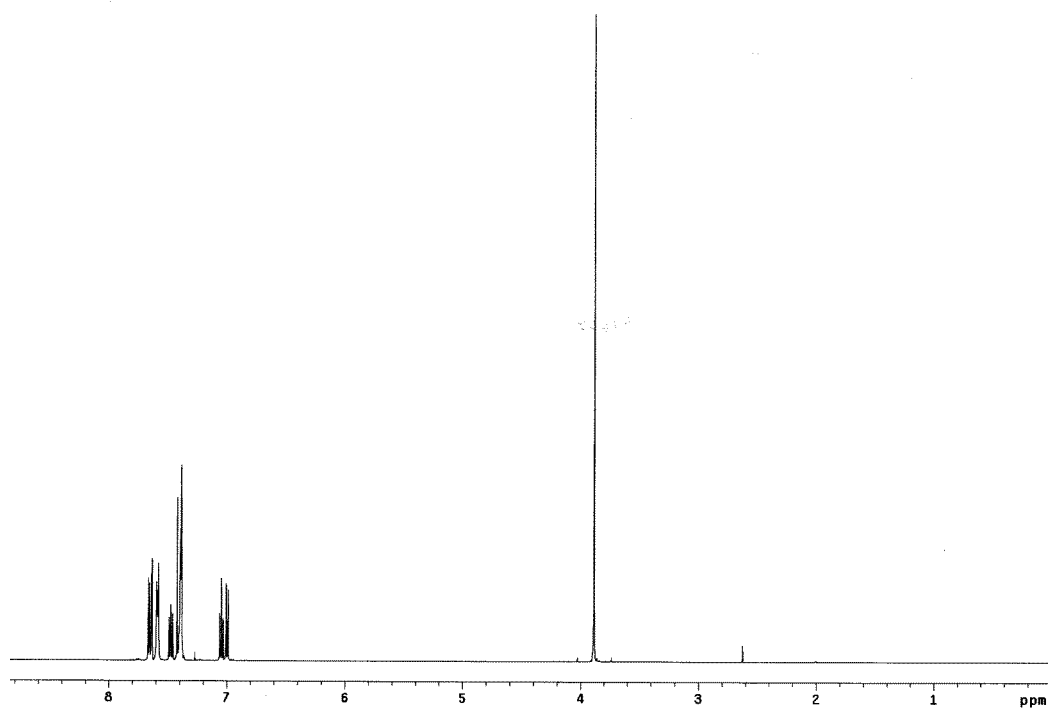
$^1\text{H}$  NMR for compound **291b** (500 MHz,  $\text{CDCl}_3$ )



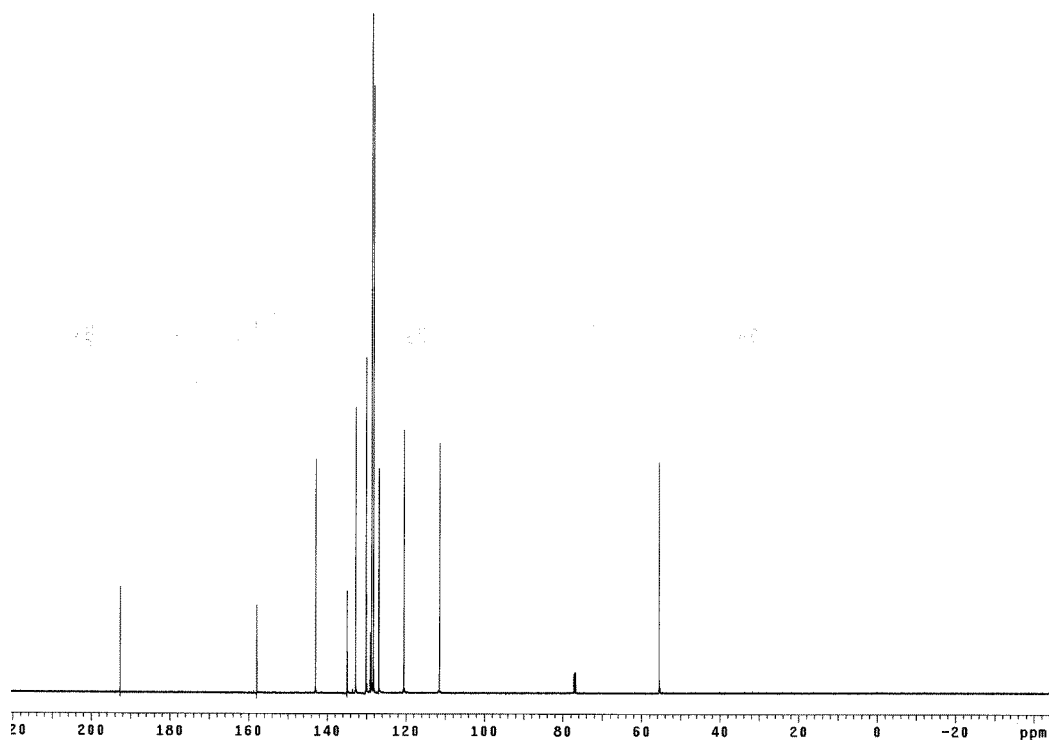
$^{13}\text{C}$  NMR for compound **291b** (125 MHz,  $\text{CDCl}_3$ )

**(E)-1-(2-Methoxyphenyl)-3-phenylprop-2-en-1-one (291c).** <sup>6-8</sup>

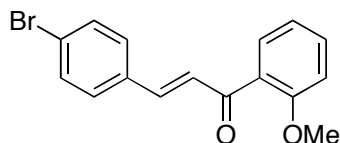
1-(2-Methoxyphenyl)-3-phenyl-2-propene-1-one was prepared according to the reported procedure. The chalcone was obtained as a yellow oil (2.9 g, 60% yield).  $\delta_{\text{H}}$  (500 MHz,  $\text{CDCl}_3$ ): 3.89 (s, 3H), 6.99 (d,  $J= 8.3$  Hz, 1H), 7.04 (td,  $J= 7.6$  Hz,  $J= 0.9$  Hz, 1H), 7.38-7.42 (m, 5H), 7.47 (td,  $J= 7.3$  Hz,  $J= 1.7$  Hz, 1H), 7.57-7.59 (m, 2H), 7.63-7.66 (m, 2H);  $\delta_{\text{C}}$  (125 MHz,  $\text{CDCl}_3$ ): 192.7, 157.9, 142.9, 134.9, 132.7, 130.1, 130.1, 129.0, 128.7, 128.2, 126.8, 120.5, 111.4, 55.5;  $m/z$  (ESI): theoretical mass  $(\text{M}+\text{H})^+$ : 239.1072; found : 239.1139



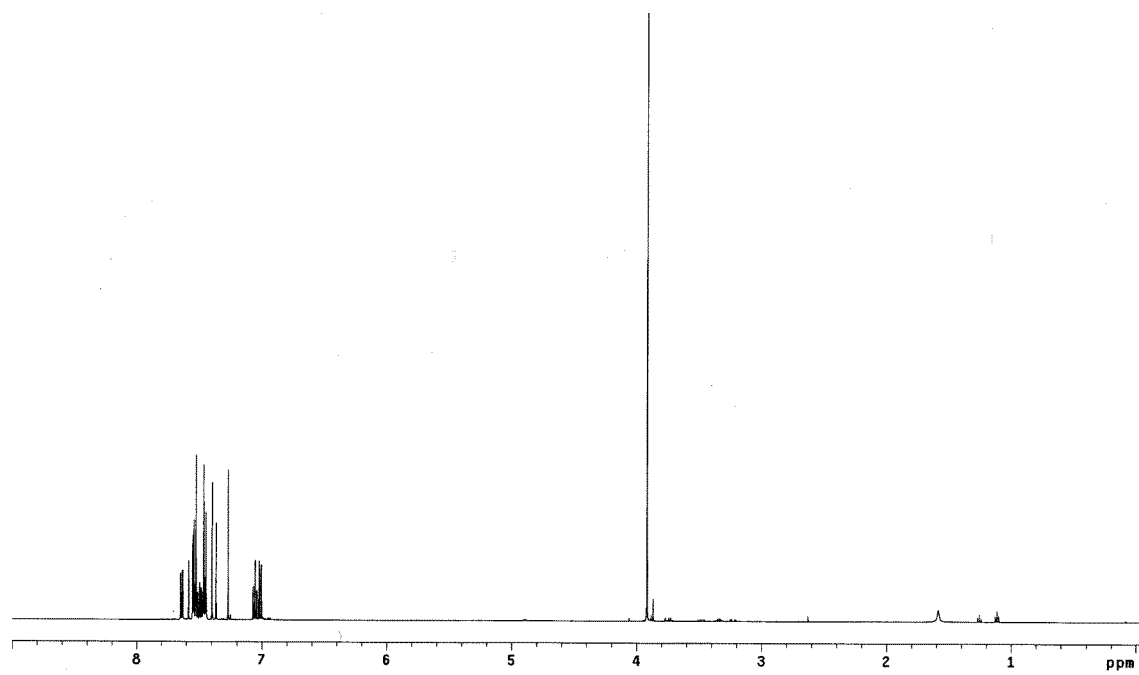
$^1\text{H}$  NMR for compound **291c** (500 MHz,  $\text{CDCl}_3$ ).



$^{13}\text{C}$  NMR for compound **291c** (500 MHz,  $\text{CDCl}_3$ )

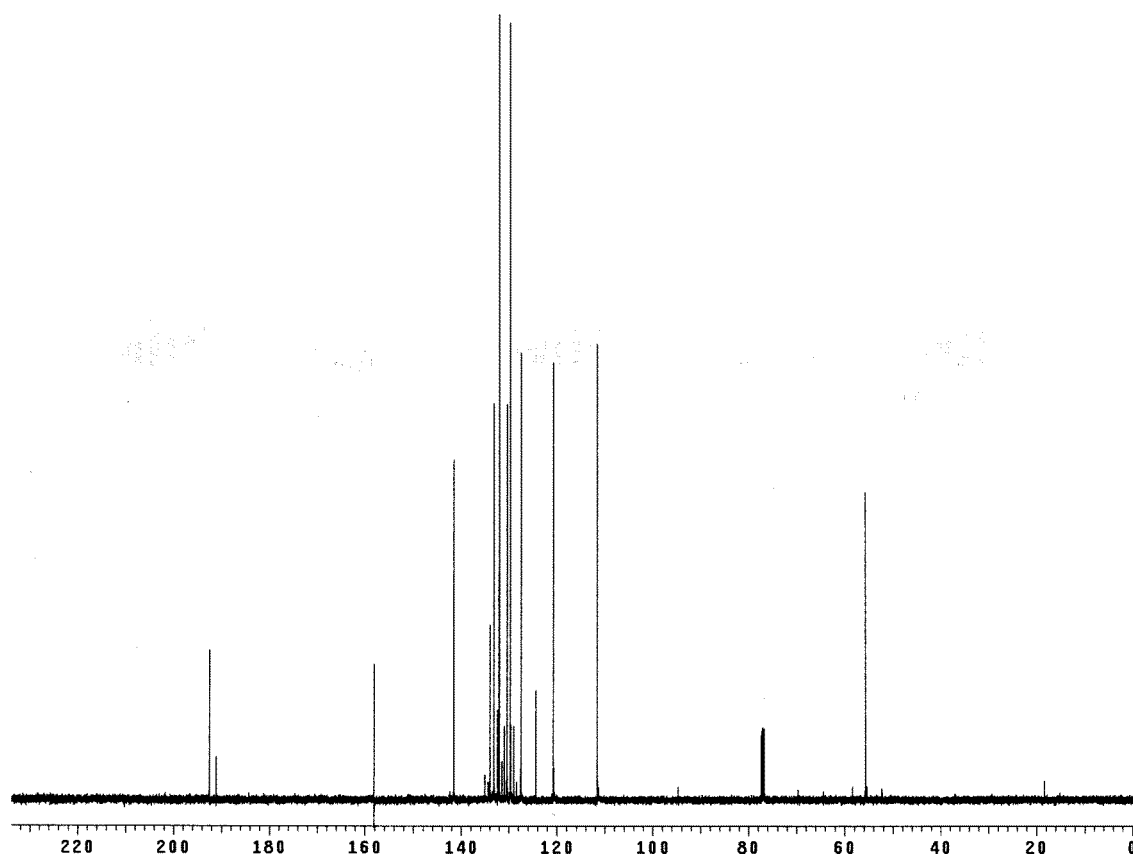
**3-(4-Bromophenyl)-1-(2-methoxyphenyl)prop-2-en-1-one (291d).**

A solution of acetophenone (3.20 g, 0.027 mol) in ethanol (27 mL) was added gradually to an aqueous solution of 10% KOH (80 mL) at 0 °C. After stirring for 30 min, 4-bromobenzaldehyde (5.00 g, 0.027 mol) was added to the solution and stirred at 0 °C for an additional 15 min. The reaction mixture was then allowed to warm up to room temperature and stirred for 12h. The product precipitated from the reaction mixture over the course of the reaction. It was filtered and washed with water to afford the desired product as a white solid (8.05 g, 94 %). Both isomers (*E*) and (*Z*) were obtained.  $\delta_{\text{H}}$  (500 MHz,  $\text{CDCl}_3$ ): 7.64 (dd,  $J= 7.6$  Hz,  $J= 1.9$  Hz, 1H), 7.58-7.45 (m, 6H), 7.38 (d,  $J= 15.8$  Hz, 1H), 7.05 (td,  $J= 7.6$  Hz,  $J= 0.9$  Hz, 1H), 7.01 (d,  $J= 8.3$  Hz, 1H), 3.91 (s, 3H);  $\delta_{\text{C}}$  (125 MHz,  $\text{CDCl}_3$ ): 192.6, 158.1, 142.1, 141.6, 134.1, 133.1, 132.2, 132.1, 130.4, 129.7, 129.0, 127.5, 125.7, 124.4, 120.8, 111.6, 55.57;  $m/z$  (HR-ESI): theoretical mass ( $\text{M}+\text{H}^+$ ): 317.0099; found : 317.0231-319.0198 (Br isotope).

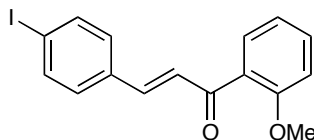


$^1\text{H}$  NMR for compound **291d** (500 MHz,  $\text{CDCl}_3$ )

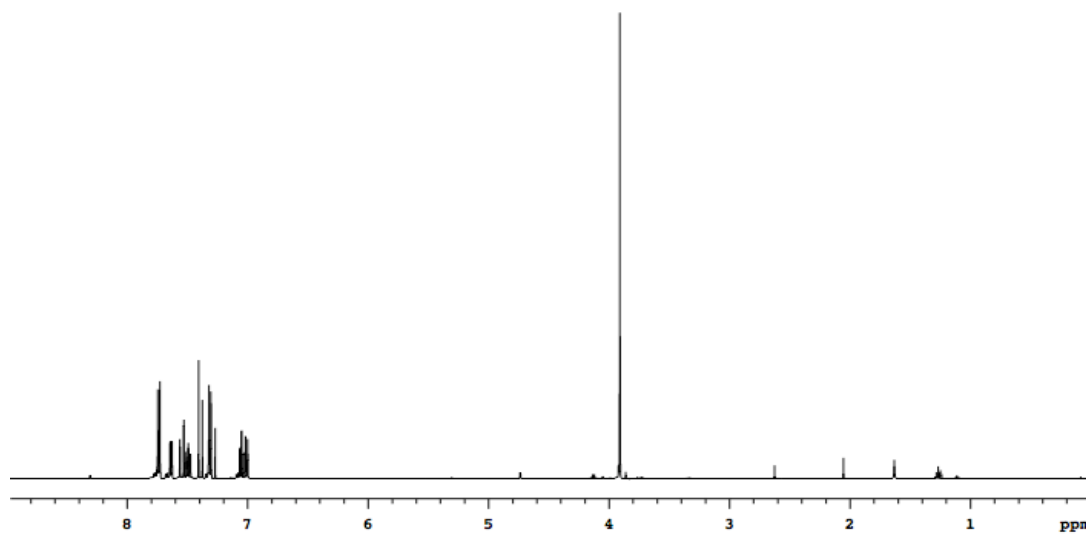




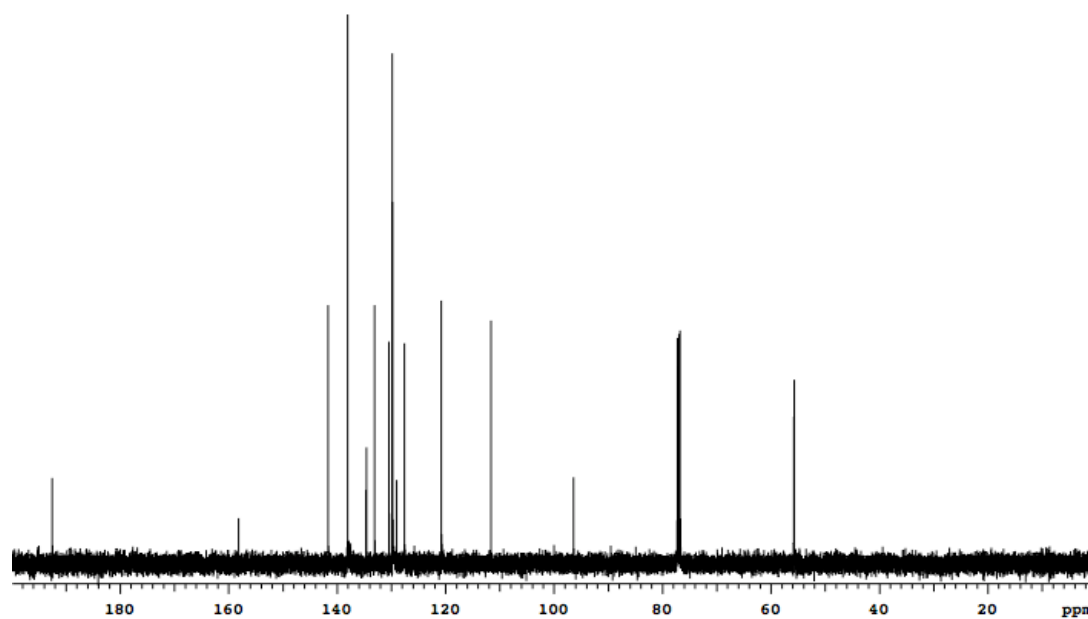
$^{13}\text{C}$  NMR for compound **291d** (125 MHz,  $\text{CDCl}_3$ )

**(E)-3-(4-iodophenyl)-1-(2-methoxyphenyl)prop-2-en-1-one (291e).**

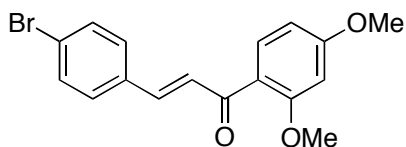
A solution of 2-methoxyacetophenone (1.43 g, 0.011 mol) in ethanol (11 mL) was added gradually to an aqueous solution of 10% KOH (32 mL) at 0 °C. After stirring for 30 min, 4-iodobenzaldehyde (2.0 g, 0.009 mol) was added to the solution and stirred at 0 °C for an additional 15 min. The reaction mixture was then allowed to warm up to room temperature and stirred for 12h. The product precipitated from the reaction mixture over the course of the reaction. It was filtered and washed with water to afford the desired product as a white solid (2.8 g, 85%).  $\delta_{\text{H}}$  (500MHz,  $\text{CDCl}_3$ ): 7.74 (d,  $J = 8.3$  Hz, 2H), 7.64 (dd,  $J = 7.6$  Hz,  $J = 1.7$  Hz, 1H), 7.56 – 7.37 (m, 3H), 7.32 (d,  $J = 8.3$  Hz, 2H), 7.05 (td,  $J = 7.6$  Hz,  $J = 1$  Hz, 1H), 7.01 (d,  $J = 8.3$  Hz, 1H), 3.91 (s, 3H);  $\delta_{\text{C}}$  (125MHz,  $\text{CDCl}_3$ ): 192.5, 158.1, 141.6, 138.0, 134.6, 133.1, 130.4, 129.8, 129.0, 127.8, 120.8, 111.6, 96.4, 55.7.



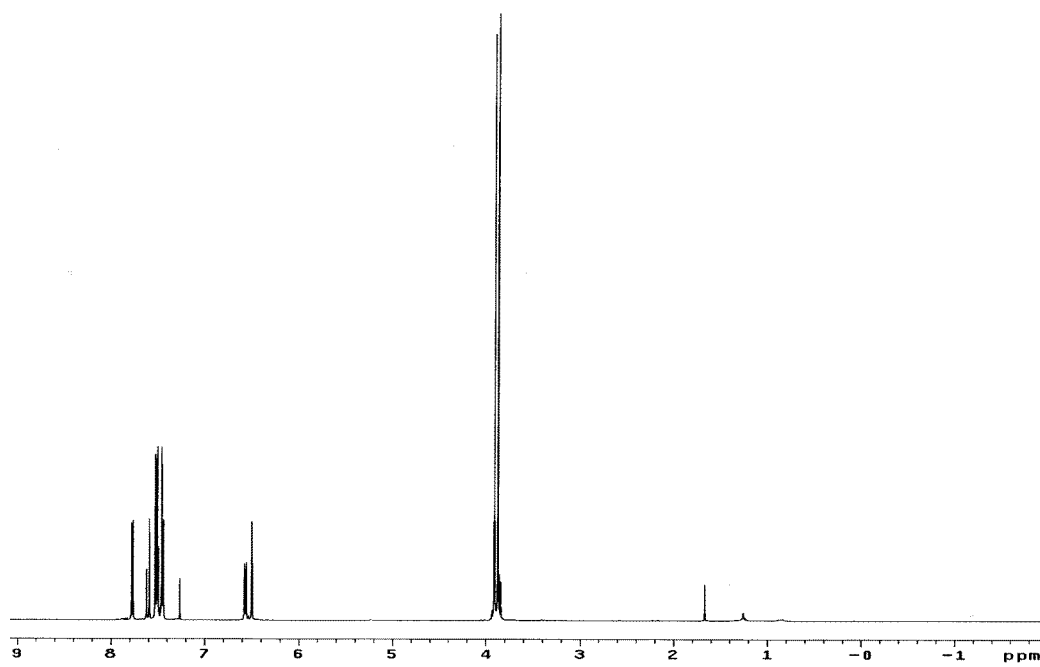
$^1\text{H}$  NMR for compound **291e** (500 MHz,  $\text{CDCl}_3$ )



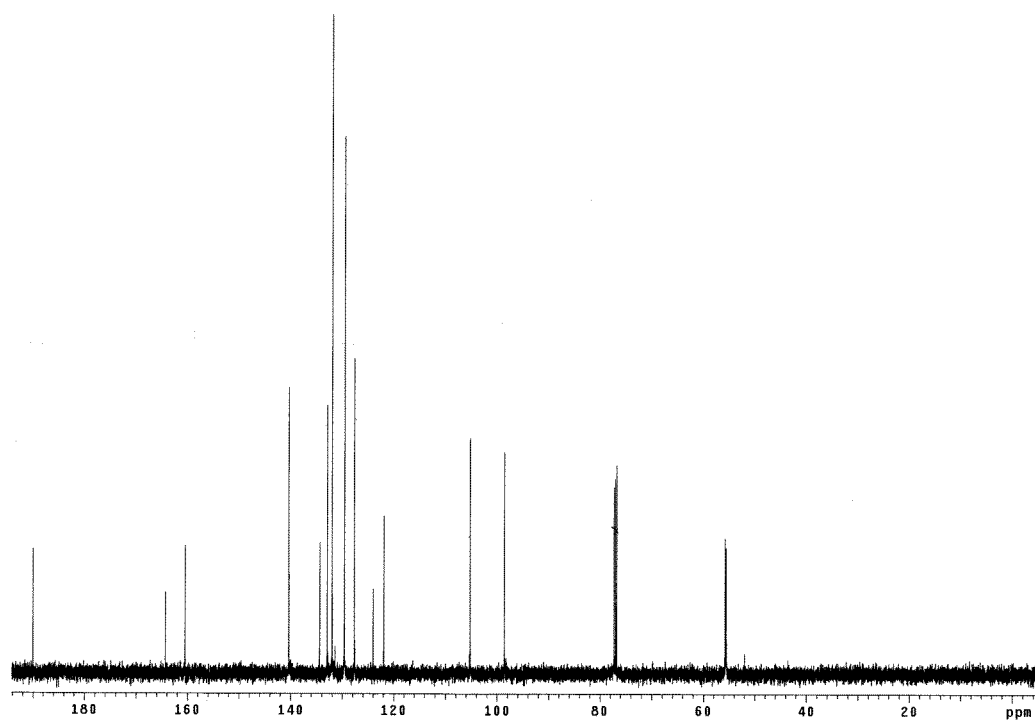
$^{13}\text{C}$  NMR for compound **291e** (125 MHz,  $\text{CDCl}_3$ )

**3-(4-Bromophenyl)-1-(2,4-dimethoxyphenyl)prop-2-en-1-one (291f).**<sup>9,10</sup>

A solution of 2,4-dimethoxyacetophenone (1.95 g, 0.011 mol) in ethanol (11 mL) was added gradually to an aqueous solution of 10% KOH (32 mL) at 0 °C. After stirring for 30 min, 4-bromobenzaldehyde (2.00 g, 0.011 mol) was added to the solution and stirred at 0 °C for an additional 15 min. The reaction mixture was then allowed to warm up to room temperature and stirred for 12h. The product precipitated from the reaction mixture over the course of the reaction. It was filtered and washed with water to afford the desired product as a white solid (2.8 g, 73%).  $\delta_{\text{H}}$  (500 MHz,  $\text{CDCl}_3$ ): 7.77 (d,  $J$ = 8.8 Hz, 1H), 7.44-7.62 (m, 6H), 6.57 (dd,  $J$ = 8.8 Hz,  $J$ = 2.4 Hz, 1H), 6.50 (d,  $J$ = 2.2 Hz, 1H), 3.88 (s, 3H), 3.91 (s, 3H);  $\delta_{\text{C}}$  (125 MHz,  $\text{CDCl}_3$ ): 190.0, 164.3, 160.4, 140.3, 134.4, 132.9, 131.9, 129.6, 127.7, 124.0, 121.9, 105.2, 98.6, 55.7, 55.5;  $m/z$  (HR-ESI): theoretical mass ( $\text{M}+\text{Li}$ )<sup>+</sup>: 353.0365; found : 353.0384-355.0366 (Br isotope).

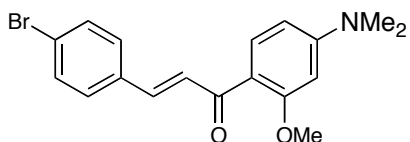


$^1\text{H}$  NMR for compound **291f** (500 MHz,  $\text{CDCl}_3$ ).



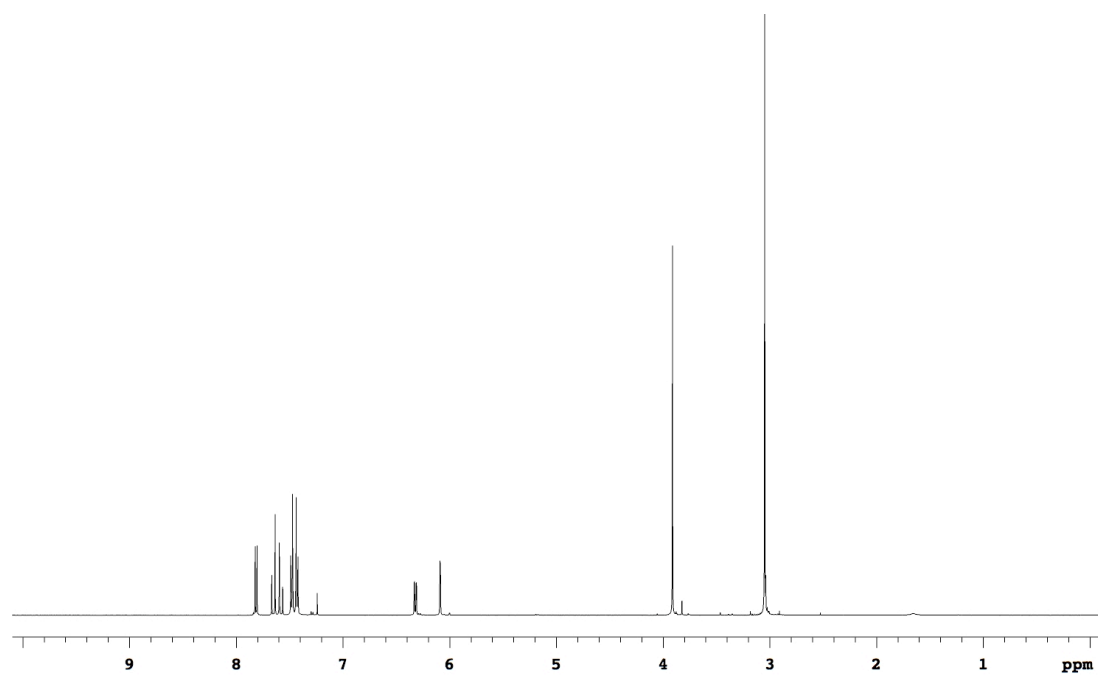
$^{13}\text{C}$  NMR for compound **291f** (125 MHz,  $\text{CDCl}_3$ ).

**(E)-3-(4-Bromophenyl)-1-(4-(dimethylamino)-2-methoxyphenyl)prop-2-en-1-one (291g).**

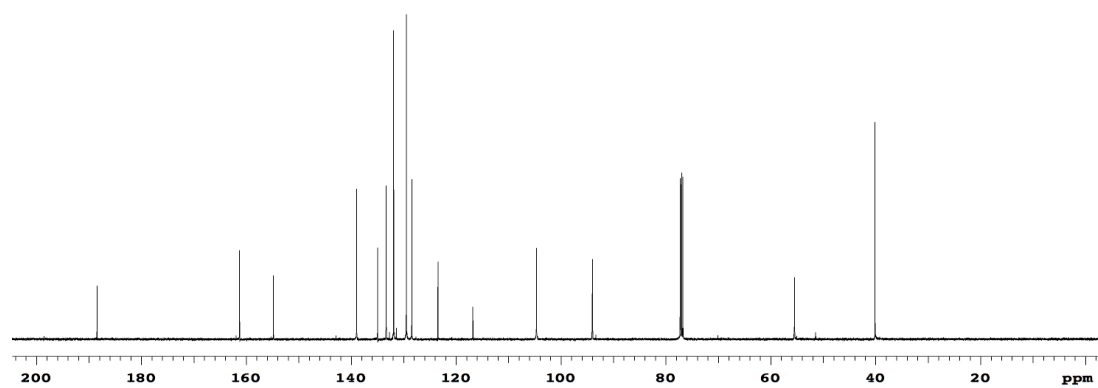


NaOH (776mg, 19.4mmol) was added to a solution of bromobenzaldehyde (1.44g, 7.8mmol) and 1-(4-dimethylamino-2-methoxyphenyl)ethanone (1.5g, 7.8mmol) in 20 mL MeOH. The reaction mixture was stirred at room temperature for 24h. The solid was collected on a filter and washed with cold MeOH to afford the title compound (2.5 g, 89%) as a light yellow solid.  $\delta_{\text{H}}$  (500MHz, CDCl<sub>3</sub>): 7.81 (d, J = 8.9 Hz, 1H), 7.62 (m, 2H), 7.45 (m, 4H), 6.32 (dd, J = 8.9 Hz, J = 2.4 Hz, 1H), 6.09 (d, J = 2.4 Hz, 1H), 3.91 (s, 3H), 3.05 (s, 6H);  $\delta_{\text{C}}$  (125MHz, CDCl<sub>3</sub>): 188.4, 161.3, 154.8, 139.0, 135.0, 133.3, 131.9, 129.5, 128.4, 123.5, 116.8, 104.7, 94.0, 55.5, 40.1; m/z (HR-ESI) theoretical mass (M+Li)<sup>+</sup> C<sub>18</sub>H<sub>18</sub>BrLiNO<sub>2</sub> 366.0681; found 366.0584.

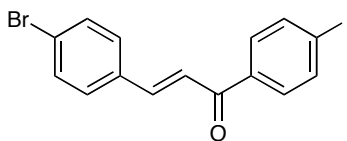




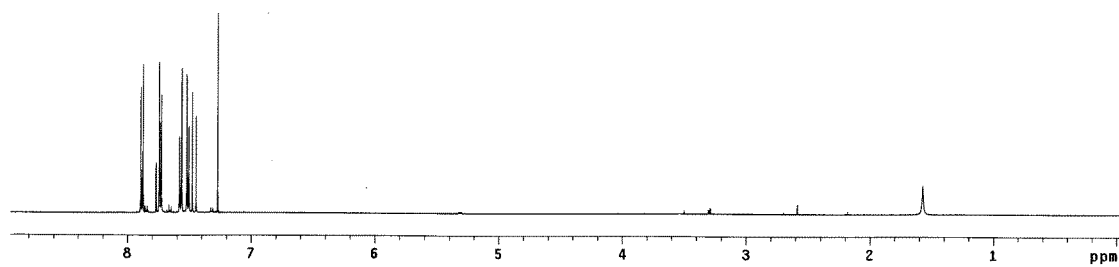
$^1\text{H}$  NMR for compound **291g** (500 MHz,  $\text{CDCl}_3$ ).



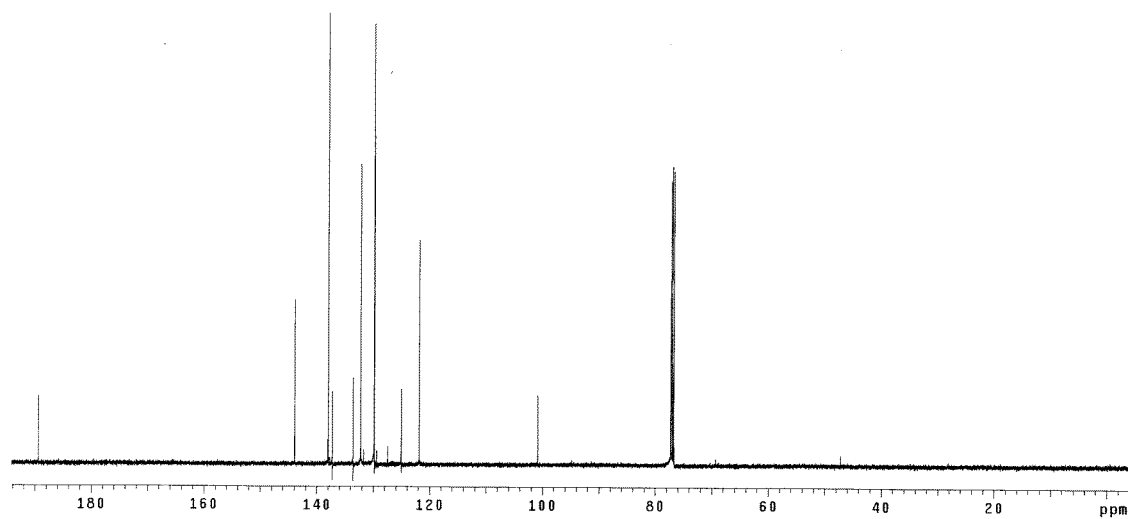
$^{13}\text{C}$  NMR for compound **291g** (125 MHz,  $\text{CDCl}_3$ ).

**(E)-3-(4-bromophenyl)-1-(4-iodophenyl)prop-2-en-1-one (291h).**<sup>11</sup>

4-Bromobenzaldehyde (20.0 g, 0.11 mol), 4-iodoacetophenone (26.6 g, 0.11 mol) and sodium hydroxide (0.432 g, 0.01 mol) were dissolved in a 1:1 mixture of methanol:water (400 mL) and stirred under reflux for 12 h. After cooling to room temperature, the product was filtered and washed with methanol. The title product was obtained as a white solid (42.7 g, 96%).  $\delta_{\text{H}}$  (500 MHz,  $\text{CDCl}_3$ ): 7.88 (d,  $J$ = 8.6 Hz, 2H), 7.75 (d,  $J$ = 15 Hz, 2H), 7.73 (d,  $J$ = 8.6 Hz, 2H), 7.51 (d,  $J$ = 8.6 Hz, 2H), 7.45 (d,  $J$ = 15 Hz, 2H);  $\delta_{\text{C}}$  (125 MHz,  $\text{CDCl}_3$ ): 189.4, 143.9, 137.9, 137.2, 133.6, 132.3, 129.9, 129.8, 125.1, 121.9, 100.8.



$^1\text{H}$  NMR for compound **291h** (500 MHz,  $\text{CDCl}_3$ )

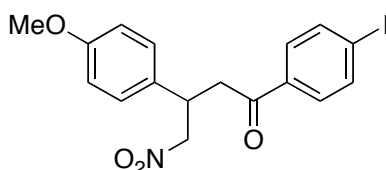


$^{13}\text{C}$  NMR for compound **291h** (125 MHz,  $\text{CDCl}_3$ )

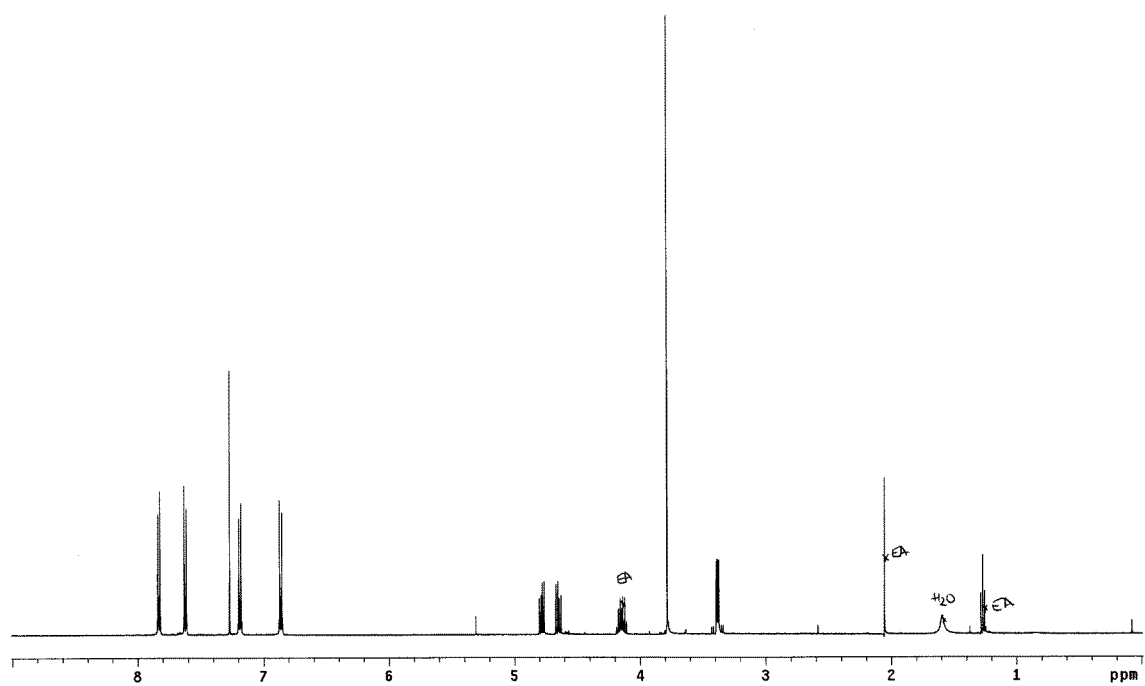
## General Procedure For The Synthesis of Michael Adduct 292a – g

A solution of chalcone (8.5 mmol), nitromethane (170 mmol) and KOH (1.7 mmol) in ethanol (8.5 mL) was heated at reflux for 12 h. After cooling to room temperature, the solvent was removed *in vacuo* and the oily residue obtained was extracted twice with ethyl acetate. The combined organic layers were washed with brine, dried over sodium sulfate and concentrated to give the target compound as a yellow solid in quantitative yield.

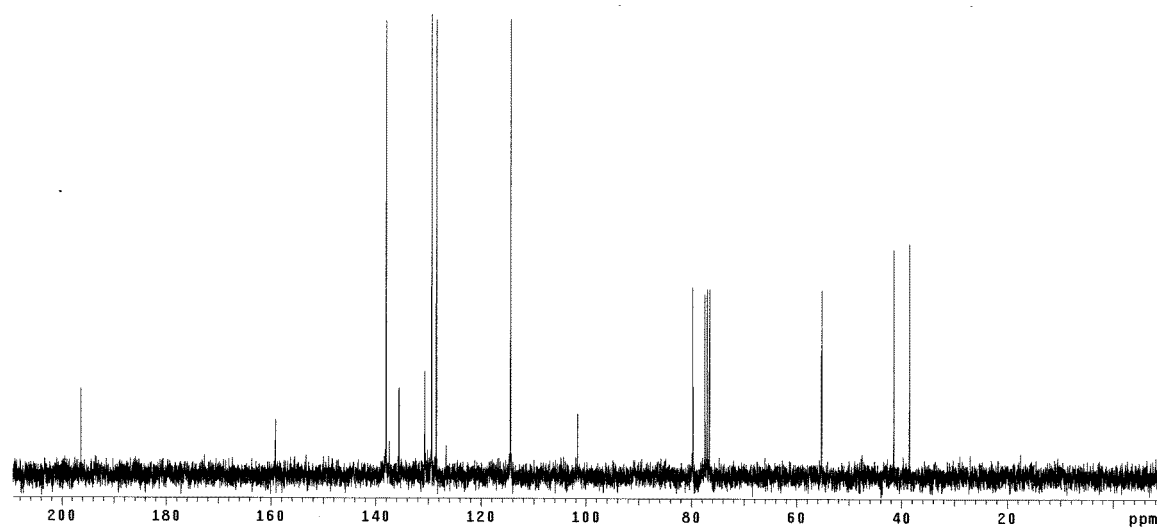
### 1-(4-iodophenyl)-3-(4-methoxyphenyl)-4-nitrobutan-1-one (292a).



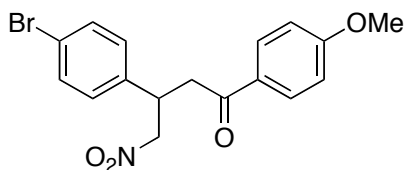
$\delta_{\text{H}}$  (500 MHz,  $\text{CDCl}_3$ ): 7.82 (d,  $J= 8.3$  Hz, 2H), 7.61 (d,  $J= 8.3$  Hz, 2H), 7.18 (d,  $J= 8.8$  Hz, 2H), 6.86 (d,  $J= 8.8$  Hz, 2H), 4.78 (dd<sub>AB system</sub>,  $J= 12.5$  Hz,  $J= 6.8$  Hz, 1H), 4.64 (dd<sub>AB system</sub>,  $J=12.5$  Hz,  $J=7.8$  Hz, 1H), 4.15 (apparent quint,  $J=7.1$  Hz, 1H), 3.77 (s, 3H), 3.37 (dd<sub>AB system</sub>,  $J= 7.3$  Hz,  $J= 1.2$  Hz, 2H);  $\delta_{\text{C}}$  (125 MHz,  $\text{CDCl}_3$ ):196.3, 159.1, 138.0, 135.6, 130.7, 129.3, 128.4, 114.4, 101.6, 79.7, 55.2, 41.5, 38.5;  $m/z$  (APCI): theoretical mass ( $M$ )<sup>+</sup>: 425.01; found : 425.1.



$^1\text{H}$  NMR for compound **292a** (500 MHz,  $\text{CDCl}_3$ )

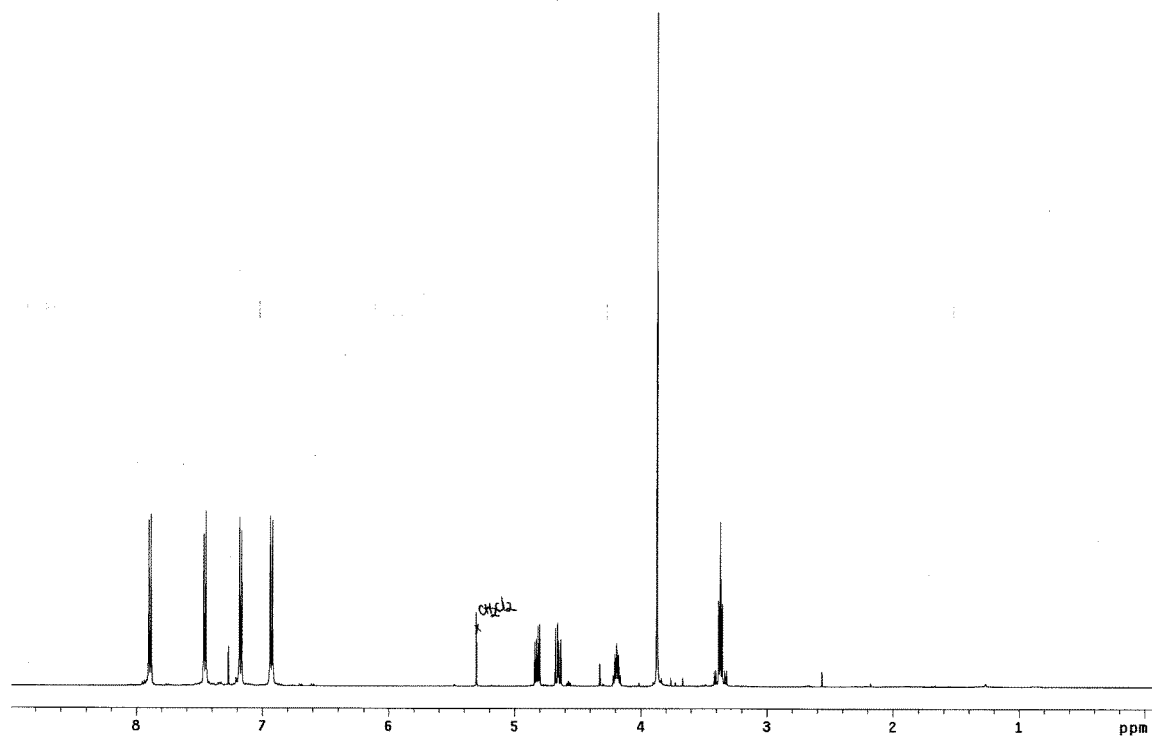


$^{13}\text{C}$  NMR for compound **292a** (125 MHz,  $\text{CDCl}_3$ )

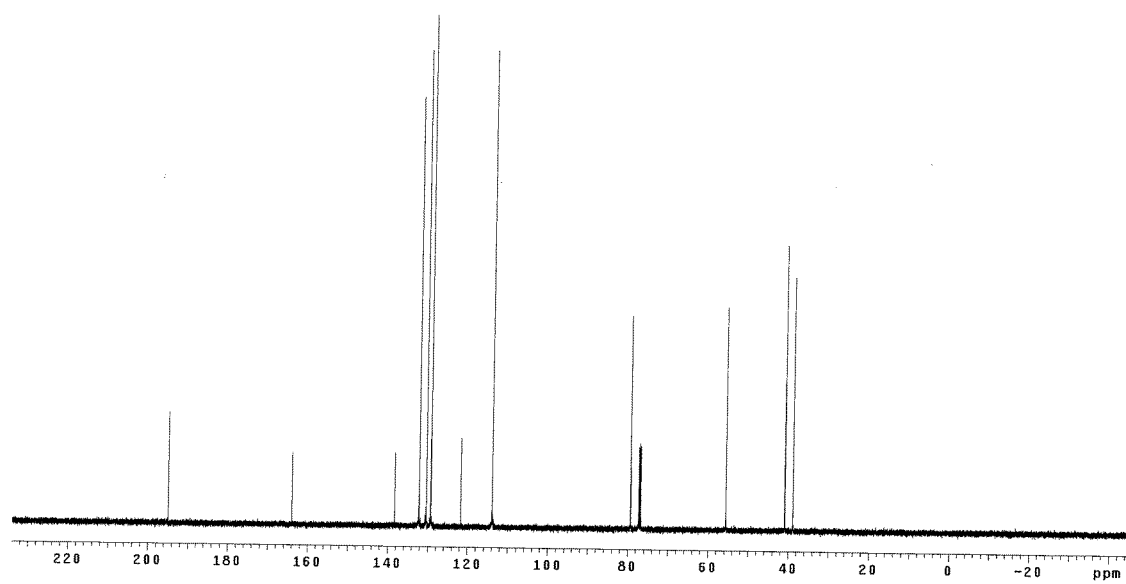
**3-(4-Bromophenyl)-1-(4-methoxyphenyl)-4-nitrobutan-1-one (292b).**

$\delta_{\text{H}}$  (500 MHz,  $\text{CDCl}_3$ ): 7.89 (d,  $J= 8.8$  Hz, 2H), 7.45 (d,  $J= 8.5$  Hz, 2H), 7.17 (d,  $J= 8.5$  Hz, 2H), 6.93 (d,  $J=8.8$  Hz, 2H), 4.8 (dd<sub>AB system</sub>,  $J= 12.5$  Hz,  $J= 6.1$  Hz, 1H), 4.65 (dd<sub>AB system</sub>,  $J= 12.5$  Hz,  $J= 8.3$  Hz, 1H), 4.19 (apparent quint,  $J= 7.1$  Hz, 1H), 3.87 (s, 3H), 3.37 (2 coalesced dd<sub>AB system</sub>,  $J= 17.6$  Hz,  $J= 6.6$  Hz, 2H);  $\delta_{\text{C}}$  (125 MHz,  $\text{CDCl}_3$ ):194.9, 163.9, 138.2, 132.1, 130.3, 129.2, 129.2, 121.7, 113.9, 79.3, 55.5, 40.8, 38.8;  $m/z$  (APCI): theoretical mass ( $M$ )<sup>+</sup>: 377.02; found : 377.9-379.9 (Br isotope)

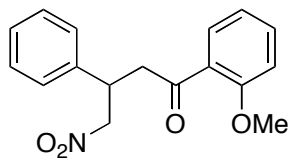




$^1\text{H}$  NMR for compound **292b** (500 MHz,  $\text{CDCl}_3$ )

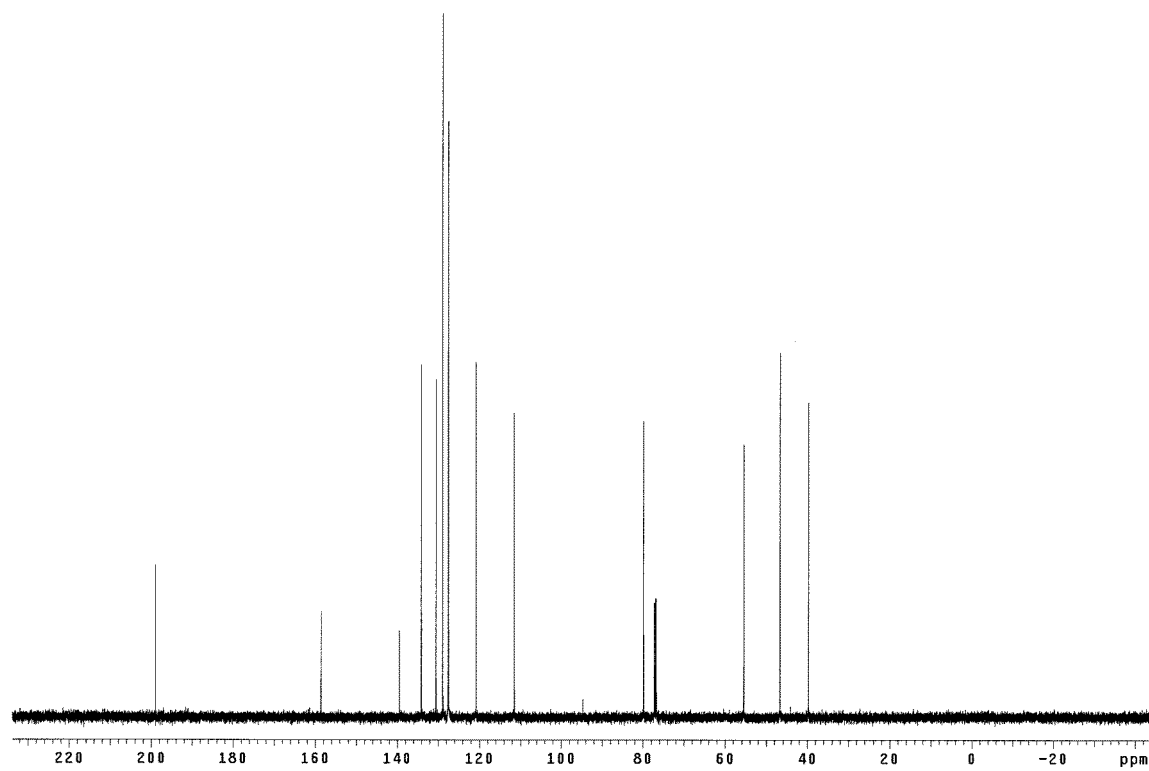


$^{13}\text{C}$  NMR for compound **292b** (125 MHz,  $\text{CDCl}_3$ ).

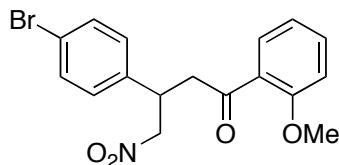
**1-(2-methoxyphenyl)-4-nitro-3-phenylbutan-1-one (292c).**

$\delta_{\text{H}}$  (500 MHz,  $\text{CDCl}_3$ ): 7.62 (dd,  $J= 7.8$  Hz,  $J= 1.9$  Hz, 1H), 7.48 (td,  $J= 7.3$  Hz,  $J= 1.9$  Hz, 1H), 7.34-7.30 (m, 2H), 7.25-7.24 (m, 3H), 7.00-6.96 (m, 2H), 4.8 (dd,  $J= 1.2$  Hz,  $J= 7.6$  Hz, 1H), 4.65 (dd,  $J= 8.3$  Hz,  $J= 1.2$  Hz, 1H), 4.18 (quint,  $J= 7.1$  Hz, 1H), 3.89 (s, 3H), 3.46 (dd,  $J= 2.9$  Hz,  $J= 3.7$  Hz, 2H);  $\delta_{\text{C}}$  (125 MHz,  $\text{CDCl}_3$ ): 198.9, 158.6, 139.4, 134.0, 130.4, 128.8, 127.6, 127.5, 127.4, 120.8, 111.5, 79.9, 55.5, 46.7, 39.7;  $m/z$  (HR-ESI): theoretical mass  $(\text{M}+\text{H})^+$ : 300.1236; found : 300.1237.

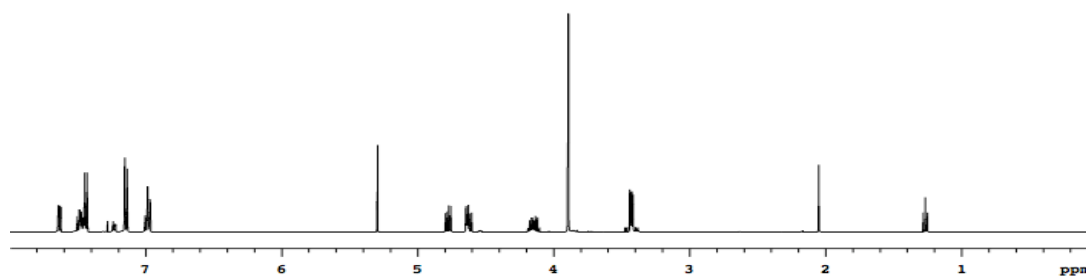




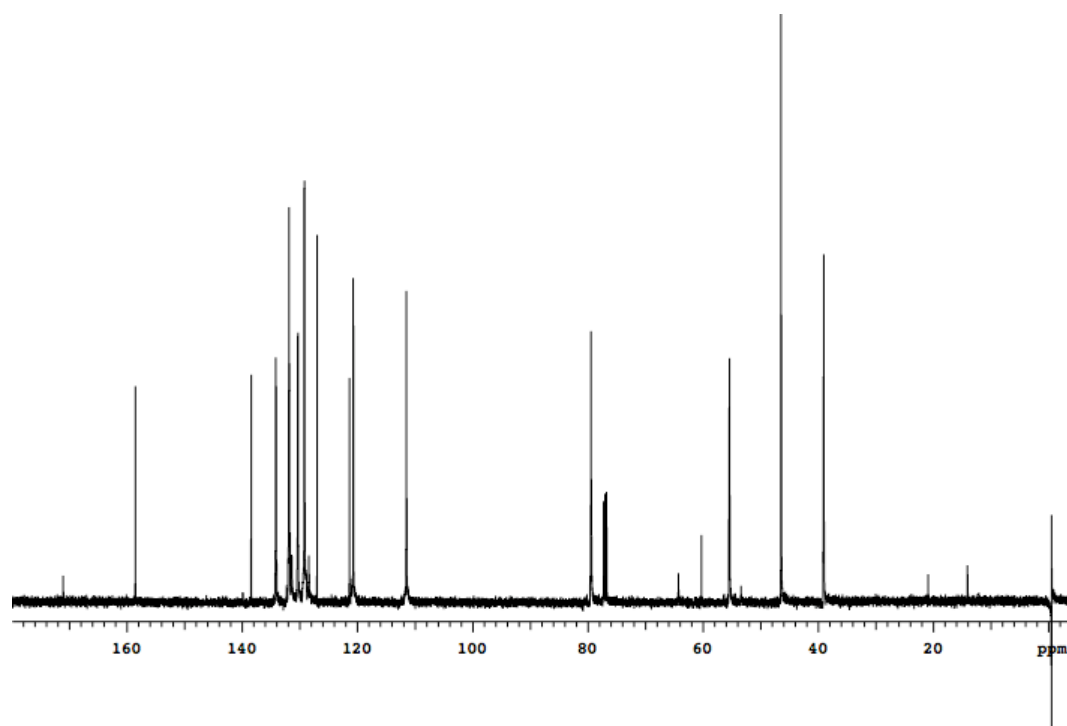
$^{13}\text{C}$  NMR for compound **292c** (125 MHz,  $\text{CDCl}_3$ )

**3-(4-Bromophenyl)-1-(2-methoxyphenyl)-4-nitrobutan-1-one (292d)**

$\delta_{\text{H}}$  (500 MHz,  $\text{CDCl}_3$ ): 7.64 (dd,  $J = 7.6$  Hz,  $J = 1.7$  Hz, 1H), 7.49 (td,  $J = 7.6$  Hz,  $J = 1.7$  Hz, 1H), 7.45 (d,  $J = 8.5$  Hz, 2H), 7.14 (d,  $J = 8.5$  Hz, 2H), 7.00-6.97 (m, 2H), 4.78 (dd<sub>AB system</sub>,  $J = 12.5$  Hz,  $J = 6.3$  Hz, 1H), 4.62 (dd<sub>AB system</sub>,  $J = 12.5$  Hz,  $J = 8.3$  Hz, 1H), 4.16 (apparent quint,  $J = 6.8$  Hz, 1H), 3.91 (s, 3H), 3.42 (dd,  $J = 6.8$  Hz,  $J = 1.7$  Hz, 2H);  $\delta_{\text{C}}$  (125 MHz,  $\text{CDCl}_3$ ): 158.5, 138.4, 134.1, 131.8, 130.3, 129.2, 127.0, 121.3, 120.7, 111.4, 79.4, 55.3, 46.4, 39.0 (signal for CO missing);  $m/z$  (HR-ESI): theoretical mass ( $\text{M}+\text{Li}$ )<sup>+</sup>: 384.0423; found : 384.0429-386.0451 (Br isotope).

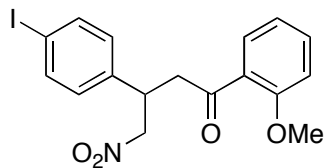


$^1\text{H}$  NMR for compound **292d** (500 MHz,  $\text{CDCl}_3$ )

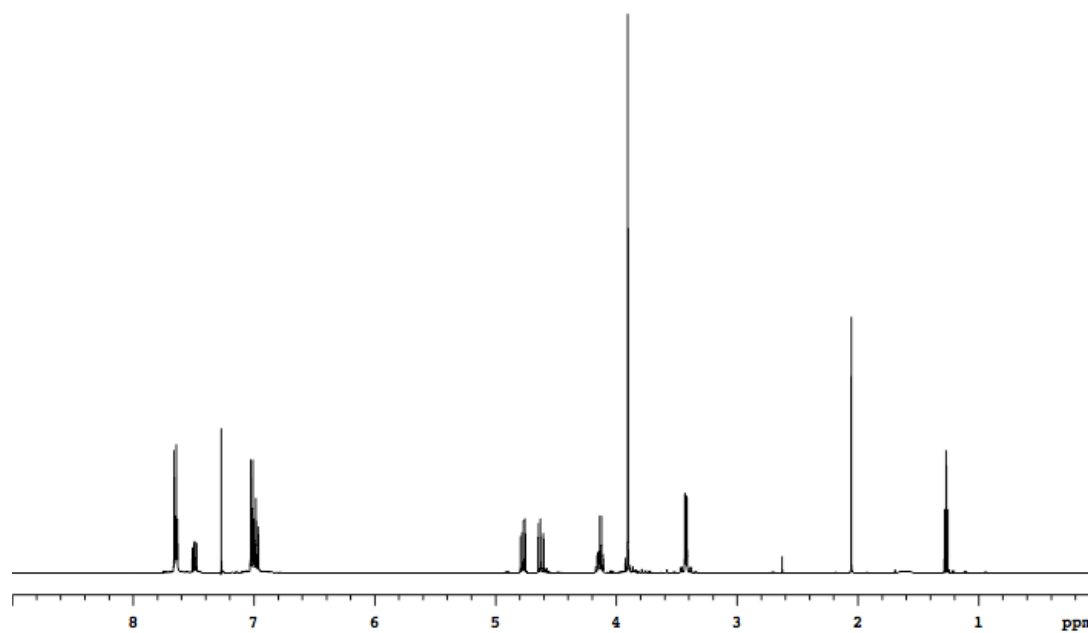


$^{13}\text{C}$  NMR for compound **292d** (125 MHz,  $\text{CDCl}_3$ )

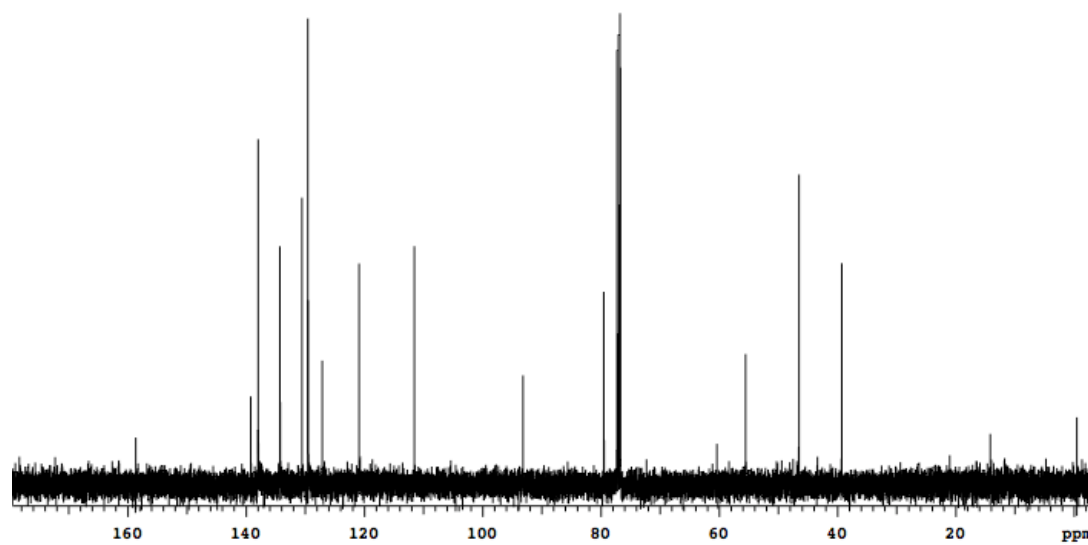


**3-(4-Iodophenyl)-1-(2-methoxyphenyl)-4-nitrobutan-1-one (292e).**

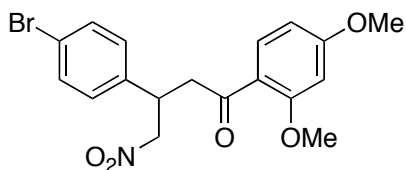
$\delta_{\text{H}}$  (500MHz,  $\text{CDCl}_3$ ): 7.66 – 7.63 (m, 3H), 7.50 (2 touching dd,  $J = 7.3$  Hz,  $J = 1.9$  Hz, 1H), 7.02 (d,  $J = 8.3$  Hz, 2H), 6.98 (t,  $J = 8.3$  Hz, 2H), 4.78 (m, 1H), 4.62 (m, 1H), 4.12 (m, 1H), 3.90 (s, 3H), 3.42 (m, 2H);  $\delta_{\text{C}}$  (125MHz,  $\text{CDCl}_3$ ): 158.6, 139.2, 137.9, 134.2, 130.5, 129.5, 127.1, 120.8, 111.5, 93.1, 79.5, 55.5, 46.5, 39.3 (C for carbonyl group not seen).



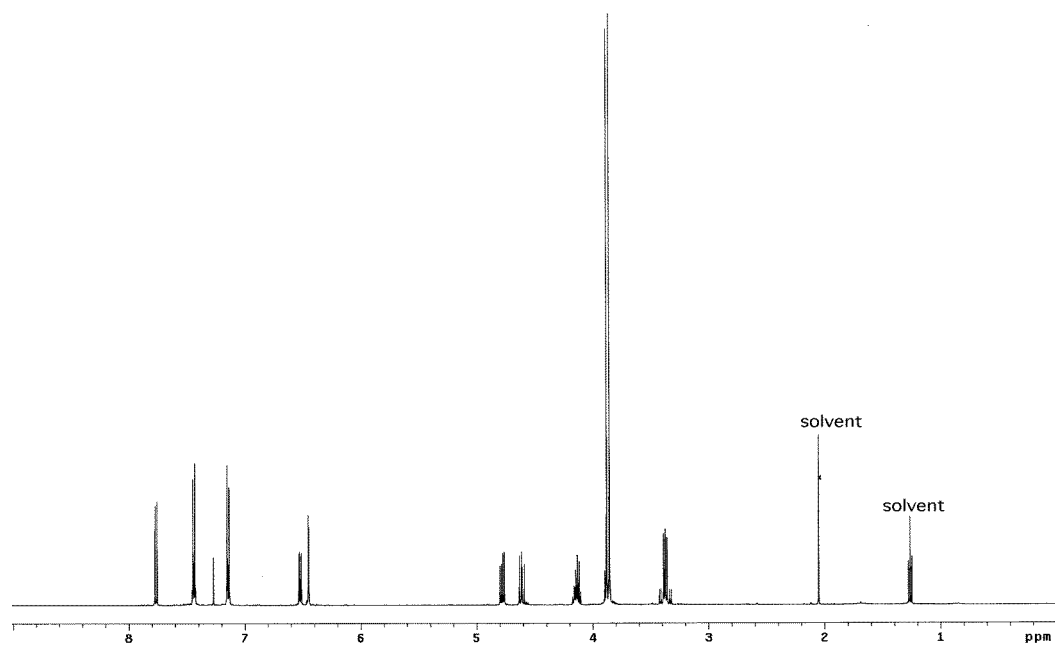
$^1\text{H}$  NMR for compound **292e** (500 MHz,  $\text{CDCl}_3$ )



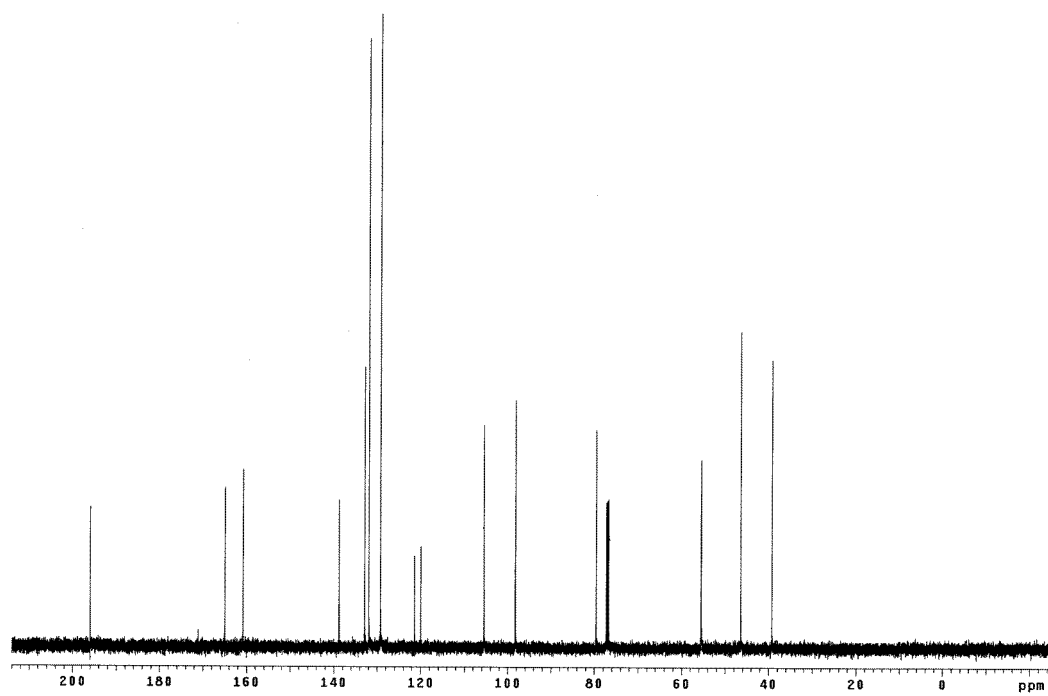
$^{13}\text{C}$  NMR for compound **292e** (125 MHz,  $\text{CDCl}_3$ )

**3-(4-Bromophenyl)-1-(2,4-dimethoxyphenyl)-4-nitrobutan-1-one (292f)**

$\delta_{\text{H}}$  (500 MHz,  $\text{CDCl}_3$ ): 7.76 (d,  $J$  = 8.8 Hz, 1H), 7.44 (d,  $J$  = 8.5 Hz, 2H), 7.14 (d,  $J$  = 8.5 Hz, 2H), 6.51 (dd,  $J$  = 8.8 Hz,  $J$  = 2.4 Hz, 1H), 6.45 (d,  $J$  = 2.2 Hz, 1H), 4.77 (dd<sub>AB system</sub>,  $J$  = 12.4 Hz,  $J$  = 6.3 Hz, 1H), 4.61 (dd<sub>AB system</sub>,  $J$  = 12.4 Hz,  $J$  = 8.8 Hz, 1H), 4.13 (apparent quint,  $J$  = 7.1 Hz, 1H), 3.87 (s, 3H), 3.85 (s, 3H), 3.39 (dd<sub>AB system</sub>,  $J$  = 17.6 Hz,  $J$  = 6.6 Hz, 1H), 3.34 (dd<sub>AB system</sub>,  $J$  = 17.6 Hz,  $J$  = 7.6 Hz, 1H);  $\delta_{\text{C}}$  (125 MHz,  $\text{CDCl}_3$ ): 196.0, 164.9, 160.8, 138.8, 132.9, 131.9, 129.2, 121.4, 119.9, 105.4, 98.2, 79.6, 55.5, 55.4, 46.4, 39.2;  $m/z$  (HR-ESI): theoretical mass ( $\text{M}+\text{Li}$ )<sup>+</sup>: 414.0528; found : 414.0537-416.0497 (Br isotope).

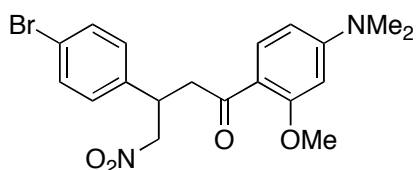


$^1\text{H}$  NMR for compound **292f** (500 MHz,  $\text{CDCl}_3$ )

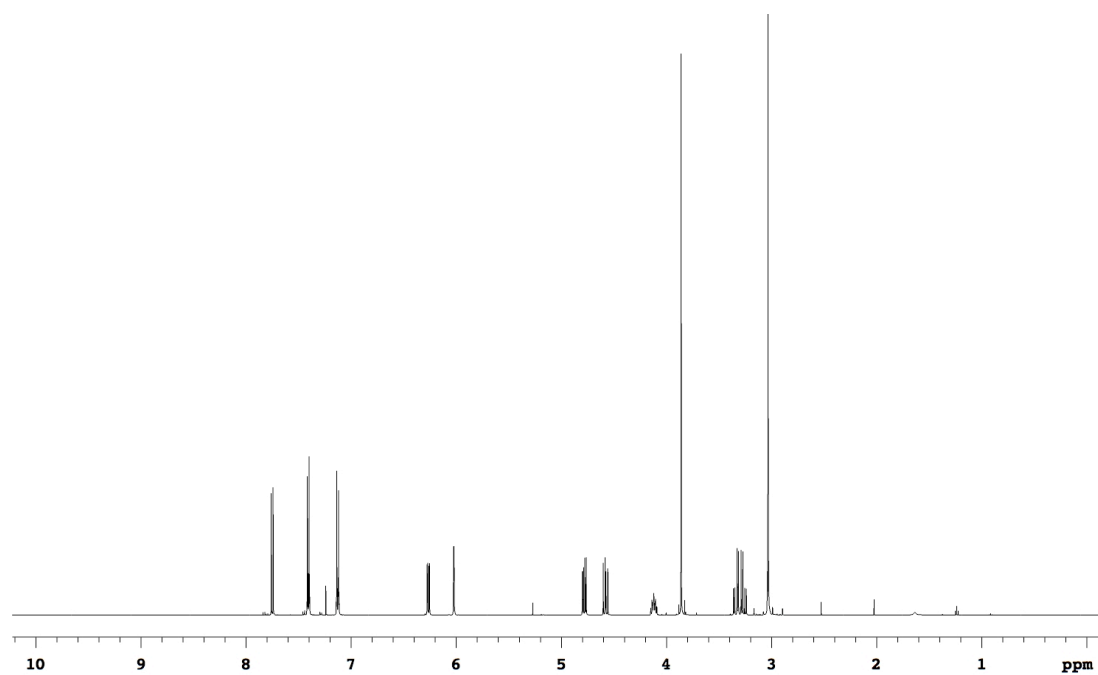


$^{13}\text{C}$  NMR for compound **292f** (125 MHz,  $\text{CDCl}_3$ )

**3-(4-bromophenyl)-1-(4-(dimethylamino)-2-methoxyphenyl)-4-nitrobutan-1-one (292g).**

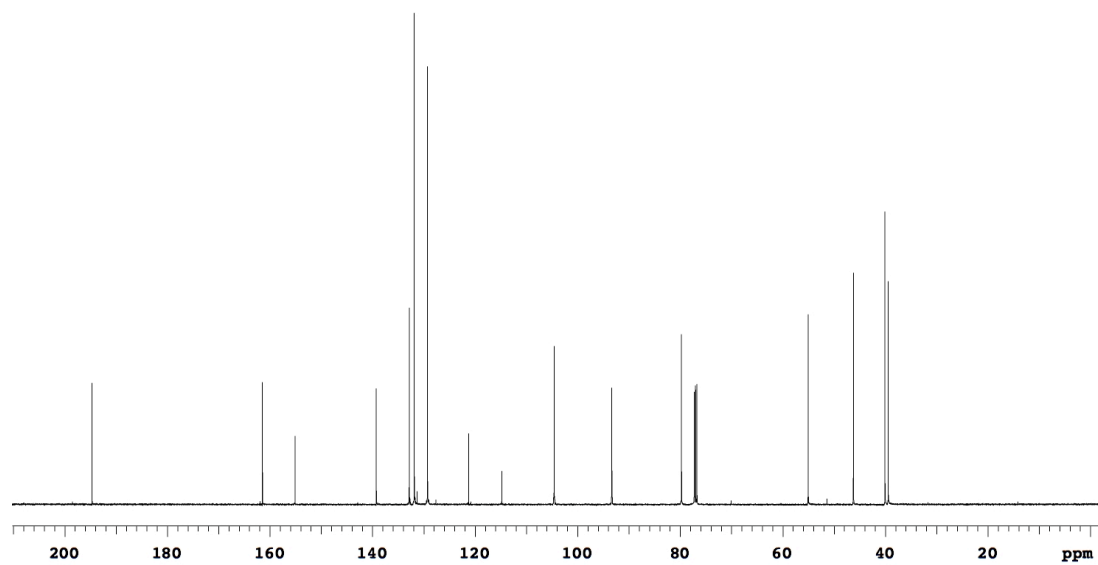


$\delta_{\text{H}}$  (500MHz,  $\text{CDCl}_3$ ): 7.75 (d,  $J = 8.9$  Hz, 1H), 7.41 (m, 2H), 7.13 (m, 2H), 6.26 (dd,  $J = 8.9$ ,  $J = 2.3$  Hz, 1H), 6.00 (d,  $J = 2.3$  Hz, 1H), 4.78 (dd<sub>AB system</sub>,  $J = 12.7$  Hz,  $J = 5.8$  Hz, 1H), 4.58 (dd<sub>AB system</sub>,  $J = 12.7$  Hz,  $J = 9.1$  Hz, 1H), 4.12 (m, 1H), 3.86 (s, 3H), 3.34 (dd<sub>AB system</sub>,  $J = 17.0$  Hz,  $J = 6.3$  Hz, 1H), 3.26 (dd<sub>AB system</sub>,  $J = 17.0$  Hz,  $J = 8.0$  Hz, 1H), 3.03 (s, 6H);  $\delta_{\text{C}}$  (125MHz,  $\text{CDCl}_3$ ): 194.7, 161.5, 155.1, 139.3, 132.8, 131.9, 129.3, 121.2, 114.8, 104.6, 93.3, 79.7, 55.1, 46.2, 40.1, 39.4.



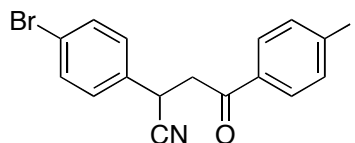
$^1\text{H}$  NMR for compound **292g** (500 MHz,  $\text{CDCl}_3$ )



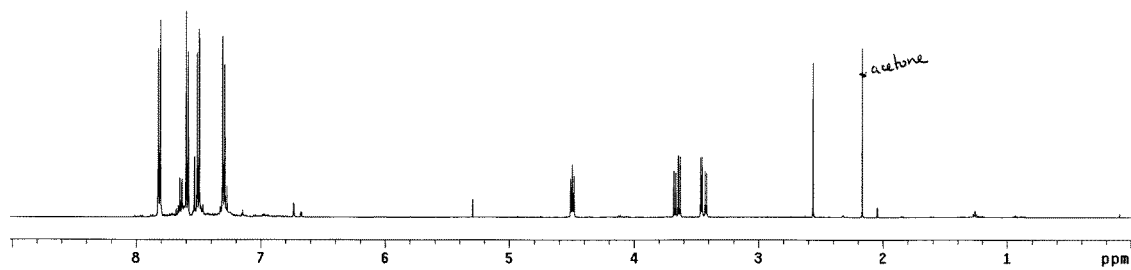


$^{13}\text{C}$  NMR for compound **292g** (125 MHz,  $\text{CDCl}_3$ )

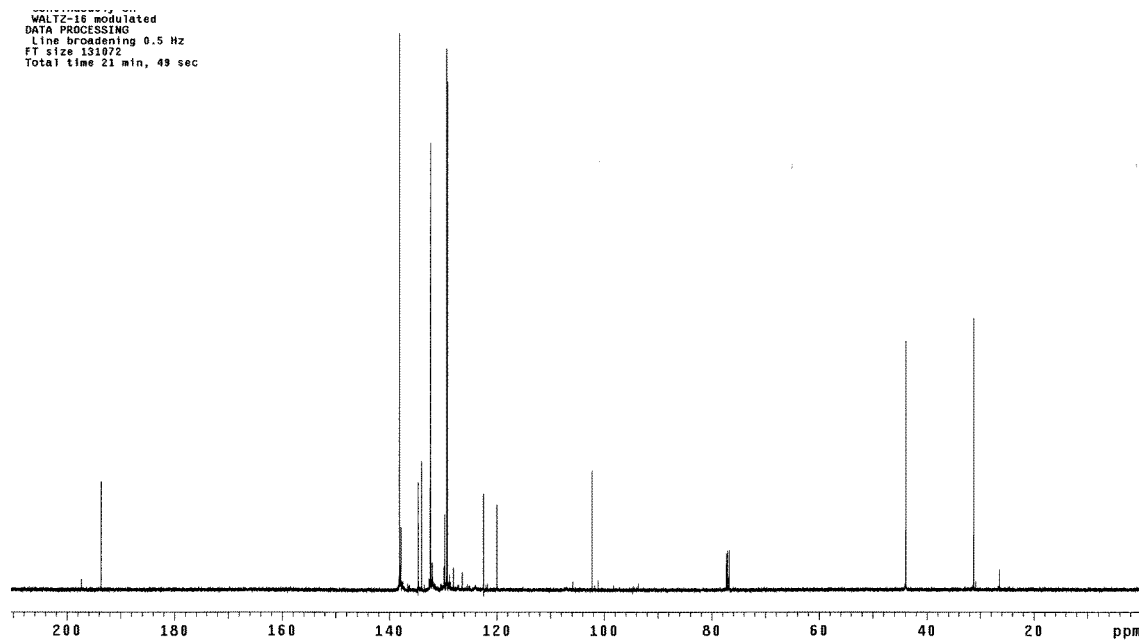
**2-(4-Bromophenyl)-4-(4-iodophenyl)-4-oxobutanenitrile (294).**



6 mL of a solution of 10% sodium carbonate was added to a solution of (*E*)-3-(4-bromophenyl)-1-(4-iodophenyl)prop-2-en-1-one **292h** (1.0 g, 2.42 mmol) and acetone cyanohydrin (0.5 g, 6.05 mmol) in acetone (20 mL). After refluxing for 12h, the reaction mixture allowed to cool to room temperature. The content of the flask was poured into an Erlenmeyer, and water was added to induce the separation of the product. Compound **7** was obtained as a yellow powder in 75 % yield (0.805 g).  $\delta_{\text{H}}$  (500 MHz,  $\text{CDCl}_3$ ): 7.82 (d,  $J$ = 8.6 Hz, 2H), 7.59 (d,  $J$ = 8.6 Hz, 2H), 7.50 (d,  $J$ = 8.3 Hz, 2H), 7.30 (d,  $J$ = 8.3 Hz, 2H), 4.49 (*apparent t*,  $J$ = 7.6 Hz,  $J$ = 6.3 Hz, 1H), 3.65 (dd<sub>AB system</sub>,  $J$ = 18.1 Hz,  $J$ = 7.6 Hz, 1H), 3.44 (dd<sub>AB system</sub>,  $J$ = 18.1 Hz,  $J$ = 6.3 Hz, 1H);  $\delta_{\text{C}}$  (125 MHz,  $\text{CDCl}_3$ ): 193.7, 138.1, 134.5, 133.9, 132.3, 129.6, 129.2, 122.4, 119.9, 98.8, 43.9, 31.2.



$^1\text{H}$  NMR for compound **294** (500 MHz,  $\text{CDCl}_3$ )

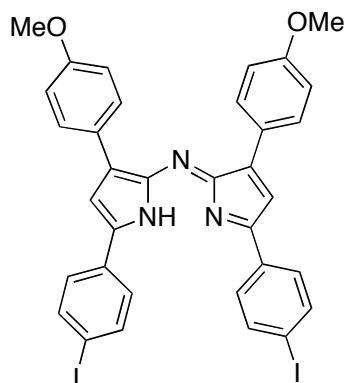


$^{13}\text{C}$  NMR for compound **294** 125 MHz,  $\text{CDCl}_3$ )

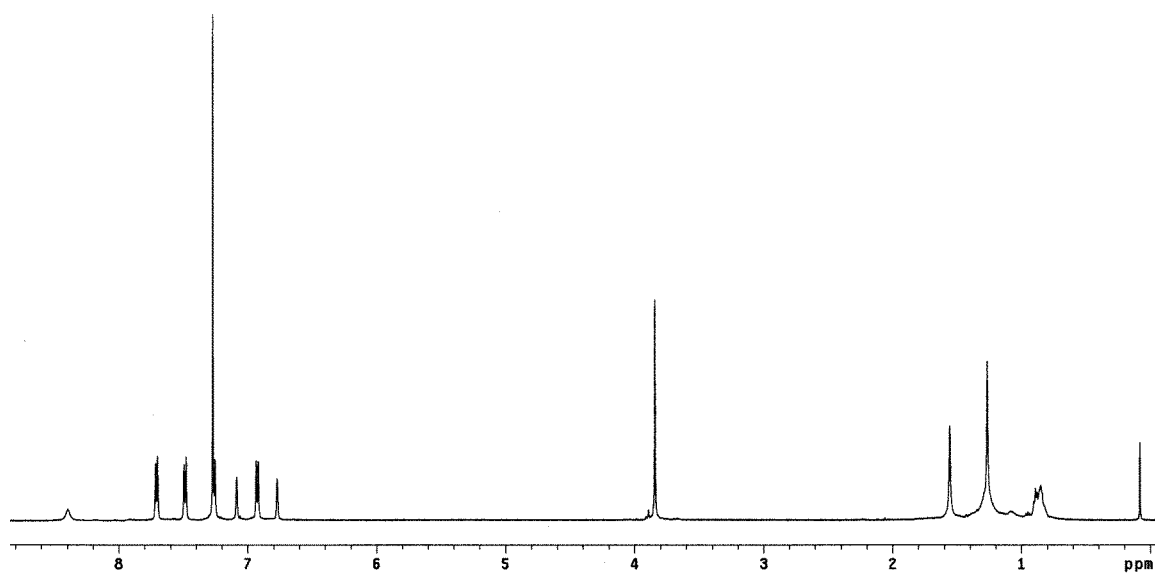
## General Procedure for the Synthesis of Azadipyrromethene 293a - g.

A 100 mL round-bottomed flask was charged with **5** (1 eq.), ammonium acetate (35 eq.), and butanol and heated under reflux for 24h. After cooling to room temperature, the solvent was concentrated to a quarter of its original volume, filtered, and the isolated solid was washed with ethanol to yield the desired product as a dark blue-black solid in about 50% yield.

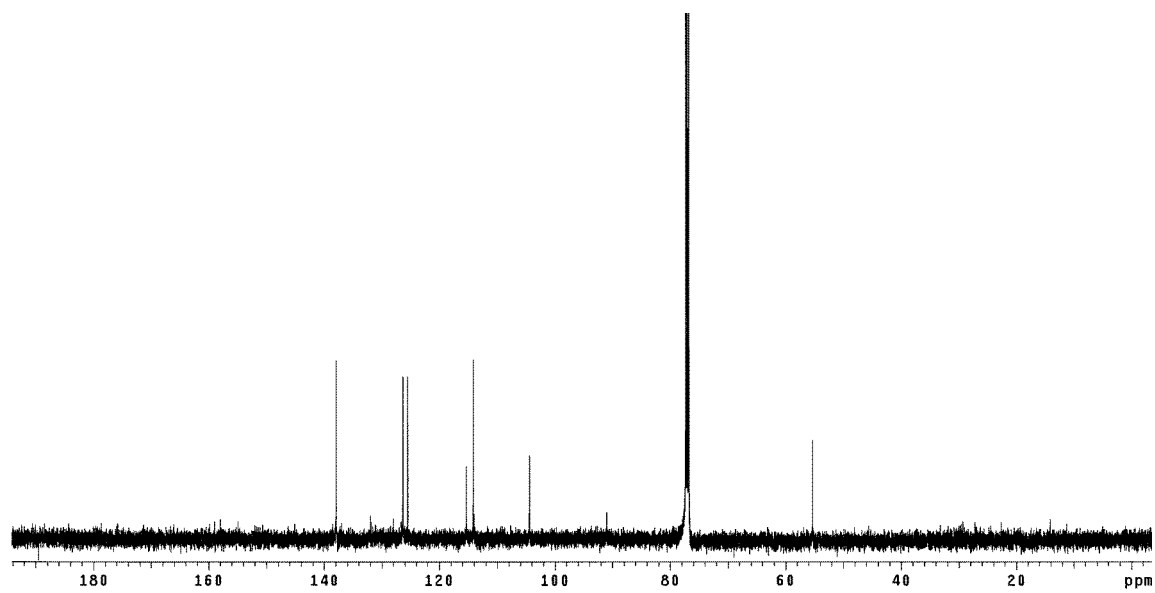
### Azadipyrromethene 293a



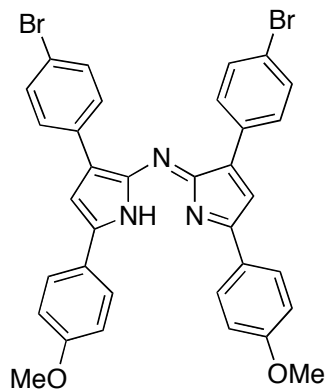
$\delta_{\text{H}}$  (500 MHz,  $\text{CDCl}_3$ ): 3.96 (s, 6H), 7.04 (d,  $J=8.3$  Hz, 2H), 7.08 (t,  $J=7.3$  Hz, 2H), 7.33-7.44 (m, 10H), 8.07 (d,  $J=7.3$  Hz, 4H), 8.13 (d,  $J=7.8$  Hz, 2H);  $\delta_{\text{C}}$  (75 MHz,  $\text{CDCl}_3$ ): 137.9, 126.3, 125.5, 115.3, 114.1, 104.4, 55.3 ; m/z (APCI): theoretical mass ( $M$ )<sup>+</sup>: 762.01; found: 762.1. Because of poor solubility or aggregation, a good  $^{13}\text{C}$  spectrum could not be obtained.



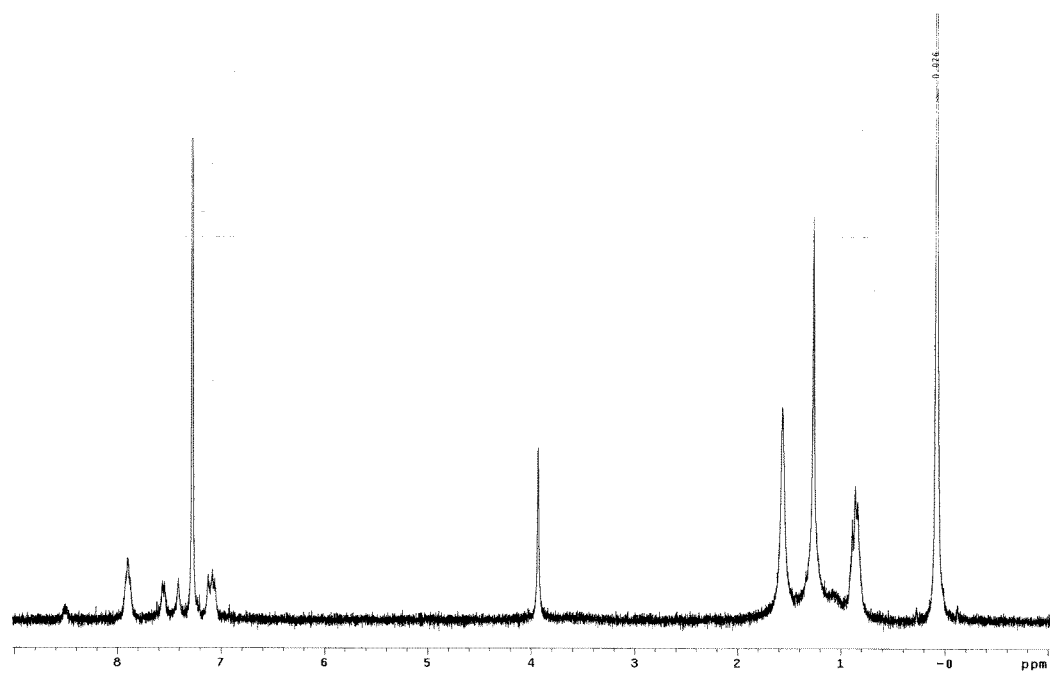
$^1\text{H}$  NMR for compound **293a** (500 MHz,  $\text{CDCl}_3$ ).



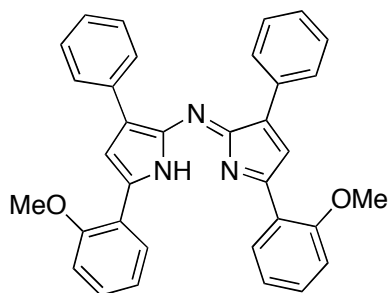
$^{13}\text{C}$  NMR for compound **293a** (125 MHz,  $\text{CDCl}_3$ ).

**Azadipyrromethene 293b**

$\delta_{\text{H}}$  (500 MHz,  $\text{CDCl}_3$ ): 8.13 (d,  $J=7.8$  Hz, 2H), 8.07 (d,  $J=7.3$  Hz, 4H), 7.33-7.44 (m, 10H), 7.08 (t,  $J=7.3$  Hz, 2H), 7.04 (d,  $J=8.3$  Hz, 2H), 3.96 (s, 6H);  $m/z$  (ESI): theoretical mass  $(\text{M}+\text{H})^+$ : 666.03; found: 666.3-668.2 (Br isotope). Attempt to take nmr in  $\text{CDCl}_3$  only gave broad signals probably because of aggregation.

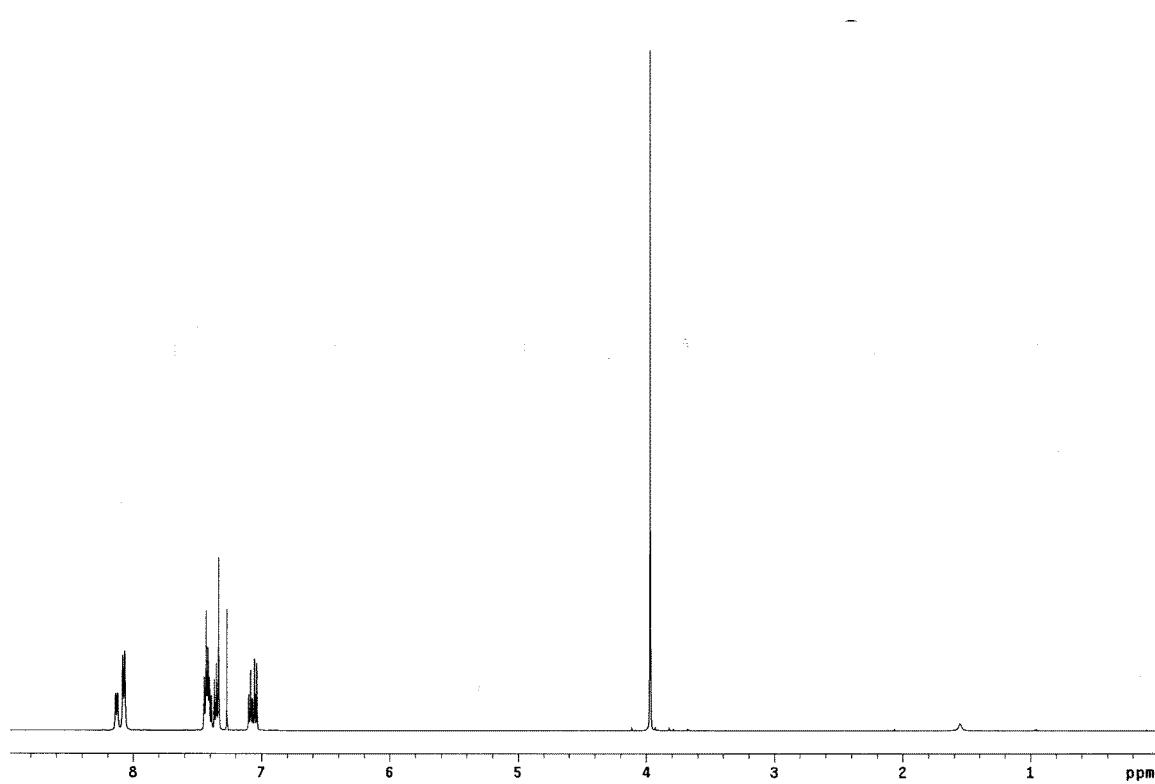


$^1\text{H}$  NMR for compound **293b** (500 MHz,  $\text{CDCl}_3$ ).

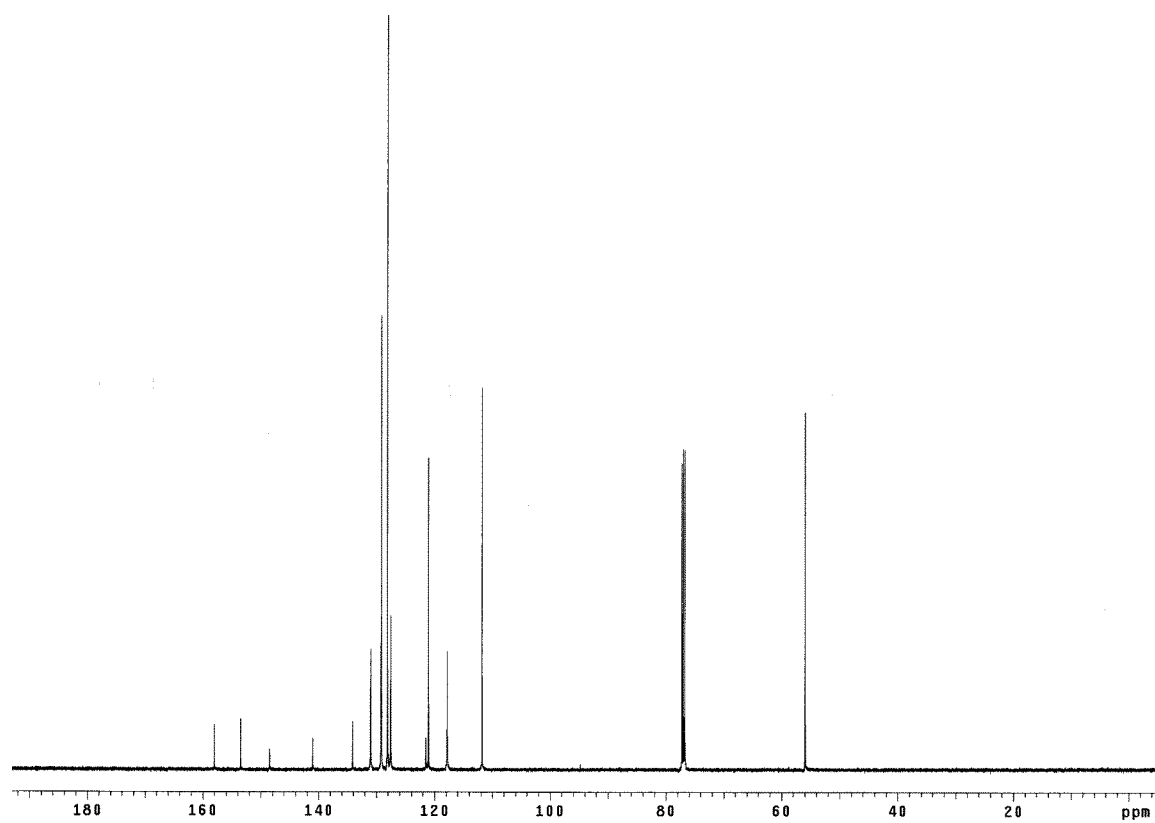
**Azadipyrromethene 293c**

$\delta_{\text{H}}$  (500 MHz,  $\text{CDCl}_3$ ): 8.13 (d,  $J = 7.8$  Hz, 2H), 8.07 (d,  $J = 7.3$  Hz, 4H), 7.44-7.33 (m, 10H), 7.08 (t,  $J = 7.3$  Hz, 2H), 7.04 (d,  $J = 8.3$  Hz, 2H), 3.96 (s, 6H);  $\delta_{\text{C}}$  (125 MHz,  $\text{CDCl}_3$ ): 158.0, 153.5, 148.5, 141.0, 134.1, 130.9, 129.1, 128.1, 127.9, 127.5, 121.4, 121.0, 117.8, 111.8, 55.9;  $m/z$  (HR-ESI): theoretical mass  $(\text{M}+\text{H})^+$ : 510.2182; found: 510.2174.

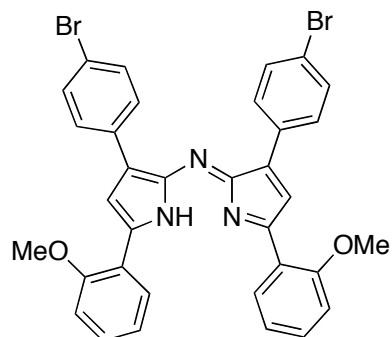




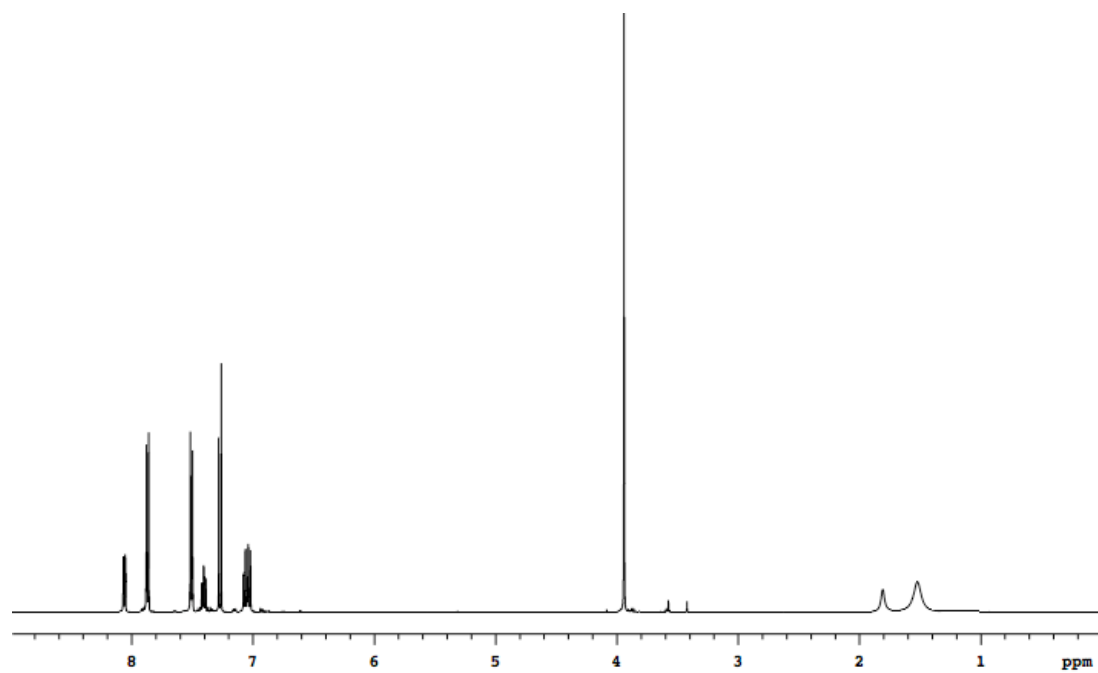
$^1\text{H}$  NMR for compound **293c** (500 MHz,  $\text{CDCl}_3$ ).



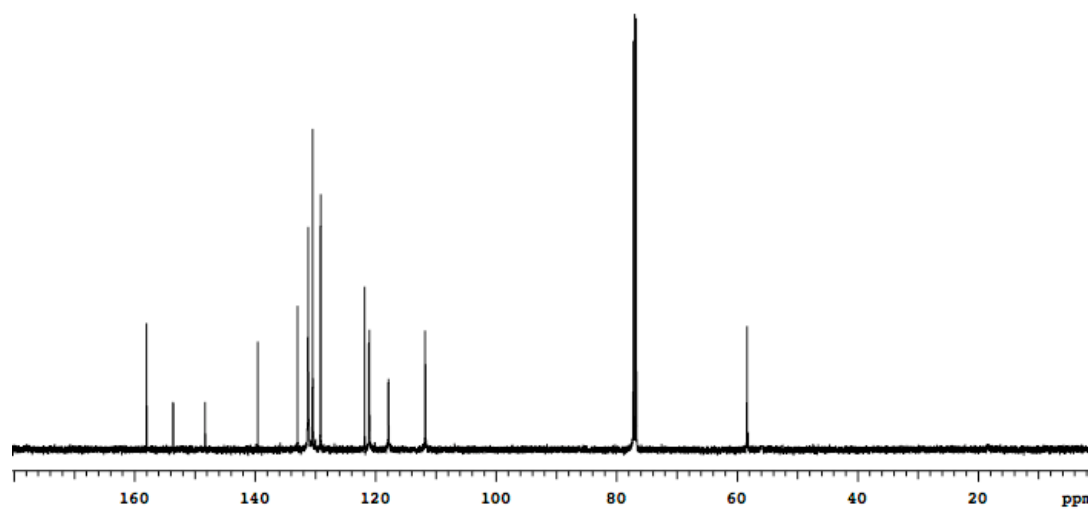
$^{13}\text{C}$  NMR for compound **293c** (125 MHz,  $\text{CDCl}_3$ ).

**Azadipyrromethene 293d**

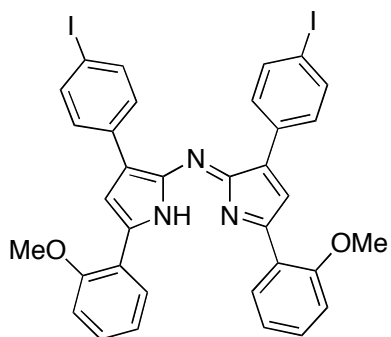
$\delta_{\text{H}}$  (500 MHz,  $\text{CDCl}_3$ ): 3.95 (s, 6H), 7.02-7.09 (m, 4H), 7.28 (s, 2H), 7.41 (dt,  $J=1.7$  Hz,  $J=7.3$  Hz, 2H), 7.51 (d,  $J=8.8$  Hz, 4H), 7.87 (d,  $J=8.5$  Hz, 4H), 8.08 (d,  $J=7.3$  Hz, 2H);  $\delta_{\text{C}}$  (125 MHz,  $\text{CDCl}_3$ ): 157.9, 153.5, 148.2, 139.5, 132.9, 131.1, 130.4, 129.1, 121.7, 121.1, 121.0, 117.9, 117.8, 111.7, 55.9;  $m/z$  (ESI): theoretical mass  $(\text{M}+\text{H})^+$ : 666.0392; found: 666.0399-668.0366 (Br isotope)



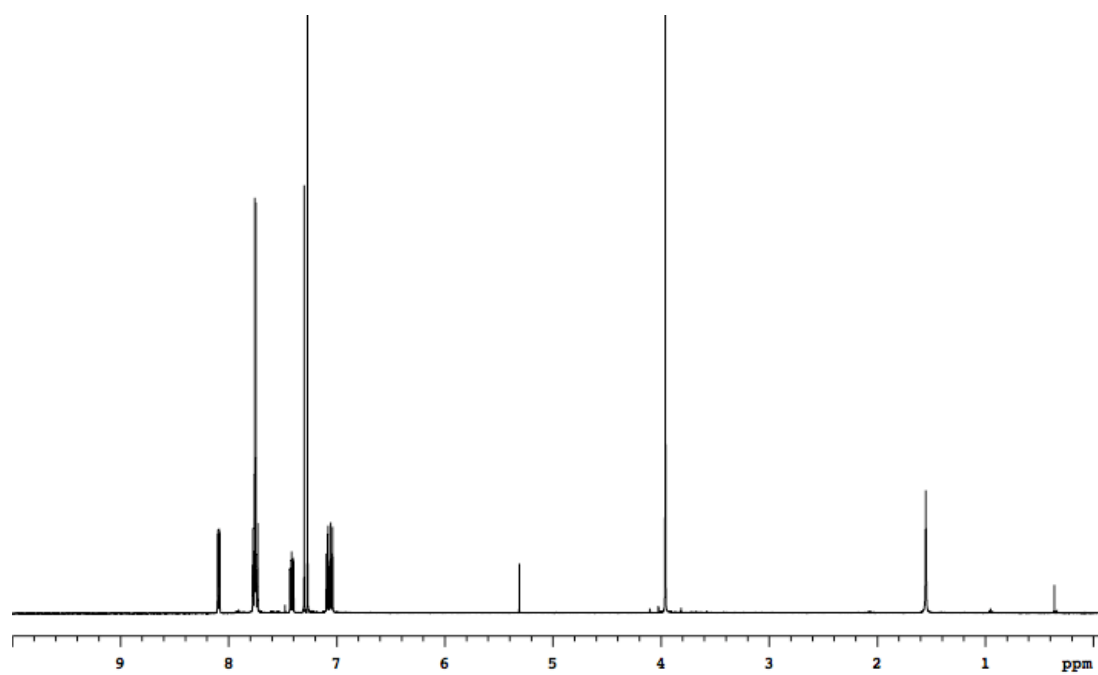
$^1\text{H}$  NMR for compound **293d** (500 MHz,  $\text{CDCl}_3$ ).



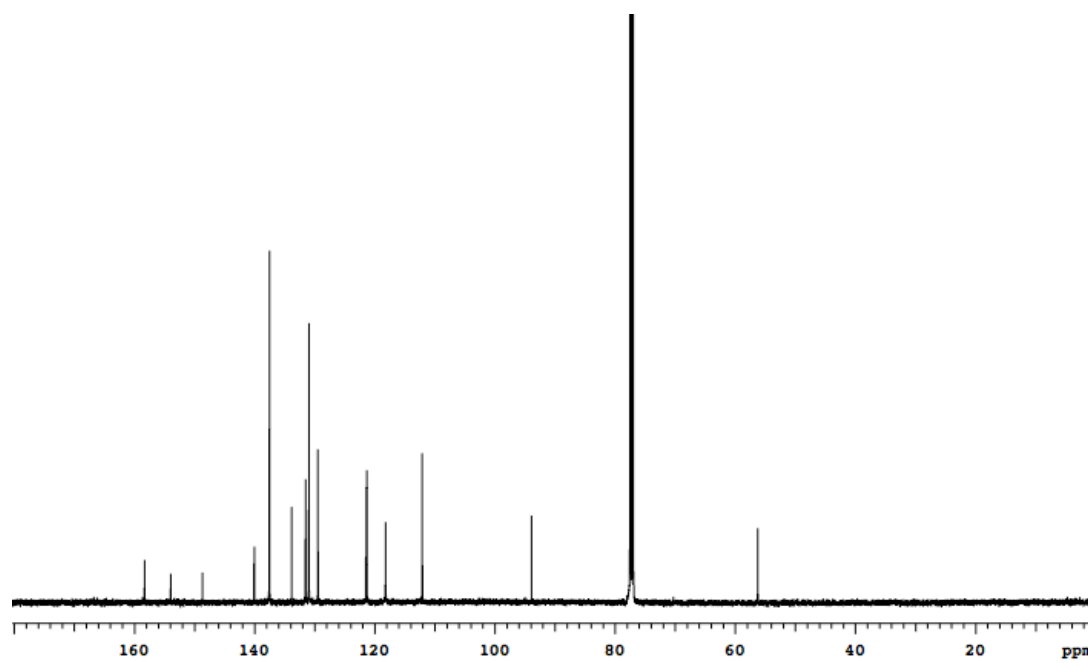
$^{13}\text{C}$  NMR for compound **293d** (125 MHz,  $\text{CDCl}_3$ ).

**Azadipyrromethene 293e**

$\delta_{\text{H}}$  (500 MHz,  $\text{CDCl}_3$ ): 8.09 (dd,  $J = 7.6$  Hz,  $J = 1.7$  Hz, 2H), 7.75 (apparent doublet of quart,  $J = 8.5$  Hz,  $J = 2.2$  Hz, 8H), 7.41 (dt,  $J = 7.3$  Hz,  $J = 1.7$  Hz, 2H), 7.30 (s, 2H), 7.08 (dt,  $J = 7.6$  Hz,  $J = 1.0$  Hz, 2H), 7.04 (d,  $J = 8.5$  Hz, 2H), 3.95 (s, 6H);  $\delta_{\text{C}}$  (125 MHz,  $\text{CDCl}_3$ ): 158.1, 153.7, 148.4, 139.8, 137.3, 133.5, 131.3, 130.7, 129.2, 121.2, 121.1, 117.9, 111.8, 93.6, 55.9.

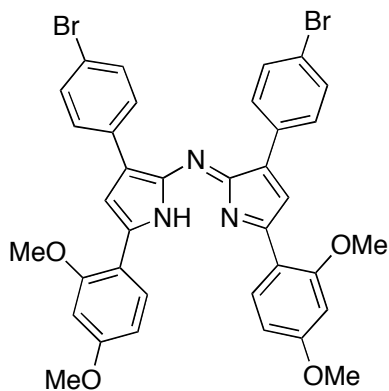


$^1\text{H}$  NMR for compound **293e** (500 MHz,  $\text{CDCl}_3$ ).

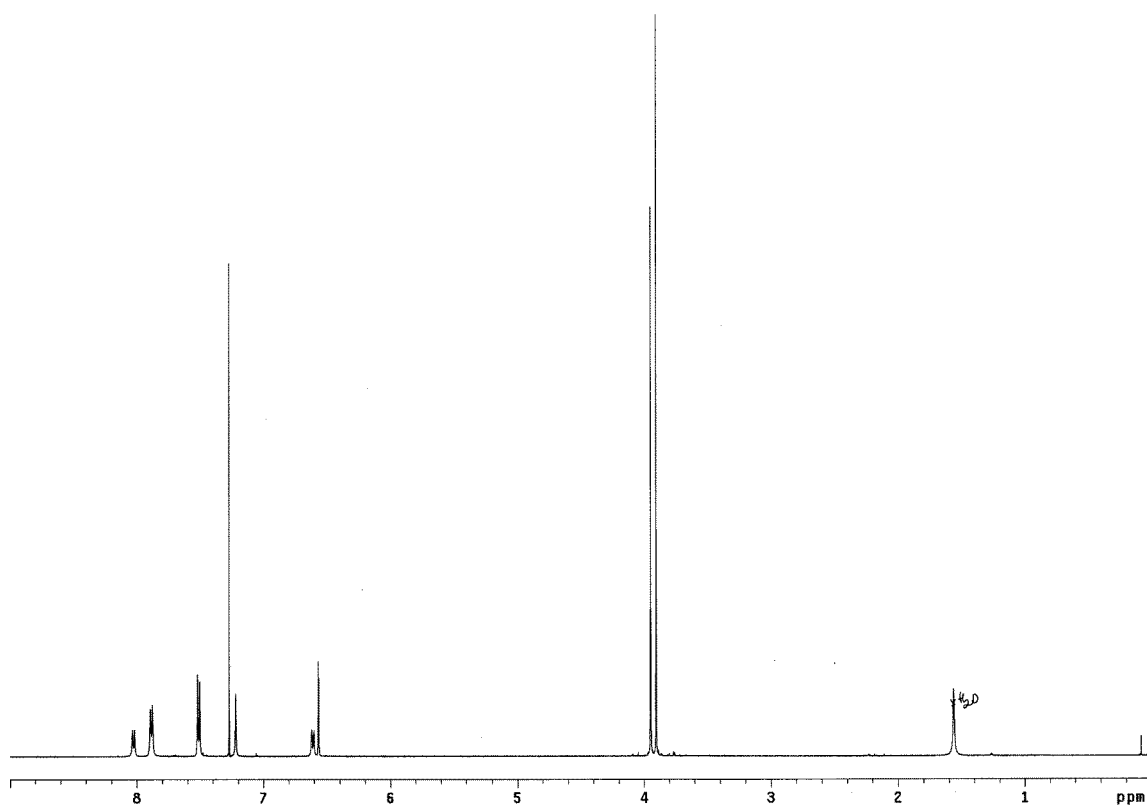


$^{13}\text{C}$  NMR for compound **293e** (125 MHz,  $\text{CDCl}_3$ ).

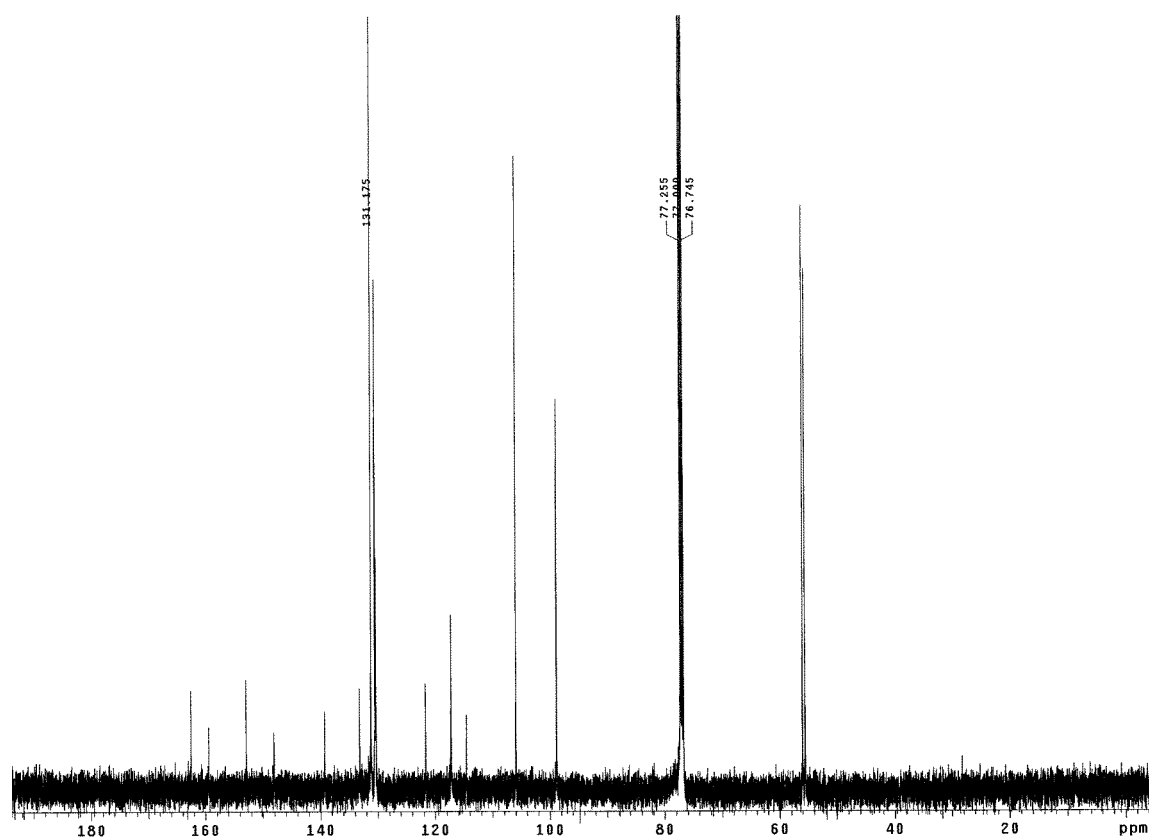


**Azadipyrromethene 293f**

$\delta_{\text{H}}$  (500 MHz,  $\text{CDCl}_3$ ): 8.03 (d,  $J=8.5$  Hz, 2H), 7.88 (d,  $J=8.3$  Hz, 4H), 7.51 (d,  $J=8.3$  Hz, 4H), 7.21 (s, 2H), 6.60 (dd,  $J=8.5$  Hz,  $J=2.4$  Hz, 2H), 6.56 (d,  $J=2.4$  Hz, 2H), 3.95 (s, 6H), 3.90 (s, 6H);  $\delta_{\text{C}}$  (125 MHz,  $\text{CDCl}_3$ ): 162.5, 159.4, 152.9, 148.1, 139.3, 133.2, 131.2, 130.5, 130.3, 121.6, 117.2, 114.5, 105.9, 98.8, 56.0, 55.6;  $m/z$  (HR-ESI): theoretical mass  $(\text{M}+\text{H})^+$ : 726.0603; found: 726.0587-728.0555 (Br isotope).



$^1\text{H}$  NMR for compound **293f** (500 MHz,  $\text{CDCl}_3$ )

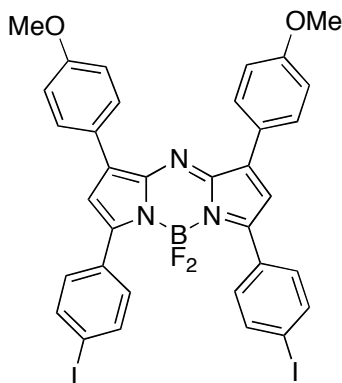


$^{13}\text{C}$  NMR for compound **293f** (125 MHz,  $\text{CDCl}_3$ ).

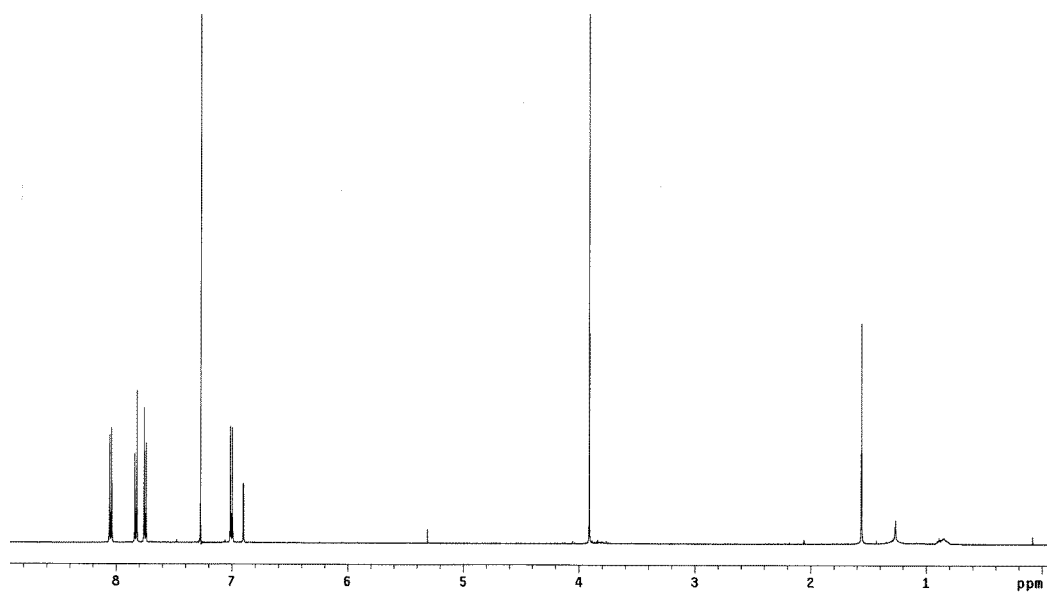
### General Procedure for the Synthesis of AzaBODIPY 288a – g .

A flame dried Schlenk flask was charged with the azapyromethene (1 eq.) and flushed with nitrogen. Dry dichloromethane and dry diisopropylethylamine (11 eq.) were then added. The solution was stirred at 25 °C for 15 min, then distilled  $\text{BF}_3 \cdot \text{OEt}_2$  (15.6 eq.) was added. After stirring at 25 °C for 24h, the mixture was washed with water, and the organic layer dried over sodium sulfate and concentrated *in vacuo* to give the target compound.

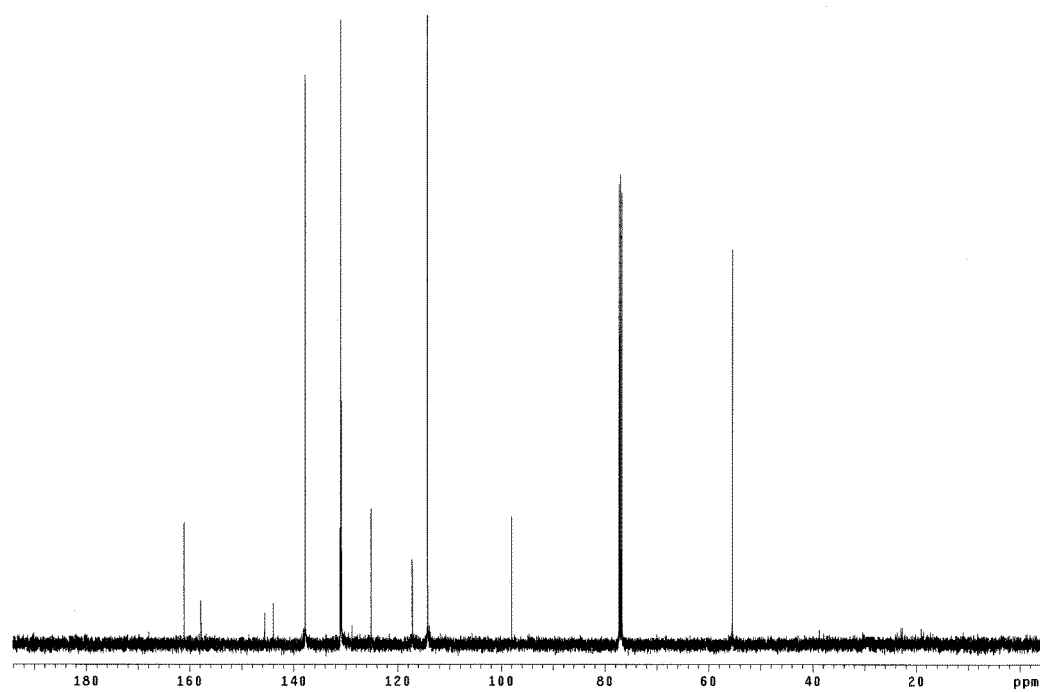
#### AzaBODIPY 288a



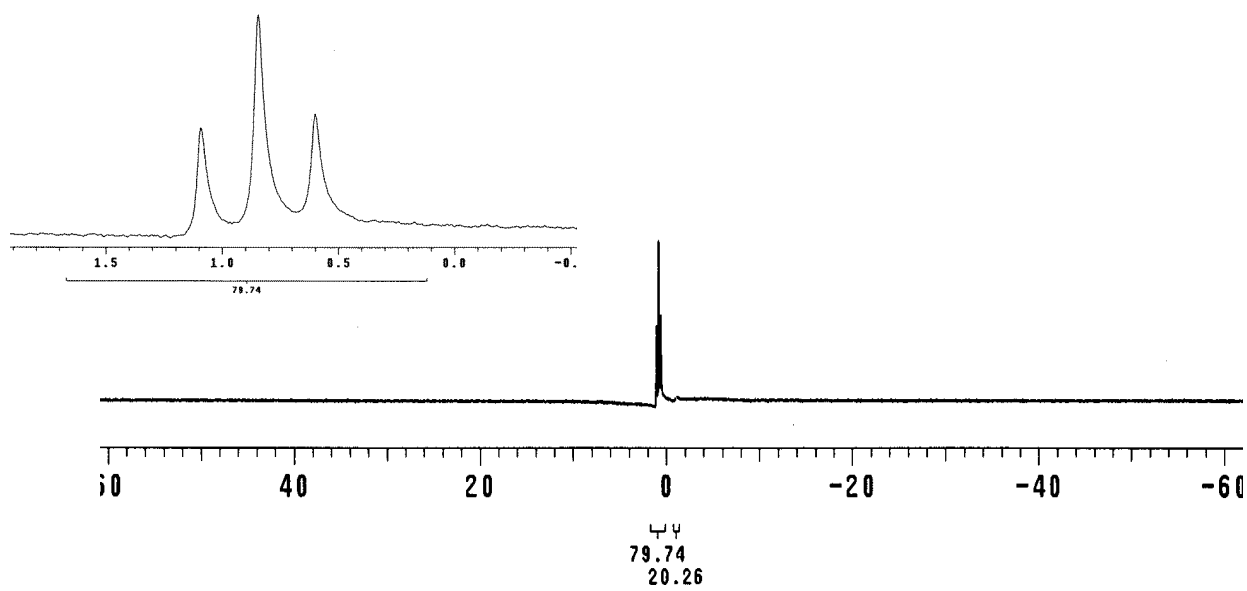
$\delta_{\text{H}}$  (500 MHz,  $\text{CDCl}_3$ ): 8.04 (d,  $J=8.8$  Hz, 4H), 7.83 (d,  $J=8.5$  Hz, 4H), 7.75 (d,  $J=8.8$  Hz, 4H), 7.00 (d,  $J=8.5$  Hz, 4H), 6.89 (s, 2H), 3.91 (s, 6H);  $\delta_{\text{C}}$  (125 MHz,  $\text{CDCl}_3$ ): 161.1, 157.9, 145.6, 144.1, 137.8, 131.1, 130.9, 130.8, 125.1, 117.2, 114.3, 98.0, 55.4;  $\delta_{\text{B}}$  (128 MHz,  $\text{CDCl}_3$ ): 0.84 (t, 1B,  $J_{\text{B-F}} = 31$  Hz);  $\delta_{\text{F}}$  (376 MHz,  $\text{CDCl}_3$ ): -134.89 (q, 2F,  $J_{\text{B-F}} = 31$  Hz); MS (maldi)  $m/z$  calcd for  $(\text{M}+\text{H})^+$   $\text{C}_{34}\text{H}_{25}\text{BI}_2\text{F}_2\text{N}_3\text{O}_2$ :810.0097; found :810.0071;  $\lambda_{\text{max abs}}$  (PhMe)/nm 680 ( $\epsilon/\text{dm}^3\text{mol}^{-1}\text{cm}^{-1}$  108 996);  $\lambda_{\text{max emis}}$  (PhMe)/nm 711;  $\Phi = 0.18$  in 1% pyridine in toluene.



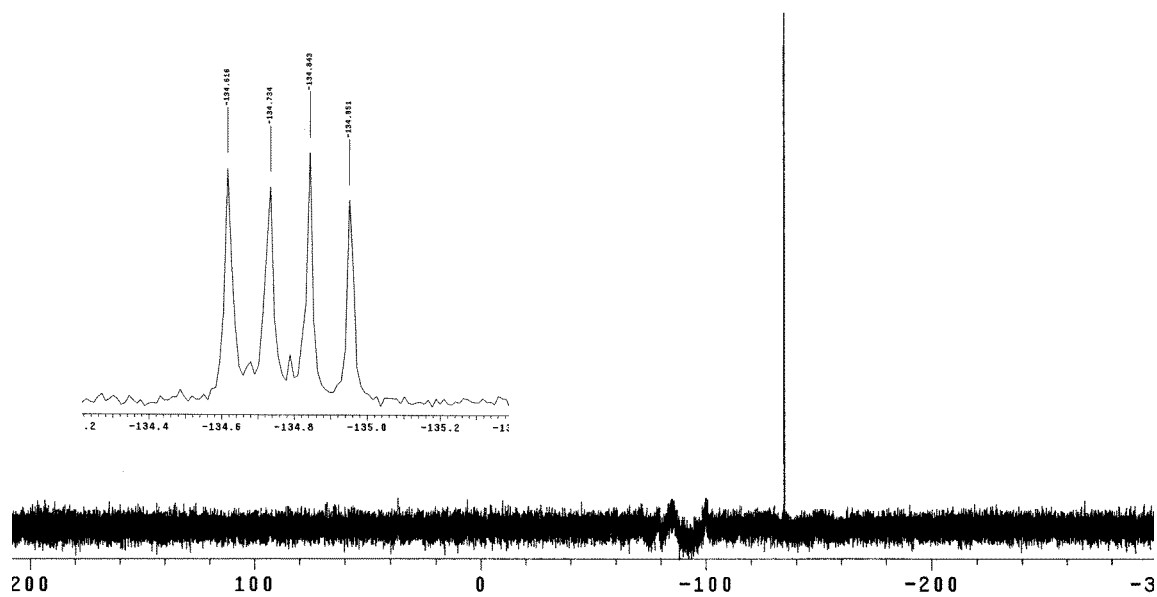
$^1\text{H}$  NMR for compound **288a** (500 MHz,  $\text{CDCl}_3$ )



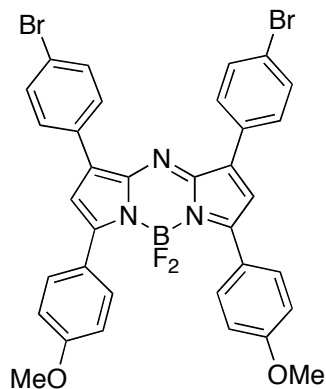
$^{13}\text{C}$  NMR  $^1\text{H}$  NMR for compound **288a** (125 MHz,  $\text{CDCl}_3$ ).



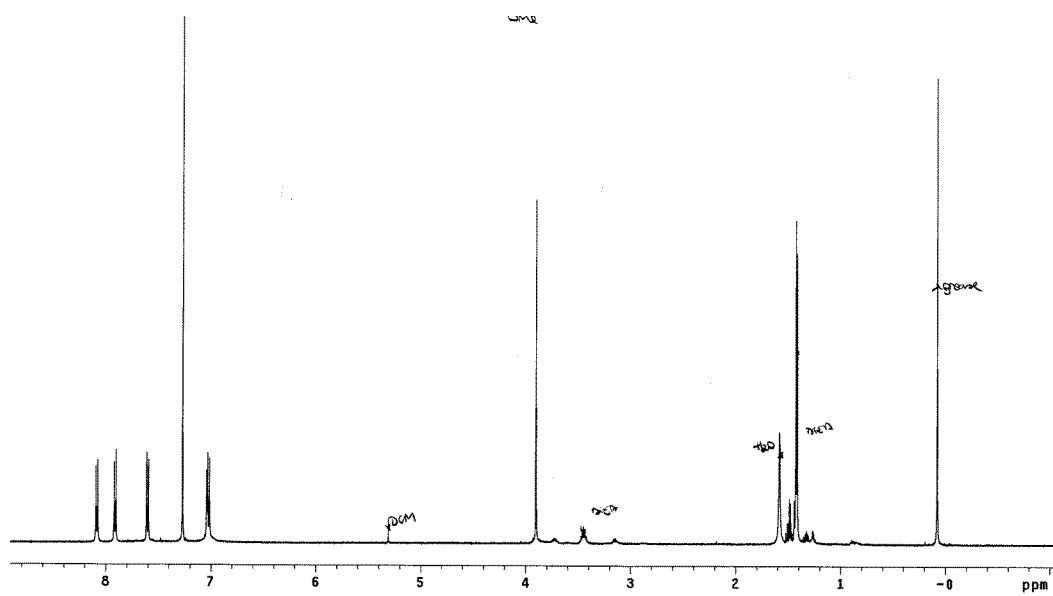
$^{11}\text{B}$  NMR for compound **288a** (MHz,  $\text{CDCl}_3$ ).



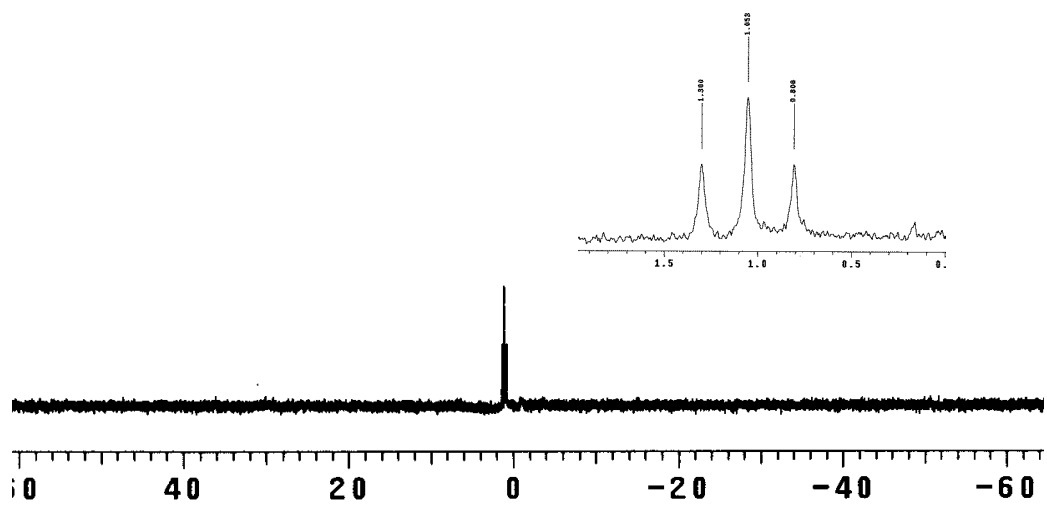
$^{19}\text{F}$  NMR for compound **288a** (MHz,  $\text{CDCl}_3$ ).

**AzaBODIPY 288b**

$\delta_{\text{H}}$  (500 MHz,  $\text{CDCl}_3$ ): 8.08 (d,  $J=8.8$  Hz, 4H), 7.91 (d,  $J=8.5$  Hz, 4H), 7.60 (d,  $J=8.5$  Hz, 4H), 7.04 (s, 2H), 7.02 (d,  $J=8.8$  Hz, 4H), 3.90 (s, 6H);  $\delta_{\text{C}}$  not taken due to poor solubility of compound;  $\delta_{\text{B}}$  (128 MHz,  $\text{CDCl}_3$ ): 1.05 (t, 1B,  $J_{\text{B-F}} = 32$  Hz);  $\delta_{\text{F}}$  (376 MHz,  $\text{CDCl}_3$ ): -132.36 (q, 2F,  $J_{\text{B-F}} = 32$  Hz); MS (ESI)  $m/z$  calcd for  $(\text{M}+\text{H})^+$   $\text{C}_{34}\text{H}_{25}\text{BBr}_2\text{F}_2\text{N}_3\text{O}_2$ : 714.03; found : 714.2-716.2 (Br isotope);  $\lambda_{\text{max abs}}$  (PhMe)/nm 702 ( $\epsilon/\text{dm}^3\text{mol}^{-1}\text{cm}^{-1}$  84 118);  $\lambda_{\text{max emis}}$  (PhMe)/nm 731;  $\Phi = 0.42$  in 1% pyridine in toluene.

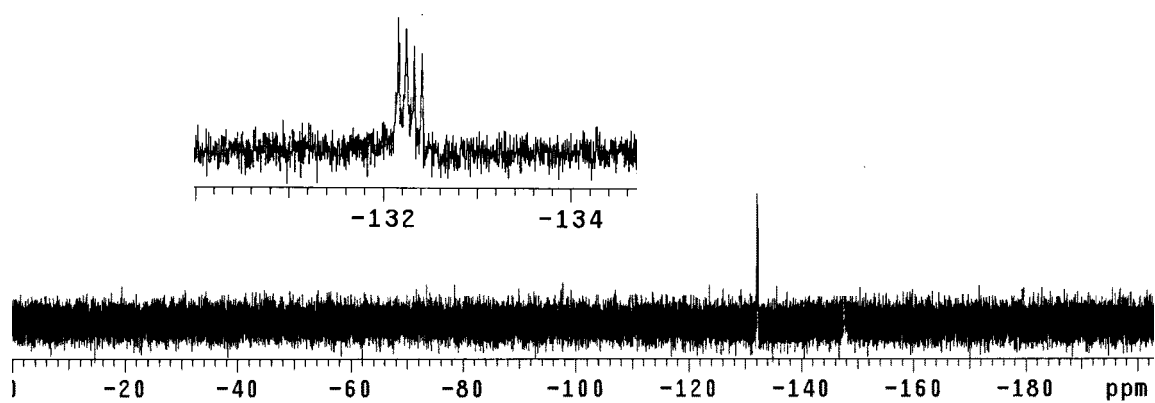


$^1\text{H}$  NMR for compound **288b** (500 MHz,  $\text{CDCl}_3$ ).



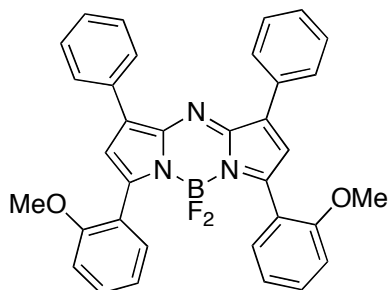
$^{11}\text{B}$  NMR for compound **288b** (500 MHz,  $\text{CDCl}_3$ ).



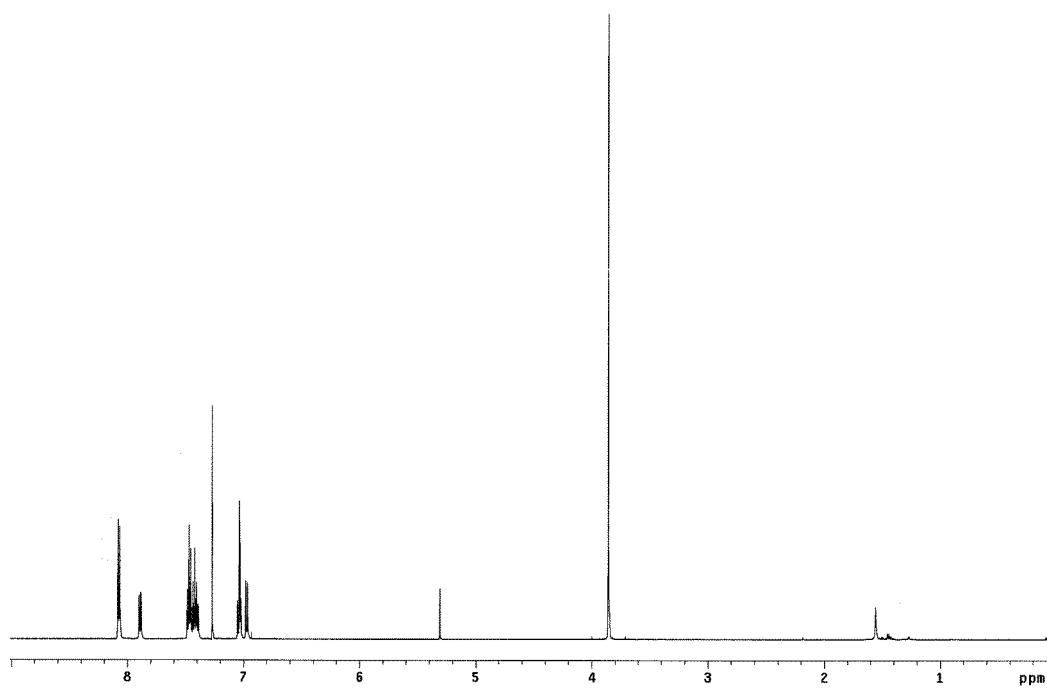


$^{19}\text{F}$  NMR for compound **288b** (500 MHz,  $\text{CDCl}_3$ ).

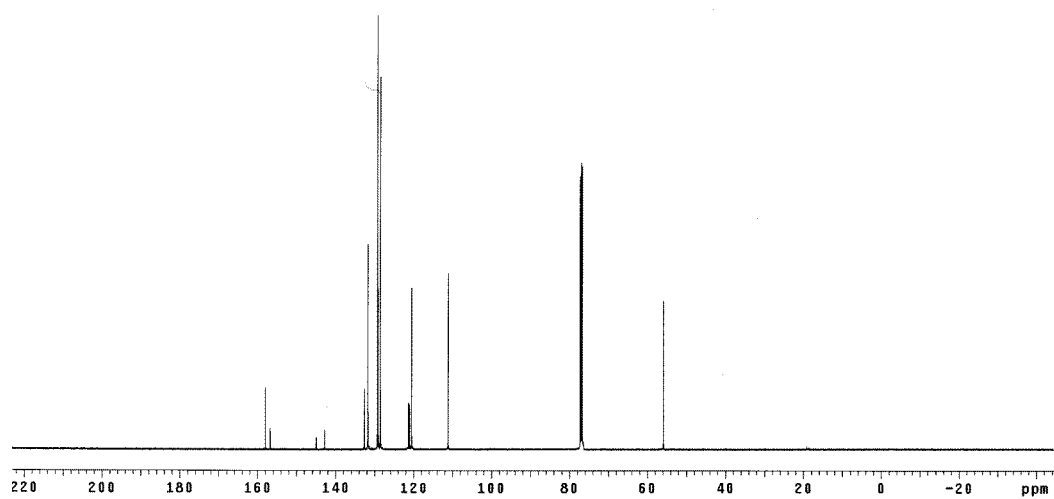
## AzaBODIPY 288c



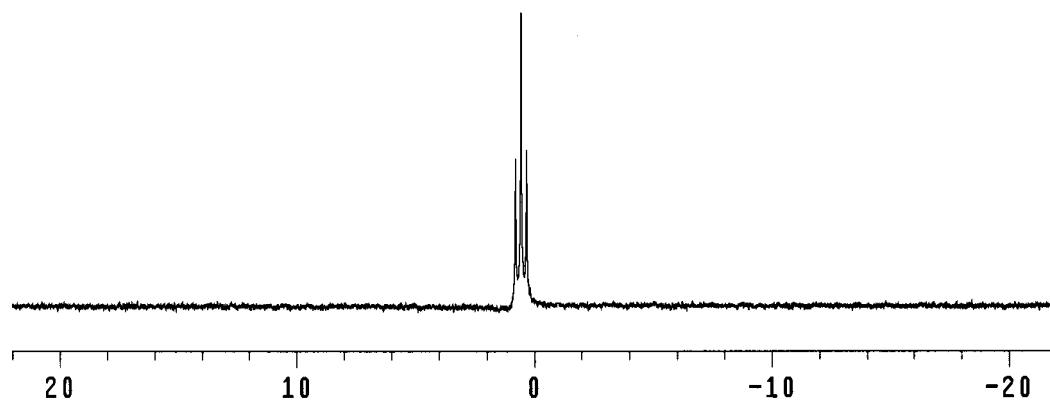
$\delta_{\text{H}}$  (500 MHz,  $\text{CDCl}_3$ ): 8.07-8.08 (m, 4H), 7.89 (dd,  $J = 7.8$  Hz,  $J = 1.7$  Hz, 2H), 7.48-7.38 (m, 8H), 7.04 (dd,  $J = 15.1$  Hz,  $J = 0.9$  Hz, 2H), 7.03 (s, 2H), 6.97 (d,  $J = 8.3$  Hz, 2H), 3.80 (s, 6H);  $\delta_{\text{C}}$  (125 MHz,  $\text{CDCl}_3$ ): 158.0, 156.7, 144.9, 142.8, 132.6, 131.7, 129.3, 129.2, 129.1, 128.5, 121.3, 121.1, 120.5, 111.1, 55.9;  $\delta_{\text{B}}$  (128 MHz,  $\text{CDCl}_3$ ): 0.558 (t, 1B,  $J_{\text{B-F}} = 30$  Hz);  $\delta_{\text{F}}$  (376 MHz,  $\text{CDCl}_3$ ): - 133.37 (q, 2F,  $J_{\text{B-F}} = 30$  Hz); HRMS (ESI)  $m/z$  calcd  $(\text{M}+\text{H})^+$   $\text{C}_{34}\text{H}_{27}\text{BF}_2\text{N}_3\text{O}_2$ : 558.2164; found : 558.2166;  $\lambda_{\text{max abs}}$  (PhMe)/nm 640 ( $\epsilon = 73\,858\text{ dm}^3\text{mol}^{-1}\text{cm}^{-1}$ );  $\lambda_{\text{max emis}}$  (PhMe)/nm 688;  $\Phi = 0.07$  in 1% pyridine in toluene.



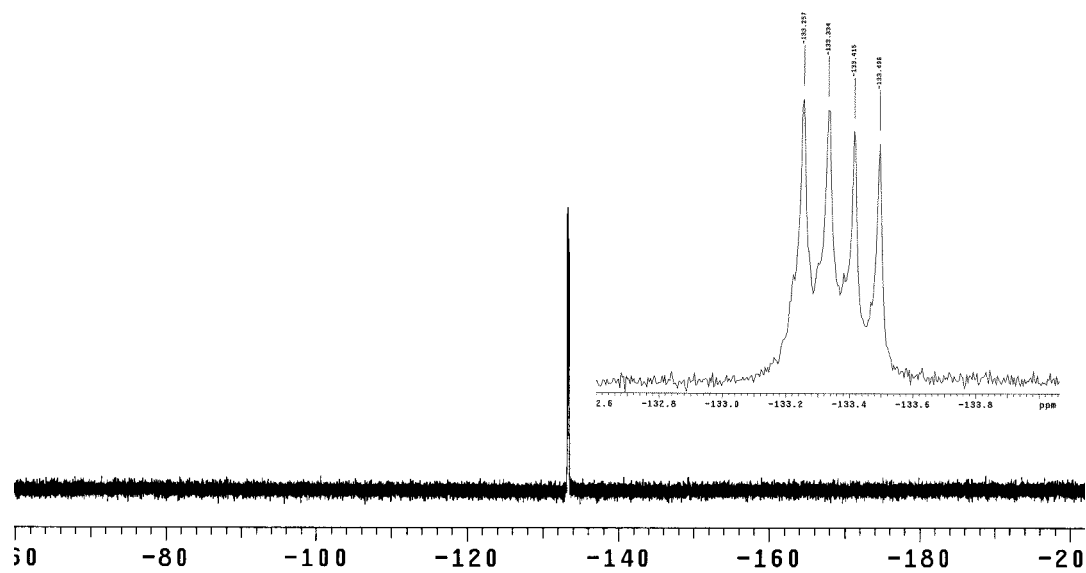
$^1\text{H}$  NMR for compound **288c** (500 MHz,  $\text{CDCl}_3$ ).



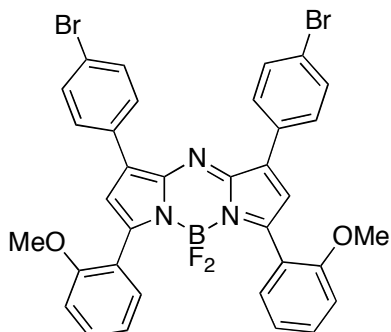
$^{13}\text{C}$  NMR for compound **288c** (125 MHz,  $\text{CDCl}_3$ ).



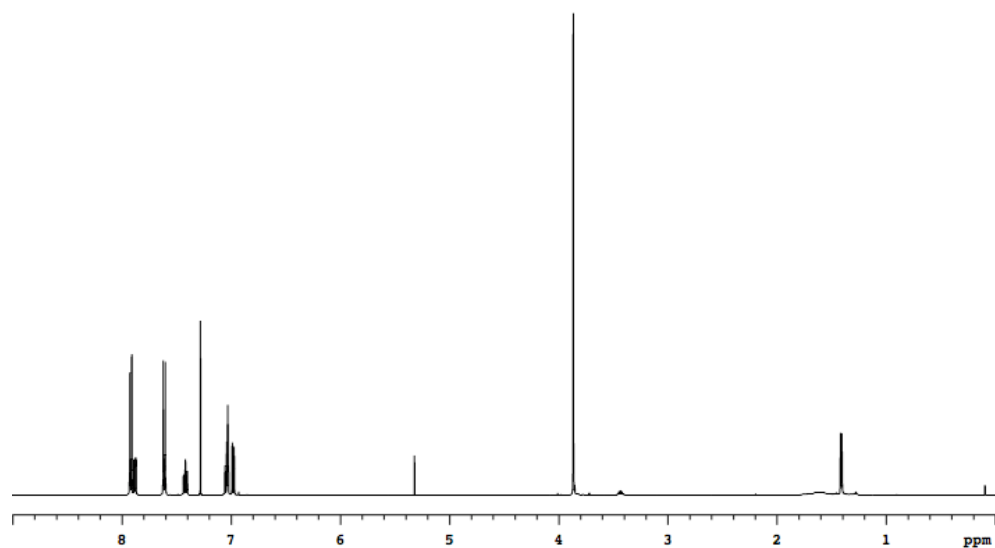
$^{11}\text{B}$  NMR for compound **288c** (MHz,  $\text{CDCl}_3$ ).



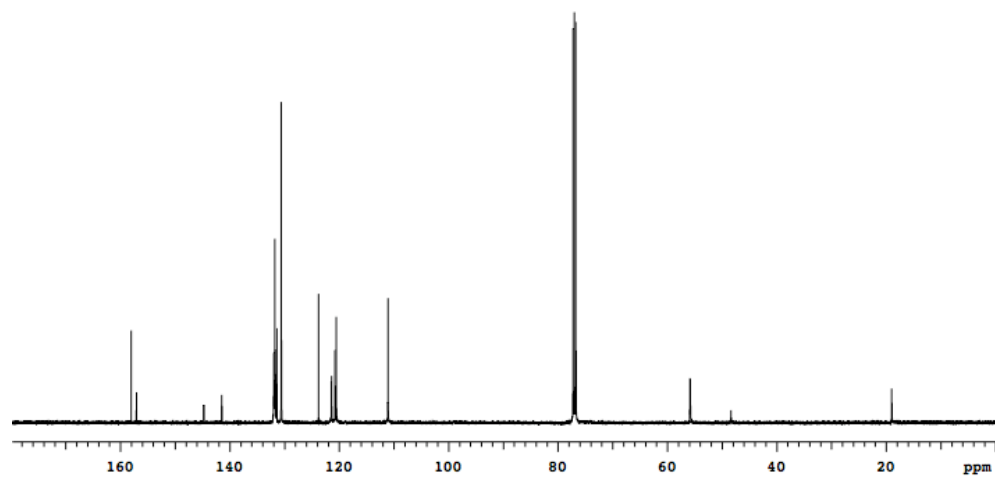
$^{19}\text{F}$  NMR for compound **288c** (MHz,  $\text{CDCl}_3$ ).

**AzaBODIPY 288d**

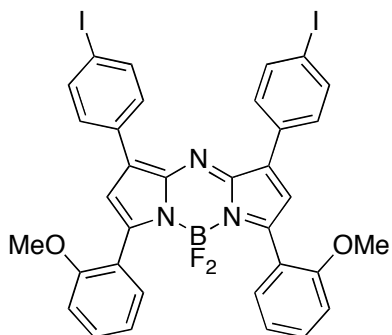
$\delta_{\text{H}}$  (500 MHz,  $\text{CDCl}_3$ ): 7.90 (d,  $J = 8.8$  Hz, 4H), 7.87 (dd,  $J = 7.6$  Hz,  $J = 1.7$  Hz, 2H), 7.60 (d,  $J = 8.8$  Hz, 4H), 7.41 (dt,  $J = 7.6$  Hz,  $J = 1.7$  Hz, 2H), 7.05-7.01 (m, 4H), 6.97 (d,  $J = 7.8$  Hz, 2H), 3.86 (s, 6H);  $\delta_{\text{C}}$  (125 MHz,  $\text{CDCl}_3$ ): 158.0, 157.0, 144.7, 141.4, 131.9, 131.8, 131.7, 131.4, 130.6, 123.7, 121.4, 120.7, 120.5, 111.0, 55.8;  $\delta_{\text{B}}$  (128 MHz,  $\text{CDCl}_3$ ): 0.51 (t, 1B,  $J_{\text{B-F}} = 30$  Hz);  $\delta_{\text{F}}$  (376 MHz,  $\text{CDCl}_3$ ): -137.46 (q, 2F,  $J_{\text{B-F}} = 30$  Hz); MS (MALDI)  $m/z$  calcd for  $(\text{M}+\text{H})^+$   $\text{C}_{34}\text{H}_{25}\text{BBr}_2\text{F}_2\text{N}_3\text{O}_2$ : 714.03; found : 714.04;  $\lambda_{\text{max abs}}$  (PhMe)/nm 650 ( $\epsilon = 55\,014 \text{ dm}^3\text{mol}^{-1}\text{cm}^{-1}$ );  $\lambda_{\text{max emis}}$  (PhMe)/nm 694;  $\Phi = 0.10$  in 1% pyridine in toluene.



$^1\text{H}$  NMR for compound **288d** (500 MHz,  $\text{CDCl}_3$ ).

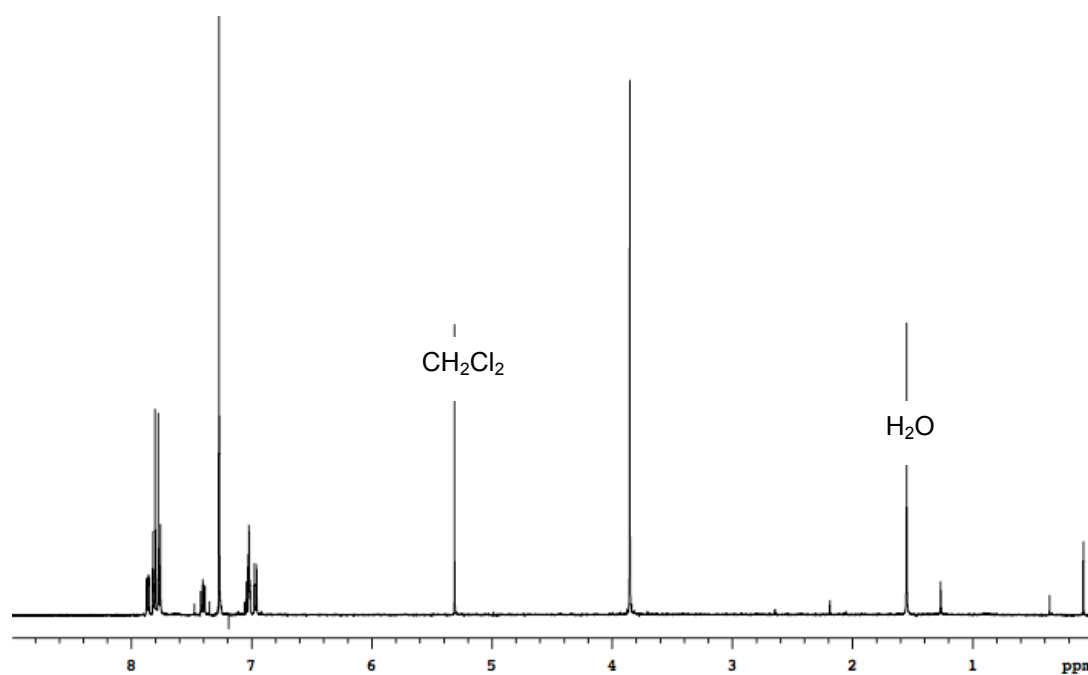


$^{13}\text{C}$  NMR for compound **288d** (125 MHz,  $\text{CDCl}_3$ ).

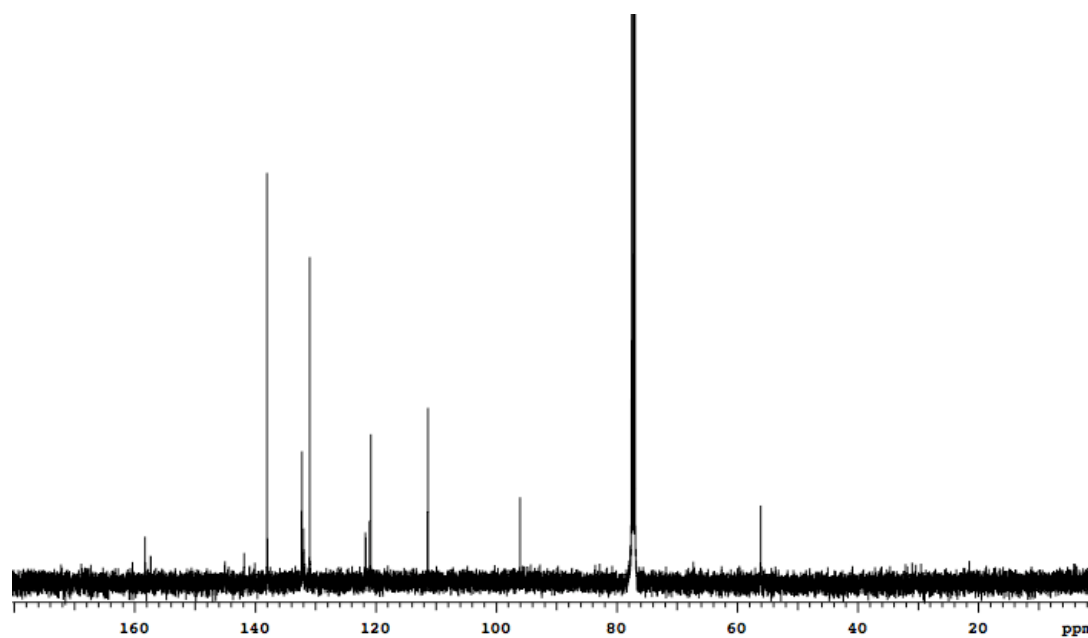
**AzaBODIPY 288e.**

$\delta_{\text{H}}$  (500 MHz,  $\text{CDCl}_3$ ): 7.86 (dd,  $J = 7.8$  Hz,  $J = 1.7$  Hz, 2H), 7.79 (apparent quart,  $J = 8.3$  Hz, 8H), 7.40 (td,  $J = 9$  Hz,  $J = 1.7$  Hz, 2H), 7.03 (td,  $J = 7.8$  Hz,  $J = 1$  Hz, 2H), 7.02 (s, 2H), 6.97 (d,  $J = 8.3$  Hz, 2H), 3.85 (s, 6H);  $\delta_{\text{C}}$  (125MHz,  $\text{CDCl}_3$ ): 158.3, 157.3, 141.9, 138.0, 132.3, 132.2, 131.9, 130.9, 121.7, 121.6, 121.0, 120.8, 111.3, 96.1, 56.2;  $\delta_{\text{F}}$  (376MHz,  $\text{CDCl}_3$ ): 45.45 (q, 2F,  $J = 31.5$  Hz). HRMS (ESI)  $m/z$  calcd for  $(\text{M}+\text{Li})^+$   $\text{C}_{34}\text{H}_{24}\text{B}_2\text{F}_2\text{N}_3\text{O}_2$  816.0179; found 816.0019;  $\lambda_{\text{max abs}}$  (PhMe)/nm 653 ( $\epsilon/\text{dm}^3\text{mol}^{-1}\text{cm}^{-1}$  71 600);  $\lambda_{\text{max emis}}$  (PhMe)/nm 701;  $\Phi = 0.10$  in 1% pyridine in toluene.



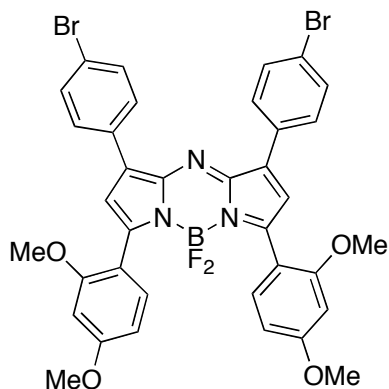


$^1\text{H}$  NMR for compound **288e** (500 MHz,  $\text{CDCl}_3$ ).

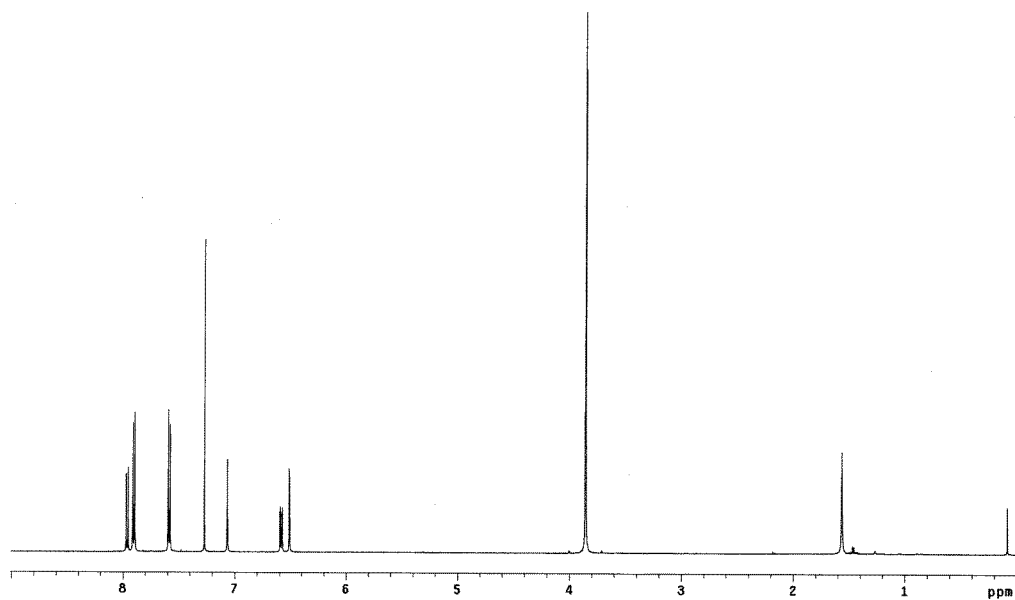


$^{13}\text{C}$  NMR for compound **288e** (125 MHz,  $\text{CDCl}_3$ ).

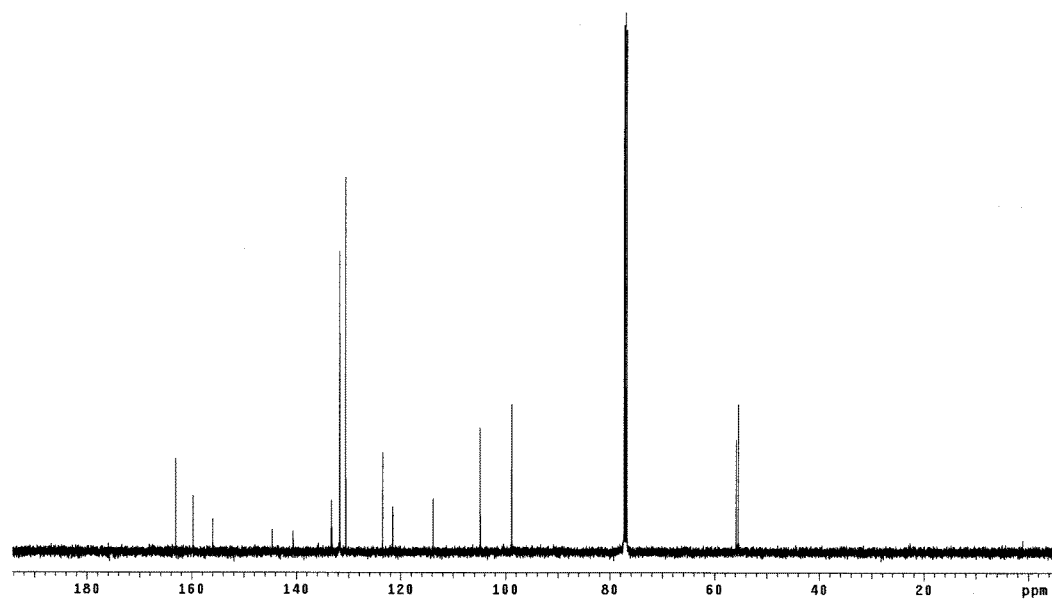
### AzaBODIPY 288f



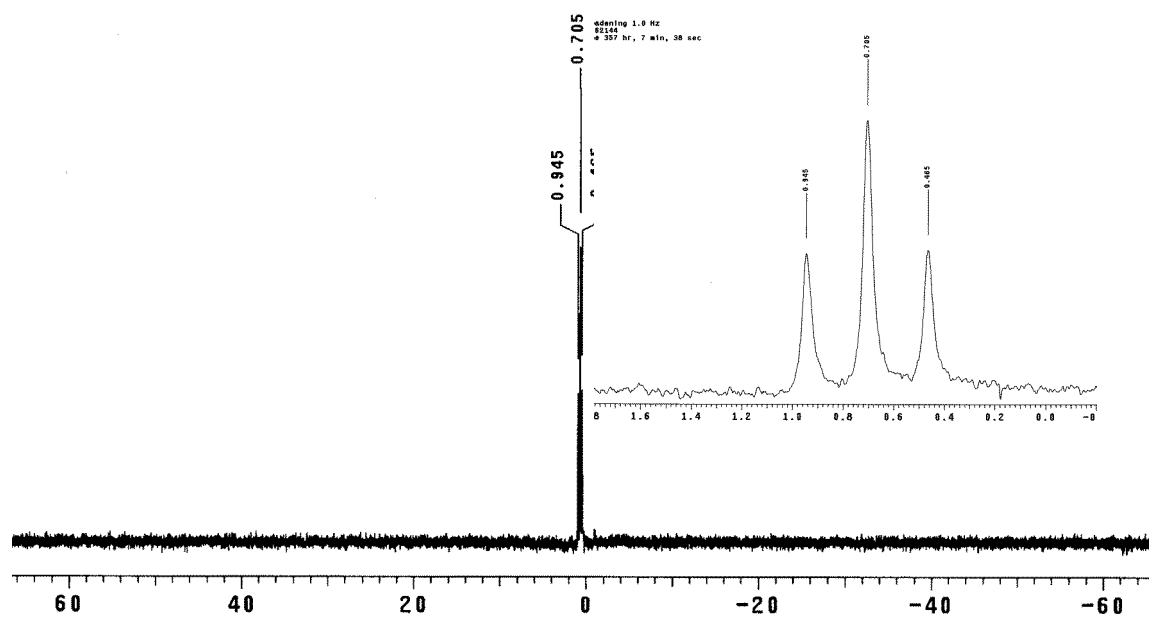
$\delta_{\text{H}}$  (500 MHz,  $\text{CDCl}_3$ ): 7.96 (d,  $J=8.8$  Hz, 2H), 7.90 (dd,  $J=1.8$  Hz,  $J=6.7$  Hz, 4H), 7.58 (dd,  $J=1.8$  Hz,  $J=6.7$  Hz, 4H), 7.06 (s, 2H), 6.58 (dd,  $J=8.8$  Hz,  $J=2.4$  Hz, 2H), 6.51 (d,  $J=2.4$  Hz, 2H), 3.86 (s, 6H), 3.85 (s, 6H);  $\delta_{\text{C}}$  (125 MHz,  $\text{CDCl}_3$ ): 163.1, 159.8, 155.9, 144.6, 140.6, 133.2, 131.7, 131.6, 130.5, 123.4, 121.5, 113.8, 104.8, 98.8, 55.8, 55.5;  $\delta_{\text{B}}$  (128 MHz,  $\text{CDCl}_3$ ): 0.71 (t, 1B,  $J_{\text{B-F}} = 30$  Hz);  $\delta_{\text{F}}$  (376 MHz,  $\text{CDCl}_3$ ): -170.14 (q, 2F,  $J_{\text{B-F}} = 30$  Hz); HRMS (ESI)  $m/z$  calcd for  $(\text{M}+\text{H})^+$   $\text{C}_{36}\text{H}_{29}\text{BBr}_2\text{F}_2\text{N}_3\text{O}_4$  774.0586; found : 774.0573-776.0550 (Br isotope);  $\lambda_{\text{max abs}}$  (PhMe)/nm 692 ( $\epsilon/\text{dm}^3\text{mol}^{-1}\text{cm}^{-1}$  66 200);  $\lambda_{\text{max emis}}$  (PhMe)/nm 738;  $\Phi = 0.20$  in 1% pyridine in toluene.



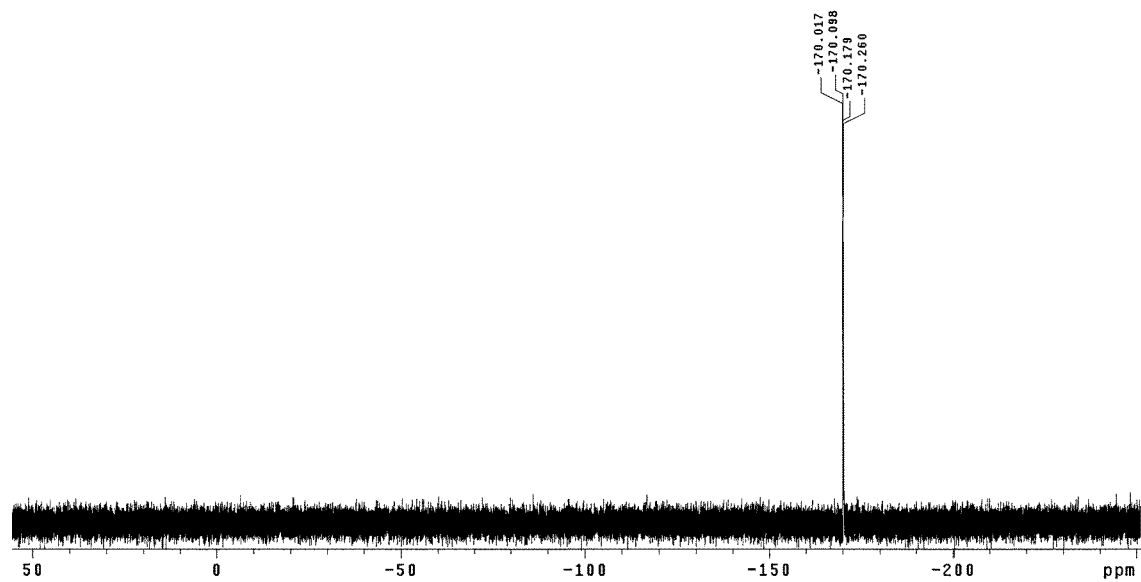
$^1\text{H}$  NMR for compound **288f** (500 MHz,  $\text{CDCl}_3$ ).



$^{13}\text{C}$  NMR for compound **288f** (500 MHz,  $\text{CDCl}_3$ ).

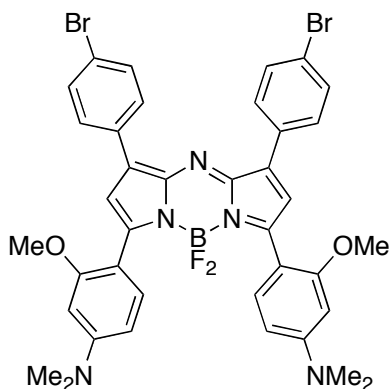


<sup>11</sup>B NMR for compound **288f** (MHz, CDCl<sub>3</sub>).



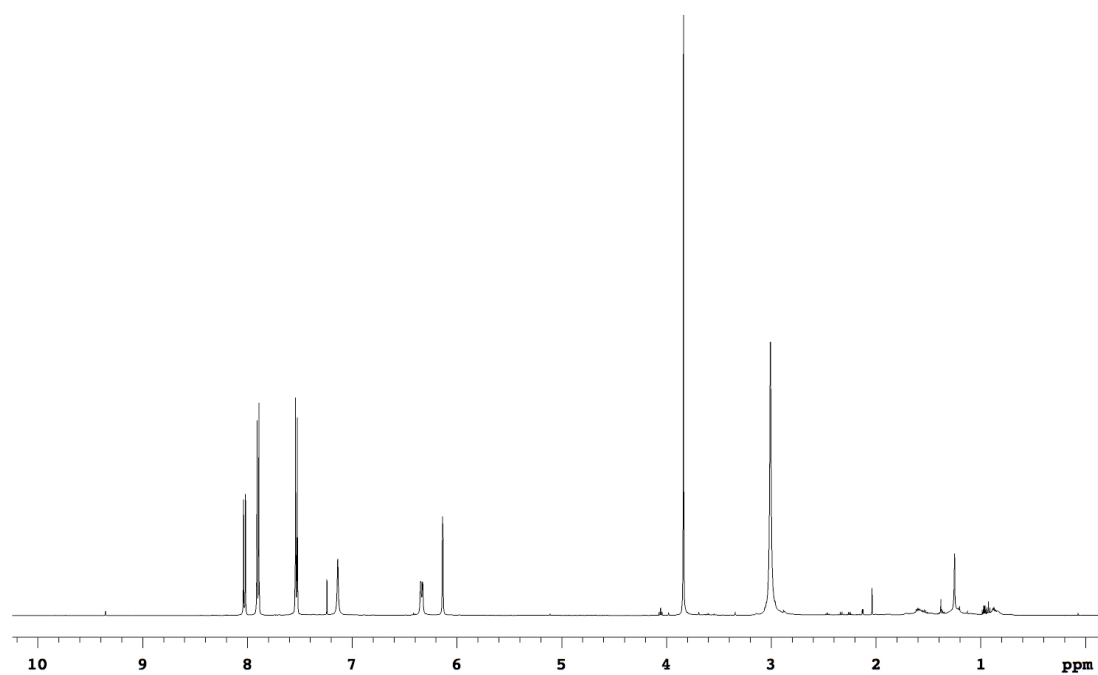
$^{19}\text{F}$  NMR for compound **288f** (MHz,  $\text{CDCl}_3$ ).

**AzaBODIPY 288g (from butyrophenone 291g).**

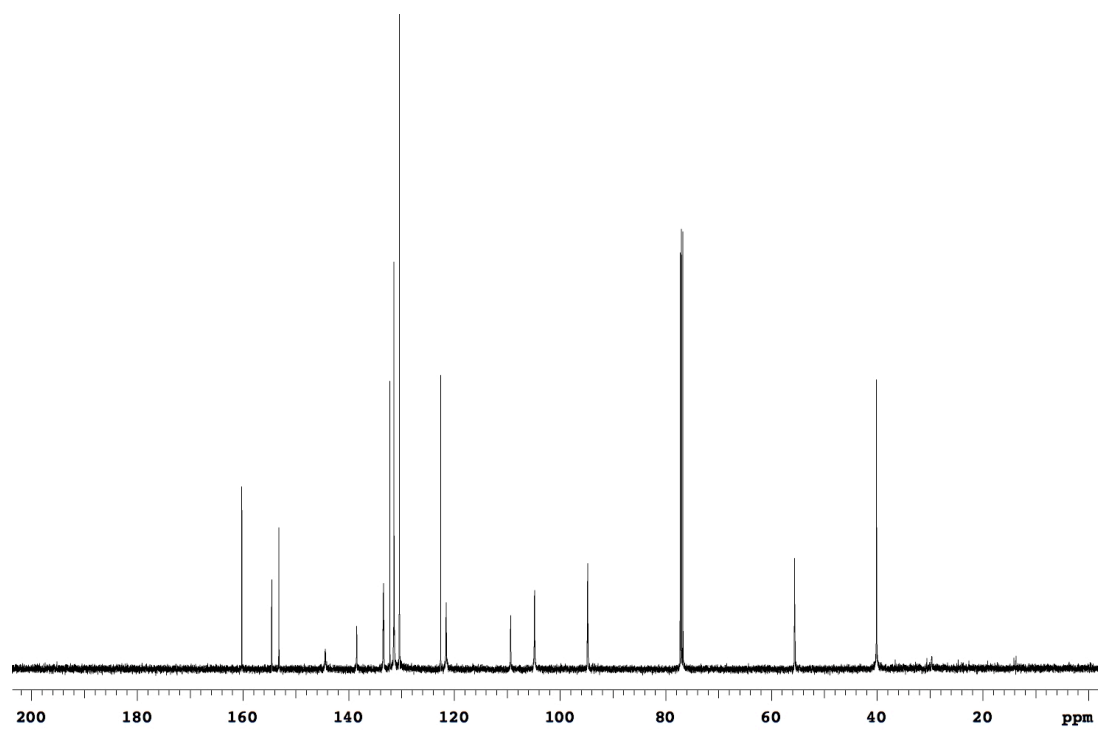


NH<sub>4</sub>OAc (17.4g, 0.23mol) was added to the solution of **5g** (2.73g, 6.5mmol) in 50mL n-BuOH. The reaction mixture was heated at reflux for 24h. After cooling to room temperature, the solution was concentrated to half its original volume. The solid was filtered and washed with cold EtOH to afford **6g** (1.0 g, 41%) as a green solid which was used in the next step without further purification. DIEA (1.8 ml, 10.3 mmol) was added to the solution of **6g** (970mg, 1.3 mmol) in 30mL dry DCM. The solution was stirred at room temperature for 15min and BF<sub>3</sub>•OEt<sub>2</sub> (1.6 ml, 12.9mmol) was added. After stirring at room temperature for 24h, the mixture was washed with water (1 x 30 mL) and brine (1 x 30 mL). The organic layer was dried over Na<sub>2</sub>SO<sub>4</sub> and concentrated under reduced pressure. The crude product was purified by flash chromatography on silica gel eluting with 2 : 3 EtOAc-hexane to afford **1g** (867mg, 84%) as a purple solid. δ<sub>H</sub> (500MHz, CDCl<sub>3</sub>): 8.03 (d, *J* = 9.2 Hz, 2H), 7.90 (d, *J* = 8.5 Hz, 4H), 7.53 (d, *J* = 8.5 Hz, 4H), 7.14 (s, 2H), 6.34 (d, *J* = 9.1 Hz, 2H), 6.13 (d, *J* = 2.3 Hz, 2H), 3.84 (s, 6H), 3.01 (s, 12H); δ<sub>C</sub> (125MHz, CDCl<sub>3</sub>): 160.2, 154.5, 153.2, 144.4, 138.5, 133.4, 132.2, 131.4, 130.4, 122.6, 121.5, 109.3, 104.8, 94.8, 55.6, 40.1; δ<sub>F</sub> (376MHz, CDCl<sub>3</sub>): 45.45 (q, 2F, *J* = 31.5 Hz). HRMS (ESI) *m/z* calcd for (M+H)<sup>+</sup> C<sub>38</sub>H<sub>35</sub>BBr<sub>2</sub>F<sub>2</sub>N<sub>5</sub>O<sub>2</sub> 800.1219; found 800.1275; λ<sub>max abs</sub> (PhMe)/ nm 798 (ε/dm<sup>3</sup>mol<sup>-1</sup>cm<sup>-1</sup> 68 610); λ<sub>max emis</sub> (PhMe)/ nm 830; Φ = 0.07 in 1% pyridine in toluene.



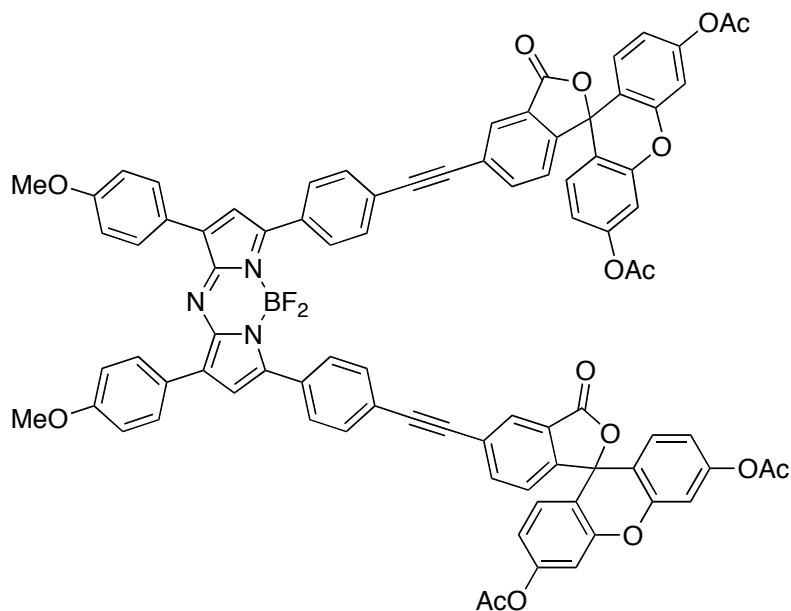


$^1\text{H}$  NMR for compound **288g** (500 MHz,  $\text{CDCl}_3$ ).



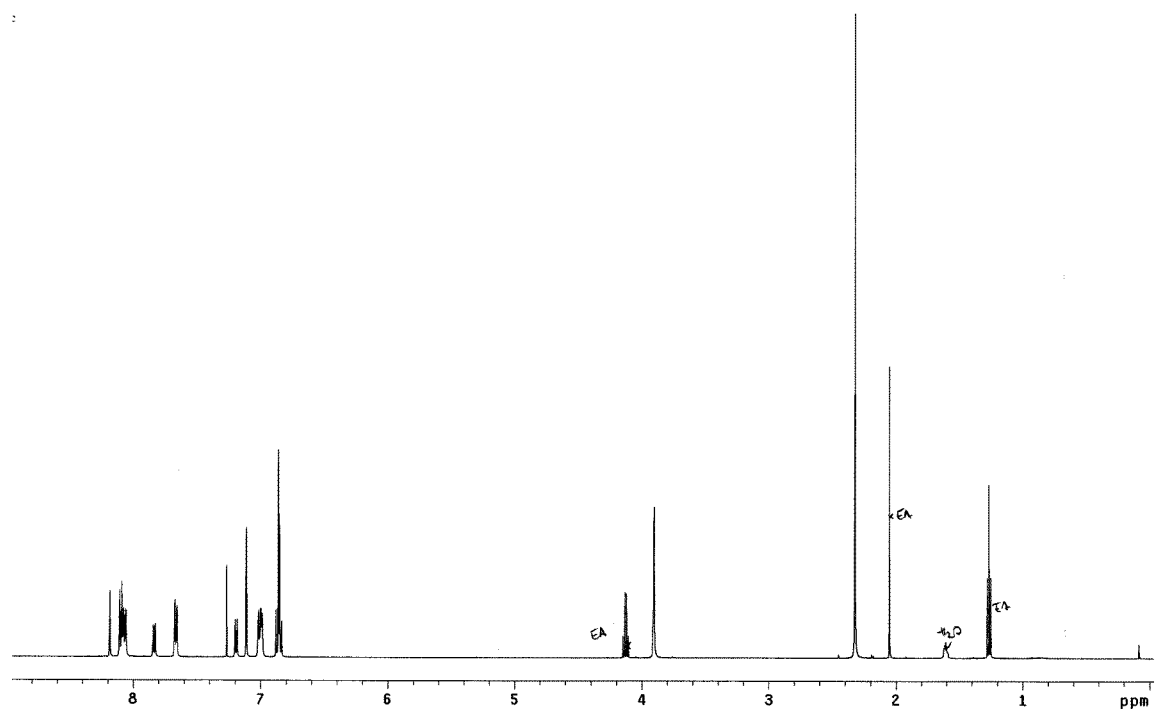
$^{13}\text{C}$  NMR for compound **288g** (125 MHz,  $\text{CDCl}_3$ ).

### Compound 298.

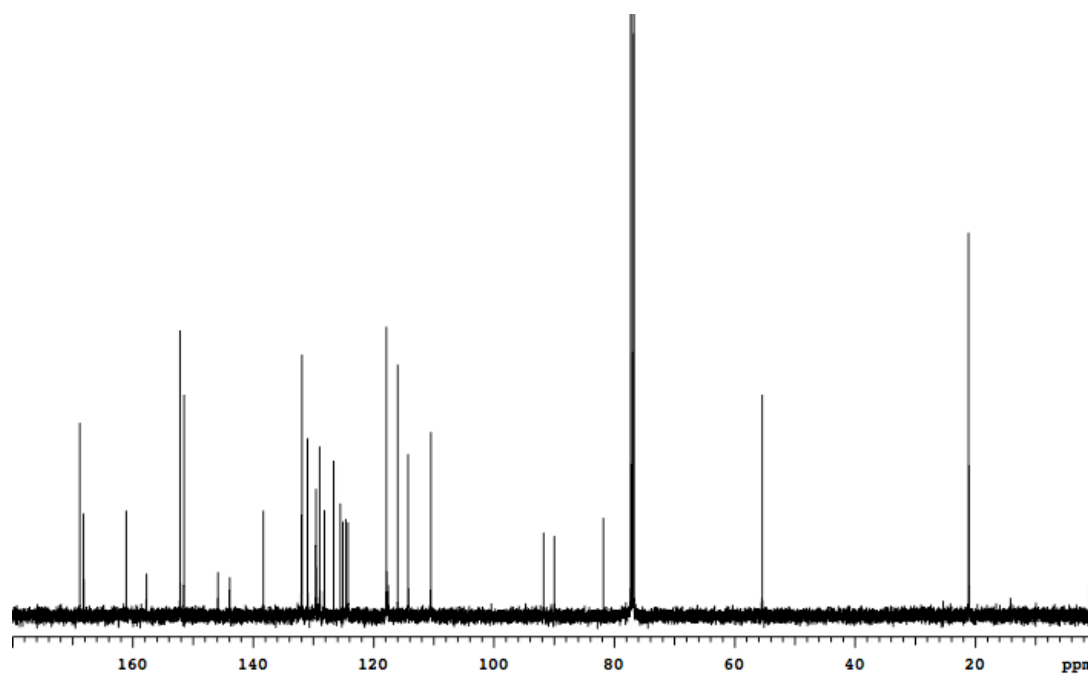


A flame dried Schlenk tube was charged with ethynyl fluorescein diacetate **296**<sup>12,13</sup> (0.24 g, 0.54 mmol), aza-BODIPY **288a** (0.2 g, 0.25 mmol), Pd (PPh<sub>3</sub>)<sub>4</sub> (17 mg, 0.025 mmol), CuI (2.4 mg, 0.012 mmol), THF (15 mL) and triethylamine (0.4 mL, 2.5 mmol). The reaction mixture was deoxygenated 3 times using the freeze-pump-thaw technique. It was then stirred at room temperature for 28h. The solvent was then removed *in vacuo*, and the residue purified by flash chromatography (dry loading). The column was first eluted with 50% Hexanes:CH<sub>2</sub>Cl<sub>2</sub> to 100% CH<sub>2</sub>Cl<sub>2</sub>, then 2% ethyl acetate:CH<sub>2</sub>Cl<sub>2</sub> to get the mono-coupling product and finally with 5% ethyl acetate:CH<sub>2</sub>Cl<sub>2</sub> to get the bis-coupling product. The bis-coupling product coeluted with the ethynyl fluorescein bis acetate homo-coupling product and is obtained in a pure form after a second flash chromatography eluted with 50% ethyl acetate:hexanes (107 mg, 30%).  $\delta_{\text{H}}$  (500 MHz, CDCl<sub>3</sub>): 8.18 (s, 2H), 8.10 (d,  $J$ = 8.1 Hz, 4H), 8.06 (d,  $J$ = 8.3 Hz, 4H), 7.83 (d,  $J$ = 8.1 Hz, 2H), 7.66 (d,  $J$ = 8.3 Hz, 4H), 7.19 (d,  $J$ = 8.1 Hz, 2H), 7.11 (d,  $J$ = 2.2 Hz, 4H), 7.02 - 6.99 (m, 6H), 6.88 - 6.83 (m, 8H), 3.91 (s, 6H), 2.32 (s, 12H);  $\delta_{\text{C}}$  (125 MHz, CDCl<sub>3</sub>): 168.8, 168.2, 161.1, 157.7, 152.2, 152.1, 151.5, 145.9, 143.9, 138.3, 131.9 (2C), 130.9, 129.6, 128.9, 128.2, 126.6, 125.5, 125.1, 124.6, 124.2, 117.8, 117.6, 115.9, 114.2, 110.5, 91.7, 89.9, 81.8, 55.4, 21.1;  $\delta_{\text{B}}$

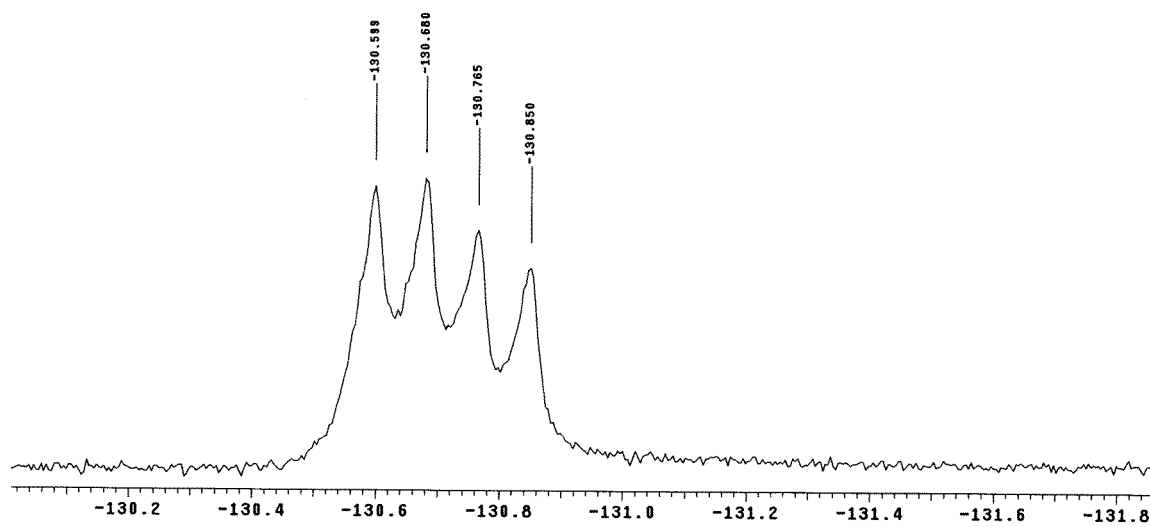
(128 MHz, CDCl<sub>3</sub>): 0.97 (t, 1B, J<sub>B-F</sub> = 31 Hz); δ<sub>F</sub> (376 MHz, CDCl<sub>3</sub>): -130.72 (q, 2F, J<sub>B-F</sub> = 31 Hz); m/z (ESI) calculated mass for C<sub>86</sub>H<sub>54</sub>BF<sub>2</sub>N<sub>3</sub>O<sub>16</sub> (M+H)<sup>+</sup>: 1434.3643; found: 1434.3638.



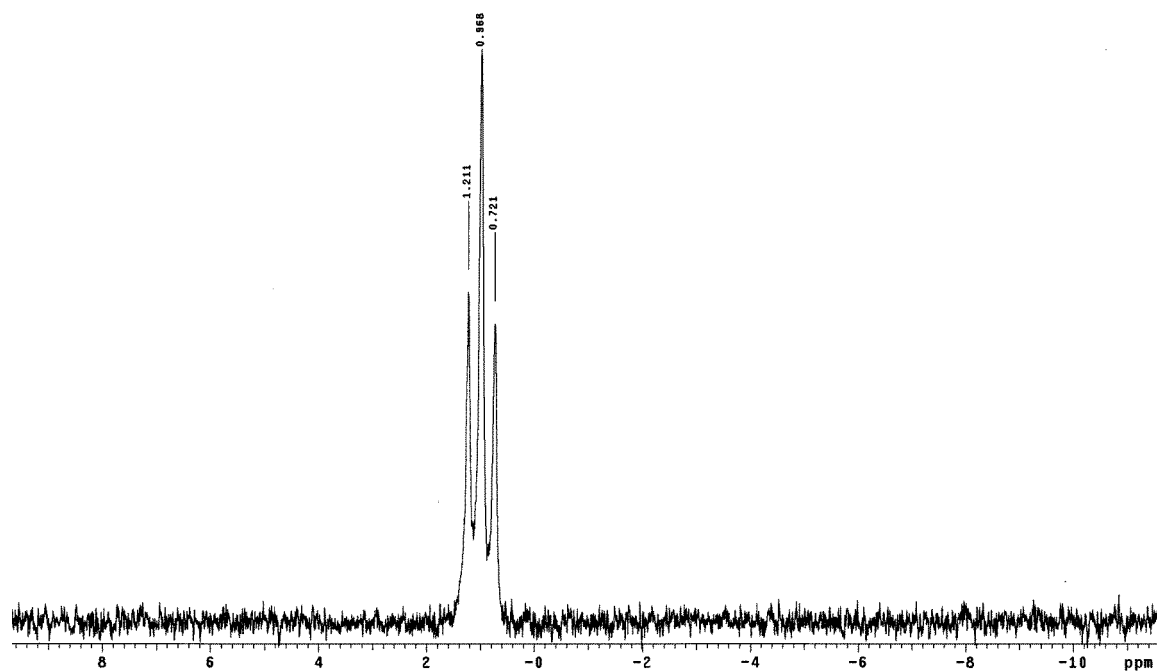
$^1\text{H}$  NMR for compound **298** (500 MHz,  $\text{CDCl}_3$ ).



$^{13}\text{C}$  NMR for compound **298** (125 MHz,  $\text{CDCl}_3$ ).



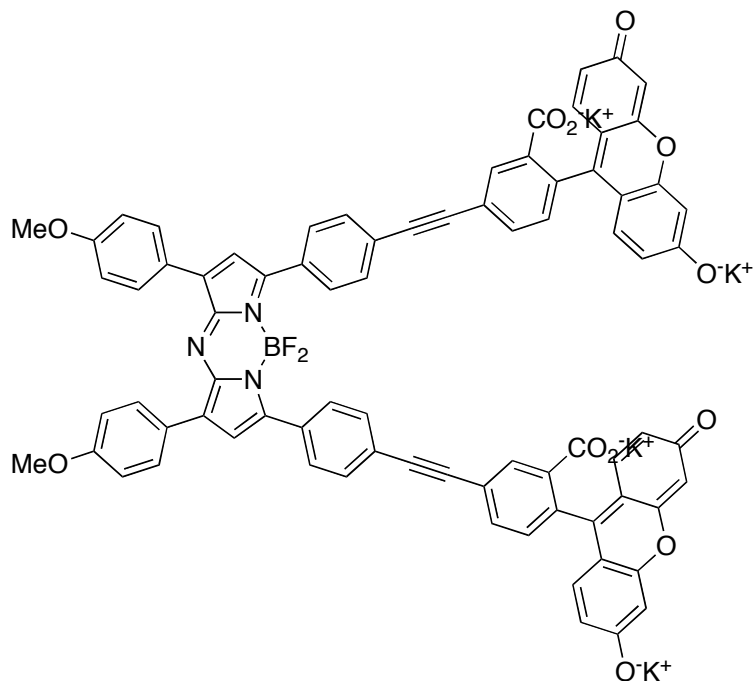
$^{19}\text{F}$  NMR for compound **298** (376 MHz,  $\text{CDCl}_3$ ).



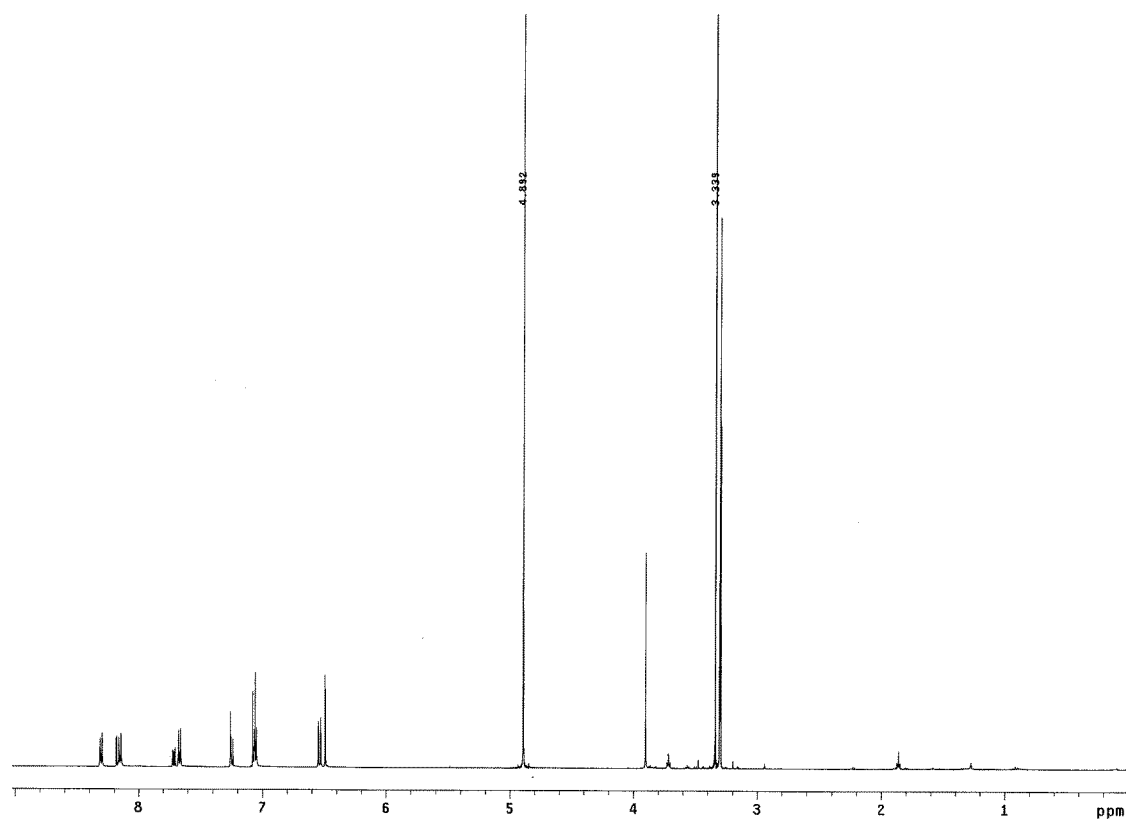
$^{11}\text{B}$  NMR for compound **298** (128 MHz,  $\text{CDCl}_3$ ).



### Compound 289.



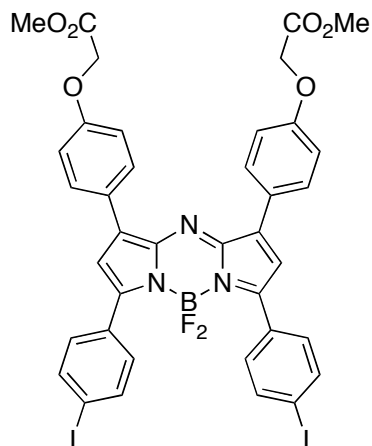
A solution of **298** in a mixture of methanol and THF (1:1) was treated with baked potassium carbonate. The reaction mixture was stirred at room temperature for 2 h. When the reaction was complete according to TLC, the solvent was removed *in vacuo* to afford the pure product.  $\delta_{\text{H}}$  (500 MHz,  $\text{CD}_3\text{OD}$ ): 8.30 (d,  $J=8.5$  Hz, 4H), 8.18 (d,  $J=1.7$  Hz, 2H), 8.15 (d,  $J=8.8$  Hz, 4H), 7.72 (dd,  $J=1.7$  Hz,  $J=7.8$  Hz, 2H), 7.66 (d,  $J=8.5$  Hz, 4H), 7.26 (s, 2H), 7.24 (d,  $J=7.8$  Hz, 2H), 7.06 (d,  $J=9.3$  Hz, 4H), 7.05 (d,  $J=8.8$  Hz, 4H), 6.54 (dd,  $J=2.2$  Hz,  $J=9.3$  Hz, 4H), 6.49 (d,  $J=2.2$  Hz, 4H), 3.90 (s, 6H);  $\delta_{\text{C}}$  (125 MHz,  $\text{CD}_3\text{OD}$ ): 182.6, 173.2, 162.6, 160.3, 159.9, 148.3, 144.6, 142.3, 134.9, 133.7, 133.6, 132.8, 132.5, 132.2, 132.1, 131.4, 131.3, 126.6, 126.2, 125.1, 124.1, 119.4, 115.3, 114.8, 113.1, 104.4, 92.1, 91.4, 55.9;  $\delta_{\text{B}}$  (128 MHz,  $\text{CD}_3\text{OD}$ ): 5.34;  $\delta_{\text{F}}$  (376 MHz,  $\text{CD}_3\text{OD}$ ): -187.46;  $m/z$  (MALDI) calculated for  $\text{C}_{78}\text{H}_{46}\text{BF}_2\text{N}_3\text{O}_{12}$ : 1267.3984;  $\lambda_{\text{max abs}}$  (50% EtOH:H<sub>2</sub>O)/nm 500 (fluorescein) and 698 (AzaBODIPY);  $\lambda_{\text{max emis}}$  (50% EtOH:H<sub>2</sub>O)/nm 530 and 733 when excited at 498 nm;  $\lambda_{\text{max emis}}$  (50% EtOH:H<sub>2</sub>O)/nm 733 when excited at 690 nm.



$^1\text{H}$  NMR for compound **289** (500 MHz,  $\text{CD}_3\text{OD}$ ).

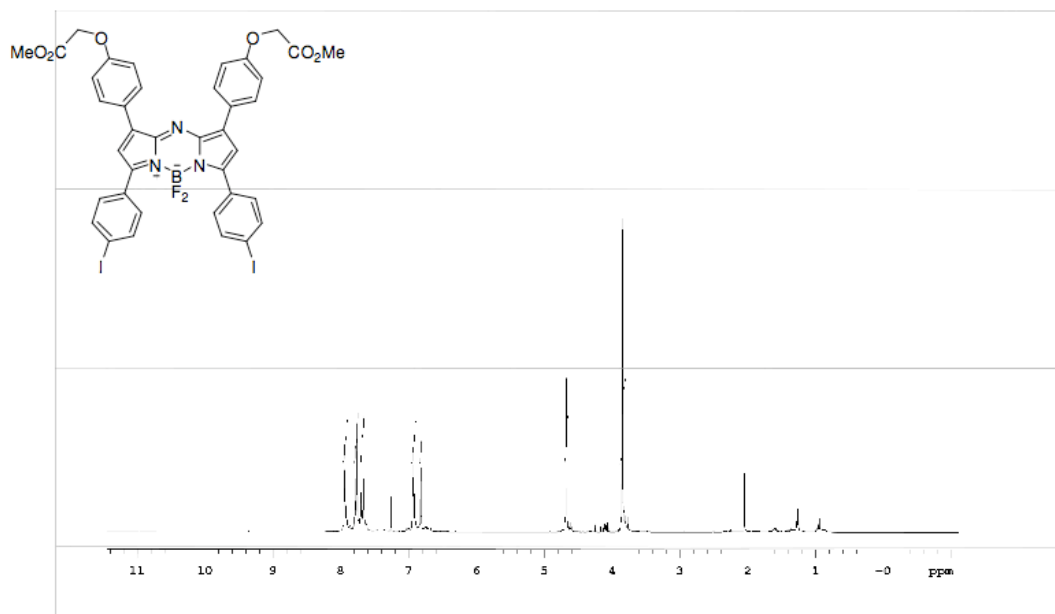


### Compound 297.

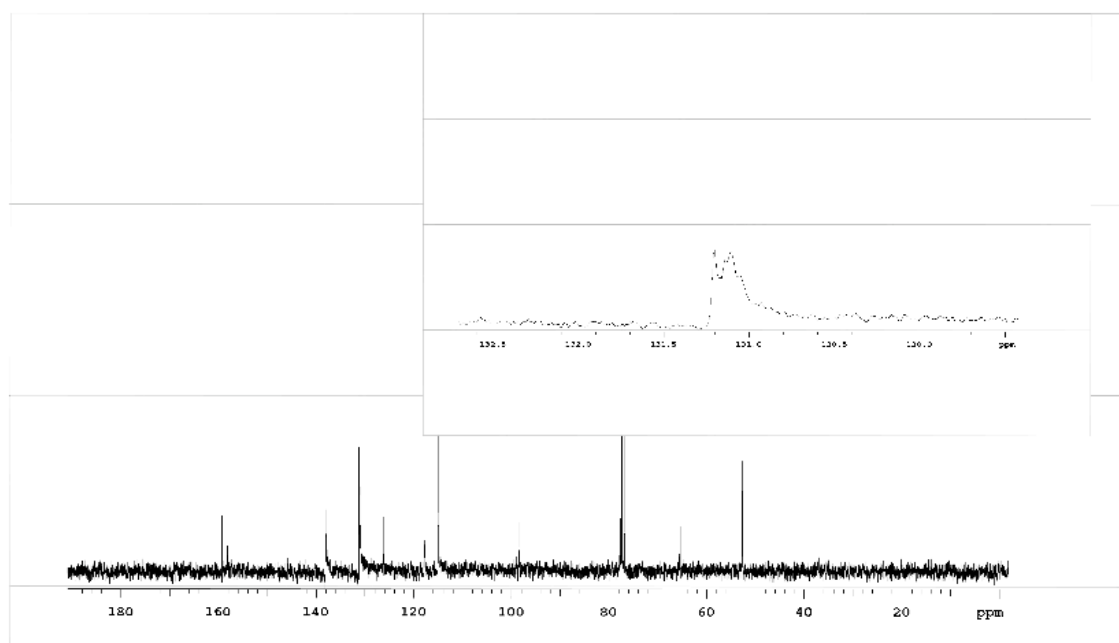


$\text{BBr}_3$  (1.0 mol solution in hexane) (4.9 mmol, 1.9 mL) was added to a solution of iodoaza-BODIPY **288a** (0.49 mmol, 0.4 g) in dry  $\text{CH}_2\text{Cl}_2$  (200 mL) at 0 °C and stirred at 25 °C for 2h. After dichloromethane was removed, EtOAc and  $\text{H}_2\text{O}$  (1:1, 300 mL) were added. The organic layer was separated, dried over anhydrous  $\text{MgSO}_4$ , filtered and finally THF (10 X 50 mL) was used to dissolve sticky material during filtration. The filtrate was concentrated and dried under vacuum. The crude product was used in next step without further purification.

$\text{NaH}$  (60% suspension in paraffin oil) (4.9 mmol, 290 mg) was added to a solution of the crude deprotected product (49.0 mmol, 383 mg; assumed quantity) and methyl bromoacetate (1.86 mmol, 1.47 mL) in dry THF (150 mL). After stirring for 12 h at 25 °C, flash silica gel was added to quench the  $\text{NaH}$  as well as to make slurry for column chromatography. The solvents were removed and chromatographed ( $\text{SiO}_2$ ; 50 % hexanes/EtOAc) to afford **297** (79 mg) in 17 % yield as a dark blue amorphous solid;  $\delta_{\text{H}}$  (500 MHz,  $\text{CDCl}_3$ ): 7.93 (d,  $J = 9.0$  Hz, 4H), 7.77 (d,  $J = 9.0$  Hz, 4H), 7.68 (d,  $J = 9.0$  Hz, 4H), 6.92 (d,  $J = 9.0$  Hz, 4H), 6.82 (s, 2H), 4.66 (s, 4H), 3.85 (s, 6H);  $\delta_{\text{C}}$  (75 MHz,  $\text{CDCl}_3$ ): 169.2, 159.2, 158.1, 143.7, 138.1, 131.1(3C), 126.2, 117.7, 115.0, 98.4, 65.4, 52.6; MS (MALDI) calcd for  $\text{C}_{38}\text{H}_{28}\text{BF}_2\text{I}_2\text{N}_3\text{O}_6$  925.0129 found 925.6324.

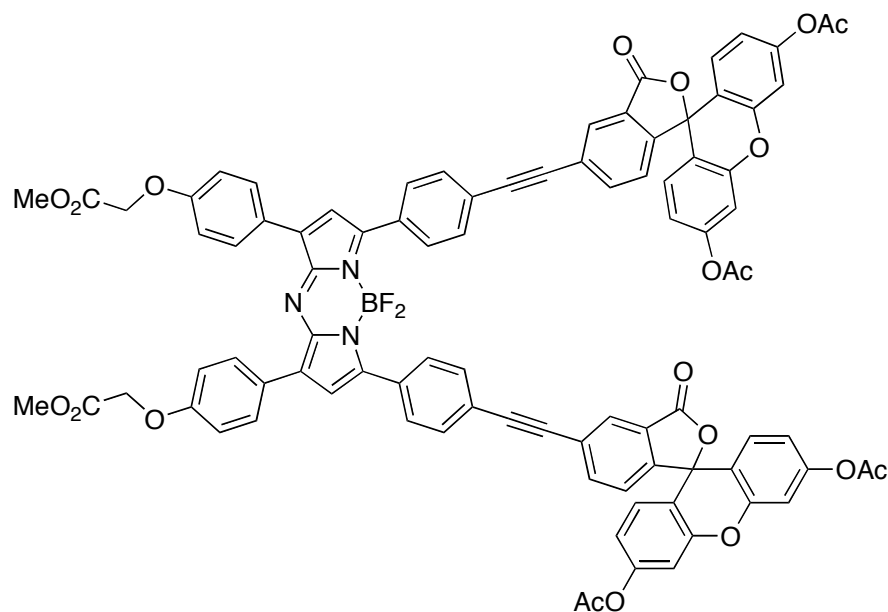


$^1\text{H}$  NMR for compound **297** (500 MHz,  $\text{CDCl}_3$ ).

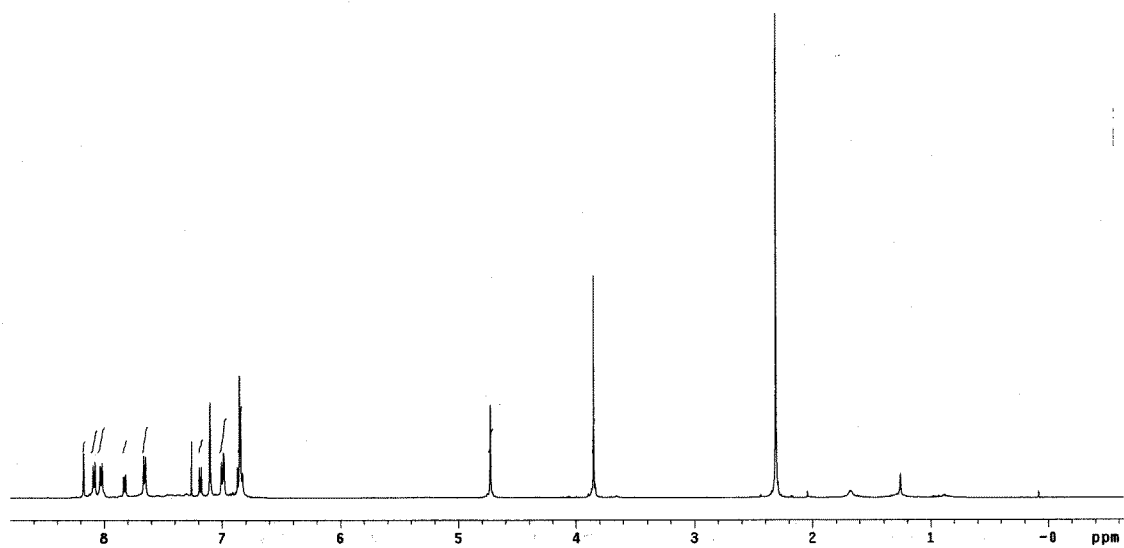


$^{13}\text{C}$  NMR for compound **297** (125 MHz,  $\text{CDCl}_3$ ).

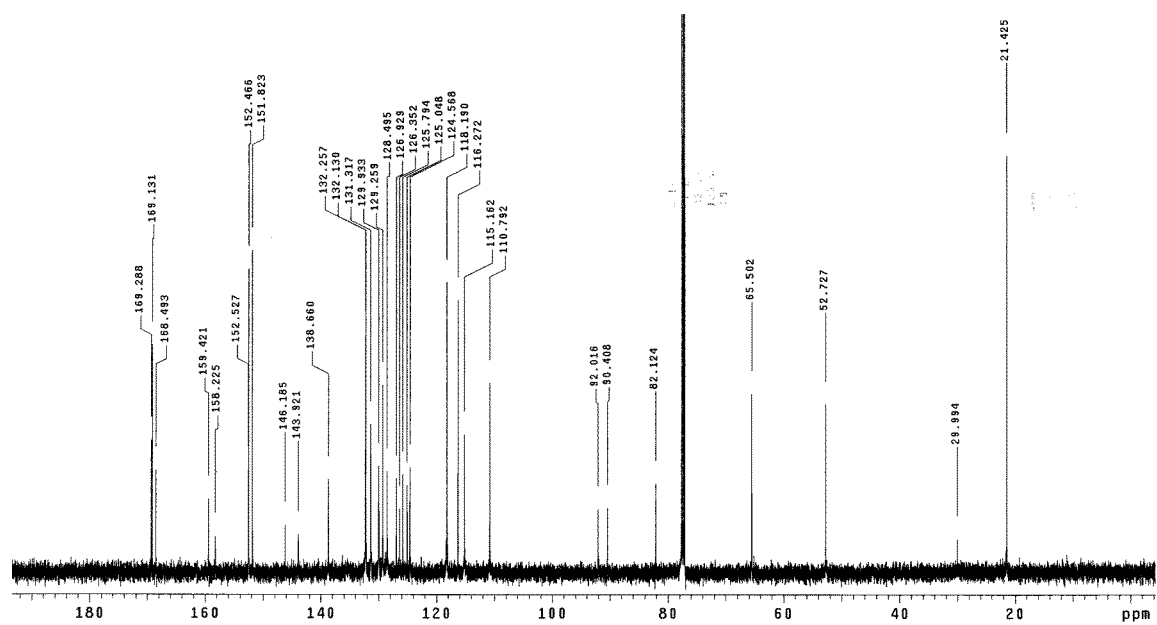
### Compound 299.



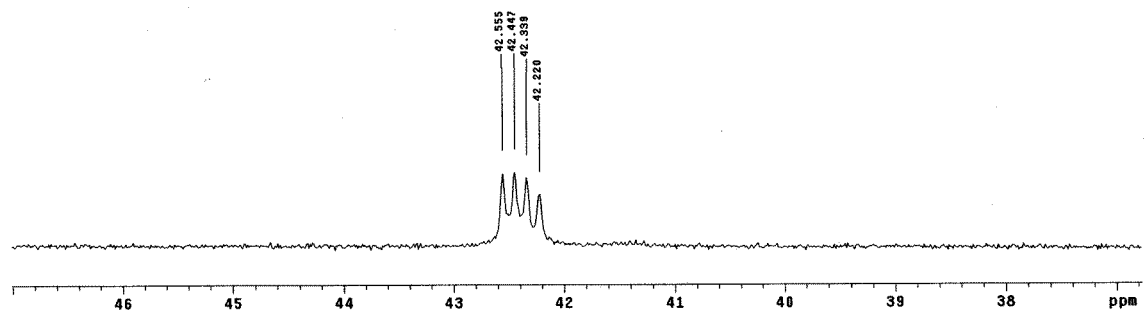
Ethynyl fluorescein diacetate **296** (0.43 mmol, 0.187 g) was added to a solution of aza-BODIPY **297** (0.085 mmol, 0.79 g), PdCl<sub>2</sub>(PPh<sub>3</sub>)<sub>2</sub> (25 mol %, 15 mg), CuI (5 mol %, 1 mg) and Et<sub>3</sub>N (1 mL) in dry THF (30 mL). The resulting solution was degassed by freeze-pump-thaw method (3 cycles). After stirring for 18 h at 40 °C, the solvents were removed and the crude residue chromatographed (SiO<sub>2</sub>; 12% EtOAc/CH<sub>2</sub>Cl<sub>2</sub>) to afford **299** (53 mg) in 40 % yield as a dark brown solid;  $\delta_{\text{H}}$  (500 MHz, CDCl<sub>3</sub>): 8.18 (s, 2H), 8.08 (d,  $J$  = 8.5 Hz, 4H), 8.02 (d,  $J$  = 8.5 Hz, 4H), 7.84-7.80 (m, 2H), 7.65 (d,  $J$  = 8.5 Hz, 4H), 7.18 (d,  $J$  = 7.5 Hz, 2H), 7.13 (d,  $J$  = 2.0 Hz, 4H), 6.99-7.01 (m, 6H), 6.84-6.85 (m, 8H), 4.73 (s, 4H), 3.85 (s, 6H), 2.31 (s, 12H);  $\delta_{\text{C}}$  (75 MHz, CDCl<sub>3</sub>): 179.3, 169.1, 168.5, 159.45, 158.2, 152.5 (2C), 151.8, 146.2, 143.9, 138.7, 132.3, 132.1, 131.3, 129.3 (2C), 129.3, 128.5, 126.9, 126.4, 125.8, 125.1, 124.6, 118.2, 116.3, 115.2, 110.8, 92.0, 90.4, 82.1, 65.5, 52.7, 21.4; IR (neat);  $\nu$  (cm<sup>-1</sup>); 1684; MS (MALDI) calcd for C<sub>90</sub>H<sub>58</sub>BF<sub>2</sub>N<sub>2</sub>O<sub>20</sub> 1549.3637 found (M-F)<sup>+</sup> 1530.1506.



$^1\text{H}$  NMR for compound **299** (500 MHz,  $\text{CDCl}_3$ ).



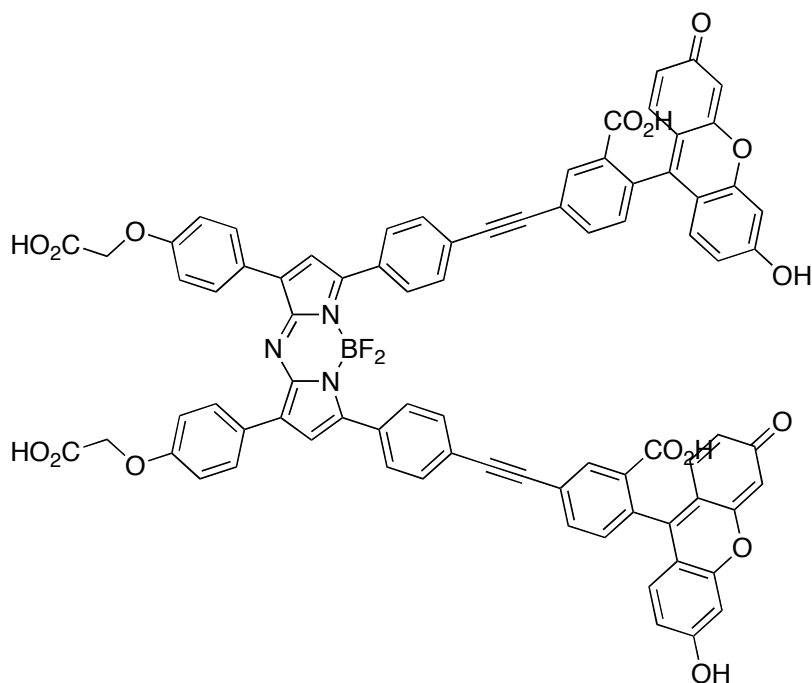
$^{13}\text{C}$  NMR for compound **299** (125 MHz,  $\text{CDCl}_3$ ).



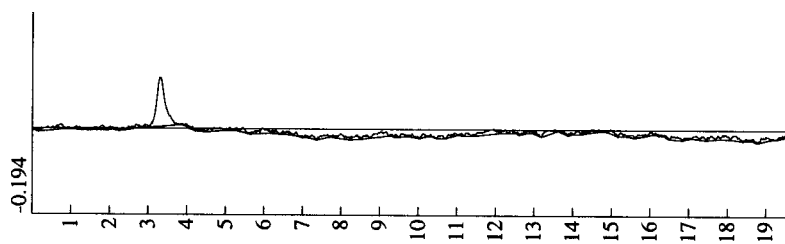
$^{19}\text{F}$  NMR for compound **299** (376 MHz,  $\text{CDCl}_3$ ).



**Compound 290.**



Solid TMSOK (0.37 mmol, 48 mg) was added to a solution of compound **299** (0.031 mmol, 48 mg) in THF (20 mL). After stirring for 2.5 h at 25 °C, the reaction mixture was neutralized with 2N HCl (1 mL) and subsequently water was added (5 mL). After stirring for 5 min, THF was removed and the aqueous layer was extracted with 25% *i*PrOH in CH<sub>2</sub>Cl<sub>2</sub> (pH = 2-3). To obtain pure product in 90 % yield (38 mg) solvents were removed and was dried under vacuum. <sup>1</sup>H and <sup>13</sup>C NMR could not be obtained because of aggregation. MS (MALDI) calcd for C<sub>80</sub>H<sub>46</sub>BF<sub>2</sub>N<sub>3</sub>O<sub>6</sub> 1353.2939 found 1354.10212 (M+H)<sup>+</sup>; Pure compound **290** (< 1 mg) was dissolved in 1:1 (CH<sub>3</sub>CN:H<sub>2</sub>O) (2 mL) and subjected to reverse phase analytical HPLC {C18, 5:95 (CH<sub>3</sub>CN:H<sub>2</sub>O) and 0.1 % TFA , t<sub>R</sub> = 16.5 min}.



C18 Reverse Phase HPLC – UV Detector ( $\lambda_{\text{max abs}}$  488 nm) – Solvent: 5/95 (CH<sub>3</sub>CN/H<sub>2</sub>O) + 0.1% TFA - retention time: 3.35 min.

- (1) Vincett, P. S.; Voigt, E. M.; Rieckhoff, K. E. *J. Chem. Phys.* **1971**, *55*, 4131-40.
- (2) Williams, A. T. R.; Winfield, S. A.; Miller, J. N. *Analyst* **1983**, *108*, 1067-71.
- (3) Buu-Hoi, N. P.; Sy, M. *Bull. Soc. Chim. Fr.* **1958**, 219-20.
- (4) Sherif, S. *Can. J. Chem* **1961**, *39*, 2563-71.
- (5) Barnes, R. P.; Goodwin, T. C., Jr.; Cotten, T. W., Jr. *J. Am. Chem. Soc.* **1947**, *69*, 3135-8.
- (6) Shadakshari, U.; Nayak, S. K. *Tetrahedron* **2001**, *57*, 8185-88.
- (7) Bloom, S. M.; Garcia, P. P. Novel Dipyrromethene Dyes. US Patent 3,691,161, 1972.
- (8) Bloom, S. M.; Garcia, P. P. Intermediates for Dipyrromethene Dyes. US Patent 3,883,555, 1975.
- (9) Liu, M.; Wilairat, P.; Go, M.-L. *J. Med. Chem.* **2001**, *44*, 4443-4452.
- (10) Liu, M.; Wilairat, P.; Go, M.-L. *J. Med. Chem.* **2002**, *45*, 1735.
- (11) Southard, G. E.; Murray, G. M. Process for preparing vinyl-substituted beta-diketones. US Patent 0069288, 2006.
- (12) Jiao, G.-S.; Thoresen, L. H.; Kim, T. G.; Haaland, W. C.; Gao, F.; Topp, M. R.; Hochstrasser, R. M.; Metzker, M. L.; Burgess, K. *Chem. Eur. J.* **2006**, *12*, 7616-26.
- (13) Jiao, G.-S.; Han, J. W.; Burgess, K. *J. Org. Chem.* **2003**, *68*, 8264-7.

## APPENDIX B

### EXPERIMENTAL DATA FOR CHAPTER III

#### General Experimental Procedures.

All chemicals were obtained from commercial suppliers and used without further purification. Thin layer chromatography was performed using silica gel 60F254 flash. Chromatography on silica gel was performed using a forced flow of the indicated solvent on EM reagents silica gel 60 (230-400 mesh). The solvents were dried/degassed by passing them down an alumina column.  $^1\text{H}$  and  $^{13}\text{C}$  NMR spectra were recorded on an Inova Instrument at 500 MHz ( $^1\text{H}$ ), 125 MHz ( $^{13}\text{C}$ ).  $^{11}\text{B}$  and  $^{19}\text{F}$  NMR spectra were recorded on a Inova 400 Broad Band instrument at 128 MHz ( $^{11}\text{B}$ ) and 376 MHz ( $^{19}\text{F}$ ). NMR chemical shifts are expressed in ppm relative to internal solvent peaks ( $\text{CDCl}_3$ : 7.27 ppm for  $^1\text{H}$  and 77.0 ppm for  $^{13}\text{C}$ ;  $\text{DMSO-}d_6$ : 2.50 ppm for  $^1\text{H}$  and 39.5 ppm for  $^{13}\text{C}$ ;  $\text{CD}_3\text{OD}$ : 3.30 ppm for  $^1\text{H}$  and 49.0 ppm for  $^{13}\text{C}$ ) and coupling constants were measured in Hz. For  $^{11}\text{B}$  NMR,  $\text{BF}_3\cdot\text{OEt}_2$  has been used as an external reference; similarly,  $\text{CFCl}_3$  was used as an external standard for the  $^{19}\text{F}$  spectra.

UV spectra were recorded in 1 cm path length quartz cuvettes on a Cary 100 Bio UV-Visible spectrophotometer at 5  $\mu\text{M}$ . Fluorescence emission spectra were recorded in 1 cm path length quartz cuvettes on a Photon Counting Spectrofluorometer PC1 SSI instrument equipped with an R928P photomultiplier tube which is sensitive up to  $\sim 850\text{-}900$  nm. Fluorescence spectra were recorded at concentrations between 1 and 5  $\mu\text{M}$ . Fluorescence quantum yield measurements were performed on the same instrument. The slit width was 0.5 nm for both excitation and emission. Relative quantum efficiencies of fluorescence of BODIPY derivatives were obtained by comparing the areas under the corrected emission spectrum of the test sample in 1% pyridine in toluene with that of a solution of zinc phthalocyanine, which has a quantum efficiency of 0.30 according to the literature.<sup>1</sup> Non-degassed, spectroscopic grade toluene and a 10 mm quartz cuvette were used. Dilute solutions ( $0.01 < A < 0.05$ ) were used to minimize reabsorption effects. The excitation wavelength was 671 nm for both compound **4** and **1**, and the reference.

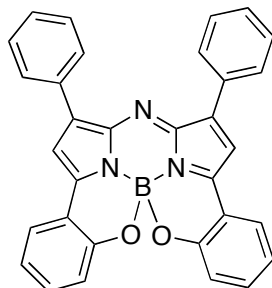
Quantum yields were determined using the equation (1):<sup>2</sup>

$$\text{equation (1)} \quad \Phi_X = \Phi_{\text{st}} (I_X/I_{\text{st}}) (A_{\text{st}}/A_X) (\eta_X^2/\eta_{\text{st}}^2)$$

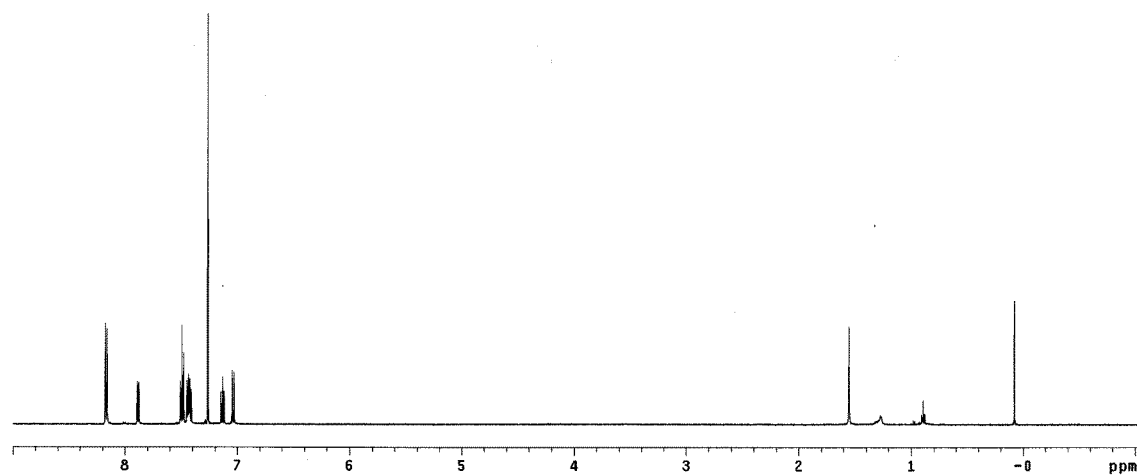
Where  $\Phi_{st}$  is the reported quantum yield of the standard,  $I$  is the integrated emission spectra,  $A$  is the absorbance at the excitation wavelength and  $\eta$  is the refractive index of the solvent used ( $\eta=1$  if same solvent). X subscript denotes unknown, and st denotes standard.

Cyclic voltammograms were recorded on a BAS-100A electrochemical analyzer using three electrodes. The working electrode consisted of 3.0 mm glassy carbon electrode. A Ag/AgCl was used as reference electrode, and a platinum coil served as a counter electrode. Tetrabutyl ammonium tetrafluoroborate was used as the electrolyte. All potentials were calibrated versus SCE by the addition of ferrocene (Fc) as an internal standard, taking  $E(\text{Fc}/\text{Fc}^+) = 0.46$  V, vs SCE. The potentials are then reported versus NHE. Measurements were obtained with solution concentrations of 1 mM in 0.1 M TBABF<sub>4</sub> in 10 mL of CH<sub>2</sub>Cl<sub>2</sub> at a scan rate of 200 mV/s.

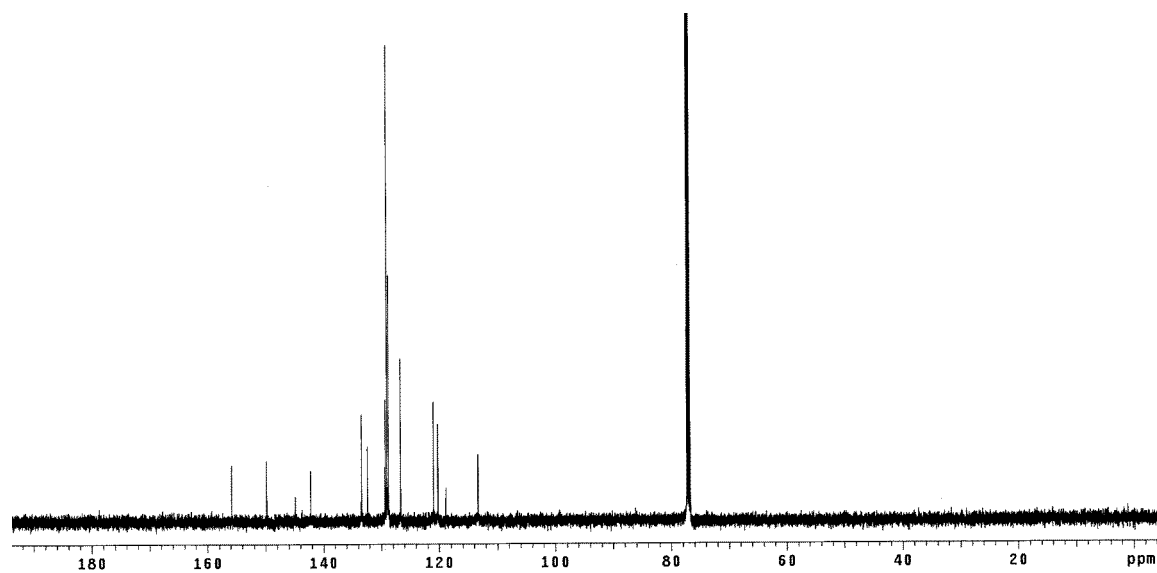
- (1) Vincett, P. S.; Voigt, E. M.; Rieckhoff, K. E. *J. Chem. Phys.* **1971**, *55*, 4131-40.
- (2) Williams, A. T. R.; Winfield, S. A.; Miller, J. N. *Analyst* **1983**, *108*, 1067-71.

**AzaBODIPY 300a**

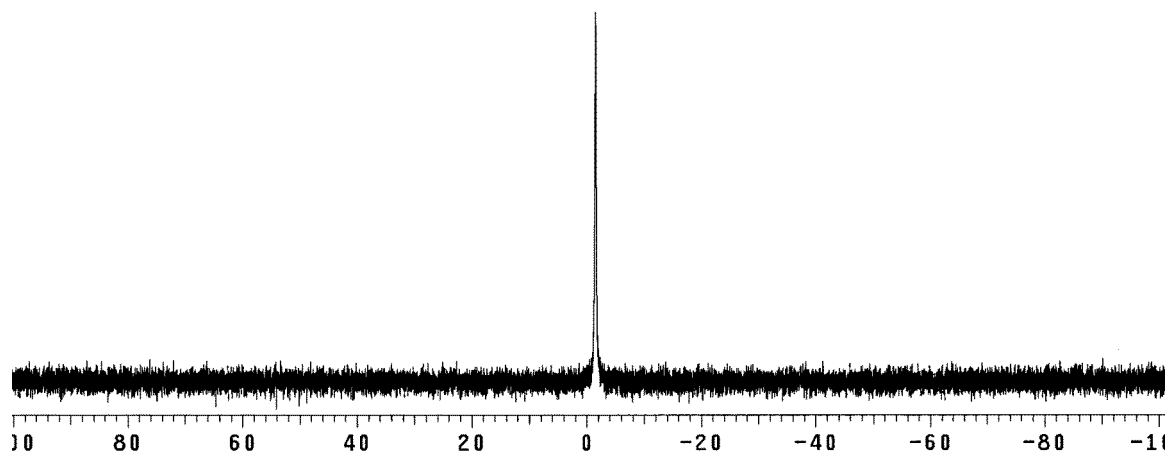
A solution of **288c** (0.09 mmol) in dry dichloromethane (2.5 mL) was cooled to 0°C, then BBr<sub>3</sub> (0.90 mmol) was added dropwise over 1 min. The solution was then allowed to reach room temperature and stirring was continued for an additional 10h. The reaction was then quenched with water at 0°C, and extracted with ethyl acetate. The combined organic layers were washed with sat'd NH<sub>4</sub>Cl, dried over sodium sulfate and concentrated *in vacuo*. The product was then purified by column chromatography on silica gel eluted with 5% ethyl acetate/hexanes to give the desired product in 62 % yield (0.03 g) as a dark solid.  $\delta_{\text{H}}$  (500 MHz, CDCl<sub>3</sub>): 8.17 (dd,  $J$ = 5.6 Hz,  $J$ = 1.5 Hz, 4H), 7.89 (dd,  $J$ = 7.8 Hz,  $J$ = 1.7 Hz, 2H), 7.51-7.41 (m, 8H), 7.26 (s, 2H), 7.13 (td,  $J$ = 7.3 Hz,  $J$ = 0.9 Hz, 2H), 7.04 (d,  $J$ = 8.3 Hz, 2H);  $\delta_{\text{C}}$  (125 MHz, CDCl<sub>3</sub>): 155.8, 149.8, 144.9, 142.2, 133.4, 132.4, 129.3, 129.0, 128.7, 126.6, 120.9, 120.2, 118.9, 113.3;  $\delta_{\text{B}}$  (128 MHz, CDCl<sub>3</sub>): -1.58 (s);  $m/z$  (HR-ESI): theoretical mass (M+H)<sup>+</sup>: 490.1727; found : 490.1722;  $\lambda_{\text{max abs}}$  (PhMe)/ 728 nm ( $\epsilon$  = 8.187 E4 dm<sup>3</sup>mol<sup>-1</sup>cm<sup>-1</sup>);  $\lambda_{\text{max emis}}$  (PhMe)/ 746 nm;  $\Phi$  = 0.51 in 1% pyridine in toluene.



$^1\text{H}$  NMR for compound **300a** (500 MHz,  $\text{CDCl}_3$ ).

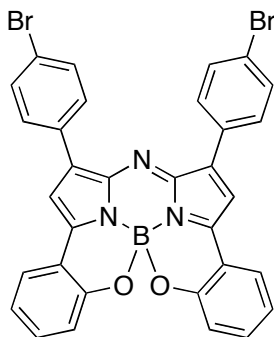


$^{13}\text{C}$  NMR for compound **300a** (125 MHz,  $\text{CDCl}_3$ ).



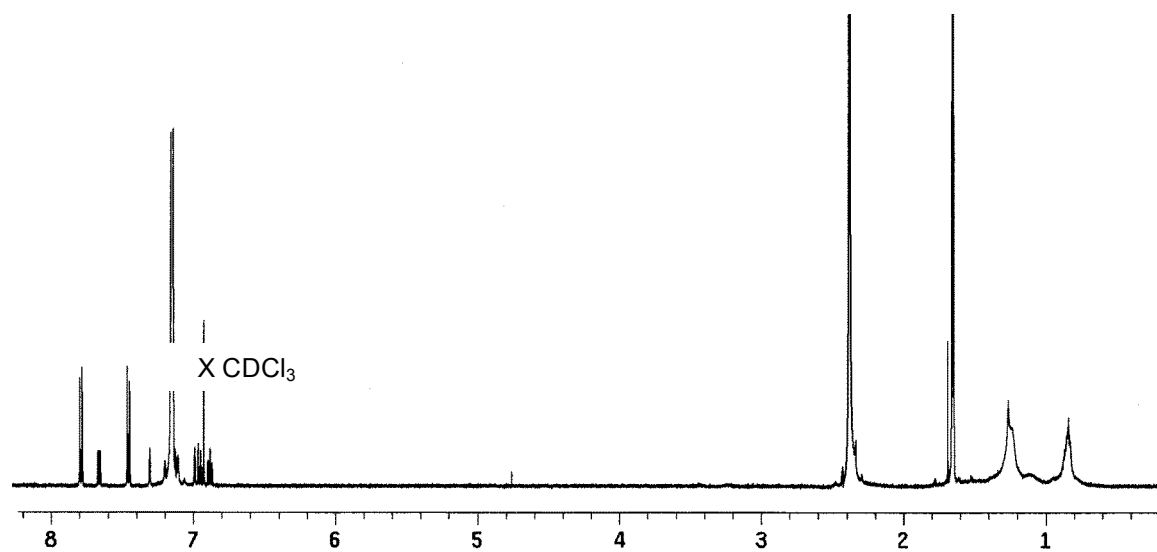
$^{11}\text{B}$  NMR for compound **300a** (128 MHz,  $\text{CDCl}_3$ ).

### AzaBODIPY 300b

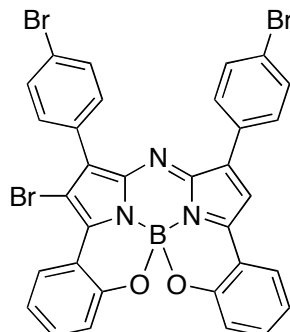


A solution of corresponding aza-BODIPY **288d** (0.07 mmol) in dry dichloromethane (10 mL) was cooled to 0°C, then BBr<sub>3</sub> (0.18 mmol) was added dropwise over 1 min. The solution was then allowed to reach room temperature and stirring was continued for an additional 10 h. The reaction was then quenched with water sat'd NH<sub>4</sub>Cl at 0°C, and extracted with ethyl acetate. The combined organic layers were washed with sat'd NH<sub>4</sub>Cl, dried over sodium sulfate and concentrated *in vacuo*. The product was then purified by column chromatography on silica gel eluted with 10% ethyl acetate/hexanes to give the desired product in 36 % yield (0.018 g) as a dark purple solid.  $\delta_{\text{H}}$  (500 MHz, C<sub>6</sub>D<sub>6</sub>): 7.80 (d,  $J$ = 8.6 Hz, 4H), 7.67 (dd,  $J$ = 7.8 Hz,  $J$ = 1.6 Hz, 2H), 7.46 (d,  $J$ = 8.6 Hz, 4H), 7.31 (bs, 2H), 7.00 (bs, 2H), 6.96 (dd,  $J$ = 7.8 Hz,  $J$ = 1 Hz, 2H), 6.89 (td,  $J$ = 7.3 Hz,  $J$ = 1 Hz, 2H);  $m/z$  (MALDI): theoretical mass ( $M$ )<sup>+</sup>: 645.0; found : 644.5, 646.5, 647.5, 648.6 (Br isotopes);  $\lambda_{\text{max abs}}$  (PhMe)/745 nm ( $\epsilon/\text{dm}^3\text{mol}^{-1}\text{cm}^{-1}$ );  $\lambda_{\text{max emis}}$  (PhMe)/760 nm;  $\Phi$  = 0.46 in 1% pyridine in toluene. Not enough sample was prepared to allow determination of the molar extinction coefficient.

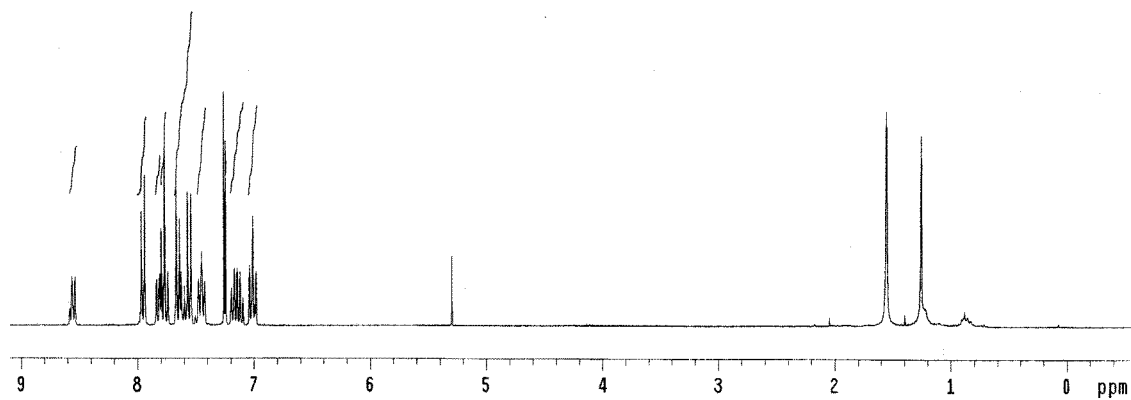




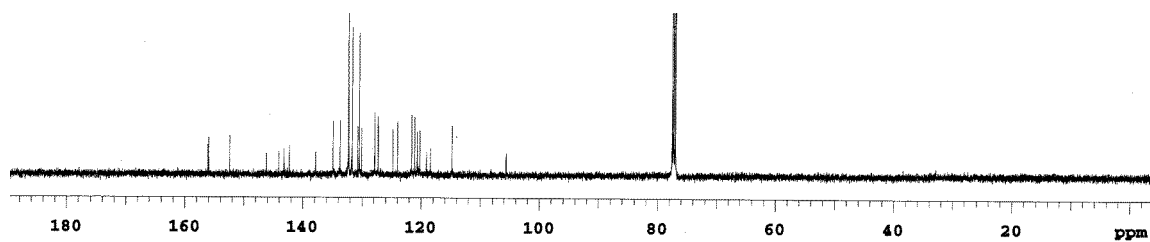
$^1\text{H}$  NMR for compound **300b** (500 MHz,  $\text{C}_6\text{D}_6$ ).

**AzaBODIPY 300c**

5% Ethyl acetate/hexanes gave rise the desired product in 41% yield (0.370 g) as a off pink dark solid.  $\delta$ H (300 MHz, CDCl<sub>3</sub>): 6.98-7.04 (m, 2H), 7.10-7.20 (m, 2H), 7.27 (s, 1H), 7.43-7.48 (m, 2H), 7.58 (d,  $J$  = 8.5 Hz, 2H), 7.67 (d,  $J$  = 8.5 Hz, 2H), 7.79 (d,  $J$  = 8.5 Hz, 2H), 7.86 (dd,  $J$  = 6.5 Hz,  $J$  = 1.5 Hz, 1H), 7.98 (d,  $J$  = 8.5 Hz, 2H), 8.56 (dd,  $J$  = 6.5 Hz,  $J$  = 1.5 Hz, 1H);  $\delta$ C (75 MHz, CDCl<sub>3</sub>):156.1, 156.0, 152.4, 146.2, 144.1, 143.2, 142.3, 137.9, 134.9, 133.7, 132.3(2C), 132.2, 131.7(2), 130.8, 130.5(2C), 130.1, 127.8, 127.3, 124.8, 124.0, 121.6, 121.1, 120.6, 120.2, 119.1, 118.4, 114.8, 105.6;  $\delta$ B (128 MHz, CDCl<sub>3</sub>): -1.73 (s);  $m/z$  (MALDI): theoretical mass (M)<sup>+</sup>: 722.9; found : 722.7, 723.7, 724.7, 725.7, 726.7, 727.7 (Br isotopes);  $\lambda_{\text{max abs}}$  (PhMe)/747 nm;  $\lambda_{\text{max emis}}$  (PhMe)/769 nm;  $\Phi$  = 0.35 in 1% pyridine in toluene. Not enough sample was prepared to allow determination of the molar extinction coefficient.

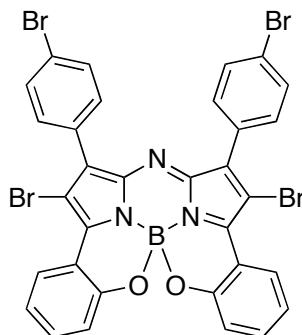


$^1\text{H}$  NMR for compound **300c** (300 MHz,  $\text{CDCl}_3$ ).

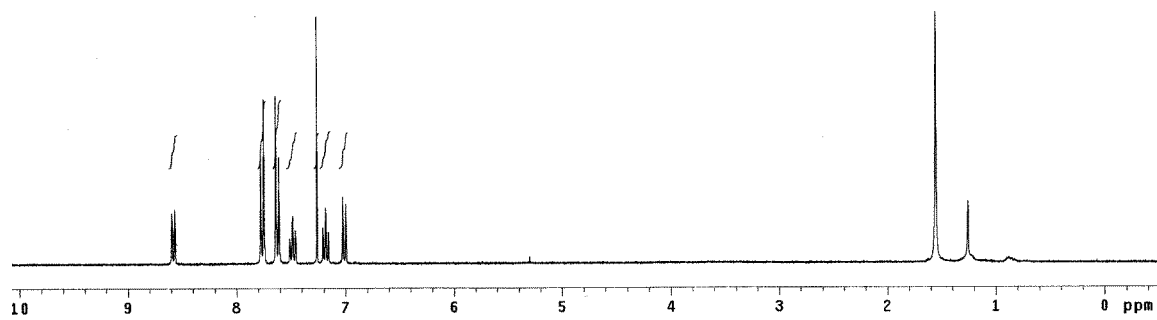


$^{13}\text{C}$  NMR for compound **300c** (75 MHz,  $\text{CDCl}_3$ ).

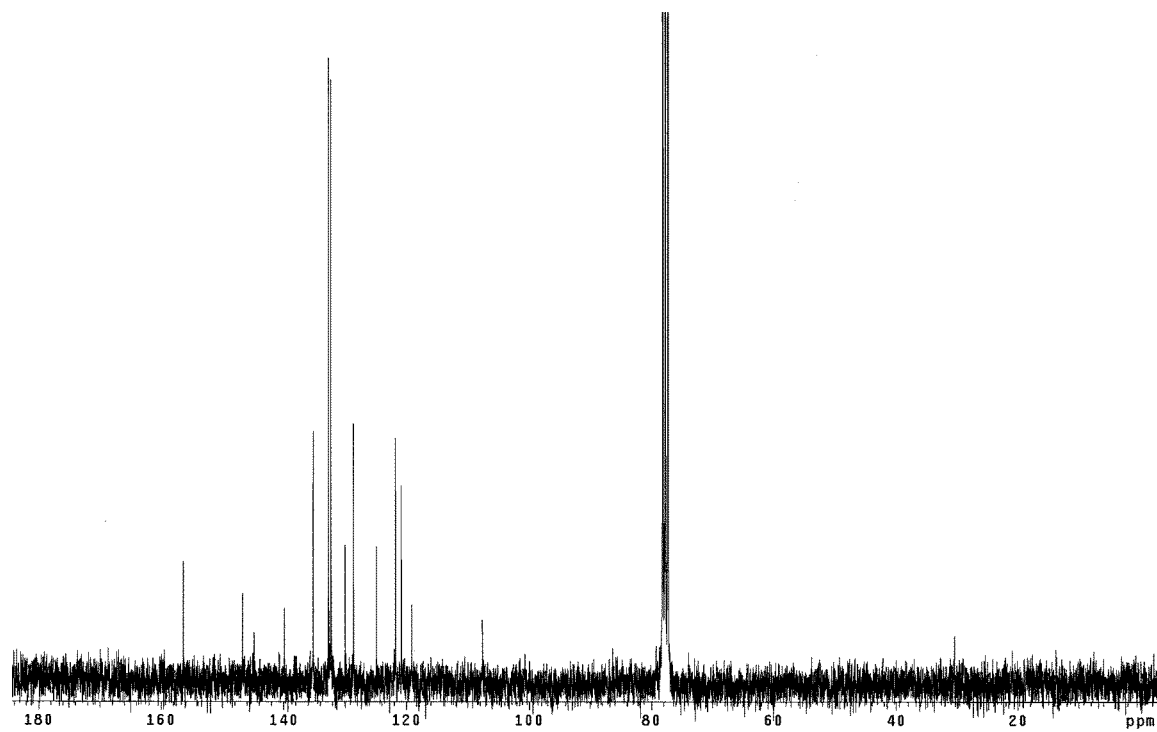
### AzaBODIPY 300d



A solution of corresponding aza-BODIPY **288d** (1.4 mmol) in dry dichloromethane (250 mL) was cooled to 0°C, then BBr<sub>3</sub> (14.0 mmol) was added dropwise over 10 min. The solution was then allowed to reach room temperature and stirring was continued for an additional 24 h. The reaction was then quenched with water sat'd NH<sub>4</sub>Cl at 0°C, and extracted with ethyl acetate. The combined organic layers were washed with sat'd NH<sub>4</sub>Cl, dried over sodium sulfate and concentrated *in vacuo*. The product was then purified by column chromatography on silica gel eluted with 5% ethyl acetate/hexanes to give the desired product in 21% yield (0.19 g) as a pink dark solid.  $\delta_{\text{H}}$  (300 MHz, CDCl<sub>3</sub>): 7.04 (d,  $J$  = 8.4 Hz, 2H), 7.16-7.20 (m, 2H), 7.45-7.48 (m, 2H), 7.62 (d,  $J$  = 7.7 Hz, 4H), 7.76 (d,  $J$  = 7.7 Hz, 4H), 8.17 (dd,  $J$  = 6.6 Hz,  $J$  = 1.5 Hz, 2H);  $\delta_{\text{C}}$  (75 MHz, CDCl<sub>3</sub>): 156.4, 146.7, 144.4, 139.8, 135.1, 132.6, 132.2, 130.0, 128.6, 124.9, 121.8, 120.8, 119.1, 107.6;  $\delta_{\text{B}}$  (128 MHz, CDCl<sub>3</sub>): -1.81 (s);  $m/z$  (MALDI): theoretical mass (M)<sup>+</sup>: 800.8 ; found : 800.6, 801.6, 803.6, 804.6, 805.6, 807.6, 808.6, 809.6 (Br isotopes);  $\lambda_{\text{max abs}}$  (PhMe)/755 nm;  $\lambda_{\text{max emis}}$  (PhMe)/776 nm;  $\Phi$  = 0.35 in 1% pyridine in toluene. Not enough sample was prepared to allow determination of the molar extinction coefficient.



$^1\text{H}$  NMR for compound **300d** (300 MHz,  $\text{CDCl}_3$ ).



$^{13}\text{C}$  NMR for compound **300d** (75 MHz,  $\text{CDCl}_3$ ).

## X-Ray Structure of Compound 300d

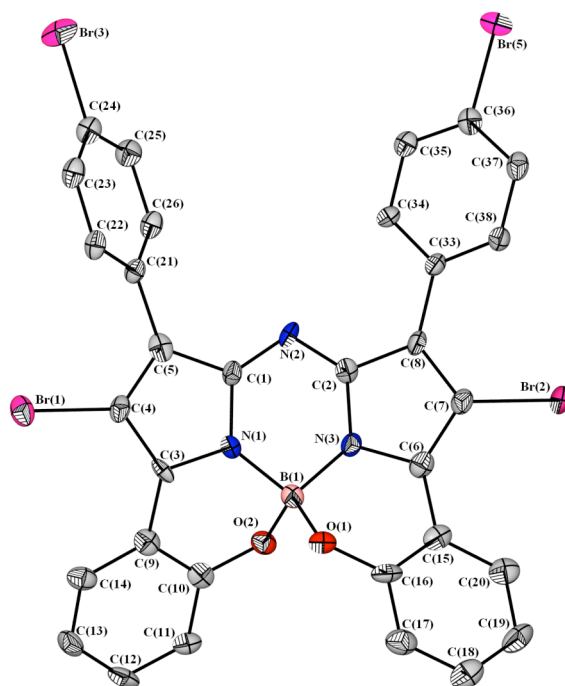


**Table 1. Crystal data and structure refinement for KBB0908.**

---

|                     |   |
|---------------------|---|
| Identification code | kbb0908   |
| Empirical formula   | C <sub>32</sub> H <sub>16</sub> B Br <sub>4</sub> N <sub>3</sub> O <sub>2</sub> |
| Formula weight      | 804.93  |
| Temperature         | 110(2) K  |
| Wavelength          | 1.54178 Å   |

**Table 1. Continued**

|                                   |   |                               |
|-----------------------------------|---|-------------------------------|
| Crystal system                    | Monoclinic                                  |                               |
| Space group                       | P2(1)/c                                     |                               |
| Unit cell dimensions              | a = 17.565(4) Å                             | $\alpha = 90^\circ$ .         |
|                                   | b = 4.9506(12) Å                            | $\beta = 105.322(11)^\circ$ . |
|                                   | c = 32.855(9) Å                             | $\gamma = 90^\circ$ .         |
| Volume                            | 2755.4(12) Å <sup>3</sup>                   |                               |
| Z                                 | 4   |                               |
| Density (calculated)              | 1.940 Mg/m <sup>3</sup>                     |                               |
| Absorption coefficient            | 7.441 mm <sup>-1</sup>                      |                               |
| F(000)                            | 1560  |                               |
| Crystal size                      | 0.12 x 0.01 x 0.01 mm <sup>3</sup>          |                               |
| Theta range for data collection   | 2.61 to 59.04°.                             |                               |
| Index ranges                      | -19 ≤ h ≤ 19, -5 ≤ k ≤ 5, -36 ≤ l ≤ 36      |                               |
| Reflections collected             | 19775                                       |                               |
| Independent reflections           | 3948 [R(int) = 0.1217]                      |                               |
| Completeness to theta = 59.04°    | 98.6 %                                      |                               |
| Absorption correction             | Semi-empirical from equivalents             |                               |
| Max. and min. transmission        | 0.9293 and 0.4688                           |                               |
| Refinement method                 | Full-matrix least-squares on F <sup>2</sup> |                               |
| Data / restraints / parameters    | 3948 / 402 / 507                            |                               |
| Goodness-of-fit on F <sup>2</sup> | 1.018                                       |                               |
| Final R indices [I > 2σ(I)]       | R1 = 0.0564, wR2 = 0.1172                   |                               |
| R indices (all data)              | R1 = 0.1030, wR2 = 0.1372                   |                               |
| Largest diff. peak and hole       | 1.139 and -2.080 e.Å <sup>-3</sup>          |                               |

**Table 2. Atomic coordinates (  $\times 10^4$ ) and equivalent isotropic displacement parameters ( $\text{\AA}^2 \times 10^3$ ) for KBB0908.  $U(\text{eq})$  is defined as one third of the trace of the orthogonalized  $U^{ij}$  tensor.**

|       | x       | y         | z       | $U(\text{eq})$ |
|-------|---------|-----------|---------|----------------|
| B(1)  | 1906(6) | 2450(20)  | 1788(3) | 26(2)          |
| Br(1) | 4433(1) | -4321(2)  | 2171(1) | 33(1)          |
| Br(2) | 133(1)  | 8807(3)   | 555(1)  | 69(1)          |
| N(1)  | 2585(4) | 696(13)   | 1728(2) | 20(2)          |
| N(2)  | 2644(4) | 2445(13)  | 1056(2) | 21(2)          |
| N(3)  | 1691(4) | 4176(14)  | 1393(2) | 22(2)          |
| O(1)  | 1183(3) | 1004(11)  | 1808(2) | 26(1)          |
| O(2)  | 2209(3) | 3861(11)  | 2188(2) | 25(1)          |
| C(1)  | 2902(5) | 786(16)   | 1387(3) | 22(2)          |
| C(2)  | 2053(5) | 4102(16)  | 1067(3) | 22(2)          |
| C(3)  | 3071(5) | -664(16)  | 2049(2) | 20(2)          |
| C(4)  | 3665(5) | -1856(16) | 1882(3) | 24(2)          |
| C(5)  | 3591(5) | -939(16)  | 1476(3) | 25(2)          |
| C(6)  | 981(5)  | 5473(17)  | 1260(3) | 26(2)          |
| C(7)  | 947(5)  | 6614(16)  | 858(3)  | 26(2)          |
| C(8)  | 1596(5) | 5750(17)  | 731(3)  | 25(2)          |
| C(9)  | 3004(5) | -145(17)  | 2469(3) | 27(2)          |
| C(10) | 2560(5) | 2220(17)  | 2518(3) | 25(2)          |
| C(11) | 2513(5) | 2950(17)  | 2922(3) | 27(2)          |
| C(12) | 2892(5) | 1480(18)  | 3268(3) | 33(2)          |



**Table 2. Continued**


---

|       |          |           |         |       |
|-------|----------|-----------|---------|-------|
| C(13) | 3344(5)  | -778(18)  | 3218(3) | 31(2) |
| C(14) | 3391(5)  | -1592(18) | 2832(3) | 29(2) |
| C(15) | 425(5)   | 4979(17)  | 1506(3) | 27(2) |
| C(16) | 546(5)   | 2693(18)  | 1770(3) | 29(2) |
| C(17) | 1(5)     | 2030(20)  | 1995(3) | 36(2) |
| C(18) | -674(6)  | 3596(19)  | 1950(3) | 38(2) |
| C(19) | -803(5)  | 5810(20)  | 1685(3) | 38(2) |
| C(20) | -270(5)  | 6553(18)  | 1466(3) | 32(2) |
| C(21) | 4168(13) | -1280(60) | 1213(7) | 21(3) |
| C(22) | 4381(9)  | -3940(30) | 1127(5) | 24(3) |
| C(23) | 4884(9)  | -4340(30) | 864(5)  | 28(3) |
| C(24) | 5183(13) | -2130(60) | 711(7)  | 26(3) |
| C(25) | 4983(9)  | 510(30)   | 780(5)  | 29(3) |
| C(26) | 4460(9)  | 870(30)   | 1035(5) | 25(3) |
| Br(3) | 5835(10) | -2930(20) | 343(6)  | 38(2) |
| C(27) | 4047(13) | -1420(60) | 1184(7) | 21(3) |
| C(28) | 4874(8)  | -1300(30) | 1342(5) | 25(3) |
| C(29) | 5376(9)  | -1630(30) | 1075(5) | 30(3) |
| C(30) | 5039(12) | -2070(60) | 656(6)  | 25(3) |
| C(31) | 4232(8)  | -2120(30) | 485(5)  | 26(3) |
| C(32) | 3737(8)  | -1730(30) | 754(4)  | 20(3) |
| Br(4) | 5773(9)  | -2280(20) | 320(5)  | 33(2) |
| C(33) | 1798(16) | 6300(70)  | 318(7)  | 21(3) |
| C(34) | 2590(8)  | 6740(30)  | 310(4)  | 22(3) |

**Table 2. Continued**

---

|       |          |          |         |       |
|-------|----------|----------|---------|-------|
| C(35) | 2774(8)  | 7250(30) | -72(4)  | 24(3) |
| C(36) | 2165(15) | 7330(70) | -434(7) | 26(3) |
| C(37) | 1379(8)  | 6880(30) | -442(4) | 27(3) |
| C(38) | 1212(8)  | 6440(30) | -53(4)  | 24(3) |
| Br(5) | 2419(11) | 8310(20) | -945(4) | 25(2) |
| C(39) | 1756(18) | 6220(70) | 314(8)  | 21(3) |
| C(40) | 2034(9)  | 4130(30) | 97(4)   | 21(3) |
| C(41) | 2199(9)  | 4650(30) | -291(4) | 25(3) |
| C(42) | 2130(18) | 7270(70) | -435(7) | 26(3) |
| C(43) | 1862(9)  | 9380(30) | -234(4) | 27(3) |
| C(44) | 1681(9)  | 8800(30) | 150(4)  | 23(3) |
| Br(6) | 2372(11) | 7660(20) | -966(4) | 29(2) |

---

**Table 3. Bond lengths [Å] and angles [°] for KBB0908.**

---

|            |           |
|------------|-----------|
| B(1)-O(2)  | 1.459(12) |
| B(1)-O(1)  | 1.474(11) |
| B(1)-N(3)  | 1.517(12) |
| B(1)-N(1)  | 1.529(12) |
| Br(1)-C(4) | 1.880(8)  |
| Br(2)-C(7) | 1.861(8)  |
| N(1)-C(3)  | 1.348(9)  |
| N(1)-C(1)  | 1.378(10) |
| N(2)-C(2)  | 1.331(10) |
| N(2)-C(1)  | 1.341(10) |
| N(3)-C(6)  | 1.367(10) |
| N(3)-C(2)  | 1.384(10) |
| O(1)-C(16) | 1.376(10) |
| O(2)-C(10) | 1.364(10) |
| C(1)-C(5)  | 1.447(11) |
| C(2)-C(8)  | 1.436(11) |
| C(3)-C(4)  | 1.429(11) |
| C(3)-C(9)  | 1.439(11) |
| C(4)-C(5)  | 1.380(12) |
| C(5)-C(27) | 1.423(18) |
| C(5)-C(21) | 1.506(17) |
| C(6)-C(7)  | 1.421(12) |
| C(6)-C(15) | 1.446(12) |

**Table 3. Continued**

---

|             |           |
|-------------|-----------|
| C(7)-C(8)   | 1.382(11) |
| C(8)-C(39)  | 1.488(18) |
| C(8)-C(33)  | 1.513(17) |
| C(9)-C(14)  | 1.403(12) |
| C(9)-C(10)  | 1.439(12) |
| C(10)-C(11) | 1.401(12) |
| C(11)-C(12) | 1.366(12) |
| C(11)-H(11) | 0.9500    |
| C(12)-C(13) | 1.406(13) |
| C(12)-H(12) | 0.9500    |
| C(13)-C(14) | 1.355(12) |
| C(13)-H(13) | 0.9500    |
| C(14)-H(14) | 0.9500    |
| C(15)-C(16) | 1.407(12) |
| C(15)-C(20) | 1.423(12) |
| C(16)-C(17) | 1.394(12) |
| C(17)-C(18) | 1.391(13) |
| C(17)-H(17) | 0.9500    |
| C(18)-C(19) | 1.379(13) |
| C(18)-H(18) | 0.9500    |
| C(19)-C(20) | 1.376(12) |
| C(19)-H(19) | 0.9500    |
| C(20)-H(20) | 0.9500    |
| C(21)-C(26) | 1.38(2)   |

**Table 3. Continued**

---

|             |           |
|-------------|-----------|
| C(21)-C(22) | 1.42(3)   |
| C(22)-C(23) | 1.404(15) |
| C(22)-H(22) | 0.9500    |
| C(23)-C(24) | 1.37(3)   |
| C(23)-H(23) | 0.9500    |
| C(24)-C(25) | 1.39(3)   |
| C(24)-Br(3) | 1.912(12) |
| C(25)-C(26) | 1.407(15) |
| C(25)-H(25) | 0.9500    |
| C(26)-H(26) | 0.9500    |
| C(27)-C(32) | 1.38(2)   |
| C(27)-C(28) | 1.41(2)   |
| C(28)-C(29) | 1.407(16) |
| C(28)-H(28) | 0.9500    |
| C(29)-C(30) | 1.37(3)   |
| C(29)-H(29) | 0.9500    |
| C(30)-C(31) | 1.38(2)   |
| C(30)-Br(4) | 1.909(12) |
| C(31)-C(32) | 1.407(15) |
| C(31)-H(31) | 0.9500    |
| C(32)-H(32) | 0.9500    |
| C(33)-C(38) | 1.37(3)   |
| C(33)-C(34) | 1.42(3)   |
| C(34)-C(35) | 1.402(15) |

**Table 3. Continued**

---

|                |           |
|----------------|-----------|
| C(34)-H(34)    | 0.9500    |
| C(35)-C(36)    | 1.37(3)   |
| C(35)-H(35)    | 0.9500    |
| C(36)-C(37)    | 1.39(3)   |
| C(36)-Br(5)    | 1.911(12) |
| C(37)-C(38)    | 1.404(15) |
| C(37)-H(37)    | 0.9500    |
| C(38)-H(38)    | 0.9500    |
| C(39)-C(44)    | 1.38(3)   |
| C(39)-C(40)    | 1.41(3)   |
| C(40)-C(41)    | 1.405(15) |
| C(40)-H(40)    | 0.9500    |
| C(41)-C(42)    | 1.37(3)   |
| C(41)-H(41)    | 0.9500    |
| C(42)-C(43)    | 1.39(3)   |
| C(42)-Br(6)    | 1.909(12) |
| C(43)-C(44)    | 1.410(15) |
| C(43)-H(43)    | 0.9500    |
| C(44)-H(44)    | 0.9500    |
| <br>           |           |
| O(2)-B(1)-O(1) | 107.8(7)  |
| O(2)-B(1)-N(3) | 116.7(7)  |
| O(1)-B(1)-N(3) | 106.8(7)  |

**Table 3. Continued**

---

|                 |          |
|-----------------|----------|
| O(2)-B(1)-N(1)  | 106.1(7) |
| O(1)-B(1)-N(1)  | 116.2(7) |
| N(3)-B(1)-N(1)  | 103.6(7) |
| C(3)-N(1)-C(1)  | 110.1(6) |
| C(3)-N(1)-B(1)  | 122.4(7) |
| C(1)-N(1)-B(1)  | 125.7(7) |
| C(2)-N(2)-C(1)  | 117.0(7) |
| C(6)-N(3)-C(2)  | 109.4(7) |
| C(6)-N(3)-B(1)  | 122.6(7) |
| C(2)-N(3)-B(1)  | 125.9(7) |
| C(16)-O(1)-B(1) | 113.0(6) |
| C(10)-O(2)-B(1) | 114.2(6) |
| N(2)-C(1)-N(1)  | 123.8(7) |
| N(2)-C(1)-C(5)  | 127.7(7) |
| N(1)-C(1)-C(5)  | 108.2(7) |
| N(2)-C(2)-N(3)  | 124.0(7) |
| N(2)-C(2)-C(8)  | 127.7(8) |
| N(3)-C(2)-C(8)  | 107.6(7) |
| N(1)-C(3)-C(4)  | 106.4(7) |
| N(1)-C(3)-C(9)  | 117.8(7) |
| C(4)-C(3)-C(9)  | 134.0(7) |
| C(5)-C(4)-C(3)  | 110.0(7) |
| C(5)-C(4)-Br(1) | 125.0(6) |

**Table 3. Continued**

---

|                  |           |
|------------------|-----------|
| C(3)-C(4)-Br(1)  | 125.0(6)  |
| C(4)-C(5)-C(27)  | 132.1(10) |
| C(4)-C(5)-C(1)   | 104.5(7)  |
| C(27)-C(5)-C(1)  | 123.4(10) |
| C(4)-C(5)-C(21)  | 127.7(10) |
| C(27)-C(5)-C(21) | 8(2)      |
| C(1)-C(5)-C(21)  | 127.1(10) |
| N(3)-C(6)-C(7)   | 107.2(7)  |
| N(3)-C(6)-C(15)  | 115.8(8)  |
| C(7)-C(6)-C(15)  | 136.0(8)  |
| C(8)-C(7)-C(6)   | 108.8(7)  |
| C(8)-C(7)-Br(2)  | 126.6(7)  |
| C(6)-C(7)-Br(2)  | 124.5(6)  |
| C(7)-C(8)-C(2)   | 106.3(7)  |
| C(7)-C(8)-C(39)  | 127.0(10) |
| C(2)-C(8)-C(39)  | 126.5(10) |
| C(7)-C(8)-C(33)  | 128.6(10) |
| C(2)-C(8)-C(33)  | 125.1(9)  |
| C(39)-C(8)-C(33) | 3(3)      |
| C(14)-C(9)-C(10) | 118.4(8)  |
| C(14)-C(9)-C(3)  | 125.5(8)  |
| C(10)-C(9)-C(3)  | 115.8(7)  |
| O(2)-C(10)-C(11) | 118.1(8)  |



**Table 3. Continued**

---

|                   |          |
|-------------------|----------|
| O(2)-C(10)-C(9)   | 122.8(8) |
| C(11)-C(10)-C(9)  | 119.0(8) |
| C(12)-C(11)-C(10) | 120.9(8) |
| C(12)-C(11)-H(11) | 119.5    |
| C(10)-C(11)-H(11) | 119.5    |
| C(11)-C(12)-C(13) | 119.5(8) |
| C(11)-C(12)-H(12) | 120.3    |
| C(13)-C(12)-H(12) | 120.3    |
| C(14)-C(13)-C(12) | 121.6(8) |
| C(14)-C(13)-H(13) | 119.2    |
| C(12)-C(13)-H(13) | 119.2    |
| C(13)-C(14)-C(9)  | 120.5(8) |
| C(13)-C(14)-H(14) | 119.7    |
| C(9)-C(14)-H(14)  | 119.7    |
| C(16)-C(15)-C(20) | 119.0(8) |
| C(16)-C(15)-C(6)  | 117.8(8) |
| C(20)-C(15)-C(6)  | 123.0(8) |
| O(1)-C(16)-C(17)  | 117.7(8) |
| O(1)-C(16)-C(15)  | 122.2(7) |
| C(17)-C(16)-C(15) | 120.1(8) |
| C(18)-C(17)-C(16) | 119.9(9) |
| C(18)-C(17)-H(17) | 120.0    |
| C(16)-C(17)-H(17) | 120.0    |
| C(19)-C(18)-C(17) | 120.1(9) |

**Table 3. Continued**

---

|                   |           |
|-------------------|-----------|
| C(19)-C(18)-H(18) | 120.0     |
| C(17)-C(18)-H(18) | 120.0     |
| C(20)-C(19)-C(18) | 121.6(9)  |
| C(20)-C(19)-H(19) | 119.2     |
| C(18)-C(19)-H(19) | 119.2     |
| C(19)-C(20)-C(15) | 119.3(9)  |
| C(19)-C(20)-H(20) | 120.4     |
| C(15)-C(20)-H(20) | 120.4     |
| C(26)-C(21)-C(22) | 119.1(13) |
| C(26)-C(21)-C(5)  | 122.6(18) |
| C(22)-C(21)-C(5)  | 118.2(18) |
| C(23)-C(22)-C(21) | 119.7(13) |
| C(23)-C(22)-H(22) | 120.2     |
| C(21)-C(22)-H(22) | 120.2     |
| C(24)-C(23)-C(22) | 118.7(13) |
| C(24)-C(23)-H(23) | 120.6     |
| C(22)-C(23)-H(23) | 120.6     |
| C(23)-C(24)-C(25) | 123.7(12) |
| C(23)-C(24)-Br(3) | 114.8(17) |
| C(25)-C(24)-Br(3) | 121.3(15) |
| C(24)-C(25)-C(26) | 116.9(13) |
| C(24)-C(25)-H(25) | 121.6     |
| C(26)-C(25)-H(25) | 121.6     |
| C(21)-C(26)-C(25) | 121.8(14) |

**Table 3. Continued**

---

|                   |           |
|-------------------|-----------|
| C(21)-C(26)-H(26) | 119.1     |
| C(25)-C(26)-H(26) | 119.1     |
| C(32)-C(27)-C(28) | 118.1(13) |
| C(32)-C(27)-C(5)  | 124.7(17) |
| C(28)-C(27)-C(5)  | 117.0(19) |
| C(29)-C(28)-C(27) | 121.4(14) |
| C(29)-C(28)-H(28) | 119.3     |
| C(27)-C(28)-H(28) | 119.3     |
| C(30)-C(29)-C(28) | 118.1(14) |
| C(30)-C(29)-H(29) | 121.0     |
| C(28)-C(29)-H(29) | 121.0     |
| C(31)-C(30)-C(29) | 122.6(12) |
| C(31)-C(30)-Br(4) | 122.9(15) |
| C(29)-C(30)-Br(4) | 114.3(16) |
| C(30)-C(31)-C(32) | 118.8(13) |
| C(30)-C(31)-H(31) | 120.6     |
| C(32)-C(31)-H(31) | 120.6     |
| C(27)-C(32)-C(31) | 121.0(13) |
| C(27)-C(32)-H(32) | 119.5     |
| C(31)-C(32)-H(32) | 119.5     |
| C(38)-C(33)-C(34) | 119.0(13) |
| C(38)-C(33)-C(8)  | 120.4(19) |
| C(34)-C(33)-C(8)  | 120.6(19) |
| C(35)-C(34)-C(33) | 120.4(13) |

**Table 3. Continued**

---

|                   |           |
|-------------------|-----------|
| C(35)-C(34)-H(34) | 119.8     |
| C(33)-C(34)-H(34) | 119.8     |
| C(36)-C(35)-C(34) | 118.0(13) |
| C(36)-C(35)-H(35) | 121.0     |
| C(34)-C(35)-H(35) | 121.0     |
| C(35)-C(36)-C(37) | 123.8(12) |
| C(35)-C(36)-Br(5) | 117.2(18) |
| C(37)-C(36)-Br(5) | 118.9(16) |
| C(36)-C(37)-C(38) | 116.9(13) |
| C(36)-C(37)-H(37) | 121.6     |
| C(38)-C(37)-H(37) | 121.6     |
| C(33)-C(38)-C(37) | 121.9(14) |
| C(33)-C(38)-H(38) | 119.0     |
| C(37)-C(38)-H(38) | 119.0     |
| C(44)-C(39)-C(40) | 119.4(13) |
| C(44)-C(39)-C(8)  | 119(2)    |
| C(40)-C(39)-C(8)  | 121.6(19) |
| C(41)-C(40)-C(39) | 120.4(13) |
| C(41)-C(40)-H(40) | 119.8     |
| C(39)-C(40)-H(40) | 119.8     |
| C(42)-C(41)-C(40) | 117.8(13) |
| C(42)-C(41)-H(41) | 121.1     |
| C(40)-C(41)-H(41) | 121.1     |
| C(43)-C(42)-C(41) | 123.8(12) |

**Table 3. Continued**

---

|                   |           |
|-------------------|-----------|
| C(43)-C(42)-Br(6) | 123.0(16) |
| C(41)-C(42)-Br(6) | 113.1(17) |
| C(42)-C(43)-C(44) | 117.3(13) |
| C(42)-C(43)-H(43) | 121.4     |
| C(44)-C(43)-H(43) | 121.4     |
| C(39)-C(44)-C(43) | 121.2(14) |
| C(39)-C(44)-H(44) | 119.4     |
| C(43)-C(44)-H(44) | 119.4     |

---

Symmetry transformations used to generate equivalent atoms:

**Table 4. Anisotropic displacement parameters ( $\text{\AA}^2 \times 10^3$ ) for KBB0908. The anisotropic displacement factor exponent takes the form:  $-2\pi^2 [ h^2 a^{*2} U^{11} + \dots + 2 h k a^* b^* U^{12} ]$**

|       | U <sup>11</sup> | U <sup>22</sup> | U <sup>33</sup> | U <sup>23</sup> | U <sup>13</sup> | U <sup>12</sup> |
|-------|-----------------|-----------------|-----------------|-----------------|-----------------|-----------------|
| B(1)  | 25(6)           | 28(6)           | 24(5)           | 6(5)            | 7(4)            | 2(5)            |
| Br(1) | 38(1)           | 25(1)           | 30(1)           | 3(1)            | 2(1)            | 7(1)            |
| Br(2) | 44(1)           | 124(1)          | 44(1)           | 36(1)           | 20(1)           | 54(1)           |
| N(1)  | 20(4)           | 19(4)           | 19(4)           | 2(3)            | 2(3)            | -1(3)           |
| N(2)  | 12(4)           | 19(4)           | 31(4)           | -5(3)           | 5(3)            | 2(3)            |
| N(3)  | 15(4)           | 27(4)           | 23(4)           | -2(3)           | 3(3)            | 0(3)            |
| O(1)  | 29(3)           | 26(3)           | 24(3)           | -2(3)           | 11(3)           | -4(3)           |
| O(2)  | 26(3)           | 28(3)           | 22(3)           | -1(3)           | 5(3)            | -4(3)           |
| C(1)  | 17(4)           | 18(4)           | 29(5)           | 7(4)            | 5(4)            | 1(4)            |
| C(2)  | 17(4)           | 21(5)           | 27(5)           | 3(4)            | 3(4)            | -7(4)           |
| C(3)  | 30(5)           | 13(4)           | 14(4)           | 6(4)            | 0(4)            | -5(4)           |
| C(4)  | 22(5)           | 19(5)           | 28(5)           | -6(4)           | 2(4)            | 6(4)            |
| C(5)  | 32(5)           | 15(4)           | 23(5)           | -8(4)           | -1(4)           | -1(4)           |
| C(6)  | 21(5)           | 25(5)           | 33(5)           | -1(4)           | 7(4)            | -4(4)           |
| C(7)  | 25(5)           | 24(5)           | 29(5)           | -2(4)           | 7(4)            | 8(4)            |
| C(8)  | 16(4)           | 28(5)           | 30(5)           | 5(4)            | 6(4)            | 6(4)            |
| C(9)  | 27(5)           | 26(5)           | 25(5)           | -4(4)           | 3(4)            | -7(4)           |
| C(10) | 19(5)           | 27(5)           | 28(5)           | 2(4)            | 4(4)            | -14(4)          |
| C(11) | 29(5)           | 27(5)           | 28(5)           | -5(4)           | 13(4)           | -4(4)           |

**Table 4. Continued**


---

|       |       |       |       |        |       |       |
|-------|-------|-------|-------|--------|-------|-------|
| C(12) | 43(6) | 39(6) | 20(5) | 7(5)   | 13(4) | -7(5) |
| C(13) | 37(6) | 31(5) | 26(5) | 12(5)  | 8(4)  | 1(5)  |
| C(14) | 33(5) | 30(5) | 26(5) | -2(4)  | 11(4) | -9(4) |
| C(15) | 24(5) | 27(5) | 30(5) | -12(4) | 8(4)  | -8(4) |
| C(16) | 30(5) | 39(6) | 24(5) | -7(5)  | 16(4) | -8(5) |
| C(17) | 37(6) | 43(6) | 28(5) | -6(5)  | 10(4) | -7(5) |
| C(18) | 33(6) | 34(6) | 50(6) | -10(5) | 17(5) | -6(5) |
| C(19) | 22(5) | 46(6) | 48(6) | -15(6) | 13(5) | -4(5) |
| C(20) | 36(6) | 28(5) | 32(5) | -9(4)  | 11(4) | -5(4) |
| C(21) | 18(5) | 16(5) | 28(5) | 0(4)   | 6(4)  | 1(5)  |
| C(22) | 21(5) | 14(5) | 34(5) | 1(5)   | 3(5)  | 0(5)  |
| C(23) | 24(5) | 20(5) | 37(5) | -3(5)  | 3(5)  | 2(5)  |
| C(24) | 25(5) | 21(5) | 32(5) | -5(5)  | 6(5)  | -2(5) |
| C(25) | 30(5) | 26(5) | 31(5) | -3(5)  | 8(5)  | 0(5)  |
| C(26) | 23(5) | 18(5) | 33(5) | -2(5)  | 5(5)  | 2(5)  |
| Br(3) | 53(3) | 12(4) | 61(3) | -3(3)  | 36(2) | 7(3)  |
| C(27) | 18(5) | 15(5) | 30(5) | 0(4)   | 5(4)  | 1(5)  |
| C(28) | 24(5) | 20(5) | 31(5) | 4(4)   | 5(4)  | 0(4)  |
| C(29) | 25(5) | 26(5) | 34(5) | -2(5)  | 0(5)  | 0(5)  |
| C(30) | 23(5) | 21(5) | 32(5) | -6(5)  | 7(5)  | 0(5)  |
| C(31) | 23(6) | 22(5) | 31(6) | -6(5)  | 3(5)  | -3(5) |
| C(32) | 13(5) | 18(5) | 29(5) | -4(5)  | 4(5)  | -3(5) |
| Br(4) | 41(3) | 11(4) | 57(3) | -5(3)  | 31(2) | 2(3)  |
| C(33) | 17(4) | 23(5) | 24(5) | -2(4)  | 6(4)  | 2(4)  |

**Table 4. Continued**

---

|       |       |       |       |       |       |        |
|-------|-------|-------|-------|-------|-------|--------|
| C(34) | 21(5) | 22(5) | 24(5) | -3(5) | 9(4)  | 2(4)   |
| C(35) | 24(5) | 20(5) | 29(5) | -3(5) | 7(4)  | 1(5)   |
| C(36) | 28(5) | 20(4) | 28(5) | -2(4) | 4(4)  | 0(4)   |
| C(37) | 27(5) | 23(5) | 29(5) | -6(5) | 1(5)  | 7(5)   |
| C(38) | 22(5) | 26(5) | 24(5) | 0(5)  | 5(4)  | 4(5)   |
| Br(5) | 45(3) | 9(4)  | 25(2) | -5(3) | 14(2) | -10(3) |
| C(39) | 17(5) | 23(5) | 24(5) | -2(4) | 6(4)  | 2(4)   |
| C(40) | 20(5) | 20(5) | 25(5) | 1(5)  | 6(4)  | -2(5)  |
| C(41) | 25(5) | 22(5) | 28(5) | -1(5) | 4(5)  | 1(5)   |
| C(42) | 28(5) | 20(5) | 27(5) | -2(4) | 5(4)  | 0(4)   |
| C(43) | 26(5) | 23(5) | 27(5) | -2(5) | 2(5)  | 9(5)   |
| C(44) | 21(5) | 25(5) | 22(5) | -1(5) | 3(4)  | 6(5)   |
| Br(6) | 51(2) | 13(4) | 26(2) | -8(3) | 15(2) | -15(4) |

---



**Table 5. Hydrogen coordinates ( $\times 10^4$ ) and isotropic displacement parameters ( $\text{\AA}^2 \times 10^{-3}$ ) for KBB0908.**

|       | x     | y     | z    | U(eq) |
|-------|-------|-------|------|-------|
| H(11) | 2213  | 4491  | 2956 | 32    |
| H(12) | 2851  | 1979  | 3541 | 40    |
| H(13) | 3623  | -1756 | 3460 | 38    |
| H(14) | 3689  | -3156 | 2806 | 35    |
| H(17) | 92    | 520   | 2180 | 43    |
| H(18) | -1047 | 3139  | 2102 | 45    |
| H(19) | -1271 | 6837  | 1654 | 45    |
| H(20) | -364  | 8101  | 1289 | 38    |
| H(22) | 4185  | -5449 | 1247 | 29    |
| H(23) | 5014  | -6114 | 794  | 33    |
| H(25) | 5189  | 1999  | 662  | 35    |
| H(26) | 4305  | 2651  | 1086 | 30    |
| H(28) | 5097  | -986  | 1634 | 30    |
| H(29) | 5933  | -1545 | 1184 | 36    |
| H(31) | 4015  | -2414 | 192  | 31    |
| H(32) | 3181  | -1686 | 638  | 24    |
| H(34) | 2999  | 6689  | 566  | 26    |
| H(35) | 3305  | 7530  | -82  | 29    |
| H(37) | 975   | 6873  | -700 | 33    |

**Table 5. Continued**

---

|       |      |       |      |    |
|-------|------|-------|------|----|
| H(38) | 678  | 6241  | -45  | 29 |
| H(40) | 2110 | 2371  | 215  | 26 |
| H(41) | 2354 | 3243  | -448 | 30 |
| H(43) | 1803 | 11150 | -350 | 32 |
| H(44) | 1504 | 10205 | 299  | 28 |

---

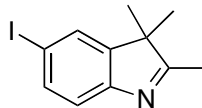
## APPENDIX C

### EXPERIMENTAL DATA FOR CHAPTER IV

#### General Procedures.

Melting points are uncorrected. High field NMR spectra were recorded on Varian Unity Plus ( $^1\text{H}$  at 300 MHz,  $^{13}\text{C}$  at 75 MHz) NMR spectrometers. Chemical shifts are reported in units of ppm relative to solvent ( $\text{CDCl}_3$ : 7.27 ppm for  $^1\text{H}$ , 77.0 ppm for  $^{13}\text{C}$ ; Acetone- $d_6$ : 2.04 ppm for  $^1\text{H}$ , 29.9 ppm for  $^{13}\text{C}$ ;  $\text{DMSO}-d_6$ : 2.50 ppm for  $^1\text{H}$ , 39.5 ppm for  $^{13}\text{C}$ ;  $\text{D}_2\text{O}$ : 4.63 ppm for  $^1\text{H}$ ;  $\text{CD}_3\text{OD}$ : 3.30 ppm for  $^1\text{H}$ , 49.0 ppm for  $^{13}\text{C}$ ; 77.0 ppm for  $^{13}\text{C}$ ;  $\text{CD}_3\text{CN}$ : 1.93 ppm for  $^1\text{H}$ , 1.3 ppm for  $^{13}\text{C}$ ). Mass spectra were obtained from the Mass Spectrometry Applications Laboratory at Texas A&M University. Thin layer chromatography was performed using silica gel (230-600 mesh).  $\text{CH}_2\text{Cl}_2$ , THF, DMF, methanol, triethylamine, and toluene were distilled from appropriate drying agents. Other chemicals were purchased from commercial suppliers and used as received.

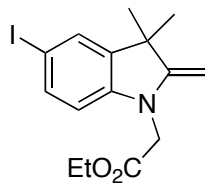
UV spectra were recorded in 1 cm path length quartz cuvettes on a Milton Roy Spectronic 3000 diode array UV spectrometer at concentrations between 1 and 10  $\mu\text{M}$ . Fluorescence emission spectra were recorded in 1 cm path length quartz cells on a SLM Aminco Fluorimeter. All fluorescence spectra were recorded at a concentration of 1.0  $\mu\text{M}$ .

**5-iodo-2,3,3-trimethyl-3*H*-indole**

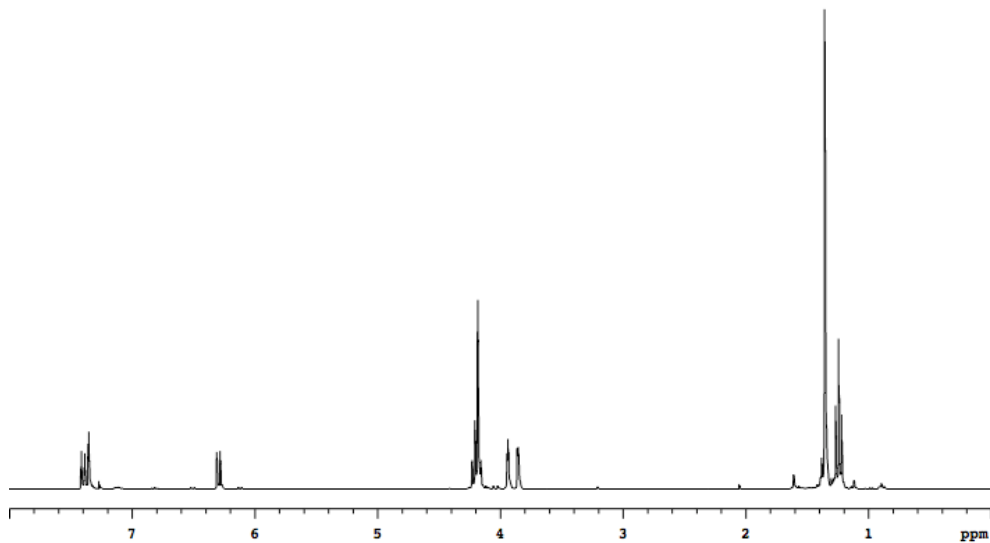
5-Iodo-2,3,3-trimethyl-3*H*-indole was synthesized according to the procedure described in the literature.[Moreau, 1974 #7750] The data obtained matched the ones reported in the literature.

$\delta_{\text{H}}$  (300 MHz,  $\text{CDCl}_3$ ): 7.45 – 7.42 (m, 2H), 7.10 (m, 1H);  $\delta_{\text{C}}$  (75.4 MHz,  $\text{CDCl}_3$ ): 187.9, 153.2, 147.9, 136.4, 130.4, 121.6, 89.7, 60.0, 53.7, 20.7, 13.9.

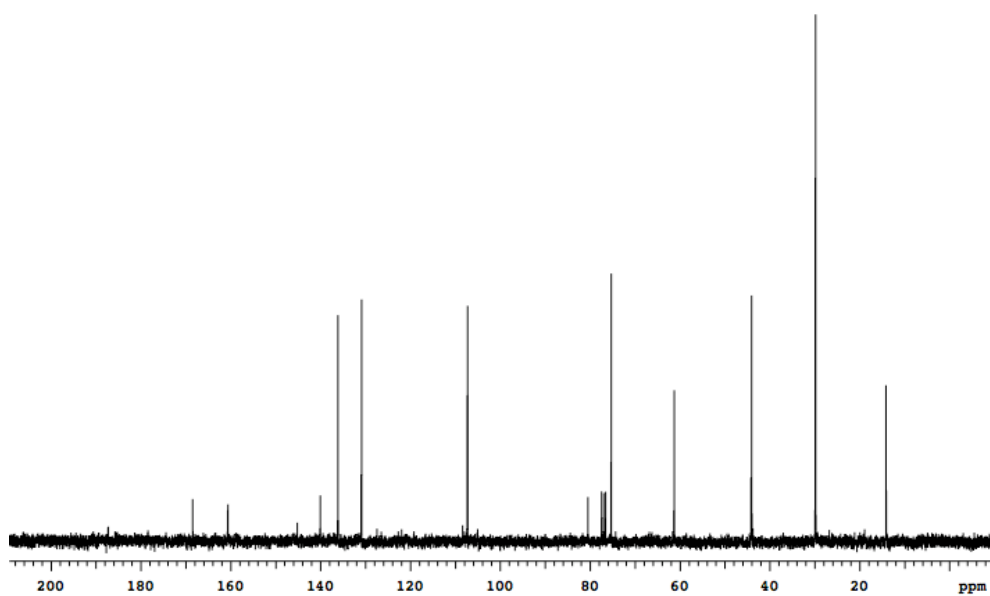
**Ethyl 2-(5-iodo-3,3-dimethyl-2-methyleneindolin-1-yl)acetate (305b)**



5-Iodo-2,3,3-trimethyl-3*H*-indole (1.00 g, 3.50 mmol) and ethyl iodoacetate (0.901 g, 4.21 mmol) were weighed into a sealed tube. The mixture was heated at 85°C for 12 h. After cooling to room temperature, 1N NaOH solution (20 mL) was added and stirred for 1 h. The reaction mixture was extracted with dichloromethane three times. The organic layers were combined and evaporated to a residue which was purified by flash column chromatography in 10% EtOAc/hexane to give the product as a brown oil (0.988 g, 76%).  $\delta_{\text{H}}$  (300 MHz,  $\text{CDCl}_3$ ): 7.40 (dd,  $J=9.0$  Hz,  $J=2.0$  Hz, 1H), 7.36 (d,  $J=2.0$  Hz, 1H), 6.30 (dd,  $J=9.0$  Hz,  $J=2.0$  Hz, 1H), 4.19 (q,  $J=8.0$  Hz, 2H), 4.19 (s, 2H), 3.94 (d,  $J=3.0$  Hz, 1H), 3.87 (d,  $J=3.0$  Hz, 1H), 1.35 (s, 6H), 1.24 (t,  $J=8.0$  Hz, 3H);  $\delta_{\text{C}}$  (75.4 MHz,  $\text{CDCl}_3$ ): 168.6, 160.8, 145.35, 140.27, 136.30, 131.07, 107.51, 80.71, 75.53, 61.47, 44.41, 44.25, 30.04, 14.34; HR-MS (MALDI) for  $\text{C}_{15}\text{H}_{19}\text{INO}_2$  ( $\text{M}+\text{H}^+$ ) calc'd 372.0461, found 372.0445.

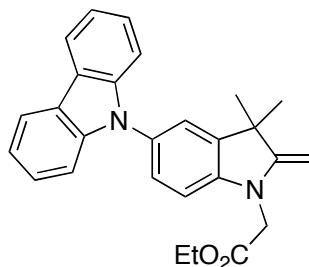


$^1\text{H}$  NMR for compound **305b** (300 MHz,  $\text{CDCl}_3$ ).



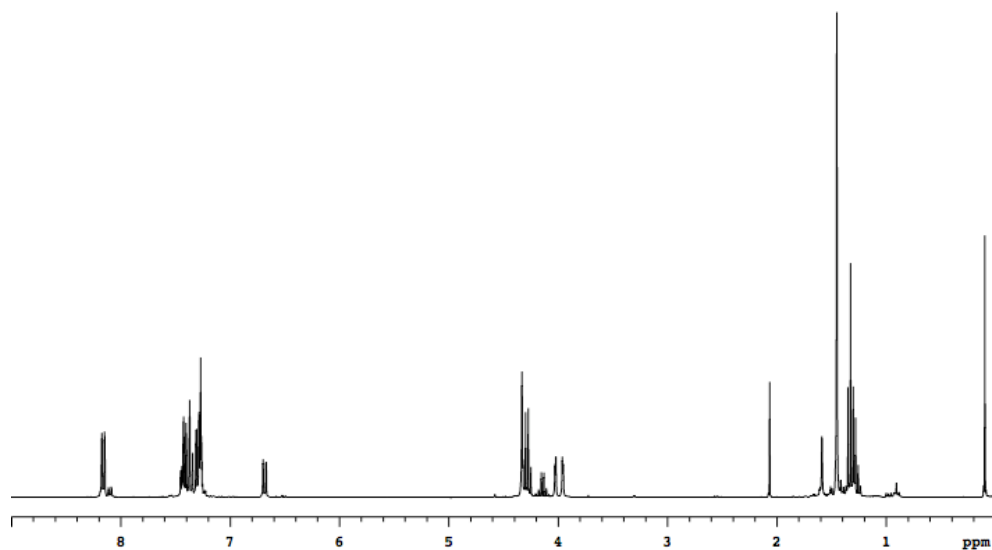
$^{13}\text{C}$  NMR for compound **305b** (75 MHz,  $\text{CDCl}_3$ ).

**Ethyl 2-(5-(9*H*-carbazol-9-yl)-3,3-dimethyl-2-methyleneindolin-1-yl)acetate  
(306b)**

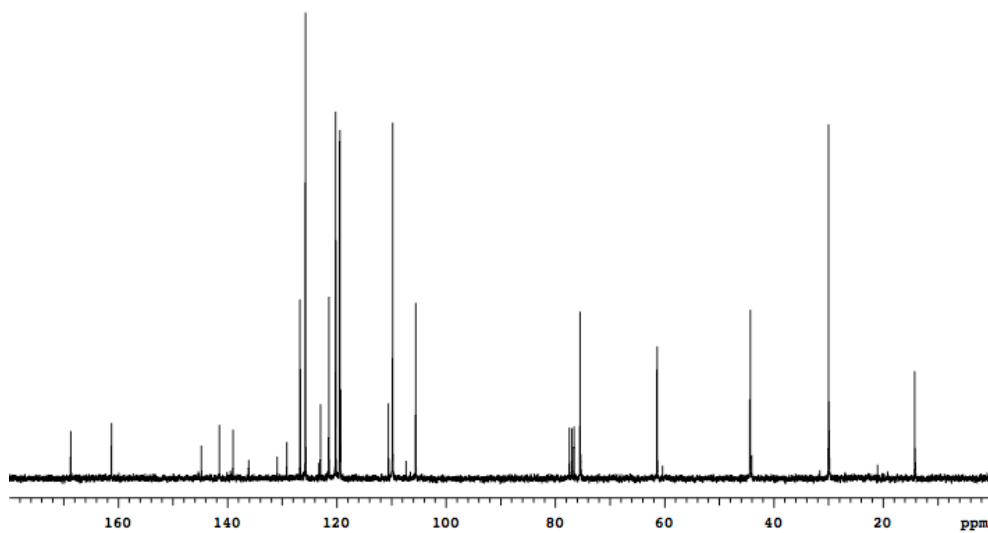


Compound **305b** (200 mg, 0.54 mmol), carbazole (90 mg, 0.54 mmol), 1,2-*trans*-diaminocyclohexane (12 mg, 0.11 mmol), CuI (5 mg, 0.03 mmol), and Cs<sub>2</sub>CO<sub>3</sub> (369 mg, 1.13 mmol) were weighed into a round-bottom flask, then dioxane (2 mL) was added. The mixture was heated at 100°C for 17 h. After cooling to room temperature, the reaction mixture was diluted with ether and filtered through a pad of celite. The residue after removal of solvent was purified by flash column chromatography using 20% EtOAc/hexane to give the product as a white solid (134 mg, 53%).  $\delta_{\text{H}}$  (300 MHz, CDCl<sub>3</sub>): 8.16 (d,  $J=8.0$  Hz, 2H), 7.43–7.26 (m, 8H), 6.68 (d,  $J=8.0$  Hz, 1H), 4.33 (s, 2H), 4.28 (q,  $J=8.0$  Hz, 2H), 4.02 (d,  $J=3.0$  Hz, 1H), 3.96 (d,  $J=3.0$  Hz, 1H), 1.45 (s, 6H), 1.32 (t,  $J=8.0$  Hz, 3H);  $\delta_{\text{C}}$  (300 MHz, CDCl<sub>3</sub>): 168.94, 161.48, 144.99, 141.71, 139.22, 136.35, 131.12, 129.38, 126.95, 125.96, 123.21, 121.67, 120.47, 120.41, 119.67, 119.54, 110.76, 110.00, 107.53, 105.79, 75.71, 61.59, 44.63, 44.52, 30.20, 14.43.



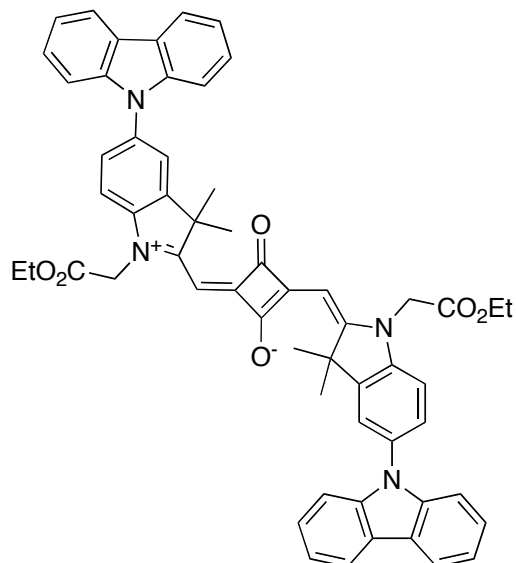


$^1\text{H}$  NMR for compound **306b** (300 MHz,  $\text{CDCl}_3$ ).

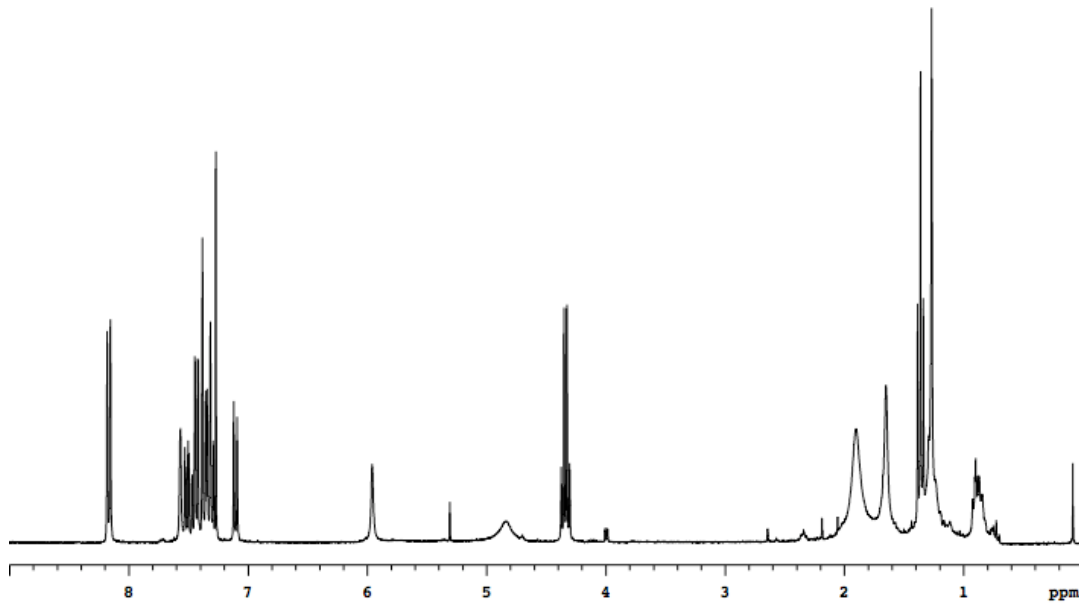


$^{13}\text{C}$  NMR for compound **306b** (75 MHz,  $\text{CDCl}_3$ ).

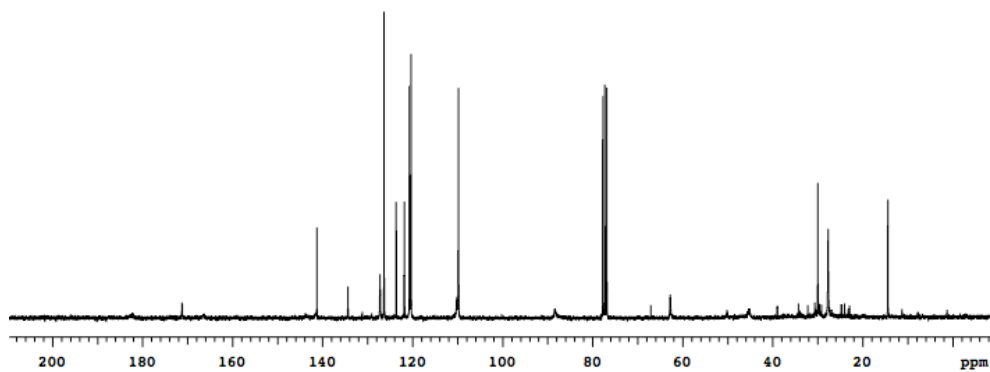
### Compound 303b



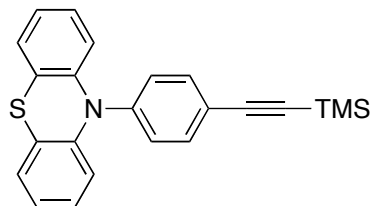
Compound **306b** (24 mg, 0.06 mmol) and squaric acid (3 mg, 0.03 mmol) were placed in a round-bottom flask. A mixture of *n*-BuOH/toluene (15 mL, 1:1 v/v) was added. The mixture was refluxed for 16 h. Water was azeotropically removed by using a Dean–Stark trap. After cooling to room temperature, the reaction mixture was filtered to give a dark-blue solid, which was further washed with ether three times (15 mg, 66%). A sample for analysis was obtained by further purification through flash column chromatography.  $\delta_{\text{H}}$  (300 MHz,  $\text{CDCl}_3$ ) 8.16 (d,  $J=8.0$  Hz, 4H), 7.56–7.27 (m, 16H), 7.10 (d,  $J=8.0$  Hz, 2H), 6.02 (s, 2H), 4.33 (q,  $J=7.2$  Hz, 4H), 1.83 (br s, 12H), 1.36 (t,  $J=7.2$  Hz, 6 H);  $\delta_{\text{C}}$  (75 MHz,  $\text{CDCl}_3$ ) 171.1, 141.2, 134.3, 127.1, 126.2, 123.5, 121.8, 121.7, 120.6, 120.3, 110.1, 109.7, 88.2, 67.0, 62.7; HR-MS (MALDI) for  $\text{C}_{58}\text{H}_{51}\text{N}_4\text{O}_6$  ( $\text{M}+\text{H}^+$ ) calcd 899.3809, found 899.3825.



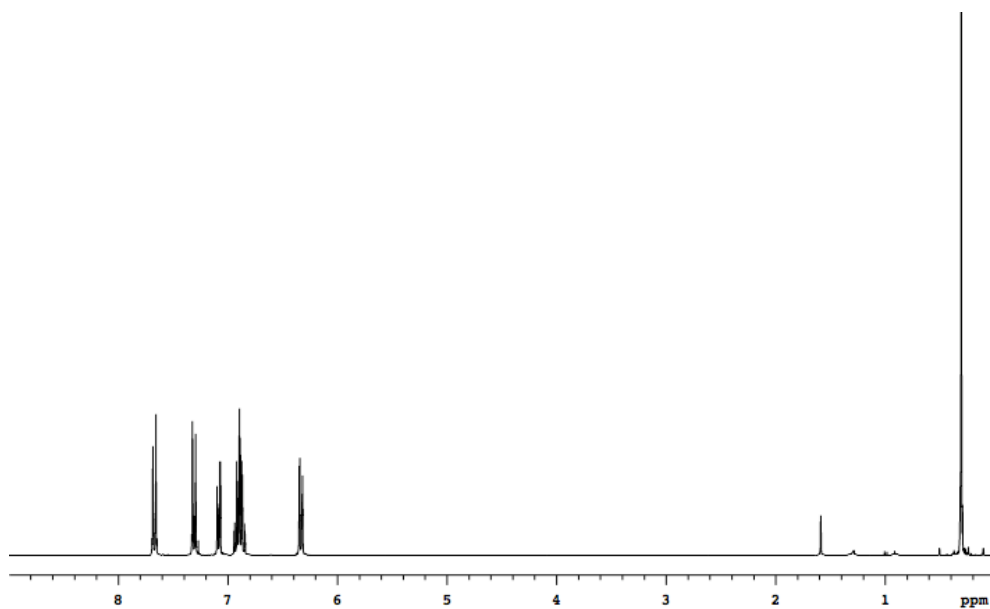
$^1\text{H}$  NMR for compound **303b** (300 MHz,  $\text{CDCl}_3$ ).



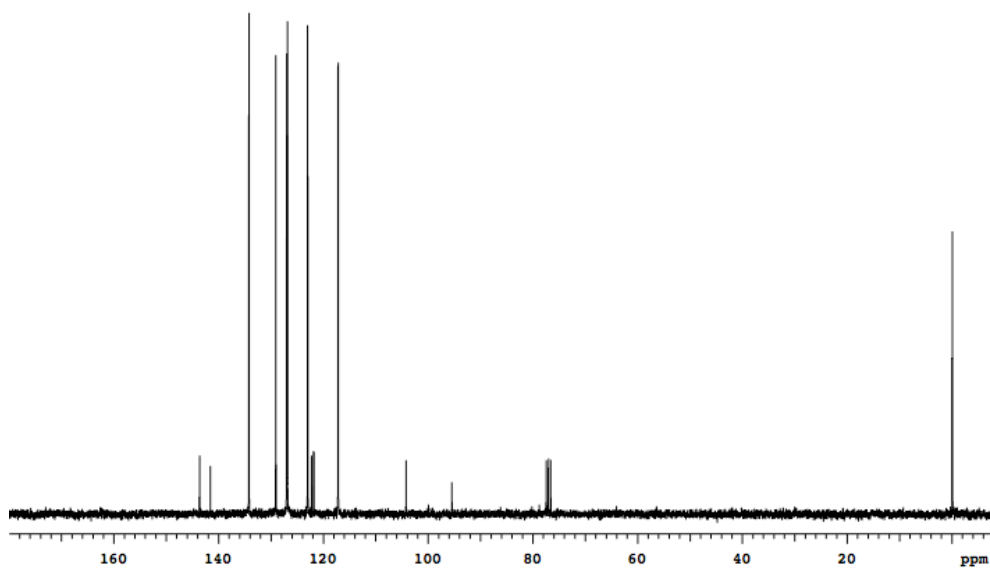
$^{13}\text{C}$  NMR for compound **303b** (75 MHz,  $\text{CDCl}_3$ ).

**Compound 311**

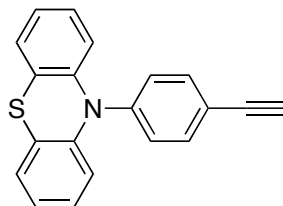
A schlenk tube equipped with a stir bar is charged with phenothiazine (1.00 g, 5.02 mmol), 4-bromophenylethynyl trimethyl silane **310** (1.15 g, 4.56 mmol),  $\text{Pd}_2(\text{dba})_3$  (0.05 g, 0.06 mmol) and sodium *tert*-butoxide (0.61 g, 6.38 mmol). The tube is purged with nitrogen, then the ligand (0.05 g, 0.18 mmol) is added inside the glove box. Toluene (5 mL) is finally added and the reaction mixture is heated at 85 °C until completion of the reaction according to tlc (~ 3 h). The reaction is then cooled to room temperature, diluted with ether and filtered over celite. After removal of the solvents, the residue obtained is purified by column chromatography eluted with 5 % ethyl acetate:hexanes. The titled compound is obtained in 34 % yield (0.57 g) as a white solid.  $\delta_{\text{H}}$  (300 MHz,  $\text{CDCl}_3$ ) 7.64 (d,  $J = 8.5$  Hz, 2H), 7.28 (d,  $J = 8.5$  Hz, 2H), 7.07 – 7.04 (m, 2H), 6.92 – 6.82 (m, 4H), 6.32 – 6.29 (m, 2H), 0.28 (s, 9H);  $\delta_{\text{C}}$  (75 MHz,  $\text{CDCl}_3$ ) 143.8, 141.7, 134.4, 129.2, 127.2, 127.0, 123.2, 122.4, 122.0, 117.4, 104.4, 95.6, 0.15.



$^1\text{H}$  NMR for compound **311** (300 MHz,  $\text{CDCl}_3$ ).

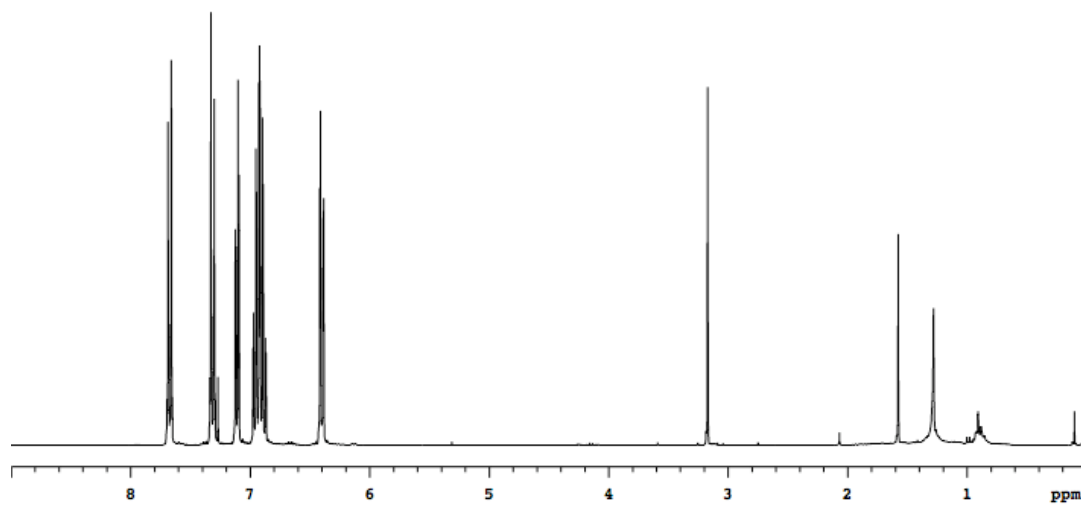


$^{13}\text{C}$  NMR for compound **311** (75 MHz,  $\text{CDCl}_3$ ).

**Compound 312**

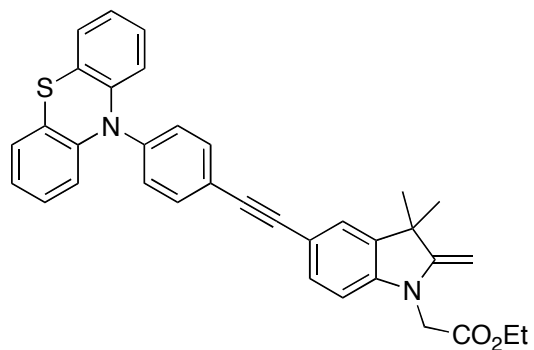
To a solution of **311** (0.57g, 1.54 mmol) in freshly distilled THF (5 mL) was added a solution of tetrabutyl ammonium fluoride (1.0 M, in THF, 2.15 mL). The reaction mixture was stirred at room temperature for 1h, and the solvent removed *in vacuo*. The residual oil obtained was then purified on silica gel with 5 % ethyl acetate:hexanes to give the desired product in 25 % (0.52 g).  $\delta_{\text{H}}$  (300 MHz,  $\text{CDCl}_3$ ) 7.64 (d,  $J= 8.5$  Hz, 2H), 7.28 (d,  $J= 8.5$  Hz, 2H), 7.09 – 7.06 (m, 2H), 6.94 – 6.83 (m, 4H), 6.38 – 6.35 (m, 2H), 3.14 (s, 1H).



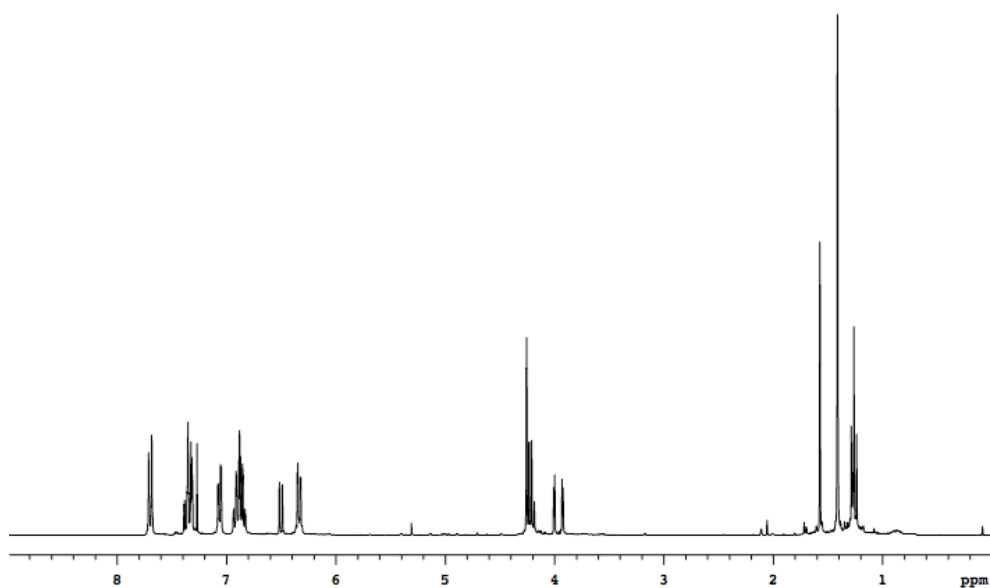


$^1\text{H}$  NMR for compound **312** (300 MHz,  $\text{CDCl}_3$ ).

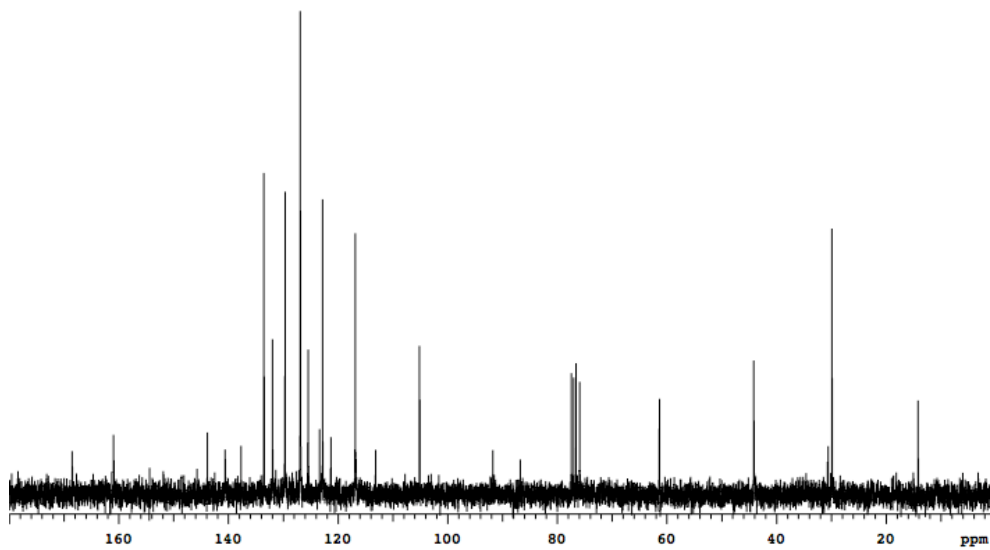
### Compound 313c



A dried-flame Schlenk tube is charged with **312** (0.07g, 0.23 mmol), **305b** (0.06g, 0.15 mmol), copper iodide (0.001 g, 0.007 mmol), Pd(PPh<sub>3</sub>)<sub>4</sub> (0.009g, 0.007 mmol), triethyl amine (0.31g, 3.02 mmol) and 2 mL of toluene. The reaction mixture is heated under nitrogen at 85 °C for 12h. After cooling to room temperature, it is then diluted with ether and filtered over celite. The solvent are removed *in vacuo* and the residual oil purified on silica gel with 30% ethyl acetate:hexanes to give the titled compound in 19% yield (0.09 g).  $\delta_{\text{H}}$  (300 MHz, CDCl<sub>3</sub>) 7.70 (d,  $J$ = 8.5 Hz, 2H), 7.38 – 7.26 (m, 4H), 7.06 (dd,  $J$ = 7 Hz,  $J$ = 1.4 Hz, 2H), 6.94 – 6.83 (m, 4H), 6.50 (d,  $J$ = 8Hz, 1H), 6.33 (dd,  $J$ = 8 Hz,  $J$ = 1.4 Hz, 2H), 4.25 (s, 2H), 4.21 (q,  $J$ = 7 Hz, 2H), 3.96 (dd,  $J$ = 22.7 Hz,  $J$ = 2.7 Hz, 2H), 1.41 (s, 6H), 1.26 (t,  $J$ =7 Hz, 3H);  $\delta_{\text{C}}$  (300 MHz, CDCl<sub>3</sub>) 168.6, 161.1, 145.9, 144.0, 140.7, 137.8, 133.7, 132.1, 129.8, 127.8, 127.0, 125.6, 123.5, 123.0, 121.5, 113.3, 105.3, 91.9, 86.9, 76.1, 61.5, 44.3, 30.8, 14.3 (2 carbons not seen).

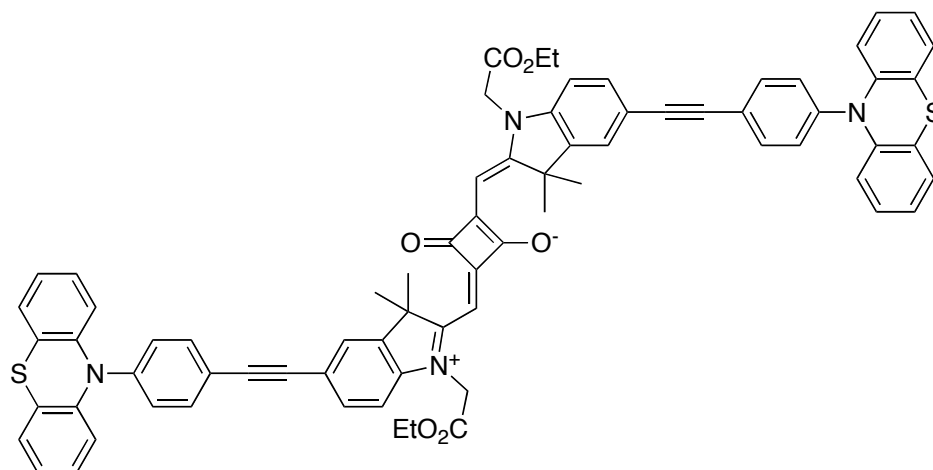


$^1\text{H}$  NMR for compound **313** (300 MHz,  $\text{CDCl}_3$ ).

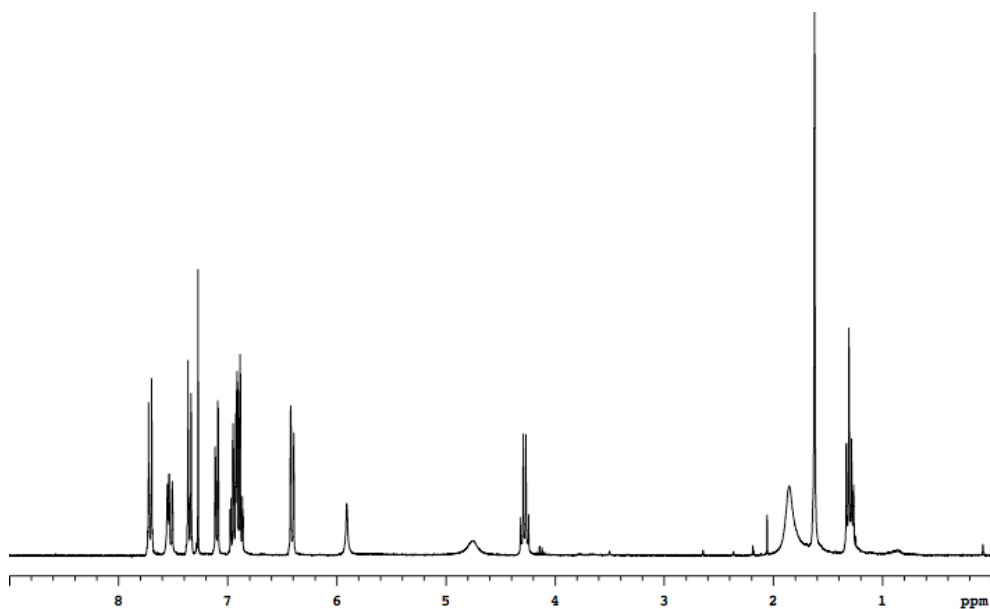


$^{13}\text{C}$  NMR for compound **313** (75 MHz,  $\text{CDCl}_3$ ).

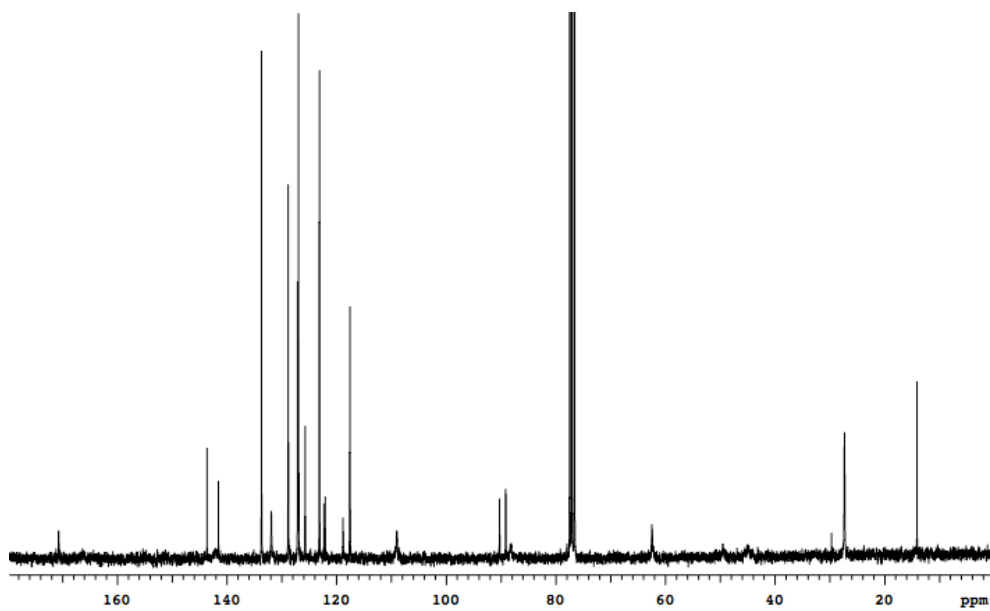
### Compound 309c



Compound **313c** (17 mg, 0.03 mmol) and squaric acid (2 mg, 0.02 mmol) were placed in a round-bottom flask. A mixture of *n*-BuOH/toluene (20 mL, 1:1 v/v) was added. The mixture was refluxed for 48 h. Water was azeotropically removed by using a Dean–Stark trap. After cooling to room temperature, the reaction mixture was filtered to give a dark-blue solid, which was further washed with ether three times. The titled compound was further purified by flash column chromatography eluted first with 40% ethyl acetate:CH<sub>2</sub>Cl<sub>2</sub> then with 20% acetone: CH<sub>2</sub>Cl<sub>2</sub> + 1% MeOH.  $\delta_{\text{H}}$  (300 MHz, CDCl<sub>3</sub>) 7.71 (d,  $J$ = 8.3 Hz, 4 H), 7.55 (bs, 2H), 7.52 (d,  $J$ = 8 Hz, 2H), 7.34 (d,  $J$ = 8.3 Hz, 4 H), 7.10 (dd,  $J$ = 1.7 Hz,  $J$ = 7.3 Hz, 4H), 6.97 – 6.86 (m, 10H), 6.41 (dd,  $J$ = 1.4 Hz,  $J$ = 7.8 Hz, 4H), 5.91 (bs, 2H), 4.28 (q,  $J$ =7 Hz, 4H), 1.62 (s, 12 H), 1.30 (t,  $J$ =7 Hz, 6H) ;  $\delta_{\text{C}}$  (75 MHz, CDCl<sub>3</sub>) 170.9, 143.9, 141.8, 133.9, 132.1, 129.1, 127.3, 127.2, 125.9, 123.4, 122.5, 122.3, 119.1, 117.8, 109.2, 90.5, 89.4, 62.7, 27.5, 14.3 (5 carbons not seen).



$^1\text{H}$  NMR for compound **309c** (300 MHz,  $\text{CDCl}_3$ ).



$^{13}\text{C}$  NMR for compound **309c** (75 MHz,  $\text{CDCl}_3$ ).

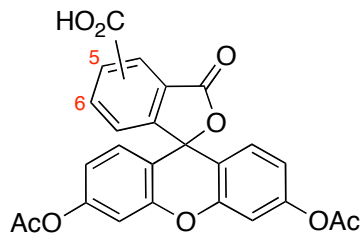
## APPENDIX D

### EXPERIMENTAL DATA FOR CHAPTER V

#### General Procedures.

Melting points are uncorrected. High field NMR spectra were recorded on Varian Unity Plus ( $^1\text{H}$  at 300 MHz,  $^{13}\text{C}$  at 75 MHz) NMR spectrometers. Chemical shifts are reported in units of ppm relative to solvent ( $\text{CDCl}_3$ : 7.27 ppm for  $^1\text{H}$ , 77.0 ppm for  $^{13}\text{C}$ ; Acetone- $d_6$ : 2.04 ppm for  $^1\text{H}$ , 29.9 ppm for  $^{13}\text{C}$ ; DMSO- $d_6$ : 2.50 ppm for  $^1\text{H}$ , 39.5 ppm for  $^{13}\text{C}$ ;  $\text{D}_2\text{O}$ : 4.63 ppm for  $^1\text{H}$ ;  $\text{CD}_3\text{OD}$ : 3.30 ppm for  $^1\text{H}$ , 49.0 ppm for  $^{13}\text{C}$ ; 77.0 ppm for  $^{13}\text{C}$ ;  $\text{CD}_3\text{CN}$ : 1.93 ppm for  $^1\text{H}$ , 1.3 ppm for  $^{13}\text{C}$ ). Mass spectra were obtained from the Mass Spectrometry Applications Laboratory at Texas A&M University. Thin layer chromatography was performed using silica gel (230-600 mesh).  $\text{CH}_2\text{Cl}_2$ , THF, DMF, methanol, triethylamine, and toluene were distilled from appropriate drying agents. Other chemicals were purchased from commercial suppliers and used as received.

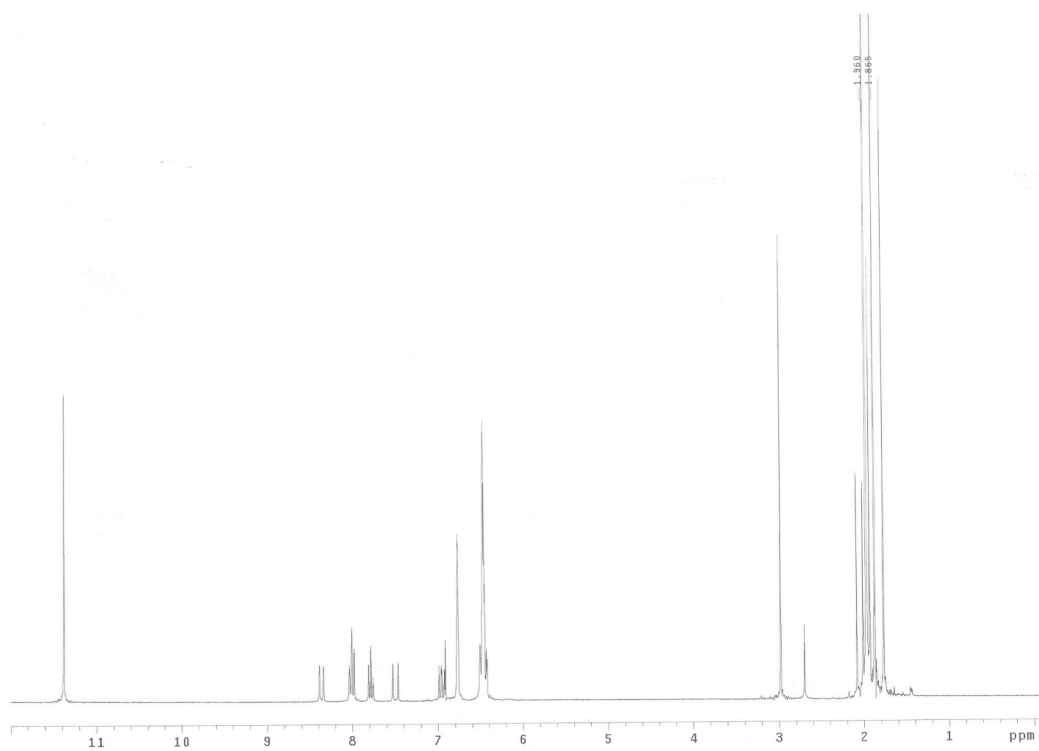
UV spectra were recorded in 1 cm path length quartz cuvettes on a Milton Roy Spectronic 3000 diode array UV spectrometer at concentrations between 1 and 10  $\mu\text{M}$ . Fluorescence emission spectra were recorded in 1 cm path length quartz cells on a SLM Aminco Fluorimeter. All fluorescence spectra were recorded at a concentration of 1.0  $\mu\text{M}$ .

**Carboxy-fluorescein diacetate (5- and 6-isomers, 334)**

Trimellitic anhydride (10g, 52 mmol) was added to a solution of resorcinol (11.5g, 104 mmol) in methanesulfonic acid (1M). The resulting mixture was heated under dry nitrogen at 80 – 85 °C for 48h. The cooled mixture was poured into 7 volumes of ice water, and filtered. The product is then dried *in vacuo* at 60 °C to constant weight.

The dried fluorescein was then converted to the diacetate by refluxing in acetic anhydride for 2 h. After cooling, the solvent was removed and the residue dried *in vacuo*. The product obtained was used such as in the next step.

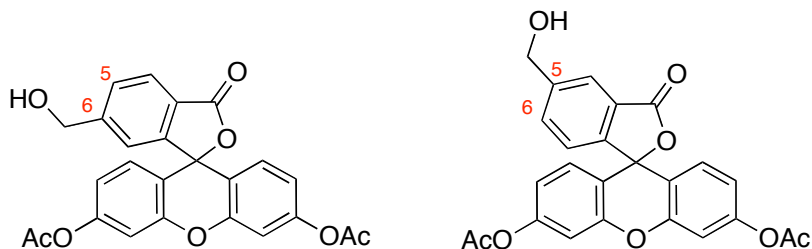
Crude  $\delta_{\text{H}}$  (CDCl<sub>3</sub>, 300 MHz) 11.2 (s, 2H), 8.36 (d,  $J= 14.3$  Hz, 1H), 8.03 – 7.97 (m, 2H), 7.80 – 7.75 (m, 1H), 7.49 (d,  $J=18.4$  Hz), 6.98 – 6.91 (m, 2H), 6.77 (s, 3H), 6.50 – 6.42 (m, 8H), 1.96 (s, 6H), 1.86 (s, 6H).



Crude <sup>1</sup>H NMR for compound **334** (300 MHz, CDCl<sub>3</sub>).



### 5- and 6-(Hydroxymethyl)fluorescein Diacetate (335)



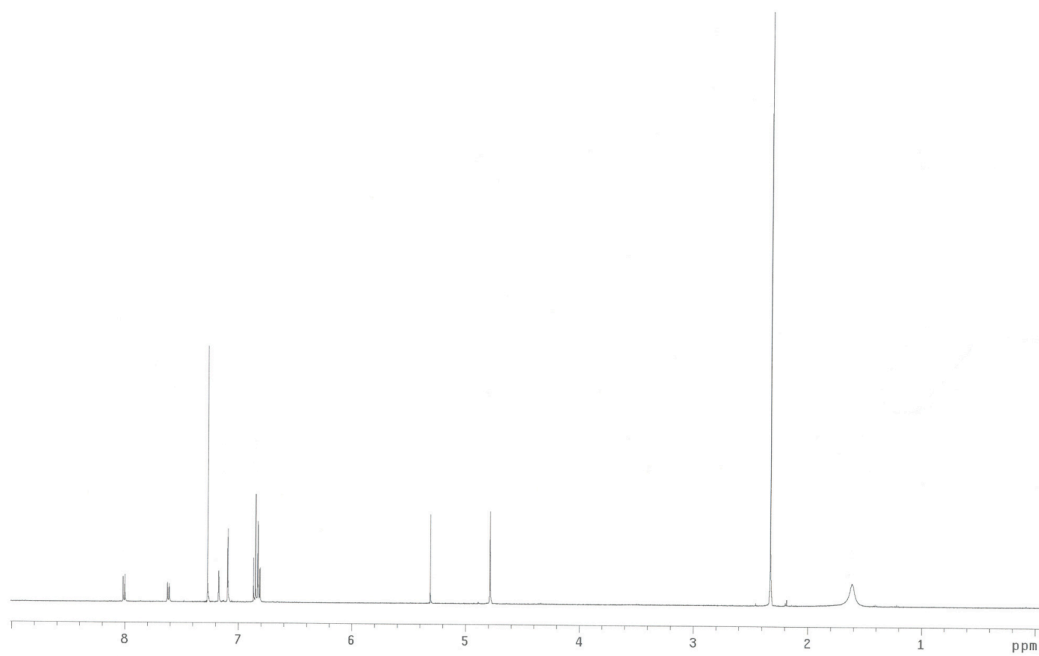
5- (6)-Carboxyfluorescein diacetate **334** (3.83 g, 8.3 mmol) and triethylamine (1.3 mL, 9.1 mmol) were dissolved in THF (40 mL) under a nitrogen atmosphere and cooled to 0 °C. Ethyl chloroformate (0.9 mL, 9.1 mmol) was added at once and the mixture stirred for 1 h. Afterward, the mixture was filtered and added to a sodium phosphate buffer (23 mL, 1 M, pH 6) which had been cooled to 0 °C. NaBH<sub>4</sub> (0.755 mg, 20 mmol) in water (7.5 mL) was then added portionwise with efficient stirring over 5 min. The reaction was then immediately poured into cold water (125 mL) and extracted with ethyl acetate (3 x 75 mL). The extracts were washed with saturated sodium chloride (2 x 30 mL), dried over anhydrous sodium sulfate, and evaporated to give the mixed 5- and 6- (hydroxymethyl) fluorescein diacetate. The isomers were separated by column chromatography eluted with CH<sub>2</sub>Cl<sub>2</sub>/Et<sub>2</sub>O (9:1). The first eluting compound was the 6-isomer (0.55 g, 15 %), the second eluting compound was the 5-isomer (0.94 g, 25 % )

*6-isomer*: δ<sub>H</sub> (300 MHz, CDCl<sub>3</sub>) 7.98 (d, *J*= 8 Hz, 1H), 7.58 (dd, *J*= 8Hz, *J*= 1.2 Hz, 1H), 7.15 (s, 1H), 7.08 (d, *J*= 2 Hz, 2H), 6.85 – 6.79 (m, 4H), 4.78 (s, 2H), 2.30 (s, 6H); δ<sub>C</sub> (75 MHz, CDCl<sub>3</sub>) 169.0, 168.8, 153.6, 151.9, 151.3, 149.5, 128.9, 128.1, 125.1, 124.8, 121.3, 117.7, 116.3, 110.3, 81.4, 64.1, 21.0.

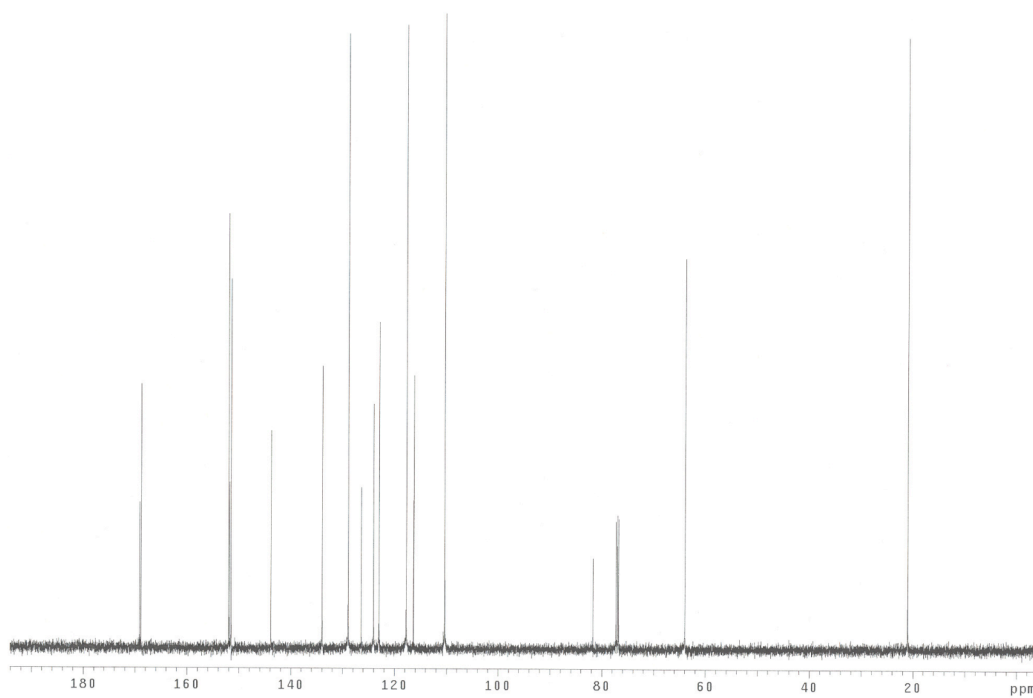
*5-isomer*: δ<sub>H</sub> (500 MHz, CDCl<sub>3</sub>) δ 8.03 (d, *J*= 8 Hz, 1H), 7.67 (dd, *J*= 8Hz, *J*= 1.2 Hz, 1H), 7.14 (d, *J*= 8 Hz, 1H), 7.08 (d, *J*= 2 Hz, 2H), 6.82 – 6.78 (m, 4H), 4.82 (s, 2H), 2.30 (s, 6H); δ<sub>C</sub> (125 MHz, CDCl<sub>3</sub>) δ 169.1, 168.8, 151.9, 151.8, 151.4, 143.8, 133.9, 128.8, 126.3, 124.0, 122.9, 117.6, 116.3, 110.3, 81.7, 63.9, 21.0.

These data matches the ones reported in the literature.<sup>1</sup>

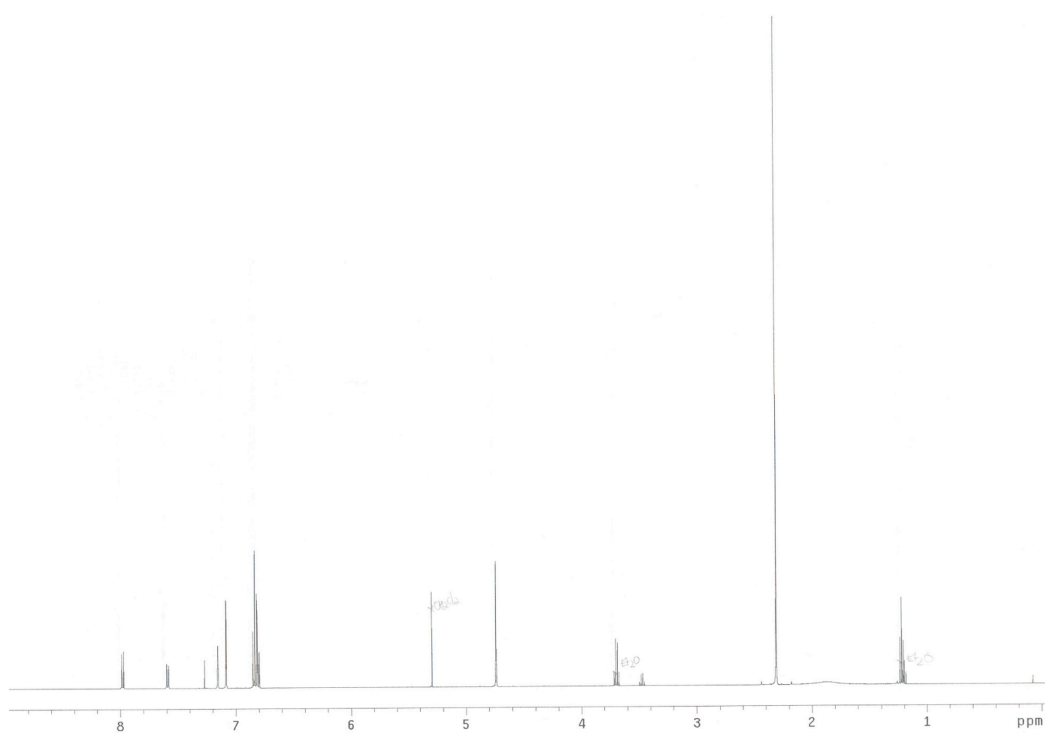
(1) Mattingly, P. G. *Bioconjugate Chem.* **1992**, *3*, 430-1.



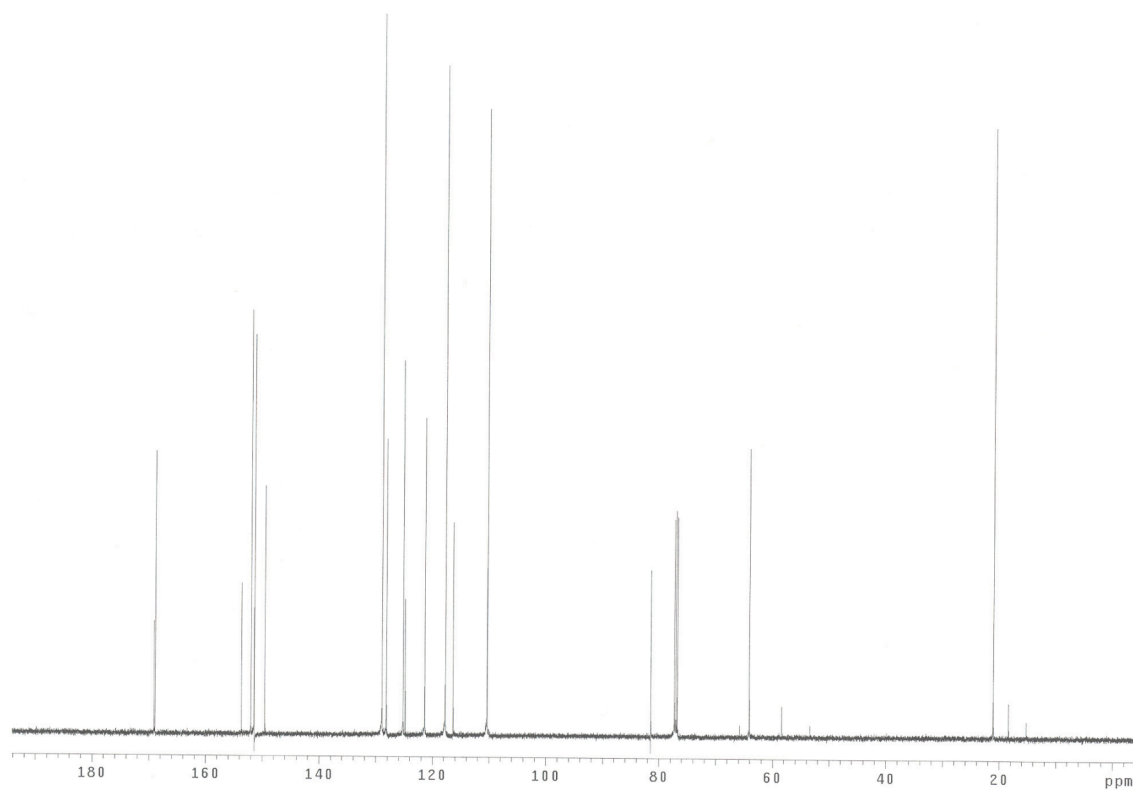
$^1\text{H}$  NMR for compound **335** (5-isomer) (500 MHz,  $\text{CDCl}_3$ ).



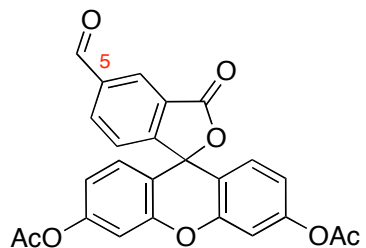
$^{13}\text{C}$  NMR for compound **335** (5-isomer) (125 MHz,  $\text{CDCl}_3$ ).



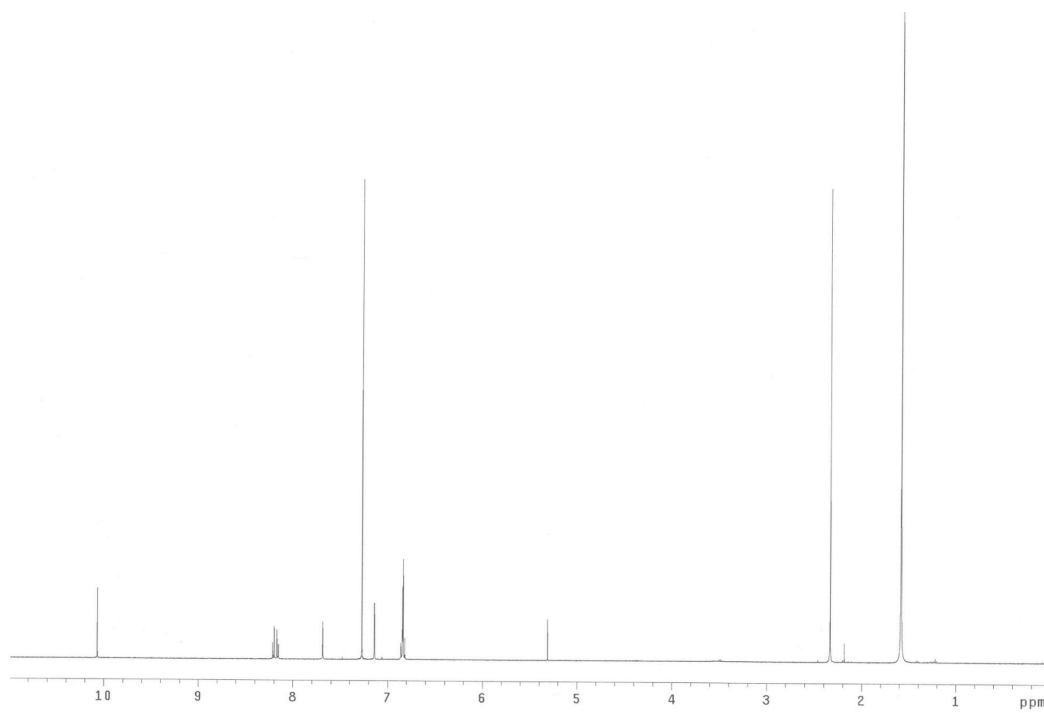
$^1\text{H}$  NMR for compound **335** (6- isomer) (300 MHz,  $\text{CDCl}_3$ ).



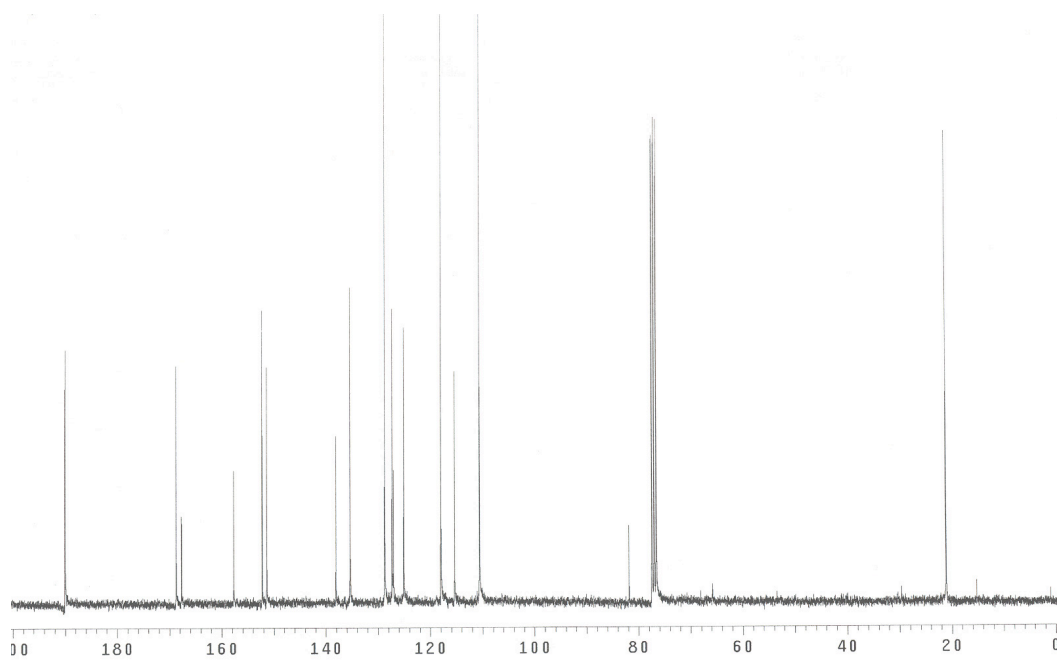
$^{13}\text{C}$  NMR for compound **335** (6- isomer) (75 MHz,  $\text{CDCl}_3$ ).

**5- Carboxyaldehyde Fluorescein Diacetate (332)**

PCC (0.67 g, 3.1 mmol) was added to a suspension of 5-(hydroxymethyl) fluorescein diacetate **335** (0.94 g, 2.1 mmol), molecular sieves 4Å, celite in 50 mL of CH<sub>2</sub>Cl<sub>2</sub>. After stirring at room temperature for 30 min, the reaction mixture is filtered over a pad of silica. The desired product was obtained as an off white solid (0.76 g, 82%) after the solvent was evaporated.  $\delta_{\text{H}}$  (500 MHz, CDCl<sub>3</sub>) 10.1 (s, 1H), 8.21 – 8.15 (m, 2H), 7.68 (s, 1H), 7.14 (d, 2H,  $J= 2\text{Hz}$ ), 6.86 – 6.81 (m, 4H), 2.33 (s, 6H);  $\delta_{\text{C}}$  (125 MHz, CDCl<sub>3</sub>) 190.0, 168.7, 167.6, 157.7, 152.2, 151.3, 138.0, 135.3, 128.6, 127.2, 127.0, 125.0, 117.9, 115.3, 110.6, 81.8, 21.0; MS (APCI) for C<sub>25</sub>H<sub>16</sub>O<sub>8</sub> (M+H<sup>+</sup>) calcd 445.39, found 445.0.



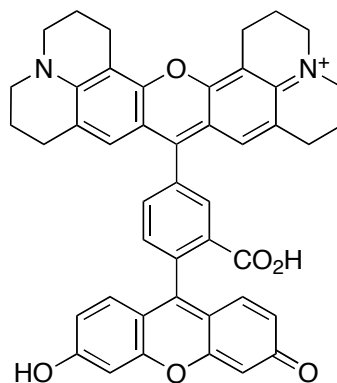
$^1\text{H}$  NMR for compound **332** (500 MHz,  $\text{CDCl}_3$ ).



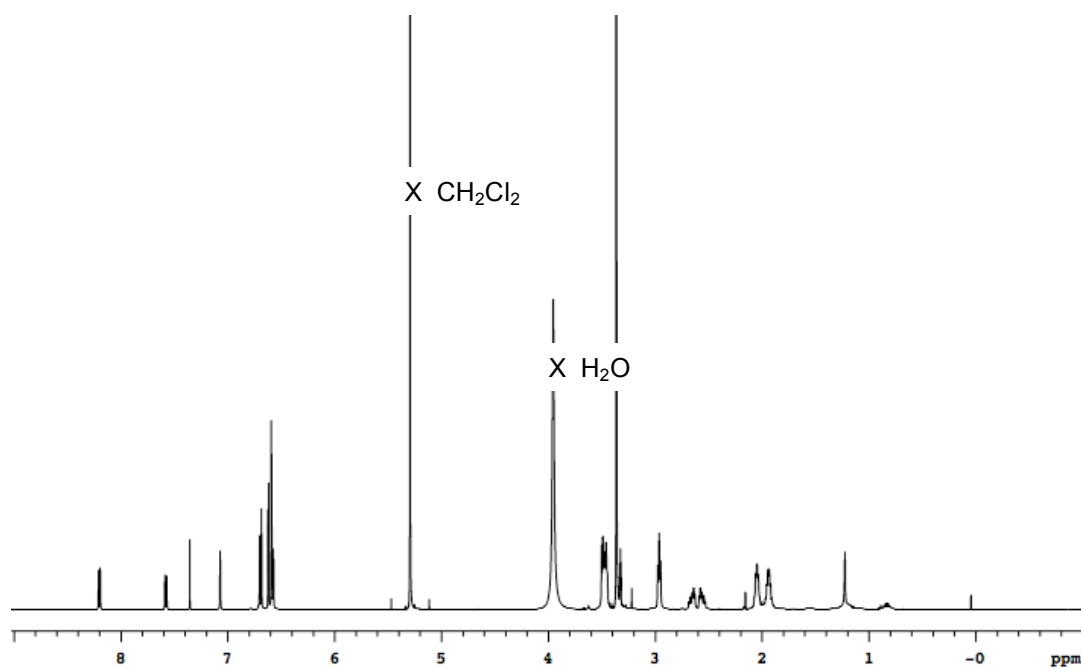
$^{13}\text{C}$  NMR for compound **332** (125 MHz,  $\text{CDCl}_3$ ).



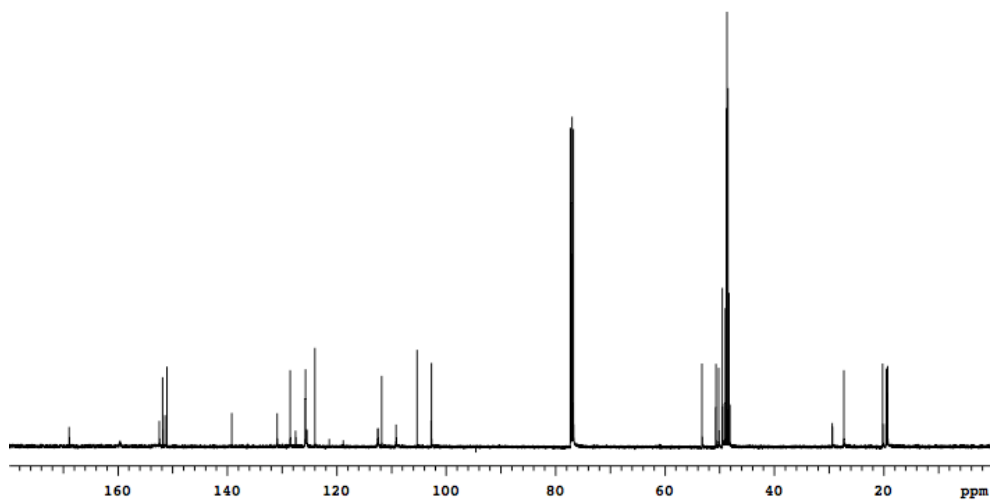
### Compound 330



5-Carboxyaldehyde fluorescein diacetate **332** (50 mg, 0.1 mmol) and 8-hydroxyjulodione (42 mg, 0.2 mmol) in 2 mL of trifluoromethane sulfonic acid were heated at 85 °C for 12h. The cooled reaction mixture was then extracted with 25% iPrOH:CHCl<sub>3</sub> (3 x 25 mL). The combined organic layer were concentrated to half, and then oxidized with chloranil (50 mg) for 30 min. The solution was filtered over celite, and the solvent evaporated. The residue was purified by column chromatography with 5% MeOH:CH<sub>2</sub>Cl<sub>2</sub>. A sample for analysis was obtained by further purification by HPLC.  $\delta_{\text{H}}$  (500 MHz, 1:1 CDCl<sub>3</sub>:CD<sub>3</sub>OD)  $\delta$  8.20 (d, 1H,  $J = 7.8$  Hz), 7.58 (dd, 1H,  $J = 7.8$  Hz,  $J = 1.5$  Hz), 7.07 (s, 1H), 6.70 – 6.57 (m, 8H), 3.50 - 3.37 (m, 8H), 2.96 (t, 4H,  $J = 6.1$  Hz), 2.67 – 2.63 (m, 2H), 2.58 – 2.54 (m, 2H), 2.07 – 2.05 (m, 4H), 1.96 – 1.92 (m, 4H);  $\delta_{\text{C}}$  (125 MHz, 1:1 CDCl<sub>3</sub>:CD<sub>3</sub>OD)  $\delta$  169.2, 152.8, 152.1, 151.7, 151.4, 139.5, 131.2, 128.8, 127.8, 126.0, 125.8, 124.3, 112.8, 112.1, 109.0, 53.5, 51.0, 50.5, 27.6, 20.5, 19.9, 19.6; MS (ESI - pos) for C<sub>45</sub>H<sub>37</sub>N<sub>2</sub>O<sub>6</sub><sup>+</sup> (M<sup>+</sup>) calcd 701.26, found 701.4.

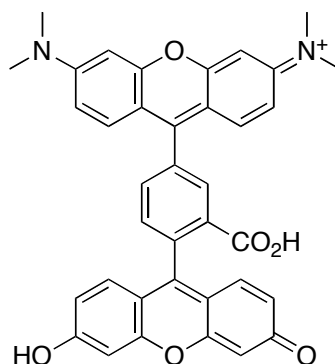


$^1\text{H}$  NMR for compound **330** (500 MHz, 1:1  $\text{CDCl}_3$ : $\text{CD}_3\text{OD}$ ).

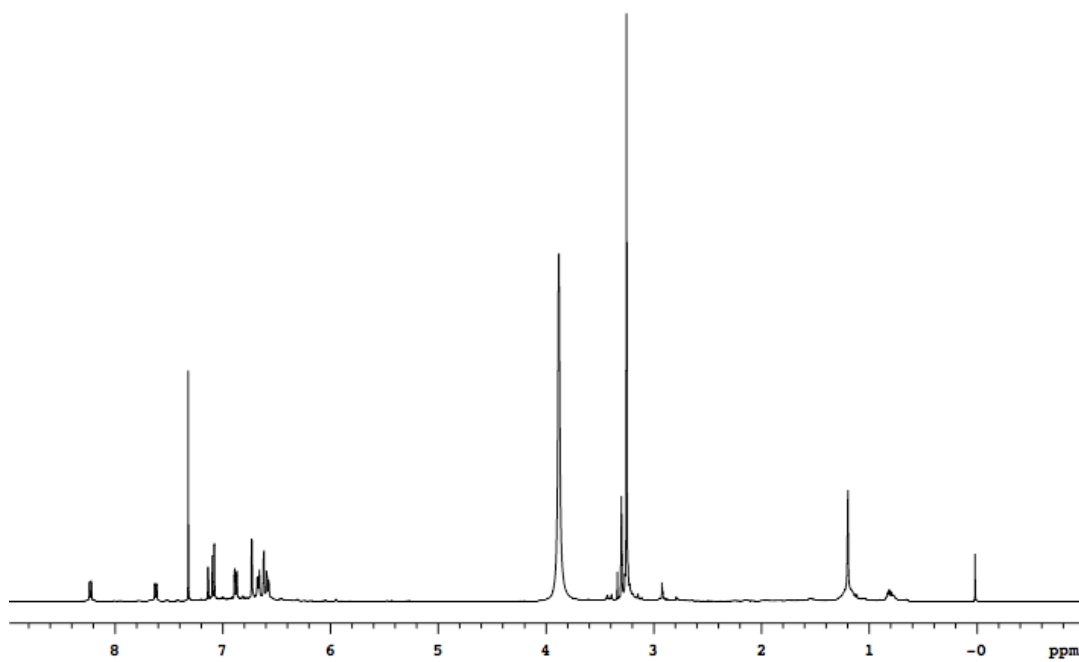


$^{13}\text{C}$  NMR for compound **330** (125 MHz, 1:1  $\text{CDCl}_3$ : $\text{CD}_3\text{OD}$ ).

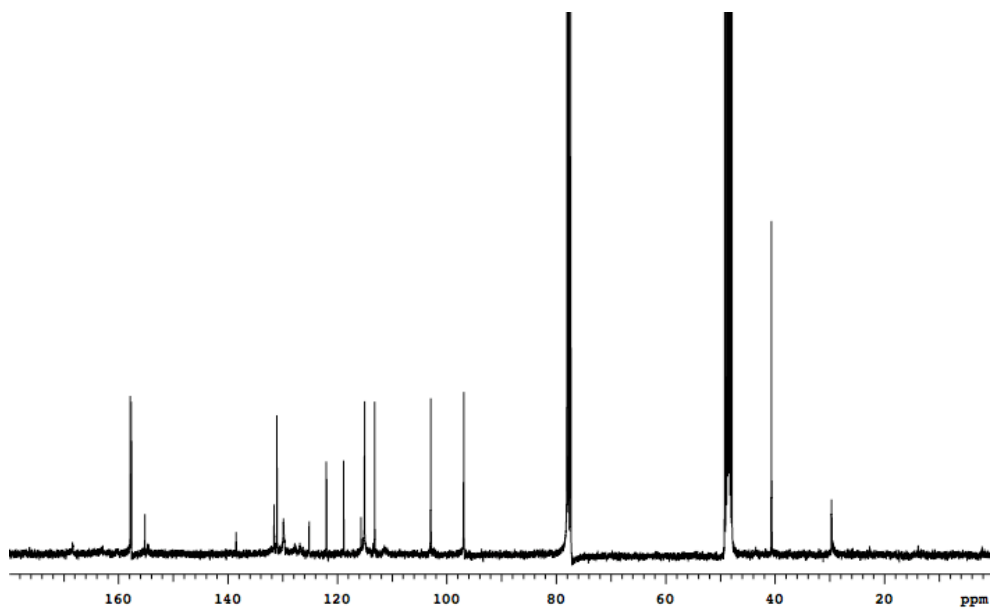
### Compound 331



5-Carboxyaldehyde fluorescein diacetate **332** (50 mg, 0.1 mmol) and 3-dimethylaminophenol (31 mg, 0.2 mmol) in 2 mL of trifluoromethane sulfonic acid were heated at 85 °C for 12h. The cooled reaction mixture was then extracted with 25% iPrOH:CHCl<sub>3</sub> (3 x 25 mL). The combined organic layer were concentrated to half, and then oxidized with chloranil (50 mg) for 30 min. The solution was filtered over celite, and the solvent evaporated. The residue was purified by column chromatography with 5 to 10 % MeOH:CH<sub>2</sub>Cl<sub>2</sub>. A sample for analysis was obtained by further purification by HPLC.  $\delta_{\text{H}}$  (500 MHz, CD<sub>3</sub>OD) 8.11 (s, 1H), 7.84 (dd,  $J$ = 8 Hz,  $J$ = 2 Hz, 1H), 7.50 (d,  $J$ = 8 Hz, 1H), 7.44 (d,  $J$ = 9 Hz, 2H), 7.16 (dd,  $J$ = 9 Hz,  $J$ = 2 Hz, 2H), 7.03 (d,  $J$ = 2 Hz, 2H), 6.81 (d,  $J$ = 8 Hz, 2H), 6.71 (d,  $J$ = 2 Hz, 2H), 6.61 (dd,  $J$ = 8 Hz,  $J$ = 2 Hz, 2H), 3.34 (s, 12H);  $\delta_{\text{C}}$  (500 MHz, 1:1 CDCl<sub>3</sub>:CD<sub>3</sub>OD)  $\delta$  157.8, 157.6, 155.1, 138.4, 131.5, 131.0, 129.8, 125.1, 121.9, 118.8, 115.6, 115.0, 113.1, 102.9, 96.8, 40.6 ; MS (ESI - pos) for C<sub>37</sub>H<sub>29</sub>N<sub>2</sub>O<sub>6</sub><sup>+</sup> (M<sup>+</sup>) calcd 597.2, found 597.1973.



$^1\text{H}$  NMR for compound **331** (500 MHz,  $\text{CD}_3\text{OD}$ ).



$^{13}\text{C}$  NMR for compound **331** (125 MHz, 1:1  $\text{CDCl}_3$ :  $\text{CD}_3\text{OD}$ ).

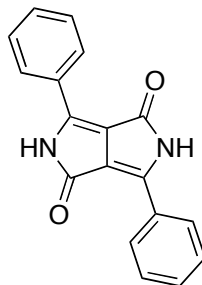
## APPENDIX E

### EXPERIMENTAL DATA FOR CHAPTER VI

#### General Procedures.

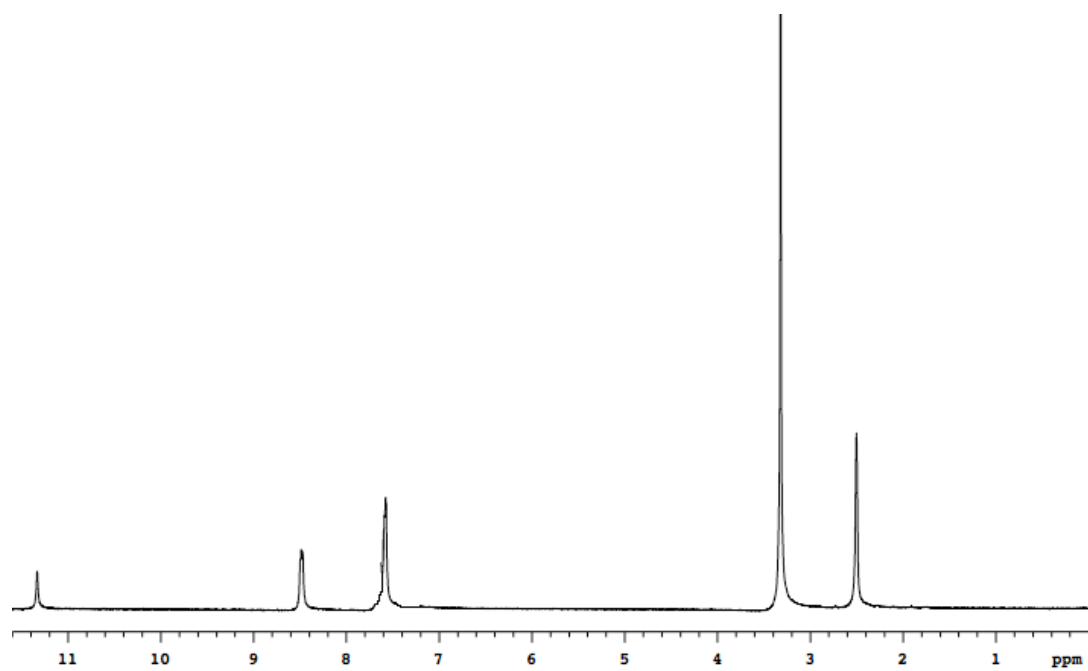
Melting points are uncorrected. High field NMR spectra were recorded on Varian Unity Plus (1H at 300 MHz, 13C at 75 MHz) NMR spectrometers. Chemical shifts are reported in units of ppm relative to solvent (CDCl<sub>3</sub>: 7.27 ppm for 1H, 77.0 ppm for 13C; Acetone-d<sub>6</sub>: 2.04 ppm for 1H, 29.9 ppm for 13C; DMSO-d<sub>6</sub>: 2.50 ppm for 1H, 39.5 ppm for 13C; D<sub>2</sub>O: 4.63 ppm for 1H; CD<sub>3</sub>OD: 3.30 ppm for 1H, 49.0 ppm for 13C; 77.0 ppm for 13C; CD<sub>3</sub>CN: 1.93 ppm for 1H, 1.3 ppm for 13C). Mass spectra were obtained from the Mass Spectrometry Applications Laboratory at Texas A&M University. Thin layer chromatography was performed using silica gel (230-600 mesh). CH<sub>2</sub>Cl<sub>2</sub>, THF, DMF, methanol, triethylamine, and toluene were distilled from appropriate drying agents. Other chemicals were purchased from commercial suppliers and used as received.

UV spectra were recorded in 1 cm path length quartz cuvettes on a Milton Roy Spectronic 3000 diode array UV spectrometer at concentrations between 1 and 10  $\mu$ M. Fluorescence emission spectra were recorded in 1 cm path length quartz cells on a SLM Aminco Fluorimeter. All fluorescence spectra were recorded at a concentration of 1.0  $\mu$ M.

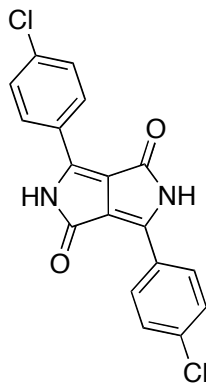
**3,6-Diphenylpyrrolo[3,4-c]pyrrole-1,4(2H,5H)-dione (342a)**

To a 25 mL round bottom flask was added benzonitrile (2.6 g, 25 mmol), potassium tert-butoxide (8.4 g, 75 mmol) and tert-butanol (12 mL). This mixture was heated to 108 - 110 °C. Then, diethyl succinate (2.3 g, 13 mmol) was slowly added over a period of time of 2 hours. The reaction mixture was then allowed to be stirred for an additional 2 hours at 108 – 110 °C, while the ethanol generated during the reaction is distilled off. After cooling, the resulting dark red solid is then transferred to a 125 mL erlenmeyer flask and 35 mL of MeOH and 4.4 mL of acetic acid were added consecutively. The red solution is then filtered, the solid washed several times with MeOH then dried overnight in vacuo. The product was obtained as a red solid in 4 % yield (0.27 g).  $\delta_{\text{H}}$  (300 MHz,  $\text{dmsO-}d_6$ ) 7.57 (bs, 6H), 8.47 (bs, 4H), 11.32 (bs, 2H); mp > 300 °C

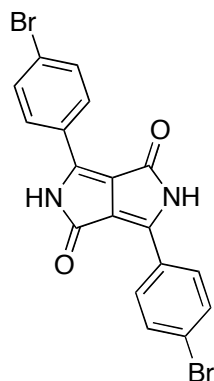




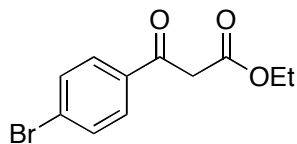
$^1\text{H}$  NMR for compound **342a** (300 MHz,  $\text{dms0-d}_6$ )

**3,6-Bis(4-chlorophenyl)pyrrolo[3,4-c]pyrrole-1,4(2H,5H)-dione (342b).**

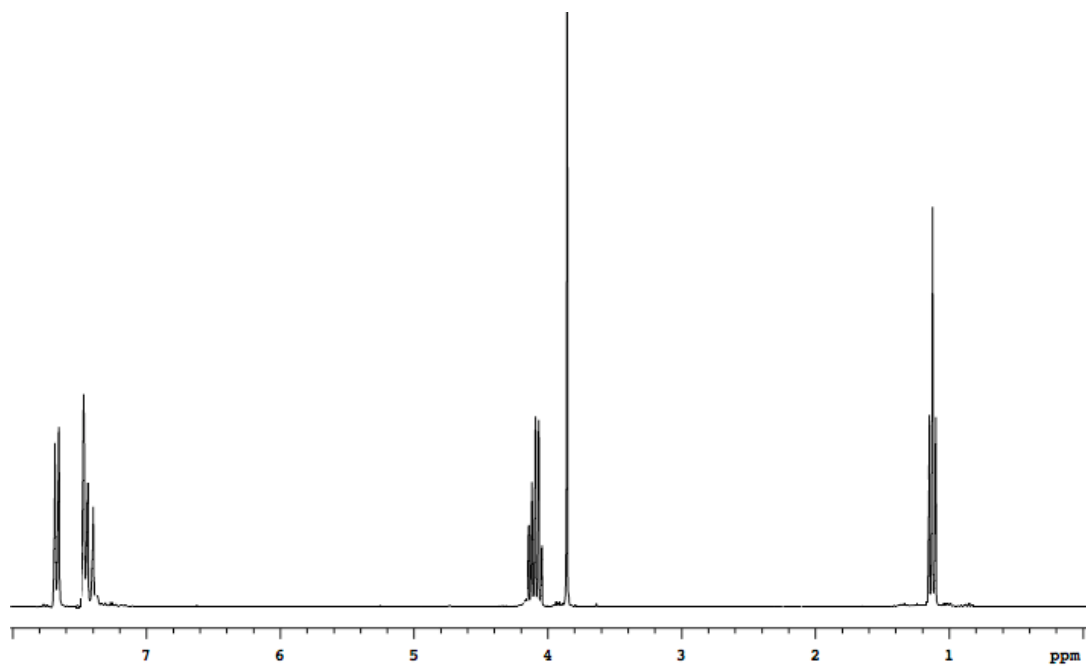
To a 3 necks 250 mL round bottom flask was added 4-chlorobenzonitrile (5.0 g, 36.3 mmol), potassium tert-butoxide (12.2 g, 109.0 mmol) and tert-butanol (30 mL). This mixture was heated to 108 - 110 °C. Then, diethyl succinate (3.3 g, 18.9 mmol) was slowly added over a period of time of 2 hours. The reaction mixture was then allowed to be stirred for an additional 2 hours at 108 – 110 °C, while the ethanol generated during the reaction is distilled off. After cooling, the resulting dark red solid is then transferred to a 125 mL erlenmeyer flask and 40 mL of MeOH and 5 mL of acetic acid were added consecutively. The red solution is then filtered, the solid washed several time with MeOH and ethyl acetate then dried overnight in vacuo. The product was obtained as a dark purple solid in 11 % yield (1.5 g); mp > 300 °C.

**3,6-Bis(4-bromophenyl)pyrrolo[3,4-c]pyrrole-1,4(2H,5H)-dione (342c).**

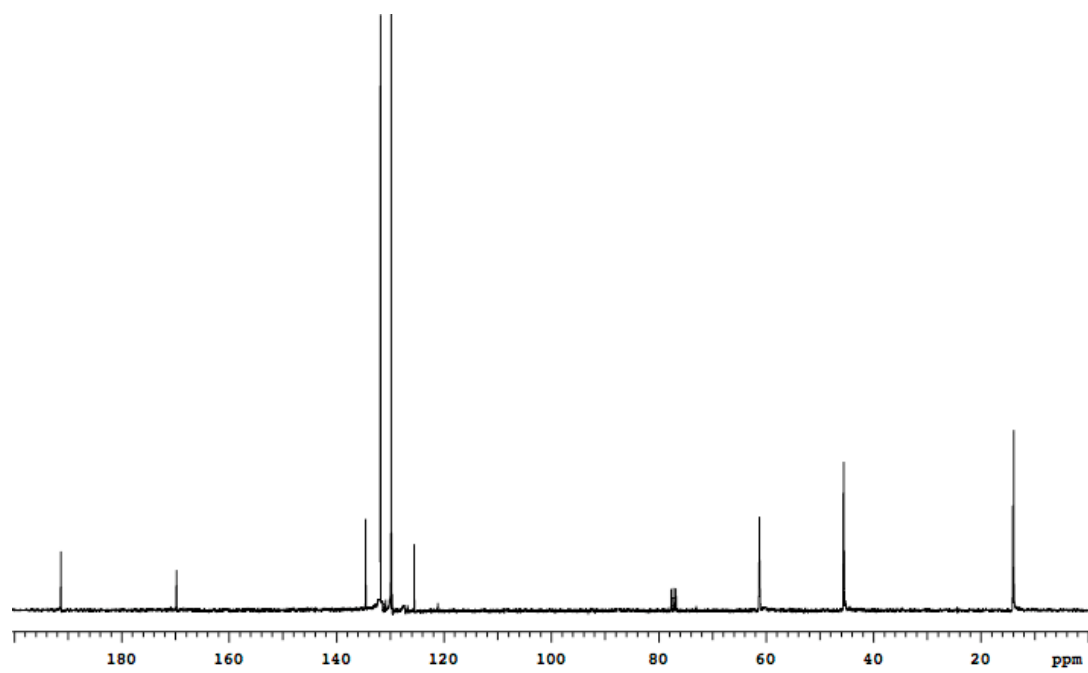
To a 3 necks 250 mL round bottom flask was added 4-bromobenzonitrile (5.0 g, 27.5 mmol), potassium tert-butoxide (9.2 g, 82.4 mmol) and tert-butanol (40 mL). This mixture was heated to 108 - 110 °C. Then, diethyl succinate (2.5 g, 14.3 mmol) was slowly added over a period of time of 2 hours. The reaction mixture was then allowed to be stirred for an additional 2 hours at 108 – 110 °C, while the ethanol generated during the reaction is distilled off. After cooling, the resulting dark red solid is then transferred to a 125 mL erlenmeyer flask and 40 mL of MeOH and 5 mL of acetic acid were added consecutively. The red solution is then filtered, the solid washed several time with MeOH and ethyl acetate then dried overnight in vacuo. The product was obtained as a dark purple solid in 7 % yield (0.85 g); mp > 300 °C.

**Ethyl 3-(4-bromophenyl)-3-oxopropanoate (343).**

Ethyl acetate (4 g, 45.5 mmol) is added dropwise to a cooled solution (-78 °C) of freshly prepared LDA. The resulting mixture is stirred for an additional 10 min, then 4-bromobenzoyl chloride (10 g, 45.5 mmol) is added. Stirring at -78 °C is continued for another 10 min, then the reaction is quenched with addition of 30 mL of 20 % HCl. The reaction mixture is then allowed to warm up to room temperature. The organic layer is separated and washed with a solution of sodium bicarbonate. The solvent is removed in vacuo, and the residue distilled (bp 129 – 131 °C at 0.6 mm Hg) to give the title product in 67 % (8.3 g) as a clear oil.  $\delta_{\text{H}}$  (300 MHz,  $\text{CDCl}_3$ ): 7.69 (d,  $J = 8.5$  Hz, 2H), 7.48 (d,  $J = 8.5$  Hz, 2H), 4.12 (q,  $J = 7.6$  Hz, 2H), 3.87 (s, 2H), 1.14 (t,  $J = 7.6$  Hz, 3H);  $\delta_{\text{C}}$  (75 MHz,  $\text{CDCl}_3$ ): 191.1, 169.6, 134.3, 131.3, 129.6, 125.3, 61.0, 45.3, 13.6.

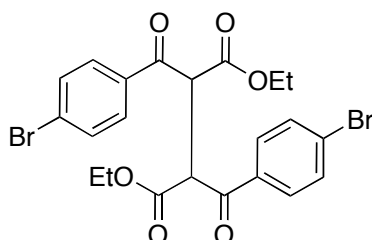


$^1\text{H}$  NMR for compound **343** (300 MHz,  $\text{CDCl}_3$ ).



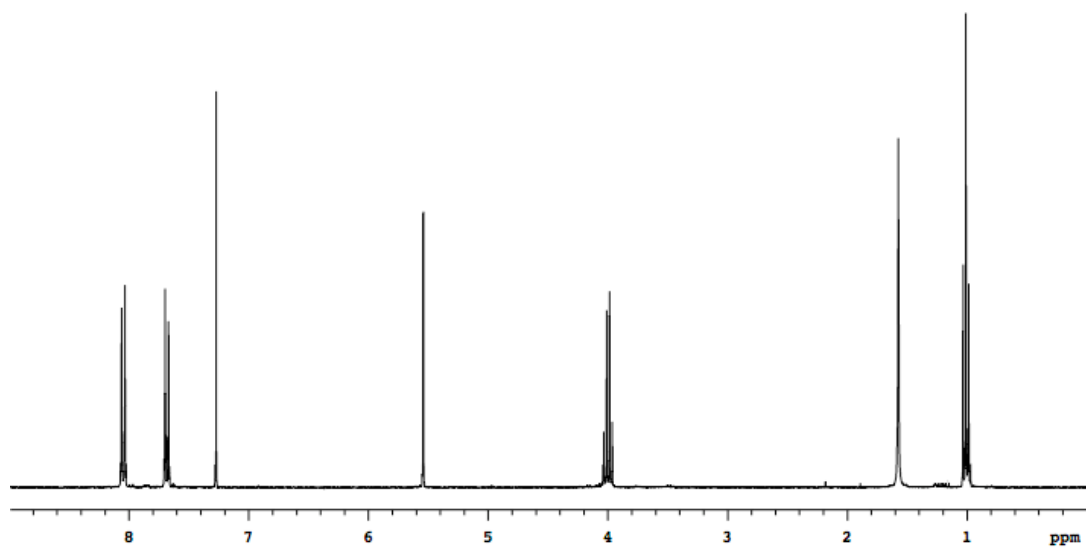
$^{13}\text{C}$  NMR for compound **343** (75 MHz,  $\text{CDCl}_3$ ).

**Compound 344.**



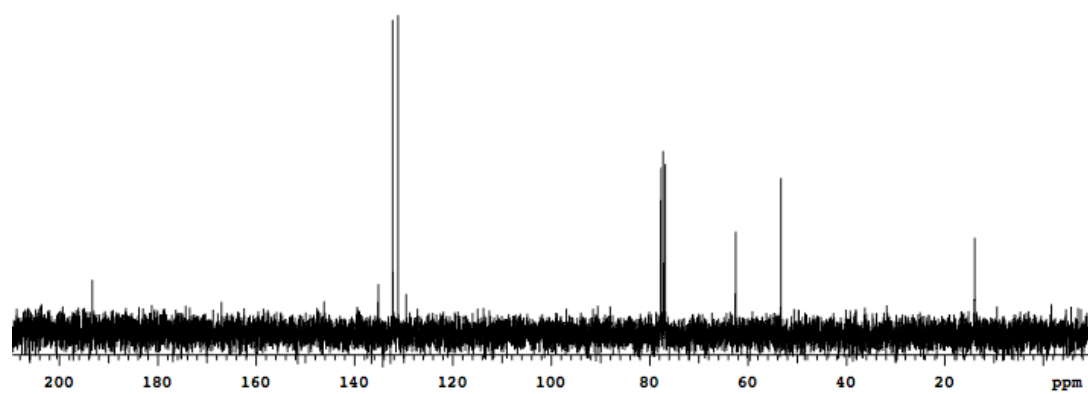
Compound **343** was prepared as described in the literature.<sup>1</sup> After sodium metal (0.28 g, 12.2 mmol) was dissolved in absolute ethanol, ethyl 3-(4-bromophenyl)-3-oxopropanoate (3 g, 11.1 mmol) was added at room temperature for 1 hour. The corresponding sodium salt of  $\beta$ -ketoester, obtained by removing the solvent under reduced pressure at room temperature, was suspended in dry ether and a solution of iodine (1.4 g, 5.5 mmol) in dry THF was added dropwise with vigorous stirring. Stirring was continued for 2 days. The dimerized  $\beta$ -ketoester was obtained by simple filtration and distillation. The reaction mixture was stirred at room temperature for 2 days, the iodine.  $\delta_{\text{H}}$  (300 MHz,  $\text{CDCl}_3$ ): 8.04 (d,  $J = 9$  Hz, 4H), 7.68 (d,  $J = 9$  Hz, 4H), 5.54 (s, 2H), 3.99 (q,  $J = 7.7$  Hz, 4H), 1.01 (t,  $J = 7.7$  Hz, 6H);  $\delta_{\text{C}}$  (75 MHz,  $\text{CDCl}_3$ ): 193.2, 136.0, 132.2, 131.1, 130.1, 62.7, 53.5, 14.1.

(1) Queignec, R.; Kirschleger, B.; Lambert, F.; Aboutaj, M. *Synth. Commun.* **1988**, *18*, 1213-

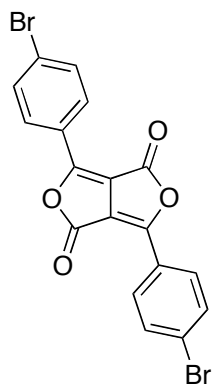


$^1\text{H}$  NMR for compound **344** (300 MHz,  $\text{CDCl}_3$ ).

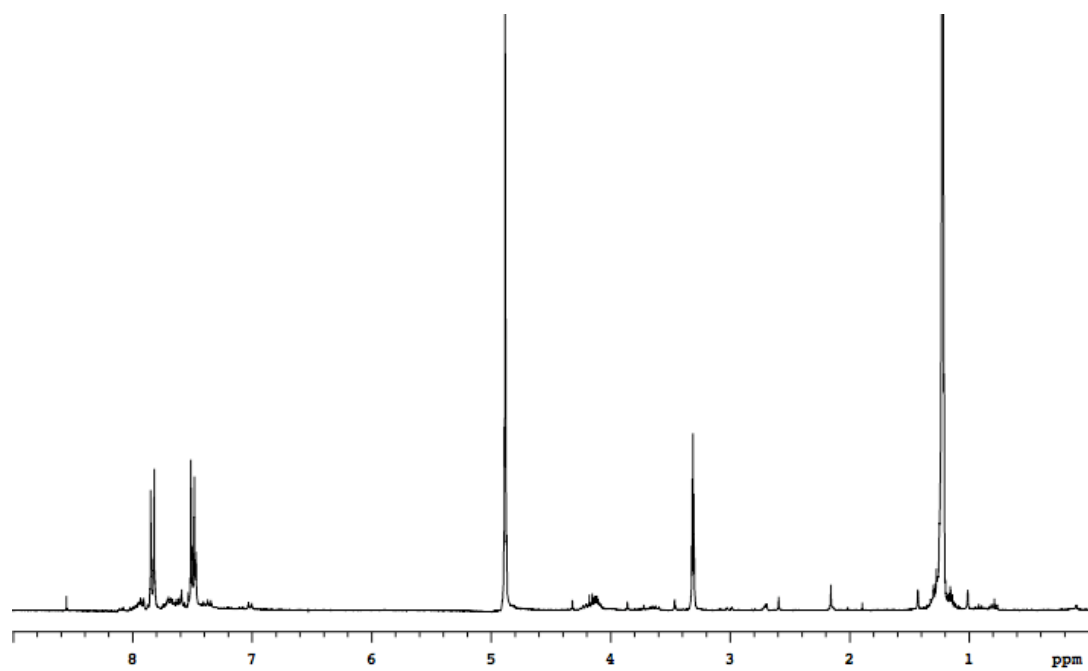




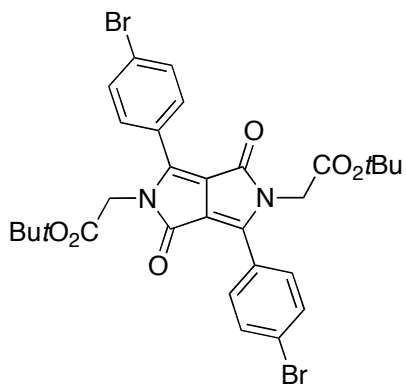
$^{13}\text{C}$  NMR for compound **344** (75 MHz,  $\text{CDCl}_3$ ).

**Compound 345**

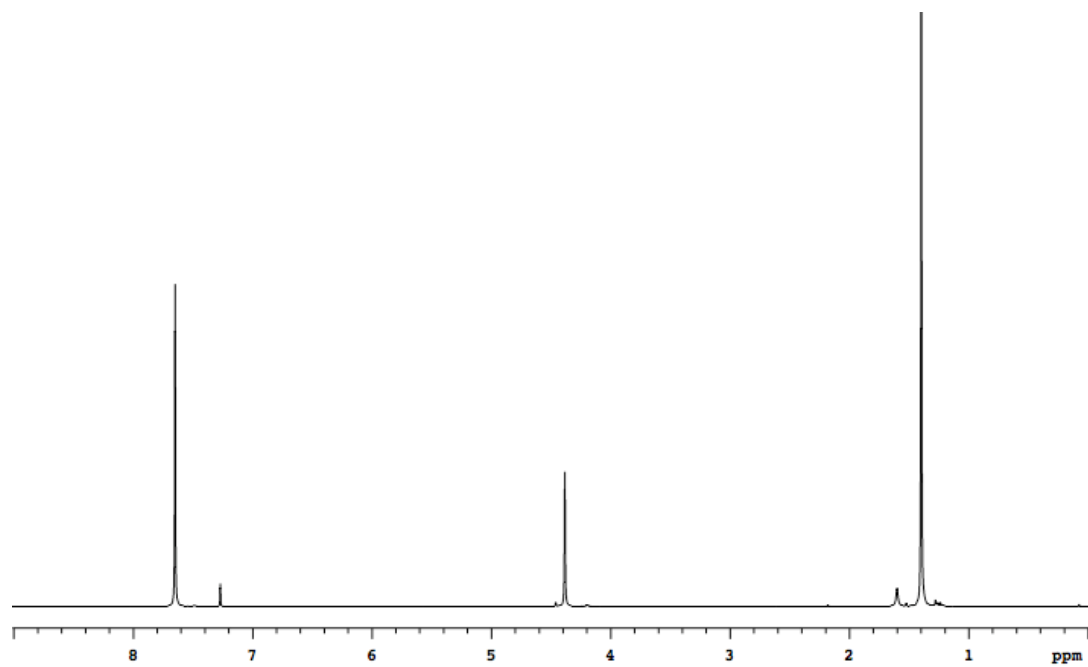
Compound **344** (50 mg, 0.2 mmol) and potassium tert-butoxide (4 mg, 0.4 mmol) in tert-butanol were stirred at room temperature for 4h. The solvent was then removed and the product was obtained as a yellow solid in 60 % crude yield (25 mg). Crude  $\delta_{\text{H}}$  (300 MHz,  $\text{CD}_3\text{OD}$ ): 7.82 (d,  $J = 9.2$  Hz, 4H), 7.48 (d,  $J = 9.2$  Hz, 4H).



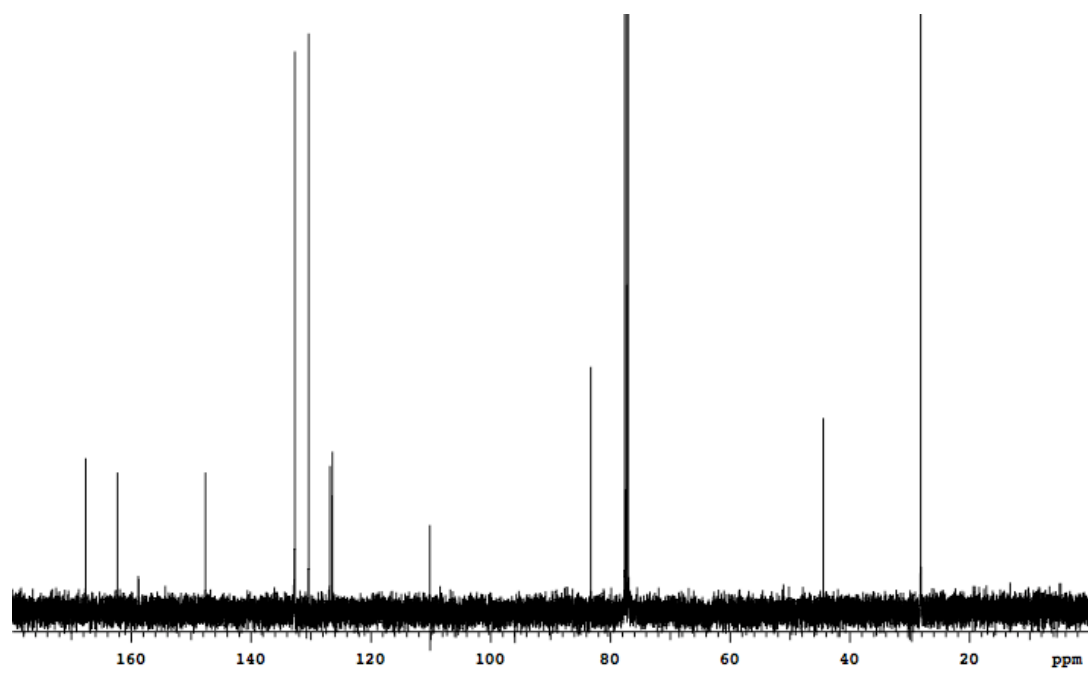
Crude <sup>1</sup>H NMR for compound **345** (300 MHz, CD<sub>3</sub>OD).

**Compound 346.**

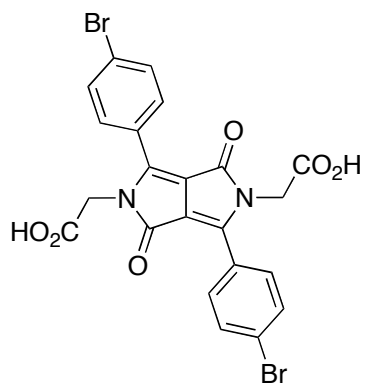
Sodium tert-butoxide was freshly prepared by reacting sodium metal (1.89 g, 82.40 mmol) in freshly distilled tert-butanol (100 mL) at 70 °C, under nitrogen. The solution was heated up to 100 °C, then a solution of 4-bromobenzonitrile (10.00 g, 54.94 mmol) in tert-butanol (100 mL) was added to it. The reaction mixture was stirred for 10 minutes, then diethyl succinate (4.78 g, 27.47 mmol) was added over a 15 minutes period. Stirring is continued for 4 hours, then bromo-tert-butyl acetate (16.07 g, 82.40 mmol) was added dropwise. After addition, the reaction mixture was stirred for another hour at 100 °C. The solution was finally allowed to cool to room temperature, and the product was isolated by filtration (14.4 g, 77 % yield).  $\delta_{\text{H}}$  (500 MHz,  $\text{CDCl}_3$ ) 7.65 (s, 8H), 4.38 (s, 4H), 1.39 (s, 18H);  $\delta_{\text{C}}$  (125 MHz,  $\text{CDCl}_3$ ) 167.3, 161.9, 147.3, 132.3, 130.0, 126.5, 126.1, 109.8, 82.9, 44.1, 27.8; HR-MS (ESI/TOF) for  $\text{C}_{30}\text{H}_{30}\text{Br}_2\text{N}_2\text{O}_6$  ( $\text{M}+\text{H}^+$ ) calc'd 673.05, found 673.0479.



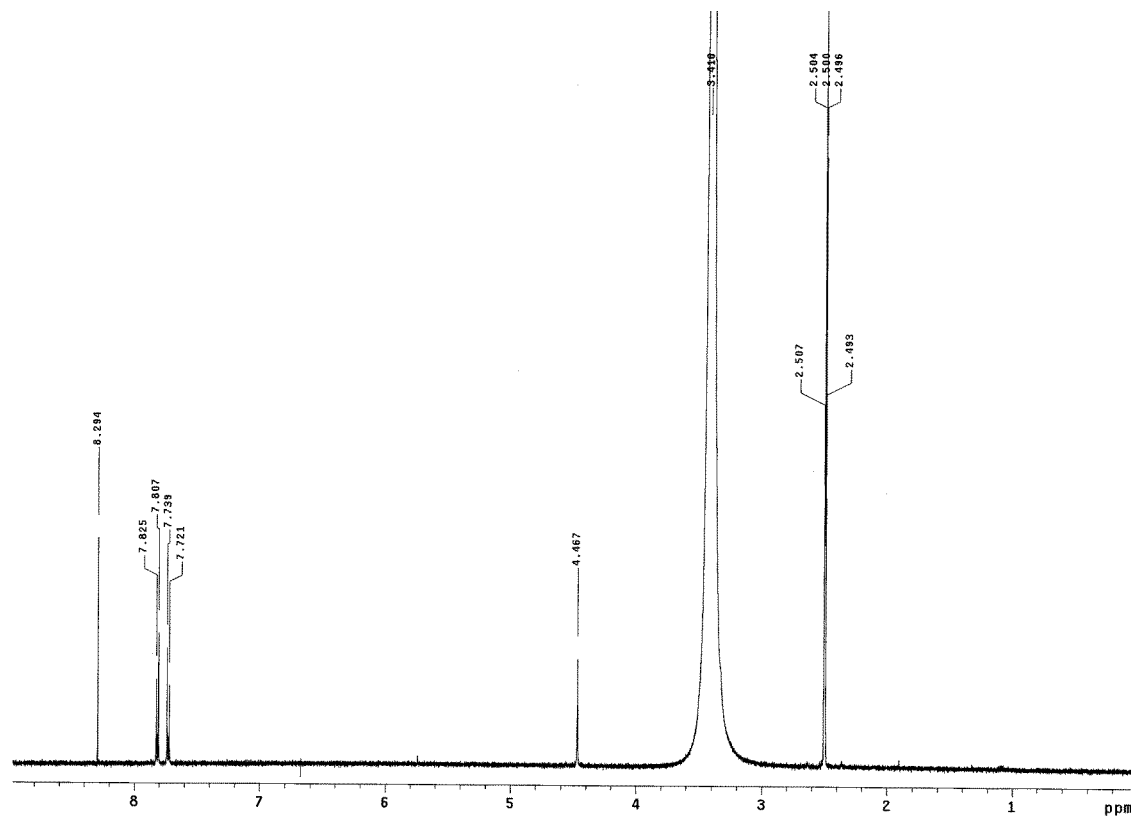
$^1\text{H}$  NMR for compound **346** (500 MHz,  $\text{CDCl}_3$ ).



$^{13}\text{C}$  NMR for compound **346** (125 MHz,  $\text{CDCl}_3$ ).

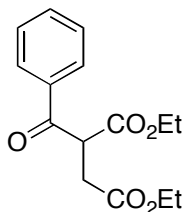
**DPP 347.**

DPP **346** (1 g, 1.49 mmol) was treated with 200 mL of a cocktail mixture of 95% TFA, 2.5 % water and 2.5 % TIS at room temperature for 1 hour. The solvents were then removed in vacuo and the residual solid was rinsed several times with hexanes. The product was obtained in near quantitative yield.  $\delta_{\text{H}}$  (500 MHz, dms $\text{-d}_6$ ): 8.29 (s, 1H), 7.81 (d,  $J = 9.0$  Hz, 4H), 7.73 (d,  $J = 9.0$  Hz, 4H), 4.46 (s, 4H); HR-MS (ESI-neg) for  $\text{C}_{22}\text{H}_{13}\text{Br}_2\text{N}_2\text{O}_6$  ( $\text{M-H}^+$ ) calc'd 558.91, found 560.8798; HR-MS (ESI-pos) for  $\text{C}_{22}\text{H}_{14}\text{Br}_2\text{N}_2\text{O}_6$  ( $\text{M+H}^+$ ) calc'd 563.16, found 562.9524; Analytical HPLC: 95 % purity.

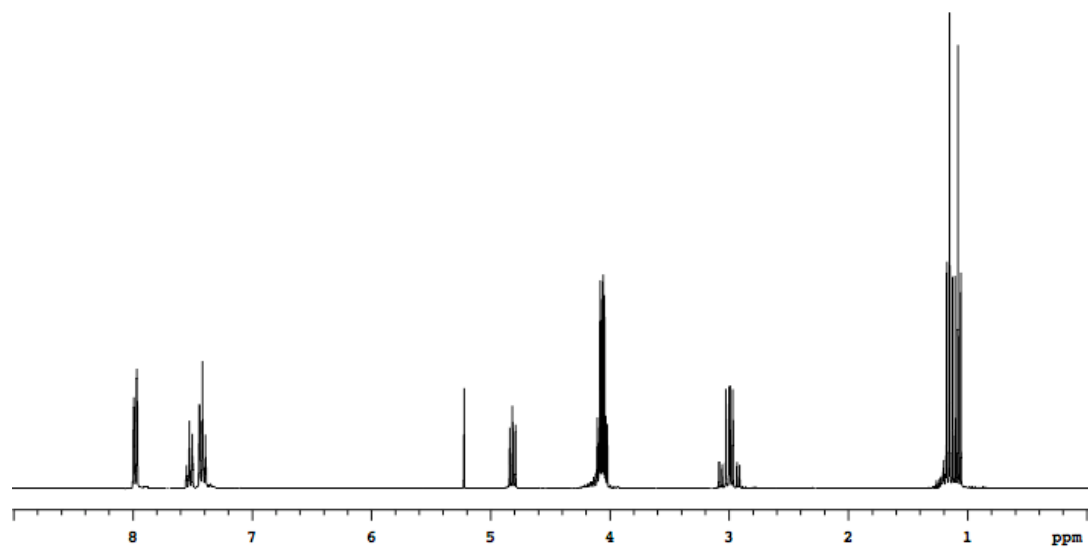


$^1\text{H}$  NMR for compound **347** (500 MHz,  $\text{dms0-d}_6$ ).

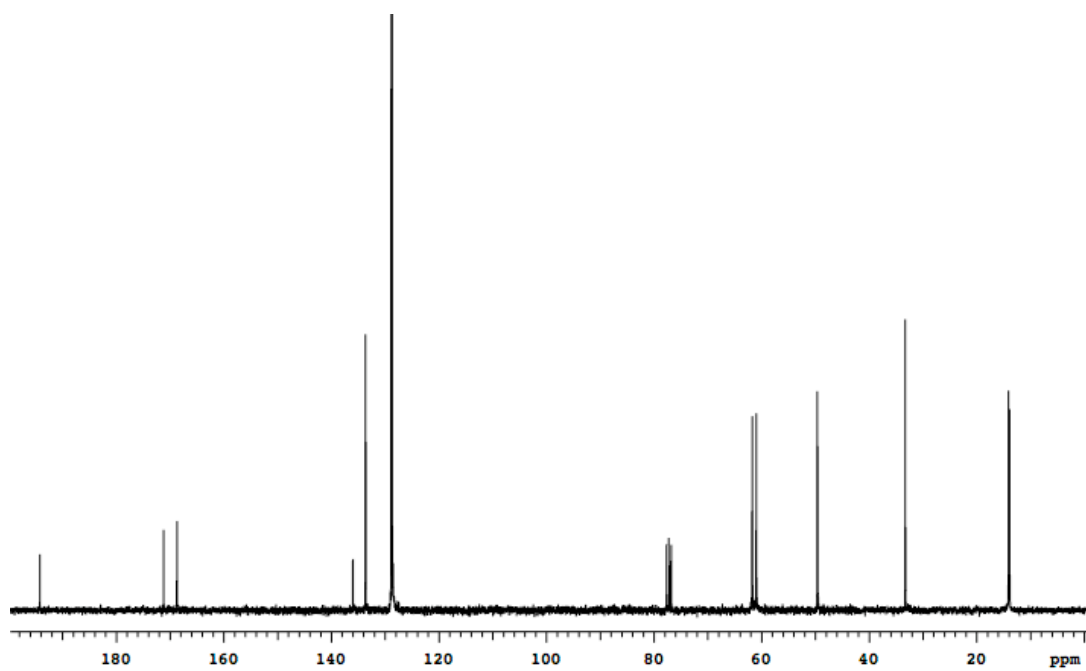


**Diethyl benzoylsuccinate (348).**

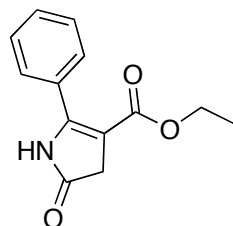
Diethyl benzoyl succinate was synthesized as described in the literature.<sup>1</sup> A suspension of ethyl benzoylacetate (5.0 g, 25 mmol),  $K_2CO_3$  (5.2 g, 38 mmol), NaI (0.94 g, 6 mmol), and ethyl bromoacetate (4.6 g, 28 mmol) was heated at 65 °C for 2 h. After cooling to room temperature, the residual solid is filtered and washed several time with  $CH_2Cl_2$ . The combined filtrates were evaporated to dryness under reduced pressure affording the titled compound (6.5 g, 93%) as a yellow oil. A sample was extra purified by column chromatography on silica gel ( $CH_2Cl_2$ ) affording 4b as a colorless to green oil.  $\delta_H$  (300 MHz,  $CDCl_3$ ): 8.01 (d,  $J = 7.3$  Hz, 2H), 7.56 – 7.52 (m, 1H), 7.43 (t, 2H,  $J = 7.3$  Hz), 4.83 (app t,  $J = 8$  Hz, 1H), 4.02 – 4.12 (m, 4H), 2.92 – 3.10 (m, 2H), 1.15 (t,  $J = 7.7$  Hz, 3H), 1.08 (t,  $J = 7.7$  Hz, 3H);  $\delta_C$  (75 MHz,  $CDCl_3$ ): 193.9, 170.9, 168.4, 135.7, 133.4, 128.6, 128.2, 61.5, 60.7, 49.4, 33.0, 13.8, 13.6. All spectral data match those reported.



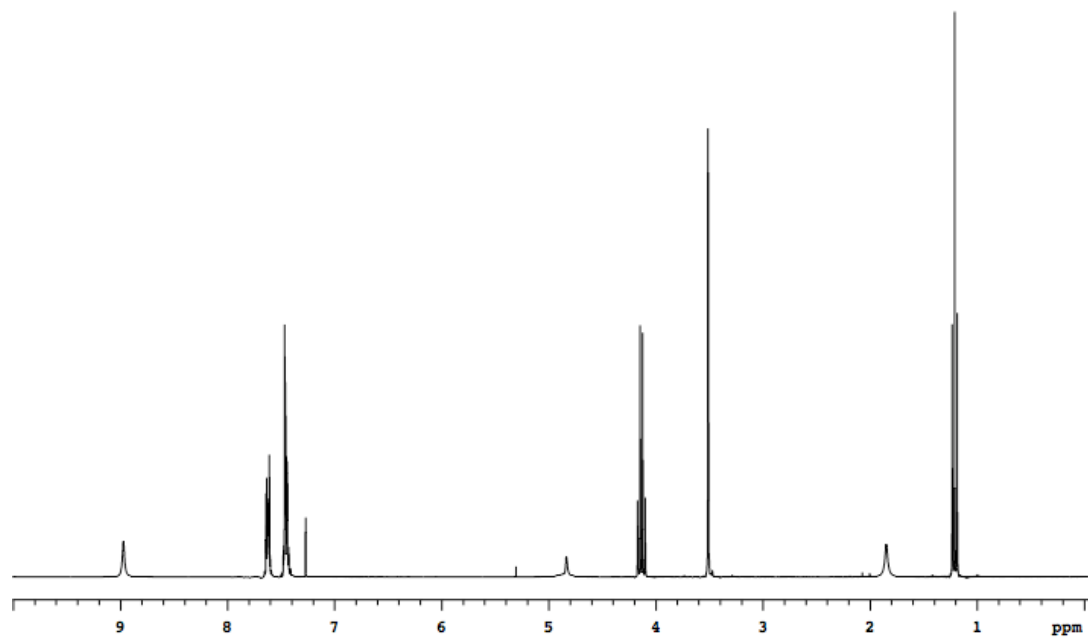
$^1\text{H}$  NMR for compound **348** ( $\text{CDCl}_3$ , 300 MHz).



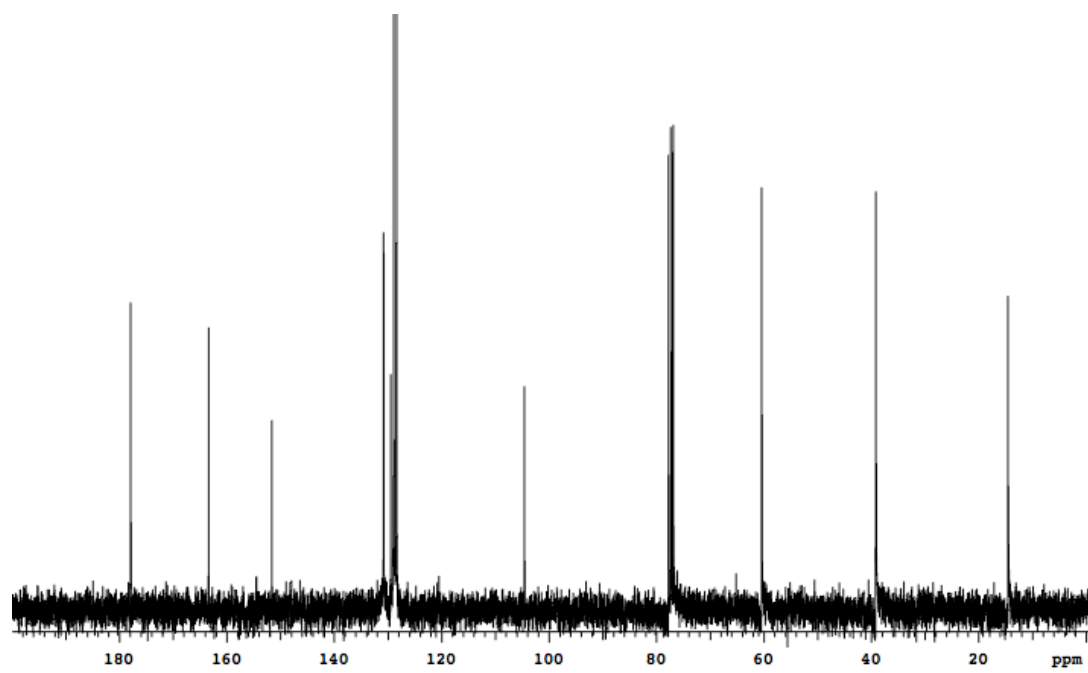
$^{13}\text{C}$  NMR for compound **348** ( $\text{CDCl}_3$ , 75 MHz).

**Ethyl 4,5-dihydro-5-oxo-2-phenyl-1H-pyrrole-3-carboxylate (349).**

A solution of diethylbenzoyl succinate **348** (28.44 g, 102.18 mmol), ammonium acetate (63.00 g, 817.50 mmol) in glacial acetic acid (20 mL) was heated at reflux for 16h. After cooling, the reaction mixture is poured into 200 mL of ice, and the product is filtered, and washed with water. Recrystallization from  $\text{CH}_2\text{Cl}_2$  gives ethyl 4,5-dihydro-5-oxo-2-phenyl-1H-pyrrole-3-carboxylate as a pale green solid in 35 % yield (8.40 g).  $\delta_{\text{H}}$  (300 MHz,  $\text{CDCl}_3$ ): 8.97 (bs, 1H), 7.64 – 7.60 (m, 2H), 7.47 – 7.44 (m, 2H), 4.13 (q,  $J = 7.1$  Hz, 2H), 3.51 (s, 2H), 1.21 (t,  $J = 7.1$  Hz, 3H);  $\delta_{\text{C}}$  (75 MHz,  $\text{CDCl}_3$ ): 177.6, 163.1, 151.3, 130.5, 129.1, 128.6, 128.1, 104.3, 60.1, 38.8, 14.2. All spectral data match those reported.

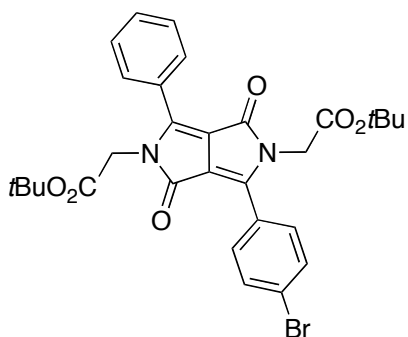


$^1\text{H}$  NMR for compound **349** (300 MHz,  $\text{CDCl}_3$ ).

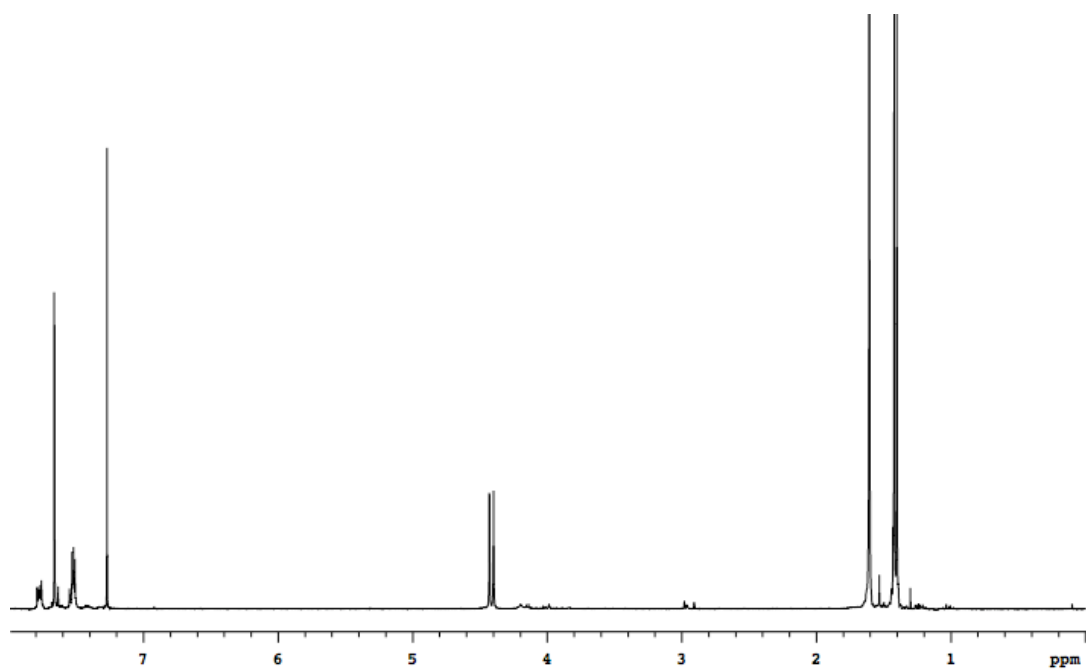


$^{13}\text{C}$  NMR for compound **349** (75 MHz,  $\text{CDCl}_3$ ).

## DPP 350

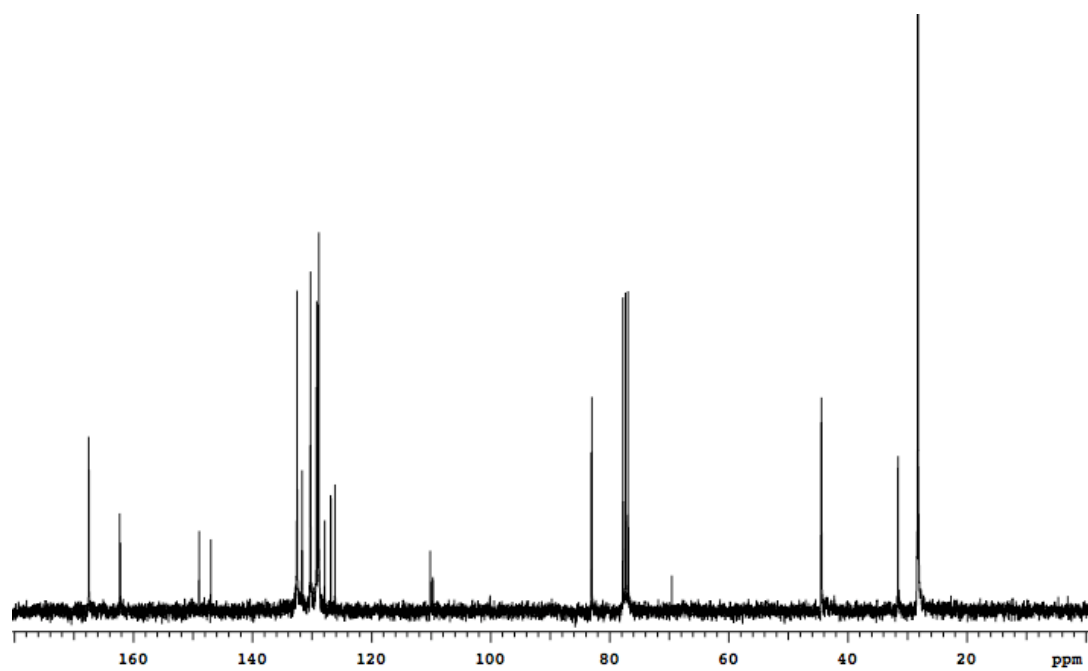


Sodium tert-butoxide is freshly prepared by reacting sodium metal (0.89 g, 38.92 mmol) in freshly distilled tert-butanol 50 mL) at 70 °C, under nitrogen. The solution is heated up to 100 °C, then a solution of 4-bromobenzonitrile (4.72g, 25.95 mmol) in tert-butanol is added to it. The reaction mixture is stirred for 10 minutes, then ethyl 4,5-dihydro-5-oxo-2-phenyl-1H-pyrrole-3-carboxylate (3.0 g, 12.9 mmol) is added over a 15 minutes period. Stirring is continued for 4 hours, then bromo-tert-butyl acetate (7.60 g, 38.92 mmol) is added dropwise. After addition, the reaction mixture is stirred for another hour at 100 °C. After cooling to room temperature, water (~ 100 mL) is added. The solution is allowed to stand for 1 hour, then the product is isolated by filtration and dried in vacuo overnight (5.2 g, 67 % yield).  $\delta_{\text{H}}$  (500 MHz,  $\text{CDCl}_3$ ): 7.76 – 7.73 (m, 2H), 7.64 (s, 4H), 7.50 – 7.48 (m, 3H), 4.42 (s, 2H), 4.39 (s, 2H), 1.40 (s, 9H), 1.38 (s, 9H);  $\delta_{\text{C}}$  (75 MHz,  $\text{CDCl}_3$ ): 167.5, 162.3, 148.9, 146.9, 132.5, 131.6, 130.2, 129.2, 128.8, 127.8, 126.8, 126.1, 110.1, 109.6, 83.1, 44.4, 28.3.

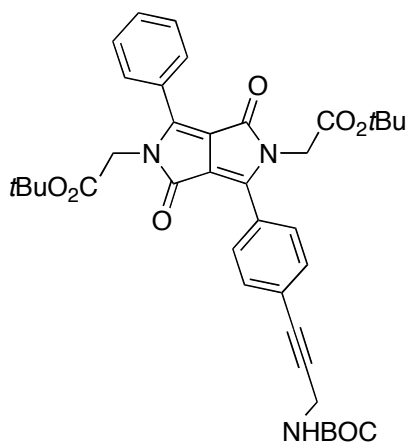


$^1\text{H}$  NMR for compound **350** (500 MHz,  $\text{CDCl}_3$ ).

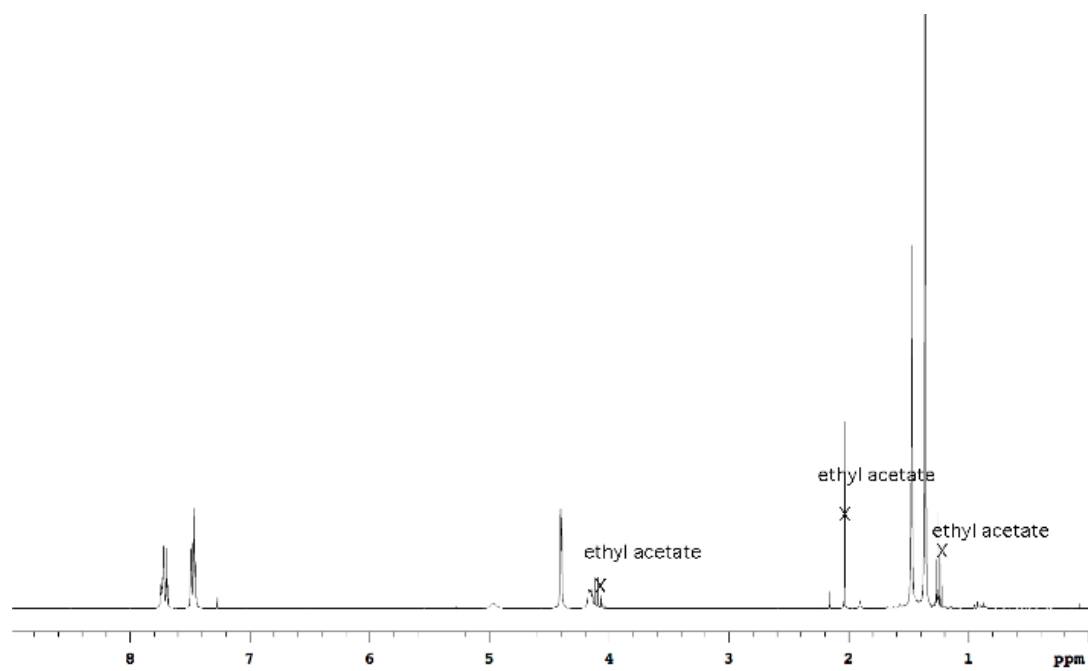




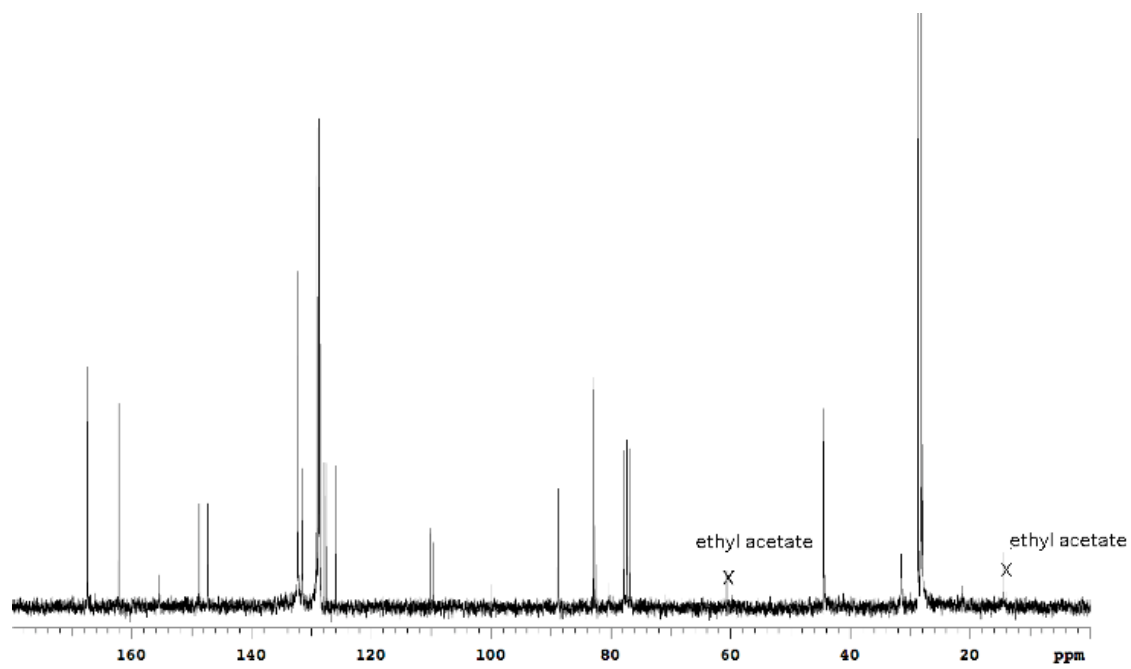
$^{13}\text{C}$  NMR for compound **350** (125 MHz,  $\text{CDCl}_3$ ).

**DPP 351.**

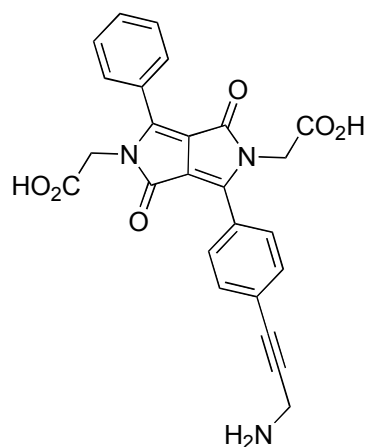
A solution of DPP **350** (0.5 g, 0.84 mmol), N-BOC propargyl amine (0.1 g, 0.67 mmol), Pd (PPh<sub>3</sub>)<sub>4</sub> (0.03 g, 5 mol%), CuI (0.005 g, 5 mol%), and triethyl amine (1.12 g, 11.07 mmol) in freshly distilled toluene (10 mL) was heated at 90 °C for 12h. After cooling to room temperature, ether was added, and the reaction mixture was filtered over celite. The solvent were removed in vacuo, and the residue was purified by column chromatography, with 30 % ethyl acetate: hexanes as solvent. The title compound was isolated in 58 % yield (0.2 g).  $\delta_{\text{H}}$  (300 MHz, CDCl<sub>3</sub>): 7.72 – 7.69 (m, 4H), 7.49 – 7.45 (m, 5H), 4.99 (bs, 1H), 4.40 (s, 4H), 4.15 (bs, 2H), 1.47 (s, 9H), 1.36 (s, 8H);  $\delta_{\text{C}}$  (75 MHz, CDCl<sub>3</sub>): 167.1, 161.8, 155.1, 148.4, 146.9, 131.9, 131.2, 128.8, 128.4, 128.2, 127.5, 127.2, 125.6, 109.7, 109.4, 88.5, 82.5, 82.2, 44.1, 31.2, 28.3, 27.7.



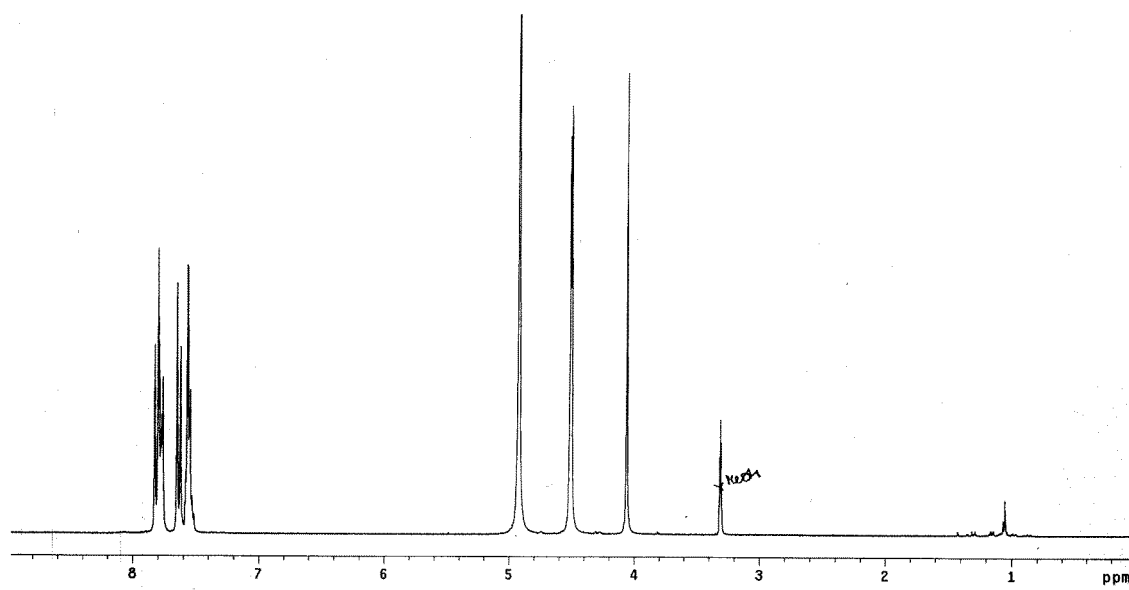
$^1\text{H}$  NMR for compound **351** (300 MHz,  $\text{CDCl}_3$ ).



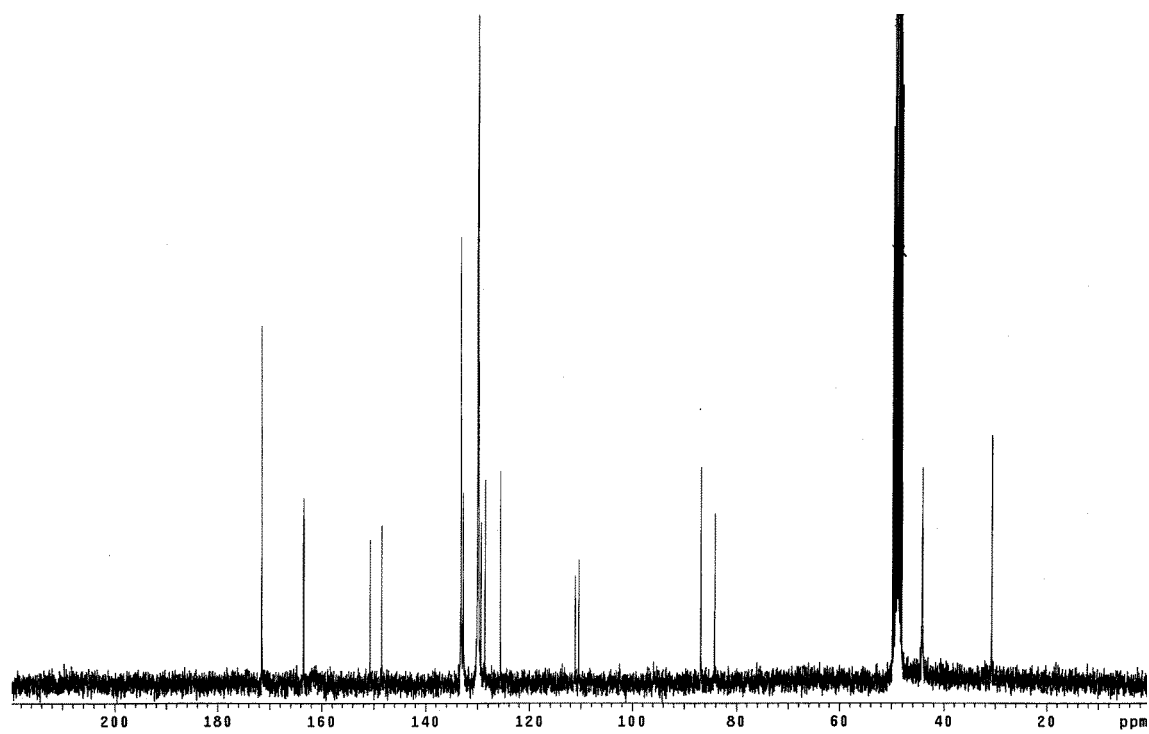
$^{13}\text{C}$  NMR for compound **351** (75 MHz,  $\text{CDCl}_3$ ).

**DPP 352.**

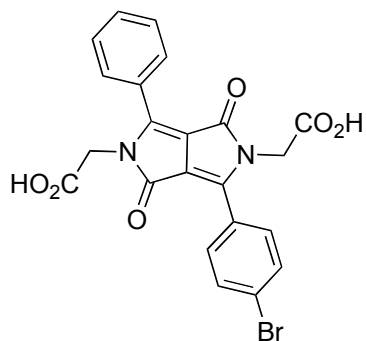
DPP **351** (50 mg, 0.07 mmol) is treated with a cocktail mixture of 95% TFA, 2.5 % water and 2.5 % TIS at room temperature until completion of reaction according to tlc (~ 2 hours). Ether is added to the reaction mixture to precipitate the product. The product is then filtered and dried in vacuo. The solvents were then removed in vacuo and the residual solid was rinsed several times with hexanes. The product was obtained in near quantitative yield.  $\delta_{\text{H}}$  (300 MHz,  $\text{CD}_3\text{OD}$ ): 7.82 – 7.79 (m, 4H), 7.65- 7.56 (m, 5H), 4.51 (s, 4H), 4.06 (s, 2H);  $\delta_{\text{C}}$  (75 MHz,  $\text{CD}_3\text{OD}$ ): 171.5, 163.5, 150.7, 148.4, 133.2, 132.7, 130.0, 129.9, 129.3, 128.6, 125.6, 111.1, 110.4, 86.8, 84.2, 44.2, 30.7; HR-MS (ESI-pos) for  $\text{C}_{25}\text{H}_{19}\text{N}_3\text{O}_6$  ( $\text{M}+\text{H}^+$ ) calc'd 458, found 458.1222; HPLC purity : 96.7 %.



$^1\text{H}$  NMR for compound **352** (300 MHz,  $\text{CD}_3\text{OD}$ ).

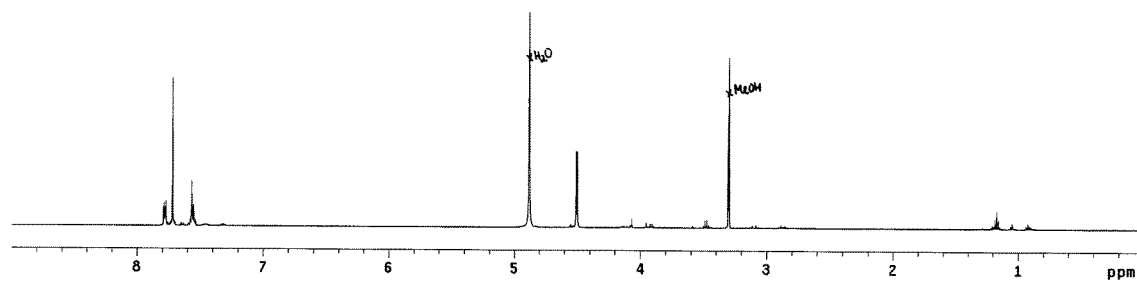


$^{13}\text{C}$  NMR for compound **352** (75 MHz,  $\text{CD}_3\text{OD}$ ).

**DPP 353.**

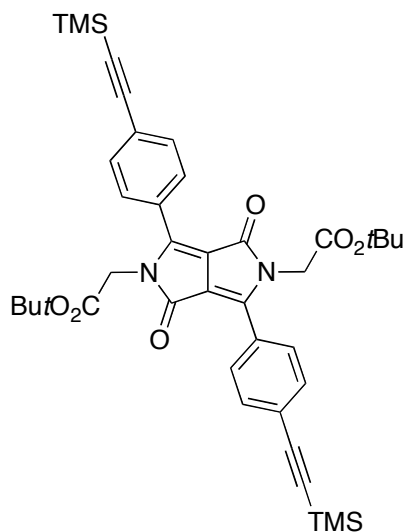
DPP **350** (50 mg, 0.08 mmol) was treated with a cocktail mixture of 95% TFA, 2.5 % water and 2.5 % TIS at room temperature until completion of reaction according to tlc (~ 2 hours). Ether was then added to the reaction mixture to precipitate the product. The product was then filtered and dried in vacuo. The solvents were then removed in vacuo and the residual solid was rinsed several times with hexanes. The product was obtained in near quantitative yield.  $\delta_{\text{H}}$  (500 MHz, CD<sub>3</sub>OD): 7.78 – 7.77 (m, 2H), 7.72 (s, 4H), 7.56 – 7.55 (m, 3H), 4.51 (s, 2H), 4.49 (s, 2H); MS (ESI-neg) for C<sub>22</sub>H<sub>15</sub>BrN<sub>2</sub>O<sub>6</sub> (M-H<sup>-</sup>) calc'd 481, found 481.1 – 483.0 (Br isotope).



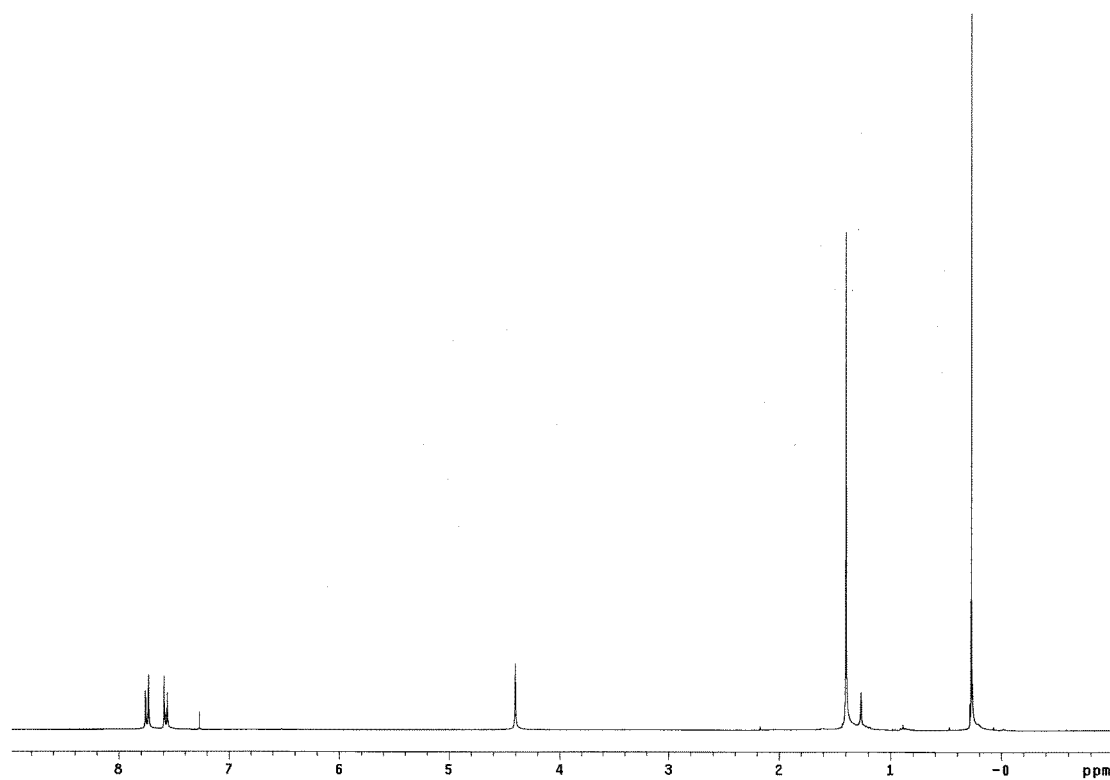


$^1\text{H}$  NMR for compound **353** (500 MHz,  $\text{CD}_3\text{OD}$ )

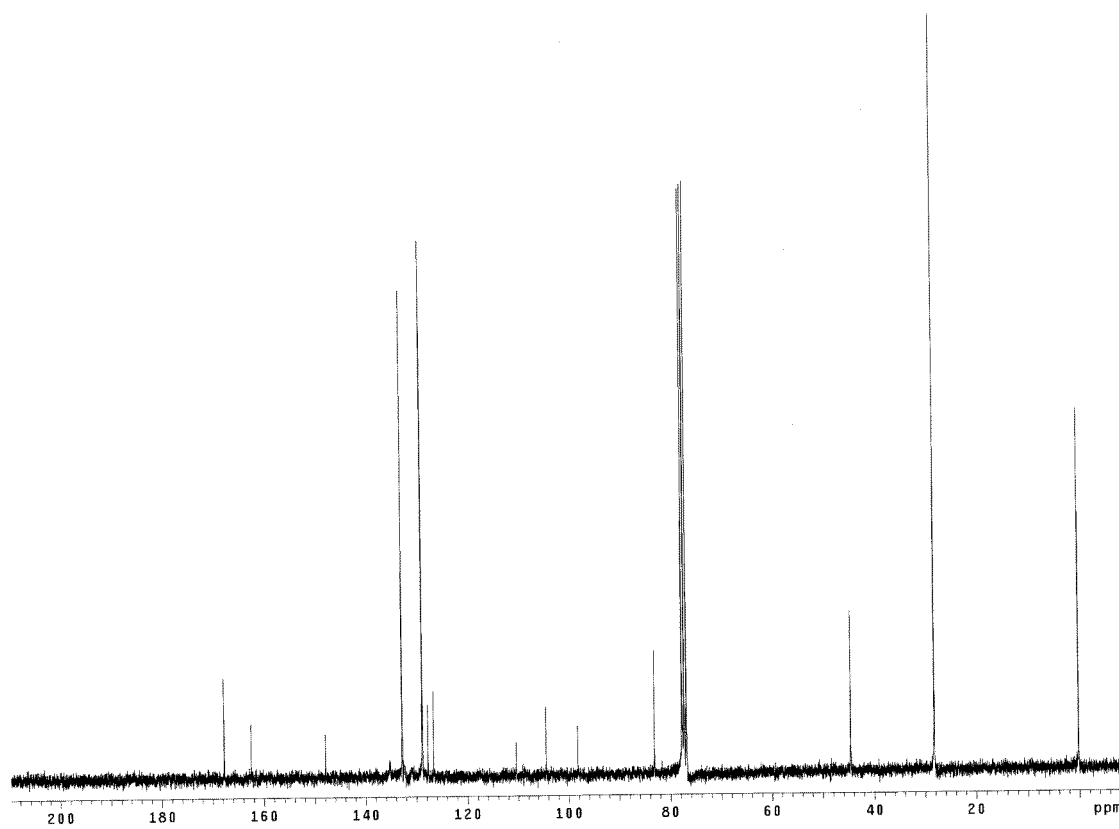
## DPP 354.



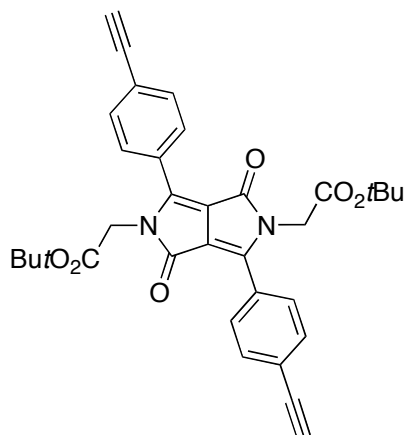
DPP **346** (5.00g, 7.41 mmol), TMS acetylene (4.37 g, 44.5 mmol), Pd(PPh<sub>3</sub>)<sub>4</sub> (0.86 g, 0.74 mmol), CuI (0.14 g, 0.74 mmol) and triethylamine (29.6 g, 296.6 mmol) in freshly distilled toluene was heated at 85 °C for 5h. After cooling to room temperature, ether was added and the reaction mixture was filtered over celite. The solvent was removed and the residue purified by chromatography on silica gel, with Hexanes, then 10% Ethyl acetate:Hexanes as solvent. 1,4-Bis(trimethylsilyl)buta-1,3-diyne was obtained from the elution with hexanes as the major product of the reaction. The title compound was obtained in 20 % yield (1.04 g).  $\delta_{\text{H}}$  (300 MHz, CDCl<sub>3</sub>): 7.74 (d,  $J$  = 8.7 Hz, 4H), 7.58 (d,  $J$  = 8.7 Hz, 4H), 4.40 (s, 4H), 1.40 (s, 18H), 0.27 (s, 18H);  $\delta_{\text{C}}$  (75 MHz, CDCl<sub>3</sub>): 167.6, 162.4, 147.8, 132.7, 128.7, 127.6, 126.5, 110.4, 104.4, 98.2, 83.1, 44.6, 28.1, 0.1.



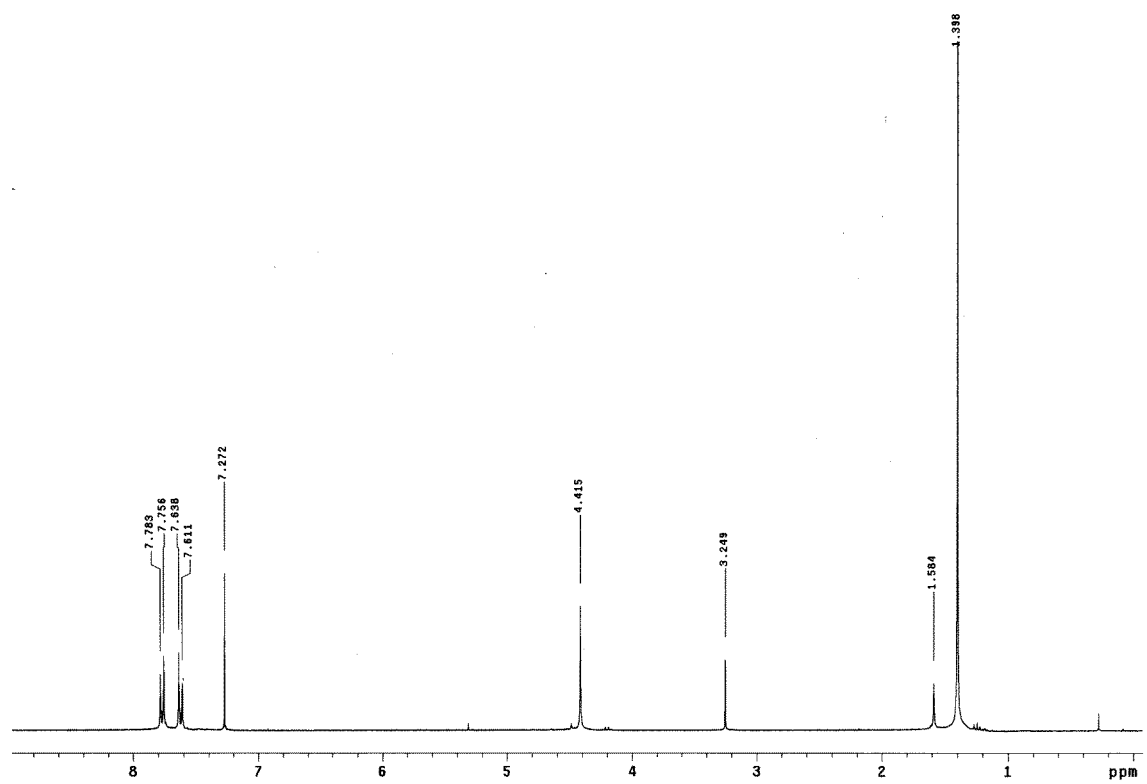
$^1\text{H}$  NMR for compound **354** (300 MHz,  $\text{CDCl}_3$ ).



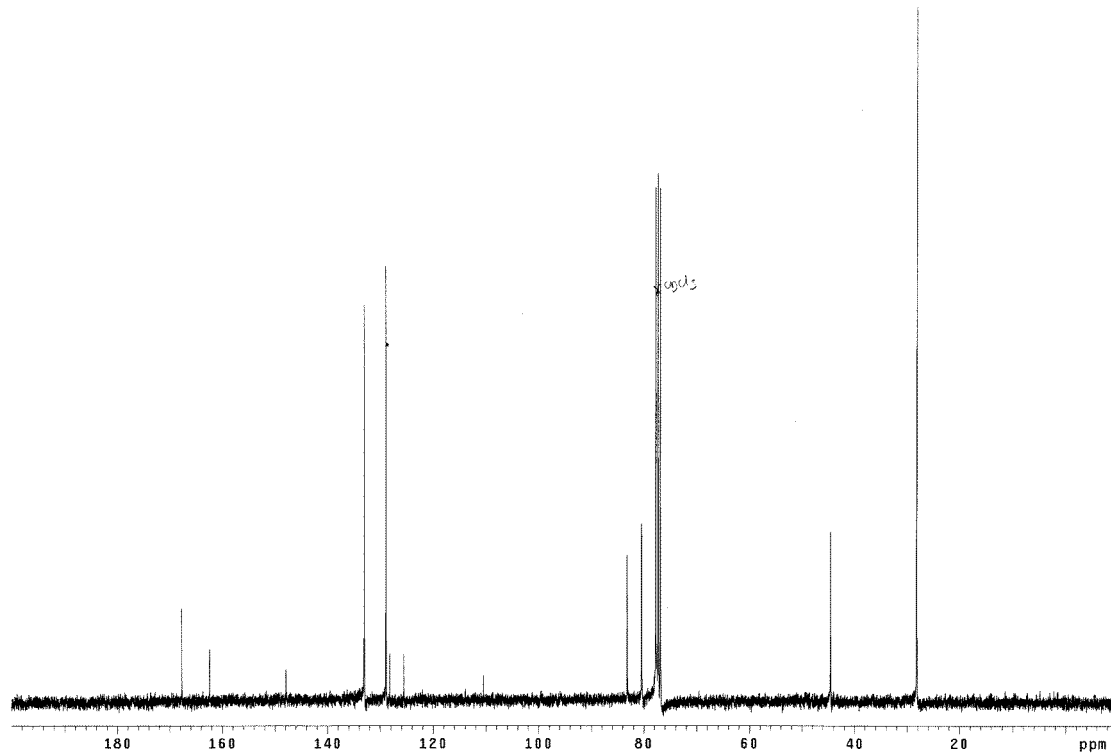
$^{13}\text{C}$  NMR for compound **354** (75 MHz,  $\text{CDCl}_3$ ).

**DPP 355.**

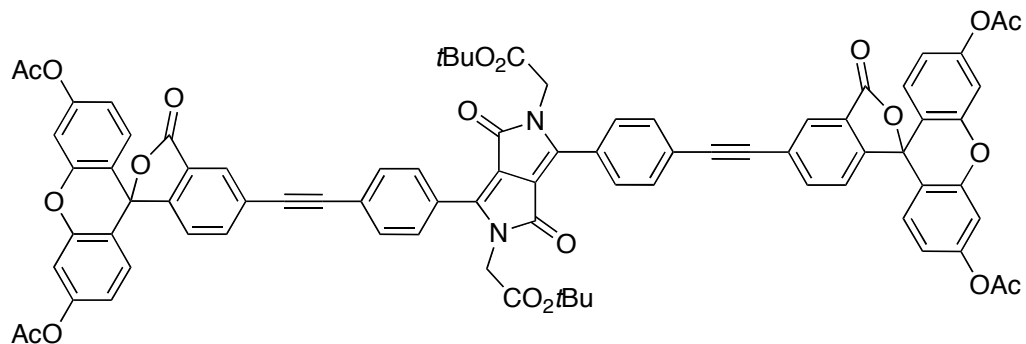
A solution of DPP **354** (0.4 g, 0.6 mmol) in freshly distilled CH<sub>2</sub>Cl<sub>2</sub> (10 mL) is cooled to - 78 °C. Then tetrabutylammonium fluoride (1.7 mL, 1.7 mmol) is added. Stirring is continued for 5 min, then the reaction is quenched with acetic acid (0.06 mL). After removal of the solvents, the crude residue is purified on silica gel, with CH<sub>2</sub>Cl<sub>2</sub> as eluent. The title compound is obtained in 64% yield (0.2 g).  $\delta_{\text{H}}$  (300 MHz, CDCl<sub>3</sub>): 7.75 (d,  $J$  = 8.1 Hz, 4H), 7.61 (d,  $J$  = 8.1 Hz, 4H), 4.39 (s, 4H), 3.25 (s, 2H), 1.39 (s, 18H);  $\delta_{\text{C}}$  (75 MHz, CDCl<sub>3</sub>): 167.6, 162.4, 147.9, 132.9, 128.9, 128.1, 125.5, 110.4, 83.1, 80.4, 44.5, 28.2; HR-MS (ESI-pos) for C<sub>34</sub>H<sub>32</sub>N<sub>2</sub>O<sub>6</sub> (M+H<sup>+</sup>) calc'd 564.23, found 565.2275.



$^1\text{H}$  NMR for compound **355** (300 MHz,  $\text{CDCl}_3$ ).

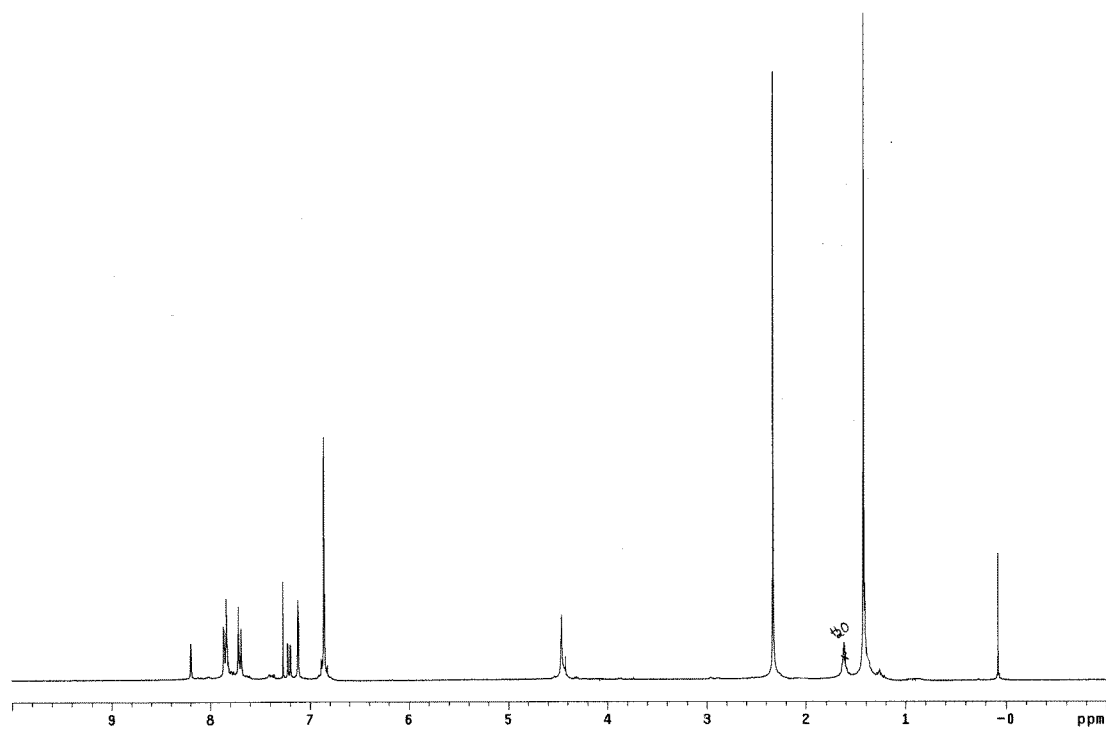


$^{13}\text{C}$  NMR for compound **355** (75 MHz,  $\text{CDCl}_3$ ).

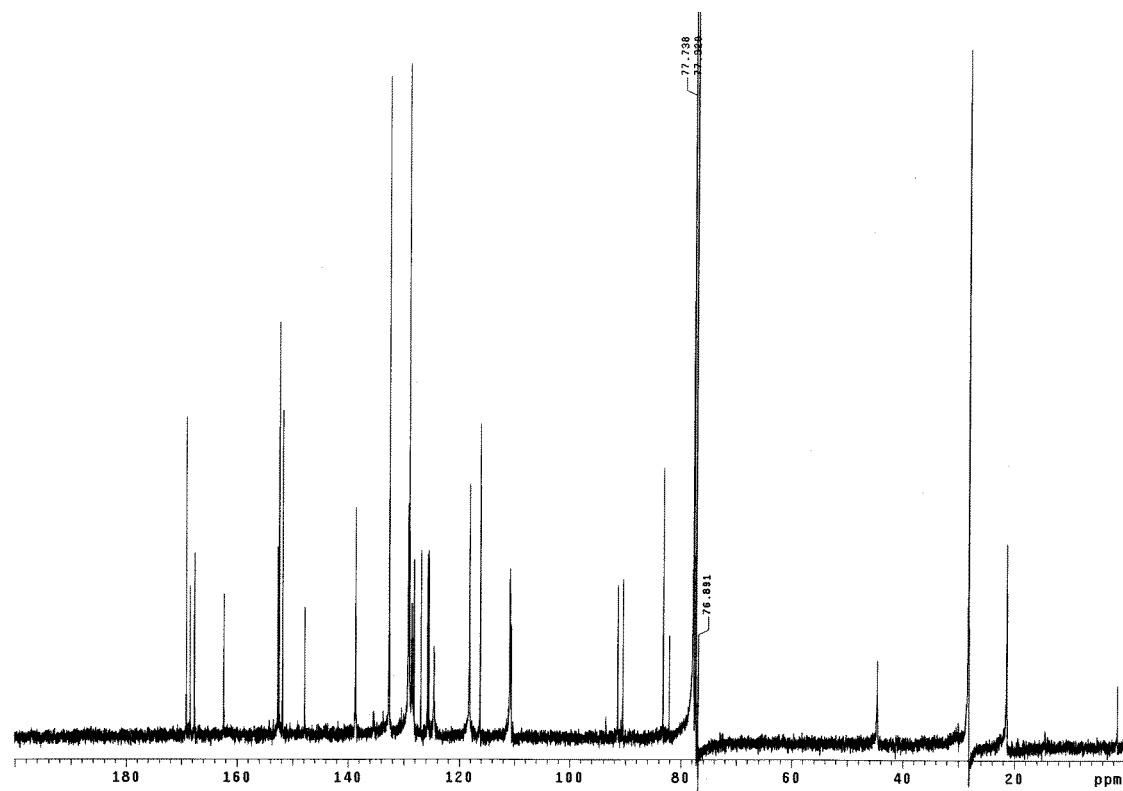
**Bis Fluorescein diacetate-DPP cassette 356.**

A solution of DPP **355** (0.100 g, 0.18 mmol), bromo-fluorescein diacetate (0.117 g, 0.24 mmol), Pd(PPh<sub>3</sub>)<sub>4</sub> (0.007 g, 0.006 mmol), CuI (0.001 g, 0.006 mmol) and triethylamine (0.238 g, 2.36 mmol) in dry THF (10 mL) was heated at 50 °C for 2 hours. After cooling to room temperature, the solvent was removed under reduced pressure and the residue purified by chromatography with 50% ethyl acetate/ Hexanes to give 0.050 g (10%) of the title compound.  $\delta_{\text{H}}$  (300 MHz, CDCl<sub>3</sub>): 8.19 (s, 2H), 7.84 (d,  $J$  = 11.4 Hz, 6H), 7.70 (d,  $J$  = 8.7 Hz, 4H) 7.20 (d,  $J$  = 7.8 Hz, 2 H), 7.11 (m, 4H), 6.85 (m, 8H), 4.46 (s, 4H), 2.32 (s, 12H), 1.42 (s, 18H);  $\delta_{\text{C}}$  (75 MHz, CD<sub>3</sub>OD): 169.1, 168.4, 167.6, 162.4, 152.7, 152.4, 151.8, 147.8, 138.6, 132.6, 129.2, 129.0, 128.5, 128.2, 126.9, 125.7, 125.5, 124.6, 118.1, 116.2, 110.8, 110.7, 110.5, 91.4, 90.4, 83.2, 82.1, 44.6, 28.2, 21.4.



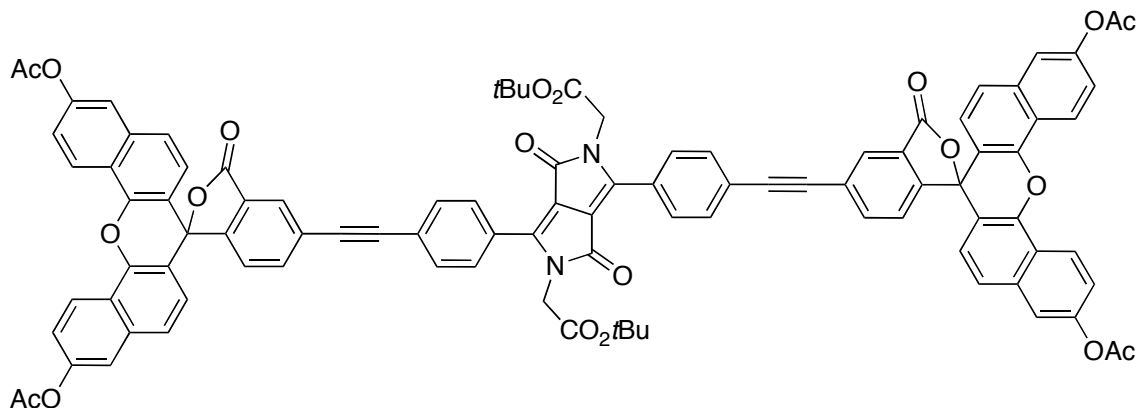


$^1\text{H}$  NMR for compound **356** (300 MHz,  $\text{CDCl}_3$ ).

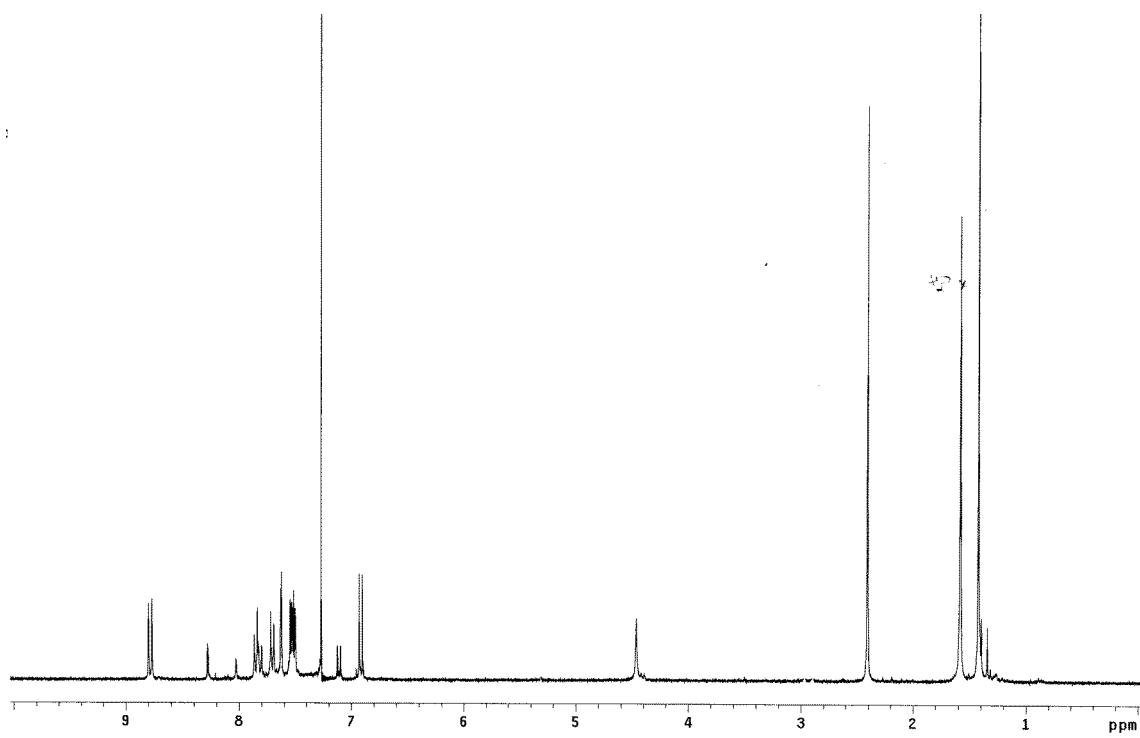


$^{13}\text{C}$  NMR for compound **356** (75 MHz,  $\text{CDCl}_3$ ).

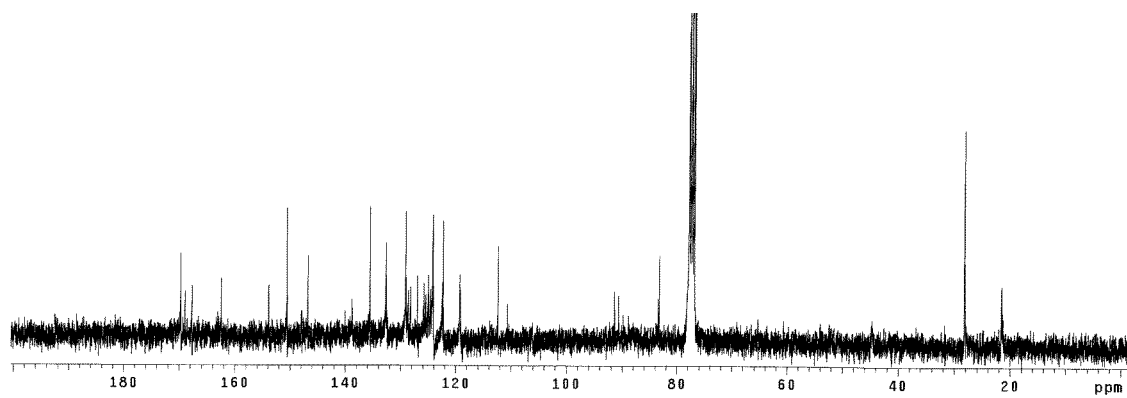
**Bis Naphthofluorescein diacetate - DPP cassette 357.**



A solution of DPP **355** (0.095 g, 0.17 mmol), bromo-naphthofluorescein diacetate (0.200 g, 0.34 mmol), Pd(PPh<sub>3</sub>)<sub>4</sub> (0.009 g, 0.008 mmol), CuI (0.002 g, 0.008 mmol) and triethylamine (0.34 g, 3.36 mmol) in dry DMF (10 mL) was heated at 80 °C for 2 hours. After cooling to room temperature, the solvent was removed under reduced pressure and the residue purified by chromatography with 20% Hexanes/dichloromethane then 2% MeOH/dichloromethane to give 0.244 g (91%) of the title compound.  $\delta_{\text{H}}$  (300 MHz, CD<sub>3</sub>OD): 8.88 (d,  $J$  = 9.0 Hz, 4H), 8.27 (s, 2H), 7.86 – 7.79 (m, 6 H), 7.71 (d,  $J$  = 8.1 Hz, 4H), 7.62 (d,  $J$  = 2.1 Hz, 4H), 7.54 – 7.49 (m, 10H), 7.11 (d,  $J$  = 8.1 Hz, 2H), 6.92 (d,  $J$  = 8.7 Hz, 4H), 4.46 (s, 4H), 2.41 (s, 12H), 1.42 (s, 18H);  $\delta_{\text{C}}$  (75 MHz, CD<sub>3</sub>OD): 169.6, 168.9, 167.6, 162.4, 153.8, 150.5, 146.7, 138.7, 135.5, 132.6, 129.0, 128.6, 128.2, 126.9, 125.8, 125.4, 124.9, 124.5, 124.1, 122.4, 122.2, 119.2, 112.3, 110.6, 91.3, 90.6, 83.4, 83.2, , 44.4, 28.7, 20.3; MS (ESI-pos) for C<sub>98</sub>H<sub>68</sub>N<sub>2</sub>O<sub>20</sub> (M+H<sup>+</sup>) calc'd 1593.44, found 1594.27.



$^1\text{H}$  NMR for compound **357** (300 MHz,  $\text{CDCl}_3$ ).



$^{13}\text{C}$  NMR for compound 357 (75 MHz,  $\text{CDCl}_3$ ).

**VITA**

**Name** Aurore Loudet

**Permanent Address** Quartier Castelviel  
31580 Villeneuve Lecussan, France

**Professional Address** Chemistry Department  
c/o Dr. Kevin Burgess  
Texas A&M University PO Box 30012  
College Station, TX 77845

**Education** 2000-2007 Ph.D., Chemistry, Texas A&M University  
College Station, TX

1999-2000 Master, Chemistry, Universite Paul Sabatier  
Toulouse, France

1995-1999 B.S., Biochemistry, Universite Paul Sabatier  
Toulouse, France

**Experience** 1999-2000 Graduate Research Assistant  
Universite Paul Sabatier, Toulouse, France

2000-2007 Graduate Research Assistant  
Texas A&M University, College Station, TX